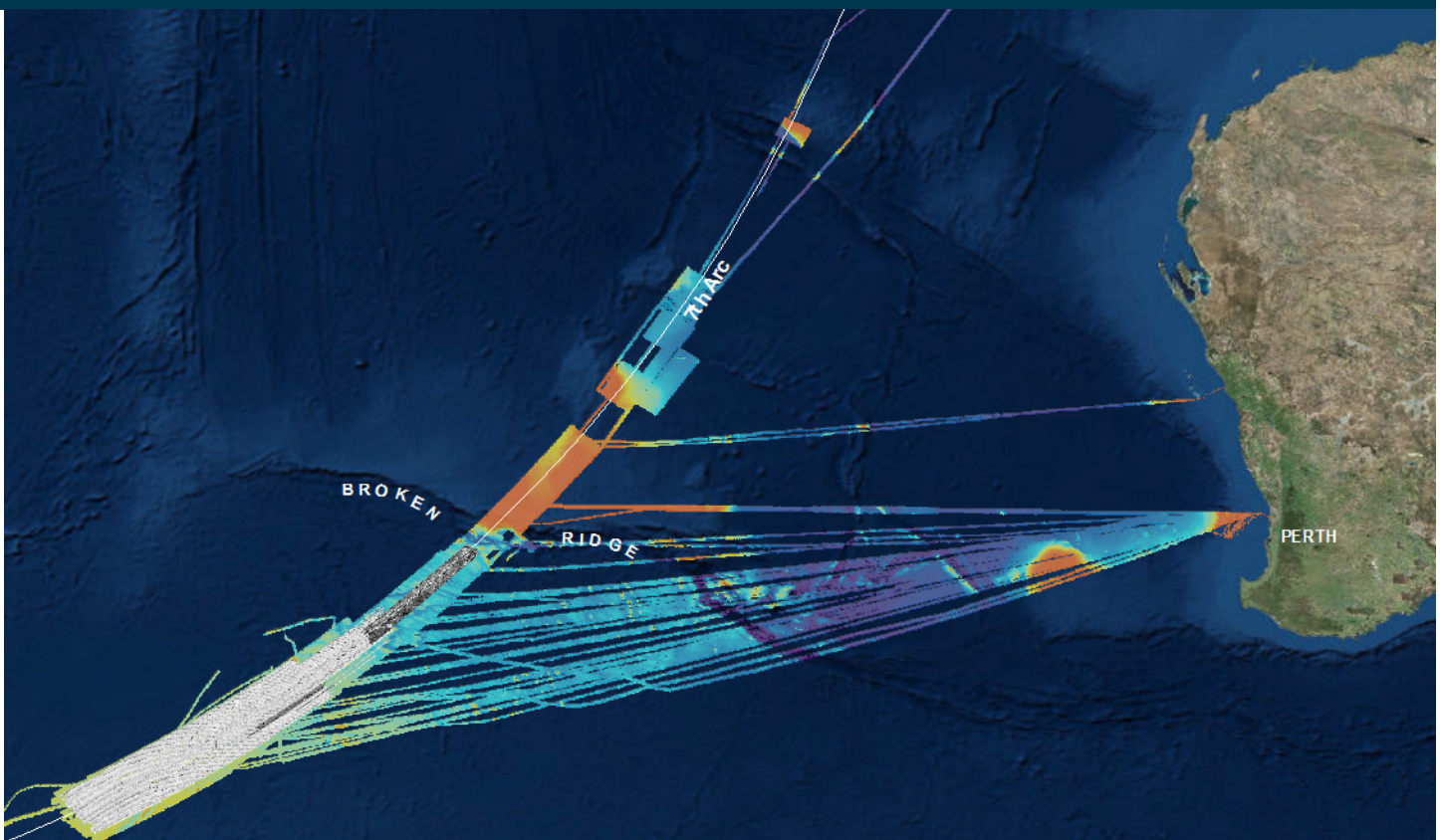




Australian Government
Australian Transport Safety Bureau

The Operational Search for MH370

3 October 2017



Investigation

ATSB Transport Safety Report
External Aviation Investigation
AE-2014-054
Final – 3 October 2017

Released in accordance with section 25 of the *Transport Safety Investigation Act 2003*

Publishing information

Published by: Australian Transport Safety Bureau
Postal address: PO Box 967, Civic Square ACT 2608
Office: 62 Northbourne Avenue Canberra, Australian Capital Territory 2601
Telephone: 1800 020 616, from overseas +61 2 6257 4150 (24 hours)
Accident and incident notification: 1800 011 034 (24 hours)
Facsimile: 02 6247 3117, from overseas +61 2 6247 3117
Email: atsbinfo@atsb.gov.au
Internet: www.atsb.gov.au

© Commonwealth of Australia 2017



Ownership of intellectual property rights in this publication

Unless otherwise noted, copyright (and any other intellectual property rights, if any) in this publication is owned by the Commonwealth of Australia.

Creative Commons licence

With the exception of the Coat of Arms, ATSB logo, and photos and graphics in which a third party holds copyright, this publication is licensed under a Creative Commons Attribution 3.0 Australia licence.

Creative Commons Attribution 3.0 Australia Licence is a standard form license agreement that allows you to copy, distribute, transmit and adapt this publication provided that you attribute the work.

The ATSB's preference is that you attribute this publication (and any material sourced from it) using the following wording: *Source:* Australian Transport Safety Bureau

Copyright in material obtained from other agencies, private individuals or organisations, belongs to those agencies, individuals or organisations. Where you want to use their material you will need to contact them directly.

Addendum

Page	Change	Date

Executive summary

On 8 March 2014, a Boeing 777 aircraft operated as Malaysia Airlines flight 370 (MH370) was lost during a flight from Kuala Lumpur in Malaysia to Beijing in the People's Republic of China carrying 12 crew and 227 passengers. The search for the missing aircraft commenced on 8 March 2014 and continued for 1,046 days until 17 January 2017 when it was suspended in accordance with a decision made by a tripartite of Governments, being Malaysia, Australia and the People's Republic of China.

The initial surface search and the subsequent underwater search for the missing aircraft have been the largest searches of their type in aviation history. The 52 days of the surface search involving aircraft and surface vessels covered an area of several million square kilometres. A sub surface search for the aircraft's underwater locator beacons was also conducted during the surface search.

The underwater search started with a bathymetry survey which continued as required throughout the underwater search and has mapped a total of 710,000 square kilometres of Indian Ocean seafloor, the largest ever single hydrographic survey. The high resolution sonar search covered an area in excess of 120,000 square kilometres, also the largest ever search or survey of its kind. Despite the extraordinary efforts of hundreds of people involved in the search from around the world, the aircraft has not been located.

Regardless of the cause of the loss of MH370, there were no transmissions received from the aircraft after the first 38 minutes of the flight. Systems designed to automatically transmit the aircraft's position including the transponder and the aircraft communications addressing and reporting system failed to transmit the aircraft's position after this time period. Subsequent analysis of radar and satellite communication data revealed the aircraft had actually continued to fly for a further seven hours. Its last position was positively fixed at the northern tip of Sumatra by the surveillance systems operating that night, six hours before it ended the flight in the southern Indian Ocean.

The challenge which faced those tasked with the search was to trace the whereabouts of the aircraft using only the very limited data that was available. This data consisted of aircraft performance information and satellite communication metadata initially, and then later during the underwater search, long-term drift studies to trace the origin of MH370 debris which had been adrift for more than a year, and in some cases, more than two years. The types of data, and the scientific methods used for its analysis, were never intended to be used to track an aircraft or pin point its final location.

On 28 April 2014, the surface search for MH370 coordinated by the Australian Maritime Safety Authority (AMSA) was concluded and the Australian Transport Safety Bureau (ATSB) assumed responsibility for conducting the underwater search for the aircraft. The underwater search area was initially defined at 60,000 square kilometres, and was increased in April 2015 when the Tripartite Governments (Malaysia, Australia and the People's Republic of China) agreed to expand the search area to 120,000 square kilometres. The primary objective of the underwater search was to establish whether or not the debris field of the missing aircraft was in the area of seafloor defined by expert analysis of the aircraft's flight path and other information. If a debris field was located, the search needed to confirm the debris was MH370 by optical imaging, and then map the debris field to enable planning for a subsequent recovery operation.

Once underwater search operations commenced in October 2014, the MH370 debris field could potentially have been located at any time. A recovery operation would need to have commenced as soon as possible after the debris field was located and the Tripartite governments had agreed on the next steps. The ATSB's role was therefore to also put in place the arrangements and plans necessary for a rapid recovery operation to occur at short notice.

The underwater search applied scientific principles to defining the most probable area to be searched through modelling the aircraft's flight path and behaviour at the end of the flight. The flight path modelling was based on unique and sophisticated analysis of the metadata associated with the periodic automated satellite communications to and from the aircraft in the final six hours of the flight. The end-of-flight behaviour of the aircraft, when MH370 was considered to have exhausted its fuel, has been analysed and simulated.

In 2015 and 2016, debris from MH370 was found on the shores of Indian Ocean islands and the east African coastline. The debris yielded significant new insights into how and where the aircraft ended its flight. It was established from the debris that the aircraft was not configured for a ditching at the end-of-flight. By studying the drift of the debris and combining these results with the analysis of the satellite communication data and the results of the surface and underwater searches, a specific area of the Indian Ocean was identified which was more likely to be where the aircraft ended the flight.

The understanding of where MH370 may be located is better now than it has ever been. The underwater search has eliminated most of the high probability areas yielded by reconstructing the aircraft's flight path and the debris drift studies conducted in the past 12 months have identified the most likely area with increasing precision. Re-analysis of satellite imagery taken on 23 March 2014 in an area close to the 7th arc has identified a range of objects which may be MH370 debris. This analysis complements the findings of the First Principles Review and identifies an area of less than 25,000 square kilometres which has the highest likelihood of containing MH370.

The ATSB's role coordinating the underwater search involved the procurement and management of a range of sophisticated and highly technical services. Management of the underwater search was aimed at ensuring high confidence in the acquisition and analysis of the sonar search data so that areas of the seafloor which had been searched could be eliminated. A comprehensive program was implemented to ensure the quality of the sonar coverage. A thorough sonar data review process was used to ensure areas of potential interest were identified and investigated.

During the early stages of the procurement, careful consideration was given to the methods available for conducting a large scale search of the seafloor. Water depths were known to be up to 6,000 m with unknown currents and unknown seafloor topography. Search operations would also have to be conducted in poor weather conditions and in a very remote area far from any land mass. Planning focused on selecting a safe, efficient and effective method to search the seafloor in an operation with an indeterminate timeframe.

The mapping of the seafloor in the search area revealed a challenging terrain for the underwater search which used underwater vehicles operating close to the seafloor. While the deep tow vehicles selected as the primary search method proved to be very effective, the seafloor terrain necessitated the use of a range of search methods including an autonomous underwater vehicle to complete the sonar coverage.

The underwater search area was located up to 2,800 km west of the coast of Western Australia and the prevailing weather conditions in this area for much of the year are challenging. Crews on the search vessels were working for months at a time in conditions which elevated the operational risks. The ATSB ensured that these risks to the safety of the search vessels and their crews were carefully managed.

At the time the underwater search was suspended in January 2017, more than 120,000 square kilometres of seafloor had been searched and eliminated with a high degree of confidence. In all, 661 areas of interest were identified in the sonar imagery of the seafloor. Of these areas, 82 with the most promise were investigated and eliminated as being related to MH370. Four shipwrecks were identified in the area searched.

The intention of this report is to document the search for MH370, in particular, the underwater search including; where the search was conducted (and why), how the search was conducted, the results of the search and the current analysis which defines an area where any future underwater

search should be conducted. The report also includes a safety analysis which is focused on the search rather than on discussing the range of factors which may have led to the loss of the aircraft.

The Government of Malaysia is continuing work on their investigation of the facts and circumstances surrounding the loss of MH370 aircraft consistent with their obligations as a member State of ICAO. The Malaysian investigation is being conducted in accordance with the provisions of ICAO Annex 13, Aircraft Accident and Incident Investigation.

The search, recovery and investigation of the loss of Air France flight AF447, in the South Atlantic Ocean in 2009, and the loss of MH370 have led to some important learnings related to locating missing aircraft on flights over deep ocean areas. Requirements and systems for tracking aircraft have been enhanced and will continue to be enhanced. Steps are being taken to advance other aircraft systems including emergency locator transponders and flight recorder locator beacons.

The ATSB acknowledges the extraordinary efforts of the hundreds of dedicated professionals from many organisations in Australia and around the world who have contributed their time and efforts unsparingly in the search for MH370.

The reasons for the loss of MH370 cannot be established with certainty until the aircraft is found. It is almost inconceivable and certainly societally unacceptable in the modern aviation era with 10 million passengers boarding commercial aircraft every day, for a large commercial aircraft to be missing and for the world not to know with certainty what became of the aircraft and those on board.

The ATSB expresses our deepest sympathies to the families of the passengers and crew on board MH370. We share your profound and prolonged grief, and deeply regret that we have not been able to locate the aircraft, nor those 239 souls on board that remain missing.

Contents

Executive summary	i
Contents	iv
Background	1
The search program	2
Investigation	2
Search	3
Recovery	4
Governance	4
Communications and media	6
Search funding	7
Search actual costs	7
History of the flight	9
Kuala Lumpur to waypoint IGARI	9
Waypoint IGARI to waypoint MEKAR	10
Waypoint MEKAR onwards	11
Aircraft Information	13
Airframe	13
Engines	14
Auxiliary Power Unit	14
Flight crew and passengers	14
The surface search	15
Malaysian led surface search	15
East of the Malay Peninsula	15
West of the Malay Peninsula	16
Northern and southern corridors announced	17
Australian led surface search	19
Initial southern Indian Ocean surface search area	20
Satellite imagery debris detections	23
Refined surface search area	25
Second refinement surface search area	29
Debris sightings and recoveries	33
Surface search coverage and confidence	34
The acoustic search for the underwater locator beacons	36
Underwater locator beacons	36
Acoustic detections	38
HMS Echo	38
Haixun 01	38
Ocean Shield	39
Analysis of acoustic detections	40
Marine animal tracking devices	41
Sonobuoys	41
Autonomous underwater vehicle search	41
The underwater search	43
Defining the initial underwater search area	43
Initial priority search area	43
Mapping the seafloor in the search area	45
Bathymetric survey	45

Geology of the search area	48
Bathymetry processing	50
Backscatter analysis	51
Selecting the search method/systems	52
The search tender	53
Synthetic Aperture Sonar	59
Other search coverage considerations	59
Validating the search systems	60
Underwater search chronology	62
The priority search area refined southwards	63
Underwater search commences	64
Search area extension	69
Generalised flight dynamic model	71
Complete Bayesian analysis	72
Last refinement to underwater search area	75
ATSB contractor reports	77
Area searched	77
Search area probability density functions	77
Quality assurance of the sonar data	83
Sonar coverage	86
Data processing and information dissemination – a new approach	89
Sonar contacts	90
Confidence in the search results	95
Other search area considerations.....	98
Pilot in Command's flight simulator	98
Controlled glide or ditching	99
Aircraft debris	102
Marine ecology examinations	107
Australian beach searches	107
Debris drift analysis	112
Hydroacoustic analysis	114
Satellite imagery analysis	116
Contrails analysis	117
Reanalysis of satellite imagery	118
External contributions	119
Other search considerations – risk mitigation.....	121
Weather	121
Weather forecasting and recording	122
Real time weather records	124
Weather events impacting search operations	125
Mitigation of weather impact on search operations	128
Health, safety and environment	129
Operational safety	130
Remote area operations	130
Remote area risk mitigation	130
Incident recording and reporting	131
Significant HSE incidents	131
Significant equipment related incidents	132
Impact of fishing vessels in the search area	132

Recovery planning	134
Planning for recovery	134
The investigations	136
Disaster Victim Identification	136
Safety analysis.....	137
Introduction	137
Search, rescue, and recovery	138
Search, rescue, and recovery phases	139
Normal flight	139
Aircraft in distress	144
Surface search	144
Underwater locator beacon search	145
Sonar search	147
Summary	147
Records of previous searches	149
Related searches	149
Previous safety recommendations	150
Malaysian Air Accident Bureau	150
Bureau d'Enquêtes et d'Analyses pour la sécurité de l'aviation civile (BEA)	150
Aviation industry statements	151
Safety actions	151
International Civil Aviation Organization	151
Inmarsat	152
Malaysia Airlines	152
Airservices Australia	152
Joint committee	152
Conclusions	153
Flight tracking	153
Emergency locator transmitters	153
Drift measurements	154
Visual and radar search aids	154
Underwater locator beacons	154
Other considerations	155
ATSB safety recommendations.....	156
Search and rescue information	156
Aircraft tracking	156
Sources and submissions	157
Sources of information	157
References	158
Submissions	159
Appendices	161
Appendix A: Search vessels	
Appendix B: Identification of the most probable final location of flight MH370 (Issue 2) – Joint Investigation Team paper - 26 April 2014	
Appendix C: Burst Frequency Offset (BFO) Doppler Model Development	
Appendix D: Fugro Survey Pty Ltd Search for Malaysian Airlines Flight MH370 All Vessels Reconnaissance Bathymetric Survey, Deep Tow Wide Area Survey and AUV Wide Area Survey Volume 7 – Summary Report	
Appendix E: Phoenix International Holdings Inc. Malaysia Airlines Flight 370 (MH370) Search End of Contract Report	

Appendix F: Chemical investigations on barnacles found attached to debris from the MH370 aircraft found in the Indian Ocean

Appendix G: Summary of Analyses Undertaken on Debris Recovered During the Search for Flight MH370

Appendix H: Analysis of Low Frequency Underwater Acoustic Signals Possibly Related to the Loss of Malaysian Airlines Flight MH370

Appendix I: Results of analysis of Scott Reef IMOS underwater sound recorder data for the time of the disappearance of Malaysian Airlines Flight MH370 on 8 March 2014

Appendix J: Seismic and hydroacoustic analysis relevant to MH370

Glossary	423
Abbreviations	427
Australian Transport Safety Bureau	429
Purpose of safety investigations	
Developing safety action	

Background

On 8 March 2014, a Boeing 777-200ER aircraft, registered 9M-MRO and operated as Malaysia Airlines flight 370 (MH370) disappeared during a flight from Kuala Lumpur to Beijing, carrying 12 Malaysian crew members and 227 passengers.

At the request of the Malaysian Government, the Australian Government accepted responsibility for initial search operations in the southern part of the Indian Ocean on 17 March 2014. A surface search by aircraft and surface vessels in the Indian Ocean, coordinated by the Australian Maritime Safety Authority (AMSA), and an acoustic sub-surface search for the aircraft's flight recorder underwater locator beacons, found no debris nor signals associated with MH370.

The Malaysian Government, as the International Civil Aviation Organization (ICAO) Annex 13 state of registry for Malaysia Airlines, was responsible for the overall strategic approach to the search for MH370 and the associated investigation. The majority of the passengers on board MH370 were from Malaysia and the People's Republic of China, however due to the proximity of the search area to Australia, and the request from Malaysia to Australia to lead search operations, Malaysia, the People's Republic of China and Australia agreed to collaborate in relation to the overarching search strategy. This cooperation is referred to as the Tripartite arrangement.

On 30 March 2014, the then Prime Minister of Australia, the Hon Tony Abbott MP, established the Joint Agency Coordination Centre (JACC) to coordinate the Australian Government's support for the search for missing flight MH370. The JACC was the coordination point for whole-of-Australian Government information, messaging and international engagement, including keeping the families of those on board and the general public informed of the progress of the search.

At the conclusion of the surface search on 28 April 2014, the Australian Prime Minister offered that Australia could continue to lead search operations. Tripartite meetings in May 2014 agreed to this arrangement and the ATSB was tasked to lead an intensified and continuous underwater search of an initial area of 60,000 square kilometres (km²). Subsequent Tripartite meetings in August 2014 agreed that Australia, through the ATSB, would also lead a recovery operation if and when the aircraft was located and a recovery was deemed suitable by the Tripartite.

A Memorandum of Understanding on Cooperation between the Governments of Australia and Malaysia in relation to MH370 (the MOU) provided a mechanism to formalise agreements on cooperation between the two governments. The then Australian Deputy Prime Minister and Minister for Infrastructure and Regional Development, the Hon Warren Truss MP, and Malaysian Minister for Transport Dato' Seri Liow Tiong Lai signed the MOU on 28 August 2014.

The MOU included a number of supplemental arrangements as annexures detailing the scope of work and responsibilities for specific areas of cooperation regarding MH370. The areas of cooperation included search, recovery, disaster victim identification, investigation, dealing with the debris site, and facilitating interactions with the next of kin. The MOU, and associated annexures, was deemed to have come into effect on 17 March 2014 for a period of three years.

On 16 April 2015, Tripartite Ministers met, considered next steps for the search and agreed that:

- If MH370 was not positively located in the initial 60,000 km² search area that the search would be expanded to an area of 120,000 km².
- When MH370 was located, a recovery operation would proceed with priorities for the recovery operation to include:
 - the aircraft's flight recorders
 - selected wreckage
 - where possible, human remains.

On 22 July 2016, Tripartite Ministers met and agreed that should the aircraft not be located in the search area, and in the absence of credible new evidence leading to the identification of a specific location of the aircraft, the search would be suspended, not ended, upon completion of the 120,000 km² search area. However, should credible new information emerge that can be used to identify the specific location of the aircraft, consideration would be given to determining next steps.

On 17 January 2017, in accordance with the decision made at the Ministerial Tripartite meeting in July 2016, the Tripartite countries issued a Joint Communiqué to announce the suspension of the underwater search following the completion of the 120,000 km² search area.

The search program

The operational search for MH370 (search program) was a large-scale complex international operation involving multiple assets in a dynamic environment. The search program encompassed a number of component activities, all of which were interdependent but with the unifying goal of ensuring the Australia (through the ATSB) fulfilled its obligations under Annex 13 of the Convention on International Civil Aviation (the Chicago Convention) and the MOU with Malaysia. Figure 1 depicts the search program objectives and the component activities.

Figure 1: Search program objectives

Program Goal	To assist the Malaysian Government in its investigation to find answers to the disappearance on 8 March 2014 (0022 local time Malaysia) of the Boeing 777-200ER aircraft registered 9M-MRO and operated as Malaysia Airlines Flight 370 (MH370)				
<i>In accordance with Annex 13 to the Convention on International Civil Aviation (Annex 13) and the Memorandum of Understanding on Cooperation between the Government of Australia and the Government of Malaysia in relation to MH370 (the MOU)</i>					
Program Objectives	Assist the Malaysian Government with its Investigation into the disappearance of MH370	To locate MH370 within the defined search area or determine to a high degree of confidence its absence from the defined search area			To coordinate the recovery of MH370 and human remains in accordance with Tripartite directions
		<i>MOU Annexure 1: Search for MH370</i>			<i>MOU Annexure 3: Recovery</i>
Program Component Activities	Assist in the conduct of the Annex 13 Investigation	Define the search area	Map the search area to enable underwater search	Conduct the underwater search	Prepare for and coordinate the recovery of MH370
		Quality assurance and data management			
	Program governance and assurance				
Program End State	ATSB has fulfilled its obligations under International Civil Aviation Organization (ICAO) Annex 13, the extant MOU and supplemental arrangements and agreements				

Source: ATSB

Investigation

The primary goal of the ATSB search program was to assist the Malaysian Government's Annex 13 safety investigation into the circumstances surrounding the aircraft's disappearance. Recovery and analysis of the cockpit voice recorder (CVR) and flight data recorder (FDR) in particular, would assist in determining the events leading to the loss of MH370.

Investigations conducted in accordance with Annex 13 of the International Civil Aviation Organization's Chicago Convention are for the sole purpose of the prevention of accidents and incidents, not to apportion blame nor to provide a means of determining liability.

Australian assistance has been provided in accordance with Annex 13 protocols. The ATSB has provided assistance to the Malaysian Annex 13 investigation since the initial stages of the search for MH370. The appointment of an Australian accredited representative to the Malaysian ICAO Annex 13 safety investigation team for MH370 was formalised on 1 April 2014. The Malaysian Annex 13 investigation team also includes accredited representatives from aviation investigation agencies in the United States, the United Kingdom, the People's Republic of China, France, Indonesia and Singapore.

The final results of Malaysia's Annex 13 Investigation are yet to be published by the Ministry of Transport Malaysia.

Search

The underwater search consisted of three component activities as outlined in Figure 1, defining the search area, conducting underwater mapping of the search area to enable the underwater search and conducting the underwater search.

Definition of the search area

The key component objectives were to:

- review the available data to determine the most likely location of MH370
- define the search area, initially for an area of up to 60,000 km², extended to an area of up to 120,000 km² in April 2015, for the purpose of conducting an underwater search for MH370 within Australia's search and rescue region in the Indian Ocean.

This aspect of the underwater search was the most challenging with analysis to refine the underwater search area being performed concurrently with search activities for the entire period of the search.

The work of many organisations and individuals from Australia and around the world was coordinated by the ATSB. Of particular note was the contribution of members of the search strategy working group (SSWG) including; Inmarsat, Thales, Boeing, the Air Accidents Investigation Branch (AAIB) of the United Kingdom, the National Transportation Safety Board (NTSB) of the United States, the Defence Science and Technology Group¹ (DST Group) and the Department of Civil Aviation Malaysia. Other significant contributors were the Commonwealth Scientific and Industrial Research Organisation (CSIRO) and Geoscience Australia.

Underwater mapping of the search area

The key component objective was to obtain a topographic map of the search area detailing the contours, depths and composition of the seafloor to enable safe navigation of underwater search equipment and prioritisation of search zones.

The method chosen to map the seafloor was a bathymetric survey. A combination of vessels contracted by the ATSB and vessels provided by the Tripartite governments were used to conduct the bathymetric survey.

The majority of bathymetric survey data was acquired from June to December 2014. However, as the underwater search progressed and the area increased from an area of 60,000 km² to 120,000 km², further bathymetric data was acquired.

Early in the underwater search the ATSB established a National Collaboration Framework Head Agreement and Project Agreement for technical assistance with Geoscience Australia. This was a key relationship for the ATSB, used to facilitate many technical aspects of the underwater search. This included the analysis, quality assurance and storage of all underwater search data including the bathymetric survey data.

¹ Formerly the Defence Science and Technology Organisation

Underwater search

The key underwater search objectives were to:

- search for, locate and positively identify MH370 within the defined search area on the seafloor
- obtain optical imaging (photography or video) of the aircraft debris field if MH370 was located, and, if possible, recover the flight recorders

or

- positively eliminate areas searched within the defined search area for the presence of MH370 with a high degree of confidence.

Coordinating the underwater search involved the procurement of search services and overseeing all aspects of the underwater search from vessel tasking to data analysis, quality assurance and management. Fugro Survey Pty Ltd (Fugro Survey) was contracted by the ATSB to provide vessels, personnel and equipment, initially to conduct a bathymetric survey and later, underwater search services.

Phoenix International Holdings Inc. (Phoenix International) and their subcontractors Hydrospheric Solutions Inc., were initially contracted by the Malaysian Government (and later in the search by the ATSB) to provide search services including the synthetic aperture sonar equipped SLH PS-60 ProSAS (ProSAS) deep tow vehicle for underwater search operations.

Details of the vessels used in the search are included in appendix A.

Quality assurance and data management

Overseeing the acquisition, analysis and management of the search data was an essential component of the search program. Early in the search, the ATSB appointed a sonar data Quality Assurance Manager with significant experience in underwater search and recovery operations to provide advice on the procurement of search services and manage the acquisition and analysis of all search data.

Systems for monitoring the performance of the search contractors were implemented including stringent performance standards, testing of search systems and oversight of all operations by expert ATSB client representatives on each search vessel. Search data was subjected to multiple levels of independent analysis and review to ensure quality, coverage and identification of all seafloor anomalies of potential interest.

Recovery

A key program objective was to prepare for a recovery operation, pending the location and positive identification of the MH370 debris field, in accordance with decisions made by the Tripartite governments in August 2014 and May 2015.

This involved planning, preliminary procurement activity and the formulation of a range of agreements with Australian and Malaysian Government agencies, including the Australian Federal Police, Western Australia Police and the Royal Malaysian Police, in order to coordinate and facilitate the recovery of evidence relevant to the investigations into the disappearance of MH370.

Governance

Program governance and assurance was a component activity under the search program that covered all other components. The ATSB is an independent Commonwealth government agency accountable to the Minister for Infrastructure and Transport and forms part of the Infrastructure and Regional Development Portfolio.

The search program forms a temporary division within the ATSB organisational structure with a specific set of objectives and accountability for the efficient, effective and ethical use of the overall search program budget provided by the Tripartite governments. Whilst the Chief Commissioner of

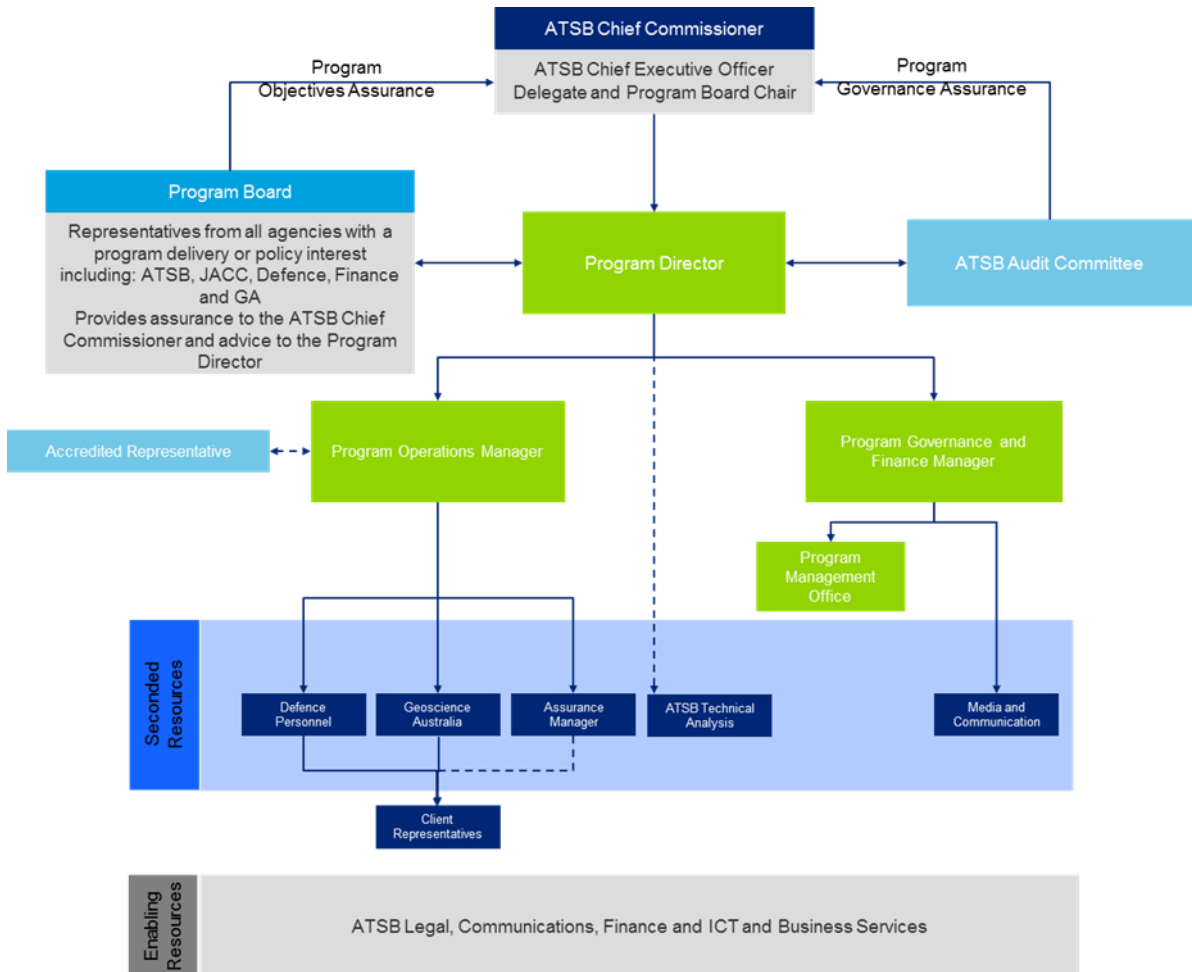
the ATSB, who is also Chief Executive Officer, is ultimately accountable to the Minister of Infrastructure and Transport for the search program, management of the search program was delegated to a full time Program Director, reflecting the scale and complexity of this program.

Given the overall program budget of approximately \$200 million, two program assurance mechanisms were implemented to provide assurance to the Chief Commissioner of effective program resource management.

- A program board, comprising the ATSB executive and representatives of key program stakeholders, provided guidance, advice and critical review of the search program. The program board was advisory rather than a decision making body due to the agile and dynamic nature of the operational environment, which required detailed technical decisions in short timeframes. The program board terms of reference were developed to support the role of the board.
- The ATSB’s audit committee provided a review of program governance mechanisms through rolling audits of key program components, conducted by the ATSB’s auditors. Details of the planned audits were outlined in the ATSB Internal Audit Annual Plans for each financial year. The ATSB’s audit committee was focused on ensuring the program complied with all relevant legislation and policy and made efficient, effective and ethical use of public funds.

Figure 2 outlines the governance structure and lines of accountability for the search program as at January 2017.

Figure 2: Governance structure



Source: ATSB

Communications and media

At times the ATSB's search program drew on the resources of the rest of the agency including the operational (investigation and technical resources), legal, finance, Information and Communications Technology and business services areas. Managing the significant volume of correspondence in relation to the search for MH370 required dedicated media and communications staff in the search team as the disappearance of MH370 has and continues to draw worldwide attention. The ATSB has received and processed over 3,500 pieces of correspondence, which include theories and queries from members of the public, scientists and academics, questions and requests for interviews and access from local and international press.

Website

When the ATSB assumed responsibility for coordinating the underwater search, a new MH370-specific section was added to the ATSB's website, www.atsb.gov.au/mh370. This section was designed to provide information and resources for all levels of interest. This included factsheets on various elements of the search, photographs and films, technical investigation reports and the archive of daily operational search updates.

Factsheets

The search for MH370 in the southern Indian Ocean involved a substantial amount of technical analysis and tasking, both to identify and refine the search area, and the practical elements of the conduct of the search itself. In an effort to provide the public with a clear understanding of the processes and resources, the ATSB published factsheets covering different elements of the search. These included:

- *MH370: Aircraft Debris and Drift Modelling*
- *MH370: Sonar Contacts*
- *Considerations on defining the search area – MH370*
- *Mapping the seafloor – Bathymetric survey – MH370*
- *The intensified underwater search for MH370*
- *MH370: Bathymetric Survey*
- *MH370: Multibeam Sonar*
- *MH370: Burst Timing Offset (BTO) Characteristics*
- *MH370: Update to Signalling Unit Logs*

The ATSB's website also provided links to works that collaborating agencies/bodies had published elsewhere:

- *The Search for MH370* (an article by Chris Ashton, Alan Shuster Bruce, Gary Colledge and Mark Dickinson of Inmarsat, published in The Journal of Navigation.)
- *MH370 – drift analysis: Trajectories of Global Drifter Program drifters* (an article by David Griffin of CSIRO)
- *The Use of Burst Frequency Offsets in the Search for MH370* (an article by Ian Holland of Defence Science and Technology Group.)
- *Bayesian Methods in the Search for MH370* (a book by Sam Davey, Neil Gordon, Ian Holland, Mark Rutten, and Jason Williams that encompassed the expert analysis of available data by the Defence Science and Technology Group.)

Technical Investigation Reports

As part of Australia's role in leading the search and as an accredited representative to Malaysia's Annex 13 investigation, the ATSB opened an external investigation, *AE-2014-054: Assistance to Malaysian Ministry of Transport in support of missing Malaysia Airlines flight MH370 on 7 March 2014 UTC*.

As part of that external investigation, the following reports have been published on the ATSB website:

- *MH370 – First Principles Review* (published 20 December 2016)
- *MH370 – Search and debris examination update* (published 2 November 2016, amended 2 December 2016)
- Debris examination reports 1, 2, 3, 4 and 5
- *MH370 – Definition of Underwater Search Areas* (published 3 December 2015, amended 10 December 2015)
- *MH370 – Flight Path Analysis Update* (published 8 October 2014)
- *MH370 – Definition of Underwater Search Areas* (published 26 June 2014, amended 18 August 2014, amended 30 July 2015).

The website also hosts the CSIRO reports; *The search for MH370 and ocean surface drift*, parts I, II and III and the Geoscience Australia report; *Summary of imagery analyses for non-natural objects in support of the search for Flight MH370*.

Search funding

Funding and resource contributions for the underwater search have been provided by the Governments of Malaysia, Australia and the People’s Republic of China as outlined in Table 1.

Table 1: Resources available to the ATSB for search activities

Country	Contribution	Percentage of available resources
Malaysia ²	A\$115m	58%
Australia ^{3 4 5}	A\$63m	32%
The People’s Republic of China ^{6 7}	A\$~20m	10%
Overall Available Resources	A\$198m	100%

Source: ATSB

Search actual costs

The estimated actual costs of the Australian led underwater search for MH370 to 30 June 2017 are detailed in Table 2. These costs cover the financial years 2013-14 through to 2016-17.

-
- ² During 2014-15 Malaysia also directly funded the provision of a vessel (*GO Phoenix*) and search system as part of the underwater search. This vessel and equipment contributed to the search from September 2014 through to June 2015. The contract for the provision of these services was directly with Malaysia and the value of this contribution is not included in the figures above.
 - ³ The funding contribution provided by Australia is outlined in Budget Measure ‘Malaysia Airlines Flight MH370 – Search’ as announced in the 2014-15 Budget. Details are provided in Budget Paper No. 2 2014-15 and the 2014-15 Portfolio Budget Statements for the Infrastructure and Regional Development Portfolio.
 - ⁴ A funding measure was also provided by Australia and outlined in Budget Measure ‘Malaysia Airlines Flight MH370 – International Contribution’ as announced in the 2015-16 Budget. Details are provided in Budget Paper No. 2 2015-16 and the 2015-16 Portfolio Budget Statements for the Infrastructure and Regional Development Portfolio. The measure consisted of \$43.9 million in 2014-15 and \$50.0 million in 2015-16 with the cost of the measure fully offset by financial contributions to the search by the People’s Republic of China and Malaysia.
 - ⁵ A further funding contribution of \$3 million provided by Australia outlined in Budget Measure ‘Malaysia Airlines Flight MH370 - additional contribution - extension’ in the 2016-17 Mid-Year Economic and Fiscal Outlook (MYEFO).
 - ⁶ In November 2015 the People’s Republic of China offered \$20 million as a resource contribution to the search. This contribution included the search vessel, *Dong Hai Jiu 101*.
 - ⁷ During the early part of the search the People’s Republic of China provided the vessel *Zhu Kezhen* to undertake underwater mapping services. The value of this contribution is not included in the figures above.

Table 2: Estimated actual search costs to 30 June 2017

Search Phase	Cost area	Estimated actual cost to 30 June 2017
Underwater Search – ATSB Lead Program Components:	Underwater Search	A\$170m
	Bathymetry (Underwater Mapping)	A\$20m
	Program Management	A\$7m
	Other sub-components (Definition of search area, Recovery preparation, Investigation Support)	A\$1m
Total – Underwater Search Program Components:		A\$198m

Source: ATSB

Costs for the search by Australian Government agencies (Commonwealth and State) over and above the funding provided in the Budget Measures have been absorbed by the respective agencies and are not included in the actual costs in Table 2.

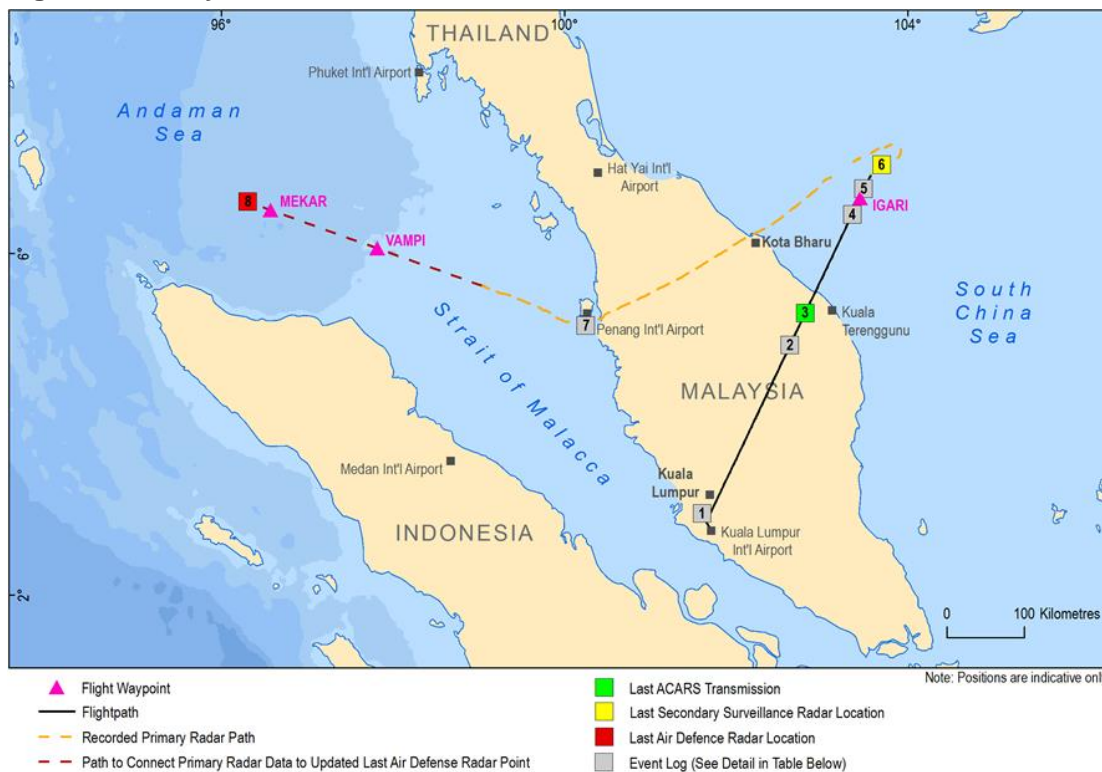
History of the flight

Kuala Lumpur to waypoint IGARI

On 7 March 2014 at 1642 UTC⁸, a Boeing 777-200ER aircraft, registered 9M-MRO and operating as Malaysia Airlines flight 370 (MH370), departed from runway 32R at Kuala Lumpur International Airport on an international scheduled passenger flight to Beijing, People’s Republic of China. On board the aircraft were 239 persons, comprising 12 crew and 227 passengers.⁹

Following take-off, the aircraft was cleared by air traffic control (ATC) at Kuala Lumpur Air Traffic Control Centre to climb to 18,000 ft (FL180)¹⁰. The crew were approved to cancel the Standard Instrument Departure and track direct to the Instrument Flight Rules (IFR) waypoint IGARI (Figure 3).

Figure 3: History of recorded events



Source: ATSB, using Ministry of Transport Malaysia data

Subsequently, the aircraft was cleared to climb to FL250 and then to the planned cruising level of FL350. At 1701:17, the Pilot-in-Command (PIC) of MH370 reported maintaining FL350.

At 1707:29, the Aircraft Communications Addressing and Reporting System (ACARS) transmitted the flight’s first ‘B777 position report’ via the aircraft’s satellite communication system. Information in this report included the total fuel load of 43,800 kg, enough fuel for MH370 to remain airborne until approximately 0012. A position report was normally transmitted every 30 minutes, however the report at 1707:29 was the last ACARS report received from the aircraft.

Prior to the aircraft reaching waypoint IGARI, which denoted the border of the Vietnamese flight information region, Kuala Lumpur Air Traffic Control Centre instructed the crew to contact Ho Chi

⁸ Coordinated Universal Time (UTC) is used throughout this report. Malaysia time (MYT) was UTC +8 Hrs.

⁹ A more detailed history of the flight has been published by the Ministry of Transport Malaysia and is available here: www.mh370.gov.my/index.php/en/media2/transcript/category/13-mh370-safety-investigation-public

¹⁰ Flight levels give an approximate altitude in hundreds of feet. FL180 is approximately 18,000 ft.

Minh Air Traffic Control Centre (Vietnam) on a radio frequency of 120.9 MHz. At 1719:30, the PIC of MH370 acknowledged the instruction with ‘Good night Malaysia Three Seven Zero.’ This was the last recorded radio transmission from the aircraft.

Waypoint IGARI to waypoint MEKAR

The aircraft was fitted with a transponder that permitted ground-based secondary surveillance radars (SSR) to track it. A subsequent review of recorded ATC radar data revealed that the aircraft passed waypoint IGARI at 1720:31 and that the Mode S transponder symbol of the aircraft was not detected on Malaysian ATC radar after 1720:36. A matching SSR target captured by Vietnamese radar at Conson Island was no longer detected after 1720:33¹¹.

Some radars, called primary surveillance radars (PSR), can detect an aircraft without relying on a transponder, usually at a much shorter range than SSR. Recordings from a civilian PSR at Kota Baru in the north of Malaysia and a military PSR on Penang Island jointly showed a target that matched the time and location of MH370’s last SSR position. While the recorded primary radar data was not continuous, the target could be followed with no ambiguity with other radar returns in the area. The limited fidelity of the PSR tracking data allowed the aircraft’s speed, location, and altitude to be approximated from IGARI onwards.

From IGARI, the aircraft apparently made a 40° turn to the right and then a 180° turn to the left to track almost directly back across the Malay Peninsula, in the general direction of Penang Island. The aircraft passed over or near IFR waypoints ABTOK, KADAX and GOLUD (which are within 3 NM of each other) and later PUKAR.

The aircraft made a slow right turn south of Penang Island. A mobile telephone registered to the aircraft’s first officer was detected by a mobile telecommunications tower at Bandar Baru Farlim Penang at 1752:27, when the aircraft was south of Penang. There was no record of communications having been made or attempted using this telephone.¹²

Radar data shows the aircraft then headed to the northwest, eventually aligning with published air route N571 from IFR waypoint VAMPI. The validity of this section of the radar data was verified using the track of a commercial flight that followed N571 about 33 NM behind MH370. The aircraft continued to the northwest until a final radar position for the aircraft was recorded approximately 10 NM beyond IFR waypoint MEKAR at 1822:12 (Figure 3). There were no reports of the aircraft being detected by any radar after this time. Key events are summarised in Table 3.

Table 3: Key recorded events

Recorded Event	Time (UTC)
Event 1: MH370 departed Kuala Lumpur International Airport	1642
Event 2: PIC reported maintaining FL350	1701:17
Event 3: ACARS report transmitted	1707:29
Event 4: Last radio transmission from MH370	1719:30
Event 5: Aircraft passed over waypoint IGARI	1720:31
Event 6: Last recorded secondary surveillance radar position	1721:13
Event 7: First officer’s mobile phone detected by Penang communications system	1752:27
Event 8: Last primary surveillance radar position	1822:12

Source: Ministry of Transport Malaysia, Royal Malaysian Police

¹¹ From 1739:03 onwards, Malaysian and Vietnamese controllers attempted to contact the aircraft by radio without success. A distress phase was formally initiated by Malaysian ATC at 2232:00.

¹² This information was obtained by the Royal Malaysian Police and reported to the Ministry of Transport Malaysia. Though a formal report was not available to the ATSB, information relevant to the search was shared.

Waypoint MEKAR onwards

At 1825:27, about three minutes after the last primary radar return, the aircraft’s satellite data unit (SDU) initiated a log-on sequence via the Inmarsat Indian Ocean Region I-3 satellite to the ground station in Perth, Western Australia. The log-on sequence and timings of subsequent SDU communications were recorded by the Inmarsat ground station, including several automated handshakes¹³ initiated by either the ground station or the aircraft, and two unanswered ground-to-air satellite telephone call attempts (made by the aircraft operator in an attempt to contact the aircraft). This information showed that the flight continued for almost six hours after the last radar return (Table 4).

Table 4: Satellite communications after passing waypoint MEKAR

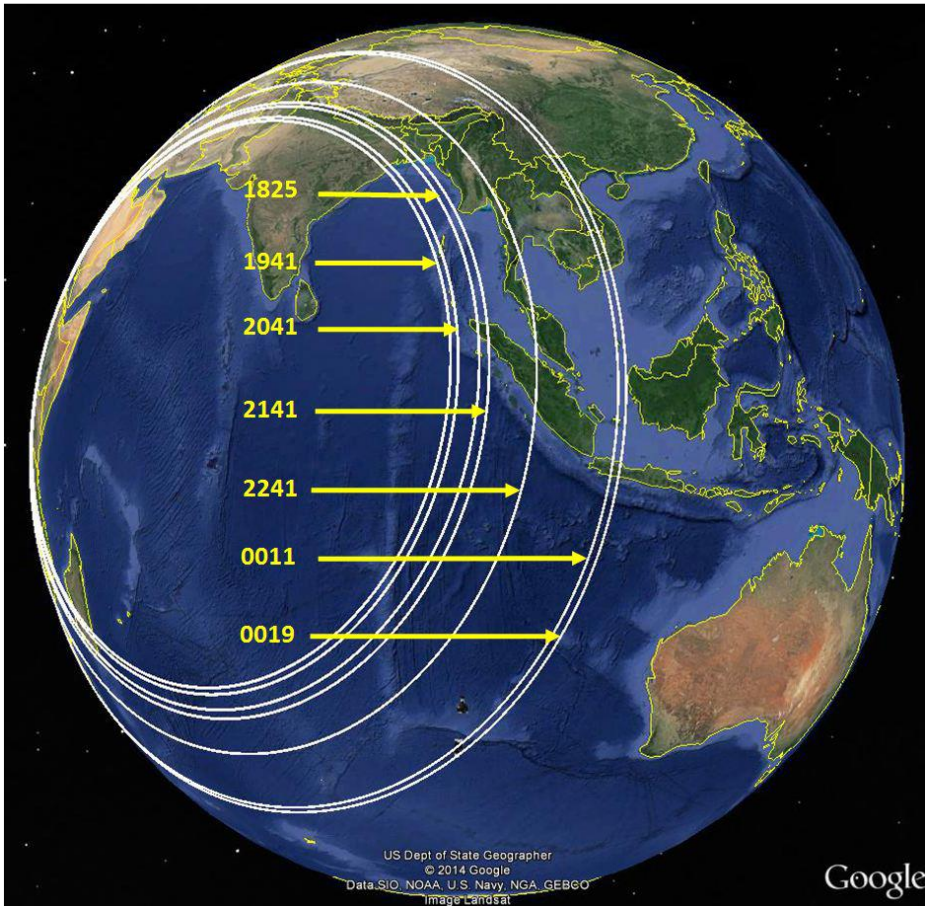
Recorded SDU communications	Time (UTC)
Handshake 1 initiated by the aircraft	1825:27
Unanswered ground to air telephone call	1839:52
Handshake 2 initiated by the ground station	1941:00
Handshake 3 initiated by the ground station	2041:02
Handshake 4 initiated by the ground station	2141:24
Handshake 5 initiated by the ground station	2241:19
Unanswered ground to air telephone call	2313:58
Handshake 6 initiated by the ground station	0010:58
Handshake 7 initiated by the aircraft	0019:29
Aircraft did not respond to log-on interrogation from the satellite earth ground station (failed handshake).	0115:56

Source: Inmarsat

As part of routine logging, Inmarsat recorded the burst timing offset (BTO) and burst frequency offset (BFO) information for each handshake. Though not intended for this purpose, the BTO could be used to find the distance between the aircraft and the satellite at the time of each handshake. A series of seven rings, joining points on the earth’s surface equidistant from the satellite, shows the range of possible locations of the aircraft at the time of each handshake (Figure 4). By taking the maximum speed of the aircraft into account, the BTO derived rings could be reduced in length to arcs (there are some areas of the rings the aircraft simply could not have reached).

¹³ In satellite communications, a handshake is a series of signalling messages that establish or maintain a communication channel.

Figure 4: BTO ring solutions for MH370



Source: Google earth, annotated by ATSB

The BFO was influenced by the speed of the aircraft relative to the satellite which is affected by the aircraft position, direction and speed of travel, and the satellite’s own movement. Analysis of the BFO metadata revealed that the aircraft headed south from some point beyond waypoint MEKAR to a region in the southern Indian Ocean. This analysis was later supported by studying¹⁴ the drift of MH370 debris which was found on the shorelines of eastern African nations in 2015 and 2016.

Analysis of the last satellite communication at 0019.29, which was an unscheduled log-on request from the aircraft, determined that it was probably the result of the aircraft having exhausted its fuel and then being powered by the auxiliary power unit. Based on the last transmitted fuel status and aircraft performance data the time that this occurred generally aligned with the expected time of fuel exhaustion. It was concluded that the aircraft probably impacted the ocean relatively close to the time this last transmission was made, which is referred to as the 7th arc.

The methodologies for calculating the aircraft’s possible flight paths were outlined in the ATSB’s reports:

- *MH370 – Definition of Underwater Search Areas* (released 26 June 2014, amended 18 August 2014, amended 30 July 2015)
- *MH370 – Flight Path Analysis Update* (released 8 October 2014)
- *MH370 – Definition of Underwater Search Areas* (released 3 December 2015, amended 10 December 2015)

¹⁴ Refer to the CSIRO reports prepared for the ATSB: *The search for MH370 and ocean surface drift- parts I, II and III*.

- *MH370 – Search and debris examination update* (released 2 November 2016, amended 2 December 2016)
- *MH370 – First Principles Review* (released 20 December 2016)

Aircraft Information

The aircraft operating flight MH370 was a Boeing 777-2H6¹⁵ER model, powered by two Rolls-Royce Trent 800 Turbofan engines (Figure 5).

Figure 5: 9M-MRO, the aircraft operating Malaysia Airlines flight MH370 on 8 March 2014



Source: Seth Jaworski

Airframe

Manufacturer:	Boeing Company
Model:	777-2H6ER
Serial number:	28420
Registration:	9M-MRO
Date of manufacture:	29 May 2002
Date of delivery:	Delivered new on 31 May 2002
Certificate of airworthiness:	M.0938 valid to 2 June 2014
Certificate of registration:	M.1124 issued 23 August 2006 Replacement of Certificate issued 17 June 2002
Last maintenance check:	A1 Check on 23 February 2014 at 53,301:17 hours and 7,494 cycles
Total airframe hours/cycles:	53,471.6 hours/7,526 cycles (as of 7 March 2014)

Source: Malaysia Airlines

¹⁵ H6 denotes the unique Boeing customer code for 737, 747 and 777 aircraft purchased by Malaysia Airlines.

Engines

Manufacturer:	Rolls-Royce	
Model:	RB211 Trent 892B-17	
	Engine 1 (Left)	Engine 2 (Right)
Serial number:	51463	51462
Date of construction:	November 2004	October 2004
Date installed:	8 May 2013	15 June 2010
Last Shop Visit:	6 September 2010 to 21 November 2010	5 February 2010 to 14 April 2010
Time in Service:	40,779 hours, 5,574 cycles (as of 7 March 2014)	40,046 hours, 5,508 cycles (as of 7 March 2014)

Source: Malaysia Airlines

Auxiliary Power Unit

Manufacturer:	Allied Signal
Model:	GTCP 331-500B
Serial number:	P1196
Auxiliary Power Unit hours:	22,093 (as of 7 March 2014)

Source: Malaysia Airlines

Flight crew and passengers

The passenger manifest for MH370, supplemented by information confirmed by INTERPOL, identifies the nationalities of passengers and crew on board the flight (Table 5).

Table 5: Nationalities of passengers and crew on board MH370

Nationality	Passengers	Crew
Chinese	153	
Malaysian	38	12
Indonesian	7	
Australian	6	
Indian	5	
French	4	
American	3	
New Zealander	2	
Ukrainian	2	
Canadian	2	
Russian	1	
Chinese Taipei	1	
Dutch	1	
Iranian	2 (travelling under stolen Austrian and Italian passports)	

Source: Malaysia Airlines flight MH370 flight manifest and INTERPOL

The surface search

The surface search for MH370 lasted from 8 March 2014 until 28 April 2014 and was initially a search and rescue operation. The intent was to locate the aircraft as quickly as possible in order to rescue any potential survivors. The areas searched were based on information from a range of sources and progressively refined analysis in relation to the aircraft’s most likely flight path.

Early in the surface search the Malaysian Government convened the Joint Investigation Team (JIT) comprising experts from the People’s Republic of China, France, Malaysia, United Kingdom, United States and Malaysian Government officials. Soon after, a satellite communications working group (SATCOM WG) was also formed and included experts from Inmarsat and Thales. These groups of experts worked together to provide advice to the Malaysian Government on the surface search areas.

By the end of the surface search an area of several million square kilometres had been searched by aircraft and surface vessels in the South China Sea, Andaman Sea, Bay of Bengal and Indian Ocean, however no items of debris from MH370 were recovered or positively identified.

The following section sets out the chronology of the surface search, the search assets used, the areas of focus at different times and the information or analysis used to define each area.

Malaysian led surface search

Search operations commenced on the day that MH370 went missing, 8 March 2014, and were led by Malaysian and Indonesian authorities in areas around Malaysia until 23 March 2014.

East of the Malay Peninsula

Initially search and rescue (SAR) operations were coordinated by Kuala Lumpur Aeronautical Rescue Coordination Centre (KL ARCC) and were conducted to the east of the Malay Peninsula in the South China Sea between 8 and 15 March 2014 (Table 6). This area was based largely on the last contact with the aircraft and where the SSR transponders ceased to operate.

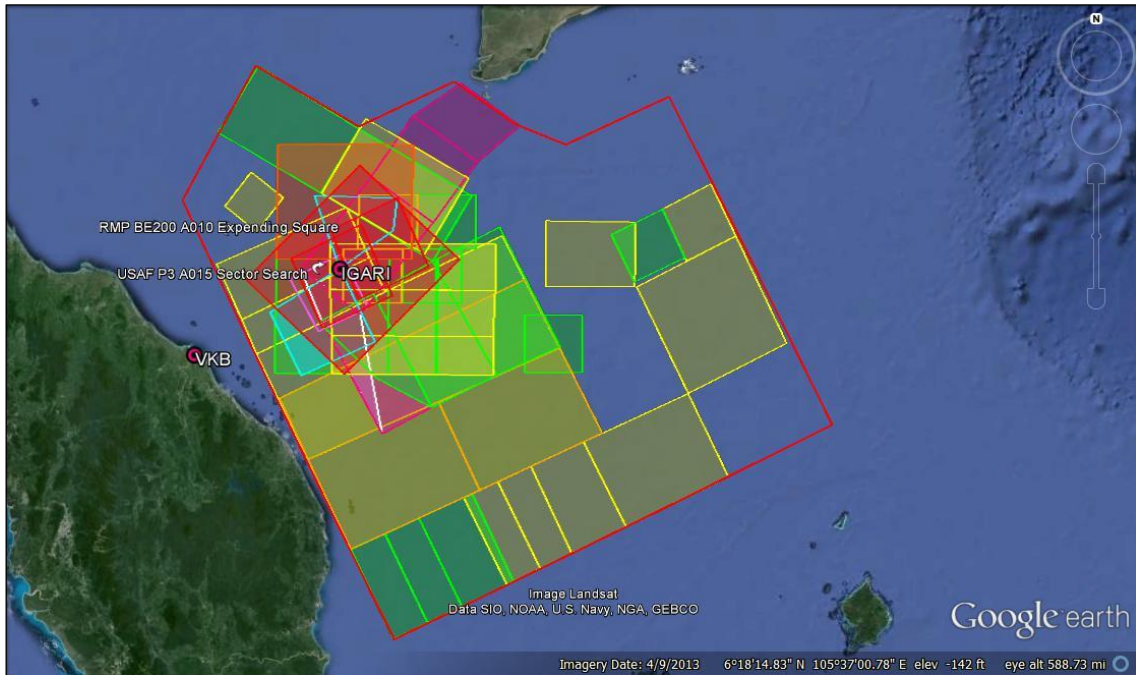
Table 6: Initial surface search SAR operations east of Malaysia

Dates:	8–15 March 2014
Event:	Malaysia (KL ARCC) initial surface search area.
Search area location:	East of Malay Peninsula (South China Sea).
Search activity:	Aerial and surface search.
Guiding advice:	Malaysia Air Defense.
Data used in planning search area refinement:	Malaysia Air Defense secondary surveillance radar data. Track BD764 7 March 2014 1642:07–1728:37 UTC recorded at 10 second intervals.
Search equipment:	28 aircraft from the People’s Republic of China (2), Japan (5), Malaysia (10), Singapore (4), Thailand (1), United States (2) and Vietnam (4). 34 vessels from the People’s Republic of China (7) Malaysia (19), Singapore (3), United States (3) and Vietnam (2).
Search area:	573,000 km ²

Source: DCA Malaysia

The areas covered during the search operations in the South China Sea are shown in Figure 6.

Figure 6: Surface search east of the Malay Peninsula 8 to 15 March 2014



Source: Google earth, annotated by DCA Malaysia

West of the Malay Peninsula

From 8 to 15 March 2014, the same time as the surface search in the South China Sea east of the Malay Peninsula, SAR operations coordinated by the Royal Malaysia Air Force, were conducted to the west of the Malay Peninsula (Table 7).

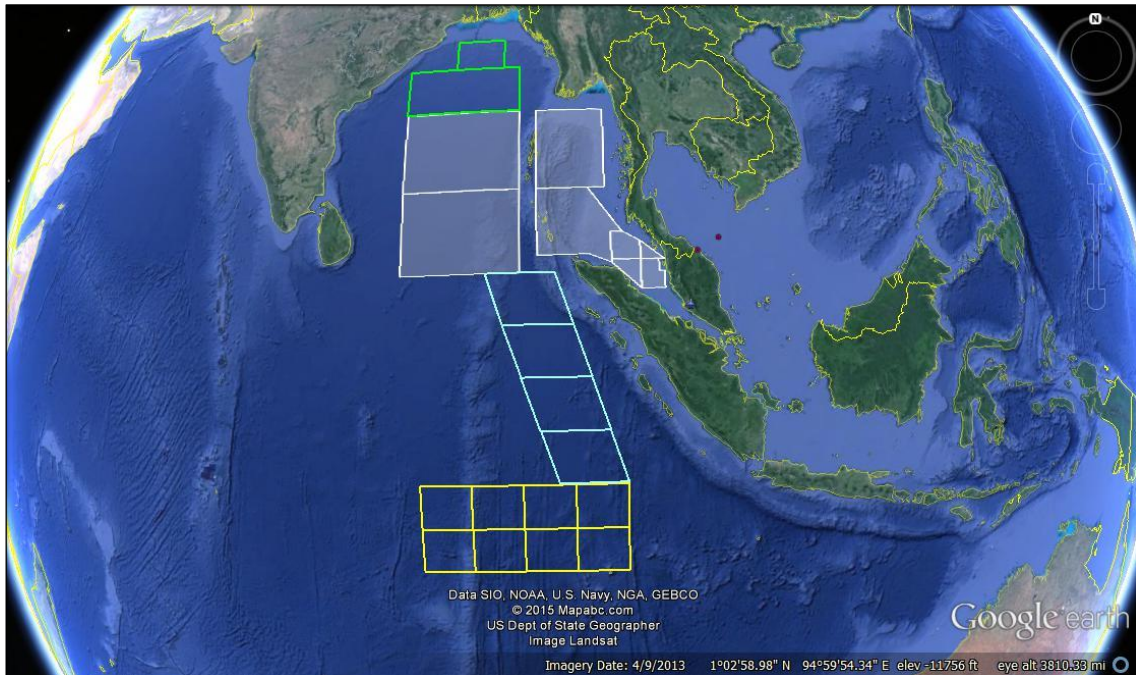
Table 7: Initial surface search SAR operations west of Malaysia

Dates:	8–15 March 2014
Event:	Malaysia (Royal Malaysia Air Force) initial surface search area.
Search area location:	West of Malay Peninsula (Strait of Malacca, Andaman Sea and the Bay of Bengal) and West of Sumatra.
Search activity:	Aerial and surface search.
Guiding advice:	Malaysia Air Defense.
Data used in planning search area refinement:	Malaysia Air Defense primary radar data. Track BE144 7 March 2014 1729:09–1802:59 UTC recorded at 10 second intervals.
Search equipment:	36 aircraft and 35 vessels from Australia, Bangladesh, the People’s Republic of China, India, Indonesia, Malaysia, New Zealand, Republic of Korea, Singapore, Thailand, United Arab Emirates and the United States.
Search area:	4,560,000 km ²

Source: DCA Malaysia

These search operations were undertaken in the Strait of Malacca, Andaman Sea, Bay of Bengal and west of Sumatra from 8 to 15 March 2014 (Figure 7, areas subject to search operations shown in white and blue). This area was searched based on the primary radar data which indicated an unidentified aircraft had flown up the Strait of Malacca, thought to be MH370.

Figure 7: Surface search areas west of the Malay Peninsula 8 to 15 March 2014

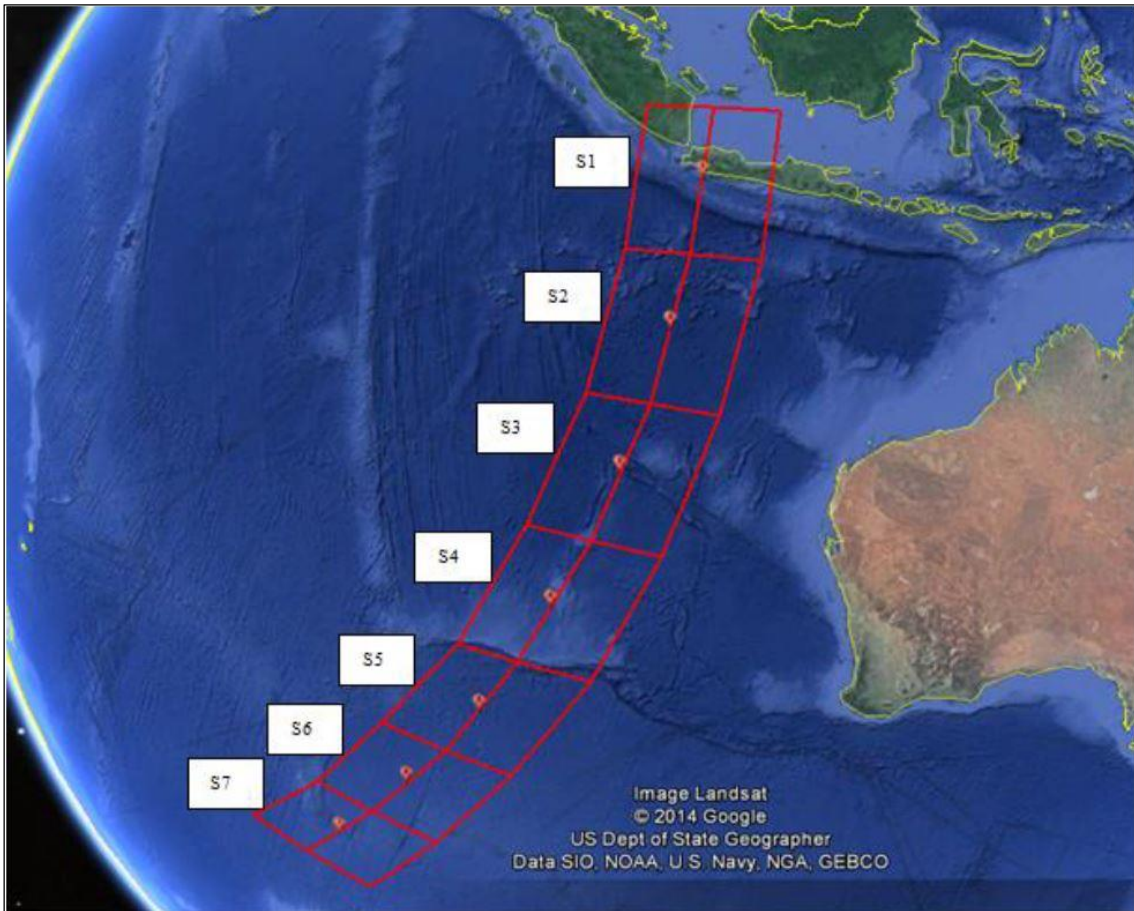


Source: Google earth, annotated by DCA Malaysia

Northern and southern corridors announced

In the first week of the surface search an analysis of Inmarsat satellite communication (SATCOM) data for MH370 indicated that the aircraft had flown for a further six hours after the final radar capture at the northern tip of Sumatra. The initial satellite data analysis indicated that the aircraft had flown along one of two corridors; one to the north in the direction of Kazakhstan or one to the south to the Indian Ocean. This new information led to the suspension of SAR operations to the east and west of the Malay Peninsula on 15 March 2014.

Figure 8: Southern corridor



Source: Malaysia, ICAO Third Meeting of the Asia/Pacific Regional Search and Rescue Task Force (APSAR/TF/3) Working Paper 06, Maldives, 25 – 29 January 2015

An aerial search coordinated by KL ARCC and Badan SAR Nasional (BASARNAS), the Republic of Indonesia National Search and Rescue Agency, was conducted within the southern corridor indicated by the SATCOM data from 18 to 23 March 2014 (Table 8).

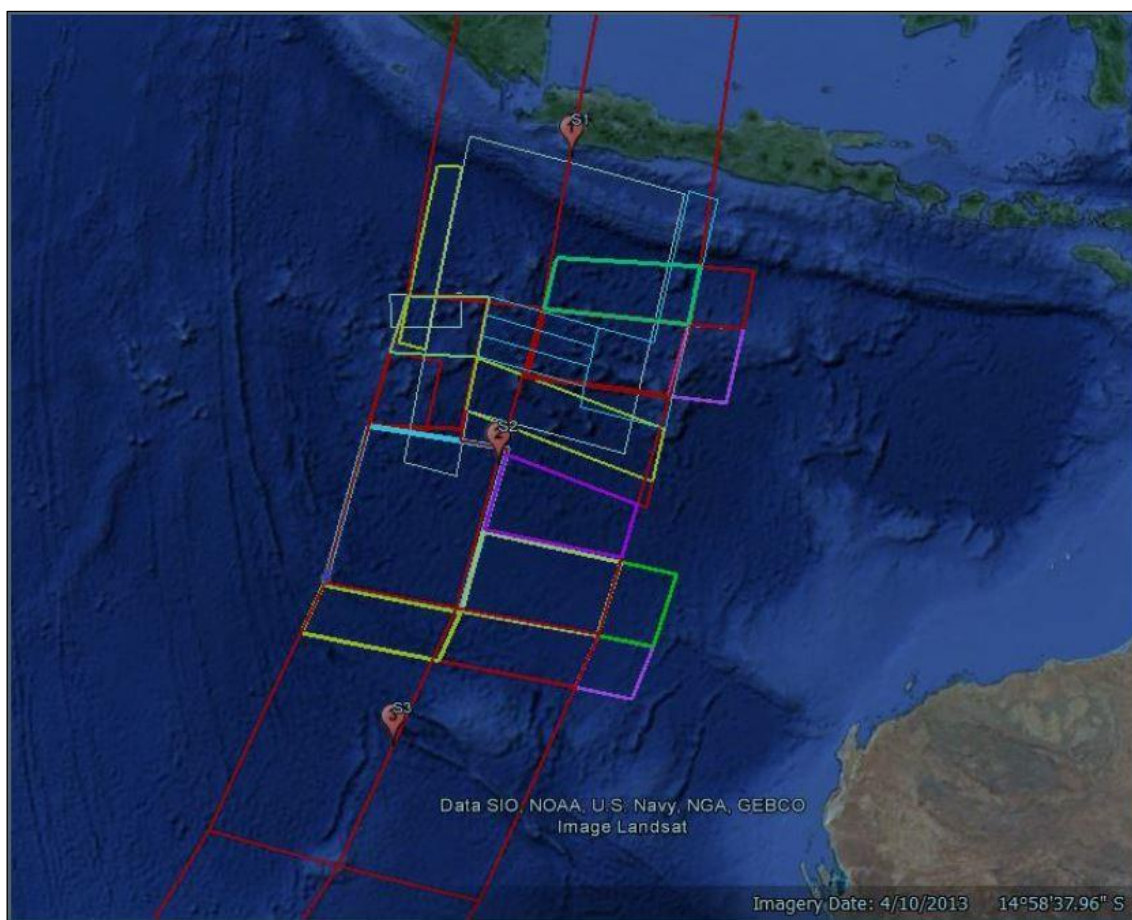
Table 8: SAR operations southern corridor

Dates:	18–23 March 2014
Event:	Malaysia (KL ARCC) and Indonesia (BASARNAS) refined surface search area.
Search area location:	Within S1-S3 (Malaysian designation – refer Figure 8 and Figure 9) of the southern corridor.
Search activity:	Aerial search
Guiding advice:	Timing information obtained from satellite data and aircraft performance data was used to identify a northern and southern corridor along which MH370 may have flown with probable final location close to the 6 th arc.
Data used in planning search area refinement:	MH370 Inmarsat satellite data unit logs and advice from SATCOM WG and data compiled by the JIT.
Search equipment:	Eight aircraft from India, Japan, Malaysia, Republic of Korea, United Arab Emirates and the United States.
Search area:	1,630,000 km ²

Source: DCA Malaysia

By 24 March 2014, further analysis of the SATCOM data established that the data was only consistent with flight paths along the southern corridor ending in the southern Indian Ocean.

Figure 9: KL ARCC and BASARNAS S1, S2 and S3 search areas (18-23 March 2014)



Source: Malaysia, ICAO Third Meeting of the Asia/Pacific Regional Search and Rescue Task Force (AP SAR/TF/3) Working Paper 06, Maldives, 25 – 29 January 2015

Australian led surface search

On 17 March 2014, with the southern corridor extending into the Indian Ocean and the Australian search and rescue region, Australia assumed responsibility for coordinating the SAR operation for the aircraft, at Malaysia’s request. The Australian Maritime Safety Authority (AMSA) was responsible for coordinating this activity using aircraft and surface vessels operating from Western Australia until 28 April 2014. AMSA continued to take advice on the areas to search from the JIT and SATCOM WG based on the progressive analysis of the Inmarsat satellite communication logs and other aircraft performance analysis.

The surface search was focused on the identification and recovery of any debris from the aircraft floating on the sea surface. When AMSA took over the coordination of the surface search nine days had passed since the aircraft went missing. It was therefore necessary to define the areas to be searched by aircraft and surface vessels based on the analysis indicating where the aircraft may have ended the flight and the calculated drift of a range of possible types of floating debris in the days after 8 March 2014.

A drift modelling working group was set up by AMSA, comprising a number of organisations including: CSIRO, Asia-Pacific Applied Science Associates, the United States Coastguard, the Bureau of Meteorology and Global Environmental Modelling and Monitoring Systems to ensure that best practice drift modelling was put in place for the surface search. The drift modelling was also informed by the deployment of self-locating datum marker buoys (SLDMB) from aircraft and

vessels throughout the surface search. A SLDMB is a drifting surface buoy fitted with a GPS that is used to measure surface ocean currents. The marker buoy has an expected lifetime of over 20 days once deployed in the ocean. Similarly, real-time wind and wave data from the search area was used to continuously update the drift models.

Initial southern Indian Ocean surface search area

The initial Australian led MH370 surface search area was determined to be a 600,000 km² area of the southern Indian Ocean approximately 2,500 km from Perth, Western Australia (Table 9). The area was determined by assuming the aircraft had made a southern turn shortly after the last radar capture at the northern tip of Sumatra and flew until fuel exhaustion.

Table 9: Initial southern Indian Ocean surface search SAR operations

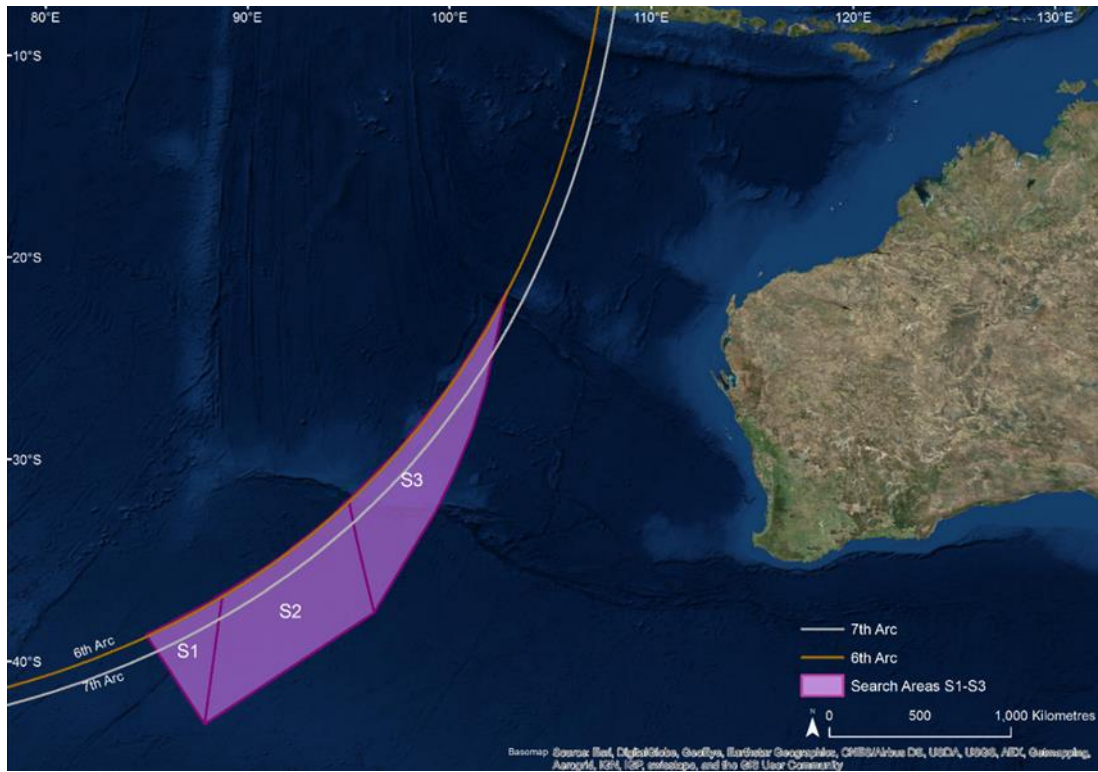
Dates:	18–19 March 2014
Event:	Australia (AMSA) initial surface search area.
Search area location:	S1/S2 ¹⁶
Search activity:	Aerial visual and radar search.
Guiding advice:	MH370 Inmarsat satellite data unit logs and advice from SATCOM WG to AMSA. Data compiled by the JIT in conjunction with NTSB.
Data used in planning search area refinement:	The actual satellite location. Turn south occurred at the northern tip of Sumatra. Performance predictions based on speed and range only with no wind consideration. Only positional information from Malaysian primary radar data. Length of arc to the south constrained by maximum aircraft groundspeed Lateral navigation set to 'track' mode. Two speeds provided 'best fit' with longest and straightest tracks reaching the 6 th arc. Assumed speed and altitude to last radar point were final ACARS values.
Search equipment:	Aircraft from Australia, New Zealand and the United States. Two merchant vessels responded to urgency broadcast and transited to and through search area.
Search area:	Refer to Table 10.

Source: ATSB

Search areas in the southern Indian Ocean designated S1, S2 and S3 (Figure 10) were defined from estimates of the aircraft's performance and endurance. In particular, two hypothetical speeds (469 and 475 knots) that resulted in the longest, straightest tracks that reached the 6th arc derived from the SATCOM data. These tracks intersected the arc in areas S1 and S2, so they were used to define the initial search area.

¹⁶ JIT designation of search areas with S1 in the south (see Figure 10) as used by AMSA and ATSB

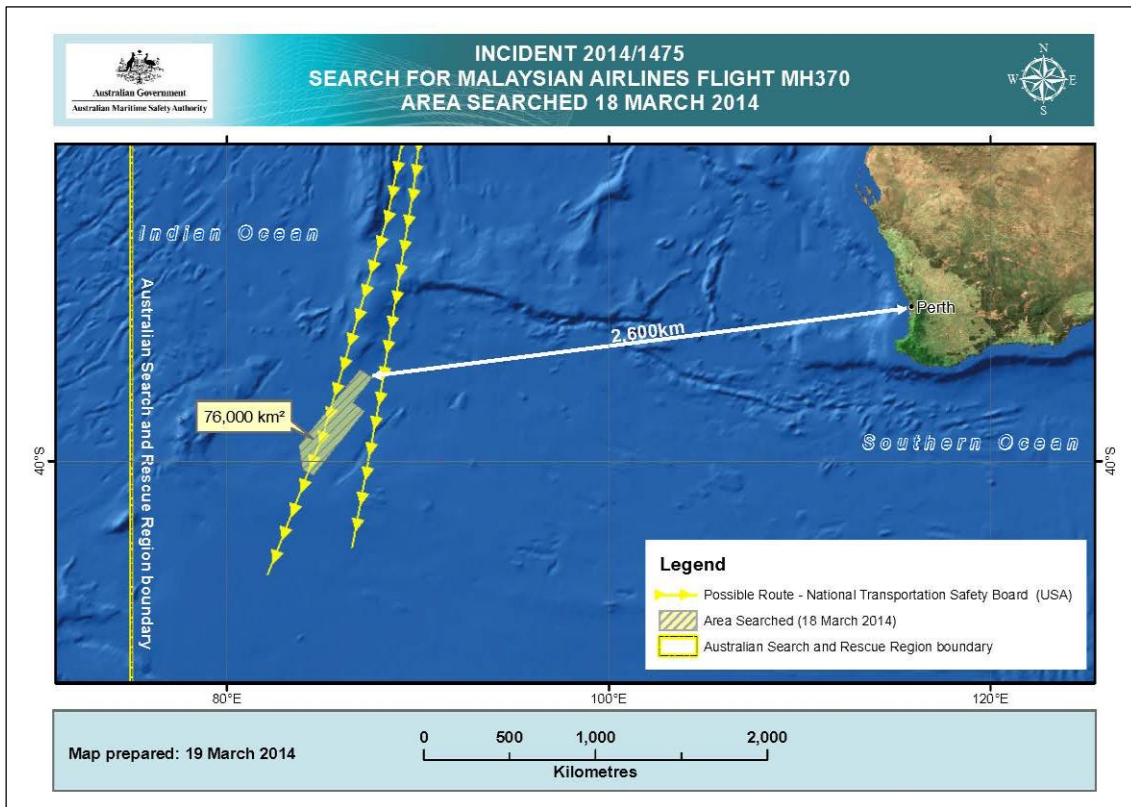
Figure 10: Possible southern final positions S1–S3 based on MH370 maximum range



Source: ATSB, using JIT data

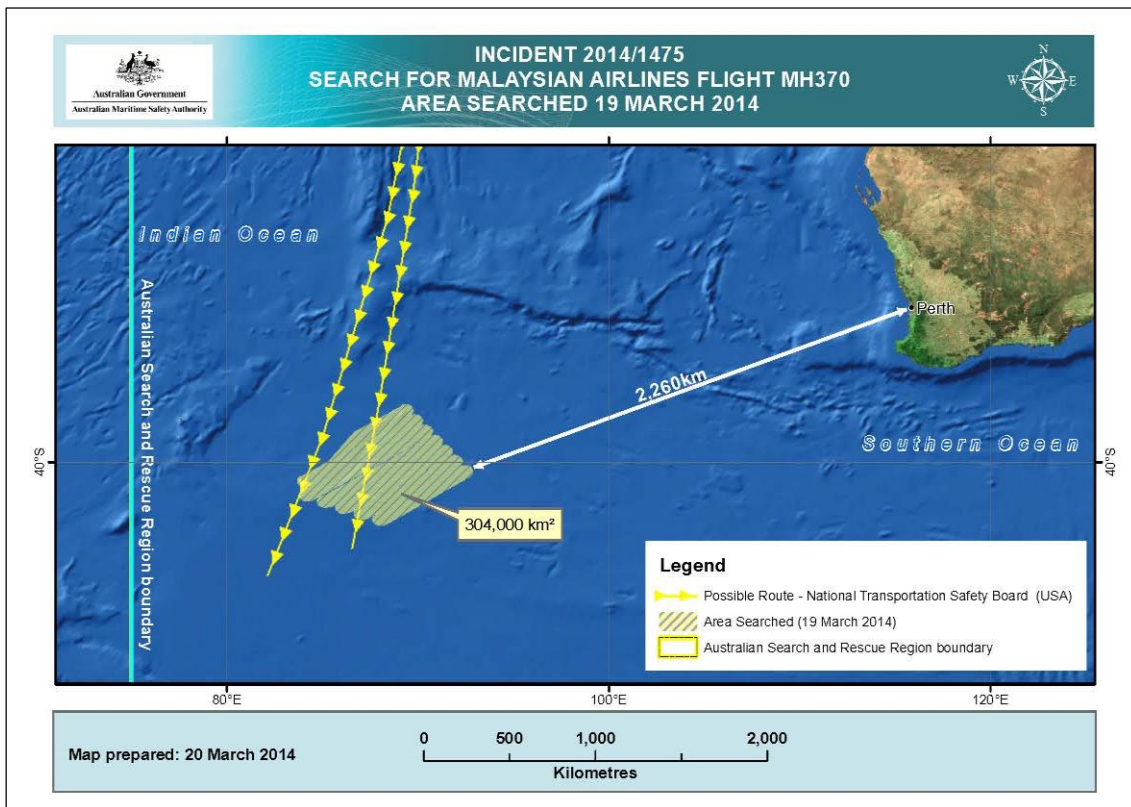
On 18 and 19 March 2014, areas S1 and S2 were corrected for drift which provided the surface search areas for those days (Figure 11 and Figure 12).

Figure 11: Area searched 18 March 2014



Source: AMSA

Figure 12: Area searched 19 March 2014



Source: AMSA

Table 10: Search area information 18 to 19 March 2014

Date	Drifted splash point area	Search Area (km ²)	Track spacing (NM)	Aircraft	Vessels	SLDMB drop	Sightings
18-Mar-14	Initial JIT Analysis (S1/S2)	65,938	40	1	2		
19-Mar-14	Initial JIT Analysis (S1/S2)	320,855	40	4	1	1	

Source: AMSA

Satellite imagery debris detections

While the initial surface search activity in the southern Indian Ocean was based on the analysis of the aircraft’s possible flight paths and maximum endurance, other information was being actively sought including satellite imagery. AMSA, working with the Australian Geospatial-Intelligence Organisation, had requested governments with low earth orbiting satellites to gather imagery in and around the MH370 search area (see section on Satellite imagery analysis). Imagery was analysed for possible aircraft debris and the information was passed to Australian Geospatial-Intelligence Organisation and AMSA.

From 16 to 27 March 2014, a number of potential debris sightings were made in satellite imagery including seven in the region of 43–45°S, 90–97°E. The objects were estimated to be between 5 m and 24 m in length. The surface search was refocused to this area to investigate these sightings and subsequent aerial sightings (Figure 13 and Table 11).

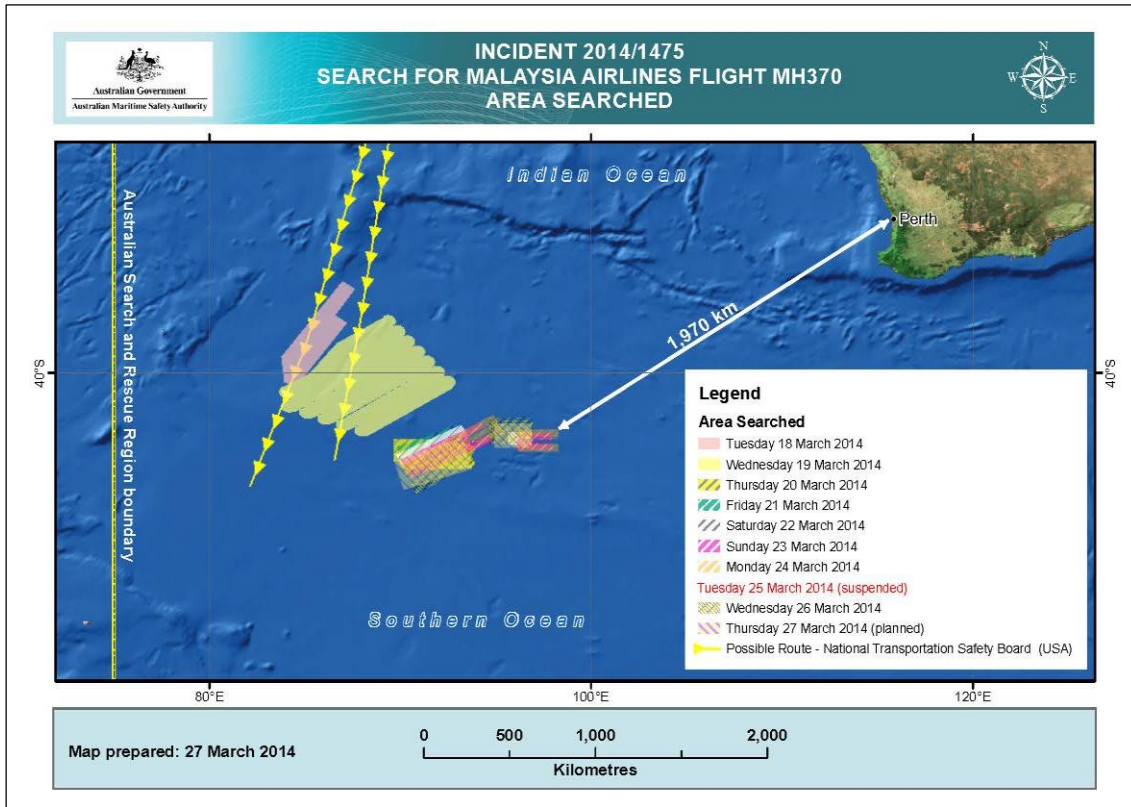
Search activity transitioned to a search and recovery operation from 25 March 2014.

Table 11: Satellite imagery search area

Dates:	20–27 March 2014
Event:	Australia (AMSA) satellite imagery search area.
Search area location:	Approximately 42°S–46°S
Search activity:	Satellite visual and radar search (multiple nations). Aerial and surface visual/ radar search. Datum marker buoys deployed by air to assist in future drift modelling.
Guiding advice:	MH370 Inmarsat satellite data unit logs and advice from SATCOM WG to AMSA Commercial satellite imagery of objects possibly related to MH370 received by AMSA.
Data used in planning search area refinement:	Assessment of commercial satellite imagery indicates possible debris approximately 148 km southeast of the initial search area.
Search equipment:	Aircraft from Australia, New Zealand, United States, Japan, the People’s Republic of China and the Republic of Korea. Vessels from Royal Australian Navy (RAN) and the People’s Republic of China.
Search area:	Refer to Table 12.

Source: ATSB

Figure 13: Cumulative area searched from 18 to 27 March 2014



Source: AMSA

Table 12: Search area information 20 to 27 March 2014

Date	Drifted splash point area	Search Area (km ²)	Track spacing (NM)	Aircraft	Vessels	SLDMB drop	Sightings
20-Mar-14	Satellite imagery (SE of S1/S2)	67,827	40/9	5	1	3	4
21-Mar-14	Satellite imagery (SE of S1/S2)	22,869	2	6	1		1
22-Mar-14	Satellite imagery and aerial (SE of S1/S2)	40,178	3	7	3	1	6
23-Mar-14	Satellite imagery and aerial (SE of S1/S2)	59,138	3/4	9	1		9
24-Mar-14	Satellite imagery and aerial (SE of S1/S2)	72,501	3/4/5	10	1	1	6
25-Mar-14	Satellite imagery and aerial (SE of S1/S2)	0 ¹⁷	N/A	1	0	3	
26-Mar-14	Satellite imagery and aerial (SE of S1/S2)	74,420	2/3/4	11	5		3
27-Mar-14	Satellite imagery and aerial (SE of S1/S2)	0 ¹⁸	2/5	9	5		

Source: AMSA

¹⁷ No aviation search due to weather.

¹⁸ No aviation search due to weather.

There were also possible debris detections from 20 to 23 March 2014, by French satellites at a location 80 to 150 km west of the 7th arc (these are discussed further in the Satellite imagery analysis section).

Refined surface search area

By 27 March 2014, following further analysis, the JIT had more confidence in MH370's speeds derived by the primary radar data captured around Malaysia. The analysis indicated that the aircraft's rate of fuel burn was higher during this segment of the flight than first thought and therefore its maximum range was decreased. The most probable track moved north to the S3 area and two new search areas designated S4 and S5 were defined (Figure 14). The corresponding drifted areas during this period of the surface search were areas A and B (Figure 15).

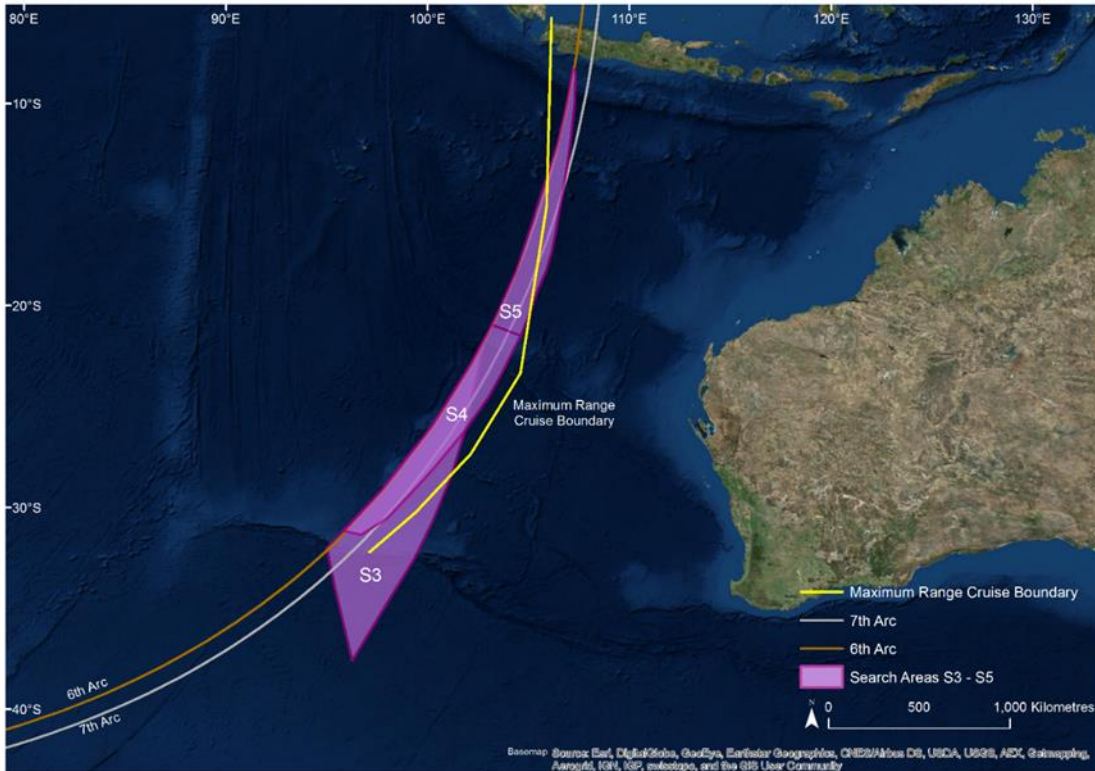
The fuel analysis also provided more confidence that the 7th arc represented the point of fuel exhaustion for the aircraft so a recommendation was made to search in a north-easterly direction along the 7th arc from the S3/S4 area boundary (Table 13).

Table 13: Refined surface search area

Dates:	28 March – 3 April 2014
Event:	Australia (AMSA/ATSB) refined surface search area.
Search area location:	S3/S4 overlap drifted Area A, S3/S4 overlap, drifted Area B.
Search activity:	Aerial and surface visual and radar search of areas drifted from the 7th arc by drifting group comprising AMSA, Global Environmental Modelling and Monitoring Systems, CSIRO, Asia-Pacific Applied Science Associates and United States Coast Guard. Satellite search (multiple nations) of areas drifted from the 7th arc.
Guiding advice:	S3/S4 starting from southerly region of S4. MH370 Inmarsat satellite data unit logs and advice from SATCOM WG. Briefing by the JIT by telephone from Kuala Lumpur on 27 March 2014 to ATSB embedded team at AMSA.
Data used in planning search area refinement:	Greater confidence in increased speeds from primary radar thus increased fuel burn. More confidence that 7th arc was fuel exhaustion point.
Search equipment:	Aircraft from Australia, New Zealand, United States, Japan, the People's Republic of China, Republic of Korea and Malaysia. Vessels from the RAN and the People's Republic of China.
Search area:	Refer to Table 14.

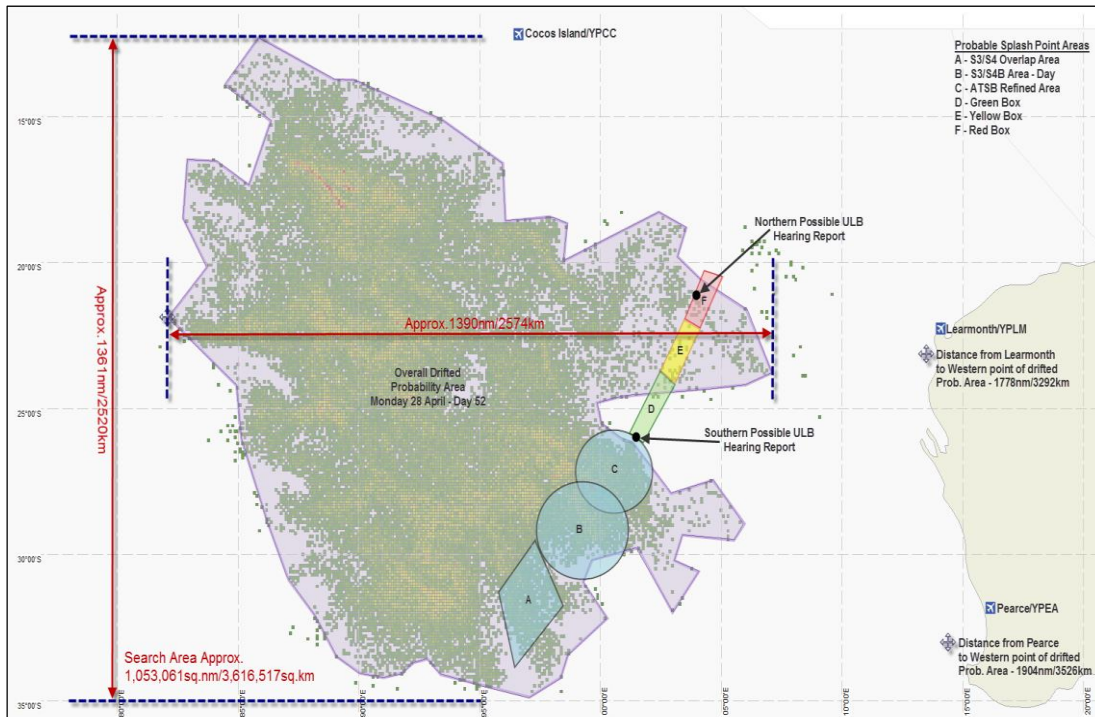
Source: ATSB

Figure 14: Defined search areas 27 March 2014 (including 7th arc and maximum range cruise boundary)



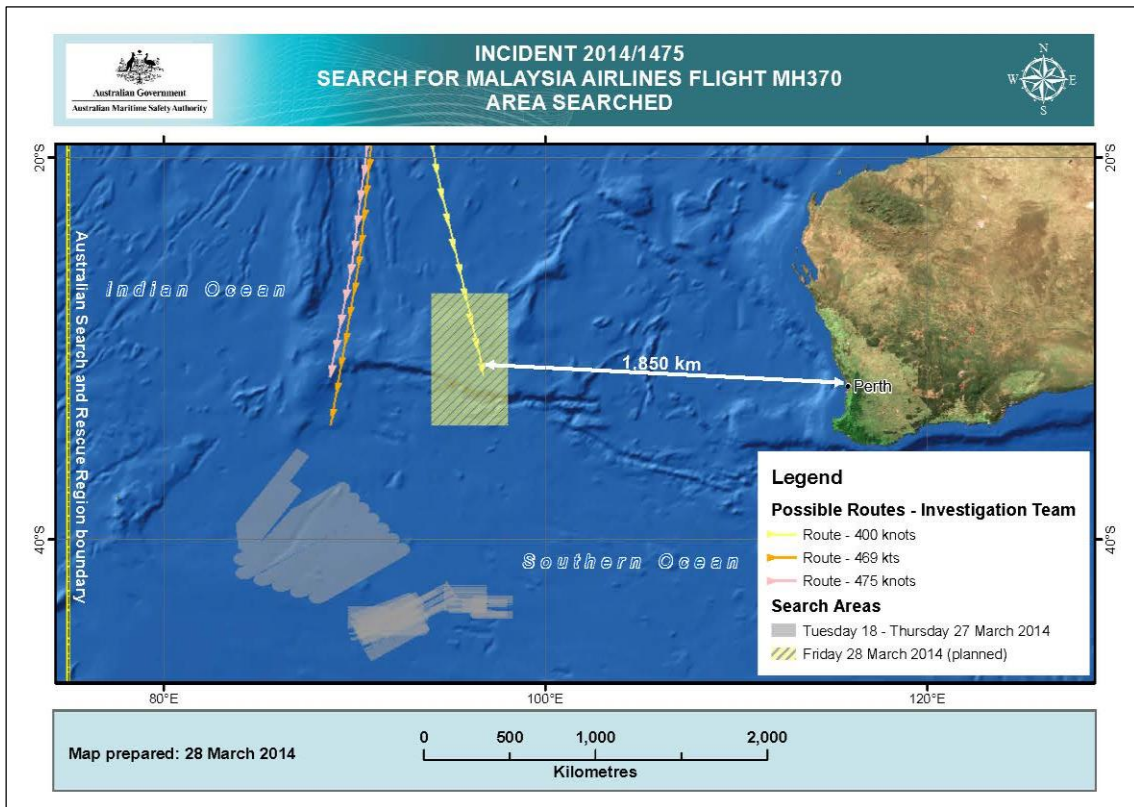
Source: ATSB, using JIT data

Figure 15: Original and drifted search areas 28 March 2014 to 28 April 2014



Source: AMSA

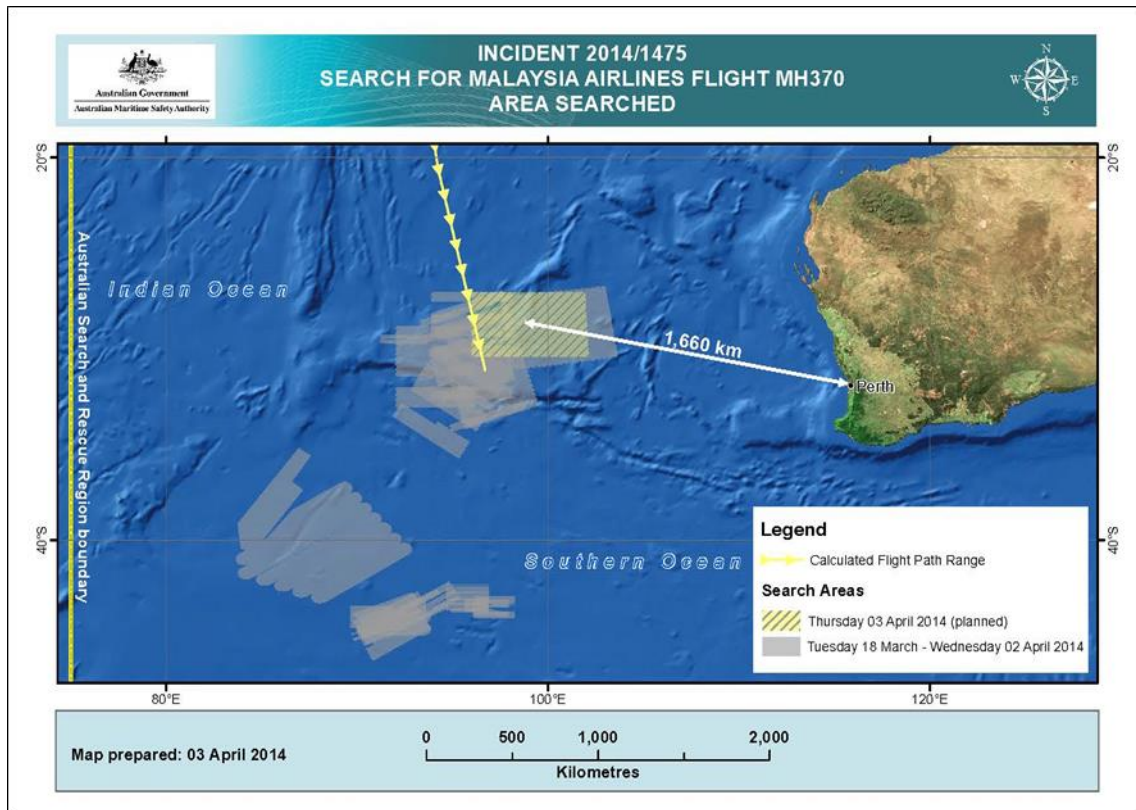
Figure 16: Move to refined area 28 March 2014 – planned and cumulative area searched



Source: AMSA

On 28 March 2014 a search of the drifted S3/S4 overlap area (Area A) was commenced. More than 50 objects were sighted and reported on that day (Table 14). Examination of images and recovery of items by surface vessels did not identify any items considered associated with MH370. A search of drifted Area B (Figure 15) within area S4 was undertaken on 2 and 3 April 2014.

Figure 17: Area searched and planned to 3 April 2014



Source: AMSA

Table 14: Search area information 28 March 2014 to 3 April 2014

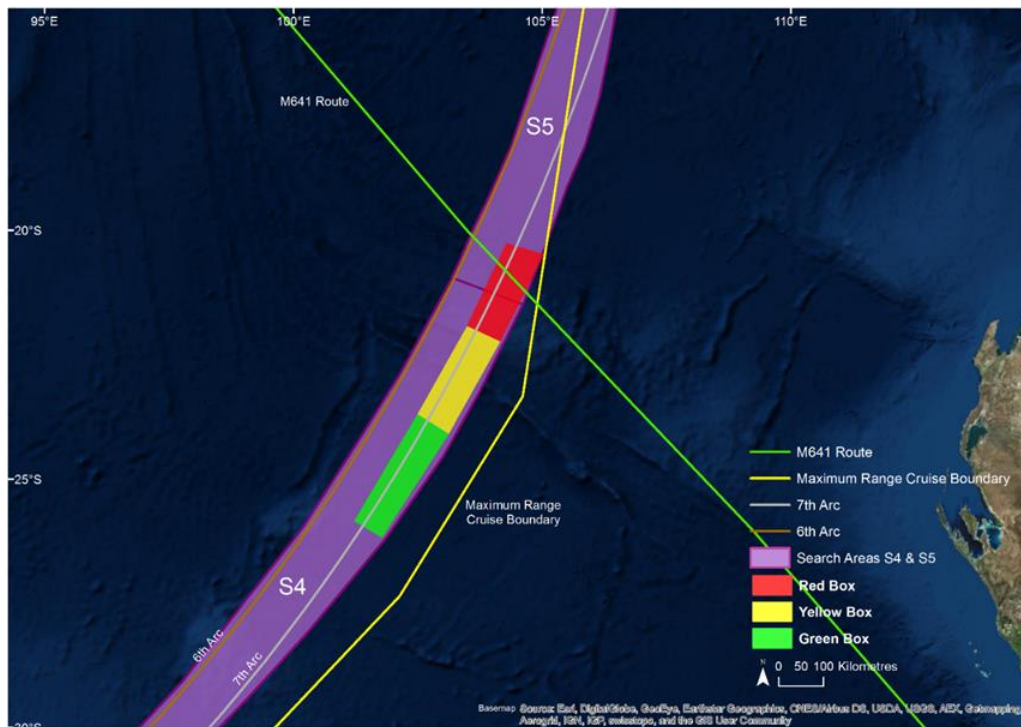
Date	Drifted splash point area	Search Area (km ²)	Track spacing (NM)	Aircraft	Vessels	SLDMB drop	Sightings
28-Mar-14	JIT 1A (S3/S4 overlap) Area A	298,636	14	10	6	3	50
29-Mar-14	JIT 1A (S3/S4 overlap) Area A	274,705	15	8	6	6	16
30-Mar-14	JIT 1A (S3/S4 overlap) Area A	251,009	12	10	8	1	5
31-Mar-14	JIT 1A (S3/S4 overlap) Area A	164,087	16	10	9	4	
1-Apr-14	JIT 1A (S3/S4 overlap) Area A	223,143	12	11	9	1	4
2-Apr-14	JIT 1A (S3/S4) Area B	236,966	15	9	9		
3-Apr-14	JIT 1A (S3/S4) Area B /JIT 1B - red box F	283,329	15/10/4	9	9	3	3

Source: AMSA

Second refinement surface search area

A second refinement to the SATCOM data analysis was provided by the JIT on 1 April 2014 which indicated the most probable aircraft path crossing at the S4/S5 area boundary. On 2 April 2014 further aircraft performance and flight path analysis starting further to the northwest of Sumatra had the effect of moving the most probable area to the northeast along the 7th arc into areas S4 and S5. Probable impact areas red, yellow and green were then defined (Figure 18). A 20,000 km² priority red area and lower probability yellow and green search areas extending to the southwest along the 7th arc were also defined.

Figure 18: Defined areas at 2 April 2014 showing red, yellow and green boxes, air route M641 and maximum range cruise boundary



Source: ATSB, using JIT data

This analysis was used to guide the remainder of the surface search. Other areas of interest possibly indicating the location of MH370 were incorporated into the search as they became available. The S4/S5 drifted areas C, D, E and F were searched during this period (Figure 15 and Table 15).

Table 15: Second refinement to surface search area

Dates:	3–28 April 2014
Event:	Second refinement to surface search area.
Search area location:	S3/S4 overlap drifted Area A (3 April). S3/S4 overlap drifted Area B (3–7 April). Drifted red box (3–7 April). Drifted <i>Ocean Shield</i> flight recorder underwater locator beacon (ULB) hearing report (8–12 April). Drifted <i>Haixun 01</i> ULB hearing report (13–17 April). Drifted yellow box (18–20 April). Drifted S3/S4 ATSB refined area (21–28 April). S4/S5 starting at S4/S5 boundary and defined by red/ yellow/green areas.
Search activity:	Aerial and surface visual and radar search of areas drifted from 7th arc by expert drifting group of AMSA, Global Environmental Modelling and Monitoring Systems, CSIRO, Asia-Pacific Applied Science Associates and United States Coast Guard. Satellite search (multiple nations) of areas drifted from the 7th arc coordinated by Australian Geospatial-Intelligence Organisation with areas advised by AMSA/ATSB.

<p>Guiding advice:</p>	<p>Areas S4 and S5 starting at S4/S5 boundary and defined by red/yellow/green areas.</p> <p>MH370 Inmarsat satellite data unit logs and advice from SATCOM WG.</p> <p>Briefing by the JIT on 2 April 2014 from United Kingdom, United States, Kuala Lumpur to AMSA (ATSB and NTSB embedded).</p> <p>Follow-up written briefing (refer JIT report at appendix B).</p> <p>Curtin University report (appendix H) on possible hydroacoustic event in search area (4 and 10 April 2014).</p> <p>Reported acoustic detections <i>Haixun 01</i> (4–5 April 2014).</p> <p>5 April advice from JIT by email on effect of eclipse (resultant cooling and doppler correction) on Inmarsat’s IOR-3 satellite on the signal frequency translation. This resulted in an increase to 425 knots groundspeed and shift to green zone.</p> <p>Reported ULB detections <i>Ocean Shield</i> (5-10 April 2014).</p> <p>MH370 PIC Microsoft flight simulator data analysis provided to AMSA/ ATSB by Australian Federal Police (19 April 2014).</p>
<p>Data used in planning search area refinement:</p>	<p>Based on the satellite timing data, the aircraft will be located near the 7th arc. Two scenarios were developed 1A and 1B based on the considered extents of the turn to the south.</p> <p style="padding-left: 40px;">Scenario 1A had the aircraft fly south immediately after the first arc.</p> <p style="padding-left: 40px;">Scenario 1B had the aircraft passing waypoint LAGOG before flying south.</p> <p>The 1B scenario had the aircraft passing close to a northwest point (8° 35.719’N, 92°35.145’E) at 1912. This was an initial qualitative assessment of the possible radar coverage from multiple data sources. This point was speculated and used as the furthest point west the aircraft was likely to have flown.</p> <p>The measured doppler profile closely matched that expected from an aircraft travelling in a southerly direction.</p> <p>One analysis showed that the best fit for the doppler frequency was at a ground speed of 400 knots, with slightly 'less' best fits at 375 and 425 knots.</p> <p>A Monte Carlo style analysis, using a number of different starting positions on the second arc also gave a best fit at 400 knots. A most probable speed range of 375 to 425 knots was selected.</p> <p>One analysis used a combination of aircraft performance and doppler data, obtained from the satellite, to generate a range of probable best fit tracks. This work was supported by a root mean square analysis.</p> <p>Flight planning carried out by Malaysia Airlines independently showed that there was sufficient fuel on board the aircraft to reach the positions determined by the analysis.</p> <p>The length of the 7th arc that defined the most probable area was obtained from the overlay of the results of all approaches.</p> <p>Given the probable battery life of the ULBs and the number of assets available to conduct the underwater search, it was decided to break the underwater search for the ULBs into three smaller areas (red, yellow and green).</p> <p>The width of the areas was defined by the probable position of the 7th arc, half of the glide range (40 NM) and the area the towed pinger locator (TPL) could cover before the ULB batteries expired.</p> <p>The area that was crossed by air route M641 was classified as red (Priority 1), the next two priorities, yellow and green, were then defined moving south along the arc from this position.</p>
<p>Search equipment:</p>	<p>Aircraft from Australia, New Zealand, United States, Japan, the People’s Republic of China, the Republic of Korea and Malaysia.</p> <p>Vessels from the RAN, Royal Malaysian Navy, Royal Navy, United States Navy and the People’s Republic of China.</p>
<p>Search area:</p>	<p>Refer to Table 16.</p>

Source: ATSB

The S4/S5 area boundary on the 7th arc was considered the best starting point due to convergence of a number of candidate paths using independent techniques and because airways route M641 (Figure 16) passed through that location. The equivalent groundspeed of hypothetical flight paths ending in this region was about 363 knots. At this time, drifted Area B was being searched.

On 3 April 2014 the surface search (one mission) of a drifted red area was commenced. This continued until 6 April 2014 when further advice was received from the JIT regarding the cooling effect of an eclipse on the satellite, shifting the calculated groundspeed up to 425 knots and moving more probable paths to the green zone. The aerial search on that day was revised in response to that information.

Sonobuoys were deployed by Royal Australian Air Force P3 Orion aircraft to passively listen for underwater locator beacons. As information relating to the possible location of MH370 was provided to the ATSB, the location of the surface, satellite search and sonobuoy drops were adjusted.

The following items of interest influenced the search areas defined during this period:

- The People’s Republic of China vessel *Haixun 01* reported possible underwater locator beacon (ULB) detections (4 to 5 April 2014) (See The acoustic search for the underwater locator beacons section).
- Curtin University reported a possible hydrophone detection (4 and 10 April 2014) (See Hydroacoustic analysis section).
- *Ocean Shield* reported possible ULB detections (6 to 10 April 2014) (See The acoustic search for the underwater locator beacons section).
- Five data points were recovered from the PIC’s home flight simulator (19 April 2014) (See Pilot in Command’s flight simulator section).

Table 16: Search area information 3 to 7 April 2014

Date	Drifted splash point area	Search Area (km ²)	Track spacing (NM)	Aircraft	Vessels	Sonobuoy drop area	SLDMB drop	Sightings
3-Apr-14	JIT 1A (S3/S4) Area B /JIT 1B - red box F	283,329	15/10/ 4	9	9		3	3
4-Apr-14	JIT 1B - yellow/red Box E and F	253,299	20/15/ 8	13	9		4	7
5-Apr-14	JIT 1B - yellow/red Box E and F	196,898	14/9	9	9			
6-Apr-14	JIT 1B - yellow/red Box E and F	216,309	15/10	10	11	For Defence To Provide		2
7-Apr-14	JIT 1B - yellow/red Box E and F	189,655	15/10	12	11	RSCU102 and RSCU104		1

Source: AMSA

Following the reported acoustic detections made by *Haixun 01* and *Ocean Shield* on 8 April 2014 the search areas were redefined (Table 17).

Table 17: Search area information 8 to 17 April 2014

Date	Drifted splash point area	Search Area (km ²)	Track spacing (NM)	Aircraft	Vessels	Sonobuoy drop area	SLDMB drop	Sightings
8-Apr-14	10 NM radius <i>Ocean Shield</i> ULB hearing report	77,333	4	11	13	RSCU105 approximately 360 NM to the south of the three main search areas.	1	8
9-Apr-14	10 NM radius <i>Ocean Shield</i> ULB hearing report	75,424	4	12	14	RSCU104 approximately 350 NM to the southeast of the three main search areas.	1	5
10-Apr-14	10 NM radius <i>Ocean Shield</i> ULB hearing report	57,923	4	11	13	RSCU102 and RSCU105 in the vicinity of <i>Ocean Shield</i> 250 NM east of the visual search area.		
11-Apr-14	10 NM radius <i>Ocean Shield</i> ULB hearing report	42,977	4/3	12	12	RSCU102, RSCU103 and RSCU105 in the vicinity of <i>Ocean Shield</i> approximately 260 NM east of the visual search area.		1
12-Apr-14	10 NM radius <i>Ocean Shield</i> ULB hearing report	41,393	4	7	13	RSCU103 in the vicinity of <i>Ocean Shield</i> approximately 315 NM east of the eastern search area.		1
13-Apr-14	10 NM radius <i>Haixun 01</i> ULB hearing report - green box D	57,466	5	9	13	RSCU102 and RSCU105 in the vicinity approximately 204 NM south east of the eastern search area.	1	1 4
14-Apr-14	10 NM radius <i>Haixun 01</i> ULB hearing report - green box D	47,706	5	9	11	RSCU102 and RSCU103 in the vicinity approximately 300 NM south east from the centre of the eastern search area.	1	
15-Apr-14	<i>Haixun 01</i> ULB hearing report - green box D	49,715	5	9	11	RSCU104 and RSCU105 approximately 600 NM north east from the centre of the eastern search area.		
16-Apr-14	<i>Haixun 01</i> ULB hearing report - green box D	33,199	5	14	11	RSCU102, RSCU103 and RSCU104 approximately 600 NM north east from the centre of the eastern search area.		1 3
17-Apr-14	<i>Haixun 01</i> ULB hearing report - green box D	41,579	5	12	12	RSCU103 and RSCU105 approximately 566 NM north east from the centre of the eastern search area.		

Source: AMSA

The search areas were again refined from 18 April 2014 following the completion of the search in acoustic detection areas to focus on other areas of interest (Table 18).

Table 18: Search area information 18 to 28 April 2014

Date	Drifted splash point area	Search Area (km ²)	Track spacing (NIM)	Aircraft	Vessels	Sonobuo y drop	SLDMB drop	Sightings
18-Apr-14	Yellow box E	35,078	5	9	13			2
19-Apr-14	Yellow box E	48,190	7/5	8	12			
20-Apr-14	Yellow box E	41,229	5	8	11			
21-Apr-14	S3/S4 ATSB refined area C	49,492	4	8	11			12
22-Apr-14	S3/S4 ATSB refined area C	31,627	4	4	11			
23-Apr-14	S3/S4 ATSB refined area C	32,680	4	5	10			4
24-Apr-14	S3/S4 ATSB refined area C	51,923	4	8	11			
25-Apr-14	S3/S4 ATSB refined area C	49,241	4	6	11			
26-Apr-14	S3/S4 ATSB refined area C	56,206	4	7	11			15
27-Apr-14	S3/S4 ATSB refined area C	0	N/A	0	11			
28-Apr-14	S3/S4 ATSB refined area C	42,839	4	6	11			

Source: AMSA

Details of the daily surface search coverage up to 31 March 2014 can be found on the [AMSA website](#).

On 31 March 2014, the search for MH370 transitioned to an investigation phase with the surface search still coordinated by AMSA as part of a larger interagency response which included ATSB, the Australian Departments of Defence, Foreign Affairs and Trade and Infrastructure and Regional Development headed by the Joint Agency Coordination Centre (JACC).

Search operations coordinated by AMSA were undertaken from 18 March to 29 April 2014 (42 days). A total of 21 aircraft and 19 vessels from Australia, the People’s Republic of China, Japan, Malaysia, New Zealand, the Republic of Korea, United Kingdom and the United States were involved in the AMSA-led surface search.

An animation showing the daily progress of the aerial surface search areas is available for viewing on the [ATSB YouTube Channel](#)

Debris sightings and recoveries

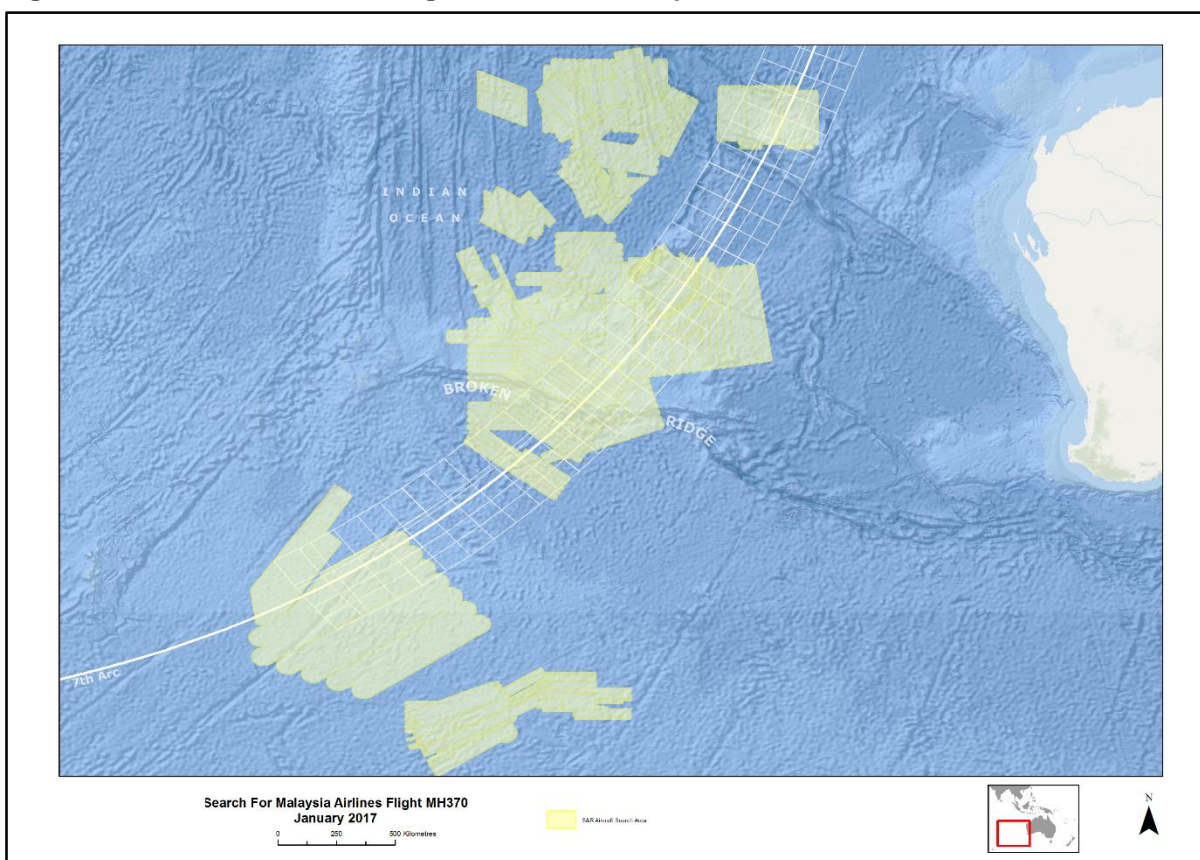
During the surface search a number of floating objects in the drifted search areas were reported by aircraft, including wooden pallets and fishing equipment. None of these items were assessed as being associated with MH370. Over thirty items of debris were recovered by surface search vessels. All of these items were considered unlikely to be associated with MH370.

Surface search coverage and confidence

The area covered during the various phases of the AMSA-led surface search by air, sea and satellite up to 28 April 2014 is shown in Figure 19.

Daily coverage confidence was analysed by AMSA with consideration of reports of coverage and visibility conditions in the assigned search area. AMSA has extensive experience with search and rescue operations, enabling them to ascertain if the assigned area had been searched to a high level of confidence. Coverage confidence was low on some days due to poor weather or the large size of the search areas relative to the number of search assets available. On occasions, the postulated location of impact changed (as analysis of the aircraft’s flight path accounted for new information) before the drifted search area was searched to high confidence.

Figure 19: Surface search coverage 18 March to 28 April 2014

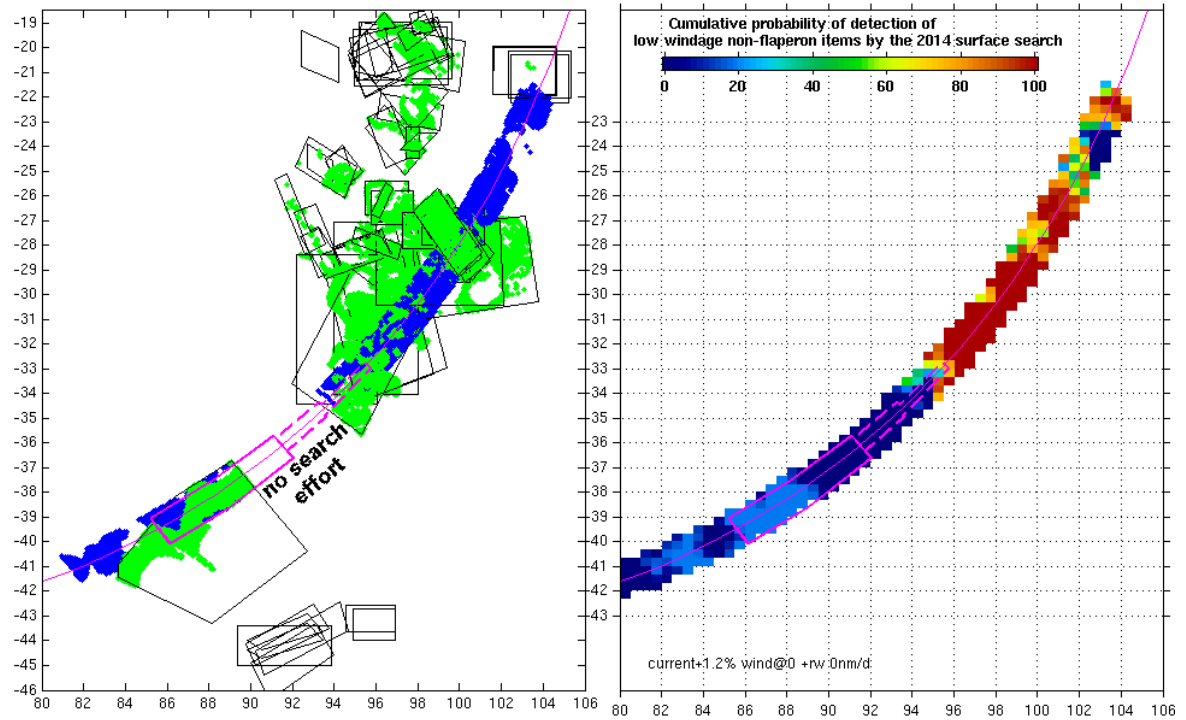


Source: ATSB, using AMSA data

CSIRO re-assessed the effectiveness of the surface search in terms of how it informed the underwater search. To do this, they re-assessed the degree of overlap of the drifted search areas with their updated estimates of where the debris field might have been, for a large number of potential impact sites distributed along the 7th arc from latitudes 21°S to 41°S and for items of debris with a range of susceptibility to the wind (leeway). For further details, see www.marine.csiro.au/~griffin/MH370/

Figure 20 shows that the first few days of the surface search was, with hindsight, fairly ineffective. This was because the number of search assets was low on the first day and because on following days the search was conducted much farther away from the 7th arc than the debris could have drifted, assuming now that the impact was within 25 NM of the 7th arc. In contrast, the northward move of the search on 28 March resulted in a high probability of detecting debris if the impact had been somewhere between about latitudes 26°S and 32.5°S. This phase of the surface search was therefore of high value to the underwater search because it adds to the weight of evidence suggesting that searching the seafloor north of about 32.5°S is unlikely to be successful.

Figure 20: Probability of detection for the surface search



The acoustic search for the underwater locator beacons

During the early stages of the AMSA-led surface search, efforts were also underway to mobilise a search for MH370’s flight recorder underwater locator beacons (ULBs). United States Navy ULB detection equipment, including a towed pinger locator system and an autonomous underwater vehicle to investigate any detections, was shipped from the United States and mobilised on the Australian defence vessel *Ocean Shield*. The People’s Republic of China vessel *Haixun 01*, equipped with a hand held hydrophone (underwater microphone) system and the United Kingdom defence vessel *HMS Echo* equipped with a hull-mounted hydrophone system were also used in the acoustic search. Later Royal Australian Air Force P-3C Orion aircraft also dropped sonobuoys in the search area to listen for MH370’s ULBs.

The acoustic search started on 2 April and continued until 17 April 2014 (the date of the last sonobuoy drop) by which time it was considered that the ULB batteries would have been exhausted. The acoustic search for the ULBs also included a limited underwater search using the autonomous underwater vehicle on *Ocean Shield* which was completed on 28 May 2014.

Underwater locator beacons

An underwater locator beacon (ULB)¹⁹ was attached to both the flight data recorder (FDR) and cockpit voice recorder (CVR) on board MH370. ULBs, also known as ‘pingers’, are battery operated acoustic transmitters which activate when immersed in water.

ULBs fitted to flight recorders (Figure 21) are designed to operate in water depths up to 6,000 m and emit a 10 millisecond sound pulse at a frequency of 37.5 kHz every second for a minimum of 30 days²⁰ when activated.

Figure 21: Typical crash protected recorder configuration with ULB



Source: ATSB

¹⁹ The underwater locator beacons installed were Dukane Model DK100

²⁰ The ULB manufacturer predicted maximum life of the batteries once activated was 40 days

An activated ULB attached to a flight recorder enables a diver, or underwater vehicle, equipped with a hydrophone to detect and locate the recorders within a known underwater debris field. ULBs have also been used to locate an entire aircraft debris field as they can be detected from a distance of 2,000 m to 3,000 m, or further in favourable conditions. This is greater than the range of many mapping sonar systems (for example side scan sonar) which may be used to search for an aircraft debris field. This means an initial search for a ULB, rather than the aircraft debris field, can be an efficient way to search a large area quickly.

Many conditions influence the actual range and ability to detect a ULB. Underwater environmental factors such as thermoclines²¹, high ambient noise or marine life in the area affect the detectability of a ULB. Impact damage can also affect the ULB housing, acoustic transducer, internal electronics, or battery functionality. The ULB could also be covered by sediment or shielded by surrounding debris on the seafloor. The surface support vessel can also be a source of noise which can affect ULB detection. Ships and their equipment are typically acoustically noisy and this can result in interference or false detections. Care is required to isolate any potential sources that may emit a similar acoustic sound or mask a real ULB signal.

The equipment used to detect a ULB signal is typically comprised of a hydrophone(s) with associated electronics to filter and amplify the acoustic pings allowing for either audible or visual detection by an operator. The detectability of a ULB signal is influenced by the hydrophone system being used to listen for it. Operators must ensure the hydrophone is operating correctly and potential sources of interference are monitored closely. Newer systems digitise and record the signal allowing for real time processing or post processing using specific software.

The method commonly used in shallow water is an immersed hydrophone mounted on a simple pole connected to a headset. The operator listens at defined locations as the hydrophone is rotated through different directions. This was the technique used by *Haixun 01*.

For deep water, a towed pinger locator (TPL) equipped with a hydrophone is towed behind a vessel close to the seafloor. A TPL system was used by *Ocean Shield* (Figure 22) which comprised the TPL, tow cable and winch and the electronics needed to process the acoustic data at the surface. Power to, and data from, the TPL was transmitted continuously via the tow cable. The TPL was also fitted with a test ULB which could be used to test the correct system operation, by emitting 10 seconds of pings, when the TPL was operating at depth.

²¹ A distinct layer in a large body of water, such as an ocean or lake, in which temperature changes more rapidly with depth than it does in the layers above or below.

Figure 22: Towed pinger locator on board *Ocean Shield*



Source: RAN

Sonobuoys were also used in the search for MH370's ULBs. The sonobuoys were released from the search aircraft and left to drift to listen for a ULB. The sonobuoys are equipped with a hydrophone, which is streamed to a depth of 300 m below the buoy and a radio transmitter which allows acoustic data to be relayed back to the aircraft for processing when it is within range. This system was used by a P-3C Orion aircraft operated by the Royal Australian Air Force.

Acoustic detections

By 2 April 2014, search vessels equipped to listen for MH370's ULBs, including *Ocean Shield*, *HMS Echo* and *Haixun 01*, were en route to, or near the 7th arc. Flight path analysis at the time indicated that the most probable points at which MH370 crossed the 7th arc were the red/yellow/green areas (Figure 18). The search for the ULBs commenced at the boundary between areas S4 and S5 within the red box on the 7th arc.

HMS Echo

On 2 April 2014, *HMS Echo* reported a possible ULB detection close to the 7th arc and the S4/S5 boundary. The hull-mounted system on the vessel was designed to provide high accuracy deep water positioning of subsea transponders operating between 27 kHz and 30.5 kHz. The hydrophone system had been retuned to 37.5 kHz by the crew of *HMS Echo* to enable detection of a ULB. On 3 April 2014, following tests, this detection was discounted as being an artefact of the ship's sonar equipment.

Haixun 01

On 4 April 2014, crew from the People's Republic of China vessel *Haixun 01* reported detections at the southern end of the green zone at 25.975°S, 101.461°E. The crew were operating the hydrophone from one of the ship's rescue boats in an area where ocean depths were approximately 4,500 m. *Haixun 01*'s crew reported a pulsed signal with a frequency of 37.5 kHz for 15 minutes, repeating once per second. A second detection at the same frequency was made the next day, 3 km west of the first detection, for 90 seconds with a much weaker signal than the previous day.

On 6 and 8 April 2014, *HMS Echo* attempted to reacquire the detections reported by the crew of *Haixun 01*. However they were unsuccessful and concluded that the detections were unlikely to be MH370's ULBs due to the water depth, surface noise and the hydrophone equipment being used by the crew of *Haixun 01* which had a practical detection range of about 2,000 m according to the manufacturer. A submarine was also tasked to investigate the area and was also unable to identify any ULB transmissions.

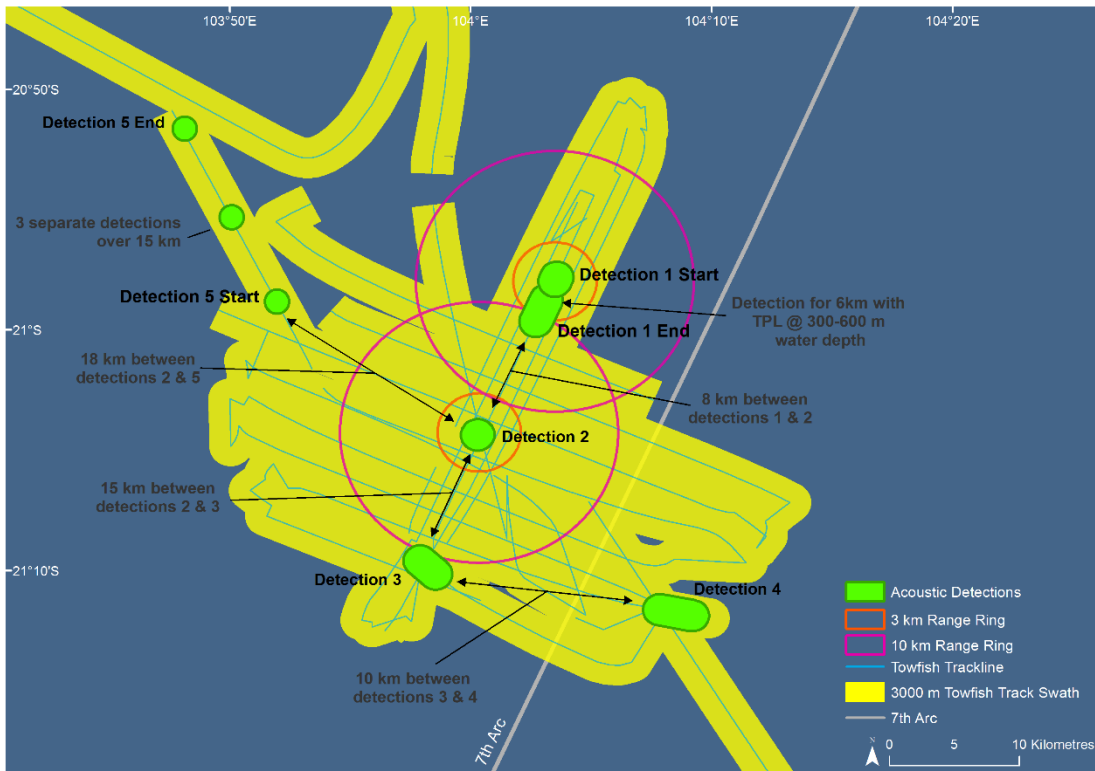
Ocean Shield

Also on 4 April 2014, *Ocean Shield* commenced acoustic search operations in the red area (Figure 16) using two United States Navy TPLs (01D and 03S) operated by Phoenix International mission crew. The 01D TPL when initially deployed exhibited acoustic noise and was replaced with the 03S TPL. This TPL was deployed on 5 April and shortly after, whilst descending, detected an acoustic signal at a frequency of approximately 33 kHz for approximately 2 hours and 20 minutes. Two additional TPL search lines were run over this area with no further detections noted. However three additional detections were recorded at different locations, one on 5 April and two on 8 April. At these three distinct locations two frequencies were identified for each detection area, each around ~33 kHz and ~42 kHz. Additional TPL search lines were run over these areas with no further detections noted.

On 10 April 2014, a fifth detection²² was recorded which consisted of three separate intermittent detections over a four hour period. However the operational log at the time notes the detections were a broad 32 kHz to 35 kHz signal and were suspected of originating from a malfunction within the TPL. For this reason, the TPL was recovered and no further search lines were run with either TPL system over this area. All five reported detections were made while using the 03S TPL and when the TPL was recovered following the fifth and final detection, the test ULB mounted on the 03S TPL was disconnected. Following the recovery the alternate 01D TPL system was then used for another four days with no further detections noted. An overview of the acoustic detections along with the TPL coverage is shown in Figure 23.

²² The fifth detection was not reported at the time but was in subsequent reporting from the operator.

Figure 23: Ocean Shield TPL detections with distance between each and TPL coverage polygons



Source: ATSB, using Phoenix International data

Analysis of acoustic detections

A review of the *Ocean Shield* acoustic detections was undertaken independently by various specialists including the ULB manufacturer, DST Group, Air Accidents Investigation Branch (United Kingdom), NTSB, Curtin University and Australian Joint Acoustic Analysis Centre. The analyses determined that the signals recorded were not consistent with the nominal performance of a Dukane DK100 ULB. Some analysts noted that the acoustic signals detected may be consistent with a damaged ULB however the calculated offsets (by the manufacturer) to the frequency, pulse width, and pulse repetition rate, for a damaged ULB, did not fully match any of the recorded detections.

It was noted that if damage had occurred to both ULBs it would be highly unlikely that the resulting offset frequency would be the same for each. However it was also noted that environmental factors could affect both ULB's frequency equally. Given the uncertainty it was decided that a seafloor search using the autonomous underwater vehicle (AUV) on board *Ocean Shield* should be performed to fully investigate the detections by looking for an aircraft debris field on the seafloor. The second possible ULB detection was deemed to be the most promising and this was the area of focus for the AUV search.

After the TPL equipment had been demobilised from *Ocean Shield*, Phoenix International performed a full test on TPL system 03S to identify and/or eliminate any possible sources for the acoustic detections during the search for MH370's ULBs. One of the tests performed showed that a simulated faulty 'self-test' cable, with a high resistance short circuit, would activate the test ULB mounted on the TPL. The faulty 'self-test' cable also caused the output frequency from the test ULB to shift from 37.5 kHz to 33 kHz, caused broadband noise and altered the acoustic ping repetition rate. The resulting acoustic signal is similar to the detections on board *Ocean Shield* during the search for MH370's ULBs.

Phoenix International also verified during their lab testing that when this condition occurred a fully functional ULB operating at 37.5 kHz was still able to be detected by the TPL.

Phoenix International's engineering test report concluded:

The fact that none of the recorded MH370 TPL search recorded acoustic detections were repeatable after numerous attempts, coupled with the significant geographical dispersion of the sounds will continue to challenge the theory that the detections were generated by an acoustic (ULB) source on the seafloor.

Marine animal tracking devices

Acoustic tracking

Acoustic tracking devices used by the Australian research community for tracking marine animals reportedly transmit at frequencies of 69 kHz or 180 kHz. These devices are monitored by hydrophones at fixed locations around Australia generally, on the continental shelf, and can only be detected up to a range of approximately 400 m. Based on the frequency of the acoustic detections on *Ocean Shield*, which ranged between 28-42 kHz, it was considered unlikely that they originated from marine animal tracking devices.

Satellite tracking

Satellite tags are another animal tracking technology commonly used. These tags are designed to transmit their data via satellite when the animal is on the surface. It was considered unlikely this type of tag would be detected by a hydrophone as the radio frequencies used are very high and quickly attenuated by water immersion. Since 2012 whale shark tracking has also largely been achieved by deploying archival tags that record but don't transmit data.

Sonobuoys

P-3C Orion sonobuoy acoustic search capability

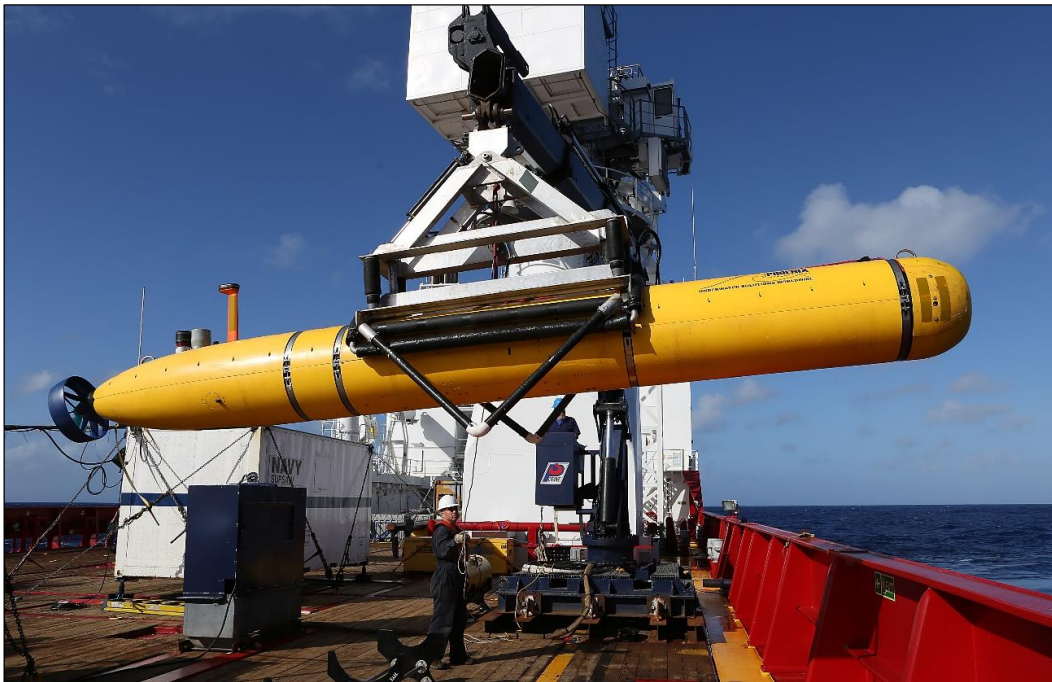
When Australia joined the international effort to locate MH370, the Australian Defence Force and Australian Defence Industry worked together to enhance the search capabilities available to the authorities coordinating the search. They developed a capability to detect a ULB signal at a range of up to 4,000 m by deploying sonobuoys from a P-3C Orion aircraft with a single sortie capable of covering an area of approximately 3,000 km².

Sonobuoy drops were undertaken from 6-17 April 2014 in the region of the 7th arc, where depths were favourable, in areas where *Ocean Shield* and *Haixun 01* had possible ULB detections. Another area targeted was based on the bearing of an event recorded shortly after 0019 UTC on 8 March 2014 at the Comprehensive Nuclear Test Ban Treaty Organization hydrophone network (data from the H01 array off Cape Leeuwin, analysed by Curtin University) and the intersection with the 7th arc (See Hydroacoustic analysis section). No acoustic detections considered to be related to ULB transmissions were detected using sonobuoys.

Autonomous underwater vehicle search

An underwater search using an autonomous underwater vehicle (AUV) commenced on 14 April 2014 in the Zenith Plateau area based on the analysis of the acoustic detections from the TPL on board *Ocean Shield*. Thirty AUV missions conducted at depths from 3,800 m to ~5,000 m were completed.

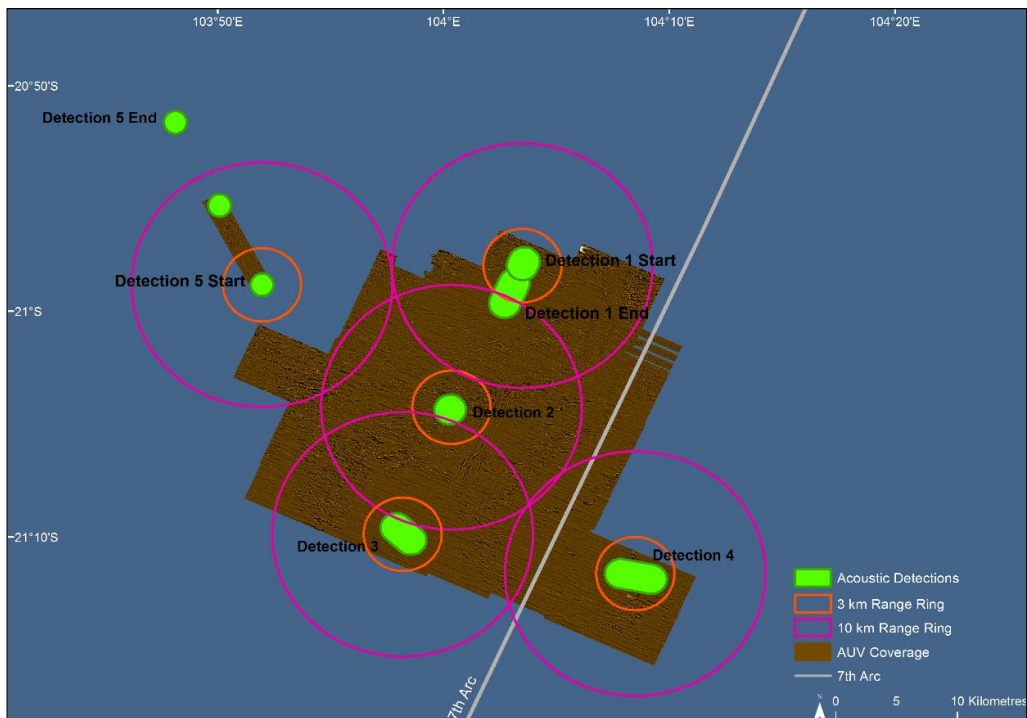
Figure 24: Phoenix International Artemis AUV on board *Ocean Shield*



Source: RAN

The AUV (Figure 24) collected 120 kHz side scan sonar data using a 400 m range scale at an altitude of 45 m. The side scan sonar tasking focused on a 10 km radius around TPL detection number two and a 3 km radius area around TPL detections one, three and four. This search was completed on 28 May 2014 and covered 860 km² with no aircraft debris detected on the seafloor. The coverage achieved by the AUV relative to the positions of the acoustic detections is shown in Figure 25. An animation of the AUV search is available for viewing on the [ATSB YouTube Channel](#).

Figure 25: *Ocean Shield* AUV coverage of acoustic detections



Source: ATSB, using Phoenix International data

The underwater search

Searching the seafloor for lost aircraft in deep water requires certain key components and thorough processes to maximise the chances of detection and success. The area to be searched must be identified with as much rigour and precision as the available information will allow. All sources of credible evidence as to how and why and where the aircraft may have ended the flight must be pursued and analysed to allow hypotheses to be formed and tested. While it is human nature to form a hypothesis and then attempt to 'fit' the evidence to that mental model, any hypothesis which is not in concert with all the evidence must be discarded, however reluctantly.

The significant challenge in finding MH370 has been defining the search area based on only limited SATCOM metadata for the final six hours of flight, and later, very long term drift studies when debris from the aircraft have been found. The total possible search area was in the order of 1,200,000 km² along the 7th arc when all possible flight paths and the potential glide range of the aircraft at the end-of-flight after fuel exhaustion are considered. To be practical, the underwater search area needed to be defined with as much precision as analysis of the available data would allow.

For the underwater search, seaworthy ships, well maintained underwater and surface equipment, and a robust program for ensuring the quality and analysis of the data collected are all critical components. All vessels used in the search for MH370 were built, crewed, operated and maintained in accordance with the appropriate international standards for international trading and/or special purpose vessels. The search equipment was tested and verified to meet the requirements stipulated by the ATSB for use in the underwater search.

During underwater search operations there were two particular areas of focus; maintaining a comprehensive program to ensure coverage of the area searched and a thorough review process for marking areas of interest, also referred to as sonar contacts. Sonar contacts were defined as any anomaly on the seafloor that appeared non-geologic in nature or unusual when compared to the surrounding seafloor. Contacts were marked to document specific points in the data which warranted further analysis or the need for additional data to be collected over the area.

Defining the initial underwater search area

Initial priority search area

On 28 April 2014, the Prime Minister of Australia announced that Australia, represented by the ATSB, would coordinate the underwater search for MH370. The ATSB subsequently formed and coordinated the Search Strategy Working Group (SSWG) to facilitate interaction with the Annex 13 investigation team flight path reconstruction group and satellite communications working group (SATCOM WG) to progress work on defining an initial underwater search area. The aim was to define underwater search areas along the 7th arc in the Indian Ocean where the SATCOM data indicated a power interruption close to the time of expected fuel exhaustion (Table 19).

An Inmarsat BFO model designated 'Differential Doppler Analysis ECLIPSE_2' was finalised in April 2014. This model incorporated all data frequency translations that Inmarsat were aware of at that time. The chronology and further information on doppler model development by Inmarsat is provided at appendix C.

Table 19: Initial priority search area

Dates:	14 June – 26 August 2014
Event:	Mapping of seafloor in proposed underwater search area of 60,000 km ² .
Search area location:	Priority and medium search areas; 27.4°S to 32.1°S along 7th arc, -20 NM, +30 NM across 7th arc.
Search activity:	Mapping of seafloor – bathymetry phase.
Guiding advice:	Initially Inmarsat's 'Differential Doppler Analysis Eclipse 2' BFO model was used to define priority, medium, wide search areas for 26 June 2014 report. The unified model released on 19 June 2014 and subsequent revisions were used in flight path modelling developments after this date.
Data used in planning search area refinement:	Effects of an eclipse on the satellite during a period of MH370 flight taken into consideration. Refined EAFC model. 1912 NW point (8° 35.719'N, 92°35.145'E) reassessed as invalid and no longer used by flight path reconstruction groups. Flight path from 2nd arc at 1941. Candidate paths with zero BTO tolerance. Candidate paths within BFO tolerance of 10Hz. Loss of control study, arc tolerance, balance of uncertainties and agreed area of 60,000km ² results in width of +30 NM, -20 NM around 7th arc.
Search equipment	<i>Fugro Equator</i> (ATSB contract survey vessel, multibeam echo sounder (MBES)) <i>Zhu Kezhen</i> (the People's Republic of China hydrographic survey vessel, MBES)
Coverage details:	Approximately 38,000 km ² completed in defined priority area 27.4°S to 32.1°S.
References	ATSB report: <i>MH370 – Definition of Underwater Search Areas</i> – 26 June 2014

Source: ATSB

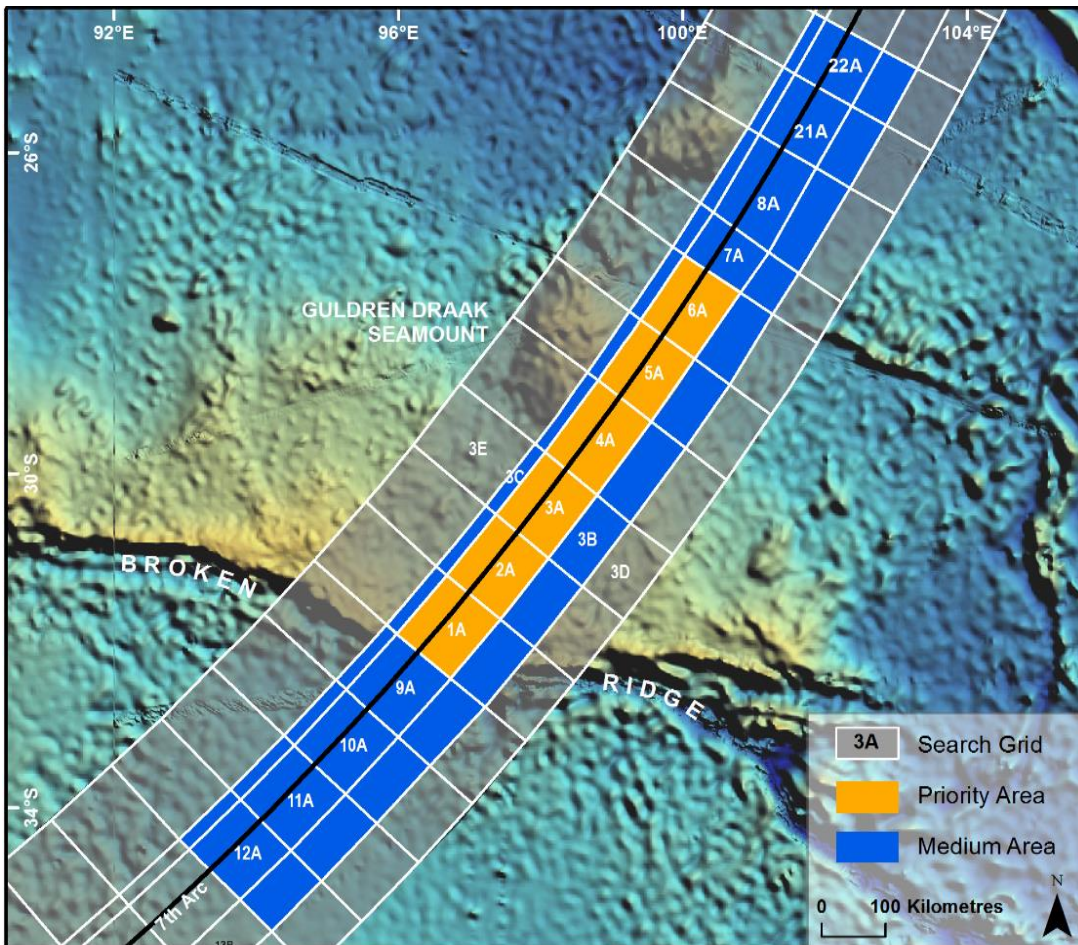
Inmarsat techniques applied to the model indicated best fit agreement for a 400 knot ground speed flight crossing the 2nd arc at latitude 2°N, ending at 28.2°S, 99.6°E at 0019 UTC. The model provided reasonable matches for a range of ground speeds between 375 and 500 knots from the estimated 2nd arc starting location, with the end-of-flight between latitudes 25°S and 37°S on the 7th arc.

Further flight path reconstruction techniques using this model were undertaken in May and June 2014 to define the initial underwater search area. The proposed underwater search area at that time was defined in ATSB report [MH370 – Definition of Underwater Search Areas](#) released on 26 June 2014. The application of the 'Eclipse 2' BFO model by the flight path reconstruction group had resulted in a shift of the most probable aircraft paths southwest along the 7th arc from the red/yellow/green area (latitudes 20.2°S–26°S) to an orange priority area (latitudes 27.4°S–32.1°S).

The report defined priority, medium and wide search areas spanning increasing lengths along and widths across the 7th arc. The priority area for the underwater search defined in June was based on the area agreed by Tripartite governments of 60,000 km². This area was equal in size to the red/yellow/green search area defined during the surface search.

The underwater search areas were designated block numbers and width letters (Figure 26). The 'A' blocks were areas of 10,000 km² each. The priority search area was therefore defined as Blocks 1A–6A.

Figure 26: The underwater search area, June 2014



Source: ATSB

A reasonable search width for a ‘loss of control’ end-of-flight scenario was determined to be 30 NM in front and 20 NM behind the 7th arc. These were the limits of the A blocks. These widths allowed an approximate search area length of 650 km along the 7th arc (orange coloured area) for a total area of 60,000 km².

Mapping the seafloor in the search area

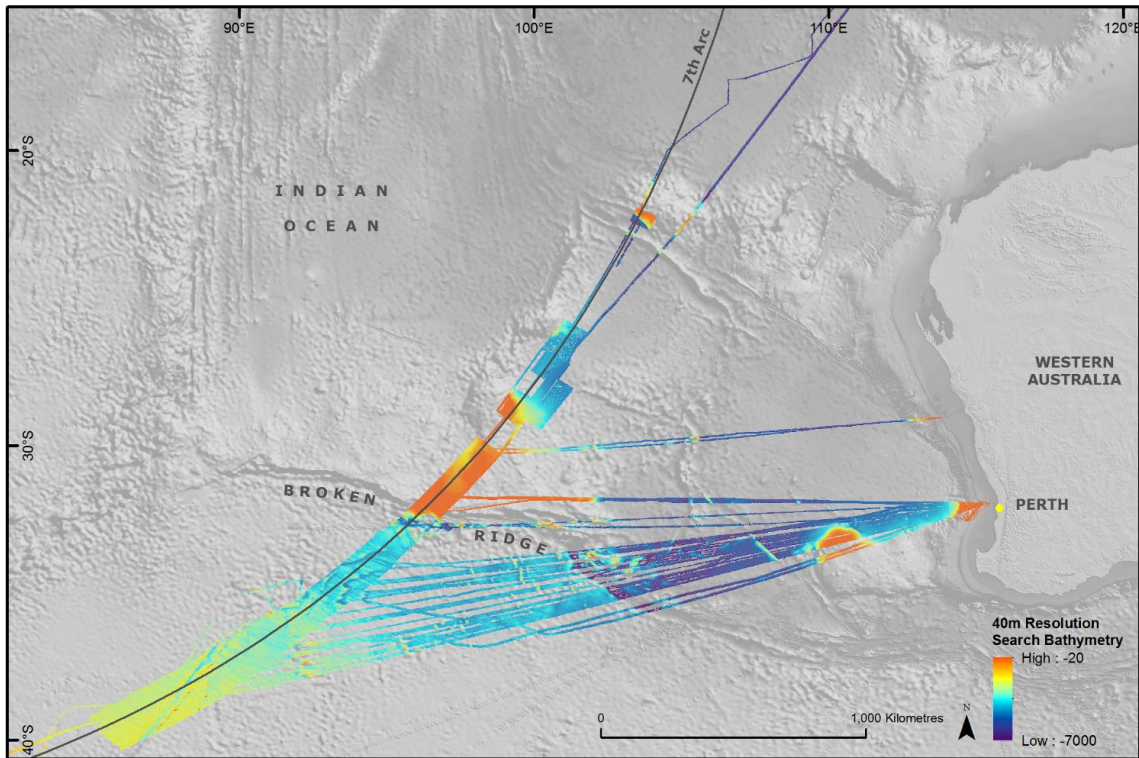
Bathymetric survey

The underwater search required a phased approach given the unknown composition and topography of the seafloor in the search area. Before the underwater search commenced, a bathymetric survey was conducted to ensure that high resolution maps were available for the safe and efficient navigation of underwater vehicles close to the seafloor. The bathymetric survey used hull-mounted multibeam sonar systems suitable for deep water wide area survey on the vessels *Fugro Equator*, *Fugro Supporter* and the People’s Republic of China vessel *Zhu Kezhen*.

The majority of the bathymetric survey was conducted from May to December 2014. Supplementary bathymetry data was intermittently acquired to expand the search area as required from December 2014 to February 2017. The bathymetric survey commenced in the underwater search area defined in June 2014 (orange area in Figure 26).

In the search area 278,650 km² of high resolution multibeam bathymetry data was collected. In all, 710,000 km² of data was collected, which includes data acquired while search vessels transited to and from port to the search area (Figure 27).

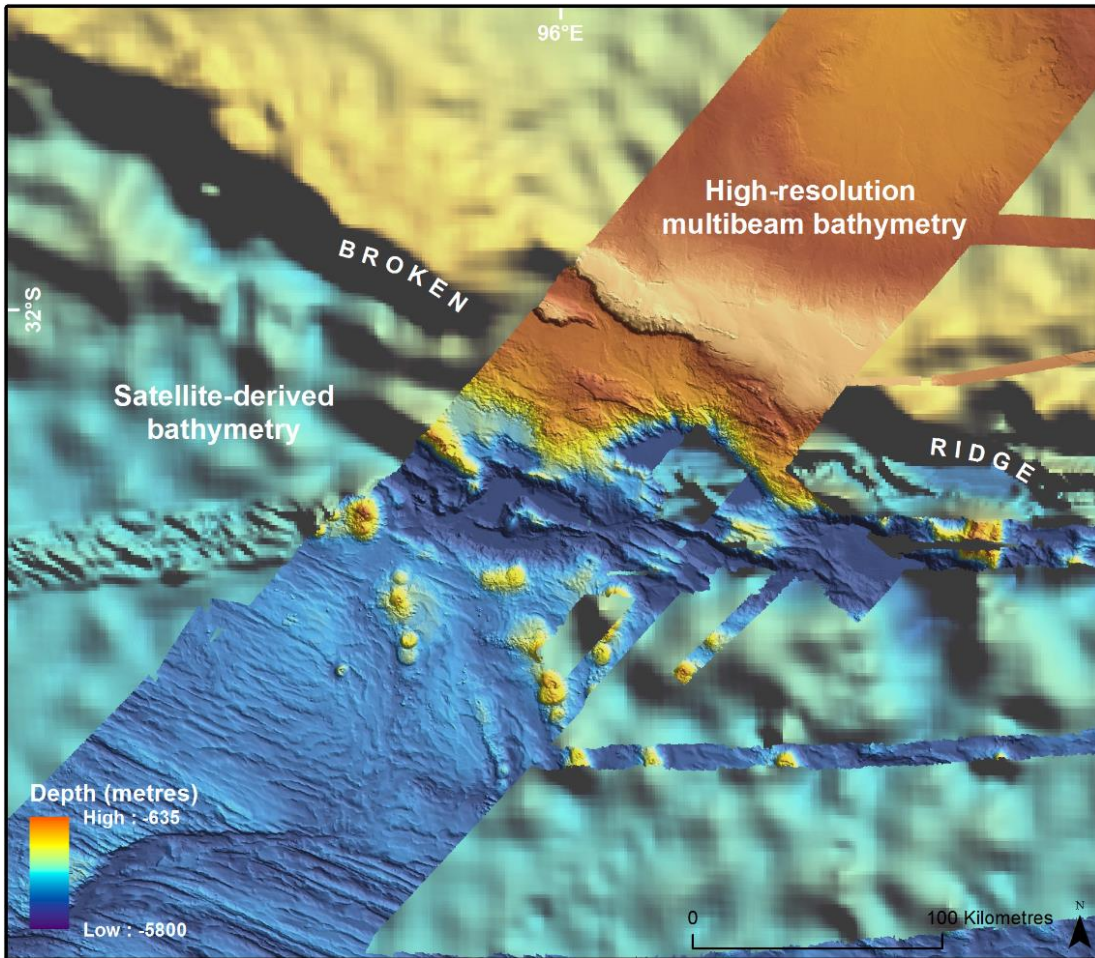
Figure 27: The 710,000 km² bathymetric survey dataset is one of the largest marine surveys ever conducted



Source: ATSB

Previous maps of the seafloor in the search area were from satellite-derived gravity data and only indicated the depth of the ocean at a coarse resolution of approximately 5 km² per pixel. The bathymetric survey acquired for the underwater search collected data at 40 m² per pixel, allowing for finer scale awareness of topography as shown in Figure 28.

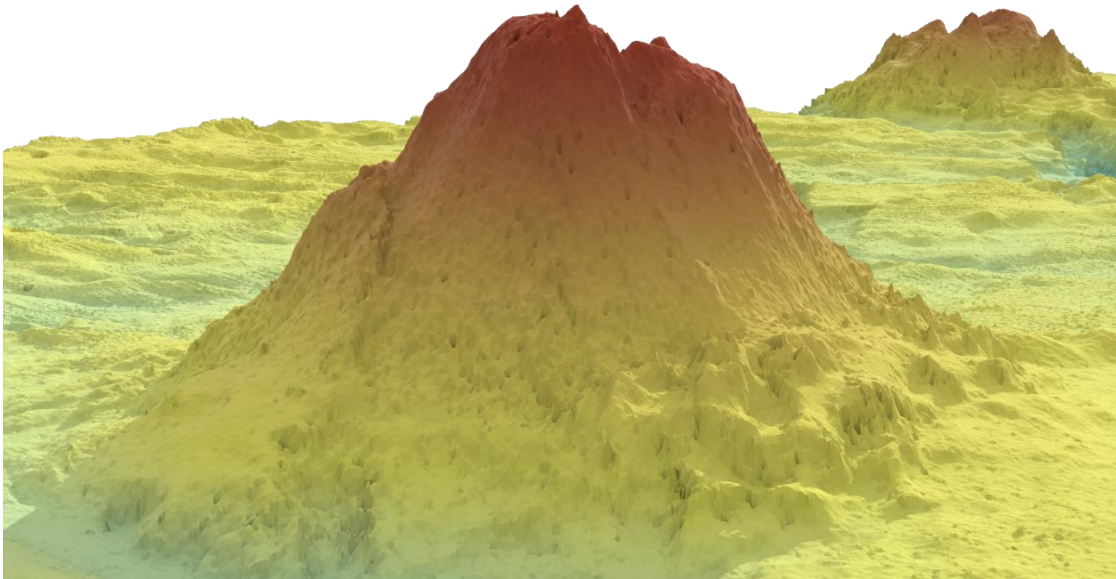
Figure 28: High resolution multibeam bathymetry data compared to low resolution satellite-derived bathymetry data



Source: ATSB

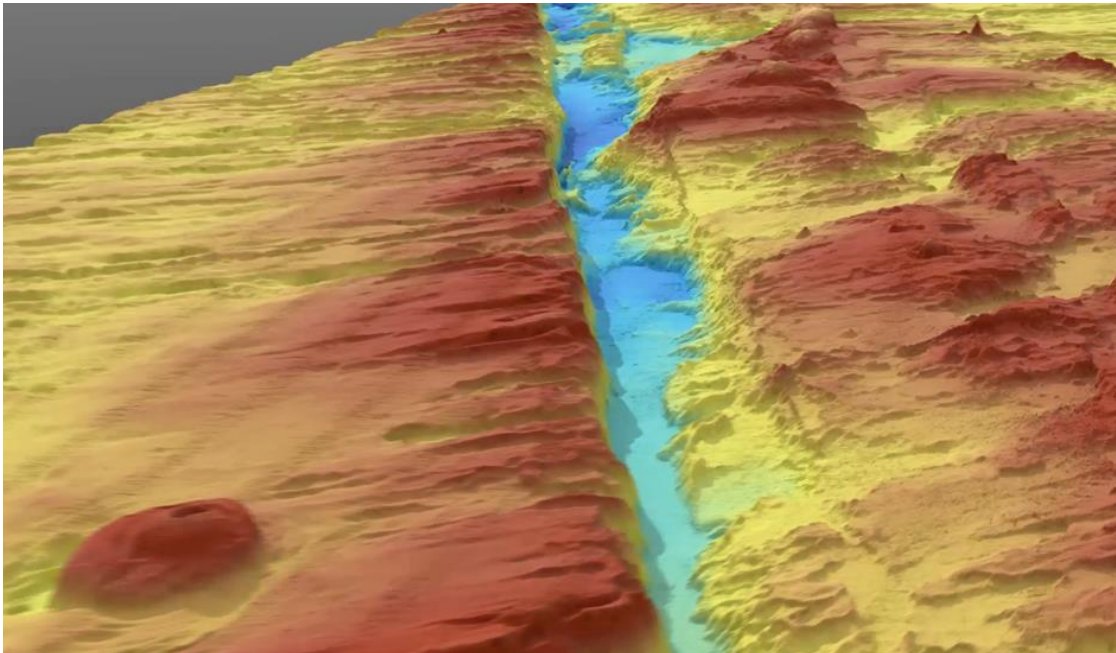
The underwater mapping revealed details about the seafloor which were not visible in the previous satellite-derived bathymetry including vast seamounts 1,500 m high and kilometres wide, deep canyons and underwater landslides of sediment that travel for kilometres along the seafloor (Figure 29 and Figure 30).

Figure 29: 2,200 m high volcano (vertical exaggeration is 3 times)



Source: Geoscience Australia

Figure 30: Geelvinck Fracture Zone, 4,500 m below sea level, fault depth 900 m (vertical exaggeration is 3 times)



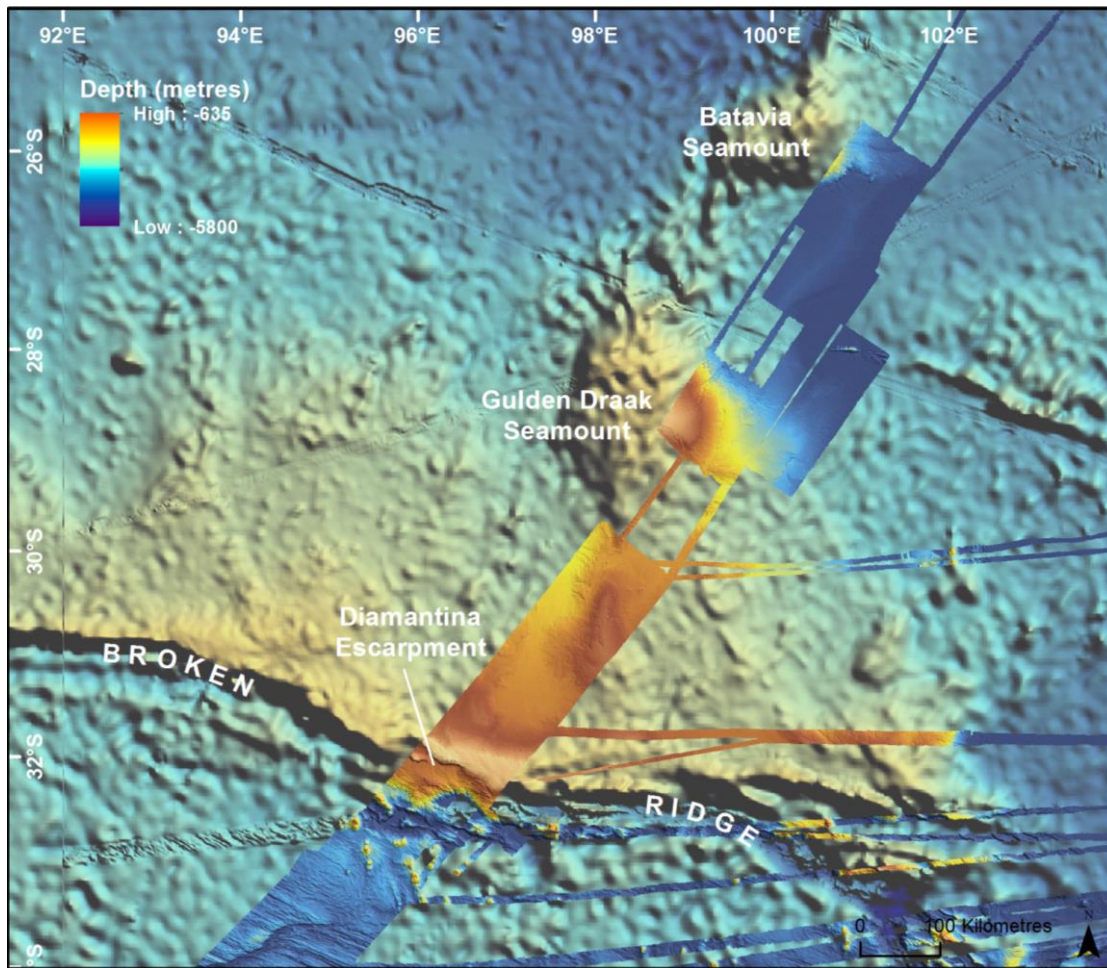
Source: Geoscience Australia

Geology of the search area²³

The major geological feature of the seafloor in the search area is Broken Ridge. It is approximately 1,200 km long and was created by tectonic forces more than 40 million years ago.

²³ From Geoscience Australia - MH370 Phase One Data Release

Figure 31: North of Broken Ridge



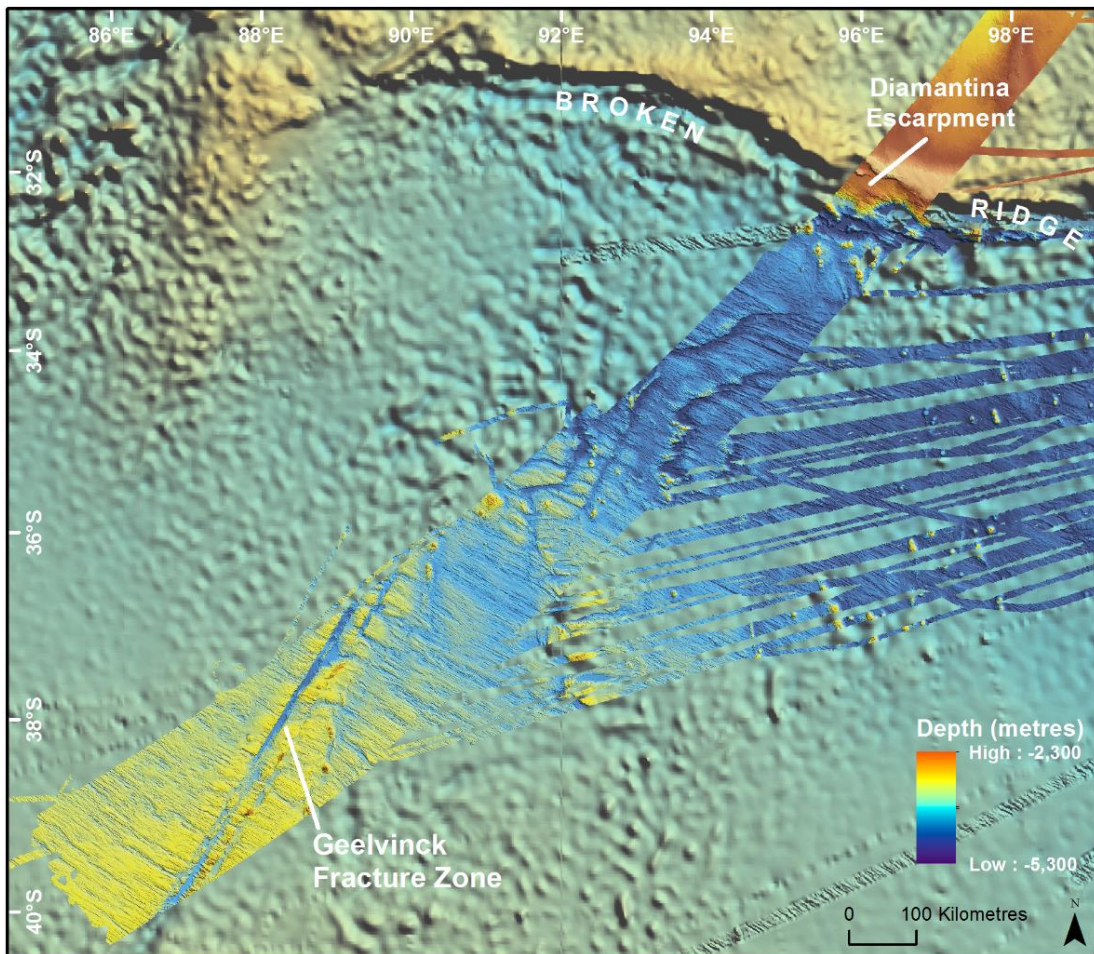
Source: ATSB

North of Broken Ridge

Here, water depths range between 635 m and 5,800 m. The seafloor north of Broken Ridge is more than 40 million years old, making it the oldest seafloor in the search area. The seafloor in this region is covered in a layer of sediment up to 300 m thick and is subject to extensive seafloor landslides, some of which are kilometres long. The Gulden Draak Seamount and the Batavia Seamount found in this part of the search area are significant due to their size (Figure 31).

Broken Ridge and the Diamantina Escarpment are a geological 'breakup zone', created approximately 40 million years ago as their tectonic plate broke apart.

Figure 32: South of Broken Ridge



Source: ATSB

South of Broken Ridge

Here, water depths range between 2,300 m and 5,300 m. The seafloor south of the Diamantina Escarpment has the youngest geology within the search area. This region of the seafloor was formed by ‘seafloor spreading’ caused by tectonic plate movements. As a result, the seafloor is highly complex, including a series of ridges, volcanoes, and valleys. The Geelvinck Fracture Zone was the result of the same tectonic motion that created Broken Ridge. It is 900 m deep and 12 km wide (Figure 32).

Bathymetry processing

The data gathered during the bathymetric survey was analysed and processed by Geoscience Australia.

High resolution multibeam data was collected using a Simrad Kongsberg EM 302 (30 kHz, *Fugro Equator*), Simrad Kongsberg EM 122 (12 kHz, *Fugro Supporter*) and a modified Reson Seabat 7150 (12 kHz, *Zhu Kezhen*).

Raw data from the Fugro Survey vessels was post-processed, and processed data from the *Zhu Kezhen* were verified, using the CARIS Hydrographic Information Processing System (HIPS) and CARIS/Sonar Image Processing Software (SIPS) v.7.1.2 SP2. The processed data were exported as ASCII XYZ point cloud files. Bathymetry data were converted into 40 m and 110 m grid formats via LASTools and Python, and imported into ArcGIS v.10.0 for spatial analysis.

More information on bathymetric surveys can be found on the Geoscience Australia website at www.ga.gov.au/

Backscatter analysis

In addition to processing and mapping the bathymetric data, Geoscience Australia analysed the backscatter data from the hull-mounted multibeam sonar, looking for anomalies in the acoustic return.

The proportion of acoustic energy returned from a rough surface is determined by the impedance contrast, sometimes referred to as 'hardness' and apparent surface roughness scale (i.e. roughness scale relative to the acoustic wave length). In general, as the impedance contrast or roughness of a surface increases, so does the intensity of backscatter returned (Figure 33).

The surface scattering coefficient is a dimensionless quantity that accounts for the intensity (power) ratio of the incident and scattered waves determined per unit area at a reference distance of 1 m. When expressed in decibels, this quantity is commonly called the backscatter strength.

Hardness of the seafloor is measured by acquiring backscatter; the reflection of acoustic signal scattering from the seafloor back to the hull-mounted multibeam sonar transducer. Measured in intensity, backscatter ranges from 10 and -70 decibels, high to low, respectively (e.g. steep slopes to soft sediment).

Figure 33: Backscatter data at 30 m resolution showing volcano with hard rocky surface



Source: Geoscience Australia

The backscatter analysis was used to identify anomalies on the seafloor. These anomalous areas were collected as a guide of potential areas of interest for the underwater search using side scan sonar.

Three classifications of area types were identified during the backscatter data analysis; navigation features, response uncertainty and potential targets (Table 20):

- Navigation features identifies areas that may be of interest for the navigation of underwater vehicles such as seafloor with high relief or large-scale irregular morphology, for example a canyon or seamount.
- Response uncertainty identifies areas of seafloor with relatively complex/highly reflective acoustic characteristics that could hinder the detection of aircraft debris.
- Potential targets identifies features that are of potential interest for further searching based on anomalies in backscatter intensity.

Table 20: Areas of interest identified in backscatter analysis

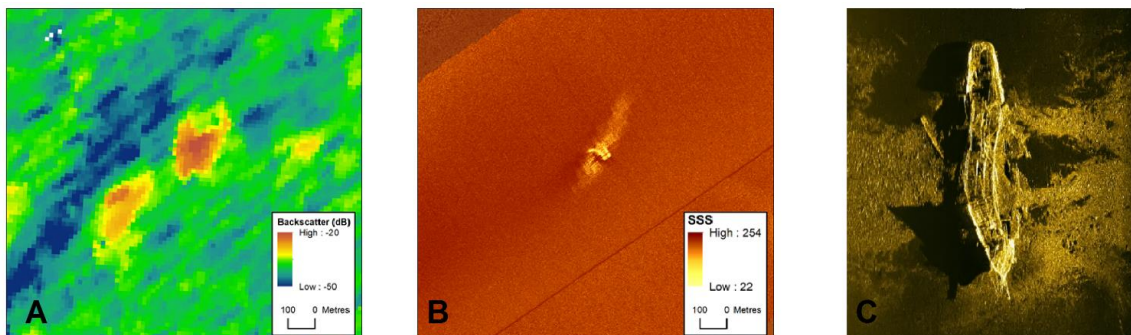
Navigation Features:	53
Response Uncertainty:	42
Potential Targets:	608

Source: Geoscience Australia

Potential targets were detected based on the anomalously high acoustic backscatter strength of small features. The identification of potential targets for fine-scale investigation was based on a line by line assessment of the backscatter strength and corresponding bathymetry data. For example, potential target areas of seafloor may have backscatter anomalies that are difficult to explain based on their corresponding geomorphology.

One potential target area is shown in Figure 34. Here, high backscatter values contrast with the surrounding seafloor of low backscatter strength. This potential target was located within the nadir region; a region in the backscatter data approximately 10 degrees to port and starboard of the ship’s track, which changes in width systematically with depth. Results from this region were not considered due to the inherent reduced quality in backscatter response. Results were discounted at the time but later compared with the side scan sonar, revealing the potential target had coincided with a shipwreck.

Figure 34: Potential target with maps showing backscatter (A), side-scan sonar (B), and man-made feature (C)



Source: Geoscience Australia (A), ATSB (B) and (C)

Selecting the search method/systems

When the surface search for MH370 concluded, it was agreed by the Tripartite governments that Australia, represented by the ATSB, would coordinate all aspects of the underwater search. This included the contracting of the necessary commercial services and also to manage the operations of all search vessels and equipment provided directly by the Governments of Malaysia and the People’s Republic of China.

The initial area to be searched was very large at 60,000 km², and became larger in April 2015 when the Tripartite governments agreed to expand the search area to 120,000 km². The main objective of the search was to establish whether or not the debris field of the missing aircraft was in the area defined by expert analysis of the aircraft flight path. If a debris field was located, the search needed to confirm the debris was MH370 by optical imaging and then map the debris field to enable planning for a subsequent recovery operation.

Careful consideration was given to available equipment and methods for conducting a large scale search of the seafloor. Water depth was expected to be up to 6,000 m with unknown currents and unknown seafloor topography. Search operations would have to be often conducted in poor weather conditions in a very remote area. While the ATSB search team hoped the aircraft would be found quickly, planning focused on selecting an efficient and effective method to search the seafloor in an operation for an indeterminate period.

The search tender

The ATSB had not previously managed an underwater search operation in such deep water nor managed a procurement of this size or complexity. Initial market research was conducted which indicated that there was a small market of mostly international marine survey/salvage companies with the capacity and capability to undertake the underwater search.

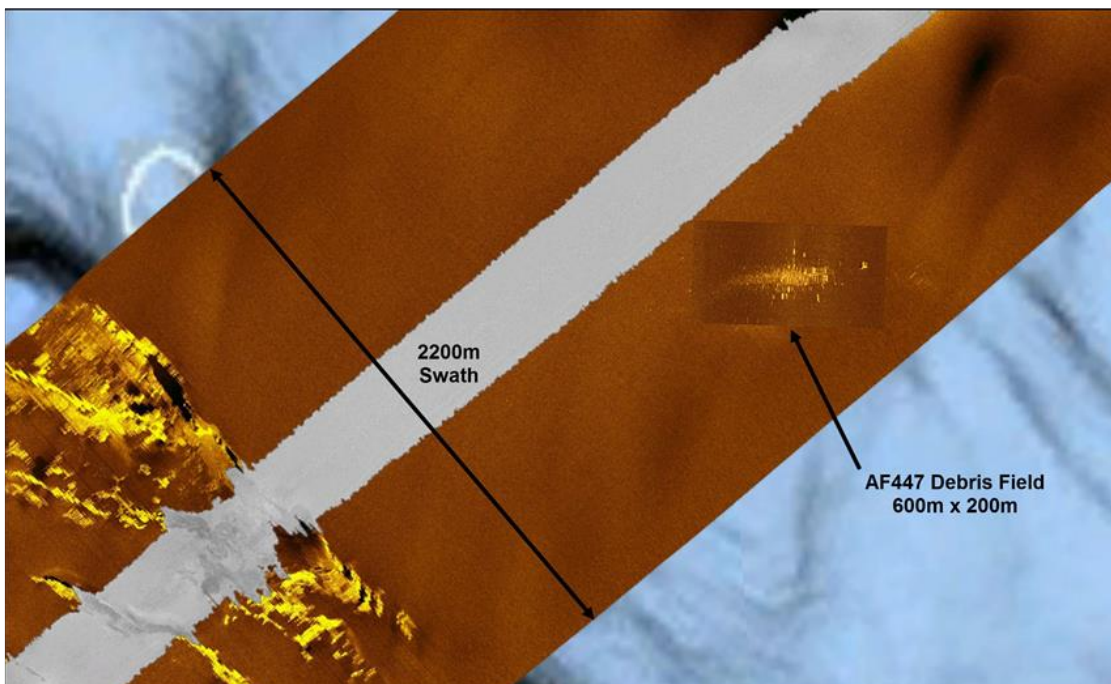
When preparing the open tender for MH370 search services, the ATSB considered all of the technical and organisational requirements to conduct an efficient, effective, and safe underwater search operation in up to 6,000 m of water, in challenging conditions. The tender focused on the underwater search equipment, vessels, personnel, past experience with similar operations, the processing, storage, transmission and security of the search data and the organisational systems and plans to be put in place to manage the search with a particular focus on risk mitigation and the health and safety of the search crews.

The ATSB's tender was for seafloor search operations to localise, positively identify, map and obtain visual imaging of the MH370 debris field. The tender was divided into two primary areas; search for and locate MH370 debris within the defined search area on the seafloor and if located, map and optically image (photograph or video) the aircraft debris field.

The search for Air France 447 (AF447) off the coast of Brazil from 2009 to 2011 is the most analogous deep water search operation for an aircraft in recent times. The ATSB consulted extensively with France's air accident investigation organisation, the Bureau d'Enquêtes et d'Analyses pour la Sécurité de l'Aviation Civile (BEA) who were responsible for the AF447 search and recovery. Woods Hole Oceanographic Institute in the United States was also consulted on the underwater search as they provided equipment and expertise for the AF447 search operations.

AF447 was an Airbus A330 aircraft, a similar size to the B777 aircraft operating flight MH370, and the wreckage was recovered from a depth of water similar to that in the MH370 search area. It was also lost in a very remote location, midway between South America and Africa in the middle of the Atlantic Ocean. The AF447 debris field was approximately 600 m x 200 m in size at a depth of 3,980 m (Figure 35).

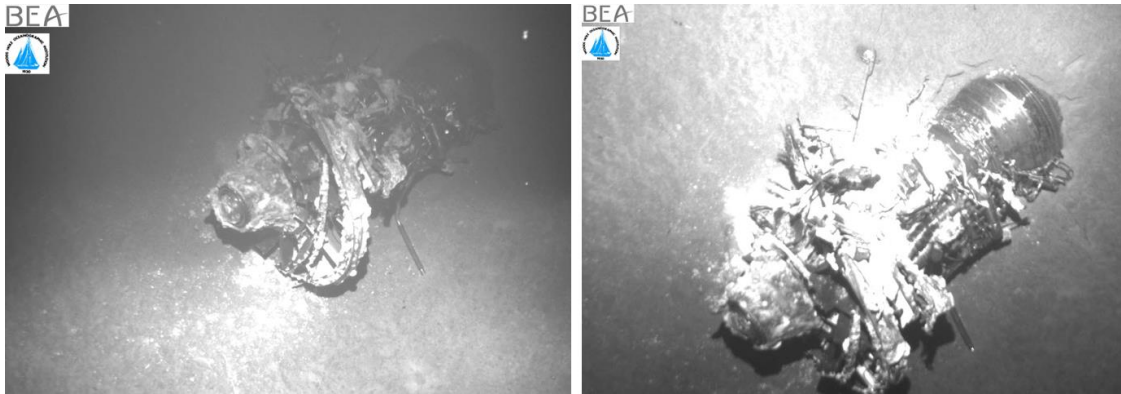
Figure 35: Air France 447 debris field overlaid to scale on a swath of MH370 deep tow vehicle sonar data



Source: ATSB, using BEA data

A key specification for the search equipment in the ATSB's tender was a feature detection capability, or resolution, of two cubic metres which was conservatively selected on the basis that this is the size of the core of B777 engines which are very robust and likely to survive a high energy impact relatively intact, as they did in the case of AF447 (Figure 36).

Figure 36: Air France 447 engines on the seafloor



Source: BEA

The tender also specified a requirement to perform a fully functional test in deep water to demonstrate that the proposed search system would reliably detect targets of two cubic metres at the sonar range scales to be used in the search. Other key tender requirements specified the necessity to mobilise the search equipment quickly and complete the search of the initial 60,000 km² in a period of 300 days.

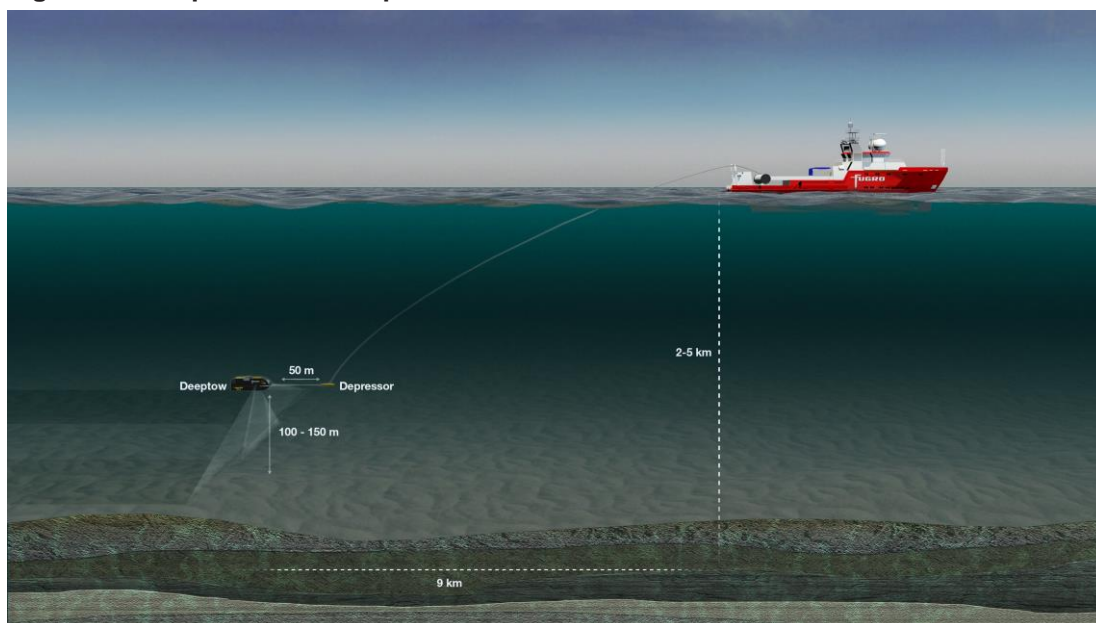
Tender responses broadly fell into two categories, those companies who offered towed side scan vehicles for primary search and detection with an alternate method to positively identify and map the debris field, usually a remotely operated vehicle (ROV) fitted with a camera. Other tenders offered autonomous underwater vehicles (AUVs) which could be used for both primary search and also positive identification and mapping using a camera. A few tenders offered both towed and autonomous search vehicles.

All tenders were assessed by a panel which included personnel who had experience in marine survey, marine salvage, marine operations, deep water search/survey and aircraft accident investigation. The tender assessment panel initially assessed each tender's compliance with the technical requirements set out in the request for tender and were not privy to the prices quoted by the tenderers. Once the tenders were ranked in merit order for the technical solutions they proposed, only then was the price considered. The intent was to ensure that the tender assessment process was weighted towards choosing the best overall technical solution.

Vehicles

There were only two choices of underwater vehicles to use in the underwater search for MH370, towed or autonomous, both had advantages and disadvantages and both types of vehicle were used in the search.

Towed vehicles are an efficient instrument platform when a search is to be conducted of a large area which can be performed in long continuous search lines where the seafloor terrain is relatively flat. Once launched from the support vessel, they can be towed for many weeks, including through periods of worse weather (than AUVs), without the need for recovery as power and data to and from the instruments on the vehicle are transmitted continuously via the tow cable. The deep tow system used in the search for MH370 is shown in Figure 37.

Figure 37: Deep tow vehicle operation

Source: Fugro Survey

Deep tow vehicles have disadvantages compared to AUVs including relatively little to no manoeuvrability and typically less accurate positioning, both of which can have an impact on the effective sonar coverage achieved in a wide area search/survey operation.

Deep tow vehicles must be positioned by changing the heading/speed/position of the tow vessel at the surface and the length of tow cable deployed. The depth of water dictates how much tow cable must be used to maintain the vehicle at a constant altitude above the seafloor for a given vessel speed. In 4,000 m of water there may be up to 8,000 m – 9,000 m of tow cable deployed which lies in a very long catenary behind the tow vessel. The response of the deep tow vehicle to changes in vessel speed, heading or position or the amount of tow cable deployed, is directly proportional to the rate each parameter is changed. The deep tow vehicle response may not be immediate but once the change begins it may happen relatively quickly and be very slow to reverse if needed.

Negotiating terrain features on the seafloor, for example a seamount where there is a steep gradient, requires the deep tow vehicle to be raised to clear the obstacle and then lowered after the obstacle is passed. This will often lead to sonar data degradation due to increased motion of the deep tow vehicle or a gap in the data termed a 'terrain avoidance holiday'. Similarly, the very long tow cable means an end-of-line turn (through 180°) onto the next search line may take up to 12 hours.

Deep tow operations are limited by the weather as a proportion of the tow vessel's pitch, heave and surge motions, in particular, are transmitted via the tow cable to the deep tow vehicle. While the very long catenary of the tow cable helps to damp these motions, any residual force at the end of the tow cable causes the deep tow vehicle to pitch and surge which can lead to sonar data quality degradation. A two body tow system (consisting of a heavy depressor connected to the end of the tow cable and a soft neutrally buoyant tether which connects the vehicle to the depressor) helps to mitigate this undesirable vehicle motion. However, depending on the weather which is forecast, decisions have to be made whether or not to recover the vehicle or continue deep tow operations based on the likely impact on the quality of the side scan sonar data and the increased risk to personnel and equipment as the sea states rise.

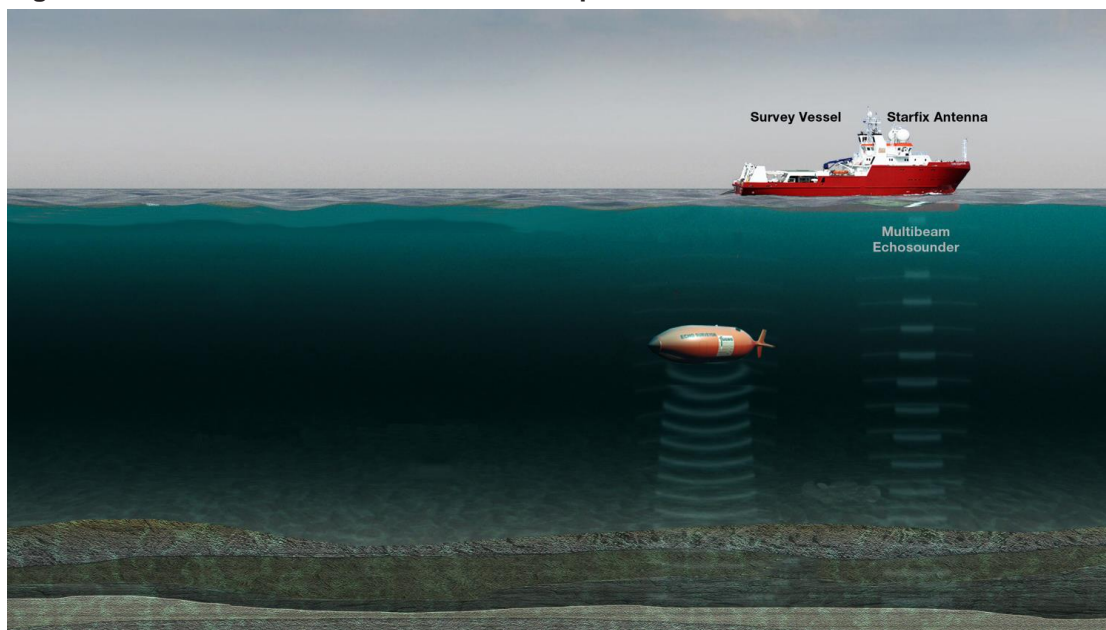
Accurately positioning an underwater vehicle in real time on a search line is critical to ensuring that the search is efficient and effective. Features identified in the sonar data must be able to be accurately georeferenced (using the vessel's position to derive the deep tow vehicle's position)

and there must be sufficient overlap in side scan sonar coverage to avoid data gaps (termed ‘off-track holidays’) between adjacent search lines. Accuracy in positioning a vehicle at depth generally diminishes as distance from the accurately known position of the vessel at the surface increases. For deep tow vehicles, factors like currents may result in the vehicle being significantly offset from the tow vessel’s track and must be compensated for by manoeuvring the vessel to maintain the required deep tow vehicle track to ensure adequate overlap between search lines.

Deep tow vehicle positioning is most often derived using one or a combination of the following; cable lay back, seafloor feature matching methods, a bottom tracking doppler velocity log (DVL), and an inertial navigation system both fitted to the vehicle, ultrashort baseline (USBL) acoustic positioning or long baseline acoustic positioning. USBL systems provide a range and bearing from the vessel to the USBL beacon which is fitted to the vehicle, or for shorter range systems, an intermediate position on the tow cable. All of these methods have inherent inaccuracies with the most accurate available long range USBL systems when coupled with an inertial navigation system and DVL achieving vehicle position accuracy in practice of approximately 50 m at a range of approximately 8-9 km.

Autonomous underwater vehicles, once programmed and launched, can be completely independent of the support vessel and are highly manoeuvrable. They can search the seafloor effectively in any pattern, not just long continuous lines, and can closely follow dynamic seafloor terrain which often leads to better overall sonar coverage. They can also achieve higher resolution sonar data given they can safely fly closer to the seafloor than a typical deep tow vehicle. Similarly when the AUV’s inertial navigation system is coupled with a DVL and USBL (or long baseline) acoustic tracking system at a relatively short range (4,000 to 5,000 m), with the support vessel tracking the AUV at the surface, or deploying a long baseline field, AUV positioning is generally more accurate than a deep tow system. Figure 38 shows an AUV operation (not to scale) with the support vessel gathering bathymetric data concurrently.

Figure 38: Autonomous underwater vehicle operation



Source: Fugro Survey

The major disadvantages of AUV’s are the need to safely launch and recover the vehicle before the batteries are exhausted, their limited duration on the seafloor per mission (typically less than 26 hours), the time to download the data which is stored on board the vehicle (or a data pod), and their relative high cost per km² compared to a deep tow vehicle equipped with the same instruments. At the time of the search tender there was also limited availability for 6,000 m rated AUVs, and multiple AUVs were needed to achieve the required search coverage rates.

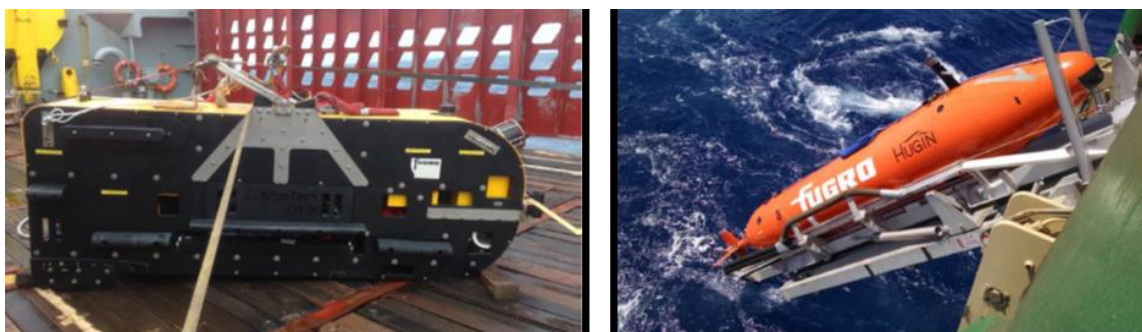
In the MH370 search area, weather for much of the year is consistently beyond safe launch and recovery limits for effective AUV operations. The exception is the summer months, December to March, when there is a much higher proportion of better weather which allows for efficient AUV operations.

At the time the search tender responses were assessed, bathymetric mapping in the search area was not complete nor was the search area fully defined. There was ongoing analysis to define the most probable area along the 7th arc where the aircraft impacted the water. Research indicated that weather was likely to be challenging for much of the year in the most likely search area and that the prevailing weather was from the southwest.

The search was likely to be able to be conducted in long lines aligned with the 7th arc which would make deep tow vehicles the most effective search method for most of the area. The weather from the southwest would also mean that the search vessels would be towing the deep tow vehicles with the weather almost directly astern or ahead, a significant advantage for maintaining the tow vessel position accurately and therefore that of the deep tow vehicle.

The decision was therefore made that deep tow vehicles represented the most efficient systems to conduct the search offered in the tender. It was concluded that choosing deep tow vehicles as the primary search method would necessitate having an AUV or ROV readily available for positively identifying sonar contacts. It was also considered that AUVs would offer further advantages as these vehicles could also be used to perform infill search work (in areas where the deep tow vehicles could not search effectively) whereas an ROV could not. Fugro Survey's underwater vehicles used in the search for MH370 are show in Figure 39.

Figure 39: Fugro Survey search vehicles: Edgetech deep tow and Kongsberg Hugin 1000 AUV

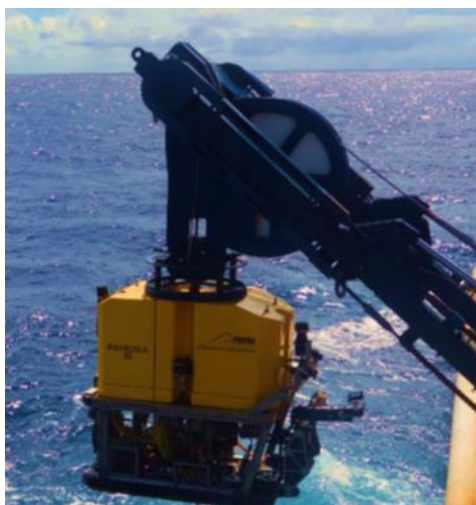


Source: Fugro Survey

Remotely Operated Vehicle

Phoenix International's *Remora III* ROV (Figure 40) was brought into the search in 2016, initially to recover the ProSAS deep tow system which was lost after a tow cable termination failure, and then later used to investigate a number of sonar contacts of potential interest. Unlike an AUV, the ROV remained tethered to, and controlled from, the support vessel. The ROV was rated to a depth of 6,000 m and was fitted with a video camera system, scanning sonar, manipulators (to gather samples), and a USBL positioning system. In good weather the ROV was able to be deployed, dive, survey and film the sonar target, return to the surface and be recovered by the vessel in 5 to 6 hours.

Figure 40: Phoenix International's *Remora III* remotely operated vehicle



Source: Phoenix International

Sonar systems

The feature detection capability of a conventional side scan sonar system is a function of several factors and operational parameters. The frequency of the sonar signal, the transmit/receive cycle (range scale), acoustic energy levels and system noise levels all factor into detection capability.

Sonar coverage rates are a function of the sonar's effective range (swath) and the speed of the sonar system over the seafloor. Lower frequency systems typically have greater range capability however longer range scales also have longer transmit cycles between 'pings' and therefore fewer 'pings' reflect off an individual target than would occur with using shorter range scales. This essentially decreases the detection capability, especially for smaller objects. Using slower tow speeds can increase the number of 'pings' on a target however this directly impacts seafloor coverage rates.

Frequency, feature detection capability, resolution required, and rate of coverage of sonar systems are all related and need to be considered and carefully weighed based on the requirements of the survey (or search). For the search for MH370 with a basic requirement to detect an object two cubic metres in size, a frequency range and associated coverage rate was selected based on the feature detection capability of the sonar system.

Another important consideration for the sonar search systems was the side scan sonar 'blind spot' in the nadir area directly beneath the vehicle. This can significantly impact the amount of overlap required between adjacent search lines and therefore the overall seafloor coverage rate.

The deep tow vehicles offered in the tender were fitted with side scan sonar transducers with a range of frequencies, often more than one. The frequencies stipulated for wide area coverage ranged from 30 kHz through to 120 kHz with corresponding vessel speeds between 1.8 and 3.0 knots. While the lower frequency systems had generally longer maximum ranges (with side scan sonar swaths up to 6 km) these systems had to be operated at less than maximum range scales in order to meet the feature detection requirement. In addition, these vehicles often did not have any instrument to cover the nadir region below the vehicle and therefore relied on very large overlaps between search lines to achieve sonar coverage in the nadir area.

The frequency of the side scan sonar on the vehicles selected by the ATSB for the search was 75 kHz. The deep tow vehicles were operated at speeds between 2.5 and 3 knots with a validated swath width of 2,000 m (which was proven to meet the feature detection requirement over the sonar test range). Data was collected over a 2,200 m swath however the last 100 m of the range on each side of the sonar was only used for aiding in assessing overlap and feature matching for position validation. Test target detection was achieved in the outer range however it was not

consistent enough to meet the feature detection requirement and was therefore not included as valid sonar coverage. Search line spacing for most of the search was set at 1,700 m which allowed up to 300 m overlap between adjacent deep tow search lines. These systems achieved coverages in excess of 200 km² per operational day during the search excluding weather, equipment downtime and end-of-line turns.

The AUV used in the search was equipped with the same side scan sonar and transducers as the deep tow vehicles and was operated at generally lower range scales for infill work but at speeds up to 3.6 knots. The sonar system was validated up to a 2,000 m swath using the same feature detection requirements and testing as the deep tow vehicles. All the vehicles contracted by ATSB for the search (deep tow and AUV) had a multibeam echo sounder (MBES) to cover the nadir area and were equipped with inertial navigation, DVL, and USBL positioning system.

Synthetic Aperture Sonar

The ProSAS deep tow vehicle (Figure 41), built and operated by Hydrospheric Solutions Inc. (Hydrospheric Solutions) was initially mobilised on *Go Phoenix* and provided to the underwater search as Malaysian Government furnished equipment. The vehicle was the latest generation of deep water (6,000 m rated) towed sonar systems. It was equipped with a 60 kHz synthetic aperture sonar (SAS) system which was able to achieve higher resolutions at longer ranges compared to traditional side scan sonar systems. The SAS processing combines data from several individual sonar ‘pings’ in a sequence with a highly accurate inertial navigation solution to build a map of the seafloor with a consistent resolution of 10 cm over the entire swath width.

The ProSAS vehicle was operated at a speed of around 1.8 knots, achieving a swath of 2,000 m (range and speed are directly related for a SAS system). The ProSAS deep tow vehicle was also equipped with a MBES to cover the nadir area and an inertial navigation, DVL, and USBL positioning system.

Later in the search (January 2016) the ProSAS deep tow vehicle was mobilised on the vessel provided by the People’s Republic of China, *Dong Hai Jiu 101*.

Figure 41: Hydrospheric Solutions ProSAS deep tow vehicle



Source: Hydrospheric Solutions

Other search coverage considerations

The search for MH370 had to be conducted over a large area as a result of the limited data available with which to reconstruct the aircraft’s flightpath or accurately determine where the aircraft may have impacted the water. A key consideration when selecting the search method was to complete the search in a reasonable time period within the constraints imposed by the weather and remoteness of the search area.

The overall rate of coverage is not only dependent on the coverage rate of the search systems when they are operational but also on the overall proportion of operational time in the search area

after discounting the time lost due to end-of-line turns (for deep tow vehicles), weather, equipment or other down time, and the time taken to transit to and from port for re-supply. The proportion of operational time in the search area is therefore maximised by extending the vessel endurance, minimising the transit time to and from the search area and minimising down time in the search area.

Operational tasking must be aimed at minimising end-of-line turns by tasking the deep tow vehicles to search on very long lines. Vessel and equipment downtime must be minimised by having well maintained and reliable vessels, equipment, sufficient spare parts and expertise on board to perform repairs while in the search area. Similarly the overall search organisation must take into account expected weather in the search area with search activity increased in the better weather months.

The request for tender, released in June 2014, stipulated a 300 day period to complete the search of the initial 60,000 km² area. At that time, the search was to be conducted in an area to the north of the underwater feature Broken Ridge. By the time the search commenced in October 2014, further search area analysis had been completed and the search area was moved 1,000 km south along the 7th arc to an area below Broken Ridge. This impacted the coverage performance targets required of the search contractor as there was additional transit time to and from port to be considered and significantly worse weather in the new search area.

To manage the coverage requirements, Fugro Survey, who were selected as prime contractor for the underwater search, decided on a deep tow vessel swing²⁴ length of 42 days to allow at least 30 possible operational days in the search area (transits were on average 5 days to and from Fremantle to the search area). The choice of industry standard Edgetech deep tow vehicles meant that spare parts and complete vehicles were also readily available. Fugro Survey maintained a complete spare deep tow system on board one of the search vessels, while a tow winch and spare tow cables were available in Perth. Equipment downtime amounted to 5.6 per cent of total time over the course of the two years of deep tow operations. Weather stand-by in the search area during deep tow operations on the Fugro Survey vessels amounted to 9.9 per cent of total time.

Validating the search systems

All underwater search systems used during the search were tested and evaluated on their object detection capabilities and overall system performance. Each system was tested at the purpose-built test range put in place by Fugro Survey off the coast of Perth. The range was in a water depth of 650 m and consisted of five steel objects ranging from 1.3 m x 1.3 m x 1.3 m to 2 m x 2 m x 2 m in size and placed on the seafloor over 1,150 m. The steel shapes consisted of two cubes, two crosses and a cylinder shape as shown in Figure 42.

²⁴ A swing is the time between port calls which includes the time to transit to and from the search area and the time in the search area.

Figure 42: Test range targets and spacing diagram



Source: Fugro Survey

After each underwater vehicle was mobilised and readied for offshore operations the vessel proceeded to the test range. Each underwater search vehicle was tested in full operation with all integrated systems expected to be used in the search area. All systems were tested and verified using their nominal operational settings. The test was concluded once the test targets were successfully detected and the sonar data quality met the requirements set out by the ATSB and was deemed fit for purpose by the ATSB’s Quality Assurance Manager and/or the ATSB client representative on board the vessel.

Verification reports were created which documented the sonar’s ability to detect the test targets through the entire swath of the SSS. Testing was performed to ensure repeatable and reliable detection of the test targets at the far range of the SSS as well as the how close to the nadir region the targets could be seen in the sonar record.

Figure 43 shows the test targets as detected with a SSS. Using a 1,000 m range scale the deep tow vehicles and AUV detected the test targets reliably. From 1,000 m to 1,100 m the test targets were seen intermittently, however there was still useful data in this far range. It was determined that the extra 100 m of range aided in feature matching used to verify overlap and coverage. However, it was maintained that only the first 1,000 m of data was accepted as fit for purpose and relied on for sonar contact detection.

The deep tow vehicle testing speed was 3 knots and the AUV speed was 3.6 knots. Testing included the MBES systems on each of the underwater vehicles. Verification of detection capability and the amount of the overlap between SSS and MBES systems was determined as the MBES was used to fill the SSS ‘blind spot’ in the nadir region directly below the deep tow vehicle and AUV. The camera on board the AUV was also tested. Figure 44 shows images of two of the

test targets on the seafloor photographed using the AUV’s camera. Target position comparisons were made along with proper operation of the deck equipment (tow winch and cable) and the processing hardware and software were also tested and verified.

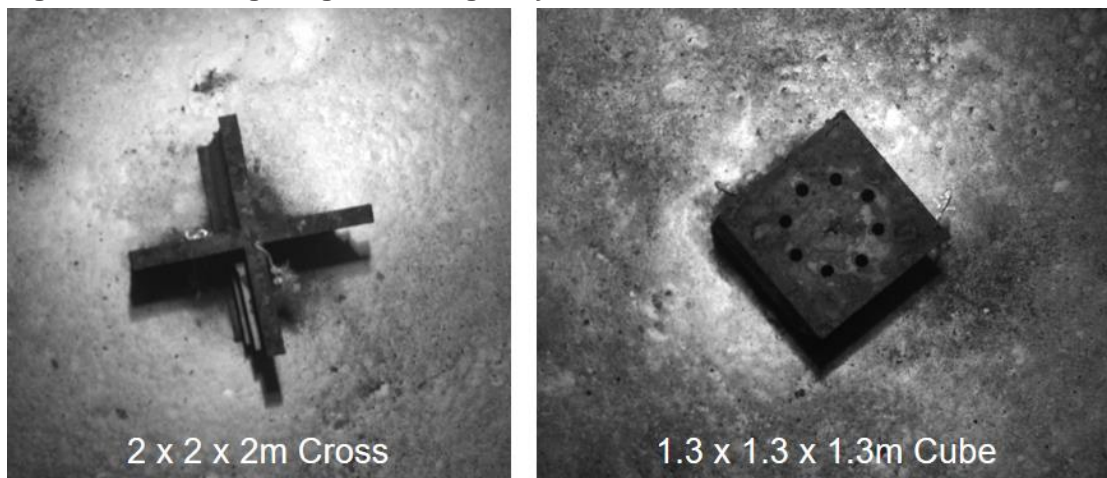
Verification testing was also performed if major repairs were carried out on the sonar systems or if the system was demobilised and mobilised again later.

Figure 43: Test range targets as imaged by deep tow vehicle side scan sonar on seafloor



Source: ATSB

Figure 44: Test range targets as imaged by AUV camera on seafloor



Source: ATSB

Underwater search chronology

Underwater search operations for MH370 lasted from 6 October 2014 until 17 January 2017. Before and during the underwater search, seafloor mapping was undertaken. The intent was to locate the aircraft debris field on the seafloor and then to commence a recovery operation. The areas searched were based on information from a range of sources, analysis which was progressively refined in relation to the aircraft’s set of most likely flight paths and analysis relating to the aircraft’s behaviour at the end-of-flight.

The SSWG formed by the ATSB at the end of the surface search brought together satellite, aircraft and data fusion specialists to progress work on defining the search area which would have the highest probability of containing MH370 to inform the underwater search. This group continued collaboration with the SATCOM WG and included experts from Inmarsat and Thales.

In June 2014 a search area of 60,000 km² was planned with an extension to the search area to 120,000 km² announced in April 2015. By the end of the underwater search an area in the order of 120,000 km² had been searched to a high confidence level by a combination of deep tow vehicles, an AUV and an ROV, however no item of debris from MH370 was located.

The following section sets out the chronology of the underwater search, the search assets used, where it was focused at different times and the information or analysis used to define those areas.

The priority search area refined southwards

While the bathymetric survey was being undertaken in the June 2014 priority search area, flight path analysis by the SSWG in July and August 2014 had focused on refinements to the 'Unified' BFO model and analysis of the BFO metadata related to the ground to air telephony call at 1839 UTC. A 'Unified 4x' BFO model (refer to appendix C) was approved by Inmarsat on 30 July 2014. This analysis redefined the priority search area of June 2014 and moved the search area south along the 7th arc (Table 21).

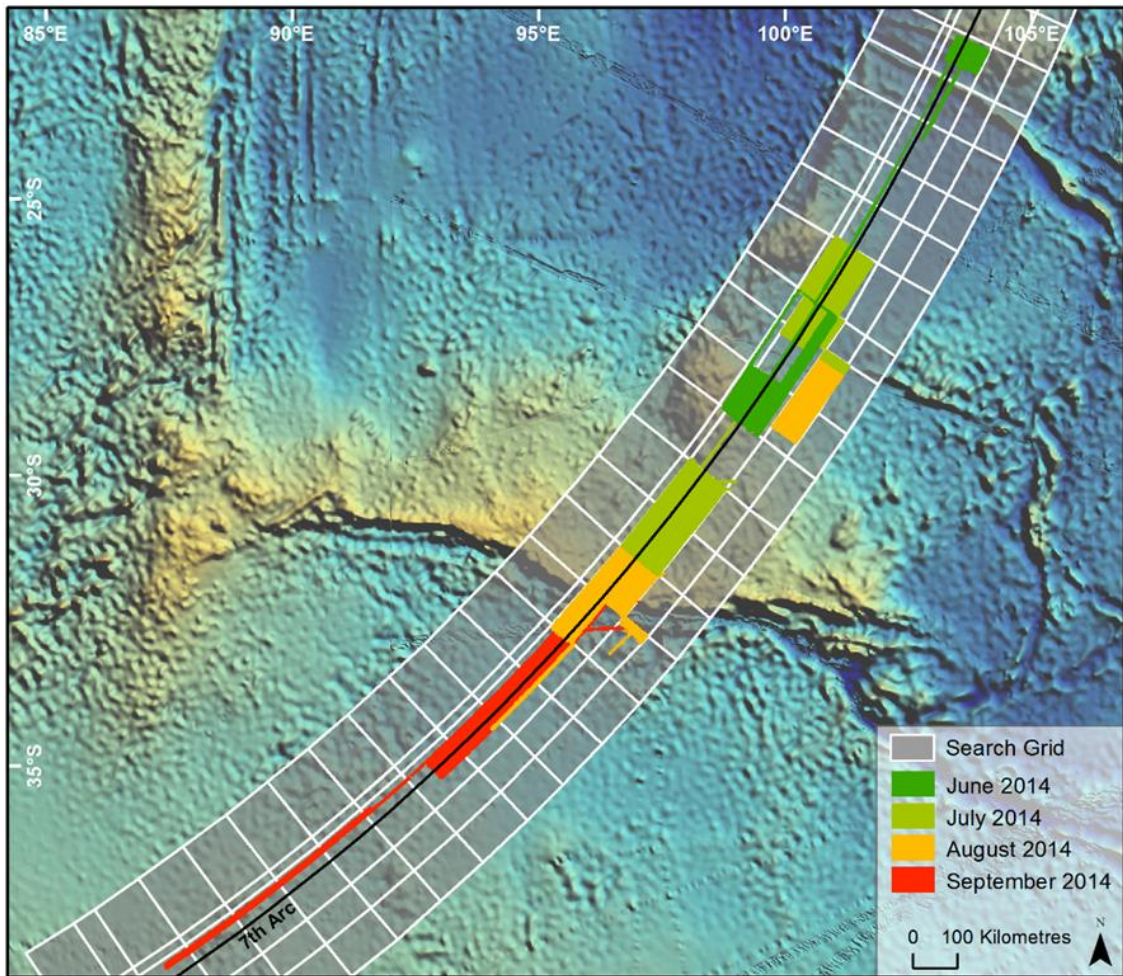
Table 21: Refined preparatory seafloor survey

Dates:	26 August – 26 September 2014
Event:	Mapping of seafloor in refined underwater search area of 60,000 km ²
Search area location:	Underwater Search Area 1, 32.8°S to 35°S and -10 NM, +13 NM across 7th arc.
Search activity:	Mapping of seafloor – bathymetry phase
Guiding advice:	Inmarsat 'BFO Analysis Unified 4x' BFO Model. Flight path reconstruction group - 4 Analyses. SSWG's analysis techniques – Constrained autopilot dynamics (south) Data error optimisation (north)
Data used in planning search area refinement:	Attempt to cover approximately 80% of highest probability flight paths derived from both constrained autopilot dynamics and data error optimisation analysis techniques.
Search equipment:	<i>Fugro Equator</i> (ATSB contracted survey vessel MBES).
Coverage details:	32.8°S to 35°S bathymetry completed ≈ 14,000 km ²
References:	Press conference – Deputy Prime Minister on 26 August 2014. ATSB report: <i>MH370 – Flight Path Analysis Update</i> – 8 October 2014.

Source: SSWG, Fugro Survey, Zhu Kezhen, ATSB

As a consequence, on 26 August 2014 *Fugro Equator* was tasked to move bathymetric survey operations south along the 7th arc to an area below Broken Ridge (red area in Figure 45). The bathymetric survey continued through September in preparation for the arrival of the first search vessel, *Go Phoenix*, in the underwater search area.

Figure 45: Bathymetry survey June to September 2014, *Fugro Equator* and *Zhu Kezhen*



Source: ATSB

Underwater search commences

On 8 October 2014, the ATSB released the report '[MH370- Flight Path Analysis Update](#)' which detailed refinements to the BFO model and flight path analysis over the preceding months. The refined BFO model designated the 'Unified 4x' model had been developed and validated, and the various flight path reconstruction techniques had been applied to the model independently by the analysis groups. The analysis resulted in two probability distributions based on two different methods of calculating the statistical match of possible flight paths with the observed BTO and BFO values; 'data error optimisation' and 'constrained autopilot dynamics' refer to Figure 54.

Table 22: Underwater search commences

Dates:	26 September 2014 – 16 April 2015
Event:	Mapping of seafloor in refined underwater search area of 60,000 km ² . Underwater sonar search commenced in refined underwater search area.
Search area location:	Underwater Search Area 1 (<i>Go Phoenix</i>), 32.8°S to 35°S along 7th arc. Underwater Search Area 2 (<i>Fugro Survey</i>), 35°S to 38.9°S along 7th arc. -20 NM, +30 NM across 7th arc.
Search activity:	Mapping of seafloor – bathymetry. Underwater search using deep tow vehicles and an autonomous underwater vehicle.
Guiding advice:	Inmarsat 'BFO Analysis Unified 4x' BFO model.

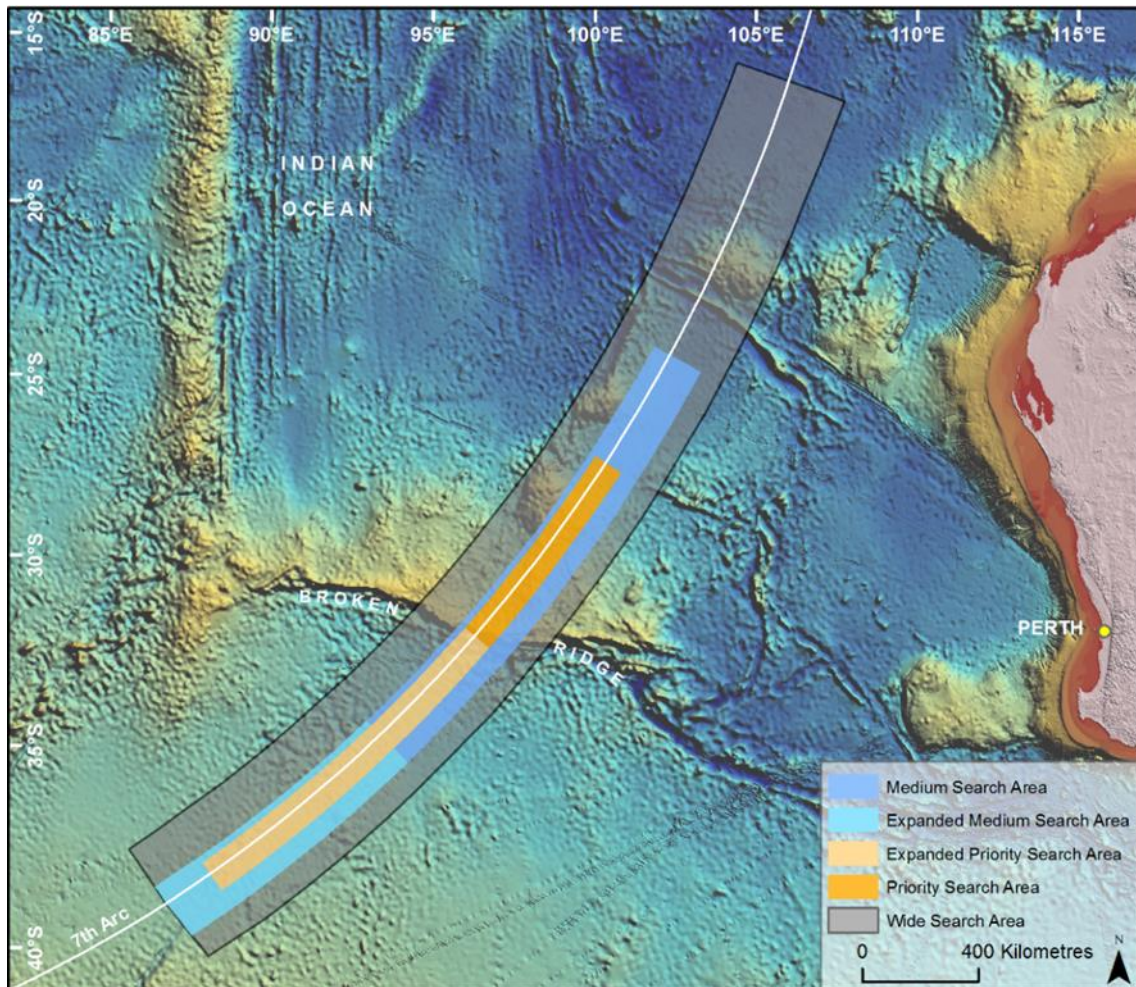
	Flight path reconstruction group - four analyses. SSWG's analysis techniques – Constrained autopilot dynamics (south) Data error optimisation (north)
Data used in planning search area refinement:	Attempt to cover approximately 80% of highest probability flight paths derived from both constrained autopilot dynamics and data error optimisation analysis techniques.
Search equipment:	<i>Fugro Equator</i> (MBES bathymetry 26 September to 18 December 2014) <i>Go Phoenix</i> (ProSAS deep tow from 6 October 2014) <i>Fugro Discovery</i> (Edgetech deep tow from 22 October 2014) <i>Fugro Equator</i> (Edgetech deep tow from 15 January 2015) <i>Fugro Supporter</i> (Hugin AUV from 29 January 2015)
Coverage details:	32.8°S to 38.9°S bathymetry completed ≈ 46,000 km ² 32.8°S to 38.9°S underwater search completed ≈ 38,000 km ²
References:	ATSB report: <i>MH370 – Flight Path Analysis Update</i> – 8 October 2014

Source: Inmarsat, SSWG, Fugro Survey, Phoenix International, ATSB

With an agreed search area of 60,000 km² it was decided to search 80 per cent of the highest probability paths crossing the 7th arc for both analyses (Table 22). This required a search area length spanning from latitudes 33.5°S to 38.3°S²⁵. An expanded priority search area south of Broken Ridge was created to accommodate this (Figure 46).

²⁵ The latitudes stated in this section are approximate and quoted at the crossing of the ATSB reference 7th arc (40,000 ft) unless otherwise stated.

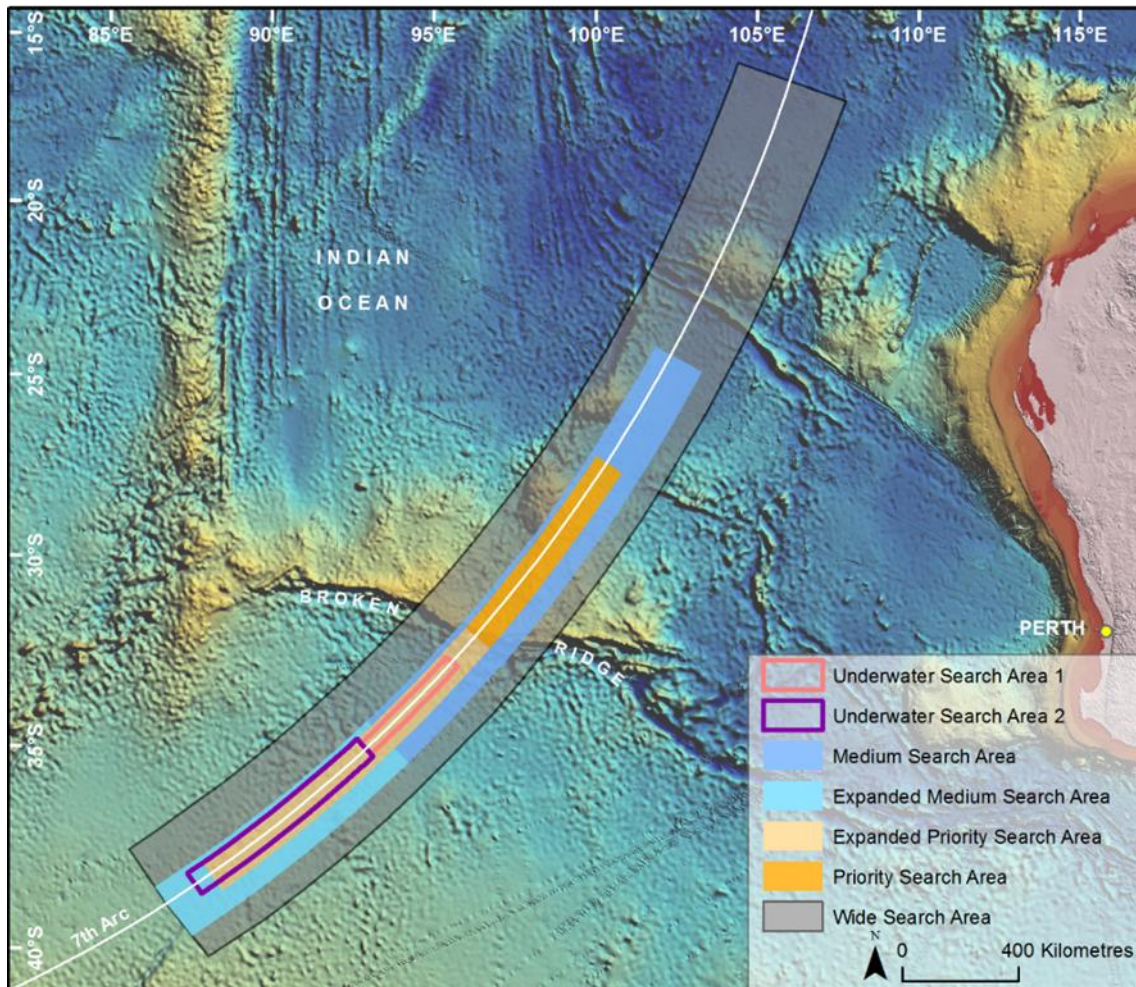
Figure 46: Priority, expanded priority and medium search areas south of Broken Ridge, 19 October 2014



Source: ATSB

Go Phoenix commenced underwater search operations using the ProSAS deep tow vehicle on 6 October 2014. The vessel was assigned a search area from latitudes 32.8°S to 35°S where bathymetry had recently been completed by *Fugro Equator*. This area was designated Underwater Search Area 1 and was an area of approximately 14,000 km². Search lines were devised for *Go Phoenix* running parallel to the 7th arc.

Figure 47: Underwater Search Areas 1 and 2 based on completed bathymetry at start of *Go Phoenix* and *Fugro Discovery* arrivals in search area

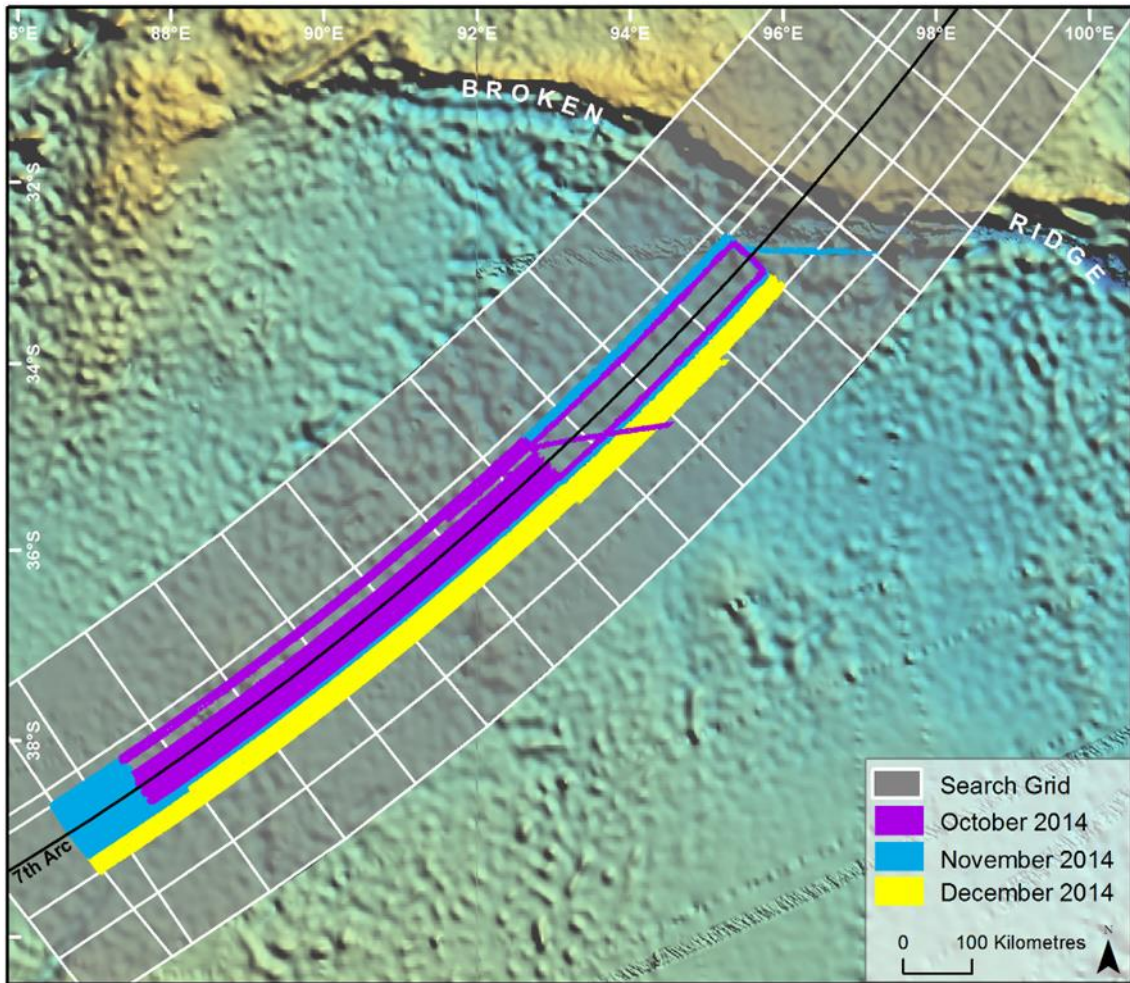


Source: ATSB

Fugro Equator completed the seafloor survey of Underwater Search Area 2 (an area of approximately 46,000 km²) during its third and fourth bathymetric survey swings. This underwater search area, from latitudes 35°S to 38.7°S along the 7th arc was then assigned to the *Fugro Survey* vessels. *Fugro Discovery* subsequently commenced underwater search operations in this area on 22 October 2014.

It was planned that *Fugro Equator* would mobilise a deep tow vehicle and commence underwater search operations in November 2014. However, technical difficulties with the tow winch on the vessel necessitated a reassignment for a further bathymetry swing in November and December focused on the southern end of Underwater Search Area 2 extending the search area to latitude 38.9°S (Figure 48).

Figure 48: Bathymetry coverage - *Fugro Equator* October to December 2014



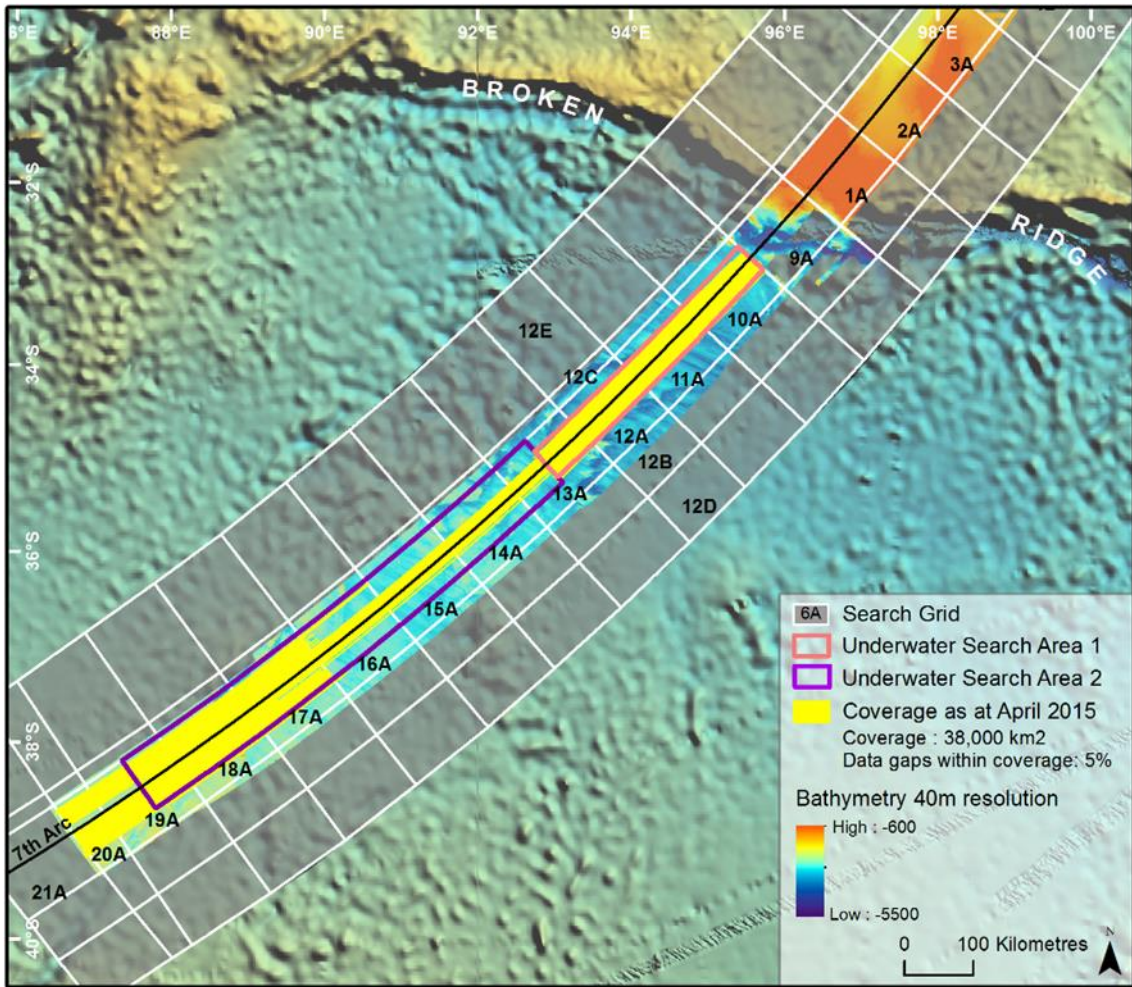
Source: ATSB

In January 2015, mobilisation of a deep tow search system on *Fugro Equator* was completed and the vessel commenced underwater search operations. In the same month *Fugro Supporter* entered the search equipped with an AUV to primarily search difficult seafloor terrain in the search area.

By 16 April 2015 an area of about 38,000 km² had been searched using three deep tow vehicles and the AUV system on board the four search vessels. *Go Phoenix* was close to completing its assigned area and the *Fugro Survey* vessels had focused on the area between latitudes 37.1°S and 38.9°S while the weather was favourable. Data gaps comprised approximately 5 per cent of the area searched (Figure 49).

During the period from November 2014 to April 2015 the four search vessels were affected by a number of tropical cyclones impinging on the search area which meant the vessels had to periodically suspend search operations to avoid storms and minimise potential damage.

Figure 49: Sonar coverage all vessels by April 2015



Source: ATSB

Search area extension

On 16 April 2015, the Governments of Malaysia, Australia and the People’s Republic of China agreed to extend the underwater search area to 120,000 km² (Table 23). This allowed an additional area to the south to be included in the search area and a widening of the search area across the 7th arc to account for a greater range of possible aircraft end-of-flight behaviours.

The ATSB created a 120,000 km² indicative search area covering the highest probability paths of the then current flight path analysis from latitudes 32.5°S to 39.1°S with arrows indicating possible search area extension directions, depending on the outcome of further refinements to the flight path analysis (Figure 50).

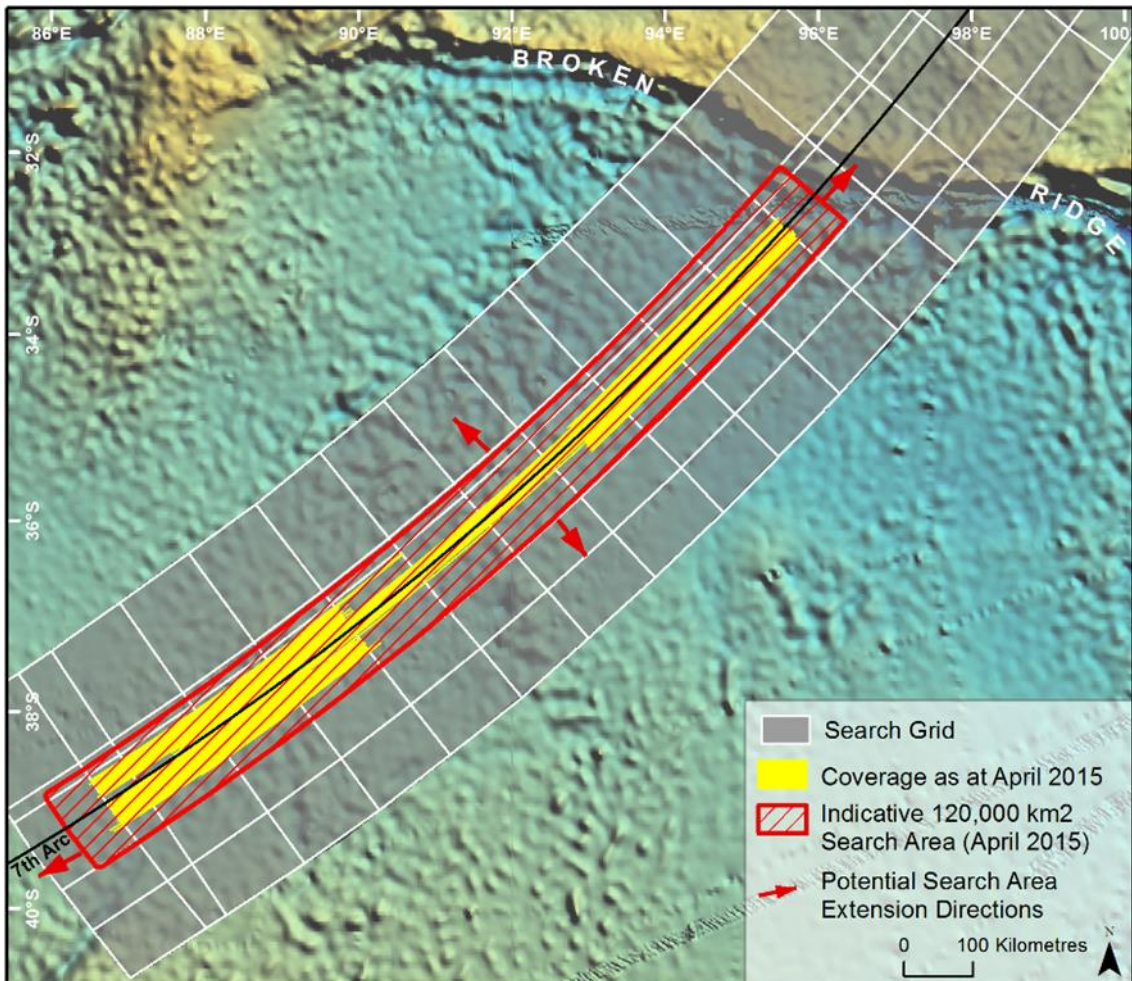
Table 23: Underwater search area expanded

Dates:	16 April 2015 – 17 July 2015
Event:	Expanded underwater search area of 120,000 km ² results in creation of indicative search area.
Search area location:	Underwater Search Area 1 (<i>Go Phoenix</i>). Indicative search area incorporating Underwater Search Area 2 (Fugro Survey). -20 NM, +30 NM across 7th arc
Search activity:	Underwater search using deep tow vehicles and autonomous underwater vehicle.

	Search area (reconnaissance) bathymetry undertaken at suitable operational times and during poor weather periods unsuitable for <i>Fugro Equator</i> deep tow vehicle operations to extend seafloor mapping to 120,000 km ² .
Guiding advice:	Tripartite governments agree to increase underwater search area to 120,000 km ² . Inmarsat 'BFO Analysis Unified 4x' BFO model. Flight Path Reconstruction Group – four analyses. SSWG's Analysis techniques – Constrained Autopilot dynamics (South) Data error optimisation (North)
Data used in planning search area refinement:	Attempt to cover approximately 80% of the highest probability flight paths derived from both constrained autopilot dynamics and data error optimisation analysis techniques.
Search equipment:	<i>Fugro Supporter</i> (Hugin AUV to 11 May 2015) <i>Go Phoenix</i> (ProSAS deep tow vehicle to 19 June 2015) <i>Fugro Discovery</i> (Edgetech deep tow vehicle) <i>Fugro Equator</i> (MBES bathymetry and Edgetech deep tow vehicle)
Coverage details:	Underwater search completed ≈ 56,750 km ²
References:	Tripartite government press conference 16 April 2015. ATSB report: <i>MH370 – Flight Path Analysis Update</i> – 8 October 2014.

Source: Inmarsat, SSWG, Fugro Survey, Phoenix International, ATSB

Figure 50: 120,000 km² indicative search area and deep tow vehicle coverage, April 2015



Source: ATSB

On 11 May 2015, after three swings of AUV operations, *Fugro Supporter* departed the search area for demobilisation in Fremantle.

On 19 June 2015, after eight swings of ProSAS deep tow vehicle operations, *Go Phoenix* departed the search area for demobilisation in Singapore following practical completion of Underwater Search Area 1.

Generalised flight dynamic model

On 17 July 2015, the decision was taken to extend deep tow search lines for *Fugro Equator* and *Fugro Discovery* to latitude 39.5°S in response to the results of DST Group’s analysis indicating high probability flight paths extending to that area (Table 24). As a result, the ATSB’s indicative search area now extended from latitude 32.8°S to 39.5°S (Figure 51). Search operations continued to be from 20 NM behind to 30 NM in front of the 7th arc with *Fugro Equator* extending coverage to latitude 39.5°S on its search lines to the east of the 7th arc.

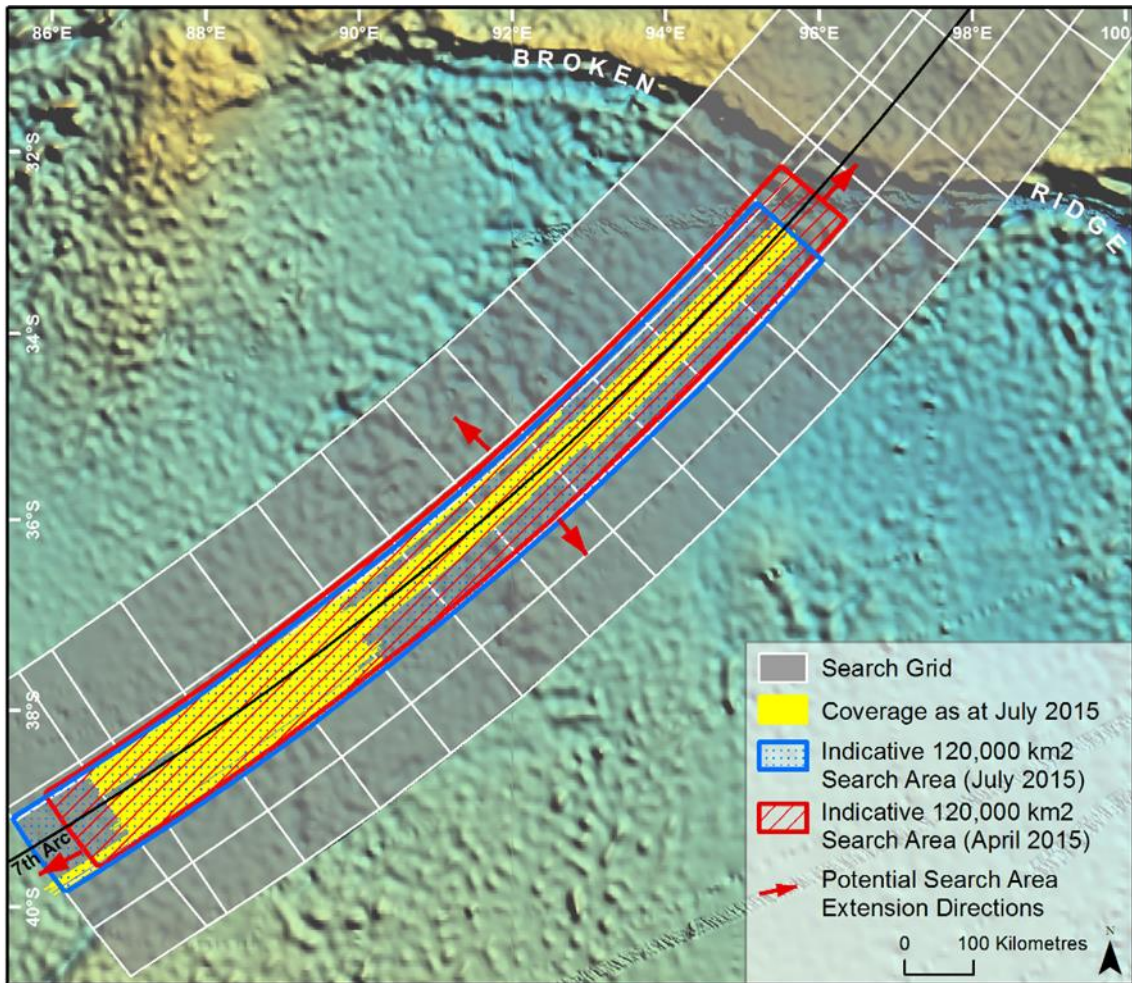
Table 24: Generalised flight dynamics

Dates:	17 July – 30 November 2015
Event:	DST Group provide continued Bayesian analysis results which extends indicative search area to the south.
Search area location:	Extended indicative search area, -20 NM, +30 NM across 7th arc
Search activity:	Underwater search using deep tow vehicle sonar systems. Search area (reconnaissance) bathymetry undertaken at suitable operational times and during poor weather periods unsuitable for <i>Fugro Equator</i> deep tow vehicle operations to extend seafloor mapping to 120,000 km ²
Guiding advice:	Inmarsat Differential Doppler Unified 4x BFO model. Flight path reconstruction group four analyses. SSWG analysis – Constrained autopilot dynamics (South) Data error optimisation (North) DST Group enhanced dynamic model results.
Data used in planning search area refinement:	DST Group developing Bayesian analysis. Consideration of possible ditching with minimal debris washed ashore.
Search equipment:	<i>Fugro Discovery</i> (Edgetech deep tow vehicle) <i>Fugro Equator</i> (MBES bathymetry and Edgetech deep tow vehicle)
Coverage details:	Underwater search area completed ≈ 75,850 km ²
References:	Tripartite governments press conference 16 April 2015. ATSB report: <i>MH370 – Flight Path Analysis Update</i> – 8 October 2014. DST Group analysis.

Source: DST Group, SSWG, Fugro Survey, ATSB

During *Fugro Discovery*’s tenth swing commencing on 29 October 2015, two separate medical evacuations of crew members were required shortly after the vessel’s arrival in the search area. This meant over 22 days in transit to and from the search area were necessary with only 8 days of underwater search operations achieved for the swing (see Health, Safety and the Environment section).

Figure 51: 120,000 km² Indicative search area and deep tow vehicle coverage, 28 July 2015

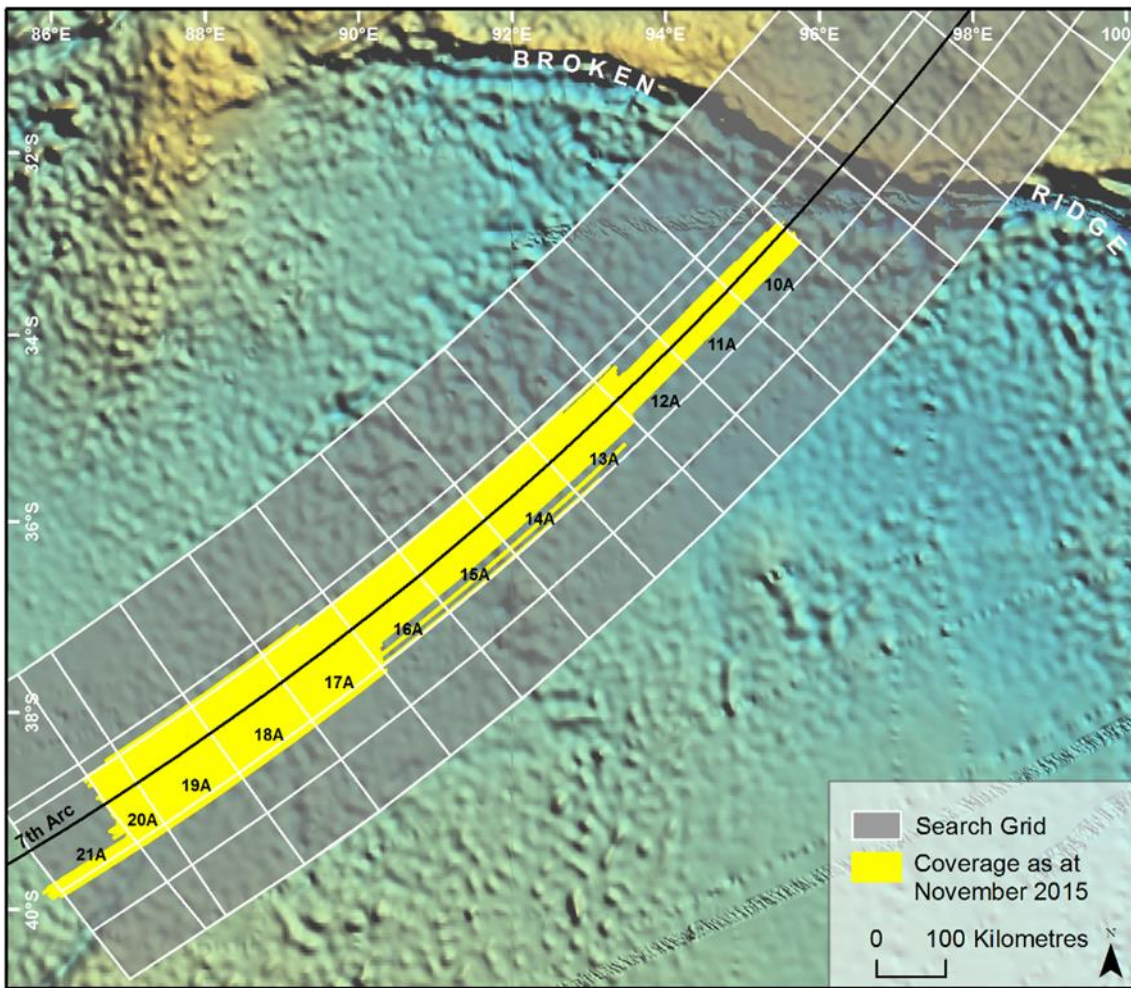


Source: ATSB

Complete Bayesian analysis

By 30 November 2015 an area of over 75,000 km² had been searched from latitudes 32.8°S to 39.5°S with about 3.8 per cent data gaps in the sonar coverage (Figure 52). *Fugro Equator* and *Fugro Discovery* were in the search area with their deep tow vehicles and *Havila Harmony* was being mobilised for AUV operations.

Figure 52: Underwater search coverage at 30 November 2015



Source: ATSB

A refined analysis of the SATCOM data undertaken by DST Group and detailed in their pre-publication draft *Bayesian Methods in the Search for MH370* was used to define a new indicative search area and promulgated in the ATSB’s report [MH370 – Definition of Underwater Search Areas](#) released on 3 December 2015 (Table 25). The indicative search area was refined by ATSB to latitudes between 36.1°S and 39.5°S to focus on the highest probability paths as shown in the heatmap generated using DST Group’s analysis and the descent kernel defined by the ATSB (Figure 56). The search area remaining to complete 120,000 km² was chosen to cover 85-90 per cent of the probability density function (PDF) along the 7th arc defined by DST Group.

Table 25: Bayesian analysis released

Dates:	30 November 2015 – 31 August 2016
Event:	DST Group Analysis produces heatmap when descent kernel applied. Decision to search 85% of flight paths to the north and 90% of flight paths to the south.
Search area location:	Indicative Search Area extended and application of descent kernel to DST Group probability density function and -40 NM, +40 NM across 7th arc in the indicative search area.
Search activity:	Underwater search using deep tow vehicle sonar systems and AUV, ProSAS deep tow vehicle re-joins search on <i>Dong Hai Jiu 101</i> . Search area (reconnaissance) bathymetry undertaken at suitable operational times and during poor weather periods unsuitable for <i>Fugro Equator</i> deep tow vehicle operations.
Guiding advice:	DST Group analysis.

	ATSB descent kernel.
Data used in planning search area refinement:	DST Group analysis. ATSB descent kernel. Consideration of both controlled and uncontrolled end-of-flight scenarios.
Search equipment:	<i>Fugro Discovery</i> (Edgetech deep tow vehicle) <i>Fugro Equator</i> (Edgetech deep tow vehicle) <i>Havila Harmony</i> (Hugin AUV) <i>Dong Hai Jiu 101</i> (ProSAS deep tow vehicle)
Coverage details:	Underwater search area completed ≈ 115,640 km ²
References:	DST Group Bayesian analysis November 2015. ATSB report: <i>MH370 – Definition of Underwater Search Areas</i> – 3 December 2015. Tripartite government meeting 22 July 2016.

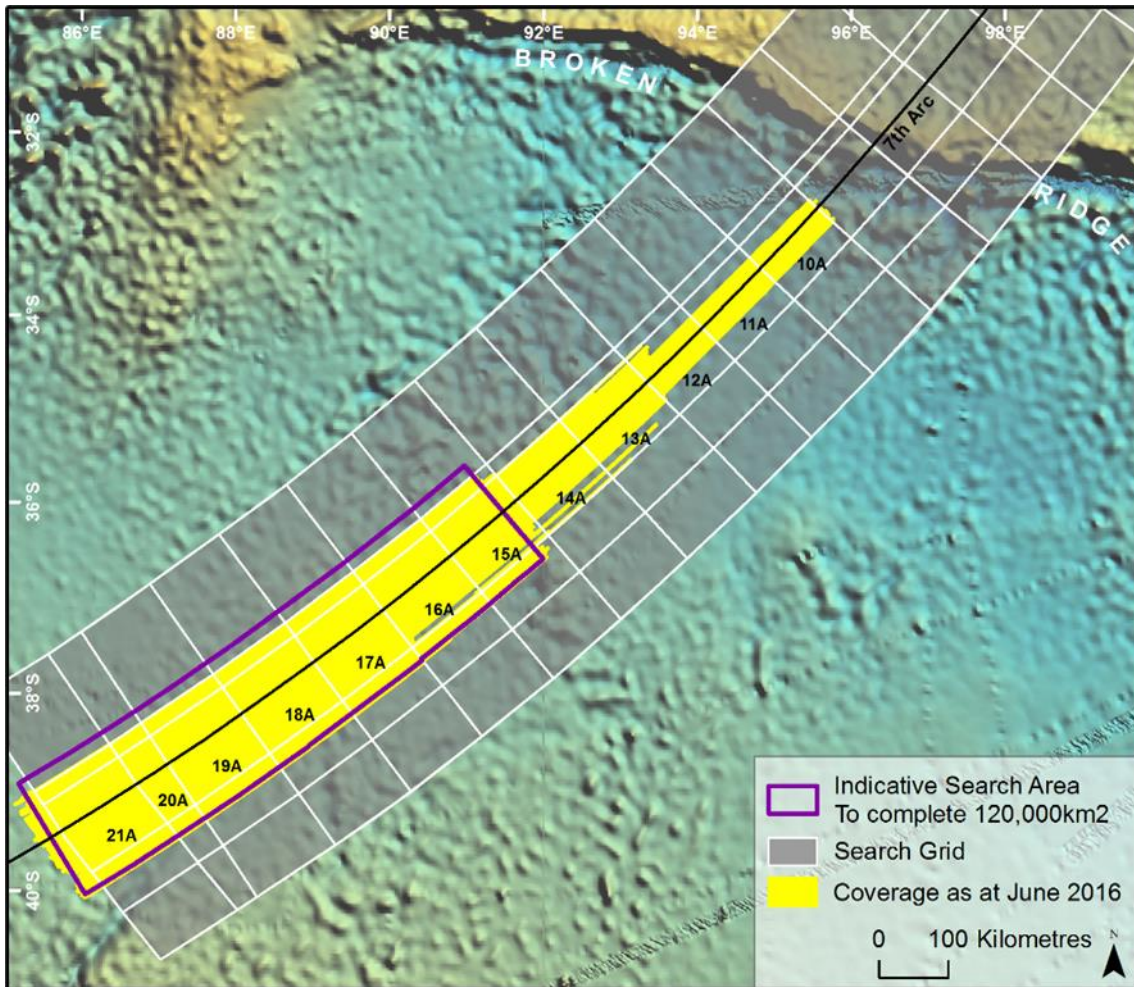
Source: DST Group, SSWG, Fugro Survey, Phoenix International, ATSB

Fugro Discovery and *Fugro Equator* continued the underwater search with deep tow vehicles and were joined in the search by *Havila Harmony* equipped with the AUV on 5 December 2015. Once again the AUV was used to search difficult areas of seafloor terrain inefficient for the deep tow vehicles to search. The vessels were tasked to complete the search of the new indicative area search area (Figure 53).

The three vessels were then joined by the People’s Republic of China rescue and salvage vessel *Dong Hai Jiu 101* with an upgraded²⁶ ProSAS deep tow vehicle which arrived in the search area in March 2016.

²⁶ During the period between operations on *Go Phoenix* and *Dong Hai Jiu 101* the ProSAS system was upgraded by Hydrospheric Solutions with an added array. This was done to improve the coverage of the ProSAS system.

Figure 53: Underwater search coverage at June 2016 showing December 2015 indicative search area



Source: ATSB

Last refinement to underwater search area

On 20 June 2016, the inboard section of MH370 right outboard wing flap was found on Pemba Island, East of Tanzania (refer to the Aircraft Debris section). This was an important development since evidence of flap extension at impact would indicate a controlled descent and thus increase the search width required in front of the arc. Conversely a retracted flap would indicate an uncontrolled end of flight scenario, close to the 7th arc.

From June to July 2016 discussions within the SSWG regarding end-of-flight ‘controlled’ or ‘uncontrolled’ descent scenarios continued and analysis using Boeing end-of-flight simulations again considered the distance beyond the 7th arc that was now a reasonable extent of an ‘uncontrolled’ descent. Further consideration of 7th arc BFO values was also underway by DST Group to see if the indicative rates of descent of the aircraft at the final arc could be ascertained.

The 7th arc width, tolerances and new simulations were incorporated into a revised descent kernel and probability map by ATSB and DST Group. The distance (prior to new simulations) recommended by the SSWG was 35 NM to the west of the 7th arc and for a ‘controlled’ scenario the search area would extend the most probable flight paths to the east of the 7th arc (Table 26).

In July 2016 *Fugro Discovery* departed Fremantle for her final swing in the search area and *Fugro Equator* commenced her penultimate deep tow swing. *Dong Hai Jiu 101* was in the search area with the ProSAS deep tow search system on board. The focus of the search was to cover gaps in

sonar data in the indicative search area, and to extend the area searched to the west of the 7th arc from 30 NM to 35 NM as recommended by the SSWG.

Table 26: Wing flap examination, BFO analysis and revised descent kernel

Dates:	August 2016 – January 2017
Event:	Examination of MH370 wing flap and DST Group BFO analysis. Analysis produces heatmap when descent kernel applied. Decision to search 85% north and 90% south of PDF.
Search area location:	Indicative Search Area extended and application of descent kernel to DST Group PDF.
Search activity:	<i>Fugro Equator</i> underwater search using Edgetech deep tow vehicle and AUV and <i>Dong Hai Jiu 101</i> mobilised with ROV. Search area (reconnaissance) bathymetry undertaken at suitable operational times and during poor weather periods unsuitable for <i>Fugro Equator</i> deep tow vehicle operations.
Guiding advice:	ATSB debris examination of wing flap. DST Group BFO analysis of final BFO sequence. ATSB revised descent kernel. DST Group revised heatmap.
Data used in planning search area refinement:	+25 NM and -25 NM from 7th arc across entire search area.
Search equipment:	<i>Fugro Equator</i> (Edgetech deep tow then Hugin AUV) <i>Dong Hai Jiu 101</i> (<i>Remora III</i> ROV)
Coverage details:	Underwater search area completed ≈ 120,000 km ²
References:	ATSB report: <i>MH370 Search and debris examination update</i> - 2 November 2016. First Principles Review, 2-4 November 2016. DST Group report: <i>The use of Burst Frequency Offsets in the search for MH370</i> , 7 Feb 2017. CSIRO report: <i>The search for MH370 and ocean surface drift</i> - 6 December 2016. ATSB report: <i>MH370 - First Principles Review</i> - 20 December 2016. Tripartite government press release 17 January 2017.

Source: DST Group, SSWG, Fugro Survey, Phoenix International, ATSB

On 22 July 2016 a Tripartite meeting (Malaysia, Australia and the People’s Republic of China) agreed that the search would be suspended upon completion of the 120,000 km² search area, should the aircraft not be located and in the absence of credible new evidence leading to the identification of a specific location of the aircraft. The underwater search coverage at that time was 113,400 km².

Poor weather conditions in the search area over this period limited the search efforts in particular for *Dong Hai Jiu 101* and a decision was made to stand the vessel down and demobilise the ProSAS search system.

Following the completion of the wing flap examination indicating that it was probably housed at the time it separated from the aircraft and the completion of DST Group’s BFO analysis indicating that the aircraft was probably in a high and increasing rate of descent the SSWG recommended the search be limited to a width of 25 NM either side of the 7th arc. This information was presented in the report [MH370 Search and debris examination update](#) on 2 November 2016.

In October *Dong Hai Jiu 101* was mobilised with Phoenix International’s ROV and tasked to investigate a range of sonar contacts.

During its final deep tow swing in September and October 2016, *Fugro Equator* was tasked to fill areas of sonar data gaps within 25 NM of the 7th arc across the entire 120,000 km² and search some new area to the west of the 7th arc within the indicative area.

In December 2016, *Fugro Equator* mobilised the AUV which was used to fill sonar data gaps within 25 NM of the 7th arc and to search the area within 25 NM and to the west of the 7th arc between latitudes 34.7°S and 36.1°S.

On 17 January 2017, *Fugro Equator* completed AUV search operations and left the search area and the Tripartite Ministers jointly announced the suspension of the search for MH370.

An animation of the progressive search coverage over the entire underwater search is available for viewing on the [ATSB YouTube Channel](#).

ATSB contractor reports

The final underwater operations reports provided to the ATSB by Fugro Survey and Phoenix International are provided in appendices D and E. These are the Fugro Survey summary report for four vessels *Fugro Equator*, *Fugro Discovery*, *Fugro Supporter* and *Havila Harmony* and Phoenix International's report for operations on *Dong Hai Jiu 101* in 2016.

Area searched

The search areas for MH370 were defined on the basis of probability. Following the final primary radar detection near the northern tip of Sumatra at 1822 UTC, the aircraft's location could not be determined with precision. For the final six hours of flight MH370's location was derived by modelling likely aircraft behaviour, under a range of assumptions, using a unique analysis of a few SATCOM metadata points. The output of this modelling was a probability density function for the aircraft's location at the time of the final SATCOM communication. This was derived using the primary radar detections, models of MH370's autopilot controlled flight dynamics, environmental information and the complete sequence of automated SATCOM communications.

Search area probability density functions

A probability density function (PDF) defines the likelihood that an event with an unknown outcome will take a particular value from within a range of possible values. The Bayesian approach to the MH370 search models the aircraft's flight path as an unknown event and then calculates the PDF of this unknown event based on the available information. For example, DST Group's PDF of November 2015 (Figure 55) indicated that it was ten times more likely that the aircraft crossed the 7th arc near 38°S than near 36°S.

When the results of the underwater sonar search are considered, if an area was searched to a high degree of confidence, the modelled flight paths which terminated at this location can be eliminated. This changes the PDF to make alternative flight paths and areas more likely to contain the aircraft. At any point in the underwater search the priority was to eliminate the highest probability areas defined by the PDF derived from the most up to date flight path analyses.

MH370 probability density functions evolution

Search area definition and analysis of available data was continuous throughout the entire search for MH370. Initial results assisted the surface search and later refinements formed the basis for the underwater search areas. The models used to define the search area and associated PDFs evolved during the search based on continuing analysis of the SATCOM data and efforts to identify the most likely behaviour of the aircraft at the end-of-flight.

In October 2014 the SSWG were using two methods to derive the flight paths and their associated probability:

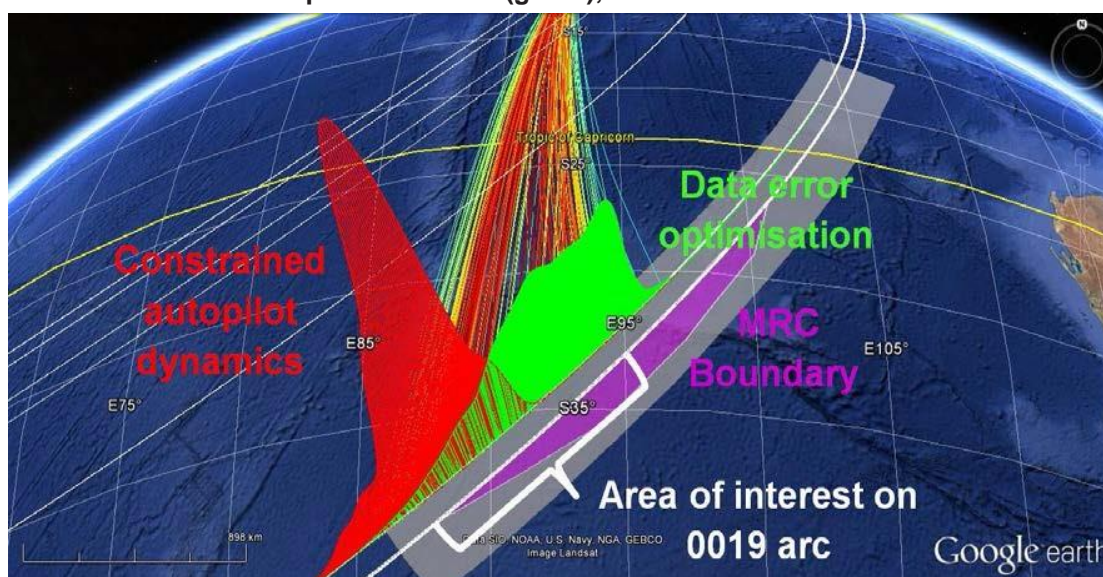
1. **Constrained autopilot dynamics** –The aircraft is assumed to have been flown using one of the autopilot modes constant magnetic heading, constant true heading, constant magnetic

track, constant true track or lateral navigation. Starting points for the trajectories are defined by the primary radar detections. All autopilot modes were considered to be initially equally likely. The aircraft is assumed to have made one deliberate manoeuvre at some time after the primary radar detections. Candidate trajectories are created for a range of possible autopilot settings (e.g. Mach number, direction). Statistical consistency with the complete sequence of BTO and BFO measurements is used to score the trajectory.

2. **Data error optimisation** – Candidate trajectories are created for a range of values of constant ground speed. All points on the 1941 UTC BTO arc that are reachable by the aircraft from the time and position of the final primary radar detection are taken as the set of possible starting points for the trajectories. Each trajectory is broken up into segments at the time of successive recorded BTO values. At these times the trajectory is allowed to change direction and the average of the directions of the track before and after the change are used to evaluate a predicted BFO measurement. The Root Mean Square error between predicted and measured BFO values from 2041 UTC onwards is used to score the trajectory.

Figure 54 shows the top 100 constrained autopilot flightpaths and their intersection with the 6th arc at 0011 UTC for each of the two trajectory scoring methods.

Figure 54: Representation of probability density functions at the 6th arc for constrained autopilot dynamic trajectories scored by statistical consistency with SATCOM (red) and minimum Root Mean Square fit to BFO (green), October 2014



Source: Google earth, annotated by SSWG

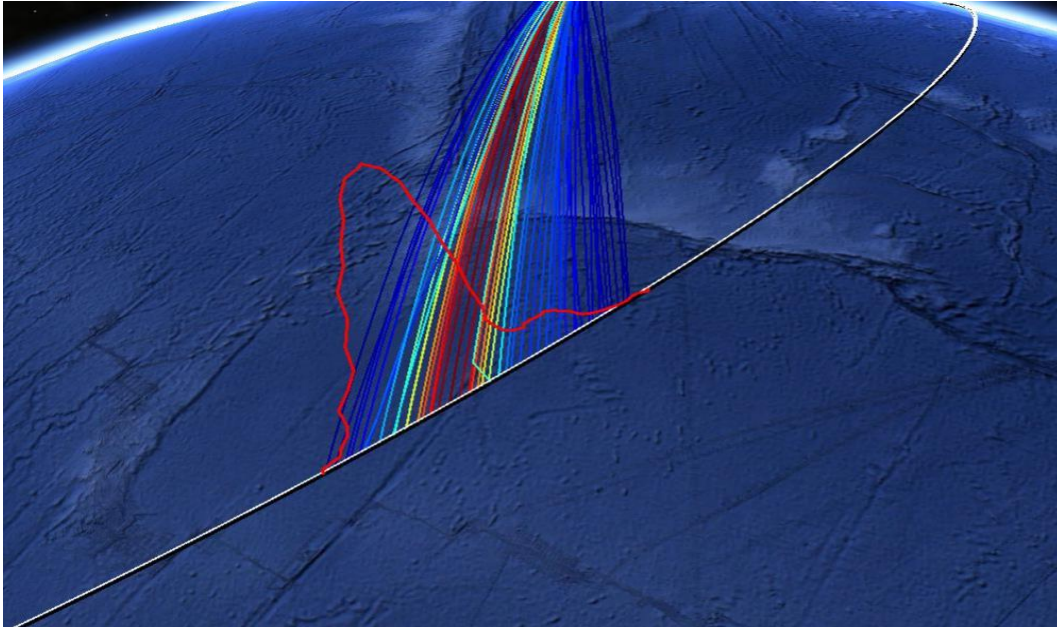
There was an overlap of the two model PDFs located between latitudes between 35°S and 39°S on the 6th arc, with latitudes between 32.5°S and 38.1°S covering 80 per cent of the probable flight paths for both analyses.

More information about the models can be found in the ATSB report [MH370-Flight Path Analysis Update](#) of 8 October 2014.

During 2015, DST Group developed and validated a more comprehensive flight path model which allowed for the possibility of more than one deliberate manoeuvre after the time of the final primary radar detection. The PDF of flight paths was calculated using numerical Bayesian methods. The procedure was validated using examples of previous flights of the accident aircraft. The resulting PDF of MH370's flight path and location at the time of the final SATCOM communication is depicted in Figure 55. This single dimension PDF was then combined with an ATSB defined search area width based on the most likely end-of-flight behaviour of the aircraft (descent kernel) to produce a PDF in two dimensions referred to as a heatmap (Figure 56). ATSB's report [MH370 -](#)

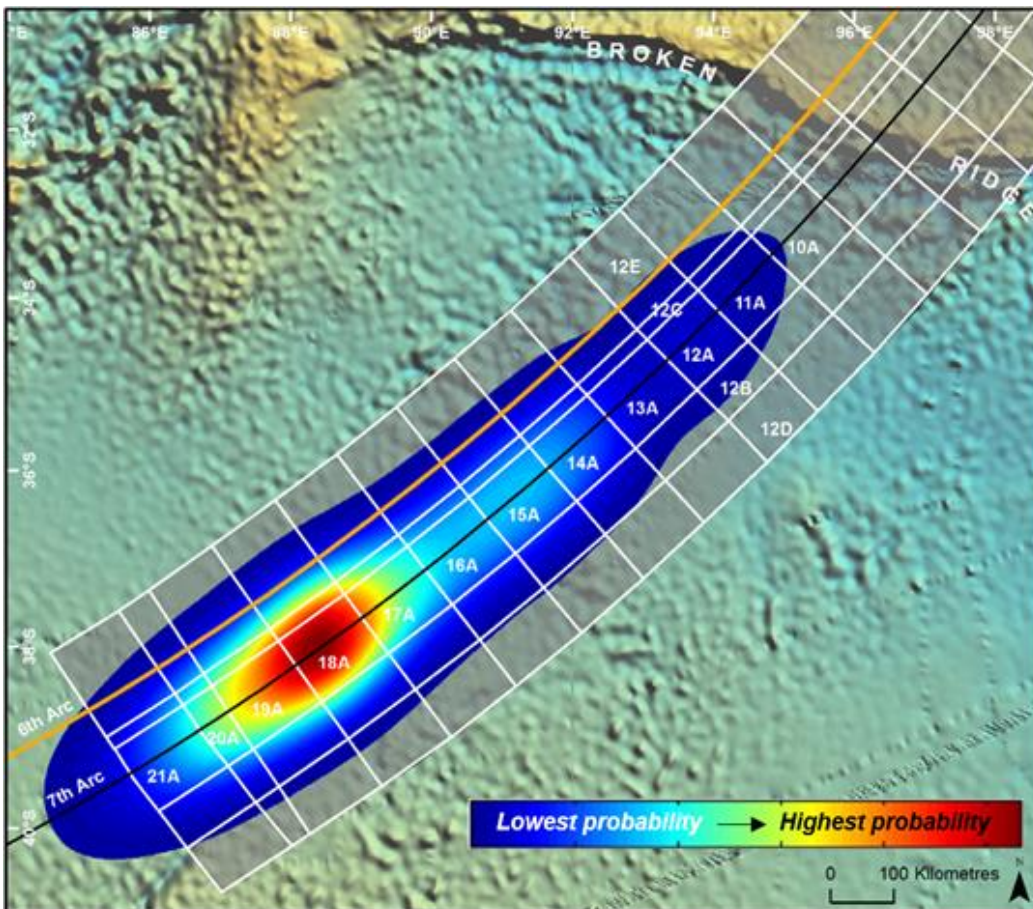
[Definition of Underwater Search Area Update](#) of December 2015 and DST Group's [Bayesian Methods in the Search for MH370](#) describe this work.

Figure 55: DST Group's flight path model probability density function (red line), November 2015



Source: Google earth, annotated by ATSB, using DST Group data

Figure 56: Two dimensional probability density function (heatmap), November 2015



Source: ATSB, using DST Group data

Figure 56 is a graphical representation of the results of the DST Group analysis with the ATSB end-of-flight scenario, with the colours in the area representing the different location probabilities from lowest (blue) to highest (red) probability.

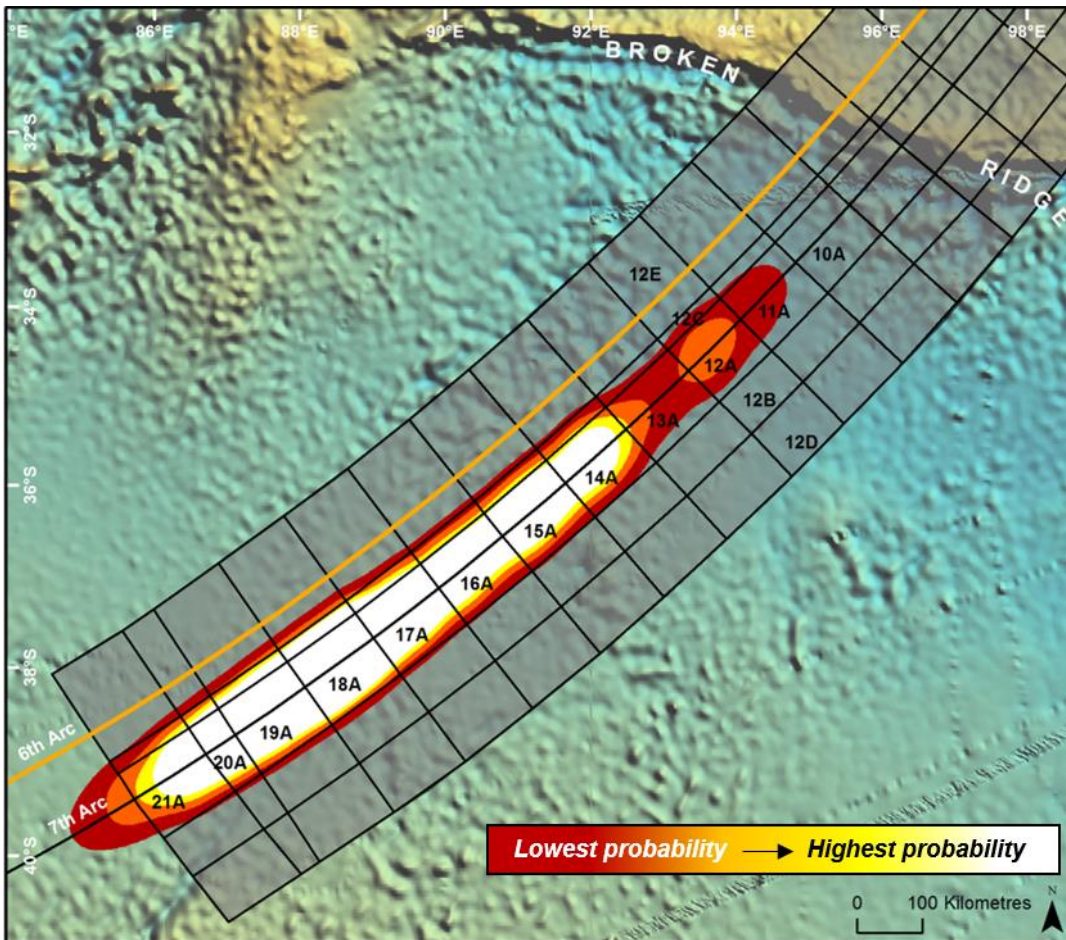
Revised probability density function – November 2016

In November 2016 experts from various organisations and agencies who had been closely involved in defining the MH370 search area met for a first principles review (the ATSB’s report of the meeting can be found here: [First Principles Review](#)). The meeting was to reassess and validate existing evidence and analysis and to identify any new analysis that may assist in identifying the location of the missing aircraft. One of the main areas of focus was the effect of the sonar search results to that time on the previously defined most probable paths and therefore the location of MH370.

At the time of the first principles review an area of nearly 120,000 km² covering more than 85 per cent of the highest probability flight paths had been searched to a level of confidence greater than 95 per cent.

The results of new analysis indicated that the end-of-flight descent kernel defining the width of the search area could be reduced to approximately 25 NM either side of the 7th arc (ATSB report: [MH370 - Search and Debris Update](#)). This information was incorporated into the DST Group’s two dimensional probability density function to produce a new heatmap (Figure 57).

Figure 57: Refined two dimensional probability density function with reduced search area width, November 2016

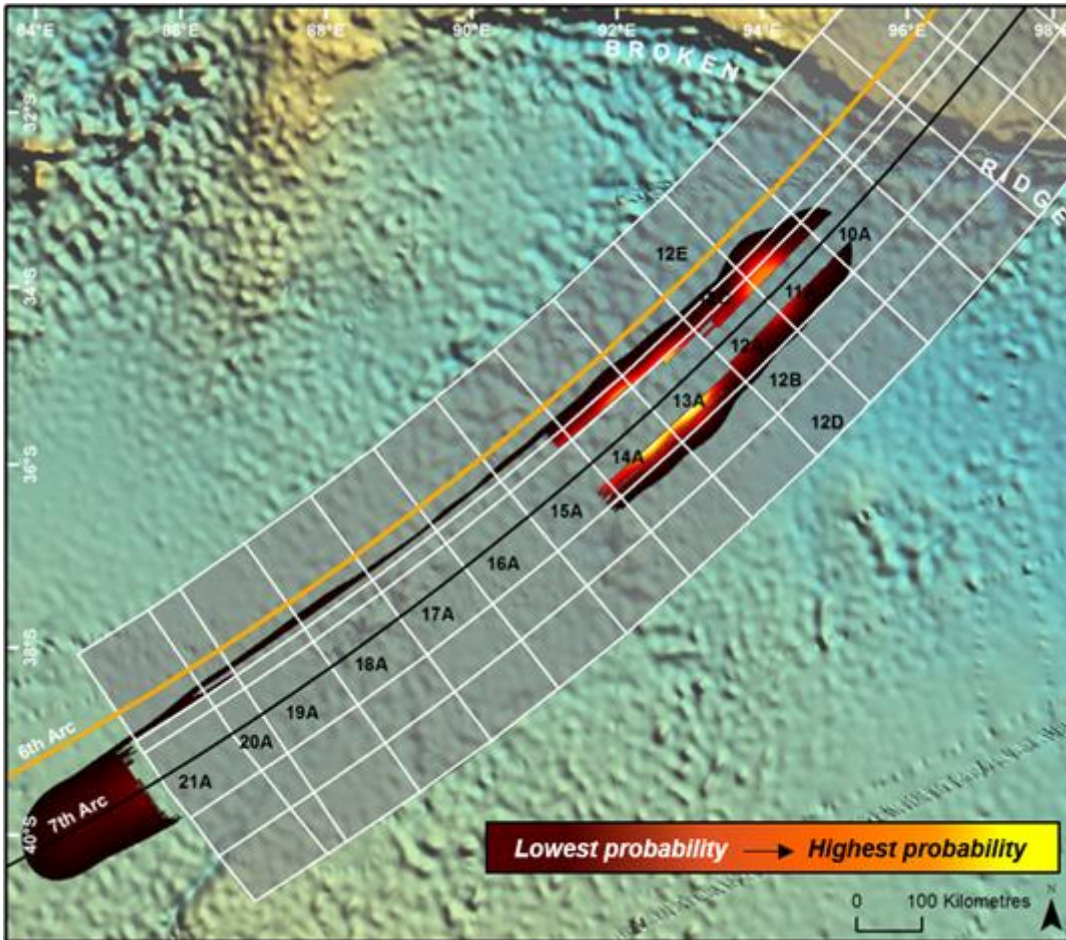


Source: ATSB, using DST Group data

Figure 57 is a graphical representation of the results of the DST Group analysis with the ATSB end-of-flight scenario taking into account search area width reduction to 25 NM. The colours in the area represent the different location probabilities from lowest (red) to highest (white) probability.

When the results of the underwater search were incorporated and considered as well as analysis from the CSIRO’s drift study of MH370 debris ([The search for MH370 and ocean surface drift](#)), which identified a range of latitudes in the search area far more likely for the origin of debris which had been recovered from the aircraft, the PDF was modified again (Figure 58).

Figure 58: A residual probability density function updated with the area searched (mask), NOVEMBER 2016



Source: ATSB, using DST Group data

Figure 58 is a graphical representation of the results of the DST Group analysis with the areas searched removed. The remaining residual probability is located in areas yet to be searched, with two clear areas of interest: north of the search area and south of the search area. The colours in the area represent the different location probabilities from lowest (brown) to highest (yellow) probability.

The effects of the completed sonar search on the PDF throughout the search can be displayed with a time sequenced animation, evolving trajectory probabilities and is available for viewing on the [ATSB YouTube Channel](#). As sonar data was acquired, to a high level of confidence, the aircraft was not in the area searched and consequently the probability of locating the aircraft in the area covered diminishes. The sonar data coverage and associated confidence are modelled into the PDF. The DST Group PDF was visualised using trajectories of probable tracks, symbolised from more likely (red) to less likely (blue).

Analysis and quality assessment of the sonar data

Analysis and quality assessment of the sonar data from the underwater search began at the time of acquisition. Data from the deep tow vehicles was transmitted continuously to the tow vessel via the tow cable. The quality of the data, position, speed and altitude of the deep tow vehicles were monitored continuously in real time by the contractor's mission crew and independently by the ATSB client representative on each search vessel.

During the summer months the vessels using the AUV monitored the vehicle's performance continuously using an acoustic data link as the AUV was not physically connected to the surface vessel. During an AUV mission the operators continuously monitored the vehicle's performance, batteries, sensors, and sonar data acquisition. When the AUV was operating on the seafloor low resolution sonar data was transmitted back to the operators to ensure data collection was occurring. Once the AUV was recovered and back on the vessel full resolution data was downloaded from all relevant sensors.

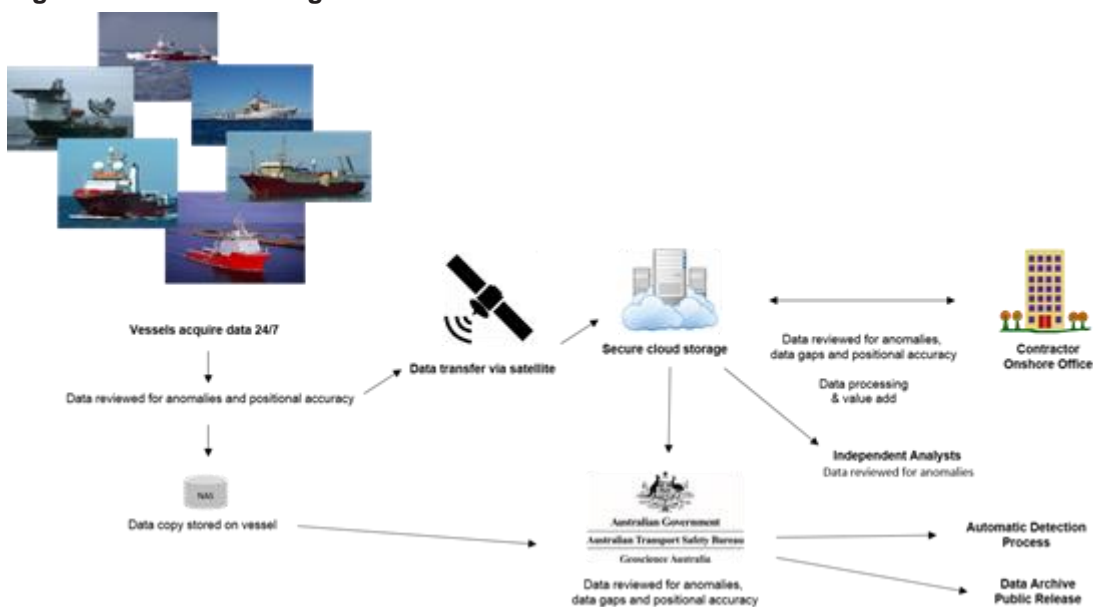
After initial data collection was complete, the positioning data was post processed on board the vessel and verified for each underwater vehicle. Sonar data was processed and analysed in more detail for sonar contacts and quality by both the mission crew and the ATSB's client representative. Checks to ensure proper coverage of the seafloor were achieved to the standards specified for each system. Sonar contacts of interest were marked and sent ashore as daily Preliminary Contact Reports.

Fugro Survey vessels then sent the relevant processed search data daily via satellite to a Fugro Survey secure data cloud. This made the data accessible to all shore-based stakeholders. The Fugro Survey Perth office then processed and analysed the data again for quality, coverage, and contacts. In addition, final products such as mosaics, raster images, plots, and geospatial databases were created and provided to the ATSB. Fugro Survey's Perth office was staffed by sonar data specialists, geophysicists, geographic information system (GIS) analysts, data managers, vessel managers and support staff.

Phoenix International and Hydrospheric Solutions operating the ProSAS deep tow vehicle used a slightly different process. After initial sonar data collection and analysis, further processing occurred to ensure subsea positioning accuracy and overall quality of data. Another review for contacts of interest was also performed. Final products were created on board the vessel which included positioning plots, analysis of coverage, mosaics, and raster images of the relevant data sets. Specific databases captured contacts of interest and sonar coverage. Contact reporting, coverage mosaics and plots were provided daily via satellite. Raw and fully processed data were stored on board until the next port call when it was provided to the ATSB.

Once the data was supplied to the ATSB all relevant search data and databases were checked for quality, coverage and contacts by the GIS team based in the ATSB's Canberra office. Data analysis and quality control was also performed by the ATSB's Quality Assurance Manager (based in the United States) and by an independent highly experienced sonar data expert also based in the United States. Figure 59 shows the data flow from vessel to final archival storage.

Figure 59: Data flow diagram



Source: ATSB

Results and assessments were compared and additional coverage maps were produced. Geoscience Australia produced bathymetric digital elevation models using the ship hull-mounted MBES data. Data was catalogued, backed up and prepared for archival storage.

Additionally, experts in the field of automatic target recognition (or detection) using sophisticated software algorithms to analyse the data were used. No new contacts have been identified to date using this technology however some existing contacts were flagged by the process. This work and process continues as the technology evolves.

Quality assurance of the sonar data

In addition to analysing the sonar data for areas of interest, there was a very careful focus on ensuring and quantifying seafloor coverage. This included proving sonar data overlap with adjacent sonar data and cataloging areas searched with systematic classifications and confidence ratings that an analyst would detect the MH370 debris field.

A historical study was conducted of available previously sonar mapped aircraft debris fields. Measurements of each field were made and aircraft size compared with any impact information available for each crash site. It was found that the area of a typical debris field for an aircraft the size of a B777, with any foreseeable crash scenario, in similar water depths similar to the MH370 search area, would be at least 100 m x 100 m and very likely to be greater than 200 m x 200 m.

The quality assurance program reviewed and monitored many aspects of the search. The following were some of the main areas of focus:

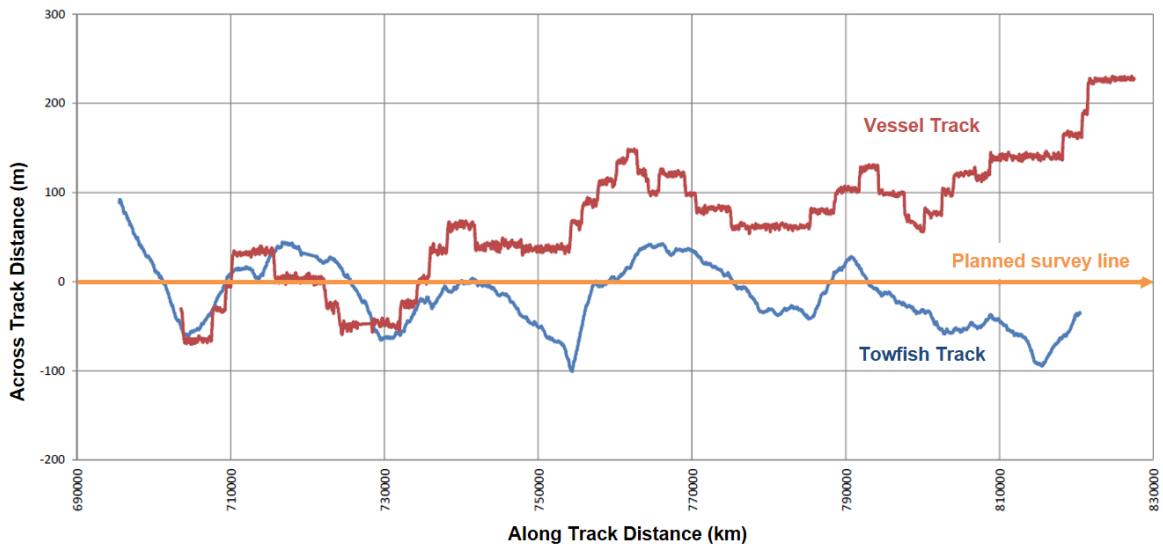
- data quality of the primary search sensors
- subsea positioning of the deep tow vehicle and AUV
- ensuring overlap between adjacent lines (or areas) of sonar data
- cataloguing all areas covered by the search systems
- reviewing the data for areas of interest (contacts)
- search methodology.

The process began with ensuring the data being collected was of the quality needed and specified by the ATSB. In short this was the ability to detect a two cubic metre object at the test range qualified range scale and vehicle altitude. Data quality was constantly monitored on board search

vessels by the equipment operators, data processors, and ATSB client representatives. It was further evaluated on shore by the data processing team, ATSB, and independent reviewer. If at any point the data quality was compromised the data coverage was reduced by narrowing the survey line spacing or the area was resurveyed. Typically any data quality or vehicle performance issues were addressed immediately on board the vessel and thus maintained operational efficiency and continuous coverage.

Ensuring the tracking system and accurate positioning of the deep tow vehicle and AUV was critical to ensuring complete sonar coverage, as this was the basis for the position being injected into all data files collected on the underwater vehicles. Figure 60 shows a typical track plot of the ship and the deep tow vehicle. This graphically represents how far the deep tow vehicle was off the planned line route and the position of the vessel relative to that planned line. Notice the ‘steps’ in the red vessel track, these were from the vessel shifting position to help ‘steer’ the deep tow vehicle down the planned route line. This allowed the operators to manipulate the deep tow vehicle position using the ship position. The graph also instantly highlighted areas where adequate overlap may be a concern with the adjacent search line.

Figure 60: Example vessel and deep tow vehicle position track plot

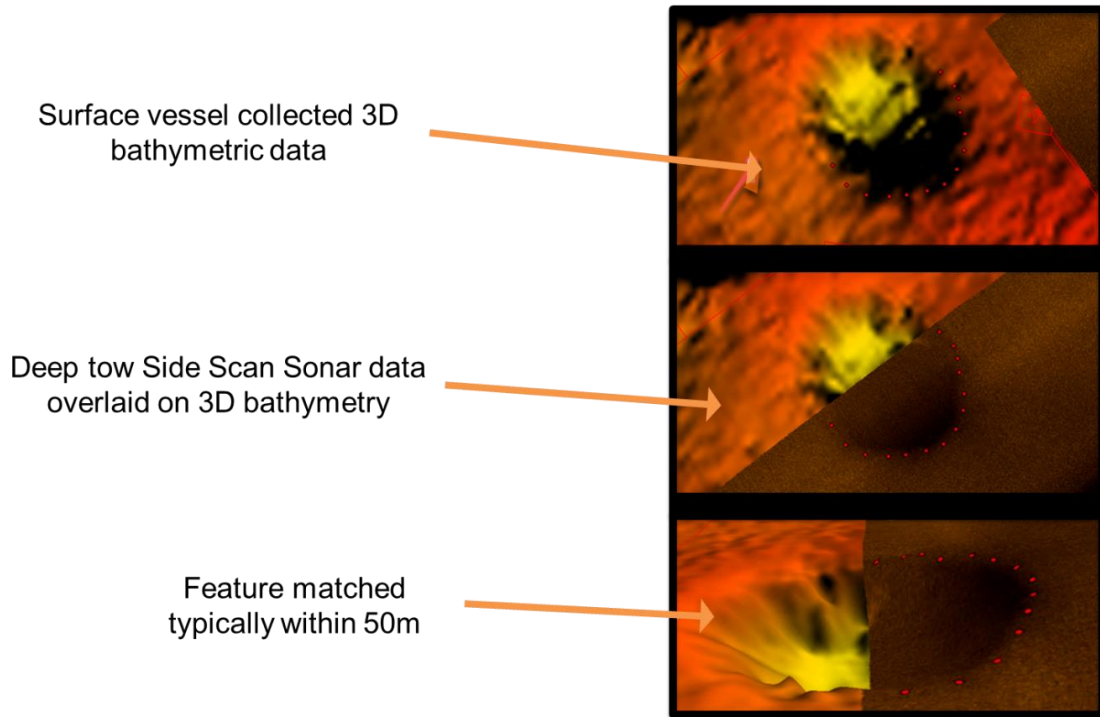


Source: ATSB

To verify the positioning of the deep tow vehicle two methods were used. The first method used the bathymetry data collected by the ship based MBES system to ground truth the sonar data. The bathymetry survey used precise motion tracking and GPS corrected positioning systems which provided reliable and accurate georeferenced MBES data to be collected in over 6,000 m of water depth. The three dimensional (3D) bathymetric maps created with the MBES data were primarily used to ensure the safe and efficient operation of the underwater vehicles, however the accuracy of the maps allowed them also to be used to verify the positioning of the sonar data.

Figure 61 shows an example of this process. The yellow area represents a depression in the seafloor, the red dots were digitised in GIS software to mark the edge of the depression within the SSS data, as indicated by the darker (black) coloured returns. This was a result of the SSS signal not being returned (reflected back) due to the seafloor sloping away. The SSS data was overlaid and draped onto the 3D bathymetric surface for comparison. If mismatched more than 50 m it was logged and the position of the SSS data was adjusted as required.

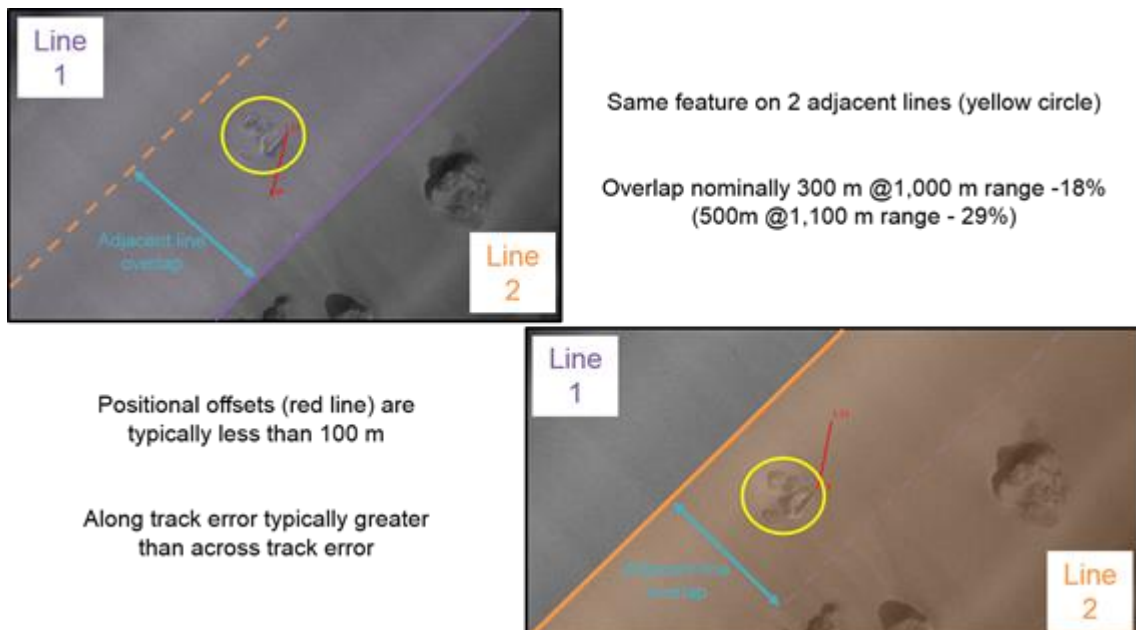
Figure 61: Example of matching side scan sonar data to a bathymetric feature



Source: ATSB

The second method used to verify the position of the deep tow vehicle was to match features between overlapping sonar data sets. This helped quantify errors in the positioning and provided a reliable 'check' of measurements for overlap between adjacent search lines. Figure 62 is an example of this. The feature circled in yellow was identified on two adjacent lines of sonar data. Selecting one discrete point within the feature allowed for a precise measurement between the lines of data using the same object. This measurement was further broken down and tabulated into along track and across track offsets. An accurate measurement was also made from the discrete point to the edge of the sonar range. This was combined with the adjacent line measurement which then gave an accurate overlap value for that point.

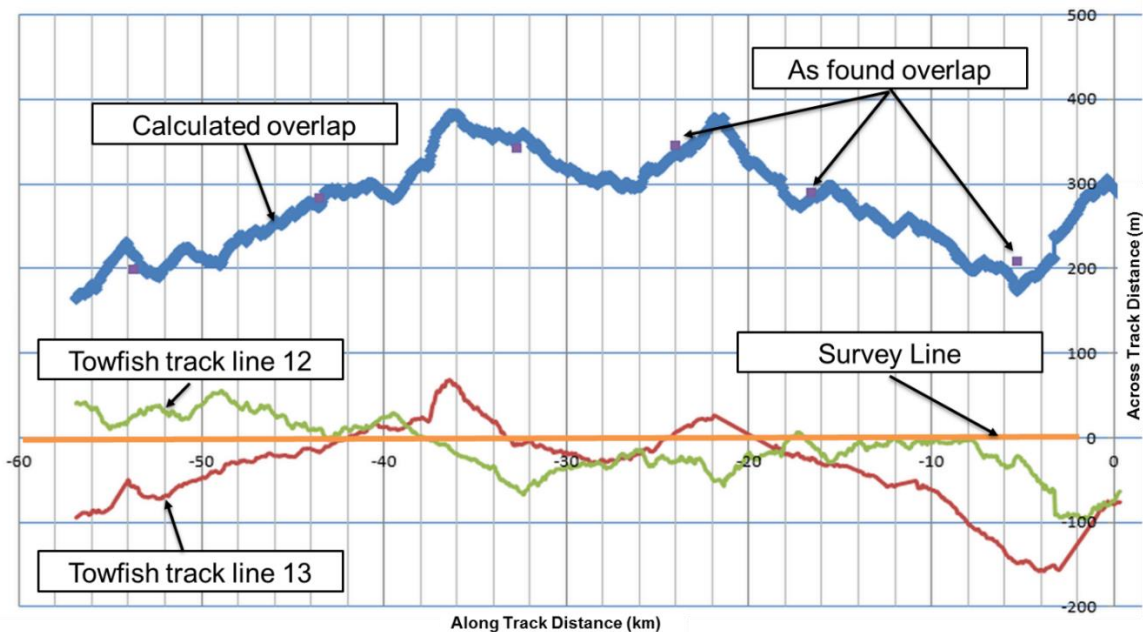
Figure 62: Example of adjacent line overlap, manual check for positional offsets



Source: ATSB

The final step in this process was to plot the findings of the overlap check, along with the actual deep tow vehicle tracks from the two adjacent lines. Figure 63 represents a plot of this process. The orange line was the planned track line. The green and red lines are two adjacent deep tow vehicle tracks, overlaid with matching distance along the track line. The blue line represents calculated overlap derived from plotting distances between the deep tow vehicle tracks. Nominally this would be 300 m using 1,000 m range scale and 1,700 m line spacing. In this example the overlap varies from 175 m to almost 400 m. In addition, the manual feature matches previously measured were plotted (purple points) and compared to the calculated overlap (blue line). Ideally these match, typical results proved to be within 50 m. This was within the ATSB’s tolerance for the positioning systems and acceptable overlap coverage.

Figure 63: Example deep tow vehicle position track for two adjacent lines, overlap value and verification points plotted



Source: ATSB

Using these techniques to verify the positioning of the deep tow vehicles established a high confidence in the position of the sonar data. With this confidence, coverage rates could be maximised allowing efficient operations while maintaining high confidence in the overall coverage. It is also the basis for accurately quantifying sonar data coverage, overlap, and seafloor areas with a lower chance of detection or no data.

Sonar coverage

The seafloor topography within the search area was such that the deep tow vehicles achieved approximately 98 per cent sonar coverage overall with a single pass. The remaining two per cent represented areas that had effectively no data. These areas were further categorised into four types of gaps in the sonar data (known as ‘data holidays’), as described below:

- Terrain Avoidance Holiday
 - Areas where the deep tow vehicle had to be raised or lowered to negotiate or avoid seafloor terrain. This normally occurred around large seamounts or fracture zones. These were marked anywhere the underwater vehicle altitude was over 300 m.
- Shadow Holiday
 - Occurred when the seafloor terrain masked the area behind it. Typically caused by a geologic obstruction which blocks the sonar signal from going further, or a high down slope gradient where no return signal was detected.

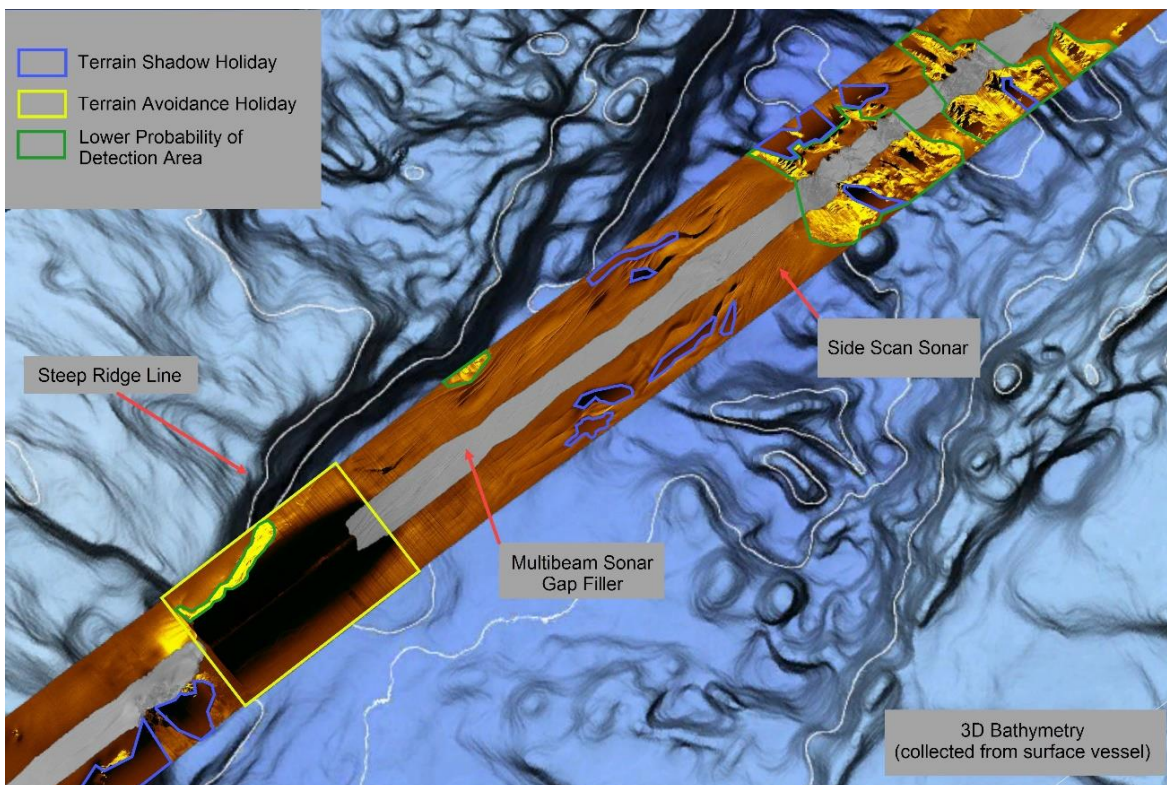
- Off-track Holiday
 - A data gap between two adjacent lines of sonar data using a valid range of 1,000 m nominally. These were rare but sometimes occurred if the ship had large deviations from the planned line or subsea currents shifted the deep tow vehicle position.
- Equipment Failure Holiday
 - Area where valid data was not collected due to equipment malfunction.

A fifth category called Lower Probability of Detection (LPD) was used when valid sonar data was collected but the detection confidence was deemed less than nominal due to complex geology, environmental conditions, or data quality degradation. For example, a large rock field on the seafloor made it more difficult to detect the presence of aircraft debris. These areas were not considered data holidays because they still consisted of valid sonar data. LPDs accounted for about two per cent of the area covered by the deep tow vehicles.

Three types of sonar data were collected, traditional side scan sonar (SSS), synthetic aperture sonar (SAS), and multibeam echo sounder (MBES). Classification of search data and holiday type were maintained with each system used. It is noteworthy that the SAS system produced an overall higher resolution image providing a greater confidence of detection in areas with complex geology. This decreased the number of LPD areas substantially within that data set.

Figure 64 is a sample representation of these data categories marked within SSS data. Areas were manually digitised using GIS software and sonar processing software. Each polygon was categorised and placed in a geospatial database. This was initially performed by the search contractor(s) and then reviewed and verified by the ATSB quality assurance team to allow for accurate assessment of overall coverage and quantify the overall confidence in the data set.

Figure 64: Deep tow vehicle sonar data draped over 3D bathymetry data showing an area of complex seafloor topography in the search area and associated sonar coverage classifications



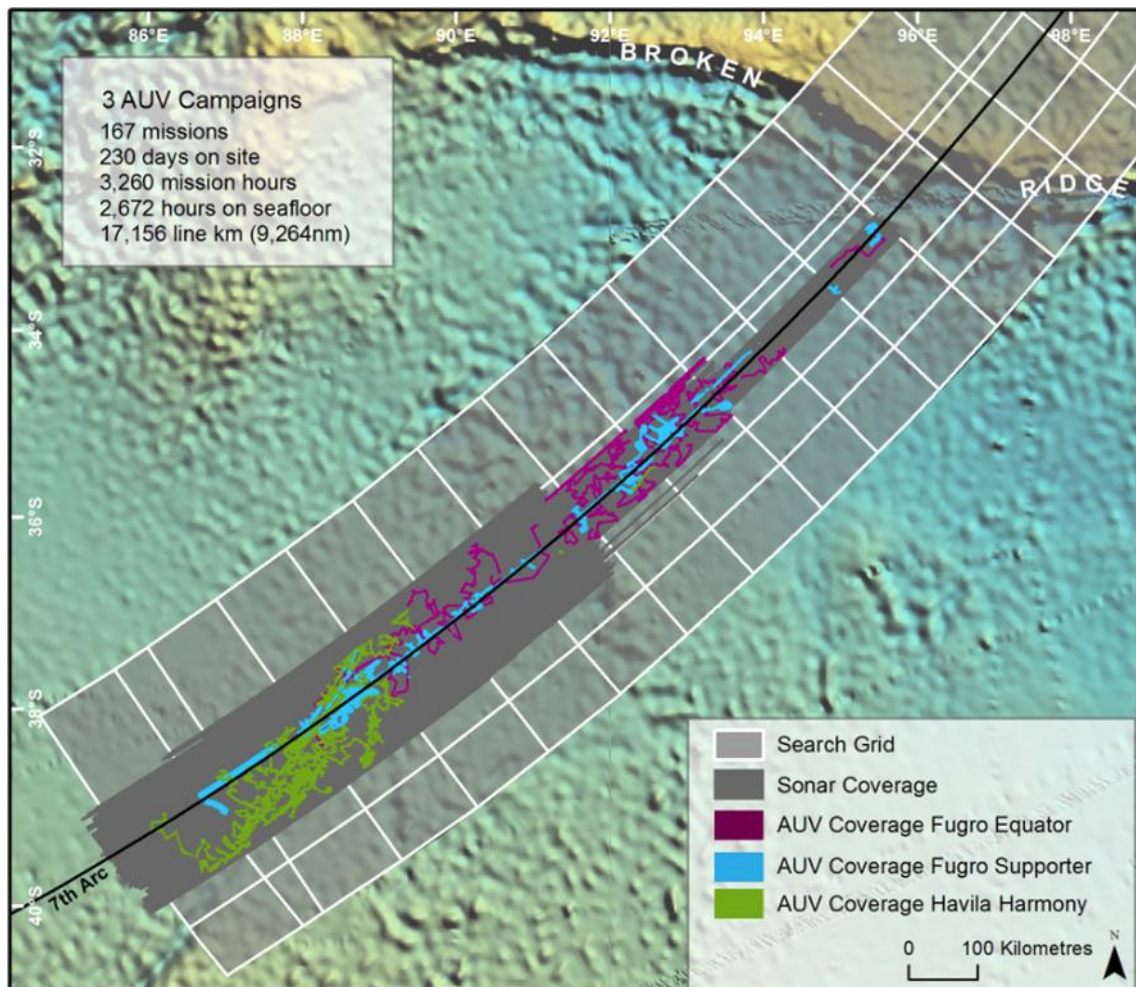
Source: ATSB

The sonar coverage geodatabase was further used to plan and execute missions performed by the AUV. With high confidence in the positioning of the search data, with each data holiday and LPD area digitised, the AUV was assigned discrete areas to infill (resurvey). Mission planning for the AUV was optimised as all areas needed to be infilled were known and precisely mapped. Data holidays were prioritised by size, grouping and proximity to the 7th arc to maximise coverage and minimise transit times between areas.

Areas designated as LPD were typically not resurveyed except in specific cases. One example was the Geelvinck Fracture Zone. This was a very large and steep ridge that transected the width of the search area and was also in a higher probability area within the search area. To ensure sufficient coverage was achieved the AUV and deep tow vehicle covered this area with multiple passes and alternate line plans.

Varying degrees of confidence were attached to LPD areas depending on interpretation of the complexity, texture, composition and topography of the seafloor. Nominally these areas were rated at 50-90 per cent likelihood that an analyst would detect the aircraft debris field. Approximately 48 per cent of LPD areas have been searched at least twice which added to the overall confidence of detection rating. Figure 65 shows an outline of all data collected by the AUV. Each colour represents one of three separate AUV campaigns over the course of the underwater search. The green area highlights a concentration of missions around the large fracture zone mentioned previously in the southern search area. A concentration of infill missions along the middle of the search area correlates with the position of the 7th arc.

Figure 65: Map showing coverage of AUV missions and statistics



Source: ATSB

Data processing and information dissemination – a new approach

During the search for MH370 Fugro developed and deployed several new technologies to improve the analysis and transfer of the sonar search data. Due to the remoteness of the search area, and the requirement for multiple vessels operating in a coordinated manner, a system was implemented in which raw sonar data was packaged and transmitted via VSAT satellite communications systems from each vessel to a secure cloud facility (Fugro term this Back2Base). This permitted simultaneous data analysis and quality control by the shore-based analysts in Fugro Survey's Perth office, GIS specialists in the ATSB's Canberra office and the ATSB's Quality Assurance Manager based in the United States.

The large volume of data and its availability on a cloud server also created the opportunity for an automation step-change in the processing of positioning, SSS and MBES data. Fugro developed 'Roames', a cloud-based system, which allowed sonar data to be automatically processed in an efficient and consistent manner. This processing system employed algorithms which significantly improved the sonar signal processing, gain curves and accuracy of the bottom tracking of the first sonar return. Improved bottom tracking and the gains applied by Roames resulted in a better interpretation of sonar data, specifically within the near nadir region²⁷ to the mid-range, however the entire sonar record benefited out to the far field.

The products resulting from the Roames processing including geo-referenced sonar mosaics, sonar point clouds and conditioned SSS data files could then be visualised in near real-time from anywhere in the world via secure link. Conventional desktop-based processing using industry standard software packages was also undertaken in parallel with the Roames processing as check on the processing results. Bottom tracking from the port and starboard channels were cross-correlated to the downward looking multibeam echo sounder to ensure the validity of the bottom detection.

Tests were conducted over the first shipwreck site, Figure 67 and Figure 68, to validate the algorithms used by the Roames system. This site provided a well-suited test area, with low-lying objects less than 25 cm high and only a few pieces of debris near 1 m in height. The wreck was spread over an area 300 m by 250 m with three larger pieces of debris that could be used for reference.

Four test lines were run directly over the shipwreck site using the deep tow vehicle at altitudes of 125 m, 130 m, 165 m and 200 m. All runs used nominal operational settings for both the SSS and MBES sensors. MBES backscatter was used to verify the position of the debris field within the SSS nadir and the tests showed that a 200 m by 200 m low lying debris field could be detected in the SSS data at an altitude of up to 200 m with a high degree of confidence over a fairly benign seafloor.

This was an important finding as early in the search it was found that the optical fibres within the deep tow vehicle tow cables experienced increasing attenuation over the course of each six week search swing. Towards the end of a swing this resulted in some areas where the tow cable failed to communicate with the required gigabit Ethernet connection for MBES operations producing a long thin data gap typically 100 m to 150 m wide, depending on the vehicle altitude. The tow cable attenuation MBES communication problem was eventually overcome using a combination of modified operational practices, maintenance procedures and alternating tow cable cables every port call ('resting' the tow cables on alternate swings).

Following field testing of the Roames system at the shipwreck debris field many of these long thin data gaps were able to be discounted. This was based on the proven detection of at least a 200 m by 200 m debris field in the nadir of the SSS data when the towfish altitude was less than 200 m, which was mostly the case. Sub-bottom profiler data was also reviewed for these areas for

²⁷ The nadir region is defined in this report as the area directly beneath the deep tow vehicle and area adjacent to the first SSS signal return.

potential anomalies to gain further confidence that a debris field had not been missed in the nadir. Areas where the seafloor was geologically complex or dynamic remained classified as data gaps or were classified as LPD. In many cases these areas were later re-investigated using the AUV to ensure search integrity.

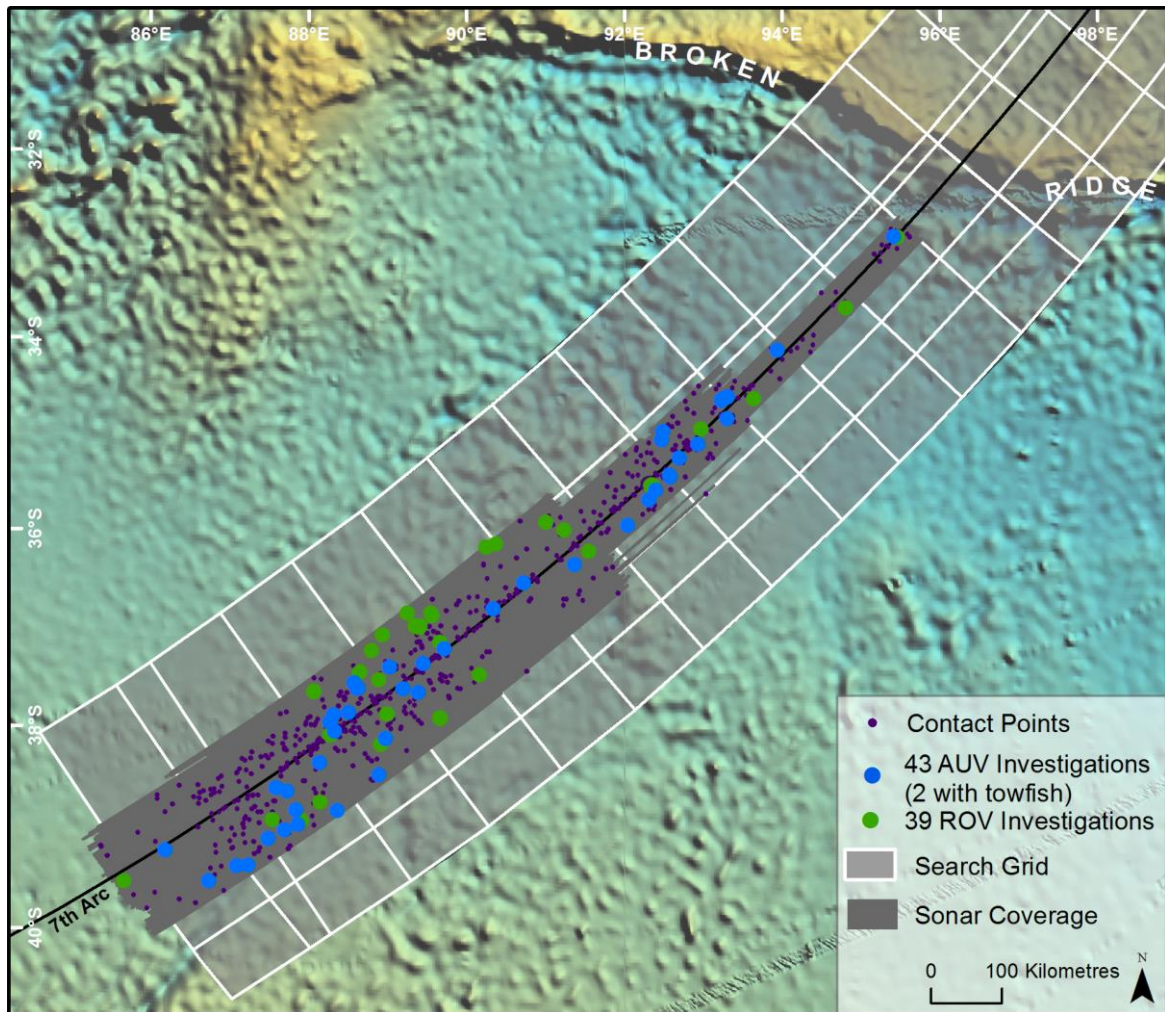
Using Fugro's cloud-based system visualisations of daily progress and data coverage were delivered through Google Earth (and other GIS applications) which provided the ATSB's search personnel with up-to-date information on the search without needing specific expertise in more complex GIS software packages. Other data delivered with the system included high resolution coverage maps, real time ship locations, line plans, track plots, weather maps, hill-shaded seafloor relief, MBES backscatter and various map layers which allowed operational decisions to be made in a timely and efficient manner. Throughout the search innovative technology was employed to improve cost-efficiency, search confidence and team safety. This technology is already being applied by Fugro to commercial and scientific marine operations across the world.

Sonar contacts

Sonar contacts (anomalous features) identified in the sonar data were classified in three ways: level 3 contacts were marked but assessed as unlikely to be related to the aircraft, level 2 contacts were marked but assessed as only possibly being related to the aircraft, and level 1 contacts were of high interest and warranted immediate further investigation. There were 618 level 3 contacts, 41 level 2 contacts, and two level 1 contacts identified and reported. The two level 1 contacts were investigated and found to be iron and coal remains of a wooden shipwreck and the other was a scattered rock field. In total, four shipwrecks were found.

Throughout the search 82 separate sonar contacts were investigated and eliminated (as being related to MH370) by the AUV, ROV, or deep tow vehicles. All investigations used either high frequency sonar or optical camera images to discount sonar contacts as related to MH370. Figure 66 shows the overall distribution and layout of the contacts that were marked and investigated.

Figure 66: Locations of contacts and secondary investigations

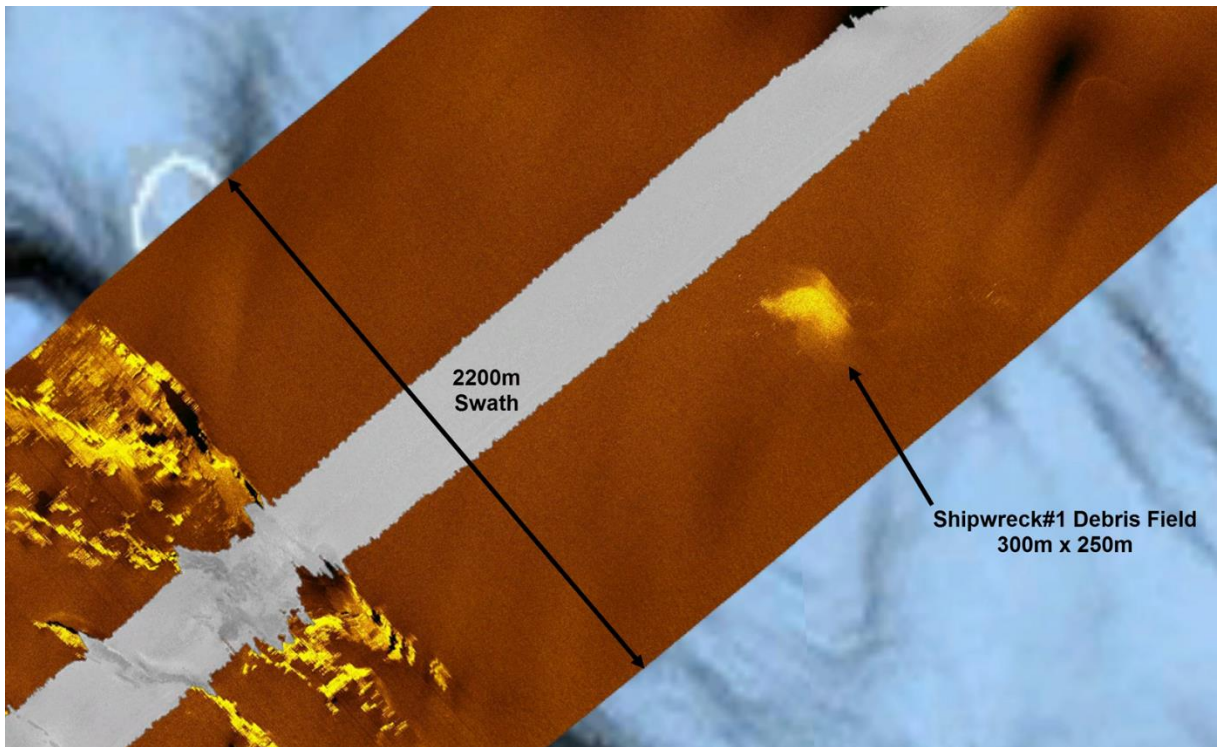


Source: ATSB

Overall these investigations and verifications provided increased confidence in the search area as they validated specific findings and provided assurance that the data analysis and interpretation were correct and accurate. This also verified the overall search methodology, providing confidence in the operations, sonar sensors and vehicles used.

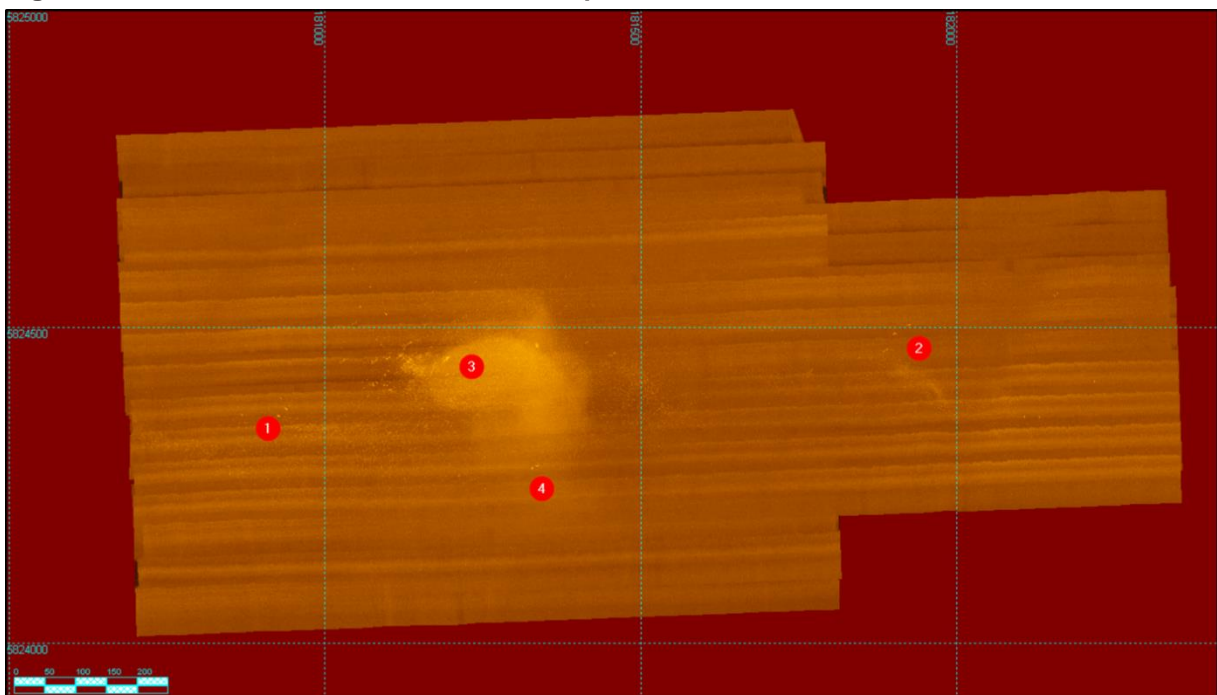
The following example was a contact highlighted as a preliminary contact on board a search vessel. This data was reviewed by the contractor’s processing team on shore, ATSB, and by independent analysis, after which it was decided to investigate further using the AUV. Figure 67 shows the first deep tow vehicle sonar line where the initial detection was made. Figure 68 shows the AUV mosaic created with several passes using 410 kHz high frequency SSS at 100 m range scale.

Figure 67: Initial deep tow vehicle sonar data, shipwreck #1 detection



Source: ATSB

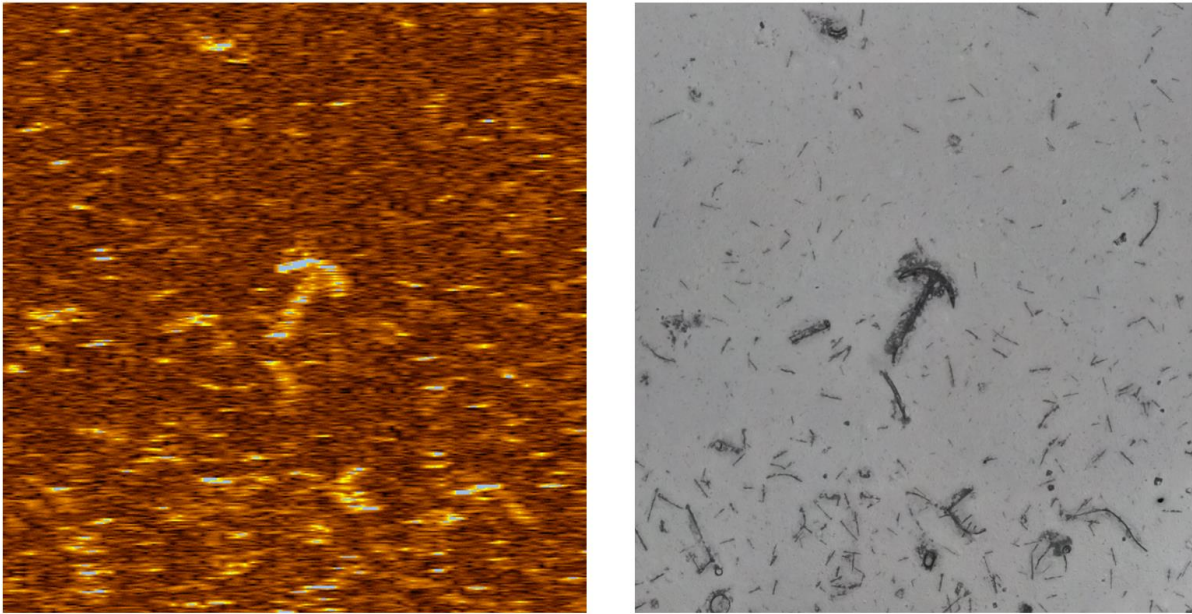
Figure 68: AUV side scan sonar mosaic of shipwreck #1 site



Source: ATSB

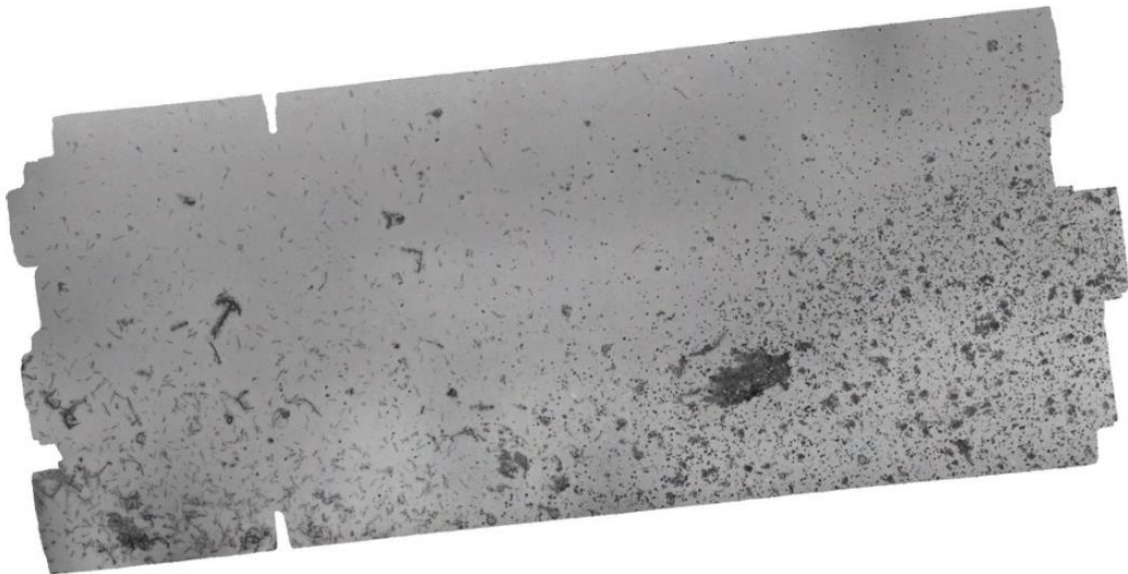
The sonar contact was suspected as being a shipwreck and confirmed by a follow-on AUV mission that collected black and white camera images. Figure 69 compares a camera image to a high frequency sonar image of an anchor highlighting the detail that was achieved using high frequency side scan sonar data and the correlation between data sets. Figure 70 is a photo mosaic created over a portion of the shipwreck site using multiple photographs taken by the AUV.

Figure 69: High resolution AUV sonar data and optical imagery of anchor



Source: ATSB

Figure 70: AUV photo mosaic subset of shipwreck #1 site

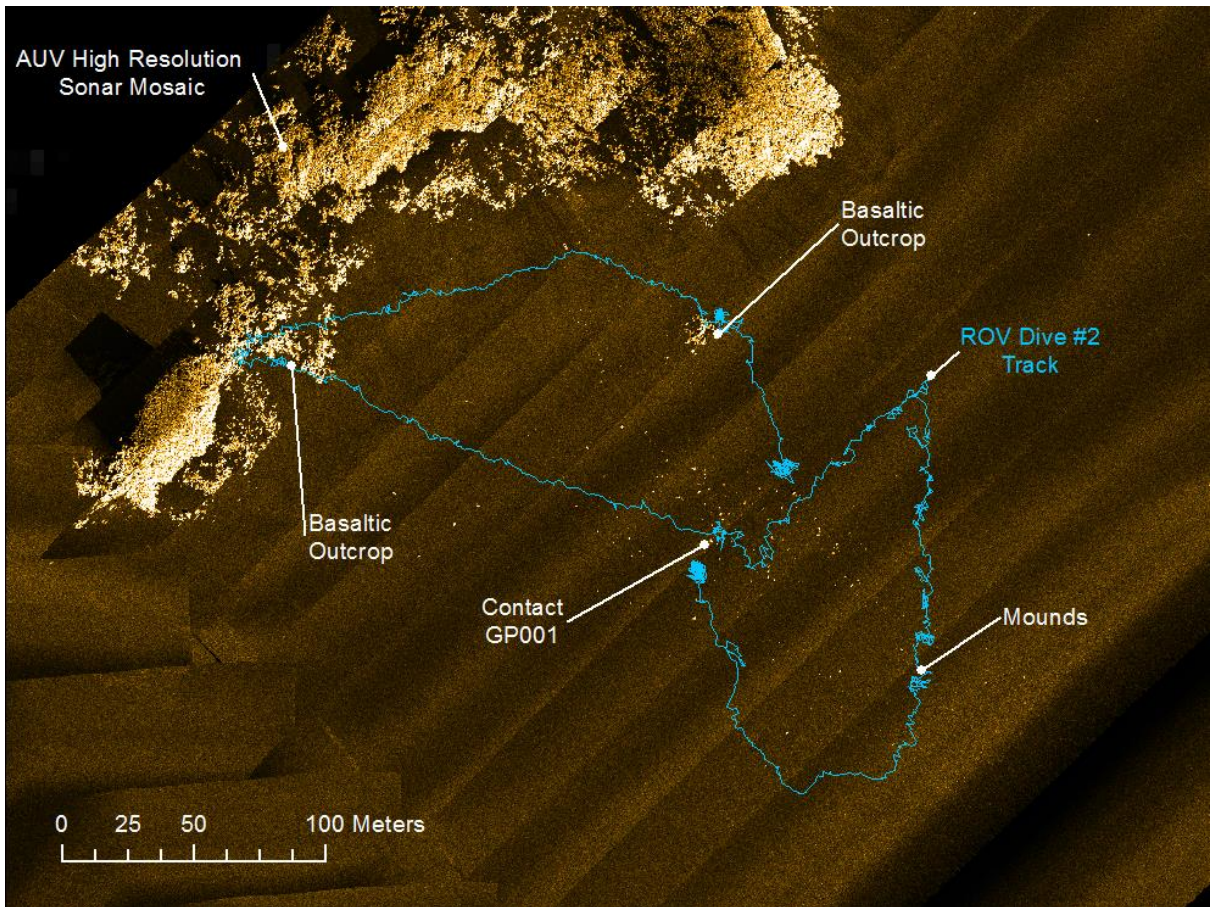


Source: ATSB

In addition to using the deep tow vehicles and the AUV to investigate areas of interest a ROV was also used. The ROV was deployed over specific sites to collect colour streaming video to confirm contacts were not related to MH370.

In total 39 discrete areas were investigated. Figure 71 shows a typical ROV track during a single investigation dive, which included a search of the immediate and surrounding area of a sonar contact. The ROV allowed for quick verification of sonar contacts, often completed in around five hours per location, with many of the contacts in difficult geologic areas within a complex and dynamic seafloor. The ROV also provided a safer alternative to using the AUV or deep tow vehicle in potentially hazardous (to the deep tow vehicle or AUV) seafloor environments. Figure 72 is a selection of man-made debris found using the ROV.

Figure 71: ROV track of typical contact investigation



Source: ATSB

Figure 72: ROV images of man-made findings



Source: ATSB

Confidence in the search results

To quantify the confidence in the search results measurable parameters were tracked and catalogued. Separating search data into categories and assessing them individually decreased generalisations across the entire data set. In addition, contact investigations, proven object detection and verification, overlapping data and positioning repeatability all provide indicators when assessing the overall confidence of the underwater search.

As detailed within the sonar coverage section the sonar data and coverage were separated into different categories. The following designations were used with a confidence of detection rating assigned, zero per cent meaning there was no confidence of detection and 100 per cent meaning complete confidence the aircraft debris field would be detected within the collected sonar data.

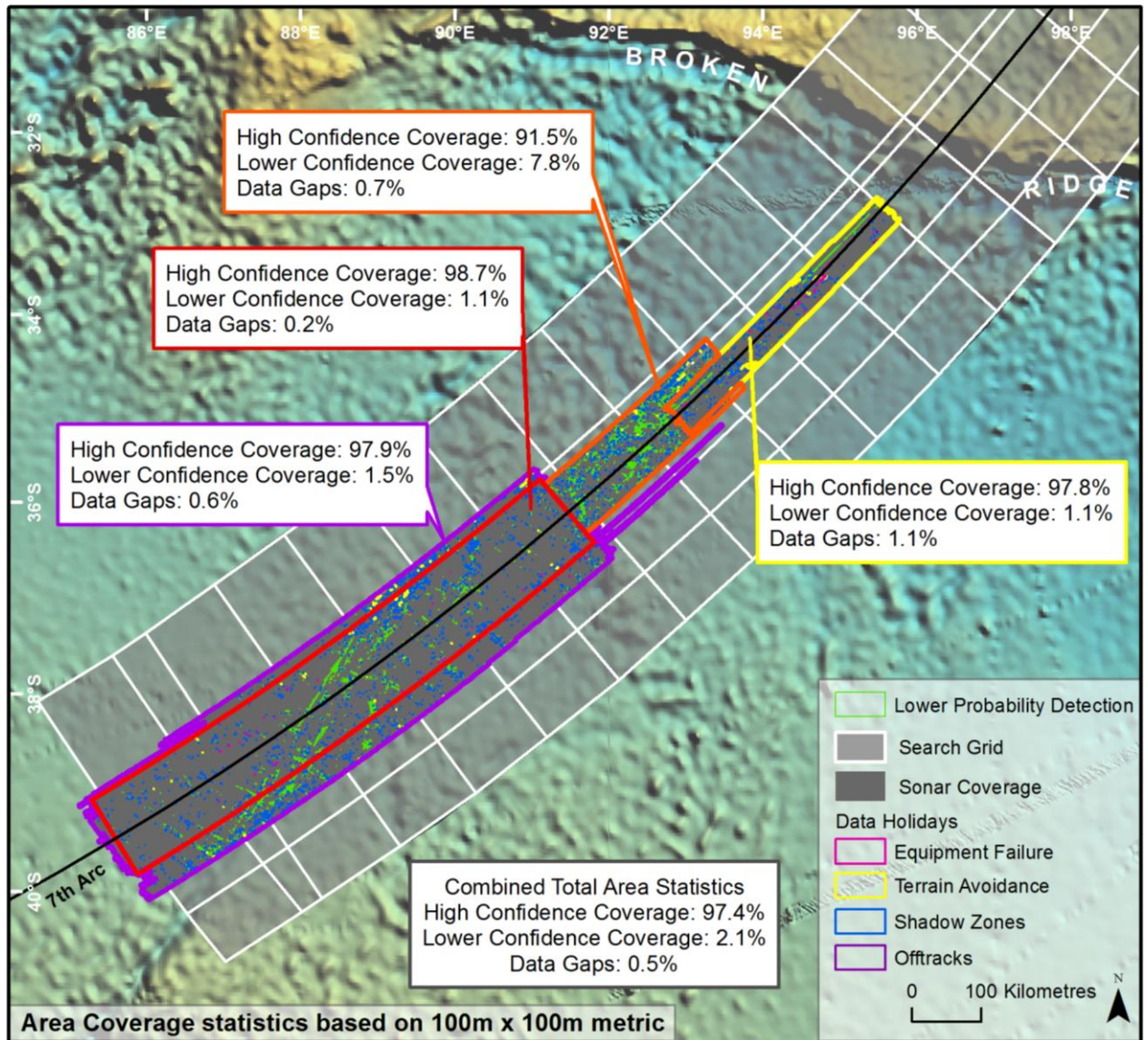
- Shadow, off-track, and equipment failure data gaps were all given zero per cent confidence of detection.
- Terrain avoidance data gaps were also given zero per cent confidence of detection.
 - Normally some useable data was within these areas, however given the higher towing altitudes and increased deep tow vehicle motion often associated with this type of holiday a conservative value of zero per cent was chosen.
- Lower probability of detection areas, these varied in the level of detection confidence.
 - A range of 50-90 per cent was used to capture this category with an overall rating of 70 per cent as the nominal value. It is worth noting that 48 per cent of these areas were searched more than once, which positively contributed to the confidence rating.
- The remaining area had good quality sonar coverage resulting in a >95 per cent confidence of detection rating.

The statistics were further broken down into four areas based on the probability of the aircraft debris field lying in the area (based on the then flight path analysis, end-of-flight, PDF) during the search. The primary difference in the overall sonar coverage for these four discrete areas was the amount of AUV time used to fill in the data gaps and the more difficult seafloor topography within each region. A description of the four areas follows:

1. Red Area: 'Indicative Search Area' out to 27.5 NM to the northwest and 25 NM to the southeast of the 7th arc.
 - Consists of deep tow vehicle SSS data, SAS data, and AUV infill data.
2. Orange Area: North of the 'Indicative Search Area' out to 23 NM to the northwest and 17 NM to the southeast of the 7th arc.
 - Consists of mainly deep tow vehicle SSS data and AUV infill data.
3. Yellow Area: Furthest north of the 'Indicative Search Area' out to 10 NM to the northwest and 13 NM to the southeast of the 7th arc.
 - Consists of mainly deep tow vehicle SAS data and AUV infill data.
4. Purple Area: Outside 27.5 NM to 36 NM to the northwest and 25 NM to 41 NM to the southeast of the 7th arc.
 - Consists of mainly deep tow vehicle SSS data.

Figure 73 summarises the overall coverage percentages and corresponding confidence of detection ratings for each area, as well as for the total combined area searched based on cataloging all data gaps and LPD areas of 100 m by 100 m size and larger.

Figure 73: Coverage statistics and associated confidence of detection, using 100 m x 100 m data gap metric



Source: ATSB

For reference, 'High Confidence Coverage' means a >95 per cent confidence of detection; 'Lower Confidence Coverage' means on average a 70 per cent confidence of detection, and 'Data Gaps' have a zero per cent confidence of detection.

For each area defined the final sonar data coverage value is determined by taking the total size of the area and subtracting out each data gap and LPD. Holidays are totaled by area (square kilometres) per individual polygon. This size attribute can be used to filter and further classify data gaps and LPDs.

It is worth noting that filtering out all data gaps and LPD areas less than 200 m by 200 m decreases the individual data gap count by 78 per cent, and LPD count by 60 per cent. Using this same metric but filtering by square kilometres reduces the total square kilometre area by 24 per cent and seven per cent respectively. This highlights that many of the data gaps and LPDs are smaller than 200 m by 200 m.

Historical analysis has shown that aircraft debris fields typically cover areas larger than 200 m by 200 m. Therefore, areas less than 200 m by 200 m can be discounted with a moderate to high degree of confidence as they are not large enough to fully contain the aircraft debris field.

However, this reduction only results in a small overall coverage increase of 0.1 per cent (data gaps) and 0.2 per cent (LPDs) respectively, hence the decision was made to maintain a conservative approach by using the 100 m by 100 m area metric.

Other search area considerations

During the course of the underwater search for MH370 the ATSB actively sought any information or analysis from credible sources which may have assisted in better understanding where the aircraft may be located. A range of information from disparate sources was carefully considered in the context of defining the most probable underwater search area. While some information and analysis did not yield any new insights or was considered and discounted on the basis of new or existing evidence or analysis, it was important to exhaust every avenue which could improve the chance of locating the aircraft.

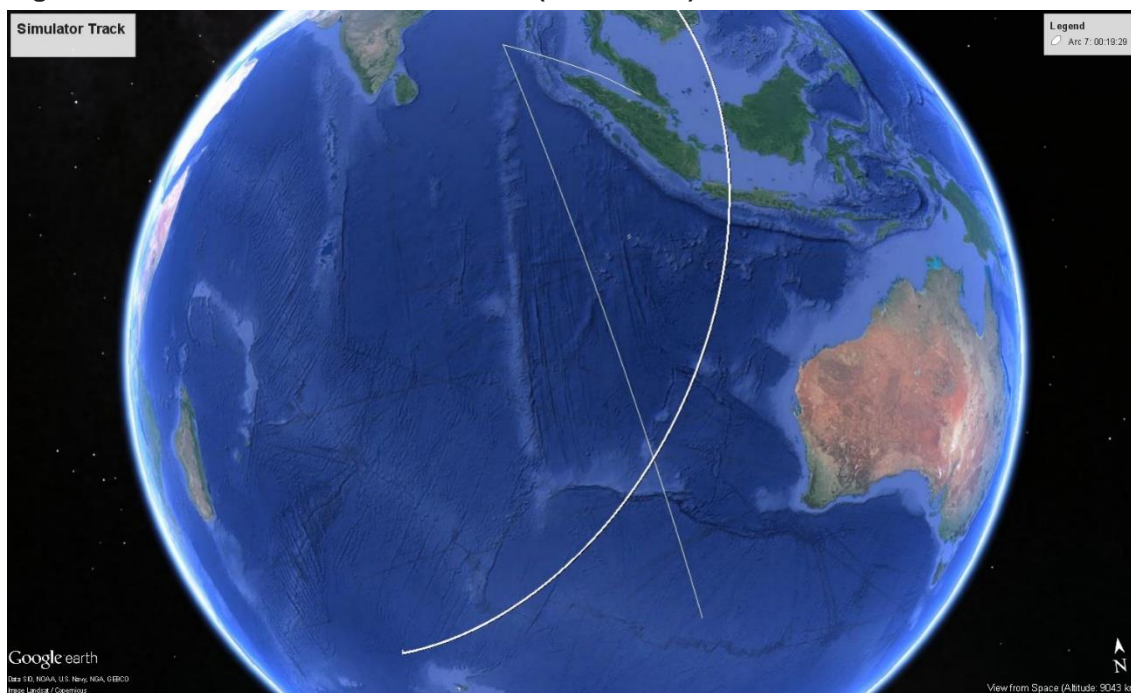
Pilot in Command's flight simulator

Data from the Pilot-in-Command's (PIC) home flight simulator was recovered and analysed in March/April 2014. This information was provided to the ATSB on 19 April 2014, during the surface search and was subsequently also analysed for relevance to the underwater search.

The simulator data was a partial reconstruction of a flight simulator session from 2 February 2014. It comprised four complete and two partial data captures of various aircraft and simulator parameters at discrete points during the simulation. The aircraft simulated was a B777-200LR. Information on the data points is summarised below:

- The initial data point indicated an aircraft at Kuala Lumpur airport.
- No useful location or aircraft information apart from simulator time was able to be recovered for the second data point.
- The next two data points indicated an aircraft tracking to the northwest along the Strait of Malacca.
- The aircraft had climbed to an altitude of 40,000 ft by the fourth data point and was in a 20° left bank, 4° nose down, on a heading of 255°.
- The final two data points were close together in the southern Indian Ocean, 820 NM southwest of Cape Leeuwin. The data indicated that the simulated aircraft had exhausted its fuel. The fifth data point was at an altitude of 37,651 ft, the aircraft was in an 11° right bank and heading almost due south at 178°.
- The data for the sixth data point was incomplete. It was 2.5 NM from the previous data point and the aircraft right bank had reduced to 3°. The aircraft was pitched nose down 5° and was on a heading of 193°. At this time there was also a user input of an altitude of 4,000 ft.

The aircraft track from the simulator data points is shown in Figure 74. The track shows the aircraft flying up the Strait of Malacca before a left turn into the southern Indian Ocean. The aircraft then tracks southeast to the fifth data point (assuming that there is no intermediate data point not captured) to fuel exhaustion at the final point. By the last data point the aircraft had flown approximately 4,200 NM. This was further than was possible with the fuel loaded on board the aircraft for flight MH370. Similarly, the simulated aircraft track was not consistent with the aircraft tracks modelled using the MH370 satellite communications metadata.

Figure 74: Simulator data indicative track (and 7th arc)

Source: Google earth, annotated by ATSB

On the day the simulation was conducted the PIC was on a rostered day of leave. The following day the PIC was rostered to fly from Kuala Lumpur to Denpasar, Bali and return the same day. On 4 February 2014 the PIC was rostered to fly from Kuala Lumpur to Jeddah, Saudi Arabia. The first three data points recovered from the simulator were consistent with the route from Kuala Lumpur to Jeddah. In the weeks between the Jeddah flight and the accident flight the PIC was rostered to fly return flights from Kuala Lumpur to; Denpasar, Beijing, Melbourne and then Denpasar again.

Six weeks before the accident flight the PIC had used his simulator to fly a route, initially similar to part of the route flown by MH370 up the Strait of Malacca, with a left-hand turn and track into the southern Indian Ocean. There were enough similarities to the flight path of MH370 for the ATSB to carefully consider the possible implications for the underwater search area. These considerations included the impact on the search area if the aircraft had been either glided after fuel exhaustion or ditched under power prior to fuel exhaustion with active control of the aircraft from the cockpit.

Controlled glide or ditching

The B777 aircraft can theoretically achieve an unpowered glide ratio of approximately 17:1. That is, for every 1,000 ft of altitude lost in an unpowered glide the aircraft can travel a distance of approximately 2.8 NM. If MH370 was at an altitude of 40,000 ft at the point of fuel exhaustion, the aircraft could be glided more than 100 NM with an average rate of descent between 2,500 and 3,000 ft/min. Simulations conducted in a B777 simulator early in the search, confirmed these results which were included in the ATSB's [MH370-Definition of Underwater Search Areas](#) report released in June 2014.

The possibility of a controlled ditching was carefully considered. Something occurred on board MH370 just before it reached the 7th arc which interrupted the power supply to the satellite data unit (SDU), (it takes a minute for the SDU to reboot after a short interruption of power). Since early in the search, analysis of the aircraft's fuel consumption and endurance, and the characteristics of the final series of SATCOM transmissions had yielded fuel exhaustion as the most likely explanation for the power interruption. However, it was considered that the SDU reboot could be explained in other ways, much less likely, if there was someone active in the cockpit and preparing the aircraft for a controlled ditching.

If the aircraft was being actively controlled during the final segment of the flight south into the Indian Ocean, a series of step climbs²⁸ (which must be initiated by someone active in the cockpit) could have resulted in enough fuel at the end of flight to perform a controlled ditching under power rather than an unpowered glide. At the time the 7th arc was generated by the aircraft logging back onto the SATCOM system, the aircraft could have been descending in a 'normal' landing configuration including full instrumentation and full hydraulic power available for all flight control surfaces including slats and flaps.

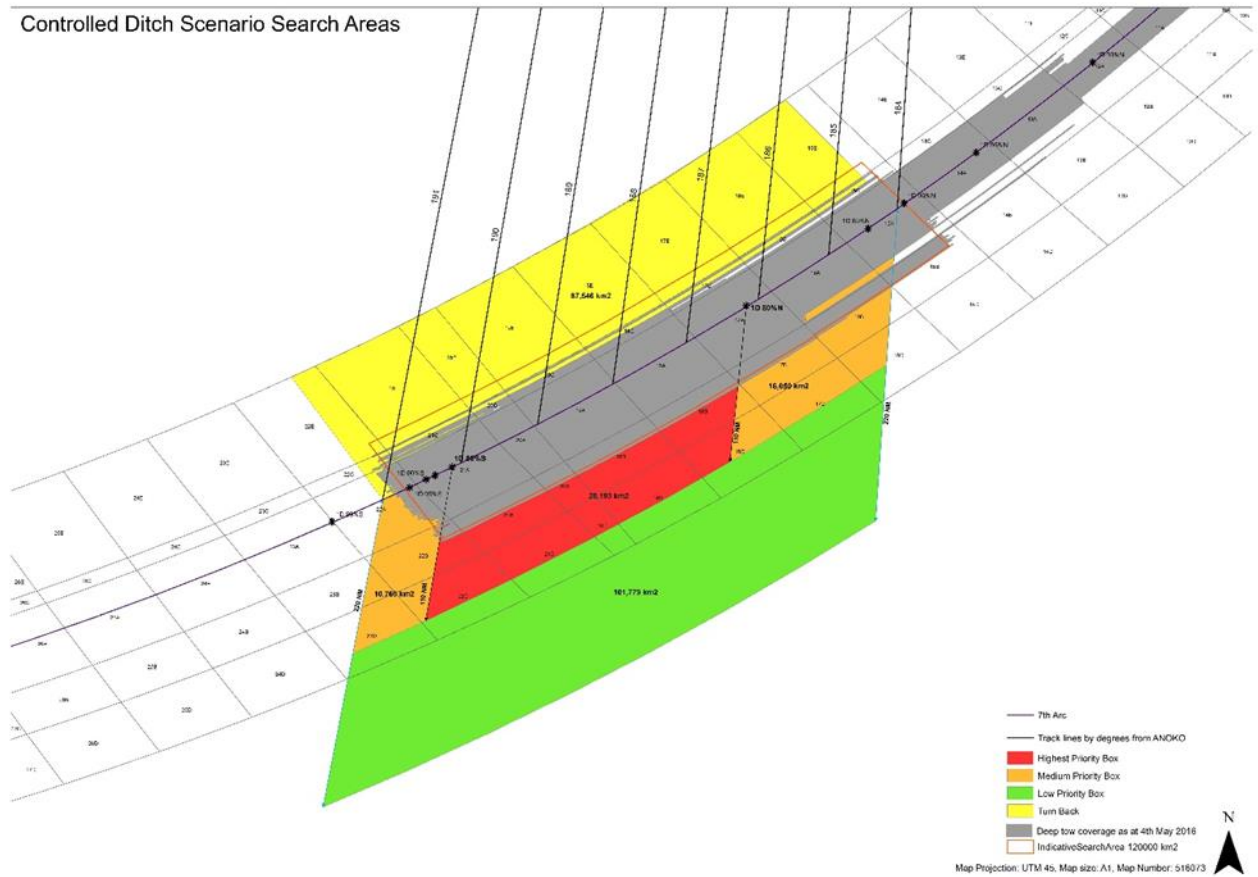
At normal rates of descent (around 2,000 ft/min) the aircraft could have flown approximately 120 NM from the top of descent (an assumed altitude of approximately 40,000 ft) to sea level. If the Boeing ditching procedure were being followed there would have been turns at lower altitudes, firstly to the southwest into the prevailing wind and finally a turn close to sea level to land the aircraft parallel to the prevailing seas.

On 8 March 2014 the sun was 6 degrees above the horizon at 0019:30 UTC as the aircraft reached the 7th arc. Sunrise had been 24.5 minutes earlier, at 2355 UTC. The surface of the ocean would have been visible in order to judge the touchdown on the sea surface. In addition, at the time the aircraft was close to fuel exhaustion, the lightest state it could be, and therefore it was possible to make a controlled ditching with the lowest possible approach speed, with flaps extended in accordance with the Boeing ditching procedure.

The most likely aircraft tracks (after the turn at the tip of Sumatra) derived from the DST Group modelling (summarised in the ATSB's [MH370-Definition of Underwater Search Areas](#) report released in December 2015) were considered at the time with a controlled descent starting just before the 7th arc, indicatively the areas of priority for searching to cover a controlled ditching (or a controlled glide) at the end of flight, as it was considered at the time, are shown in Figure 75.

²⁸ A step climb in aviation is a series of altitude gains that improve fuel economy by moving into thinner air as an aircraft becomes lighter (when fuel is burnt during the flight) and becomes capable of faster, more economical flight.

Figure 75: Indicative controlled ditch scenario search areas at July 2016



Source: ATSB

By June 2016 many pieces of aircraft debris (see following section on Aircraft debris) confirmed or very likely from MH370, had been recovered from east African shorelines. Some items were from within the fuselage. While no firm conclusions could be drawn given the limited amount of debris, the type, size and origin on the aircraft of these items generally indicated that there was a significant amount of energy at the time the aircraft impacted the water, not consistent with a successful controlled ditching.

Critically, a section of right outboard main flap (Figure 81) was found near Tanzania on 20 June 2016. The item was shipped to the ATSB for analysis. This analysis indicated that the flaps were most likely in a retracted position at the time they separated from the aircraft making a controlled ditching scenario very unlikely.

The ATSB’s [MH370-Search and Debris Examination Update](#) on the flap analysis also contained the summary of the analysis [The Use of Burst Frequency Offsets in the Search for MH370](#) performed by DST Group scientists on the final two satellite transmissions from the aircraft. This work quantified the range of possible rates of descent based on the burst frequency offsets of the SATCOM transmissions. In summary, the analysis concluded that the aircraft was descending at a rate of between 2,900 ft/min and 15,200 ft/min when the 7th arc was crossed. Eight seconds later the rate of descent had increased to between 13,800 ft/min and 25,300 ft/min²⁹. These rates of descent ruled out a controlled unpowered glide with the intent to extend range.

²⁹ It should be noted that these descent rates were derived assuming the SDU was still receiving valid track and speed labels from the ADIRU at 0019:37 UTC for use in its doppler pre-compensation algorithm.

Aircraft debris

In the search for MH370, the recovery of debris from the aircraft has provided some of the most important evidence as to what may have happened to the aircraft at the end-of-flight and where it may be located.

Looking at past aircraft accidents, there is almost always some debris left floating after an aircraft crashes in water. The debris will often include items designed to float including seat cushions, life jackets, and escape slides, but also many items of cabin fit-out, like cabin linings and tray tables, which are made of low density synthetic materials. Similarly aircraft structural components, including flight surfaces, may entrap sufficient air to remain buoyant for long periods and have also been commonly found afloat following a crash.

The amount and type of debris varies but it is usually detected and recovered within the first few weeks of the accident before it has been significantly dispersed. Over time, all floating debris will eventually decompose, become water-logged and then sink. For some items of debris this may be relatively fast. For example, items which are buoyant due to entrapped air will sink when the air is released or void spaces become filled, a process which is hastened by the action of wind and waves. Other items constructed of materials which are less permeable, like seat cushions, will float for long periods but they too will eventually sink when the material degrades through chemical and/or mechanical decomposition. This decomposition may take a very long time in the case of some synthetic materials, plastics in particular, but is quicker for items which biodegrade.

The opportunity to locate and recover debris from the sea surface diminishes rapidly over the first few weeks from the time of a crash. Thereafter, there will be some less permeable items of debris which will remain afloat for a longer period but they will be increasingly dispersed. Dispersal is directly related to the surface drift experienced by the individual items of debris which in turn is related to their physical characteristics: size, shape and density. To be found ashore, an item of debris must remain afloat long enough and be subjected to the right combination of winds, waves and currents for it to make landfall.

Modern aircraft like the B777 have many structural and cabin fitout components manufactured of composite materials. These structures are typically of sandwich construction with hard outer layers, often of fibre reinforced plastic or alloy, which are bonded to a honeycomb core. They are light (buoyant), strong and highly resistant to decomposition and therefore may float for long periods before making landfall.

During the course of the underwater search for MH370 numerous items of debris were found and reported to the ATSB originating from a range of Australian and International sources. These items ranged from pieces of mechanical wreckage through to items of clothing, food wrappings and personal items.

When reports were received by the ATSB, contact would be made with the reporter to provide instructions including:

- Note the time and location (GPS position) of the find.
- Take photographs of the debris.
- Note any numbers or distinctive markings.
- Preserve any sea life that might be attached to the item.
- Check if the item floats (this helped to eliminate objects early on).
- Handle the item as little as possible and wrap it to preserve its condition.

Once photographic and other evidence was received, a process of assessment would take place in consultation with the Malaysian Annex 13 investigation team, Malaysia Airlines and Boeing as the aircraft manufacturer. If the item was considered to be potentially MH370 related then the member of the public was advised to hand it in to local authorities to await collection, usually by the Malaysian authorities. On several occasions debris was shipped directly to the ATSB

laboratories in Canberra and analysed at the request of the Malaysian Annex 13 investigation team.

The flaperon

On 29 July 2015, more than 500 days after the aircraft went missing, a large item of aircraft debris was recovered from a beach on La Réunion Island in the western Indian Ocean. A preliminary assessment confirmed that it was possibly a flaperon (a flight control surface which has the dual functions of an aileron and flap) from a B777 aircraft. The item was taken by the French authorities on the island and shipped to Toulouse in France for examination under the control of French judicial authorities.

The examination revealed a range of part and serial numbers marked on internal components of the item which were compared with the manufacturer's records to confirm that the item was the right flaperon from the B777 aircraft operating flight MH370. The flaperon was the first item of debris positively confirmed to have come from MH370.

A number of other tests and examinations were made in France on the flaperon, including marine specimen examinations (barnacles attached to the flaperon), failure analysis of metal and composite components and flotation testing. Details of all examinations were provided to the ATSB by the French judicial authorities to assist with the search for MH370 (the public release of any reports on the flaperon examination is the responsibility of the French judicial authorities). Figure 76 shows the flaperon buoyancy testing conducted in France.

Figure 76: The flaperon buoyancy test



Source: Direction Générale de l'Armement Techniques Aéronautiques

Other parts recovered

Following the recovery of the flaperon, many more items of debris were found and recovered from beaches in Madagascar, Mauritius, Mozambique, South Africa and Tanzania late in 2015 and early 2016. Further debris items confirmed as originating from MH370 are shown in Figure 77, Figure 78, Figure 79, Figure 80 and Figure 81. Debris examination reports of these items are available on the ATSB website at www.atsb.gov.au.

Figure 77: Engine cowling section



Source: ATSB

Figure 78: Right wing flap track fairing section



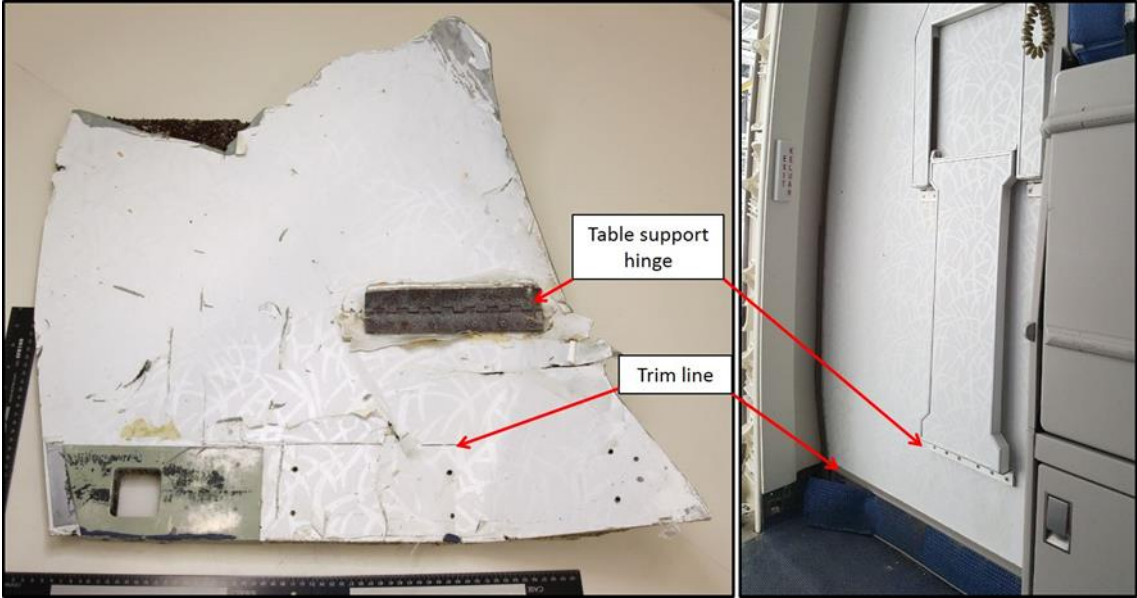
Source: ATSB

Figure 79: Right horizontal stabilizer panel section



Source: ATSB

Figure 80: Internal cabin bulkhead panel section



Source: ATSB and Ministry of Transport Malaysia

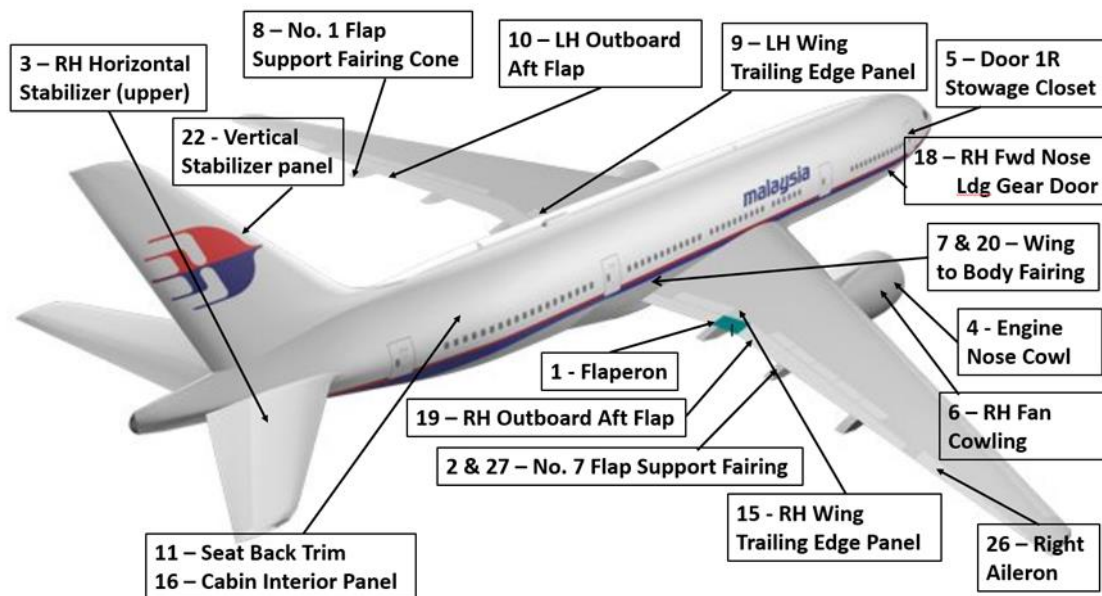
Figure 81: Right outboard flap section



Source: ATSB

Debris examination reports are available on the Ministry of Transport Malaysia website at www.mh370.gov.my. At the time of writing, 18 items were identified as being very likely or almost certain to originate from MH370, with another two assessed as probably from the accident aircraft. These are illustrated in Figure 82.

Figure 82: General locations of items recovered. Some parts could have come from different locations than shown



Source: Ministry of Transport Malaysia

Marine ecology examinations

When the flaperon was recovered from La Réunion Island there was a significant amount of marine growth attached to it. The majority of the marine organisms were a type of goose barnacle (*Lepas (Anatifera) anatifera striata*). After taking advice from an expert at the Western Australia Museum, who also identified the barnacle, the ATSB came to understand that the attachment and growth of the barnacles may reveal some evidence in relation to where the flaperon started its drift in the Indian Ocean and the passage that it took in the succeeding 500 days before it came ashore. Also, critically, that the chemical composition of the barnacle shells may yield some information about the temperature and salinity of the water where the various stages of the barnacle growth took place. For the oldest (and largest) barnacles it was thought that this may yield some evidence as to where MH370 may be located.

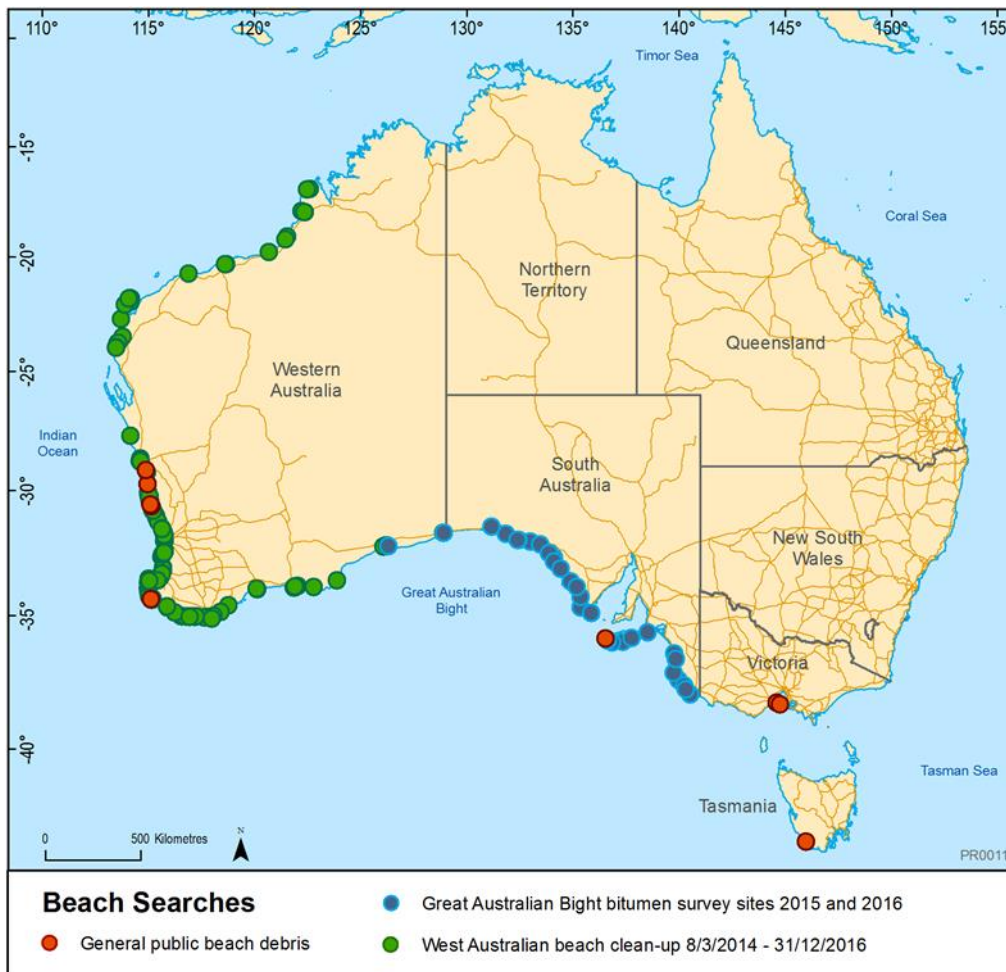
This advice was provided to the French investigation team who performed some analysis on the flaperon barnacles. Later the French investigation team provided some samples of the largest barnacles to Geoscience Australia who passed them onto a team at the Australian National University led by Dr Patrick De Deckker for further analysis. The results of the analysis were inconclusive, Dr De Deckker's report is reproduced at appendix F.

All suspected MH370 debris which were transported to the ATSB laboratories in Canberra underwent quarantine and processing at Geoscience Australia's Canberra facility en route. Processing involved photographing, examining, identifying (and removing) any organisms contained within, or attached to, the items of debris. Any items of particular interest were referred to relevant specialists for further analysis and advice. The scientific team from Geoscience Australia coordinated a range of identification and examinations which are included in appendix G.

Australian beach searches

Since the start of the search for MH370 the ATSB has been cognisant that any confirmed debris finds on the Australian coastline may be significant to the search. Initial drift modelling indicated that the most likely place for debris to come ashore in Australia in 2014-15, in particular, was the coast of Western Australia or South Australia. Various organisations and members of the public undertook searches along Australian coastlines which included actively looking for any form of debris that could possibly have originated from MH370. Australian beaches searched are depicted in Figure 83.

Figure 83: Australian beach search locations

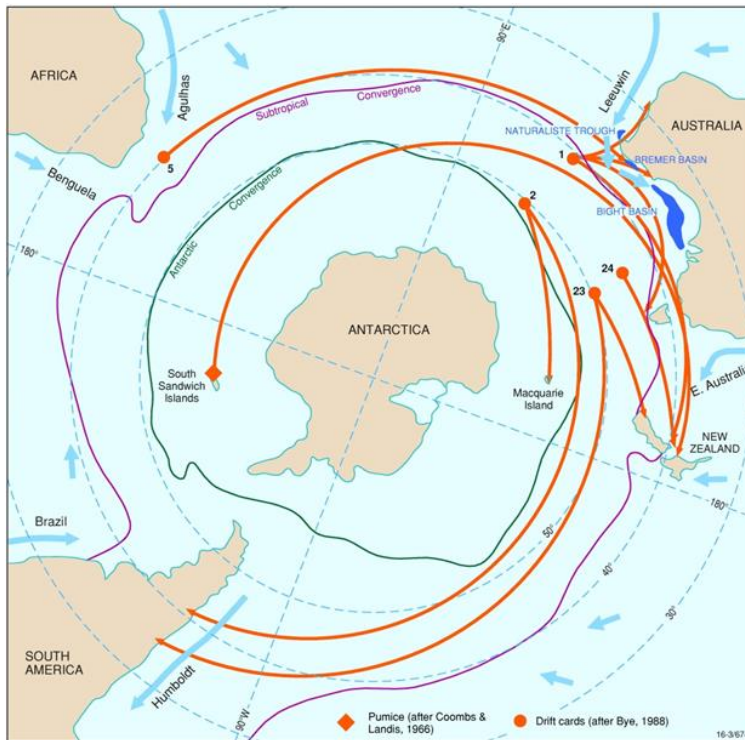


Source: ATSB. We acknowledge that the source of the West Australian beach clean-up data used in this image was the Tangaroa Blue Foundation Ltd Australian Marine Debris Initiative database with data being collected and provided by many individuals and organisations

Great Australian Bight

The University of Adelaide in conjunction with CSIRO conduct regular annual surveys of beaches sponsored by the petroleum industry stretching from the eastern coast of Western Australia, through South Australia to the western beaches of Victoria collecting bitumen from marine petroleum seeps which have drifted into the Great Australian Bight. Over time, specific beaches have been identified and targeted where the likelihood of finding bitumen washed up from global and local currents is likely. The origin of the bitumen ranges from either South East Asia, where they have drifted in the Leeuwin current down the western Australian coast, Southern Africa where they have drifted across the Indian Ocean or potentially from sedimentary basins in the Great Australian Bight. Known currents from historical research are depicted in Figure 84.

Figure 84: Known circulation of currents and bitumen samples from 40° south latitudes



Source: Padley, D 1995, 'Petroleum geochemistry of the Otway Basin and the significance of coastal bitumen strandings on adjacent southern Australian beaches', PhD thesis, University of Adelaide

Bitumen surveys were conducted in September 2015 and October 2016 (Table 27). The surveys covered various beaches across the Great Australian Bight. The University of Adelaide and CSIRO were contacted through Geoscience Australia staff (involved with the MH370 search project) and were asked to assist the ATSB by also looking for anything that could conceivably be debris from MH370.

The following beaches were searched over the two years (2015 and 2016) and no debris from MH370 was located.

Table 27: Bitumen survey beaches

Area	Beach Name	Latitude	Longitude
Limestone Coast	28 Mile Crossing	S 36.437	E 139.772
Eyre Peninsula	Avoid Bay	S 34.669	E 135.345
Kangaroo Island	Bales Beach	S 35.992	E 137.346
Limestone Coast	Beachport Conservation Park	S 37.446	E 139.963
Eyre Peninsula	Cactus Beach	S 32.077	E 132.979
Eyre Peninsula	Cape Bauer	S 32.714	E 134.094
Great Australian Bight	Delisser Sandhills	S 31.716	E 128.896
Great Australian Bight	Dogfence Beach	S 31.769	E 131.842
Eyre Peninsula	Elliston	S 33.646	E 134.888
Limestone Coast	Evans Cave (Eves Cove)	S 37.182	E 139.744
Great Australian Bight	Eyre Bird Observatory	S 32.254	E 126.301
Great Australian Bight	Eyre Well	S 31.464	E 131.144
Eyre Peninsula	Fowlers Bay West	S 32.005	E 132.440
Eyre Peninsula	Gascoigne Bay West	S 32.529	E 133.893
Limestone Coast	Geltwood Beach	S 37.659	E 140.223

Eyre Peninsula	Hanson Bay	S 36.017	E 136.853
Eyre Peninsula	Mount Drummond Beach	S 34.258	E 135.343
Limestone Coast	Nene Valley	S 37.986	E 140.514
Limestone Coast	Number 1 and 2 Rocks (Channel Rocks)	S 37.796	E 140.321
Kangaroo Island	Pennington Bay	S 35.852	E 137.745
Eyre Peninsula	Point Peter	S 32.177	E 133.440
Kangaroo Island	Sandy River	S 35.951	E 136.634
Eyre Peninsula	Scott Bay	S 32.004	E 132.389
Eyre Peninsula	Sheringah Beach	S 33.873	E 135.174
Eyre Peninsula	Sleaford Bay	S 34.882	E 135.846
Eyre Peninsula	St Mary Bay	S 32.530	E 133.856
Eyre Peninsula	St Mary Bay South	S 32.536	E 133.857
Limestone Coast	The Granites	S 36.658	E 139.854
Eyre Peninsula	Tractor Beach	S 32.869	E 134.113
Eyre Peninsula	Tyringa Beach	S 33.147	E 134.418
Limestone Coast	Waitpinga Beach	S 35.635	E 138.499
Kangaroo Island	West Bay	S 35.888	E 136.553

Source: CSIRO and the University of Adelaide

Western Australia

The Tangaroa Blue Foundation and Celestial Vision conduct regular clean-ups of Australian coastlines.

The Tangaroa Blue Foundation

The Tangaroa Blue Foundation (Tangaroa Blue) is an Australia wide not for profit organisation dedicated to removal and prevention of marine debris entering the ocean systems. Further information is available at www.tangaroablue.org.

Tangaroa Blue organise volunteer beach and coastline clean-ups for the purpose of their marine debris research program. In 2014 and again in 2015 and 2016 organisers at Tangaroa Blue were contacted to be on the lookout for MH370 related debris on the Western Australian coastline.

Between the dates of 8 March 2014, and 8 April 2015 there were a total of 387 beach clean-ups reported to Tangaroa Blue along the Western Australian coastline between the South Australian and West Australian border and north to Kalbarri. These clean-ups involved 6,095 working hours with over 17 tonnes of marine debris and rubbish collected. In 2016 just under 1,800 volunteers at 138 beach locations removed more than 88,880 items of rubbish from the Western Australian coastline as part of the 2016 West Australian Beach Clean-up.

There were many items of possible MH370 debris reported by Tangaroa Blue during these beach clean ups, all of which were assessed but none of which were confirmed as originating from MH370.

Celestial Vision

The company proprietor of Celestial Vision undertakes photography for numerous publications and regularly visits coastal locations in mid to southern Western Australia. Celestial Vision is one of the many contributors to Tangaroa Blue and undertook an active search of beaches for MH370 debris.

The searches covered an area of almost 14 hectares, at 15 sites, along a 450 km section of the Western Australian coastline, between Myalup, and Drummond Cove (north of Geraldton). Some

beaches were visited more than once. Some items of possible interest in relation to MH370 were located and assessed but none were confirmed as originating from MH370.

Investigations of beach debris found by the general public

Media reporting of MH370 has been extensive which has prompted members of the public to look for and report items of debris found on Australian beaches. All reported finds were assessed but none were confirmed as originating from MH370. Two recent examples are included below, Figure 85 and Figure 86.

Debris from Kangaroo Island, South Australia (June 2016)

A member of the public notified ATSB in early June 2016 of an unusual piece of debris found on a beach on Kangaroo Island off the South Australian coast.

The item of interest was made of a similar composite material as those washed up on the African coastlines. There was little evidence of marine growth suggesting a short period in the water but the item was brought to Canberra by ATSB staff for examination.

Figure 85: Debris found on Kangaroo Island, South Australia



Source: South Australia Police

The item was marked with a stencil “No Step” in a font not used by Malaysia Airlines and although the item was a similar construction to aircraft components the colour of the paint differed enough to eliminate the origin of the item as being from MH370.

Debris from Queenscliff, Victoria (November 2016)

A member of the public notified the ATSB in early November 2016 of an unusual piece of debris found on a beach at Queenscliff, south of Melbourne on the Bellarine Peninsula at the entrance to Port Phillip in Victoria.

Figure 86: Debris found in Queenscliff, Victoria

Source: Victoria Police

The item was constructed with a carbon composite skin over an aluminium honeycomb core and had two square panels. The photographs of the item were assessed by Malaysia Airlines and Boeing and it was concluded it did not originate from MH370.

Debris drift analysis

Debris drift studies have been used extensively throughout the search for MH370. Early drift studies during the surface search in March and April 2014 aimed to inform the deployment of aircraft and vessels in the southern Indian Ocean searching for aircraft debris floating on the sea surface. Later drift studies in 2014 aimed to complement the search area definition analysis based on the SATCOM data by providing indications of likely timings and locations of debris landfall.

Following the release of the ATSB's *MH370 - Definition of Underwater Search Areas* report on 26 June 2014, a drift model was applied by one organisation (who had been a part of AMSA's drift modelling working group during the surface search) to the wide search area defined in the report. The drift modelling was run to provide an indication of when and where the first possible debris would make landfall. This modelling indicated that the first possible landfall was on the west coast of Sumatra, Indonesia and would have occurred in the first few weeks of July 2014. Indonesian search and rescue authorities were subsequently advised of the possibility of debris washing up on their shorelines.

In November 2014, the ATSB asked CSIRO to perform a drift study based on the revised search area defined in the *MH370 - Flight Path Analysis Update* report released on 8 October 2014. The CSIRO study indicated that there was an extremely low probability that any debris from MH370 would have made landfall at that time and the results were not consistent with the other organisation's study which indicated a Sumatra landfall (the study was later found to be erroneous). The ATSB fact sheet [MH370: Aircraft Debris and Drift Modelling](#) contains more information about the initial debris and drift modelling work.

A further drift study was performed by the CSIRO following the discovery in July 2015 of the first confirmed item of debris from MH370 (the flaperon) to identify the likely point of origin. The challenge associated with all the studies of MH370 debris is to trace the origin of debris which have been adrift for long periods of time and travelled thousands of kilometres in open ocean conditions.

In April 2016 the ATSB commissioned CSIRO to perform a comprehensive drift study to determine the likely origin of the significant numbers of MH370 debris items which had been found on African shorelines since December 2015. The discovery of many items of debris from MH370 confirmed the existence of a debris field, thereby discounting the possibility of an intact aircraft, and combined with the results of the seafloor search, narrowed the range of potential aircraft impact locations. The study differed from earlier drift modelling as all sources of evidence in relation to debris were considered and a number of modelled debris items were field tested to positively establish actual rates of drift in measured wind and wave conditions. The results of this study and subsequent complementary work are detailed in a series of reports jointly published by the CSIRO and ATSB.

The first CSIRO report, [The search for MH370 and ocean surface drift](#), was released on 20 December 2016, and the analysis was based on:

- measuring the wind-driven drift rate of replica aircraft parts alongside oceanographic drifters (whose travel times across the Indian Ocean are well known)
- using an updated ocean surface current model, derived by accurate satellite measurements of small perturbations of sea level to yield estimates of surface currents, which were then validated using the global archive of oceanographic drifters.

The drift study also took into account other evidence including the:

- absence of debris findings on the Western Australian coastline
- absence of debris findings during the surface search
- July 2015 arrival time of the flaperon at La Réunion Island
- December 2015 and onwards arrival times of confirmed aircraft debris on shorelines in the western Indian Ocean.

The drift study concluded that latitudes from 36°S to 32°S, close to the 7th arc, were the most prospective as the likely point of origin of the recovered aircraft debris. The drift study identified an area near 35°S close to the 7th arc as particularly prospective, as this area was most consistent with all the evidence.

The drift study also concluded that:

- Debris originating north of 32°S, close to the 7th arc, would probably have been detected by the surface search, and that debris originating from this area would have probably arrived in Africa before December 2015.
- Debris originating south of 39°S, close to the 7th arc, would have been more likely to have arrived on the Australian coast than on eastern African coastlines.

The second CSIRO published report, [The search for MH370 and ocean surface drift – Part II](#), was released on 21 April 2017. This drift study provided further validation that the area near 35°S on the 7th arc was the most prospective point of origin for the recovered aircraft debris. This result was based on the field testing of a genuine Boeing 777 flaperon cut down to match the flaperon recovered from MH370. The new field tests showed that the net drift of the actual flaperon due to its asymmetrical shape would have been at an angle to the prevailing winds and seas which explained the July 2015 arrival at La Réunion Island with more precision.

The third CSIRO published report, [The search for MH370 and ocean surface drift – Part III](#), was released on 16 August 2017. This drift study tracks the point of origin of possible MH370 debris, identified by Geoscience Australia, in four French Pleiades satellite images captured on 23 March 2014 in an area to the west of the 7th arc (see section on Satellite imagery analysis). The study concluded:

- The most likely location of the aircraft point of impact is an area around 35.6°S, 92.8°E.
- Further possible yet lower likelihood aircraft impact locations are within about 50 km and parallel to the east of the 7th arc.

- A range of possible but lower likelihood aircraft impact locations are near 35.2°S 91.9°E on the western side of the 7th arc.

The discovery of MH370 debris in 2015 and 2016 has been the sole source of new evidence in the search for MH370 (since March 2014). The analysis of this debris, and particularly the drift studies, have yielded new insights about the likely location of the aircraft. The capture of possible debris in the French satellite imagery only two weeks after the aircraft was lost allows drift modelling results to be refined with considerable accuracy. While it cannot be concluded with certainty that the items identified in the satellite imagery are MH370 debris, the coincidence of the area identified in the drift study with all other search area analysis including the results of the surface and underwater searches is compelling.

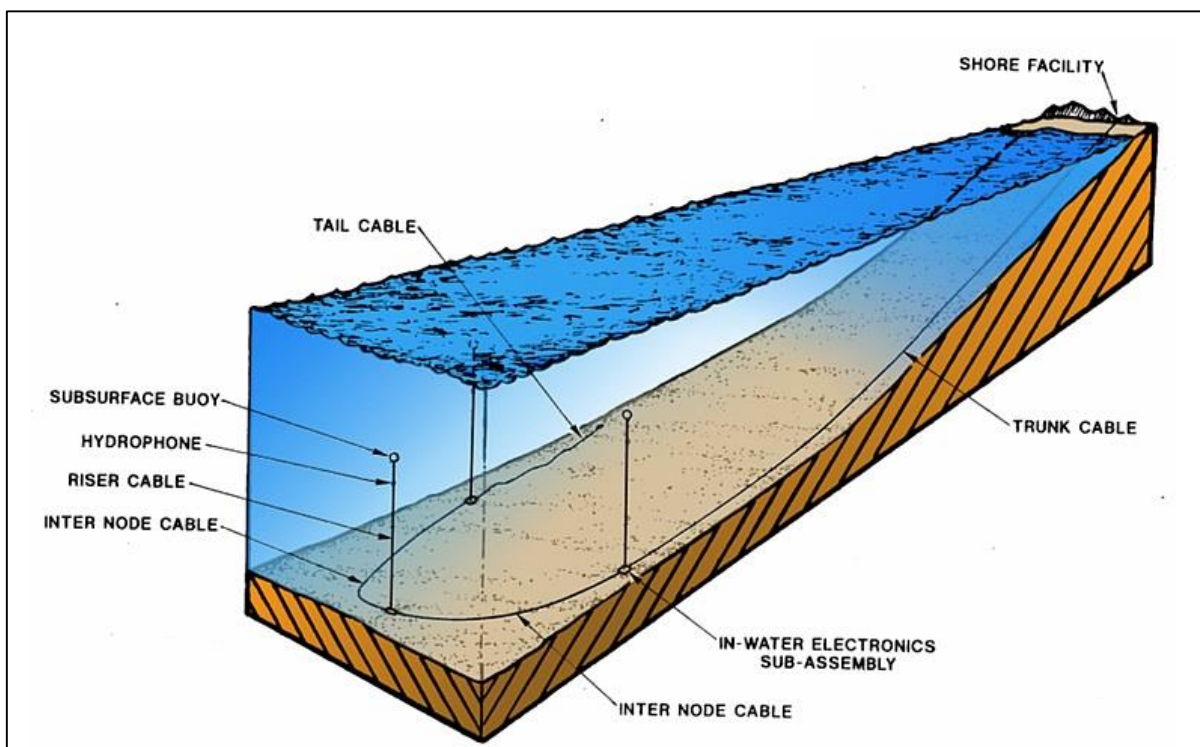
Hydroacoustic analysis

At a depth of about 1,000 m there is a layer of water where sound travel is particularly efficient. This layer is called the Sound Fixing and Ranging Channel, or SOFAR channel. Hydroacoustic monitoring makes use of this channel, and the phenomenon of sound waves being ‘trapped’ in that layer and therefore propagating over a very large distance.

As part of the United Nations Comprehensive Nuclear-Test-Ban-Treaty Organization or the Integrated Marine Observing System (IMOS), there are a network of hydrophones installed in oceans around the world. There are two of these stations located in the Indian Ocean; one installed off the coast of Perth (HA01) and one installed at Diego Garcia (HA08).

Each station consists of an array of three hydrophones separated in space (Figure 87) and connected to a shore facility via a trunk cable.

Figure 87: Diagram of a hydrophone array showing three hydrophones and connection to a shore facility



Source: Comprehensive Nuclear Test-Ban-Treaty Organization

For a given acoustic source origin, the configuration of the three hydrophone produces a different arrival time at each hydrophone. Analysis of these arrival times allows relatively accurate determination of the bearing to the sound source. The array can also give a coarse estimate of the distance from the hydrophone, however the tolerance in these calculations is large. In order to

accurately identify the origin of a signal, at least two stations are required to perform a triangulation on that signal.

After MH370 went missing, it was hypothesised that an impact with the water of a B777 could have created an acoustic source sufficiently large to propagate into the Sound Fixing and Ranging Channel and therefore to the hydrophone stations. As such, the hydroacoustic signals present in the Indian Ocean around the time of the aircraft's expected impact with water were examined to determine whether they could provide any information to help define the search area. Additional data was also received from recordings of low-frequency underwater acoustic signals from data loggers off the Western Australian coast owned by Curtin University's Centre for Marine Science and Technology (CMST).

The ATSB requested that CMST and DST Group analyse all available signals in an attempt to detect and localise underwater sounds that could be associated with the impact of the aircraft on the water or with the implosion of wreckage as the aircraft sank.

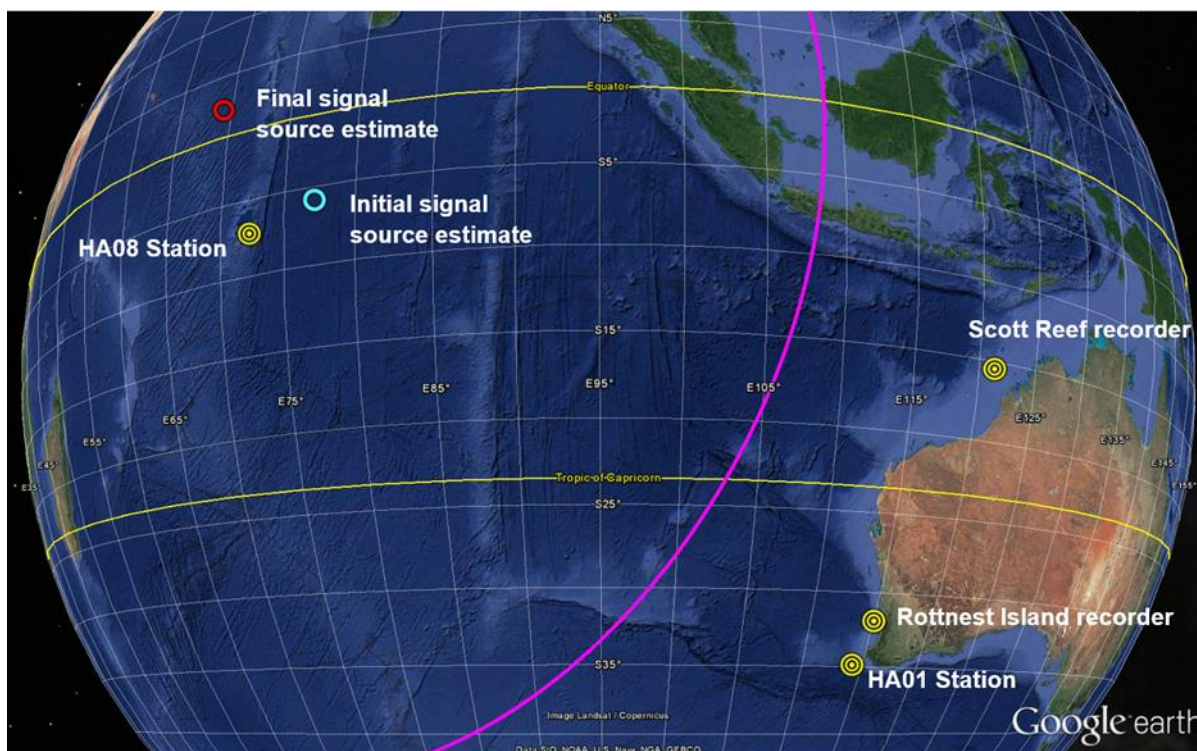
The CMST provided two reports to the ATSB:

- *Analysis of Low Frequency Underwater Acoustic Signals Possibly Related to the Loss of Malaysian Airlines Flight MH370*, CMST report 2014-30; 23 June 2014, (appendix H).
- *Results of analysis of Scott Reef IMOS underwater sound recorder data for the time of the disappearance of Malaysian Airlines Flight MH370 on 8th March 2014*; 4 September 2014, (appendix I).

The first report found one acoustic event of interest that occurred at a time that potentially linked it to MH370. This event was received on one of the Integrated Marine Observing System recorders near the Perth Canyon (RCS) and at the Comprehensive Nuclear-Test-Ban-Treaty Organization hydroacoustic station at Cape Leeuwin (HA01). A detailed analysis of these signals resulted in an estimated signal source that was compatible with the timing of the last satellite handshake with the aircraft, but incompatible with the satellite to aircraft range derived from this handshake.

The second report used data from a hydroacoustic logger from the Scott Reef to further examine the signal of interest. Based on this further data, the source was identified as being likely of geological origin and originating from the Carlsberg Ridge (source shown in Figure 88 as a red circle).

Figure 88: Locations of the hydroacoustic stations and the estimated signal source locations



Source: Google earth, annotated by ATSB using Curtin University Centre for Marine Science and Technology data

The Los Alamos National Laboratory in the United States also published an analysis of the hydroacoustic signals (appendix J). The conclusions of this report were that there was a possible candidate arrival at HA01 that indicated the southern portion of the search area. The analysis highlighted that this signal was problematic due to its close proximity in time to the arrival at the station of an acoustic signal from an ice event from Antarctica.

CMST, acting as advisor to the ATSB, reviewed all the submitted and published analyses including the Los Alamos National Laboratory report. The result of this review did not identify any further signals of interest.

At the first principles review, the complete hydroacoustic data analysis results were presented. Meeting participants determined that hydroacoustic analysis did not contribute any useful new information to the search.

Satellite imagery analysis

During the initial stages of the search for MH370 there was a concerted effort to identify MH370, or a possible condensation trail from the aircraft, in any available satellite imagery captured over the Malay Peninsula and the Strait of Malacca. Available satellite imagery for the Indian Ocean was also later analysed for the time of the flight and some hours after. The aircraft was not identified in any of this imagery although some possible condensation trails were identified and analysed.

During the subsequent surface search in the Indian Ocean, AMSA, with the assistance of the Australian Geospatial-Intelligence Organisation, made requests of foreign governments including France, Italy, Germany, Thailand, the People's Republic of China and the United States to capture imagery (in various electromagnetic spectra including radar, optical and infrared) using their low earth orbiting satellites in the region of the MH370 search area. The intent was to cover as wide an area as possible with the satellites in the hope that aircraft debris floating on the ocean surface

could be identified in order to focus the aerial and surface vessel search. This request was made around 15 March 2014, a week after the aircraft went missing.

In the first week of the surface search satellite imagery was provided to AMSA in which possible debris had been identified. The area was in the region of 43-45°S, 90-97°E and this area was extensively searched by aircraft between 20 and 27 March 2014 without locating any MH370 related debris.

From 20 to 23 March 2014 possible debris was also detected in satellite imagery well to the north of the area being searched at the time. These satellite images of possible debris, both radar and optical, were captured much closer to the 7th arc in the region of 34-35.5°S, 90-92°E but the area was never searched by air. At the time of these detections, the surface search was focused elsewhere and there were two merchant vessels transiting through the area who had been warned to be on the lookout for debris. No reports of debris were received from these vessels.

Contrails analysis

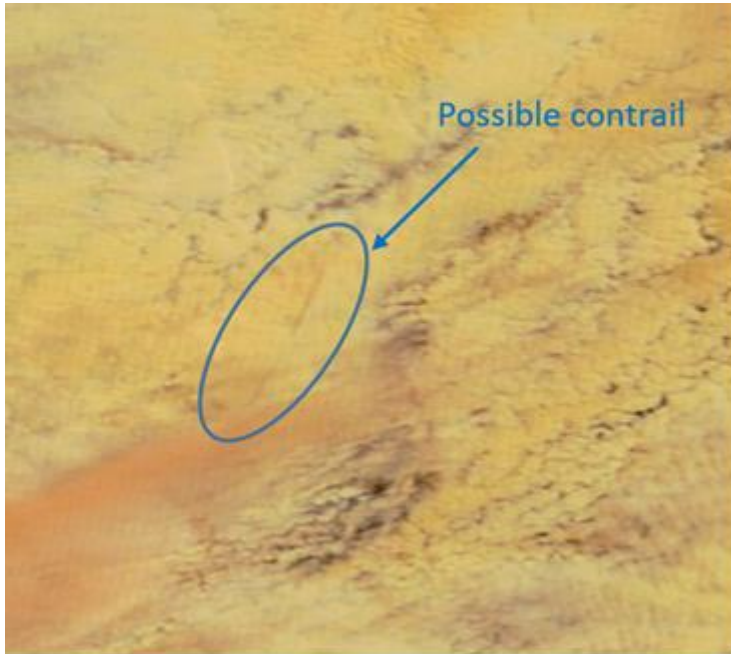
In April 2014, scientists³⁰ from the National Aeronautics and Space Administration (NASA) in the United States analysed satellite imagery in the Indian Ocean looking for possible MH370 condensation trails (contrails). Their approach was to examine all available polar-orbiting satellite imagery available along possible MH370 flight tracks between 1900 UTC on 7 March 2014 and 0500 UTC on 8 March 2014. They also examined atmospheric temperature and moisture profiles to determine the potential for contrail formation at these times and locations.

One possible contrail was identified in NASA's Terra satellite Moderate Resolution Imaging Spectroradiometer (MODIS) instrument data at 0445 UTC on 8 March at 45.5°S, 84°E with an orientation from north-northeast to south-southwest, Figure 89. It was concluded that atmospheric conditions at the time were suitable for contrail formation. The position and orientation of the possible contrail, when cloud motion was accounted for over the previous four hours, were found to be broadly consistent with the assumptions about MH370's flight path at the time.

The possible contrail was analysed in the Terra MODIS data captured at several different wavelengths, and also using other satellite imagery captured around the same time in the area, and it was concluded that the possible contrail was probably a shadow from some other feature or a cloud edge.

³⁰ Dr Patrick Minnis, Kristopher Bedka, Doug Spangenberg and David Duda, NASA

Figure 89: Terra satellite MODIS image, 0445 UTC, 8 March 2014 at 45.5°S, 84°E



Source: NASA, annotated by ATSB

Later in the underwater search, the NASA scientists also provided an assessment of a third party analysis of possible condensation trails in satellite imagery captured at the northern tip of Sumatra around the time of the flight of MH370. They concluded after studying a range of satellite imagery for the area at the time that what had been identified as possible contrail was probably a nearly linear discontinuity in the stratocumulus cloud deck.

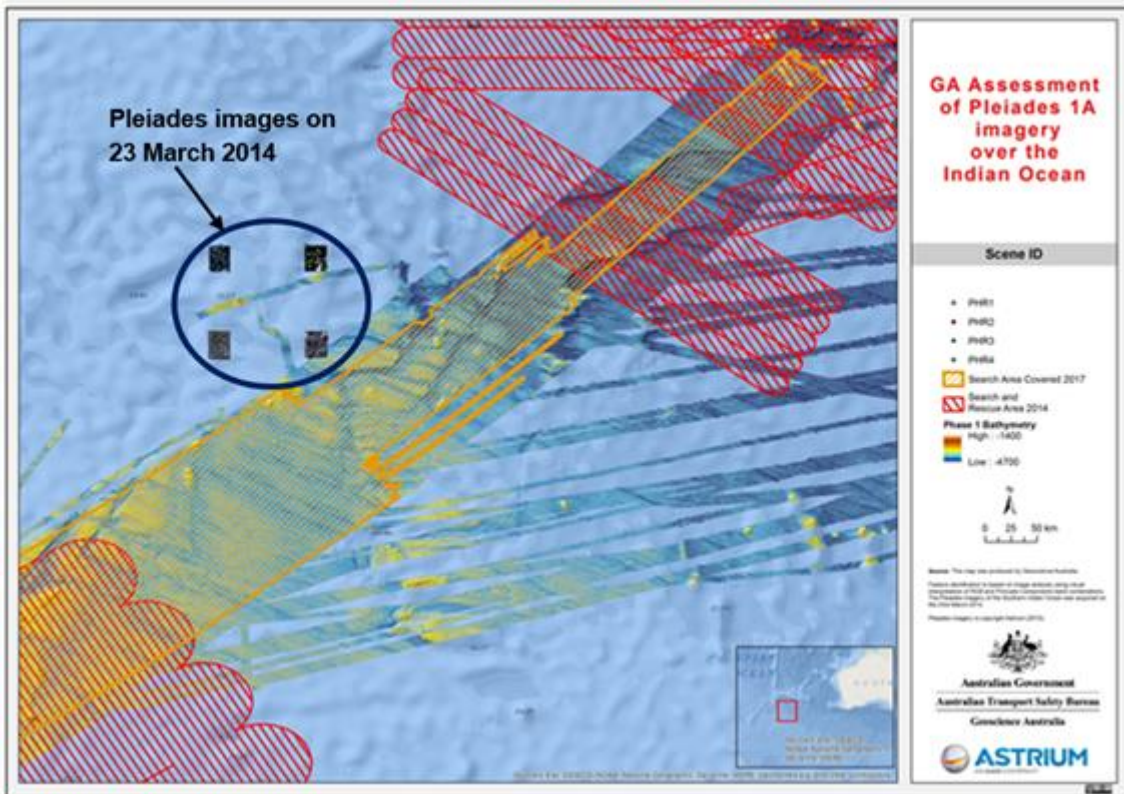
Reanalysis of satellite imagery

At the time the surface search commenced in the southern Indian Ocean on 18 March 2014, it was not known with certainty whether or not there was any debris still adrift in the search area nor the composition of that debris. The discovery of a range of MH370 debris on eastern African shorelines in 2015 and 2016 confirmed that debris was adrift at the time of the surface search, and importantly, the size, shape, colour and composition of some debris items. The discovery of this debris prompted the reanalysis of aerial surface search debris sightings and available satellite imagery based on the now known physical characteristics of some of the items.

Early in 2017 the French Ministry of Defence provided the ATSB with four native resolution optical satellite images from their Pleiades satellite constellation. The four images were captured on 23 March 2014 to the northwest of the 7th arc (Figure 90) in an area not searched by aircraft during the surface search. The area where the satellite images were captured was also significant as it was where MH370 debris was likely to have drifted, initially to the northwest, in the two weeks after MH370 was lost if the aircraft had impacted the water close to the 7th arc around latitude 35°S.

If debris could be identified within the satellite imagery it would provide very strong support to the range of other analyses indicating that the aircraft had impacted the water close to the 7th arc around latitude 35°S, specifically the CSIRO debris drift studies: [The search for MH370 and ocean surface drift](#) and [The search for MH370 and ocean surface drift-Part II](#). The original French analysis in March 2014 had identified four possible objects which may be debris in the satellite images. The ATSB asked Geoscience Australia to reanalyse the images and determine whether the images included objects that were potentially man-made in origin.

Figure 90: Location of four Pleiades satellite images, surface and underwater search areas



Source: Geoscience Australia, annotated by ATSB

Geoscience Australia’s analyses included semi-automatic workflows and a comprehensive analysis using manual visual interpretation, with the optical data subjected to a principle components analysis to help distinguish potential objects from their surroundings. On 16 August 2017 the ATSB released Geoscience Australia’s report: [Summary of imagery analyses for non-natural objects in support of the search for Flight MH370](#), which concluded that the four satellite images contain at least 70 identifiable objects, with twelve being assessed as probably man-made and a further 28 objects assessed as possibly man-made. The resolution of the images at 0.5 m² was insufficient to conclude with certainty that any of the objects were debris from MH370 however some objects show geometric shapes that do not conform with wave patterns or other expected natural phenomena.

The ATSB passed the results of Geoscience Australia’s analysis to CSIRO to perform a drift study to determine with greater precision where the objects identified in the imagery were likely to have been on 8 March 2014. CSIRO’s report [The search for MH370 and ocean surface drift – Part III](#), released with Geoscience Australia’s report in August 2017, analyses the origin of the objects and concludes that if any of the objects identified in the satellite imagery are from MH370 that the most likely place the aircraft impacted the ocean was 35.6°S, 92.8°E (see section on Debris drift analysis).

External contributions

Over the course of the past three years the search for MH370 has prompted significant public interest and an extraordinary amount of correspondence with the ATSB from external sources. Individuals and groups with a variety of expertise submitted their considerations, theories and analysis supporting particular search locations. The ATSB has maintained a dialogue with various individuals and groups throughout the search, monitored online discussion forums and responded

to queries from MH370 researchers. The credible analyses provided by various external contributors were considered alongside the work of the search strategy working group.

The ATSB acknowledges the extensive contributions that many individuals and groups have made during the underwater search for MH370. Many contributors have provided credible, alternate and independent approaches and analysis of the limited data available. In particular, the 'MH370 Independent Group' comprised of scientists, researchers and individuals who have cooperated across continents to advance the search for MH370. The ATSB is grateful for their work collectively and individually including Duncan Steel, Mike Exner, Victor Iannello, Don Thompson, and Richard Godfrey. The ATSB also acknowledges the extensive and detailed contributions provided by Simon Hardy, Bobby Ulich and Robin Stevens.

The search for MH370 was significantly advanced after the first debris from the aircraft was found on La Reunion Island in July 2015. The subsequent efforts of Blaine Gibson in searching for and locating MH370 debris on east African coastlines did much to raise public awareness of the importance of the MH370 debris which led to many more items of debris being handed in. Mr Gibson met and communicated with ATSB during his 2015-2016 search expeditions and he is acknowledged for his outstanding efforts in communicating his debris finds to Malaysia, ATSB, the next of kin and the wider world.

Other search considerations – risk mitigation

The underwater search was conducted continuously over more than two and a half years in a remote area up to 1,500 NM off the west coast of Australia. The search was conducted in latitudes between 33°S and 39°S, an area where the weather is often poor depending on the season and seas are very often rough and, occasionally, extreme. There were significant risks to the search vessels and their crews associated with conducting the underwater search in these conditions which needed to be carefully managed.

Weather

Large weather systems consistently moved through or near the search area. The latitude of operations at different times in the search (both surface and underwater) was a major factor in the impact of these weather systems. During the surface search the vessels and aircraft experienced a wide range of weather conditions. Typically search operations could proceed however, in choppy sea surface conditions with breaking waves the ability to detect floating debris can be more difficult.

Most of the underwater search was conducted from latitudes 33°S to 39°S in the Indian Ocean adjacent to the 7th arc. The only underwater search outside of this area was the initial TPL search followed by AUV operations around potential detection locations up near latitude 21°S. The weather proved to be moderate in this northern area, resulting in minimal weather down time. However, the southern area where the underwater search had shifted was known for adverse weather conditions at any time of year, but especially during the cyclone season (November to April) and the winter months (June to August).

The search area, particularly towards the southern end, was subject to high winds, waves, and swell as a result of winter or cyclonic activity. Efforts were therefore made to better predict and understand weather impacts and to mitigate against any potential incidents. Figure 91 shows the back deck awash on *Go Phoenix* during a typical weather event in the search area.

Figure 91: A large amount of water flooding the back deck working area of *Go Phoenix*



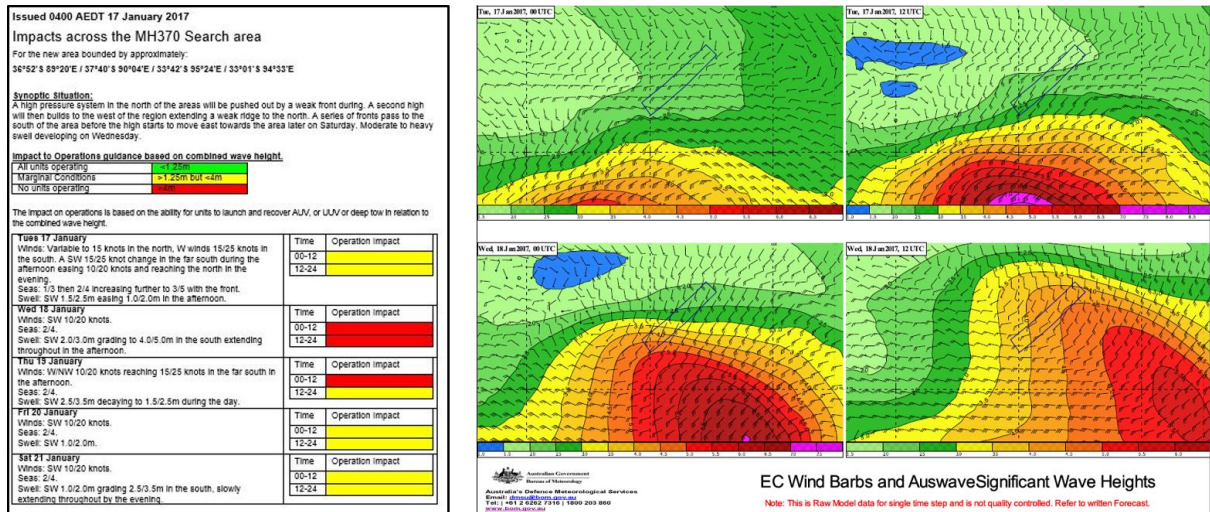
Source: Hydrospheric Solutions

Weather forecasting and recording

A comprehensive understanding of the expected weather was required to better prepare the vessels for operations and for preparing the following day's operational schedule. Forecasting the weather and sea conditions was vital for deep water search operations. Typical deep tow vehicle recoveries took around six hours so the operators could not wait until the weather was upon them, they needed to react to the forecast weather prior to its arrival.

The ATSB, vessel operators and contractors sought forecasts from various commercial and public weather sources. The ATSB utilised the services of the Australian Defence Meteorological Support Unit (DMSU), a section of the Australian Bureau of Meteorology (BOM). Forecasting extended for five days, with an example report shown in Figure 92. The report used colour banding to reflect potential impacts to operations based on forecasted significant wave/swell height and wind speeds. DMSU also produced a series of wind and sea graphics that depicted the passage of weather systems, showing wind barbs and contoured charts for significant wave heights to be expected. This was transmitted to the search vessels, contractor operations staff and ATSB daily.

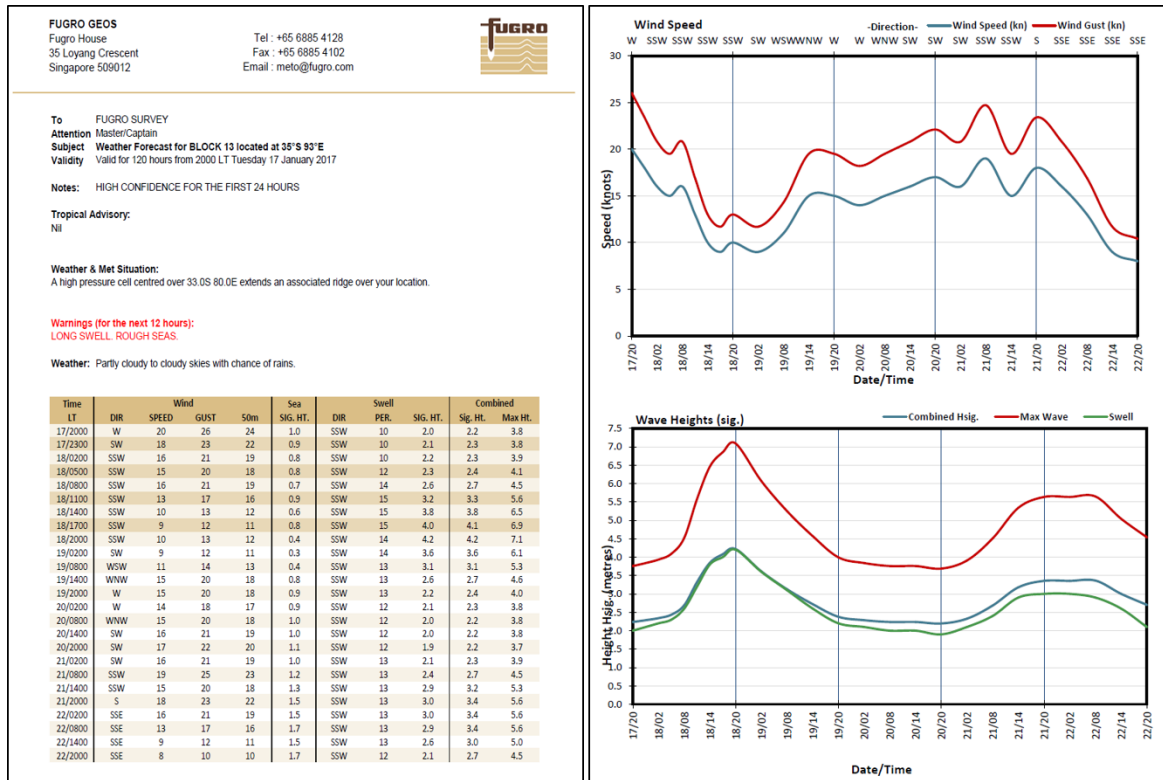
Figure 92: Example BOM Defence Meteorological Support Unit daily search area weather forecast report



Source: BOM Defence Meteorological Support Unit

Search vessel operators and contractors accessed their own weather forecasting services. Fugro Survey's GEOS weather service tabulated three hour interval predictions of wind, sea, swell and combined significant wave heights. This was also represented graphically as seen in Figure 93 and transmitted twice daily to the ATSB, contractor operations staff and search vessels.

Figure 93: Example Fugro GEOS weather service twice daily search area weather forecast report



Source: Fugro Survey

For long-term forecasts and trends in the southern Indian Ocean, climatological input was provided by the BOM and Fugro’s Metocean Division. In 2014 Fugro Survey commissioned work to provide statistical meteorological data by using information from three available locations within the region. Operational wind and wave statistics were derived from data taken from the Fugro GEOS WorldWaves database, which in turn was derived from the European Centre for Medium-Range Weather Forecasts.

Fugro Survey provided the spreadsheet shown in Figure 94 which lists the percentage of time each month that the predicted significant wave height was expected. This aggregation of long term wave height averages for the search area was key to forward planning the search activities and considering weather downtime associated with deep tow, AUV or ROV operations. The higher the significant wave height, the riskier it was to safely launch and recover the respective search system being used. For example, for AUV operations the limit for the safe launch and recovery of the vehicle was significant wave heights no larger than 3.0 m, and if the intent was to work through the month of May, statistically 70.8 per cent downtime could be expected. This is determined by adding all the figures above the intercept of 3.0 m wave height in the month of May column. By comparison, a 3.0 m wave height limitation in January could statistically expect 13.7 per cent downtime.

Figure 94: Historical significant wave heights for each month as a percentage of time

Total	100.00	100.00	100.00	100.00	100.00	100.00	100.00	100.00	100.00	100.00	100.00	100.00
11.5					0.08							
11.0												
10.5					0.24		0.16					
10.0					0.16		0.08		0.25			
9.5					0.40	0.25	0.65					
9.0					0.32	0.25	0.56	0.24	0.25			
8.5					0.32	0.42	0.97	0.16				
8.0					0.73	1.25	0.56	0.24	0.50	0.08		
7.5		0.18			1.05	1.17	2.26	0.56	0.33	0.08		
7.0					1.21	2.33	1.94	1.77	1.00	0.08		
6.5		0.09	0.32	0.17	2.18	2.33	3.87	2.50	2.08	0.81	0.08	0.16
6.0			0.24	0.33	3.23	3.17	5.65	4.27	3.08	1.69	0.17	0.16
5.5	0.24		0.73	0.92	4.27	5.83	7.18	8.15	4.83	2.74	1.17	0.32
5.0	0.16	0.09	0.65	1.83	5.81	9.58	8.71	9.03	6.58	4.19	1.75	1.53
4.5	0.65	1.24	0.81	2.92	8.55	14.50	10.65	10.48	10.83	4.44	4.33	2.18
4.0	1.29	2.13	3.79	5.92	10.40	12.58	13.39	15.89	12.17	8.47	7.83	3.31
3.5	4.35	4.34	6.37	11.42	15.16	14.83	14.92	15.08	16.17	13.55	13.00	8.39
3.0	7.02	10.99	14.44	17.42	16.69	11.42	13.87	14.76	19.17	17.74	17.92	15.56
2.5	15.65	18.71	25.08	25.08	14.68	11.83	8.71	8.71	11.42	18.95	23.83	20.40
2.0	28.47	28.37	30.73	23.00	9.76	6.00	4.27	6.77	8.50	16.29	19.17	23.71
1.5	32.26	24.29	15.08	9.75	4.19	2.08	1.61	1.37	2.58	9.44	10.00	16.61
1.0	9.92	9.57	1.77	1.25	0.56	0.17			0.25	1.45	0.75	6.45
0.5												1.21
0.0												
	Jan	Feb	Mar	Apr	May	Jun	Jul	Aug	Sep	Oct	Nov	Dec

Source: Fugro Survey

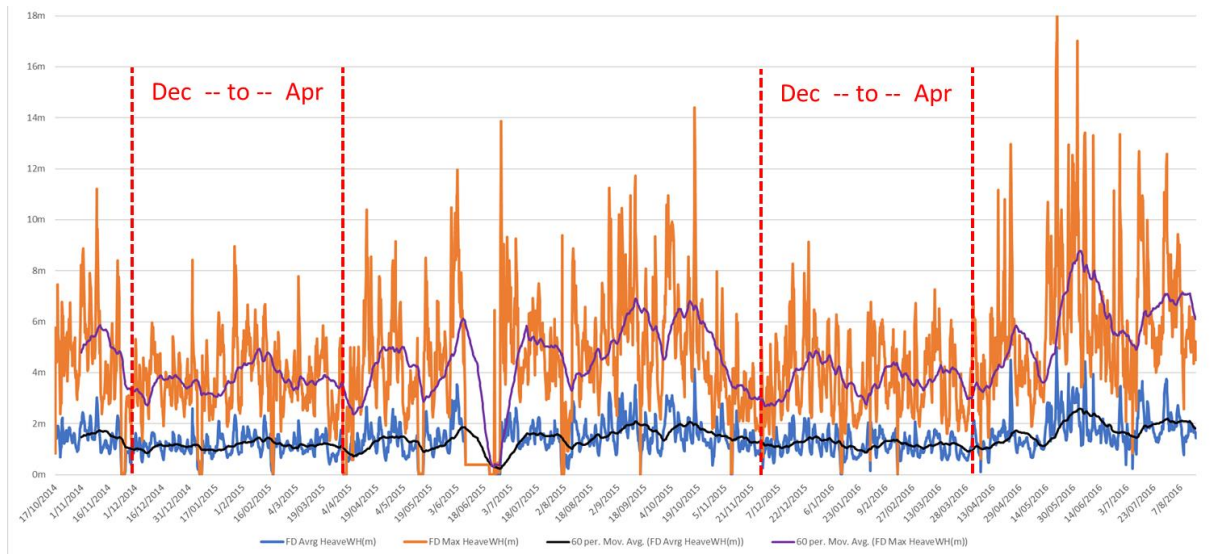
Real time weather records

Real time weather observations were recorded as part of the daily reporting requirements for most search vessels while in the search area. This occurred every watch (four hours) with the observations provided to the BOM to ground truth the satellite weather observations and climate models used by world weather and climate agencies. These observations resulted in significant improvements to the models and forecasts as the search progressed.

Additionally, on board the Fugro Survey vessels real time weather observations were recorded from a weather station, positioning systems and motion sensors. Vessel position, heading, speed, pitch, roll, heave, wind speed, wind direction, atmospheric pressure and temperature were all recorded and available in real time. On *Fugro Equator* these parameters were recorded at one second intervals, and on *Fugro Discovery* every five seconds. These parameters were also recorded on *Fugro Supporter* and *Havila Harmony*. This not only assisted the operators with making operational decisions based on the weather conditions and vessel motion at any given time, but also documented a comprehensive historical account of the weather in the search area over a nearly three year period.

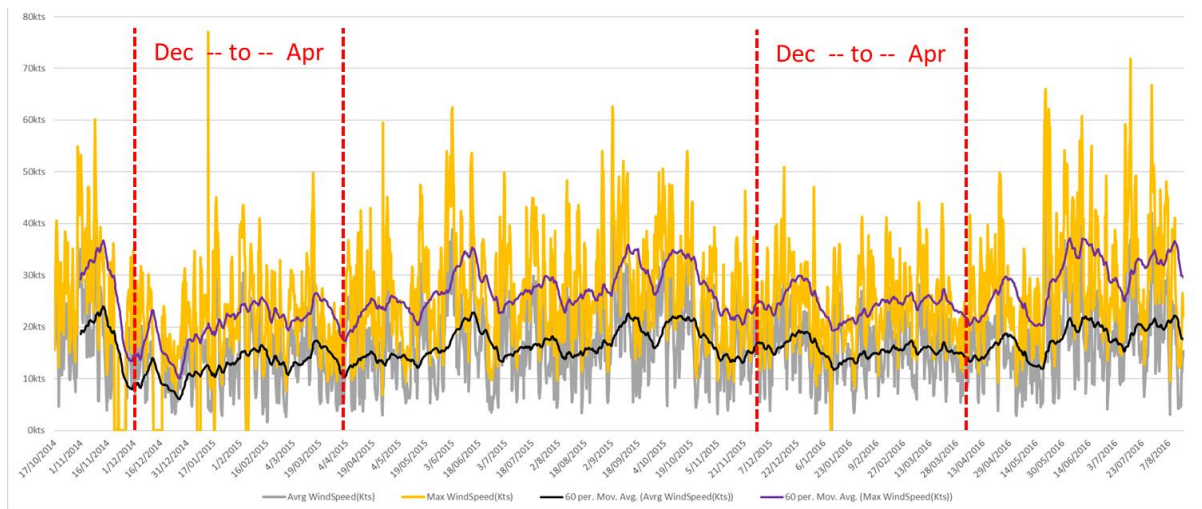
Plots of wind and heave data are included below. Figure 95 shows *Fugro Discovery's* recorded heave in metres for both peak value (orange) and average value (blue) sampled over a 6-hour period. Figure 96 shows *Fugro Discovery's* recorded wind speed in knots for both peak value (yellow) and average value (grey) sampled over a 6-hour period. Additionally, each plot has a 15 day rolling trend line (purple and black lines) to show the general monthly trends over the data collection period.

Figure 95: *Fugro Discovery* recorded heave in metres (Orange = max, Blue = average)



Source: ATSB

Figure 96: *Fugro Discovery* recorded wind speed in knots (Yellow = max, Grey = average)



Source: ATSB

Weather events impacting search operations

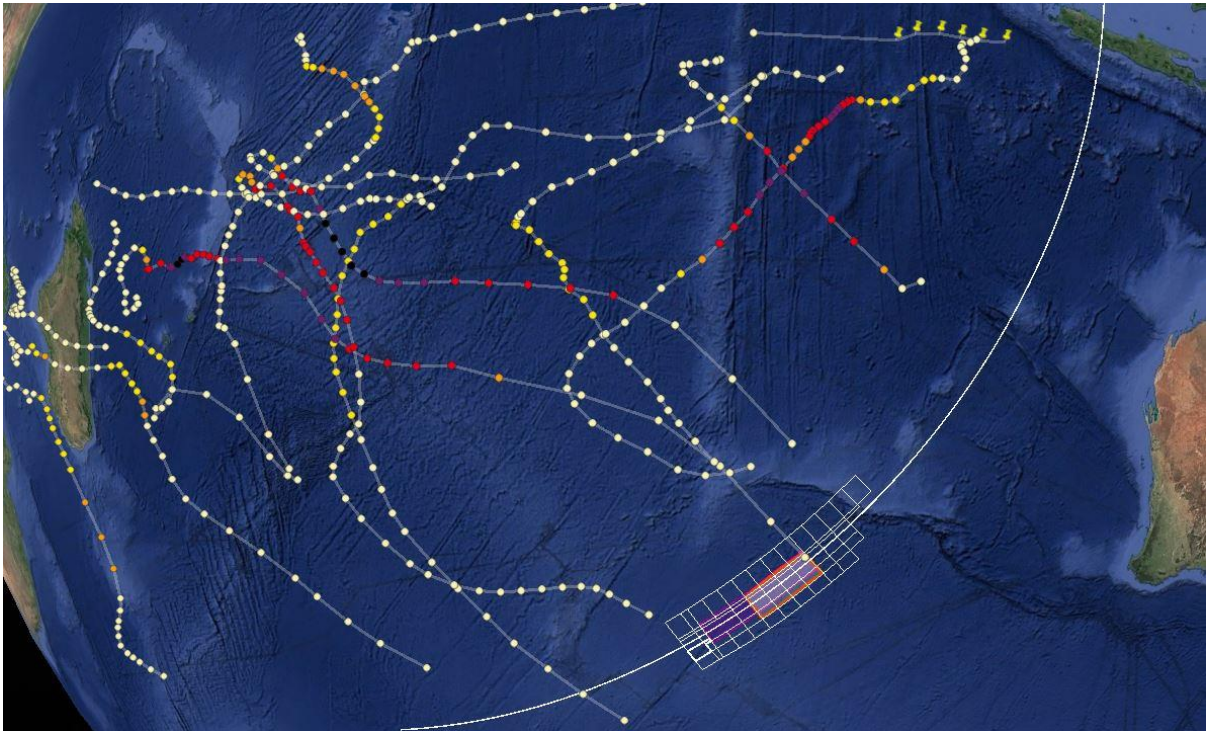
The path of tropical cyclones and tropical storms had significant impacts on vessel operations at times during the search. The cyclone season in the southern Indian Ocean is from mid-November to the end of April the following year³¹. Tropical cyclones in the southern Indian Ocean normally form in the basin between Madagascar and the Maldives before departing for other areas of the Indian Ocean.

As part of an initial assessment of cyclone and storm activity, an examination was undertaken of data from the French meteorological service on La Réunion Island, which has responsibility for issuing advisories and tracking tropical cyclones in the southern Indian Ocean basin. Archive data (1998-2015) suggested an average of 4.8 cyclones and 4.1 tropical storms per year across the entire southern Indian Ocean region.

³¹ For Seychelles and Mauritius the season ends mid-May

The 2014-15 cyclone season (Figure 97) was typical with five cyclones and six storms, whilst in 2015-16 (Figure 98) there were three cyclones and five storms reported. Even though few cyclones reached the search area the effects of a decaying cyclone or storm presented challenging conditions for the search vessels at times.

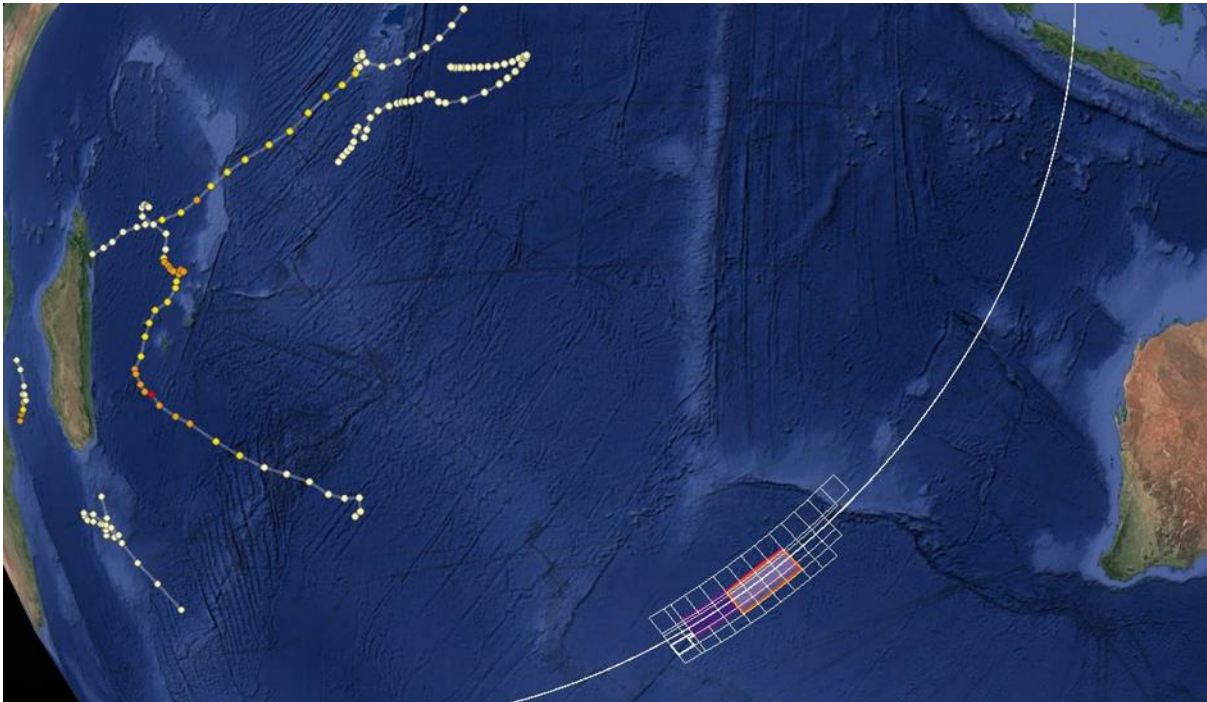
Figure 97: Tropical cyclone systems in the southern Indian Ocean 2014–15 cyclone season



Source: Google earth, annotated by ATSB using Météo-France La Réunion data

During the 2014-15 cyclone season several systems severely affected search operations. During one period, all vessels departed the search area to seek calmer waters for several days. Vessels would often have to suspend search operations, recover the deep tow equipment and patiently ride out the severe sea conditions. In comparison, the 2015-16 cyclone season was relatively benign.

Figure 98: Tropical cyclone systems in the southern Indian Ocean 2015–16 cyclone season



Source: Google earth, annotated by ATSB using Météo-France La Réunion data

Weather conditions in the winter months (June to August) also had significant impacts on vessel operations at times during the search. The onset of winter conditions coincided with the initial phase of bathymetric data collection from late May 2014. The survey vessels experienced periods of poor weather however were typically able to continue collecting data. During periods of higher significant wave heights the survey coverage rate was reduced to maintain data quality. Winter weather conditions in 2014 did not impact underwater search operations, as these commenced in latitudes between 33°S and 39°S in October 2014.

After the severe weather impacts of the 2014-15 cyclone season, winter conditions continued to bring adverse weather, although July 2015 brought unseasonal fair weather conditions resulting in better than expected underwater search coverage rates for the month.

After a relatively benign cyclone season in 2015-16, the vessels encountered consistent severe winter weather conditions. From 8 May 2016 to 16 June 2016 no underwater search operations could be performed. Surface bathymetric data could be collected successfully by *Fugro Equator* for brief periods when conditions allowed. Severe weather conditions continued with significant wave heights above the limitations for the launch and recovery of the deep tow vehicle on *Dong Hai Jiu 101*, resulting in the decision to suspend *Dong Hai Jiu 101* search operations in August after two swings with minimal underwater search time. The ProSAS search system was demobilised and the vessel went to standby at anchor off Fremantle until the weather improved in October 2016.

Fugro Equator and *Fugro Discovery* had both been subject to ‘winterisation’ modifications to improve the safety and operability of the vessels and equipment in the extreme conditions. One major improvement was to their launch and recovery systems for their deep tow vehicles which enabled them to work in higher sea states safely and effectively. Fugro Survey also designed and implemented an optional secondary recovery system for their AUV, this allowed recovery of the AUV in higher sea states. This system was transferrable and used for both *Havila Harmony* and *Fugro Equator* AUV operations.

As an example of conditions experience in the search area, on 13 July 2016 *Fugro Equator* recorded a combined wave and swell measurement of 24.03 m (trough to peak). This occurred in

a 12 hour period where four other waves over 20 m were experienced, all on a 65 m vessel whilst operating at a latitude of 38°S. Figure 99 shows *Fugro Discovery* in typical sea conditions.

Towards the end of 2016 and early 2017 the weather improved in the search area with the coming of summer. However, operations were still impacted with passing weather systems. By this time *Dong Hai Jiu 101* had mobilised an ROV and successfully completed 30 dives but there was still 47 per cent weather standby time. During this period *Fugro Equator* demobilised the deep tow system and mobilised the AUV which was able to complete all of its tasking with only 11 per cent of the time on weather standby.

The Fugro Survey vessels operated over the entire search period and in all regions of the search area with an overall weather standby time for all vessels for both AUV and deep tow vehicle operations accounting for 9.4 per cent of their total time on the search.

Figure 99: *Fugro Discovery* in the search area in typical conditions and a rare calm day



Source: Fugro Survey

Mitigation of weather impact on search operations

Aside from comprehensive weather forecasting the following actions were taken to mitigate the weather risk to search operations:

Weather avoidance

As per normal practices on board a vessel, the Captain was responsible for the safety of the vessel and the crew. The decision to depart the search area for calmer waters always lay with the vessel master and the operator.

Vessel equipment improvements

Winterisation of the search vessels meant making changes to equipment or procedures to promote safer operations in higher sea states and was implemented by Fugro Survey. This was a significant factor when working on deck but also a factor in day to day living within the vessel accommodation areas.

Variable tasking

Both *Fugro Supporter* and *Fugro Equator* were fitted with hull-mounted multibeam echo sounder systems capable of bathymetric survey in the search area and therefore had dual roles at times during the search. Both vessels were tasked to conduct bathymetric survey operations (in areas planned to be searched) whenever the sea conditions were deemed unsafe to conduct their primary tasking of underwater search operations using their deep tow or AUV systems.

Line Planning

For safety and efficiency the deep tow lines ran nearly perpendicular to the typical swell and wind direction for the search area. This allowed the vessels to steer directly into or with the seas as opposed to running parallel to them. As sea states increase running parallel to the seas will cause the vessel to roll considerably and is much harder to maintain straight track lines needed for deep tow operations.

Further mitigation actions for risks to crew safety associated with operating in such a remote area are outlined in the following Health, Safety and Environment section.

Health, safety and environment

The underwater search for MH370 presented some significant risks to the health and safety of the crews on board the search vessels. As Australia's transport safety investigator the ATSB was particularly aware of the need to ensure these risks were carefully managed and that the standard for all operations carried out by the search contractors were industry best practice. Contractors were advised that at all times the safety of the vessels and their crews must never be compromised during search operations and this was reiterated throughout the duration of the search.

The ATSB took an end-to-end approach to ensure search operations were conducted safely and contractors had appropriate systems in place to manage the safety of their staff. It started with specifying the health, safety and environment (HSE) standards which potential search contractors needed to meet. These became contracted obligations when search contracts were awarded. Finally, during search operations the contractor's compliance with the HSE standards was monitored with a comprehensive reporting system and ATSB staff on each search vessel who (amongst other things) monitored the management of safety on board the vessel.

Requirements stipulated in the request for tender for search services included that all search vessels must comply with all International Maritime Organisation instruments including the Safety of Life at Sea Convention, the International Convention for the Prevention of Pollution from Ships, and International Safety Management Code³². The contractor was also required to operate risk management and safety management systems covering all their assets, operations and personnel which were subject to regular inspection and audit by relevant regulatory authorities. In addition, if the contractor was proposing to charter search vessels from a third party, that the vessel's safety management system was appropriately bridged to the contractor's safety management system.

Search contractors were required to include full details of their safety management systems and the implementation of these systems in the context of the underwater search, in a project execution plan. All personnel embarking on search vessel operations were required to have medical fitness certificates as well as (at least) Basic Offshore Safety Induction and Emergency Training. Contractors were also required to provide effective reporting of health, safety and environment matters in their daily operational reporting to the ATSB and provide timely notice and when any incidents occurred.

Consideration was also given to managing emergencies at sea, in a remote area, due to a serious injury or illness to the contractor's personnel, vessel crew or the ATSB's client representative. Risk mitigation strategies were put in place including a requirement for qualified medical personnel to be carried on each vessel together with additional medical supplies and equipment.

Fugro Survey operated a mature whole-of-organisation quality, risk and safety management system. The system included appropriate policy and procedures and was designed to inculcate an organisational culture in which staff actively recognised and responded appropriately to risk within a supportive management framework. Responsibility for maintaining HSE standards was assigned to all employees and sub-contractors, ensuring ownership and accountability remained with every person in the organisation.

Phoenix International also operated a mature health, safety and environmental management system containing a comprehensive suite of policies and procedures. There was a particular focus on safe methods of work and the identification and mitigation of risks associated with operational tasks.

³² For international trading vessels the International Safety Management Code sets out the requirements for vessel safety management systems and compliance is audited by Classification Societies, Flag and Coastal State Authorities.

Operational safety

Both Fugro Survey and Phoenix International operated safety management systems which included a hazard analysis and job safety environmental analysis for all high risk operations on their vessels (for example launch and recovery of underwater search vehicles). Over the course of the search, Fugro Survey, in particular, implemented significant improvements to equipment and procedures used for some of these safety critical operations.

Daily meetings were conducted on each search vessel to discuss operational activities for the next 24 hours including weather updates and any deviation from agreed and approved operations. Shorter focus meetings, 'toolbox talks', were held with relevant crew prior to undertaking any operational task. Toolbox talks also facilitated the handover to the next shift of any incomplete work or new hazards identified.

Weekly safety meetings reviewed any HSE issues raised since the previous meeting, any incident reports and reviewed any proposed amendments to procedures based on job safety or hazard analysis. All personnel were encouraged to note safety observations throughout the week and the weekly safety meetings enabled a forum to discuss what worked well and highlighted areas for improvement.

Emergency drills were conducted within 24 hours of leaving port and then at least once a week during search operations, involving all crew. These drills included fire and abandon ship, man overboard, and emergency helivac. Periodic safety audits were also performed throughout the course of the search and provided confirmation of safety practices on each vessel.

Remote area operations

The weather in the search area for much of the search was poor, the search area was 5-6 days transit from the coast of Western Australia and the vessels were in the search area for protracted periods (42 day swings for Fugro Survey's deep tow vessels). The crews on board the search vessels were exposed to a level of risk not normally experienced in the marine industry. Poor weather increases the risk of a serious injury during vessel operations especially when exposure to the risk is over many weeks. Similarly the protracted period in the search area increases the chance that a serious illness may develop which may have been undiagnosed at the time the vessel departed port. Additionally, the risk of a poor outcome for the injured or ill crew member is significantly increased as a result of the protracted time needed to transport them from the search area to comprehensive medical facilities ashore.

When making operational decisions and tasking requests the ATSB and search contractors continually considered ways to mitigate the risks associated with the weather and the remoteness of the search area. Shore staff and vessel crews worked continuously to improve the safety of any operation performed at sea and while underway to and from the search area. On board the vessels safety meetings and risk assessments occurred daily or as needed during operational periods. A close working relationship between the search equipment operators (mission crew) and vessel crew helped to ensure the safety of all personnel especially during periods of rough weather.

Remote area risk mitigation

Upgraded medical support

In addition to a comprehensive medical required for all vessel crew the medical facilities on board the search vessels were upgraded. The remote and through-winter operations meant that standard medical facilities and support carried typically on the vessels as part of their normal surveys/tasks was inadequate. Doctors were embarked on all search vessels and the medical kit carried by the vessels was significantly upgraded.

Vessel scheduling

In case of an emergency in the search area mutual vessel support could be vital. Whilst vessel schedules and tasking were not routinely adjusted to guarantee there were at least two vessels working in the search area, it was always a consideration in planning tasking for the vessels. The sheer size of the search area, the patchwork of tasks outstanding as the search progressed and the operational and contractual management of the vessels meant that dual operations in close proximity could not always be achieved. However, it was strived for and achieved whenever possible.

Incident recording and reporting

The ATSB was informed of any incidents on board the search vessels via telephone or email or via daily operations reports. A register was developed to ensure all incidents which occurred during search operations were recorded and followed with the search contractors. Open incidents were followed up with the vessel project managers and while most were resolved quickly, a few remained unresolved for longer periods, pending outcomes of internal investigations or awaiting approval for procedural changes.

A summary of HSE incidents was included in both the contractor weekly operations reports and the ATSB client representative weekly reports. These provided a good way to confirm all parties were recording the same information and reconciled the activities reported on the daily operations reports, for the same reporting period.

Lagging indicators are normally seen to identify trends in past performance, assess outcomes and occurrences. These include possible near misses, crew injury and illness, equipment damage or loss, or an environmental incident. Leading indicators can reveal areas of possible weakness, be utilised to identify hazards, assist risk assessments and define risk management policy, such as vessel inductions, permits to work and safety drills.

Both Fugro Survey and Phoenix International provided a table of leading and lagging indicators, with incident narration, in their respective operational reports. These provided an overall summary of health, safety and environmental incidents throughout the underwater search (including the mapping of the seafloor), as shown in Table 28.

Table 28: Summary of MH370 HSE Lagging and Leading Indicators

Lagging Indicators	TOTAL	Leading Indicators	TOTAL
Near miss	39	JSEA ³³ s and inductions	687
Injury or Accident	9	Safety meetings	5442
Medical Treatment	13	Emergency drills	392
Equipment damage or Loss	60	Safety observations	395
Environmental incident	1	Safety inspections	344
		Marine fauna observations	29
TOTAL	122	TOTAL	7289

Source: Fugro Survey and Phoenix International

Significant HSE incidents

Although Table 28 shows 122 separate incidents across all vessels, most had little or no impact on search operations. HSE incidents which did impact on search operations during the course of the underwater search were three medical evacuations of ill or injured crew members on search vessels:

³³ Job Safety and Environmental Analysis

- On 4 November 2015 a crew member on *Fugro Discovery* advised the doctor on board that he had abdominal pains. After consulting with International SOS (travel medical service) possible appendicitis was suspected. Search operations were suspended and the vessel commenced transit to Fremantle. A medical examination on shore ruled out appendicitis and the patient made a full recovery.
- On 16 November 2015 a crew member on *Fugro Discovery* presented to the doctor on board with visual disturbance, headache, nausea and unequal pupil size. The doctor contacted International SOS who advised ‘a life threatening condition could not be ruled out’. A medivac was recommended as further tests were needed in a hospital, including CT scan, MRI and bloods. The vessel transited to Fremantle where the patient was hospitalised. After testing and a few days of rest, he was granted a permit to fly home.
- On 26 June 2016 a crew member on aboard *Dong Hai Jiu 101* fell from a top bunk and injured his right shoulder and right thigh. Although the patient’s shoulder was in a satisfactory condition after treatment, a deep cut was found in his thigh which required stitches. Further consultation on board determined the vessel’s medical facilities were not sufficient to treat a severe infection and the vessel returned to Fremantle. The patient was transferred ashore from the anchorage for further treatment and was cleared to travel home two days later.

From the mobilisation of *Fugro Equator* on 2 June 2014 (in Singapore) to undertake the bathymetry survey until the demobilisation of *Fugro Equator* on 23 January 2017 (following the final AUV campaign), underwater search operations occurred for a total of 966 days. The search operations involved two major contracted companies, six different vessels which completed a combined 59 swings (from port to search area and return to port) with rotating personnel totalling in the hundreds (including marine and survey crew, client representatives, interpreters, doctors, and equipment specialists).

Considering the remote and dangerous weather conditions encountered during the underwater search, high praise should go to the captains and marine crew for the extraordinary management of each vessel which resulted in minimum incidents involving personnel and equipment. The low number of HSE incidents over close to 1,000 days of search operations is a testament to the cooperation, resilience and good practice by all involved in the underwater search.

Significant equipment related incidents

The loss of two separate deep tow vehicles, within months of each other, significantly impacted search operations. On 24 January 2016, while running a deep tow survey line, *Fugro Discovery* lost its deep tow vehicle, when it collided with a volcano about 2,500 m below sea level. Only 4,500 m of the 10,000 m tow cable was recovered. The crew marked the approximate location of the deep tow vehicle and returned to port where the tow cable, reel and deep tow vehicle were replaced. The vessel then returned to the search area and continued normal survey operations. *Havila Harmony*, having completed its first AUV swing for the summer campaign, mobilised a remotely operated vehicle during its port call. On returning to the search area *Havila Harmony*’s crew successfully located and recovered *Fugro Discovery*’s lost deep tow vehicle by 3 February 2016.

On 21 March 2016 the ProSAS deep tow vehicle on aboard *Dong Hai Jiu 101* was lost while it was being hauled in for recovery. The tow cable termination attached to the depressor had failed. The last known position of the deep tow vehicle was marked by the mission crew and the vessel returned to Fremantle. A remotely operated vehicle was mobilised on *Dong Hai Jiu 101* in Fremantle and the vessel returned to the search area where the deep tow vehicle was located and recovered from the seafloor on 18 April 2016.

Impact of fishing vessels in the search area

Despite the remote location of the underwater search, fishing vessels were regularly encountered by the search vessels in the search area during the summer months. It was considered that

search operations could be impacted as most of the fishing vessels appeared to be working with long lines. Fishing long lines are very strong synthetic monofilament main lines tens of kilometres long which may carry thousands of baited hooks on branch lines (snoods). Once set, they are free to drift for many hours with the prevailing currents before being recovered by the fishing vessel. If a fishing line were to become entangled with a search vessel tow cable there was a real risk that a deep tow vehicle could be lost and so steps were taken by the search vessels to make contact with, identify and warn the crews of the fishing vessels. These efforts met with limited success.

After several encounters between search vessels and fishing vessels measures were taken by ATSB in an attempt to reduce the likelihood of encounters. This including the issue of NAVAREA warnings (a marine safety information or warning notice for an area issued by maritime safety authorities, in this instance the Australian Maritime Safety Authority) and direct contact with fishing vessel owners when the vessels could be identified. This too resulted in almost no success and so when fishing vessels were encountered in close proximity, the search vessels either recovered their equipment until it was safe to redeploy, or diverted their course to avoid contact (when they were performing AUV operations).

Havila Harmony's encounter with fishing gear

On 8 January 2016 *Havila Harmony* (Figure 100) was undertaking AUV operations in the search area. During the afternoon fishing vessels had been sighted within 200 m of the vessel and a notification was sent to other search vessel in the area and the ATSB. The AUV was performing a dive with the ship tracking the position of the AUV from the surface using the USBL system fitted to a pole which is hydraulically extended several metres below the hull when it is operating.

It was noted by the crew that the USBL positioning data had become inconsistent during the AUV mission. When the AUV was recovered, the crew attempted to recover the USBL pole for further inspection but were only able to raise it 11 cm before it became stuck. Unable to resolve this issue, the vessel had to return to port where it was found that the USBL pole was bent with a large amount of fishing line wrapped around it (Figure 100). The damage required *Havila Harmony* to be dry docked so the USBL pole could be replaced.

Figure 100: *Havila Harmony* and fishing line wrapped around the vessel's USBL pole



Source: Fugro Survey

Recovery planning

Once underwater search operations commenced in October 2014, the MH370 debris field could potentially have been located at any time. A recovery operation would need to commence as soon as possible after the debris field was located and the Tripartite governments had agreed on the next steps. The ATSB therefore needed to put in place the arrangements and plans necessary for a rapid recovery operation to occur at short notice.

Planning for recovery

The Governments of Malaysia, Australia and the People's Republic of China had decided that they would meet if MH370 was found, to consider issues relating to any recovery. It was decided that the ATSB would coordinate the on-water component of recovery operations, in consultation with other involved agencies. The ATSB would be responsible for overall coordination including:

- procuring recovery services (vessel(s), recovery equipment and subsea assets)
- planning operations including the tasking of vessels, assets and personnel
- liaising with the recovery contractor and their staff
- assuring the overall quality of the recovery operation services.

Considerations for the recovery of MH370 had commenced during March 2014, with a request to the French BEA to share information relating to the technical and operational support required during the recovery of AF447. Like the underwater search operation, the recovery operation for AF447 provided an example of operational challenges likely to be similar for an MH370 recovery, including the depth of water and the remoteness of the area.

The recovery of aircraft debris in deep water is generally accomplished by using a ROV (Figure 101) to either rig large items to lifting equipment or place small items in baskets or cages lowered to the seafloor and then lifting the baskets by winch or crane from the seafloor to the recovery vessel. A recovery vessel is required to have a dynamic positioning system capable of positioning the vessel for extended periods while the ROV is operating on the seafloor. For the MH370 recovery planning, weather was also a key consideration as the search area is prone to poor weather conditions for much of the year, often beyond the significant wave height limits for safe ROV operations.

Figure 101: A remotely operated vehicle on the seafloor



Source: Fugro Survey

Early in 2015 the ATSB called for expressions of interest for the MH370 recovery operation. The objective of the request for expressions of interest was to establish a shortlist of pre-qualified suppliers who could be rapidly contracted to undertake the recovery. A range of requirements were stipulated including specifications for the vessel and recovery systems (which included two ROVs).

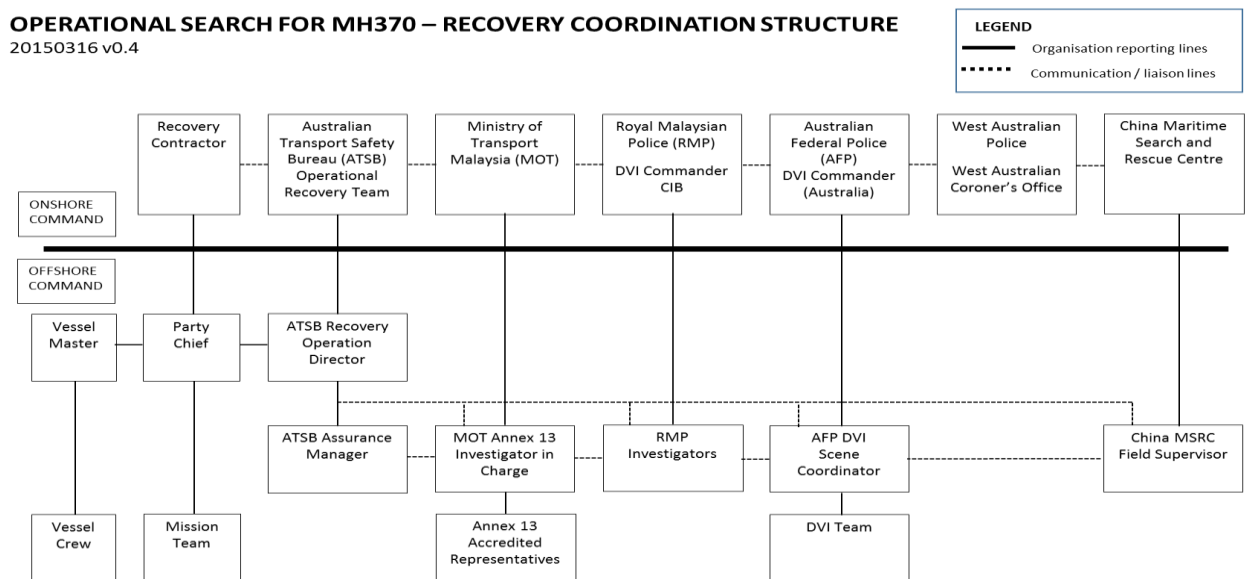
Requirements were designed around the need to support the range of activities involved in a recovery for up to 30 days at a time in a remote area offshore, working in water depths up to 6,000 m in often poor weather. The goal was to recover evidentiary material to support the Annex 13 and Royal Malaysian Police (RMP) investigations and the recovery of human remains. The large number of people required to be involved in the operation, and the requirements to process and store recovered items, also posed some logistical challenges.

The potential services included:

- mapping and capturing optical imaging of the MH370 debris field
- recovering human remains and debris from the MH370 debris field
- providing deck space and support services on board the recovery vessel for recovery equipment supplied to preserve human remains and aircraft debris
- providing accommodation on board the recovery vessel for all involved personnel
- providing data storage services and communication services to relay information to the Australian mainland.

To be prepared for the recovery operation the ATSB developed, in consultation with Malaysia and the People’s Republic of China, a detailed *MH370 Recovery Operational Plan* that would be implemented once MH370 was positively identified. To facilitate all aspects of the potential recovery operation, the ATSB also drafted a collaborative head agreement and specific project agreement with the Australian Federal Police (AFP) under the Commonwealth National Collaboration Framework, to define roles and responsibilities. The ATSB also arranged a MoU with the Australian Department of Defence to collaborate in any potential recovery operation. These arrangements were designed to assist the ATSB to coordinate the range of specialist input required for a complex deep water recovery operation as outlined in Figure 102.

Figure 102: Recovery coordination structure



Source: ATSB

The ATSB also planned for a range of other activities associated with the recovery operation and included them in the *MH370 Recovery Operational Plan*. These activities included the medical certification and premobilisation training for personnel who would be on board the recovery vessel including survival at sea and critical incident stress.

The investigations

Information about the debris field itself would only be available when MH370 was found. Part of the requirements for the underwater search were for the contractor to positively identify the debris field, map the debris field and produce a photographic mosaic of the entire field. Using this photomosaic, and prior to the commencement of a recovery operation, areas of particular interest could be identified which would form the basis for the initial priorities of the recovery operation.

During recovery operations investigation personnel are required to oversight the aircraft component recovery and legal aspects of the recovery operations. It was foreseen that investigators and representatives from the Malaysian Annex 13 investigation team, supported by representatives from Boeing, would need to be on board the recovery vessel to lead all aspects of the Annex 13 investigation. It was agreed that aircraft debris preservation procedures were to be in accordance with ICAO guidelines.

Similarly, officers from the RMP would be on board the recovery vessel to oversee the collection, processing and storage of evidence for their investigation.

The priority items for the investigations were the flight recorders (FDR and CVR) and quick access recorder. Further priority items included other potential sources of non-volatile memory such as avionics components or personal electronic devices and specific items of the aircraft structure or interior.

The initial prioritisation of debris would then be reviewed once the recovery vessel was on site, with opinions from all investigation parties considered with a view to the overall investigation. The early recovery, and initial analysis of the FDR, CVR and quick access recorder may assist the selection process. A potential expedited transfer of the FDR, CVR and quick access recorder from the recovery vessel to ATSB Canberra offices for analysis was also considered.

Disaster Victim Identification

Specialist personnel were required to oversight the recovery and repatriation of human remains in accordance with the INTERPOL Disaster Victim Identification process. Recovery of human remains would involve a multi-national and multi-jurisdictional operation led by the RMP and supported by the AFP.

Recovery planning identified that AFP Disaster Victim Identification professionals, in collaboration with Western Australia Police, PathWest Laboratory Medicine WA (Western Australian Government Pathology), Western Australia State Coroner, and RMP, would be on board the recovery vessel to coordinate the recovery of human remains, including recording and photography at the point of recovery, and appropriate transport to Western Australia.

The AFP, in collaboration with its partner agencies, planned to establish a temporary mortuary in Perth, Western Australia, to coordinate autopsies and post-mortem information.

The RMP, with the support of the AFP, would coordinate the collection of ante-mortem information, reconciliation of ante-mortem and post-mortem information, and repatriation of human remains once identified.

Safety analysis

Introduction

The disappearance of MH370 and the scale of the search for the aircraft is unprecedented in commercial aviation history. The aircraft continued to fly for almost six hours after the last time its position was positively fixed at the northern tip of Sumatra by the surveillance systems operating on the night. Whether or not the loss of MH370 was the result of deliberate action by one or more individuals, or the result of a series of unforeseen events or technical failures, it is almost inconceivable and certainly societally unacceptable in this modern aviation age with 10 million passengers boarding commercial aircraft every day, for a large commercial aircraft to be lost and for the families of those on board not to know with certainty what became of the aircraft nor those on board.

The function of the ATSB as described in the *Transport Safety Investigation Act 2003* is to improve transport safety. The ATSB considers, in relation to MH370, that it is difficult to fulfil this remit without locating the aircraft and determining the reasons for its disappearance.

MH370 was equipped with a variety of systems designed to communicate the aircraft's position during normal operations and in emergencies. These included the transponder system, the ACARS communication system, the emergency locator transmitters, and the underwater location beacons fitted to the flight recorders. All these systems complied with industry standards and were the state of the art at the time that the Boeing 777 was designed and certified and at the time the aircraft was delivered in 2002. Unfortunately, none of these systems succeeded in transmitting the aircraft's position at the end of its flight.

The search for MH370 commenced more than three years ago, on 8 March 2014. The initial surface search and the subsequent underwater search have been the largest in aviation history. The significant challenge has been to trace the whereabouts of the aircraft using the very limited available data: satellite communications metadata for the final six hours of flight – a method never intended to be used for this purpose – and long-term debris drift modelling to trace the origin of MH370 debris which had been adrift for more than a year and in some cases almost two years.

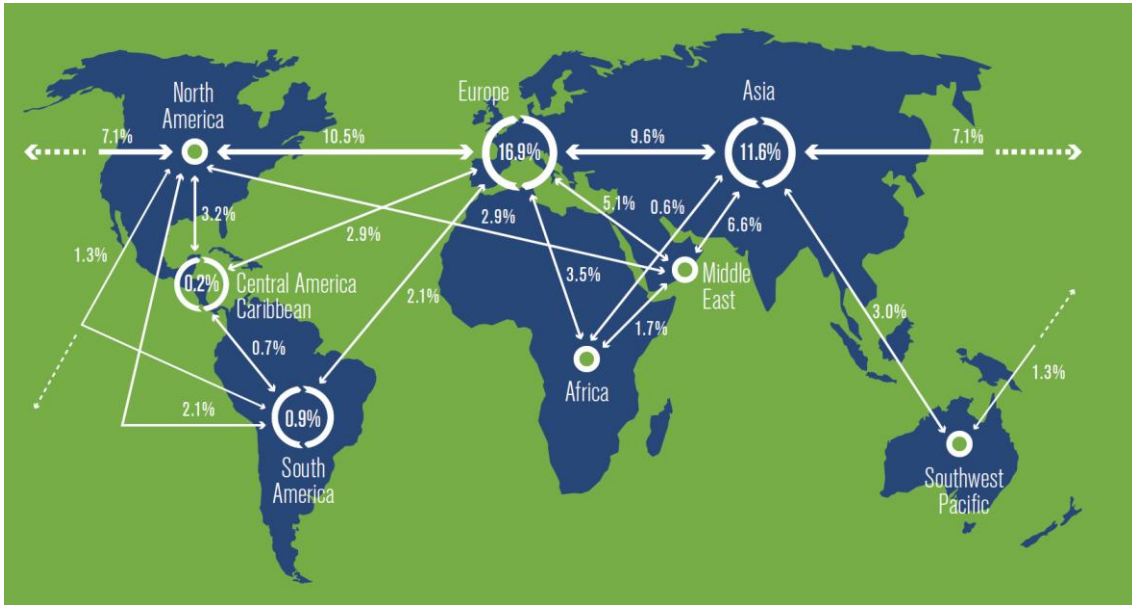
Improvements in international civil aviation regulation must be sought to ensure that this type of event is identified as soon as possible and mechanisms are in place to track and locate a commercial aircraft that is in distress or not following its filed flight plan.

The International Civil Aviation Organization (ICAO) is responsible for setting the international standards for civil aviation safety which are applied, in law, by all contracting States. The Annexes to the Convention on International Civil Aviation (the Chicago Convention) set out provisions for the safe and effective conduct of aviation activities. Among them, Annex 12 is applicable to search and rescue (SAR), though many of the factors that can determine the success of a SAR are contained in other Annexes, in particular, those for the operation of aircraft (Annex 6), aeronautical telecommunications (Annex 10) and air traffic services (Annex 11). Additionally, the outcomes of a search directly impact the effectiveness of an Annex 13 safety investigation. This in turn influences ongoing aviation safety.

Hundreds of millions of passengers are flown across transoceanic routes each year. More than 7 trillion commercial passenger-kilometres were flown in 2016, about a third of which were over major oceans (Figure 103³⁴). This safety analysis aims to broadly determine possible improvements in these areas in order to increase the efficiency and effectiveness of searches of aircraft lost in international waters.

³⁴ IATA World Air Transport Statistics, 60th Edition. A passenger-kilometre is equivalent to one passenger flown for one kilometre. It can be used as a measure of civil aviation activity and, to some extent, exposure to risk.

Figure 103: Proportion of passenger-kilometres on international, scheduled routes, 2016



Source: International Air Transport Association

Search, rescue, and recovery

The main objectives of search, rescue and recovery operations performed when a commercial aircraft has been subject to an accident are to:

- Locate, rescue and retrieve survivors and casualties.
- Provide evidence for an investigation to determine what happened:
 - to permit safety improvement
 - for the benefit of grieving families, friends, and communities.

There have been many occasions where people have survived major passenger aircraft accidents, including impacts into the sea. While survival appears most likely if an accident occurs during take-off or landing, when a rapid response is to be expected, some of these accidents occurred in relatively remote locations. In such cases, timeliness is critical because the occupants are likely to have injuries and be exposed to harsh environmental conditions. The sooner medical attention can be administered, the greater their chances of survival beyond the first few hours or days.

The purpose of an accident investigation as detailed in Para 3.1 of ICAO Annex 13 is:

The sole objective of the investigation of an accident or incident shall be the prevention of accidents and incidents.

If an aircraft is lost or missing for an extended period of time, then the amount of information available to achieve the objectives of the investigation is diminished and safety issues may not be identified and resolved as quickly.

An Annex 13 investigation authority's role is to bring about positive safety change in an objective way. It is also important to understand and consider the emotional impact of an accident that affects individuals, groups, and communities. Recovery of accident casualties is also important from a cultural perspective. A successful search and investigation provides answers that may contribute to the alleviation of grief, and in a broader sense, confidence in the safety of the global aviation industry is maintained when an accident is well understood. A rapid, successful search helps make these things possible.

Search, rescue, and recovery phases

A search consists of a number of stages that differ depending on whether the accident is over water or land. Since a search relies heavily on the information available prior to the accident, the ATSB has included consideration of pre-accident factors in this analysis.

The ATSB has divided the process into phases as summarised in Table 29.

Table 29: Search phases associated with different accident locations, and example activities associated with each phase

Phase	Accident over water	Accident over land
Normal flight	Scheduled, triggered, or continuous monitoring of aircraft position and status	Scheduled, triggered, or continuous monitoring of aircraft position and status
Aircraft in distress	Triggered monitoring of aircraft position and status following an abnormal event	Triggered monitoring of aircraft position and status following an abnormal event
Primary search	Search for survivors, casualties, and floating debris	Search for survivors, casualties, and main wreckage
Underwater locator beacon search	Wide search for submerged wreckage and ULB signals (general area)	Not applicable
Sonar search	Narrow search for submerged wreckage and casualties ('pinpointing')	Not applicable
Recovery	Recovery of casualties, wreckage and recorders.	Not applicable

Source: ATSB

Normal flight

Position tracking

Position reports (made by crew over radio, or automated data transmissions) are often the best information available to SAR authorities to define a search area. Their usefulness diminishes with time elapsed from the last report, and to some extent, whether that report was routine or indicated an emergency (this is discussed more in the following section). Knowing the maximum time from the last report to the time of the aircraft impact is critical in determining the area for the initial search. The potential search area becomes much larger when there is more uncertainty.

In cruise, an airliner travels about 8 NM per minute. In 15 minutes, an aircraft could be at any location within a 125 NM radius circle, with an area of about 170,000 km².

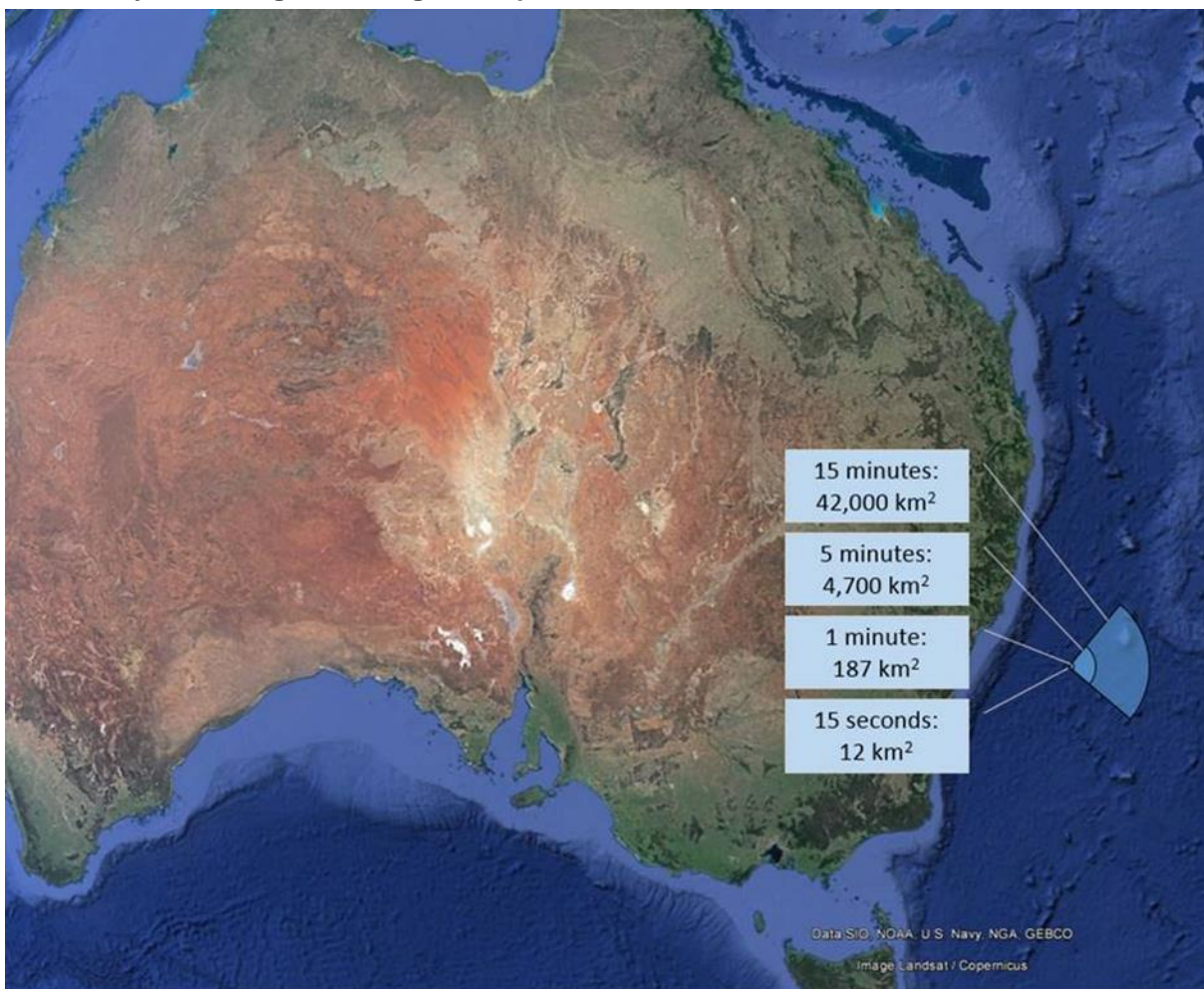
If the aircraft's track at the time of the last position report is known or can be estimated, and assuming that the aircraft is unlikely to turn more than about 45° either side of that track, this area can be reduced to a quadrant with an area of approximately 42,000 km². An indication of the effect of time uncertainty on the likely impact area is given in Table 30 and Figure 104.

Table 30: Search areas associated with time uncertainty, assuming 500 knot groundspeed

Time between position reports (mm:ss)	Radius (NM)	Maximum area (km ²)	Typical highest likelihood area (km ²)
15:00	125	168,365	42,000
10:00	83	74,829	19,000
5:00	42	18,707	4,700
1:00	8	748	190
0:30	4	187	47
0:15	2	47	12

Source: ATSB

Figure 104: Example visual representation of search areas associated with time uncertainty, assuming 500 knot groundspeed



Source: Google earth, annotated by ATSB

In the accident involving AF447, the aircraft was programmed to transmit ACARS reports (including position information) every 10 minutes. AF447 also sent an unscheduled, triggered report during the event sequence. The searchers therefore had an indication that impact with water would have been within a few minutes and almost certainly within 10 minutes. The initial search area for AF447 was 17,000 km² with the main wreckage not found until almost two years later. The investigation found that impact with water was about four minutes after the final triggered position report. As with MH370, the duration of the search was a function, to a large extent, of the level of uncertainty about the aircraft’s position at impact.

A BEA review (BEA 2011) concluded that when the aircraft position could be determined one minute prior to the accident, 95 per cent of accidents were within a 6 NM radius of that position, and 85 per cent were within 4 NM. When the aircraft position could be determined ten minutes prior to impact, none were within 20 NM. This indicates that a 10 minute interval between position reports would result in a potential search area of at least 4,300 km² in most cases.

To reduce the potential search area, position reports could either be sent at shorter intervals, or triggered by abnormal aircraft events to increase the likelihood that the most recent position report would be nearer to the accident site.

The information available for the search for MH370 was atypical because the normal aircraft position messages were not reported for the majority of the flight. MH370 was fitted with a system that would normally provide position reports via satellite every 30 minutes. During MH370 only basic handshake data and not position information was transmitted. The search area was established by a series of complex analyses of that data and refinements during the search using data not intended for that purpose.

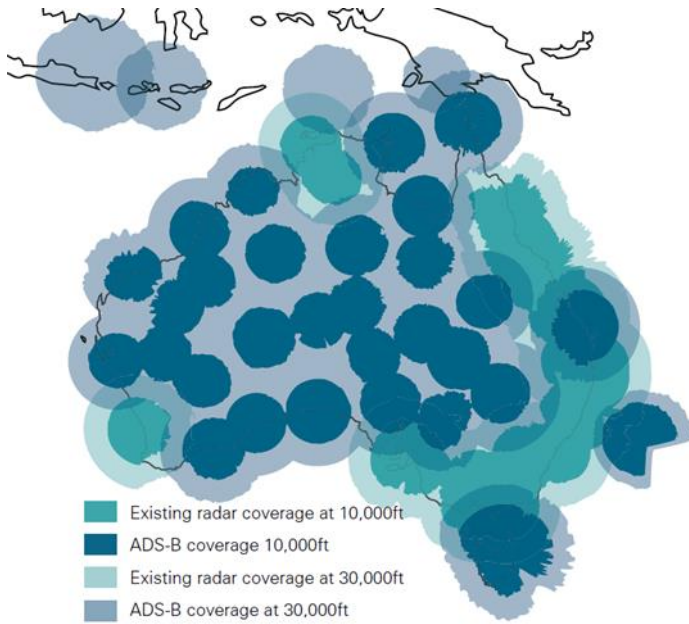
Initially, MH370 was thought to be in the seas around the Malaysian peninsula. The search did not commence in the Indian Ocean until 10 days after the flight. The delay and resulting oceanic drift led to large search areas and wide debris dispersal. By then, any debris left afloat would have drifted well over 100 km. Furthermore, unlike for most other searches, there was no single starting point. The position of MH370 at the time of the last satellite transmission could not be calculated as a particular point but lay somewhere along an arc more than 3,000 km long. The wide underwater search area, allowing for uncertainties and potential glide distance, was in the order of 1,200,000 km².

The aircraft's ACARS system had the ability to provide position reports and was configured by Malaysia Airlines to transmit position reports every 30 minutes. These were not sent for the majority of the flight. More recent position reports would have reduced this search area even if they had occurred a few hours before the end of the flight. Position reporting systems need to be both reliable and secure. Multiple sources and mechanisms to transmit position information can also be beneficial for redundancy.

Position tracking technologies

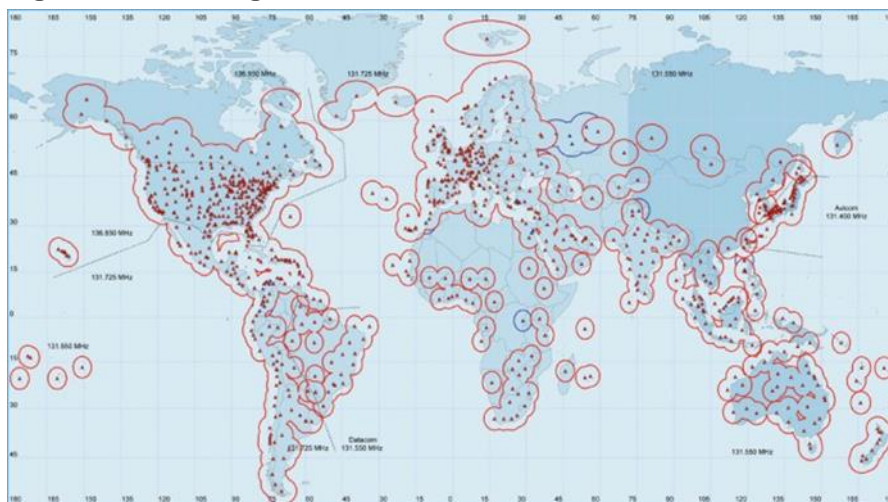
Around areas with high population density, controllers continuously track aircraft using secondary surveillance radar and Automatic Dependent Surveillance – Broadcast (ADS-B). Both of these technologies rely on aircraft and ground equipment, and only work when the aircraft is within range of the ground stations (Figure 105 and Figure 106). Aircraft-to-ground voice communications is generally accomplished over Very High Frequency (VHF) radio, which also has a limited range and is not available in oceanic areas.

Figure 105: Secondary surveillance radar (cyan) and ADS-B (blue) coverage in Australia



Source: Civil Aviation Safety Authority, modified by ATSB

Figure 106: Coverage of an ADS-B network

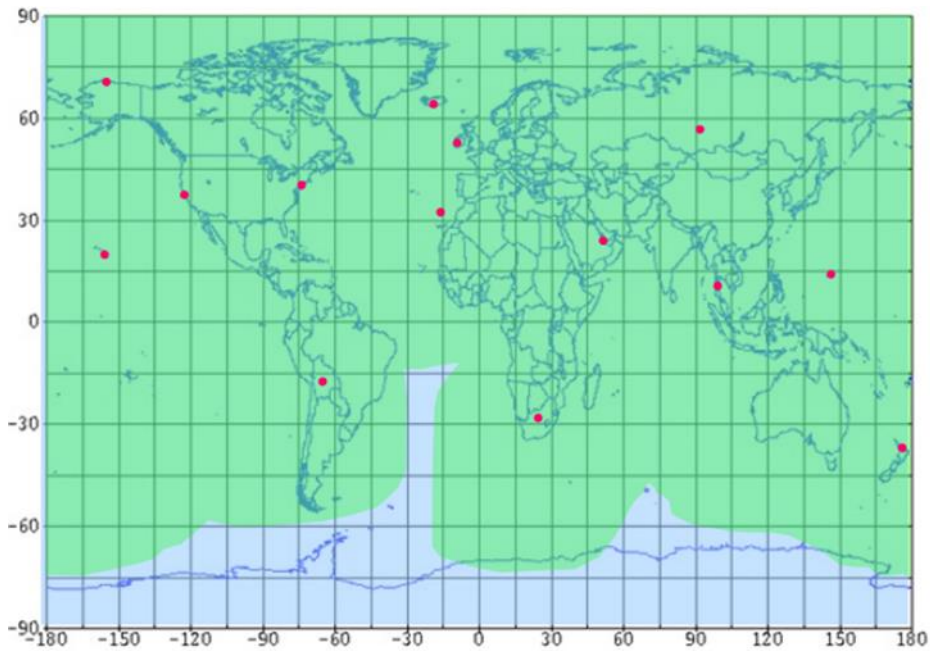


Source: SITA

If certain aircraft systems are not operational, the only way to track an aircraft outside of visual range is through the use of primary surveillance radar. Compared with secondary surveillance radar, these systems have reduced coverage, cannot positively identify an aircraft, and provide significantly degraded location and speed information.

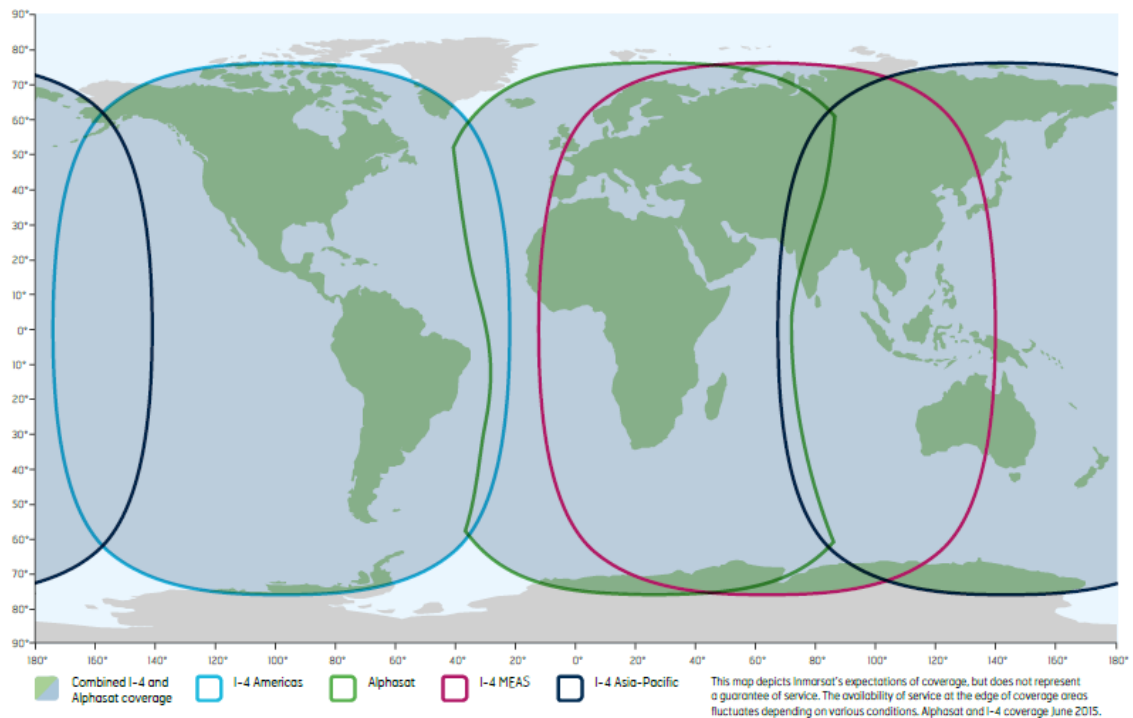
Over less populated areas and oceans, aircraft can send triggered, on-demand or scheduled position reports via satellite or long-range High Frequency radio with near-global coverage (Figure 107 and Figure 108). Both of these technologies need the equipment on board the aircraft to be operational.

Figure 107: Primary (green) and secondary (blue) coverage of a High Frequency network



Source: ARINC

Figure 108: Coverage of the Inmarsat Swift-Broadband satellite constellation



Source: Inmarsat

MH370 was within radar (both primary and secondary) and VHF range for the first part of the flight. For most of the flight over the Indian Ocean, the only available mechanisms to communicate with or locate it – that is, satellite and High Frequency radio – relied on the aircraft systems being both operational and switched on.

Aircraft in distress

Timeliness of accident detection is important in terms of narrowing the search area, and in some circumstances may also provide opportunities for positive intervention. In the case of MH370 the alert was not raised until some hours after the aircraft diverted from its planned route despite the expected handover to a different air traffic control authority and absence of scheduled ACARS reports.

However, this situation is very unusual. In general, an emergency situation in controlled airspace, particularly within range of radar or other tracking technology, is likely to be detected relatively quickly. Outside of these areas, the remote detection of abnormal conditions depends on information being transmitted from the aircraft to ground-based monitoring systems. There is often a very high pilot workload during an emergency and crews may not be willing or able to make a distress call or activate a distress signal.

The same technologies used for aircraft tracking in normal flight can also be used to detect and respond to abnormal events, such as deviation from a flight path or unusual aircraft behaviour. Currently, some aircraft can automatically transmit when certain events occur such as a change in climb or descent rate, or when there is an aircraft fault. This is likely to significantly reduce search area because a manually – or automatically – triggered position report is more likely to occur closer to the point of impact than a scheduled position report.

If there are adequate processes and assets in place to monitor this information, a timely response can be initiated. The response can be made more effective when there is more information available to draw upon, particularly the aircraft position as close as possible to the time of the accident, and information about the nature of the problem. Currently, the content and rate of automatic and manual reports, and the extent to which they are monitored for signs of abnormal events, is probably very variable.

There are significant technological hurdles that need to be overcome for all civil aircraft to continuously transmit detailed flight data and there is also a cost associated with such a systems. Nevertheless, the automatic streaming (continuous transmission) of detailed flight data may provide information of great value for both the search and investigation, possibly to an extent that recovery of the flight data recorders becomes significantly less important.

Furthermore, such data streamed from an aircraft in a distress situation or continuously throughout the flight may allow early detection and mitigation of factors that might lead to an accident. Such technology is evolving and already exists to some degree on some airframes. Initially, it may be feasible to only stream data in emergencies due to data capacity and rate limitations, but as the performance of datalink technology improves, these practices are expected to be more widely adopted in normal flight due to the potential economic and safety benefits that result from the availability of near real time flight data.

MH370's systems were capable of sending limited status data, automatically triggered by certain types of fault, via satellite or VHF radio. However, those transmission systems were not operating normally (and the aircraft was also out of range of VHF stations) for most of the flight.

Surface search

Once an aircraft is known or suspected to be subject to abnormal operations, and its exact location is not immediately apparent, a visual search is initiated. This is primarily conducted by aircraft and, if applicable, surface vessels. The purpose of this stage of the search is to find survivors and (if over water) floating debris. The size of the area to be searched is highly dependent on the information available about the aircraft's last position at this point in time.

Locating an aircraft which has impacted on land is less problematic than one in water. The wreckage doesn't sink or drift and impact usually leaves ground marks and smoke from a post-impact fire. The aircraft is more likely to have been seen if near a populated area. Weather,

terrain, and heavy foliage can be an issue, however, particularly for accidents involving small aircraft.

Accidents over water pose a different set of challenges. The aircraft usually breaks up on impact and most of it is likely to sink. Floating debris immediately begins to disperse with wind and waves and their distribution becomes wider over time. The first floating debris from AF447 was 70 km from the aircraft's last known position after 5 days. If the area is remote it may not be possible to deploy search resources quickly enough to avoid a search area that is tens of thousands of square kilometres. It is therefore imperative to obtain the best possible information about the impact location and to deploy effective search assets to the area as soon as possible to minimise the search area and maximise the likelihood of finding survivors and floating debris.

Aircraft are fitted with emergency locator transmitters (ELTs) to aid in locating an accident site. If effective, they provide accurate impact position information to monitoring satellites or nearby aircraft or surface craft. ELTs are designed to transmit locating signals on impact, and some can be manually triggered. This occurs very rarely, probably because crews understandably focus on resolving an emergency and preventing an accident rather than activating a device that cannot directly help them. ELTs that are activated on impact can often be damaged or shielded by wreckage or terrain, rendering them ineffective. Studies have indicated that ELT failure rates are in the region of 25-75 per cent though data is limited (ATSB 2013; Defence Research and Development Canada 2009; Stimson 2015).

Current-generation ELTs are not suitable for accidents on water, because they or their attached antennas are usually rendered ineffective by submersion and/or impact. It would be of significant benefit if an ELT transmission was automatically triggered whenever flight or fault conditions become significantly unsafe, prior to impact. A triggered ELT transmission provides similar benefits to triggered position reports with the additional benefit of a more rapid response because global monitoring and response systems are already proven and in operation.

An additional consideration is an ELT or similar device that is designed to float free following a water impact. This would generally drift with other debris permitting determination of the point of impact and the movement of floating debris after the impact.

There were four ELTs on board MH370. One was a fixed unit (located in the fuselage crown over the aft passenger cabin) and could have been either manually activated or automatically activated by a significant deceleration force. If activated, this unit would have transmitted a 406 MHz signal to specialised SAR satellites, and signals detectable by nearby aircraft or surface craft monitoring the relevant distress frequencies (243 MHz and 121.5 MHz).

A second ELT was portable with manual activation only, but otherwise had similar capabilities as the fixed unit, and was stowed in the forward cabin in a locker.

The other two ELTs were located in the emergency escape slides (which could be detached for use as a life raft) at door 1 left and at door 4 right. These ELTs were of a type that automatically activated on contact with water and transmitted only the 243 MHz and 121.5 MHz homing signals that are no longer monitored by satellite.

Despite the number of ELTs on board MH370, no distress transmissions were received by SAR authorities at any time during the flight. This suggests that the ELTs on board the aircraft did not transmit an emergency signal either by automatic or manual activation or by water immersion. This highlights the potential benefit of reliable, deployable and accident-resistant emergency beacon technology.

Underwater locator beacon search

The majority of aircraft wreckage usually sinks shortly after impact with the sea surface. This means that the technology with the greatest potential to assist searchers locate the main aircraft wreckage are the underwater locator beacons (ULBs) fitted to the flight recorders which commence transmitting on contact with water. The time available for searchers to locate the

aircraft debris field and the flight recorders on the seafloor is therefore limited by the battery life of the ULBs.

There are many factors which may delay the search for an aircraft's ULBs including: the accuracy of the last aircraft position data, the remoteness of the area, an initial search focused on rescuing survivors, the availability of suitable ULB detection equipment and a suitable vessel, time to mobilise the vessel, equipment and personnel and transit to the search area, and the weather in the area. All of these factors will reduce the window of opportunity to locate the ULBs before their batteries expire and limit the area that can be searched before this occurs.

As noted previously, a 10-minute position reporting interval would result in a search area of more than 4,300 km². By way of comparison, ICAO estimates that a ULB search can typically be conducted at a rate of about 100 km²/day and that a maximum of about 2,300 km² can be searched within the currently-mandated 30-day battery life (ICAO 2016).

Current generation ULBs transmit on a frequency of 37.5 kHz with a range of detection between 2 km and 3 km. This range depends on factors which affect the propagation of the ULB's acoustic transmissions through the water which include; depth, pressure, temperature and salinity and also the sensitivity of the detection equipment. Surface hydrophones are only effective in water depths up to approximately 2 km. In very deep water, a towed pinger locator (TPL) system must be used. These systems are not readily available and therefore take time to source, mobilise and transit to a search area on a suitable vessel. Furthermore, once a ULB is detected, multiple search passes with a TPL are needed to adequately triangulate the position of the ULB.

A significant complication in ULB searches is the reliability of detection, which can be affected by background noise, as well as potential for false positives from equipment on the search vessel or other transmitters such as marine science tracking devices.

The duration of the ULB search phase is influenced by how broad the search area is and how quickly the search equipment can be mobilised to the area. In the case of Air Asia 8501, the aircraft's last location was captured on radar, allowing early discovery of floating debris and an initial underwater search area of 9 km² (Kurniadi & Ng 2015). The underwater wreckage was located within days of the underwater search commencing. If the search had relied only on the position of floating debris, the underwater search may have taken considerably longer – the first floating debris found was over 50 km away (Komite Nasional Keselamatan Transportasi 2015).

ULBs can be difficult to locate due to extreme depths, or to a lesser extent, challenging underwater terrain. In this case wreckage might not be found within the limited battery life. The acoustic search for AF447's ULBs did not detect them even though vessels passed within expected detection range of the aircraft site; this may indicate that the beacons were not operational or that the signals were shielded by wreckage or silt.

In 2016, EgyptAir flight 804 impacted the Mediterranean Sea in an area with challenging underwater terrain. Due to an unusual circumstance the ELT was triggered prior to impact. With the aircraft's position known within about 5 km, and both ULBs being operational, the underwater wreckage took about a month to locate. The search came close to extending beyond the expected battery life even though it had the benefit of unusually good position information.

These accidents demonstrate that even precise impact position information may not be sufficient to provide a high level of confidence that a current-generation ULB will be located, particularly in deep or difficult waters. The benefits of having ULB devices that are as reliable, long-range and long-duration as practicalities permit are numerous. With greater battery life, the search can be extended. With greater range (using a lower frequency), more area can be searched in a given period of time. For accidents in deep waters, an extended-range ULB can also be detected by surface search equipment that is much more rapidly mobilised than a TPL or underwater vehicles.

MH370 was fitted with current-generation ULBs operating on 37.5 kHz with an expected battery life of between 30 and 40 days. Due to the very limited information available about the aircraft's location the ULB search along the 7th arc did not commence until 25 days after the flight, allowing

between 5 and 15 days to locate the beacons. Several false detections led to inefficient coverage of the search area. The search for the ULB's continued until 17 April 2014, 40 days after the flight. Subsequent refinements of the satellite data and other analyses indicated that this part of the search was concentrated too far north and well beyond the range of any current or proposed ULB type.

Sonar search

The final stage of the search is to determine the exact location of the aircraft debris field on the seafloor using sonar then optical imaging for positive identification. If a ULB is detected and its approximate location can be triangulated, this phase of the search can be relatively brief. For example, the wreckage of EgyptAir flight 804 was found about two weeks after the first ULB detection. If the location of the aircraft debris field has not been narrowed down with any other method a sonar search can take a long time and be very expensive.

The searches for AF447 and MH370 both demonstrate the extent of this effect. In the case of AF447, the aircraft's location was known to within a few minutes' flying time, with additional information available to prioritise the search area, yet an unsuccessful ULB search led to a sonar search that took four months over nearly two calendar years and at a cost of about €21 million (BEA 2012).

The sonar search for MH370 was based on even more limited information. Since there was very little information available about the aircraft's position (which partly led to the subsequent ULB search being unsuccessful) the sonar search area had to be several times greater than that for AF447. Primarily as a result of these issues, the sonar search has been unable to locate MH370 at a cost of up to A\$200 million.

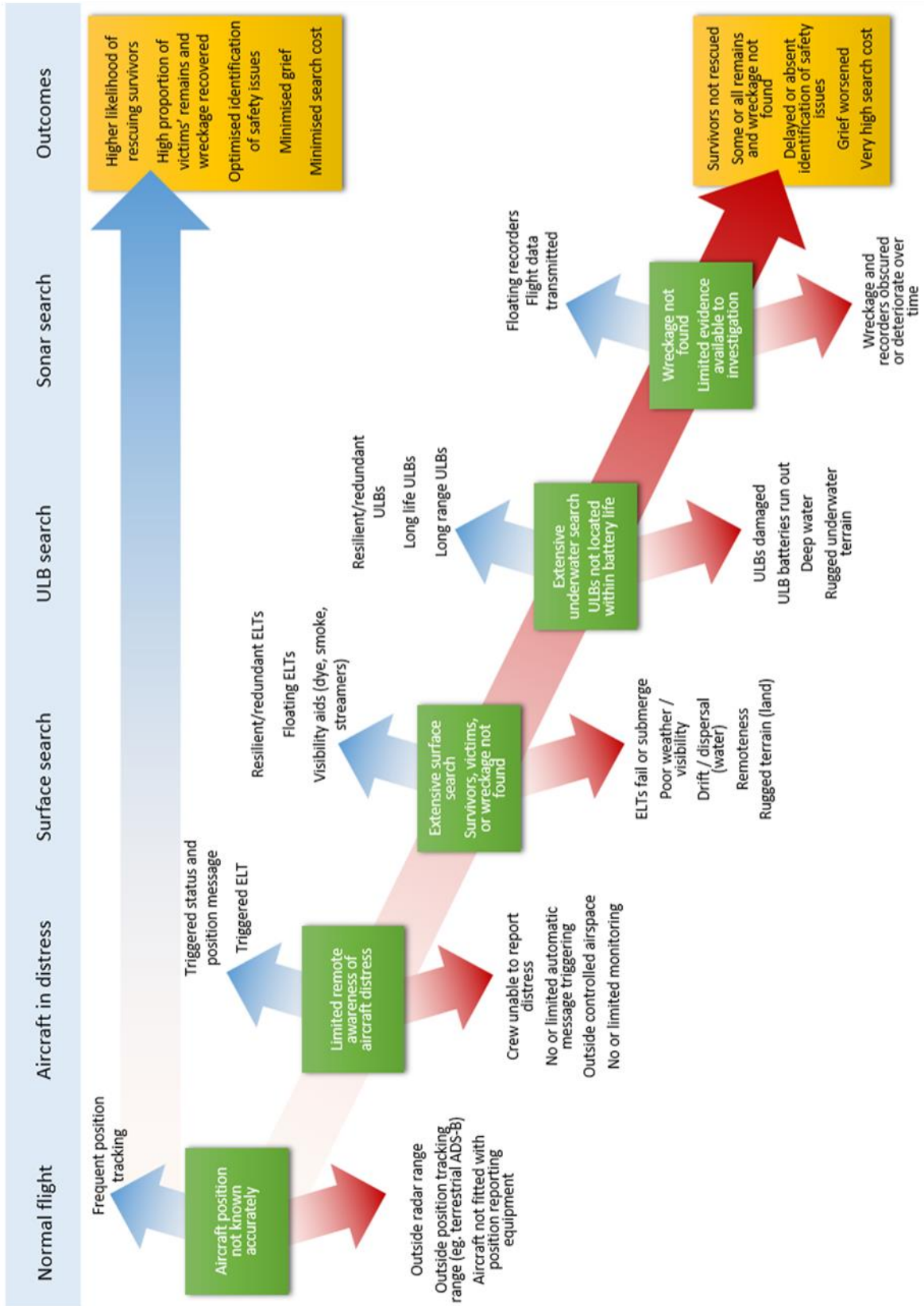
Summary

The preceding sections illustrate that issues arising early in a search can have a cumulative effect on the eventual outcome. Figure 109 illustrates the progression through each stage of a sea search, with some of the factors that help and hinder.

If an aircraft's initial position is not known with sufficient accuracy or there is a delay in responding, the area of floating debris will have drifted further from the impact point and dispersed, increasing the size required for a surface search. Debris drift modelling becomes less accurate over time and the potential location of an underwater debris field and ULBs becomes more uncertain. ULBs may not be detected before batteries become exhausted, resulting in a sonar search that needs to cover a wide area. Ultimately, every stage of the search becomes increasingly more difficult and costly.

Alternatively if the appropriate equipment, monitoring and response mechanisms are in place to capitalise on each opportunity to narrow the search area, the total search effort becomes far more manageable and has a much greater likelihood of success.

Figure 109: Factors affecting a sea search



Source: ATSB

Records of previous searches

The detailed search reports previously published by the BEA, and search information provided in some Annex 13 investigation reports such as for Asiana Airlines cargo flight 991 (Aviation and Railway Accident Investigation Board 2015) provide useful information for the benefit of planning and conducting future searches, and for pre-emptively improving search results as outlined in this report.

There is relatively limited public and official information available about the process and outcomes of some searches. It is not an explicit part of the Annex 13 guidelines for inclusion in an accident investigation report, so some reports do not address the search itself, or do so only in general terms. There is no Annex 12 requirement to publish or analyse search information. This limits the ability for researchers to determine the factors that help or hinder a search, and provide focus on factors that can be controlled.

The ATSB therefore considers it would be beneficial to include relevant and useful SAR information after an investigation. Examples of information that would be useful for future analysis include:

- last confirmed time, position, altitude, and position accuracy
- initial alert time and mechanism
- impact time and location
- initial search area and type, and search assets deployed
- underwater search area and type
- water depth, topography, and type of seafloor (such as rock, silt, sand, mixed)
- time and location of rescues
- time, location, and mechanism (such as visual, sonar, beacon detector) of important finds, including major floating debris, main wreckage, all flight recorders, and ULBs
- effectiveness of ELTs and ULBs when found (such as operational, non-operational, disconnected antenna) and other search and rescue aids.

Brief information could be included in the Annex 13 investigation report. More detailed information can be included in appendices, or separate reports, either published or held by ICAO for access by contracting States.

Related searches

In December 2009, a working group led by the BEA published a report that included details of 26 searches for aircraft lost at sea from 1980 – 2009 (BEA 2009). Since then, four more civil aircraft searches have occurred (Table 31).

Table 31: Related occurrences since December 2009

Date	Flight number	Location	Initial alert	ULB detected	Main wreckage found
19 May 2016	EgyptAir flight 804	Mediterranean Sea	ELT (triggered by electrical fault)	13 days	27 days
28 December 2015	Air Asia X flight 8501	Java Sea	Lost radar contact	Within 5 days	5 days
8 March 2014	Malaysia Airlines flight 370	Indian Ocean	Lost radio contact	No	No
28 July 2011	Asiana Airlines cargo flight 991	Korea Strait	Declared emergency over radio	No	5 days

Source: ATSB

Previous safety recommendations

Malaysian Air Accident Bureau

On 9 April 2014, the Malaysian Air Accident Bureau recommended that ICAO examine the safety benefits of introducing a standard for real-time tracking of commercial transport aircraft. At the time of writing, the Malaysian ICAO Annex 13 Safety Investigation Team advised that it had not received a formal response from ICAO to this recommendation.

Bureau d’Enquêtes et d’Analyses pour la sécurité de l’aviation civile (BEA)

Data transmission and emergency locator transmitters

The BEA directed an international working group on triggered transmission of flight data and in 2009 issued two recommendations (BEA 2009b) requesting that the European Aviation Safety Agency (EASA) and ICAO:

... study the possibility of making it mandatory for airplanes performing public transport flights to regularly transmit basic flight parameters (for example position, altitude, speed, heading).

... study the possibility of making mandatory, for airplanes making public transport flights with passengers over maritime or remote areas, the activation of the emergency locator transmitter (ELT), as soon as an emergency situation is detected on board.

In 2011, in a further update to the AF447 investigation (BEA 2011a), the BEA recommended that EASA and ICAO:

... make mandatory as quickly as possible, for airplanes making public transport flights with passengers over maritime or remote areas, triggering of data transmission to facilitate localisation as soon as an emergency situation is detected on board.

The BEA published a report by the Triggered Transmission Working Group (BEA 2011b) which advised that:

... it is technically feasible to significantly reduce the search area for wreckage by:

- Triggering transmission of appropriate data via SatCom prior to impact, and/or
- Automatically activating next generation ELTs prior to impact, and/or
- Increasing the frequency of position reports.

The working group also suggests that the location radius of 4 NM is a realistic aim for 2020.

Underwater locator beacons

On 17 December 2009, the BEA recommended (BEA 2009b) that EASA and ICAO

...extend as rapidly as possible to 90 days the regulatory transmission time for ULBs installed on flight recorders on airplanes performing public transport flights over maritime areas.

...make it mandatory, as rapidly as possible, for airplanes performing public transport flights over maritime areas to be equipped with an additional ULB capable of transmitting on a frequency (for example between 8.5 kHz and 9.5 kHz) and for a duration adapted to the pre-localisation of wreckage.

In 2012, the BEA advised (BEA 2012b)

During the acoustic searches undertaken during the first phase, the raw acoustic data from the towed pinger locators (TPL) was not recorded. Use of post-readout software would have made it possible to check if the ULB signals were present in the background noise. For future passive acoustic search systems, it appears to be essential to record this raw acoustic data.

Drift measurement buoys

On 5 July 2012, BEA issued numerous recommendations resulting from the AF447 investigation (BEA 2012), addressing several matters relevant to SAR. A recommendation addressed to ICAO recommended the amendment of ICAO Annex 12 to encourage contracting States to equip their search aircraft with buoys to measure drift and to drop them, when these units are involved in the search for persons lost at sea.

Aviation industry statements

International Air Transport Association

In an 11 November 2014 report on issues surrounding flight tracking and search activities, the IATA Aircraft Tracking Task Force (ATTF) made seven recommendations addressing aircraft tracking and coordinating responses to aircraft incidents (International Air Transport Association Aircraft Tracking Task Force 2014).

British Airline Pilots Association

On 8 March 2017, the British Airline Pilots Association (BALPA) issued a media release urging improved position tracking, including retrofitting advanced position tracking technology onto older aircraft (British Airline Pilots' Association 2017).

Safety actions

The key developments related to aircraft search in recent years are summarised here, and it is likely that other organisations have implemented additional local safety measures. It should be noted that the pace of change in aviation can be slow, especially when changes are far reaching. In addition to the time taken to determine and agree on the best approaches at an international level, it is necessary to provide state regulators, manufacturers and operators time to prepare and implement them.

International Civil Aviation Organization

In recent years, ICAO have convened several working groups and meetings to discuss issues related to aircraft tracking and search activities. Some are ongoing at the time of writing, with the following changes to ICAO Standards and Recommended Practices implemented from 2014 through 2016:

- Annex 6 Amendments 38 and 40-A introduced provisions for automatic deployable flight recorders (ADFR). These are deployable, buoyant flight data recorders that have an integrated ELT instead of a ULB.
- Annex 6 Amendment 38 also requires recorder-mounted ULBs to have increased battery life of 90 days from 1 January 2018. From the same date, most large aircraft operated on remote

oceanic routes are to be equipped with an additional airframe-mounted, long-range, 30-day ULB to supplement those fitted to the flight recorders.

- Annex 6 Amendment 40-A also introduced requirements for responding to distress alerts, and clarifications related to the use of emergency location equipment. Complementary to Amendment 40-A, ICAO Document 10054, *Manual on Location of Aircraft in Distress and Flight Recorder Data Recovery* is in development at the time of writing.

Annex 6 Amendment 39 specified aircraft to be fitted with tracking equipment from 8 November 2018, with 15-minute tracking intervals (recommended for all commercial aircraft over 27 t and mandated for aircraft over 45.5 t³⁵). This interval is to be decreased to every minute for an aircraft in distress³⁶, for aircraft certified after 1 January 2021 (recommended for new aircraft designs over 5.7 t and mandated for aircraft over 27 t). This is to provide ‘a high probability of locating an accident site to within a 6 NM radius’. In recent years the two largest regulators of aircraft manufacturers, EASA and the United States Federal Aviation Administration (FAA), implemented similar new rules governing the fitment and specification of ULBs.

Inmarsat

On 12 May 2014 Inmarsat announced the proactive provision of free ADS position reporting at 15-minute intervals to all aircraft equipped with its Classic Aero system (the system installed on MH370) which represents most long-haul commercial aircraft. Inmarsat’s more recent Swift Broadband service, which has been operational for over five years and is currently installed on more than 1,000 commercial passenger aircraft, automatically records the location of all aircraft in flight every two minutes for system optimisation purposes at no cost.

Malaysia Airlines

Malaysia Airlines plans to implement satellite-based ADS-B data monitoring and automated alerting to its existing fleet when the Aireon satellite constellation is operational in 2018. It was reported that this will not require the installation of any new equipment and will be capable of minute-by-minute reporting (Aireon 2017).

Airservices Australia

Among many other air traffic services providers worldwide, Airservices Australia have implemented a satellite ADS-C service. This enables aircraft to be tracked at 14-minute intervals in Australian airspace. According to Airservices Australia, controllers can now observe and react to any unusual flight behaviour and notify SAR agencies sooner. In the event of an abnormal situation, the reporting rate automatically increases to every five minutes. Air traffic controllers are also able to set the rate to near real-time for individual aircraft if required.

Joint committee

In 2013 the Radio Technical Commission for Aeronautics (RTCA) and European Organisation for Civil Aviation Equipment (EUROCAE) convened a joint committee (SC-229 and WG 98) to update standards addressing the latest design, performance, installation and operational issues for 406 MHz emergency beacons. In part, the committees’ scope includes the study of in-flight triggering and crashworthiness (Radio Technical Commission for Aeronautics 2016).

³⁵ As a guide, the latter category includes aircraft about the size of a Fokker 100 or larger.

³⁶ Triggering criteria is provided in EUROCAE ED-237, *Minimum Aviation System Performance Specification for Criteria to Detect In-Flight Aircraft Distress Events to Trigger Transmission of Flight Information*.

Conclusions

Flight tracking

Some of the most significant safety actions to date include:

- ICAO mandated that new aircraft types must be capable of detecting unsafe conditions, which triggers near-continuous data and position reports that can be remotely monitored.
- ICAO mandated that operators will need to track aircraft position at 15-minute intervals in normal flight.
- Airservices Australia now tracks aircraft position at 14-minute intervals within Australian airspace, and the reporting rate can be increased in response to abnormal situations.
- Inmarsat and Malaysia Airlines have voluntarily implemented a secondary means of position tracking that exploits a previously-unused capacity of existing technology.

There are some limitations to the improvements. The 15-minute position tracking interval may not reduce the search area enough to ensure that survivors and wreckage are located within a reasonable timeframe. This should be alleviated in new aircraft by the use of ADFRs and triggered, and subsequently near-continuous position reports but the former may not be widespread and the latter may not be effective when there are multiple aircraft system failures. Furthermore, until either capability is retrofitted to existing aircraft, the tracking interval would remain at 15 minutes and, with several new types already in service, there may be no significant change for many years. ATSB considers it highly desirable to find ways of implementing similar measures to existing aircraft. This can be done by increasing the rate of position reports, by implementing triggered transmissions, or recognising that there may be technical limitations of existing equipment, some combination of both.

Inmarsat and Malaysia Airlines have demonstrated that improvements to current – and previous – generation aircraft can be made with a relatively small initial outlay and minimal ongoing cost. While this approach may not provide the same level of functionality as mandated for newer aircraft, it should be applied to the existing fleets and aircraft designs that will constitute the bulk of air transport for the foreseeable future.

Given that many emergencies involve aircraft system failures and high crew workload, airborne locating systems must be designed to be automated as much as possible and resilient to failure of other systems (such as power), impact, fire, and immersion in water. For security reasons they should also be resistant to tampering and remote interference.

Emergency locator transmitters

The use of automatic deployable flight recorders (ADFR) is likely to significantly improve the information available for a search. An ADFR would have an integrated ELT that is more likely to remain operational after accidents over land and sea, and can also be used to monitor debris drift. However, partly due to technical challenges in ADFR design, there may be significant costs in developing and installing them and there are currently no rules requiring that they be installed. For this reason, other avenues should be explored to enhance ELT effectiveness in existing and future fleets.

Following the search and investigation into the loss of AF447, the BEA issued a recommendation to EASA and ICAO in regard to the activation of ELTs as soon as an emergency situation is detected on-board the aircraft. This is broadly similar in concept to the increase in position reporting rates for aircraft certified from 2021 onwards, but has the advantage of potentially being more readily retrofitted to existing fleets, and would also be more resilient to multiple aircraft system failures. International groups have been studying ways to improve ELT effectiveness.

Drift measurements

The surface search drift modelling was informed by the deployment of self-locating datum marker buoys from aircraft and vessels. Standard SAR marker buoys have an expected lifetime of around 20 days once deployed in the ocean and are fitted with a drogue. Their design attempts to minimise the effects of wind and surface waves so the buoy drifts primarily with the surface layer (top one to two metres of water) in a way analogous to a human being treading water.

Using standard SAR marker buoys to track the potential path of MH370 debris over long periods had some limitations. Their battery life needed to be longer, preferably several months at least, and the buoys needed to be designed to drift in a way similar to the debris which was recovered, on the surface and subject to the effects of both wind and surface waves.

Visual and radar search aids

Consideration could be given to installing automatically-deployed, floating search aids such as streamers or radar reflectors, particularly if it is feasible to install several, because they will tend to drift together with other debris. These could be incorporated as part of seat cushion design, or placed in frangible containers in cargo compartments and empty spaces throughout the airframe, to break loose during an impact sequence and can ultimately aid in the search for survivors, bodies, and floating wreckage. Water marking dye and smoke could also be considered, but less likely to be feasible because of their limited useful duration, and because smoke devices can themselves be hazardous.

Underwater locator beacons

Previous searches illustrate the benefit of having ULB devices that are as reliable, long-range and long-duration as practicalities permit. With greater battery life, a search can be extended if needed. With greater range, more area can be searched in a given period of time.

ICAO have mandated the introduction of ULBs that have a longer battery life and, for remote oceanic flights, have a much greater effective signal distance. The latter means that a greater area can be searched in a given period of time, and also that more assets can be deployed to searches in deeper waters where more specialised equipment was previously needed. These improvements to airborne equipment should greatly improve the likelihood of a successful underwater search.

Further improvements can be made by addressing the ways that a search is conducted. It is imperative to differentiate between ULB signals and others, and to make the most of available equipment to ensure that even very faint signals are detected. Examples of ways to accomplish both of these things are to record all measurements so that they can be reviewed later, and wherever possible, to use signal processing techniques to evaluate the validity of signal detections and maximise the detection sensitivity.

The BEA previously advised search authorities to record all acoustic data for later analysis if needed, in case a faint, ambiguous or obscured signal was not initially identified. In the case of the search for MH370, some recorded acoustic data was later analysed by several agencies to establish the validity of potential detections. Other potential detections could not be re-analysed because the data was not recorded; this meant that a search asset was diverted to the area for another scan, reducing the total area that could be acoustically searched in the limited time available. Though it made no difference to the outcome on this occasion, this kind of difficulty can be readily overcome if all search data is continuously recorded.

During the search for MH370, ATSB found that military sonobuoys can provide a rapidly-deployed and effective means to listen for ULBs over a wide area. One sortie was capable of searching an area of approximately 3,000 km². It is therefore beneficial to use this type of asset when possible.

Other considerations

As mentioned previously, the pace of change in aviation can be slow. Depending on the nature of the, as yet, undetermined reasons for the loss of MH370, it is possible that timely fulfilment of the BEA's 2009 and 2011 recommendations on transmission of flight data might have assisted in the search for MH370. On the other hand Inmarsat's voluntary and proactive inclusion of rudimentary tracking information into its satellite communications system has proven invaluable. This demonstrates how beneficial advancements can be found and implemented before the formal process is complete, and that those solutions can be simple and low-cost.

The equipment fit of current aircraft is far from uniform, and every operation is different. For example, there is less benefit in having frequent position reports if an effective distress or diversion alerting system is in place, or an aircraft is fitted with an ADFR, or if it only flies in radar-controlled airspace. Operators and manufacturers will need to find innovative ways of improving existing fleets in a way that suits their individual needs and capabilities. Regulators should support this approach.

To maximise effectiveness, an approach similar to that made for flight safety can be applied to the fitment of tracking and emergency location equipment. It is beneficial to have a level of functional overlap between systems to maximise reliability in the event of malfunction, and to reduce interdependencies for important systems.

Finally, though there are many uncontrollable factors that hinder a search, such as weather, remoteness and water depth, these factors can be managed. It is therefore critical to plan for an emergency response. Above all, a quick response can greatly assist in delivering a successful outcome. This means having the technology in place for alerting and information transfer, and the ground-based resources and processes to monitor and respond to them. Each system will be different depending on the requirements and capabilities of the operation, but the most important consideration is that the system needs to be viewed in its entirety from normal flight to finding underwater wreckage. This will make the process both effective and efficient.

ATSB safety recommendations

Malaysia is the responsible State for the ICAO Annex 13 investigation into the occurrence involving Boeing 777-200ER registered 9M-MRO and operating as Malaysia Airlines flight 370 (MH370). As a State that has participated in the investigation, Australia may also issue safety recommendations under Annex 13.

Search and rescue information

There is relatively limited public and official information available about the process and outcomes of some searches. It is not an explicit part of the ICAO Annex 13 guidelines for inclusion in an accident investigation report. Similarly there is no Annex 12 requirement to publish or analyse search information. This limits the ability for researchers to determine the factors that help or hinder a search.

Therefore the ATSB recommends that:

- ICAO encourages or mandates the publication of relevant information about search, rescue and recovery operations for the benefit of future research.
- ICAO Annex 13 investigation bodies should endeavour to publish relevant information about search, rescue and recovery operations for the benefit of future research.

Aircraft tracking

While there has been significant enhancements in the tracking of commercial aircraft in recent years there are some limitations to the improvements. The ICAO mandated 15-minute position tracking interval for existing aircraft may not reduce a potential search area enough to ensure that survivors and wreckage are located within a reasonable timeframe.

Therefore the ATSB recommends that:

- States ensure that sufficient mechanisms are in place to ensure a rapid detection of, and appropriate response to, the loss of aircraft position or contact throughout all areas of operation.
- Aircraft operators, aircraft manufacturers, and aircraft equipment manufacturers investigate ways to provide high-rate and/or automatically triggered global position tracking in existing and future fleets.

Sources and submissions

Sources of information

The sources of information used in the preparation of the report included the:

- Air Accidents Investigation Branch of the United Kingdom
- Annexes to the Convention on International Civil Aviation (Chicago, 1944)
- Australian Geospatial-Intelligence Organisation
- Australian Maritime Safety Authority
- Australian National University
- Boeing
- Bureau of Meteorology Defence Meteorological Support Unit
- Commonwealth Scientific and Industrial Research Organisation
- Curtin University Centre for Marine Science and Technology
- Defence Science and Technology Group
- Department of Civil Aviation Malaysia
- Dukane
- External contributors including members of the public reporting items of debris
- French Civil Aviation Safety Investigation Authority, BEA
- French Judicial Authorities
- French meteorological service on La Réunion Island
- French Ministry of Defence
- Fugro Survey Pty Ltd
- Geoscience Australia
- Hydrospheric Solutions Inc.
- Inmarsat
- Joint Agency Coordination Centre
- Joint Investigation Team
- Los Alamos National Laboratory (United States)
- Malaysia Airlines
- Ministry of Transport Malaysia
- National Aeronautics and Space Administration
- National Transportation Safety Board of the United States
- People's Republic of China government agencies
- Phoenix International Holdings Inc.
- Royal Australian Air Force
- Royal Australian Navy
- Royal Navy
- Scientific experts at Australian and international universities, museums and institutions
- Tangaroa Blue Foundation Ltd and Celestial Vision
- Thales
- University of Adelaide.

References

Aireon 2017, *Malaysia Airlines Enlists SITAONAIR, Aireon and FlightAware for 100% Global Flight Tracking*, media release, Aireon, Virginia, 18 April.

Australian Transport Safety Bureau 2013, *A review of the effectiveness of emergency locator transmitters in aviation accidents*, ATSB Transport Safety Report AR-2012-128, ATSB, Canberra.

Aviation and Railway Accident Investigation Board 2015, *Crash Into The Sea After An In-Flight Fire, Asiana Airlines, Boeing 747-400F, HL7604, International Waters 130 km West Of Jeju International Airport, 28 July 2011*, Aircraft Accident Report ARAIB/AAR1105, Aviation and Railway Accident Investigation Board, Sejong Special Self-governing City, Republic of Korea.

British Airline Pilots' Association 2017, *Pilots renew call for improved tracking on all aircraft on MH370 three-year anniversary*, media release, BALPA, London, 8 March.

Bureau d'Enquêtes et d'Analyses pour la sécurité de l'aviation civile 2009a, *Flight Data Recovery Working Group Report*, Technical document, BEA, Paris.

Bureau d'Enquêtes et d'Analyses pour la sécurité de l'aviation civile 2009b, *Interim Report n°2 on the accident on 1st June 2009 to the Airbus A330-203 registered F-GZCP operated by Air France flight AF 447 Rio de Janeiro – Paris*, BEA, Paris.

Bureau d'Enquêtes et d'Analyses pour la sécurité de l'aviation civile 2011a, *Interim Report n°3 On the accident on 1st June 2009 to the Airbus A330-203 registered F-GZCP operated by Air France flight AF 447 Rio de Janeiro – Paris*, BEA, Paris.

Bureau d'Enquêtes et d'Analyses pour la sécurité de l'aviation civile 2011b, *Triggered Transmission of Flight Data Working Group Report*, Technical document, BEA, Paris.

Bureau d'Enquêtes et d'Analyses pour la sécurité de l'aviation civile 2012a, *Final Report On the accident on 1st June 2009 to the Airbus A330-203 registered F-GZCP operated by Air France flight AF 447 Rio de Janeiro – Paris*, update 27 July 2012, BEA, Paris.

Bureau d'Enquêtes et d'Analyses pour la sécurité de l'aviation civile 2012b, *Sea Search Operations*, BEA, Paris.

Defence Research and Development Canada 2009, *Emergency Locator Transmitter (ELT) Performance in Canada from 2003 to 2008: Statistics and Human Factors Issues*, report prepared by J Keillor, G Newbold, A Rebane, S Roberts & J Armstrong, Technical Report DRDC Toronto TR 2009-101, Defence Research and Development Canada, Toronto.

International Air Transport Association Aircraft Tracking Task Force 2014, *Aircraft Tracking Task Force Report and Recommendations*, IATA, Montréal.

Inmarsat 2014, *Inmarsat to provide free global airline tracking service*, media release, Inmarsat, London, 12 May.

International Civil Aviation Organization 2016, *Annex 6 to the Convention on International Civil Aviation – Operation of Aircraft Part I – International Commercial Air Transport – Aeroplanes*, 10th edn, ICAO, Montréal, ATT K-1.

Komite Nasional Keselamatan Transportasi 2015, *PT. Indonesia Air Asia Airbus A320-216; PK-AXC Karimata Strait Coordinate 3°37'19"S – 109°42'41"E Republic of Indonesia 28 December 2014*, Aircraft Accident Investigation Report KNKT.14.12.29.04, KNKT, Jakarta.

Kurniadi T & Ng J 2015, 'Challenges of Sea Search and Recovery Operations - Sharing of Experience from a Recent Joint Operation', paper presented to the International Society of Air Safety Investigators Annual Seminar, Augsburg, Germany, 24-27 August.

Radio Technical Commission for Aeronautics 2016, 'Special Committee (SC) 229 – 406 MHz Emergency Locator Transmitters (ELTs) Terms of Reference', Revision 2, RTCA Paper No. 151-16/PMC-1506.

Stimson CM 2015, '2nd Generation ELT Performance Specification Development', visual presentation presented to the International SAR 2015 Conference and Exhibition, Brighton, United Kingdom, 12-13 May.

Submissions

Under Part 4, Division 2 (Investigation Reports), Section 26 of the *Transport Safety Investigation Act 2003* (the Act), the Australian Transport Safety Bureau (ATSB) may provide a draft report, on a confidential basis, to any person whom the ATSB considers appropriate. Section 26 (1) (a) of the Act allows a person receiving a draft report to make submissions to the ATSB about the draft report.

A draft of this report was provided to:

Air Accidents Investigation Branch of the United Kingdom

Australian Department of Defence

Australian Department of Finance

Australian Department of Infrastructure and Regional Development

Australian Maritime Safety Authority

Australian National University

Boeing

Bureau d'Enquêtes et d'Analyses pour la Sécurité de l'Aviation civile (France)

Chinese Maritime Safety Administration

Civil Aviation Administration of China

Commonwealth Scientific and Industrial Research Organisation

Curtin University Centre for Marine Science and Technology

Defence Science and Technology Group

Department of Civil Aviation Malaysia

Fugro Survey Pty Ltd

Geoscience Australia

Hydrospheric Solutions Inc.

Inmarsat

Joint Agency Coordination Centre

Komite Nasional Keselamatan Transportasi, Indonesia

Los Alamos National Laboratory (United States)

Malaysia Airlines Berhad

Ministry of Transport Malaysia

National Transportation Safety Board of the United States

Phoenix International Holdings Inc.

Thales

Transport Safety Investigation Bureau of Singapore

Submissions were received from:

Air Accidents Investigation Branch of the United Kingdom

Australian Department of Finance

Australian National University

Boeing

Commonwealth Scientific and Industrial Research Organisation

Defence Science and Technology Group

Fugro Survey Pty Ltd

Inmarsat

Malaysia Airlines Berhad

Ministry of Transport Malaysia

The submissions were reviewed and where considered appropriate, the text of the report was amended accordingly.

Appendices

Appendix A: Search vessels

Search vessels

Fugro Equator

At the time of involvement in the underwater search, the purpose built survey vessel, *Fugro Equator*, was operated by Fugro Survey Pty. Ltd., Australia. The ATSB contracted Fugro Survey Pty. Ltd. to provide the vessel, marine crew, survey crew and subsea equipment for search services in support of the ATSB led search operations to locate MH370. With a low acoustic signature, the vessel is fitted with a hull-mounted Kongsberg EM302 deep water multibeam echo sounder to undertake seabed mapping.

Fugro Equator involvement in the underwater search spanned from June 2014 to February 2017.

Figure 1: *Fugro Equator*



Source: Steph Turner

Ship details

Name:	<i>Fugro Equator</i>
IMO number:	9627411
Call sign:	C6ZT5
Flag:	Bahamas
Classification society:	Germanischer Lloyd
Ship type:	Research Survey Vessel
Year built:	2012
Owner(s):	Fugro Equator Inc.
Manager:	Fugro Survey Pte Ltd
Gross tonnage:	1,929 t
Deadweight:	564 t
Length overall:	65.74 m
Main engine(s):	3 x Mitsubishi S12R-MPTA
Maximum power:	3,420 kW
Service speed:	10 knots

GO Phoenix

At the time of involvement in the underwater search, the anchor handling tug supply (AHTS) vessel, *GO Phoenix*, was owned and managed by GO Marine Group Pty Ltd (GO Marine), Australia. The vessel was under charter to Phoenix International Holdings Inc. (Phoenix) who were contracted by DEFTECH, on behalf of the Malaysian Government, to provide Government Furnished Equipment (GFE) in support of the ATSB led search operations to locate MH370.

GO Marine provided the marine crew, and Phoenix provided the survey crew and subsea equipment. Phoenix subcontracted Hydrospheric Solutions Inc. (SLH) to provide survey crew and the ProSAS SLH PS-60 synthetic aperture sonar (SAS) system.

Go Phoenix involvement in the underwater search spanned from September 2014 to June 2015.

Figure 2: GO Phoenix



Source: ATSB Client Representative

Ship details

Name:	<i>GO Phoenix</i>
IMO number:	9495208
Call sign:	V7AW9
Flag:	Marshall Islands
Classification society:	Det Norske Veritas
Ship type:	Anchor Handling Tug Supply Vessel
Year built:	2013
Owner(s):	Hai Jiao 1207 Ltd
Manager:	Go Offshore Asia Pte Ltd
Gross tonnage:	7,534 t
Deadweight:	4,500 t
Length overall:	91.0 m
Main engine(s):	2 x MaK 16M32C
Maximum power:	16,000 kW
Service speed:	13 knots

Fugro Discovery

At the time of involvement in the underwater search, the survey vessel *Fugro Discovery* was operated by Fugro Survey Pty. Ltd., Australia. The ATSB contracted Fugro Survey Pty. Ltd. to provide the vessel, marine crew, survey crew and subsea equipment for search services in support of the ATSB led search operations to locate MH370.

Originally purpose built as a Norwegian Navy patrol boat, the vessel underwent a conversion before joining the Fugro fleet as a multi-role geophysical and hydrographic survey vessel.

Fugro Discovery involvement in the underwater search spanned from October 2014 to August 2016.

Figure 3: *Fugro Discovery*



Source: Fugro Survey/Oliver Edwards

Ship details

Name:	<i>Fugro Discovery</i>
IMO number:	9152882
Call sign:	3EKE6
Flag:	Panama
Classification society:	Det Norske Veritas
Ship type:	Research Survey Vessel
Year built:	1997
Owner(s):	Fugro Discovery Inc.
Manager:	Fugro Marine Services BV
Gross tonnage:	1,991 t
Deadweight:	1,350 t
Length overall:	70.0 m
Main engine(s):	1 x MaK 6M32
Maximum power:	2,638 kW
Service speed:	10 knots

Fugro Supporter

At the time of involvement in the underwater search, the survey vessel *Fugro Supporter* was operated by Fugro Survey Pty. Ltd., Australia. The ATSB contracted Fugro Survey Pty. Ltd. to provide the vessel, marine crew, survey crew and subsea equipment (AUV system) for search services in support of the ATSB led search operations to locate MH370.

Originally built as a Buoy and Lighthouse Tender, the vessel underwent a conversion before joining the Fugro fleet as a multi-purpose geophysical and hydrographic survey vessel.

Fugro Supporter involvement in the underwater search spanned from January 2015 to May 2015.

Figure 4: *Fugro Supporter*



Source: ATSB

Ship details

Name:	<i>Fugro Supporter</i>
IMO number:	8518364
Call sign:	JZKY
Flag:	Indonesia
Classification society:	Biro Klasifikasi Indonesia
Ship type:	Research Survey Vessel
Year built:	1994
Owner(s):	Suar Samudera Abadi PT
Manager:	Suar Samudera Abadi PT
Gross tonnage:	2,065 t
Deadweight:	1,152 t
Length overall:	75.39 m
Main engine(s):	3 x Caterpillar 3516TA
Maximum power:	2,760 kW
Service speed:	12 knots

Havila Harmony

At the time of involvement in the underwater search, the survey vessel *Havila Harmony* was operated by Fugro NV. The ATSB contracted Fugro Survey Pty. Ltd. to provide the vessel, marine crew, survey crew and subsea equipment (AUV system) for search services in support of the ATSB led search operations to locate MH370.

Originally built as an Offshore Supply Vessel, the vessel underwent a conversion before joining the Fugro fleet as a multi-purpose geophysical and hydrographic survey vessel, fitted with dynamic positioning (DP2).

Havila Harmony involvement in the underwater search spanned from November 2015 to March 2016.

Figure 5: *Havila Harmony*



Source: Fugro

Ship details

Name:	<i>Havila Harmony</i>
IMO number:	9343596
Call sign:	LAYW7
Flag:	NIS (Norway)
Classification society:	Det Norske Veritas
Ship type:	Offshore Support Vessel
Year built:	2005
Owner(s):	Havila Offshore Labuan Ltd
Manager:	Havila Shipping ASA
Gross tonnage:	4,724 t
Deadweight:	3,000 t
Length overall:	92.95 m
Main engine(s):	4 x Cummins QSK60-M
Maximum power:	7,600 kW
Service speed:	13.5 knots

Dong Hai Jiu 101

At the time of involvement in the underwater search, the search and rescue vessel, *Dong Hai Jiu 101*, was operated by the Dong Hai Rescue Bureau, China. The vessel and marine crew was made available by the Chinese Government to support the ATSB led search operations to locate MH370. Dong Hai Jiu translates to East China Sea.

The ATSB contracted Phoenix to provide the survey crew and subsea equipment. Phoenix subcontracted SLH to provide survey crew and the ProSAS SLH PS-60 synthetic aperture sonar (SAS) system. Phoenix also provided an ROV system.

Dong Hai Jiu 101 involvement in the underwater search spanned from January to December 2016.

Figure 6: *Dong Hai Jiu 101*



Source: ATSB

Ship details

Name:	<i>Dong Hai Jiu 101</i>
IMO number:	9654816
Call sign:	BSIN
Flag:	China
Classification society:	China Classification Society
Ship type:	Search and Rescue Vessel
Year built:	2012
Owner(s):	China Government Dong Hai Rescue Bureau
Manager:	China Government Dong Hai Rescue Bureau
Gross tonnage:	4,747 t
Deadweight:	1,759 t
Length overall:	116.95 m
Main engine(s):	2 x MAN-B&W 6L48/60CR
Maximum power:	14,400 kW
Service speed:	21 knots

Appendix B – Identification of the most probable final location of flight MH370 (Issue 2) – Joint Investigation Team paper - 26 April 2014

Note: This appendix provides a copy of the analysis as provided post a Joint Investigation Team (JIT) briefing to AMSA on 2 April 2014. The paper therefore describes the analysis and advice to 2 April 2014 and represents only a snapshot of the JIT on-going analysis to early April 2014.

The paper provides the background on BTO and BFO analysis during the Australian-led surface search in March-April 2014. The reader should consider the contents of this paper in this context only. Later published technical analysis of BTO and BFO referred to in the main report links provides the refined BTO and BFO analysis used to define underwater search areas.

At the time this paper was written the aircraft manufacturer, was providing assistance to Malaysia and the ATSB in establishing:

- possible reasons for the total communication loss between 1707 UTC and 1825 UTC (page 3)
- end-of-flight scenario theories based on the final arc as it related to possible fuel exhaustion (page 16).

No current investigations or assessments are currently being undertaken by Boeing into this.

The JIT paper analysis provided in this appendix showing a 400 knots best fit path was revised on 5 April 2014 for 425 knots as the best fit. (See Table 15 of the main report).

IDENTIFICATION OF THE MOST PROBABLE FINAL LOCATION OF FLIGHT MH 370 (ISSUE 2)

INTRODUCTION

This document records the development of a process, up to 2 April 14, to determine the most probable final location of Flight MH 370. Issue 2 was issued on 26 April 14 with some minor changes to ensure that the terminology for handshake is consistent with earlier communications. There are no changes in the resultant search areas.

Timing information obtained from satellite data and aircraft performance data was used to identify a Northern and Southern corridor along which Flight MH 370 may have flown. Doppler information from the satellite data, combined with aircraft performance data was then used to further refine the most probable final location. Finally, consideration was given to the navigation of the aircraft and the mode that it may have flown in utilising the stored routes and waypoints in its Flight Management System. This work concluded that Flight MH 370 probably ended in an area 375 nautical miles long and 40 nautical miles wide, centred approximately 900 nautical miles off the west coast of Australia, with the most probable location in the northern part of this area.

At the time of this report, further work is being carried out using the satellite data in order to further refine this position.

Timings. All timings are UTC. Malaysian time (MYT) is UTC + 8 hours.

BACKGROUND INFORMATION ON SATELLITE COMMUNICATIONS

Functions

Satellite Communications (SATCOM) provides the satellite link for the following functions:

- Audio and text communication.
- Interface with ACARS.
- In-flight Entertainment Equipment.

Technical information

The aircraft satellite communication system operates on L Band, transmits at 1.6 GHz and receives at 1.5 GHz. The Earth Station uses C Band, transmits at 6 GHz and receives at 4 GHz. During the flight of MH 370, the aircraft communicated through the Inmarsat Indian Ocean Region (IOR) I-3 satellite and the Earth Station in Perth Australia.

There are a number of channels available for messages to be sent between the satellite and Earth Station. One of the channels is called the 'common access channel', which aircraft will listen to when not engaged in a call on another channel.

If the ground station has not heard from an aircraft for an hour since the last communication then it transmits a 'log on / log off' ("ping") message on the common access frequency using the aircraft's unique identifier. If the aircraft receives its 'unique identifier' it returns a short message that it is still logged onto the network. This process has been described as a handshake.

The following timing information is recorded at the satellite Earth Station for each handshake:

- Earth Station to the Satellite,
- Satellite to the Aircraft,
- Aircraft to the Satellite,
- Satellite to the Earth Station.

During the flight of MH 370, the satellite reached its most northerly point of the inclination orbital path at approximately 19:30 hrs, after which it moved in a southerly direction increasing in velocity until it crossed the equatorial plane at 01:30 hrs. For an aircraft in the southern hemisphere the satellite appears to be moving towards it during this period and hence the Doppler frequency increases as the satellite velocity increases. For an aircraft in the northern hemisphere the satellite will appear to be moving away from it and the Doppler will decrease as the satellite's velocity increase.

INITIAL PREDICTIONS OF THE AIRCRAFT FLIGHT PATH

Initial information

MH 370 departed Kuala Lumpur international airport (KLIA) at 16:41 hrs on 7 March 14. On 8 March 14, Malaysian Airlines (MAS) established that the aircraft SATCOM had completed a handshake with the

Inmarsat satellite at 00:19 hrs. At this time MAS also estimated that there was sufficient fuel on the aircraft for it to remain airborne until 00:12 hrs.

Final seven handshakes

Apart from a period between the last ACARS message at 17:07 hrs and the handshake at 18:25 hrs on the 7 March 14, the SATCOM link was available during the flight. This interruption of the SATCOM link occurred after ACARS had stopped transmitting messages and may have occurred for a number of reasons such as cycling of the electrical power, the aircraft's antenna losing sight with the satellite or the resetting of the aircraft's Satellite Display Unit (SDU). There is no record in the satellite Earth Station log of the link having been logged-off from the cockpit through the Control Display Unit (CDU); such an activity would have been automatically captured in the Earth Station log. The reason for the loss of the SATCOM link is currently being investigated by the aircraft and equipment manufacturers.

Data from the last seven handshakes¹ was used to help establish the most probable location of the aircraft. Initially only six of these handshakes, which had been initiated by the Earth Station, were considered to be complete. The seventh and last handshake, which had been automatically initiated by the aircraft, was originally assessed as a partial handshake and was not used in the analysis. Two unanswered ground to air telephone calls had the effect of resetting the activity log and hence increased the period between the ground initiated handshakes. The significant timings used to identify the most probable final location of the aircraft are as follows:

Aircraft departs KLIA	16:41 hrs
Last ACARS transmission	17:07:48 hrs
1 st – handshake initiated by the ground station	18:28:27 hrs
Unanswered ground to air telephone call	18:39:52 hrs
2 nd – handshake initiated by the ground station	19:41:00 hrs
3 rd – handshake initiated by the ground station	20:41:02 hrs
4 th – handshake initiated by the ground station	21:41:24 hrs
5 th – handshake initiated by the ground station	22:41:19 hrs
Unanswered ground to air telephone call	23:13:58 hrs
6 th – handshake initiated by the ground station	00:10:58 hrs
7 th – handshake initiated by the aircraft	00:19:29 hrs
Aircraft did not respond to handshake from the satellite earth ground station.	01:15:56 hrs

¹ Since the 2 April 14 the seven handshakes have been redefined such that only five meet the definition originally given in this paper. This change makes no difference to the final location of the aircraft. In order to be consistent with information previously released by the Malaysian authorities, Issue 2 of this paper continues to call all seven contacts 'handshakes'.

Construction of the seven arcs

From the time that it took the signals to be sent and received by the Earth Station it was possible to determine the elevation between the aircraft and satellite at each handshake and the previous ACARS exchanges. This elevation data is plotted in Figure 1.

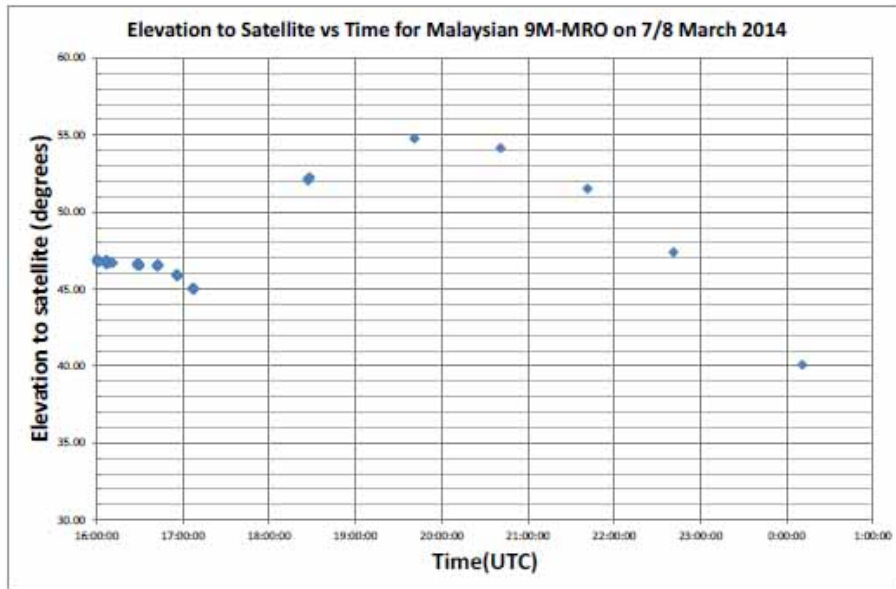


Figure 1 – Plot of the elevation of the aircraft to the satellite

This initial analysis assumed a fixed satellite location. The analysis was subsequently updated to incorporate the inclined orbit of the satellite, which reached approximately 1,200 km above and below (z-axis) the equatorial plane over a 24 hour period. On the 7 March 14, the satellite was at the most northerly point of its orbit at approximately 19:30 hrs.

The time that the seven handshakes occurred and the exact knowledge of the satellite location enabled a number of arcs to be drawn on the earth's surface at a fixed distance from the satellite - the altitude of the aircraft was not taken into account. The length of these arcs was constrained by the maximum speed of the aircraft, which was initially set at a ground speed of 652 kt. The arcs for the seven handshakes are shown at Figure 2.

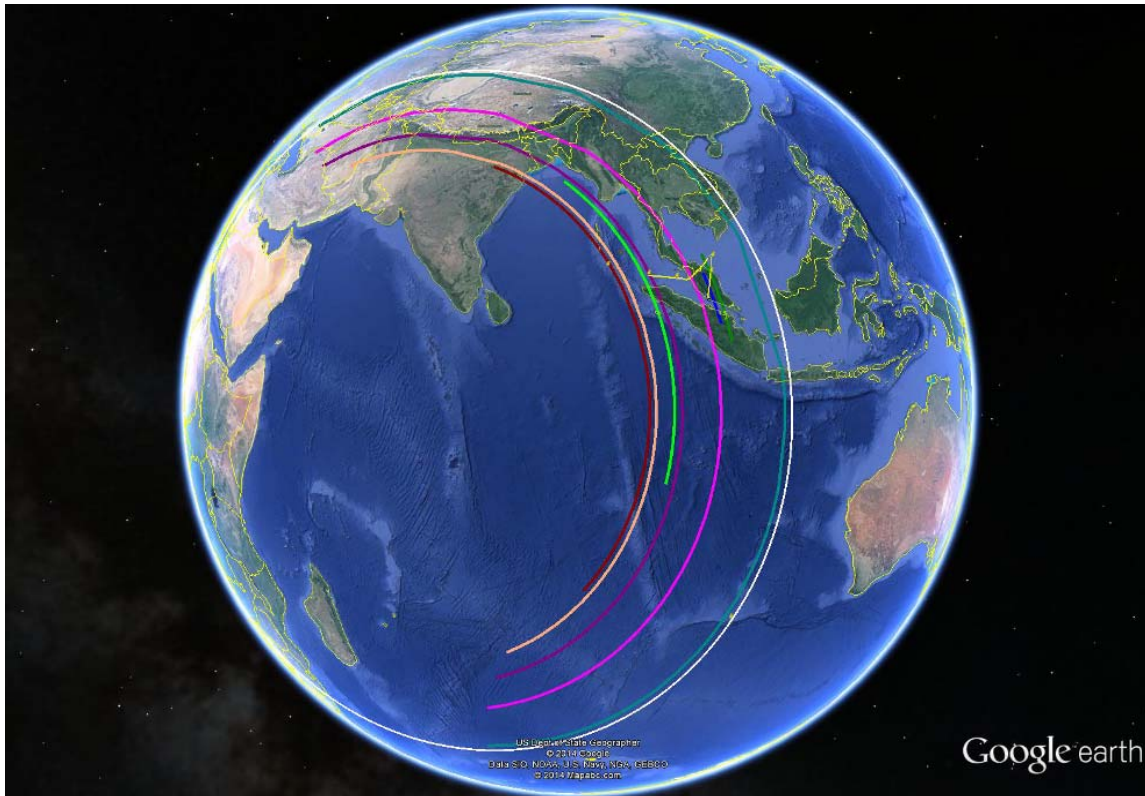


Figure 2 - Position of the arcs obtained from the 7 handshakes

Development of Northern and Southern routes

Primary radar data provided by the Royal Malaysian Air Force detected an aircraft believed to be MH 370, flying through the Straits of Malacca. At this time only the location data was used in the final location analysis as the accuracy of the speed and altitude information was not known. Therefore, for the initial calculations, the altitude and speed of the aircraft was obtained from the data in the cruise report, timed at '17:06:43 hrs' ('latitude 5.299° S and longitude 102.813° E') that had been transmitted via ACARS. The altitude was recorded as 35,000 feet and from the other recorded parameters Boeing calculated a ground speed of 473 kts. The cruise report also stated that the total fuel weight (TOTFW) at this time was 43,800 kg.

The aircraft had to cross each of the seven arcs at the time of the handshake. Using the assumption that the aircraft altitude and speed remained the same, it was possible to estimate where the aircraft would have crossed the 1st arc. This approach produced two solutions, one heading in a northerly direction and the second in a southerly direction.

Boeing undertook a number of performance calculations varying the speed and altitude to determine the range of the aircraft. The speed chosen affected where the aircraft crossed each of the arcs. This resulted in a family of solutions along the arc generated by the satellite data from the 6th handshake. These

northern and southern solutions are shown in Figure 3 and are bounded by the low and high speed flight paths which terminate on the final position arcs (6th arc).

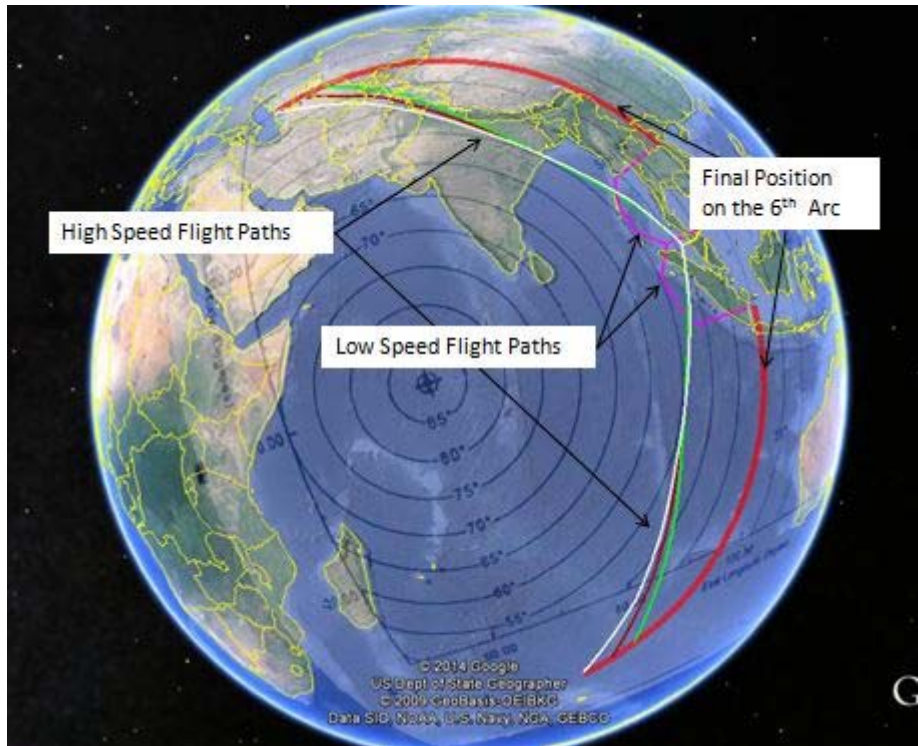


Figure 3 - Northern and southern final position arcs

PREDICTIONS BASED ON THE OFFSET BURST FREQUENCY

In order to determine if the aircraft flew the northern or southern route a second technique was developed by Inmarsat, which considered the relative velocity of the satellite to the aircraft. This technique considered the difference in frequency of the pulse sent and received by the earth station, which was defined as the Offset Burst frequency (OBF).

Use of Doppler data to help locate the aircraft

The OBF results from the position and movement of the satellite relative to the aircraft. The aircraft attempts to compensate for the Doppler generated by the aircraft's movement and the Earth Station for the movement of the satellite. The contribution to the OBF from the various Doppler contributions is shown in Figure 4.

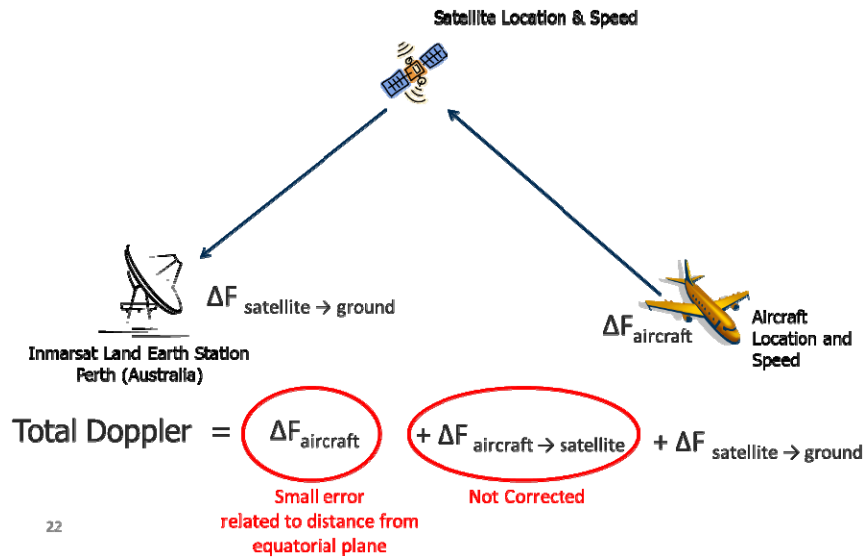


Figure 4 - Doppler contributions to OBF

The Doppler is comprised of the following components:

- The $\Delta F_{\text{aircraft}}$ component is the correction applied by the terminal for the aircraft velocity and assumes a fixed satellite position. When the satellite is furthest from the assumed position the applied frequency offset error, while not large, will be its largest. As the satellite moves towards the equatorial plane the assumed satellite position becomes closer to reality and the correction applied by the terminal become more accurate and the $\Delta F_{\text{aircraft}}$ error becomes insignificant.
- The $\Delta F_{\text{aircraft} \rightarrow \text{satellite}}$ component is at its lowest when the satellite is turning from a northerly to southerly direction. The satellite will accelerate as it heads towards the equatorial plane so the $\Delta F_{\text{aircraft} \rightarrow \text{satellite}}$ component becomes larger with time. For an object in the southern hemisphere the satellite will now be moving towards it and hence the Doppler will increase. This is what the data shows for MH 370 indicating that it had flown to the south.

The overall Doppler is therefore a combination of $\Delta F_{\text{aircraft}}$, which is largest earlier in the flight and decreases over time, and $\Delta F_{\text{aircraft} \rightarrow \text{satellite}}$, which is lowest earlier in the flight and increases over time. The maximum error for $\Delta F_{\text{aircraft}}$ is still quite small and is of the same order of magnitude as $\Delta F_{\text{aircraft} \rightarrow \text{satellite}}$ during the first few hours after the last known ACARS transmission.

The theory is that the frequency shift will be different depending where you are on the arc, the direction of travel and the speed of the aircraft. This theory has been checked against 11 other Boeing 777 aircraft, flying in various northern and southern directions.

While on the ground at Kuala Lumpur airport and during the early stage of the flight MH 370 transmitted 17 messages. At this stage the location of the aircraft and the satellite were known; therefore it was possible to calculate the system time delay for the aircraft, satellite and ground station. The OBF was calculated at each handshake and knowing the time and position of the satellite it was possible, considering the aircraft performance, to determine where on each arc the OBF would fit best.

The position that the aircraft crossed the 6th arc was dependent on the aircraft speed and the position where the aircraft turned south after flying north along the Straits of Malacca. The assumption was that the turn south occurred at the northern end of Sumatra. The analysis showed poor correlation on the northern track, but good correlation on the southern track. The analysis also indicated that using these assumptions, speeds of approximately 450 kts and 400 kts resulted in the best fit. This can be seen in Figure 5.

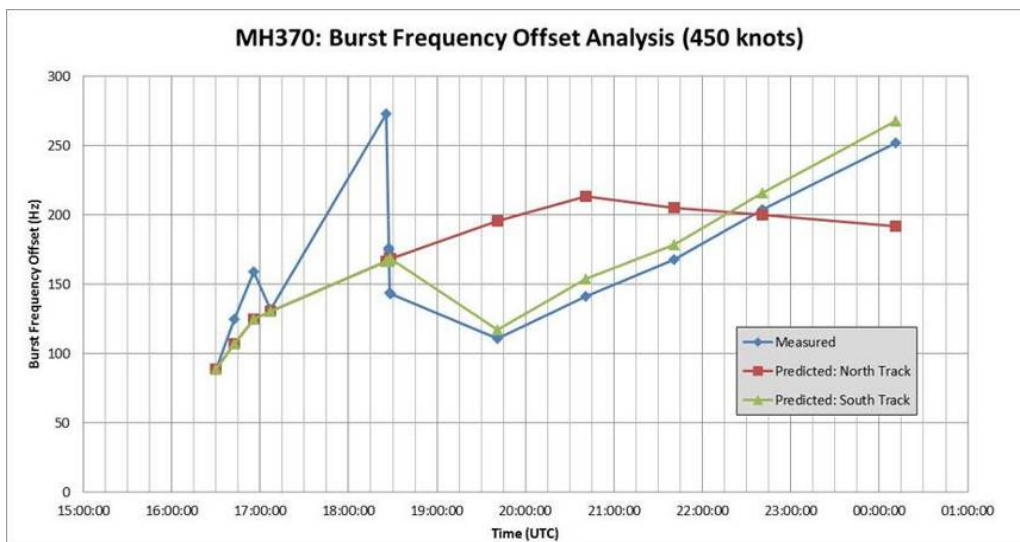


Figure 5 - Best fit OBF at 450 kts

The yellow track shown in Figure 6 is an example of a quick turn south after the final military radar contact coupled with a high speed track of 450 kts. The red track represents a more northern track after the final military radar contact followed by a 400 kts southern track. This shows a good correlation between the southern track prediction and the aircraft performance.

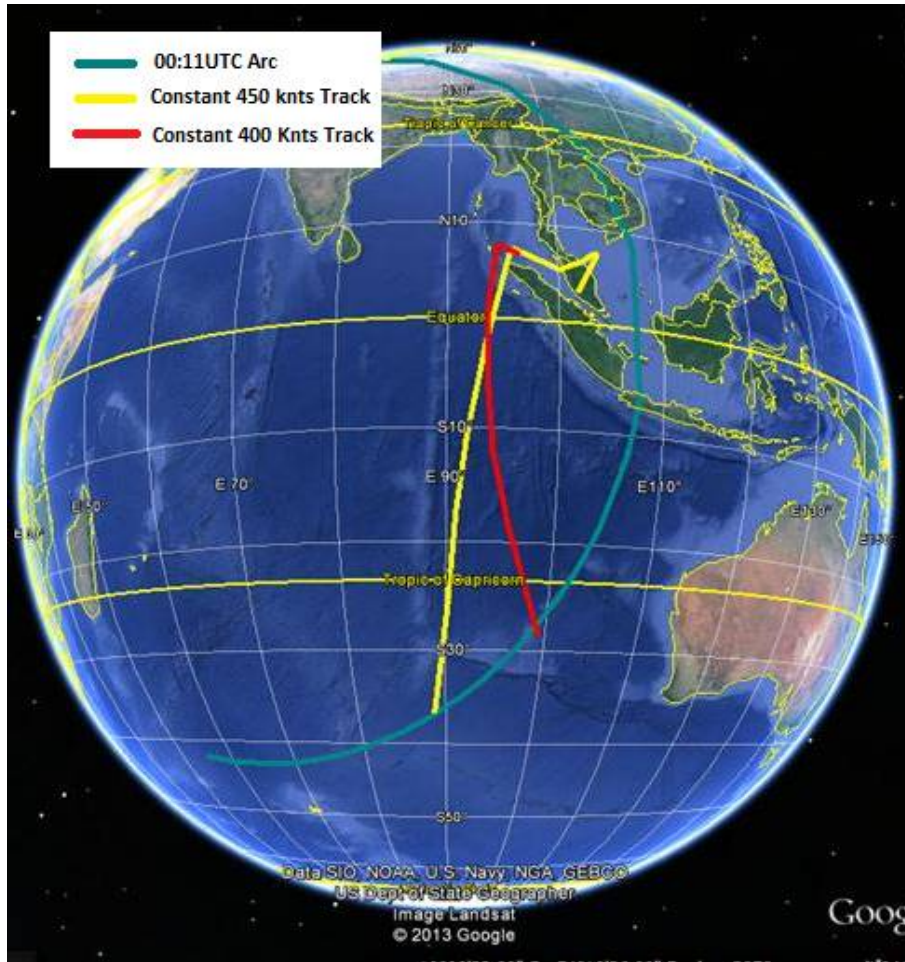


Figure 6 - Examples of southern solutions from Inmarsat analysis

It was possible to assess the accuracy of the analysis using the timing from the 17 messages transmitted from the aircraft while it was on the ground at Kuala Lumpur airport. The maximum positional error from the analysis was approximately 17 km. Inmarsat advised that the positional error of the 6th and 7th arcs would be of the same order.

No response was received from the aircraft at 01:15:56 hrs when the ground earth station sent the next log on / log off message, indicating that the aircraft was no longer logged onto the network.

This analysis established that the aircraft had not flown along the northern corridor and it was unlikely that the flight ended in the north part of the southern corridor. However the flight had to have crossed the 6th arc at 00:10:58 hrs and the 7th arc at 00:19:29 hrs. The estimation of the final position had yet to be determined.

FIRST PROPOSED SEARCH AREAS

Performance based analysis

The first proposed search areas were established by using Boeing's performance predictions and the criteria that for a track to be valid it must reach the 6th arc. The flight tracks shown in Figure 7 represent the maximum distances based on the crossing of the arcs and the speed of the aircraft. The lower boundary defined by S1 to S5 represents the maximum range of the aircraft. As the S1 and S2 areas were created by the longest and straightest tracks they initially generated the greatest interest.

First assumption on lateral navigation mode

By setting a heading for the aircraft to fly, the track would change with the increase in magnetic variation the further south the flight progressed. It was concluded that in order to be assured of flying a required track, the aircraft lateral navigation would probably have been selected to the 'track' mode. This would maintain the desired track with the increasing magnetic variation being compensated for.

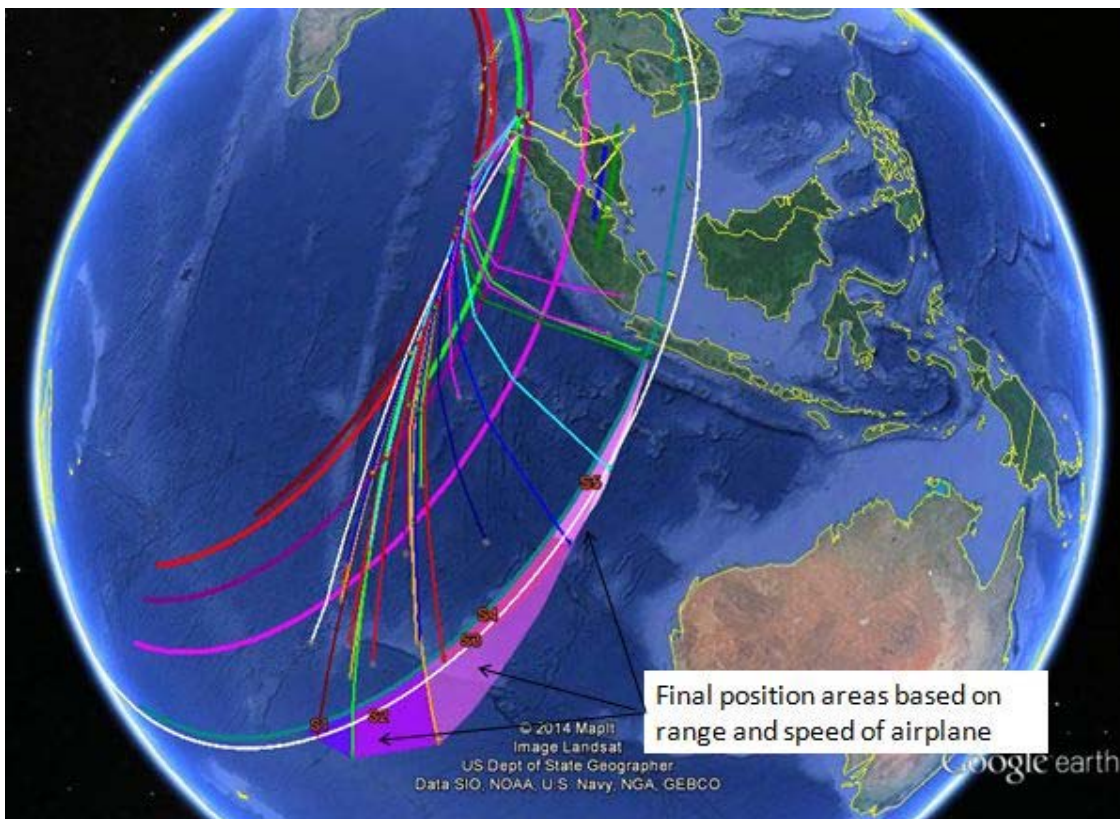


Figure 7 - Early final position locations based on aircraft performance

REFINEMENT OF INITIAL ASSUMPTIONS

Boeing's analysis of the aircraft's movement from the last ACARS reporting position and the end of the primary radar coverage showed that the aircraft had accelerated from 473 kts to 500 kts as it transited across the Malaysia Peninsular and along the Straits of Malacca. This was confirmed by the last two Royal Malaysian Air Force air defence radar returns.

Moving the aircraft's turn south to a position slightly north of Sumatra resulted in a closer fit of the Doppler at the arc defined by the first handshake. This change resulted in a decrease in range for the longest flight paths that had helped to define S1 and S2 and which now no longer reached the 6th arc. Consequently S1 and S2 were no longer considered to be locations where the flight could have ended. See Figure 8.

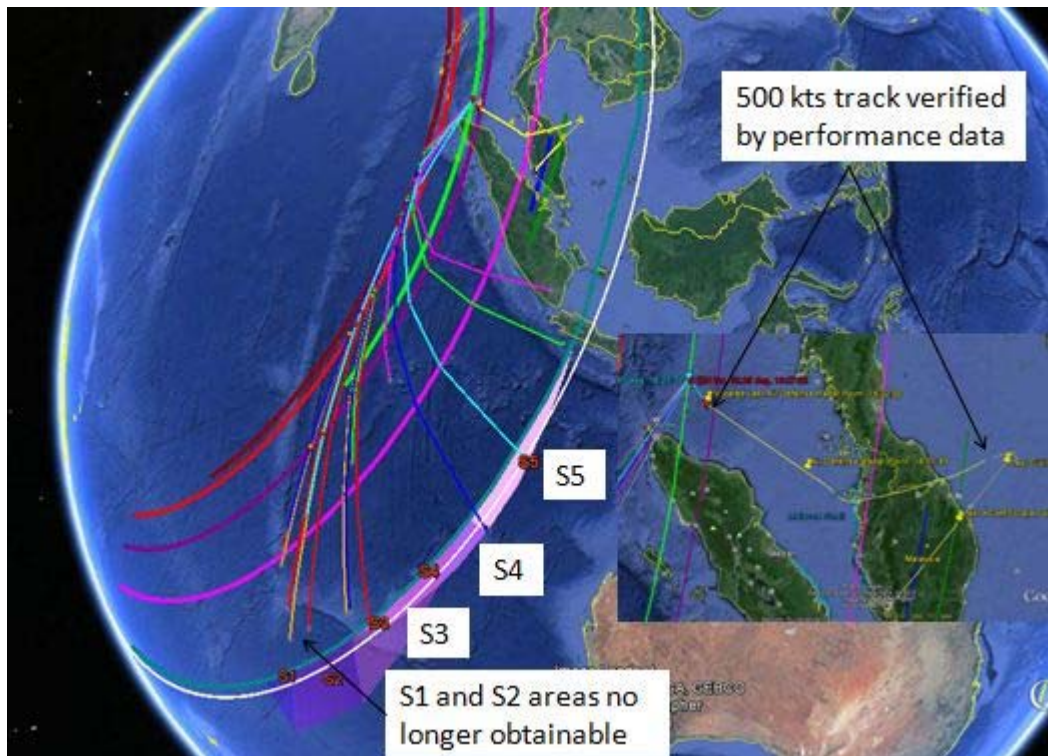


Figure 8 - Valid tracks based on Boeing analysis using Doppler and performance

THE SEVENTH HANDSHAKE

The timing offset used in the 7th handshake at 00:19:29 hrs, which had been initiated from the aircraft, was now better understood and allowed the position of the 7th arc to be defined. However, analysis of the

Doppler frequency revealed a significant difference to that predicted; actual was 2 Hz and predicted was 250 Hz.

From an analysis of the most probable reason why the aircraft had initiated the message, the working assumption was made that the 7th arc was the point at which Flight MH 370 ran out of fuel. The Doppler and performance calculations were then used to refine the final position along the arc.

SCENARIO ROUTE 1A AND 1B

In carrying out the Doppler and performance analysis, two scenarios, 1A and 1B, were developed. Scenario 1A required the aircraft to fly in a southern direction after it crossed the 1st arc. Scenario 1B required the aircraft to fly a northern route through waypoint IGREX and waypoint LAGOG, before flying south. The LAGOG waypoint was included as it was close to a supplied, high confidence position labelled '19:12Z'. The 1B scenario resulted in a reduced number of possibilities for the final position on the southern end of the 7th arc.

REFINEMENT OF INMARSAT ANALYSIS - 31 MARCH 14

Inmarsat reran their analysis using the 19:12Z position as a starting point. The analysis used ten evenly spaced points on the 2nd arc between the northern and southern limits where the aircraft could have crossed this arc. In each case the aircraft's speed across a range of 350 to 500 kts was analysed. The aircraft was also constrained to cross the arcs at the appropriate time and to travel in a straight line between the arcs, crossings at the designated speed.

The results were evaluated against the Differential Doppler predictions at the crossing of the last three arcs: handshakes 5, 6 and 7. The best fit for the aircraft tracks was found to be at 400 kts and this was independent of whether the analysis started from the new position or from the best point determined by the crossing of the 1st arc. This analysis assumed a constant speed after the 19:12Z point with the aircraft moving in a straight line between the arcs: the heading can change when the aircraft crosses an arc, but it must cross the next arc at the correct time.

Starting from position 19:12Z, the best fit is shown in Figure 9. It is within 1 Hz of the prediction for the final three data points, and results in a crossing of the 7th arc at Latitude 23.4°S, Longitude 102.8°E.

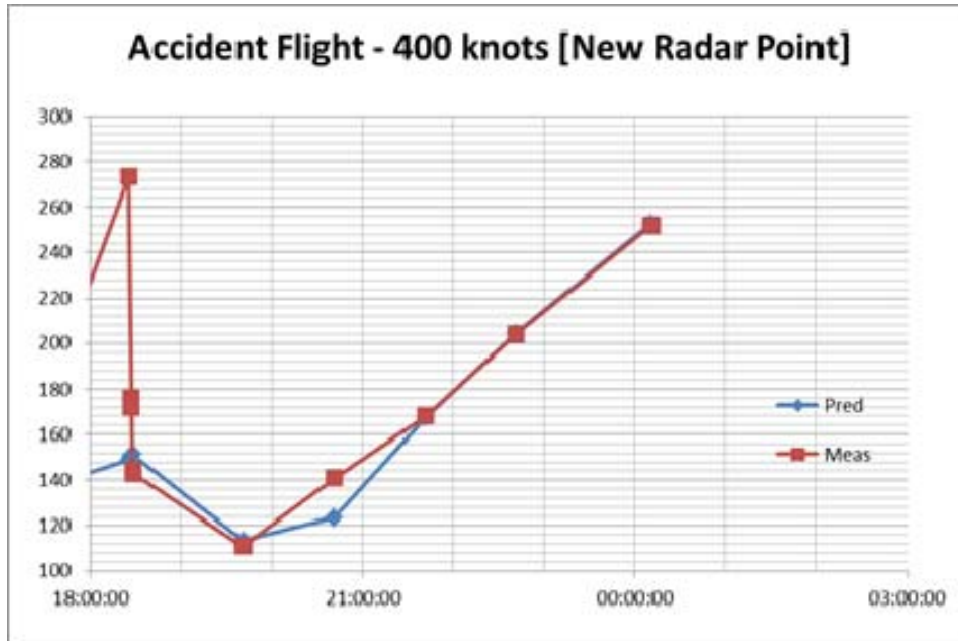


Figure 9 - Best fit for Inmarsat Doppler analysis

The higher accuracy of the satellite timing data means that the location of the arc itself is accurately known and the main error in the analysis occurs with the position of the aircraft. The analysis established that the mismatch between the measured and predicted frequency at the last handshake (7th arc) at speeds of 375 kts and 425 kts was as follows:

375 knots	20.6°S	104.2°E	[mismatch 6 Hz]
400 knots	23.4°S	102.8°E	[mismatch 1 Hz] <- best fit
425 knots	25.9°S	101.2°E	[mismatch 4 Hz]

Figure 10 shows these positions on the 7th arc.

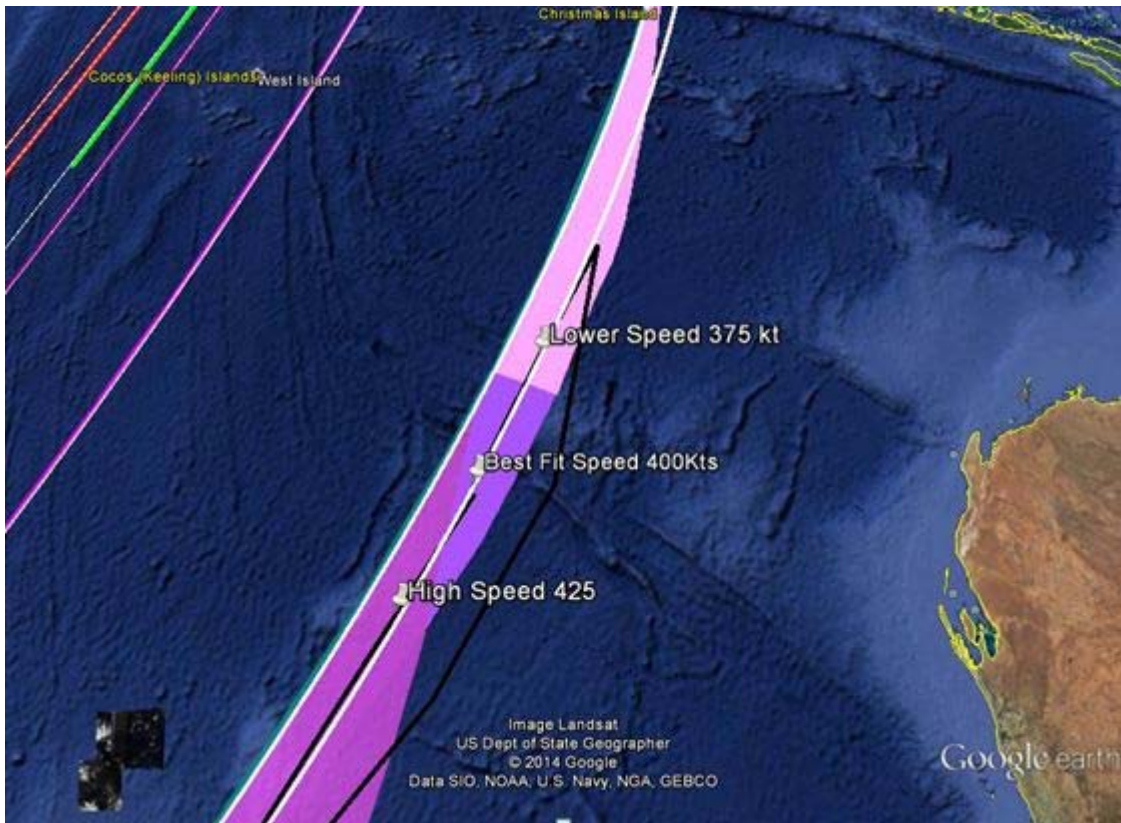


Figure 10 - Segment of the 7th arc over which Inmarsat Doppler information fits best.

As it is not known when the aircraft turned south, Inmarsat carried out an analysis using the 2nd arc crossing as the start location for a Monte Carlo style analysis. Ten different start locations on the 2nd arc were tested (equally spaced between 6°N and 4°S), at speeds ranging from 350 to 500 kts in 25 kt steps. The match with the differential Doppler curve at the final three points was used to evaluate the results.

In this analysis the track starting at the 6°N, 93.5°E crossing at the 2nd arc (19:41 hrs handshake) and terminating at 23.4°S 102.8°E crossing of the 7th arc, with a velocity of 400 kts, was the best fit. The sum of the mismatch across the last 3 arcs was 1 Hz. See Figure 11.

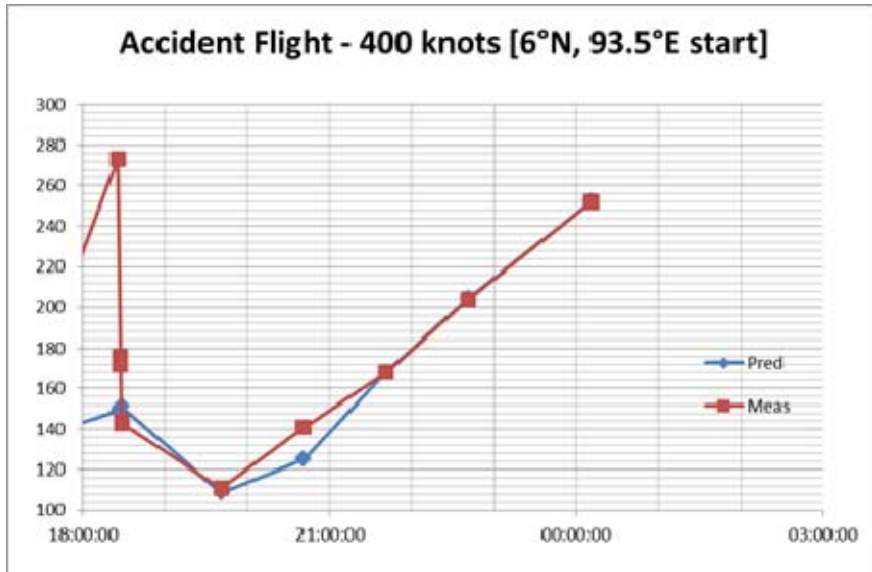


Figure 11 - Results of Inmarsat Monte Carlo style analysis

REFINEMENT OF BOEING ANALYSIS

In this refinement Boeing used the performance based flight tracks, previously identified, and compared the Doppler that these tracks generated with the Doppler information obtained from the OBF. The difference between the Doppler values was then classified as red, yellow, green or blue, with red being the ‘best fit’. This further refinement identified a higher probability of final position solutions identified by the area bounded by the black line in Figure 12. The thickness of this bounded area was determined by maximum range calculations.

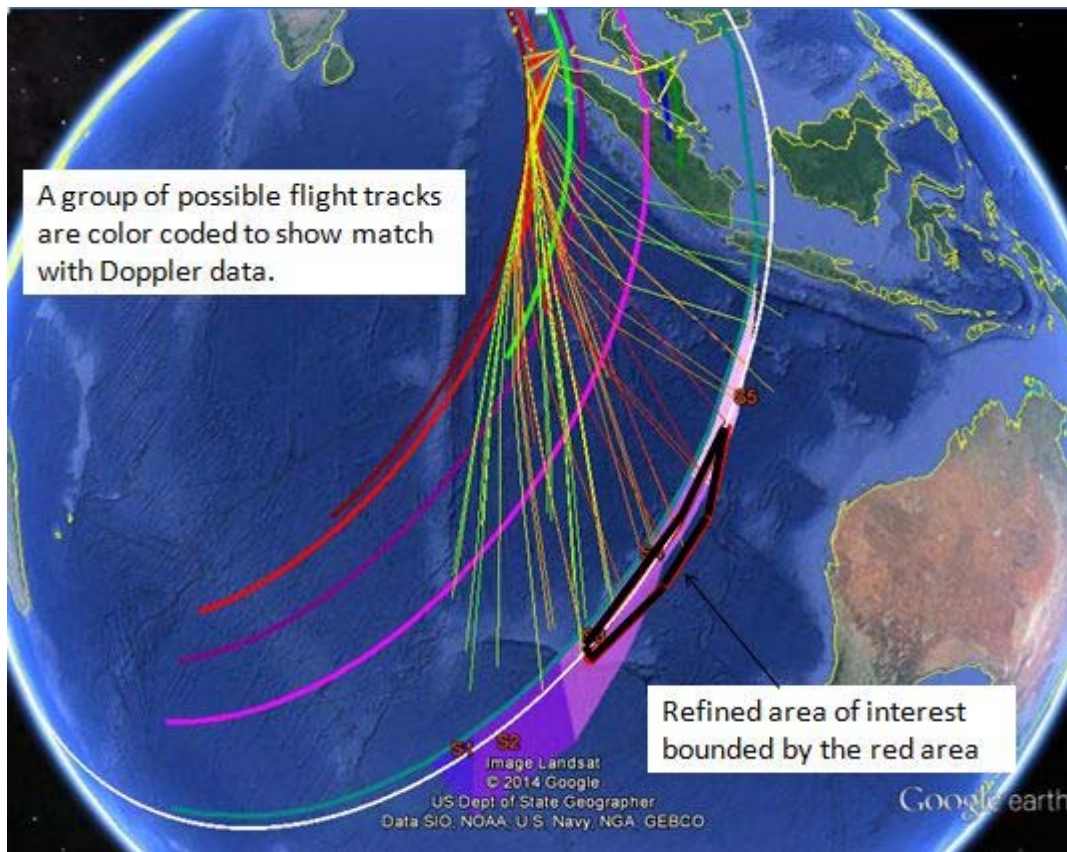


Figure 12 - Boeing combined Doppler and performance tracks

STATUS OF FLIGHT MH 370 AT SEVENTH ARC

The status of the airplane at the 7th and last arc (0:19:29 hrs), is still being assessed by Boeing. The exchange of information between the aircraft and the satellite was initiated by the aircraft's SATCOM system and does not contain the same characteristics as the previous six handshakes. There are a number of possibilities as to why the aircraft might have initiated this message.

AIR ROUTES

The track following the initial left turn off the planned route was towards Penang, from there the aircraft appeared to follow air routes to the 19:12Z position. The use of stored waypoints in the aircraft Flight Management System (FMS) suggests that the navigation was carried out using the Automatic Flight Control System (AFCS) in the lateral navigation mode. When the aircraft departed LAGOG the next major waypoint to the south was COCOS, which could be linked to the M641 air route. This would have taken the aircraft towards Perth. Once this route was set it would need no further input from the pilot for the aircraft to maintain altitude and route using the AFCS and auto throttle system. The fuel endurance would depend on the indicated airspeed selected and the flight level flown. This process allowed a

possible fixed point to be identified where both engines had flamed out at the 7th handshake. This would have been where the air route centreline crossed the 7th arc.

SIZING THE UNDERWATER SEARCH AREA

The final refinement to the underwater search area was obtained by overlaying the results of the refined Inmarsat Doppler analysis, Boeing refined Doppler and range analysis, and air route M641. The width of the area was determined by considering the error in the position of the 7th arc, the gliding range of an unpowered Boeing 777 from an altitude of approximately 30,000 feet. Consideration was also taken regarding the area that the towed underwater detector could cover before the predicted life of the batteries in the Dukane beacon expired.

The Joint Investigation Team had been advised that there were three assets available that could conduct underwater acoustic detection. Therefore the area was divided into three equal size segments along the arc with the highest priority given to the area where the air route M641 crossed the 7th arc. The proposed underwater search area, shown at Figure 13, is approximately 375 nautical miles long and 40 nautical miles wide and is defined by the following points:

U1	20° 16' 2.71" S 104° 17' 4.86" E	red, upper north west
U2	20° 29' 10.22" S 105° 01' 14.01" E	red, upper south east
U3	21° 55' 50.84" S 103° 29' 13.66" E	red/yellow, boundary north west
U4	22° 14' 21.49" S 104° 08' 34.81" E	red/yellow, boundary south east
U5	23° 42' 18.69" S 102° 29' 26.29" E	yellow/green, boundary north west
U6	24° 05' 31.73" S 103° 06' 27.22" E	yellow/green, boundary south east
U7	25° 49' 56.65" S 101° 12' 52.20" E	green, lower north west
U8	26° 09' 59.47" S 101° 46' 22.04" E	green, lower south east

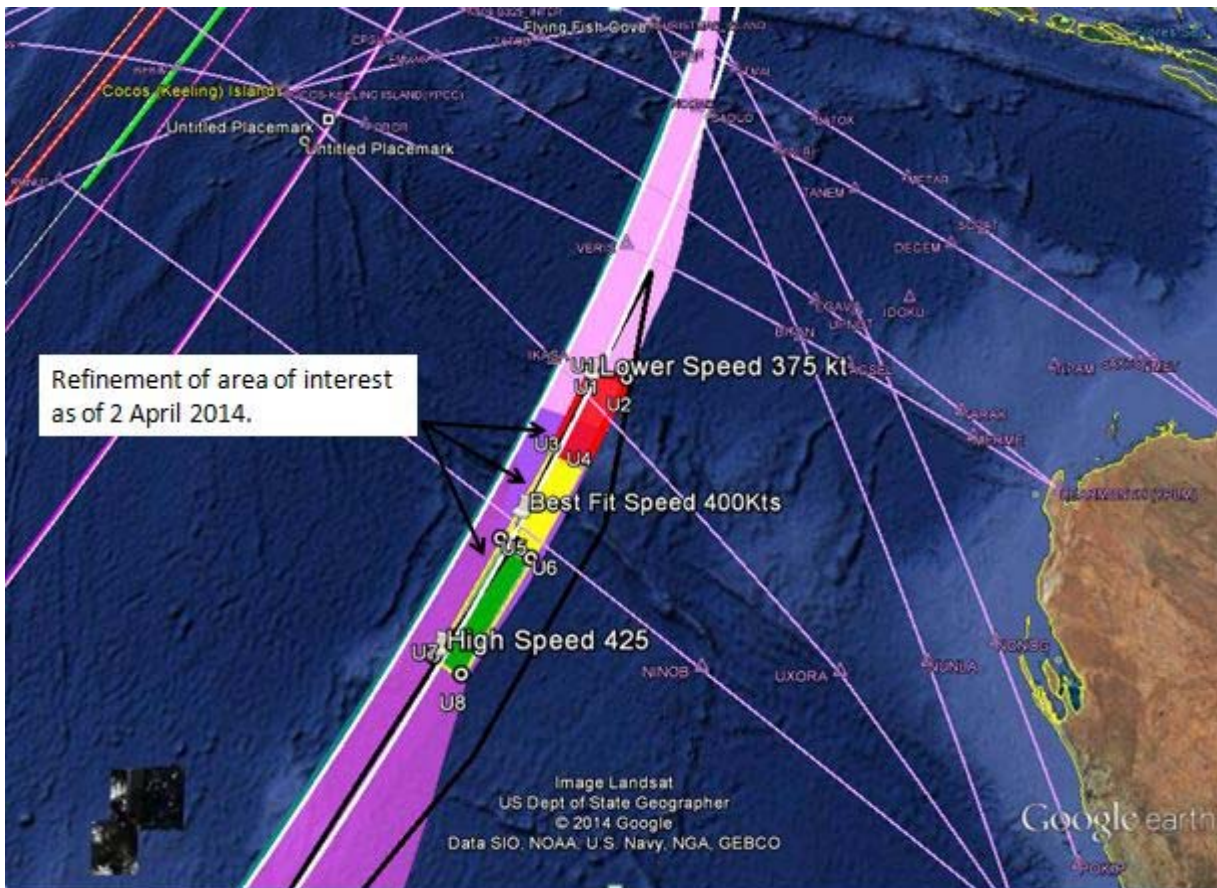


Figure 13 - Underwater search area as defined by the Joint Investigation Team on 2 April 2014

SUMMARY OF THE FACTORS USED TO DETERMINE THE UNDERWATER SEARCH AREAS

The following factors were used to determine the underwater search area.

- The flight ended after the 7th handshake, which occurred at 00:19:29 hrs on 8 March 2014.
- Based on the satellite timing data, the aircraft will be located near the 7th arc.
- The aircraft passed close to the point identified as 19:12Z.
- The measured Doppler profile closely matched that expected from an aircraft travelling in a southerly direction.
- Inmarsat analysis showed that the best fit for the Doppler frequency was at a ground speed of 400 kts, with slightly 'less' best fits at 375 and 425 kts. A Monte Carlo style analysis, using a number of different starting positions on the 2nd arc also gave a best fit at 400 kts. From this approach a most probable speed range of 375 to 425 kts was selected.

- Boeing analysis using a combination of aircraft performance and Doppler data, obtained from the satellite, to generate a range of probable best fit tracks. This work was supported by a Root Mean Square analysis that took account of a number of variables.
- Flight planning carried out by MAS independently showed that there was sufficient fuel onboard the aircraft to reach the positions determined by the Inmarsat and Boeing analysis.
- The length of the arc that defined the most probable area was obtained from the overlay of the results of the Inmarsat and Boeing approaches.
- Given the probable battery life of the Dukane beacon, and the number of assets available to conduct the underwater search, it was decided to break the underwater search area into three smaller areas.
- The width of the areas was defined by the probable position of the 7th arc, half of the glide range (40 nautical miles) and the area the towed detector could cover before the Dukane battery expired.
- The area that was crossed by air route M641 was classified as red (Priority 1), the next two priorities, yellow and green, were then defined moving south along the arc from this position.

The position and sizing of the underwater search area was based on the facts available on the 2 April 14. The analysis and underlying assumptions were constantly being reviewed and it was possible that further adjustments may be necessary.

CAUTION

The Doppler technique used as a method for determining the likely aircraft speed is sensitive to input variables and in particular the frequency compensation applied at the satellite earth ground station. As of the 2 April 14, work was still being carried out to understand these variables and the effect of the temperature variation as a result of the satellite experiencing an eclipse during the early part of the flight. Any further refinements would probably adjust the search area along the 7th arc.

Appendix C – Burst Frequency Offset (BFO) Doppler Model Development

Burst Frequency Offset (BFO) doppler model development¹

BFO doppler model summary

Inmarsat commenced work on BFO doppler modelling in the days after the aircraft went missing, with effort being ramped up once the timing analysis was essentially complete. Three significant model variants were generated, although many others were developed on the way to these three.

'Differential Doppler Analysis Release 2 (OAMS)'.

This model was finalised on 22 March 2014 and was used to generate the curves that were released to the public at that time indicating that the aircraft took a southerly route. The Differential Doppler Analysis Release 2 (OAMS) modelled:

- doppler shift associated with aircraft and satellite movement;
- Perth GES translation error based on sinusoidal model;
- satellite frequency shift during eclipse period based on pilot signal measurements.

'Differential Doppler Analysis ECLIPSE_2'.

This model was distributed to the Satcom Subgroup on 8 April 2014 and incorporated:

- Better curve fitting and smoothing of data associated with Perth and satellite frequency translation;
- all data frequency translations that Inmarsat were aware of at the time, having a good understanding and justification for them all.

This model was used for the analysis to define the initial underwater search area.²

'Differential Doppler Analysis UNIFIED_2x'.

This was distributed to the Satcom Subgroup on 19 June 2014. The Differential Doppler Analysis UNIFIED_2x':

- corrected minor timing error in OAMS data (2 min 55 seconds);
- accurately modelled Perth and Satellite frequency translation based on measured data.
- was used for the explanatory notes at Appendix G of the ATSB report released on 26 June 2014.³

¹ This appendix should be read in conjunction with the Inmarsat paper *'The search for MH370'* published in Oct 2014 that presents analysis of the satellite signals that resulted in the definition of the MH370 search area. This paper is available via a link on the ATSB website at <http://www.atsb.gov.au/mh370-pages/resources/fact-sheets/>

² As shown in Table 2 and Appendix F of *'MH370 – Definition of Underwater Search Areas'* published on 26 June 2014. Available on the ATSB website at <http://www.atsb.gov.au/mh370-pages/updates/reports/>

³ *'MH370 – Definition of Underwater Search Areas'* published on 26 June 2014 is available on the ATSB website at <http://www.atsb.gov.au/mh370-pages/updates/reports/>

BFO doppler model chronology

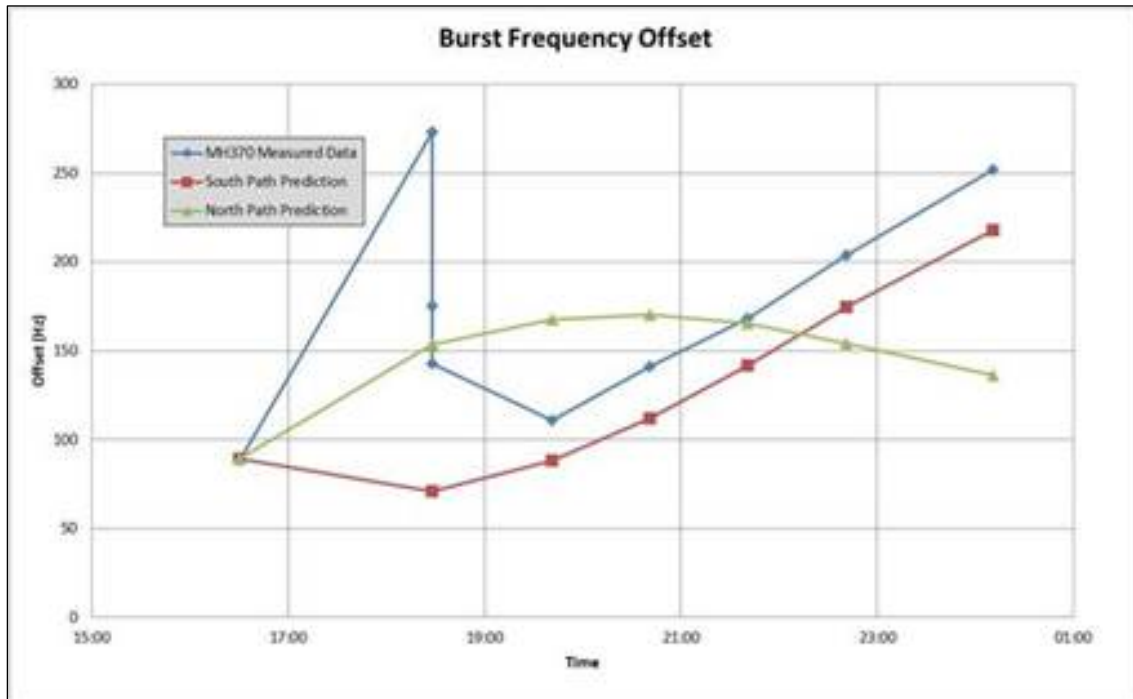
21 Mar 2014 *Differential Doppler Analysis*

First (internal to Inmarsat) release of fully worked out Doppler analysis, including AES velocity, satellite velocity, AES frequency correction, Perth GES frequency correction.

- No allowance made for satellite translation frequency variation;
- Perth GES frequency correction based on sinusoidal correction reported by GES staff.

Resultant curve indicated better fit for southern routes:

Figure 1: Differential Doppler Analysis BFO versus time (21 March 2014)

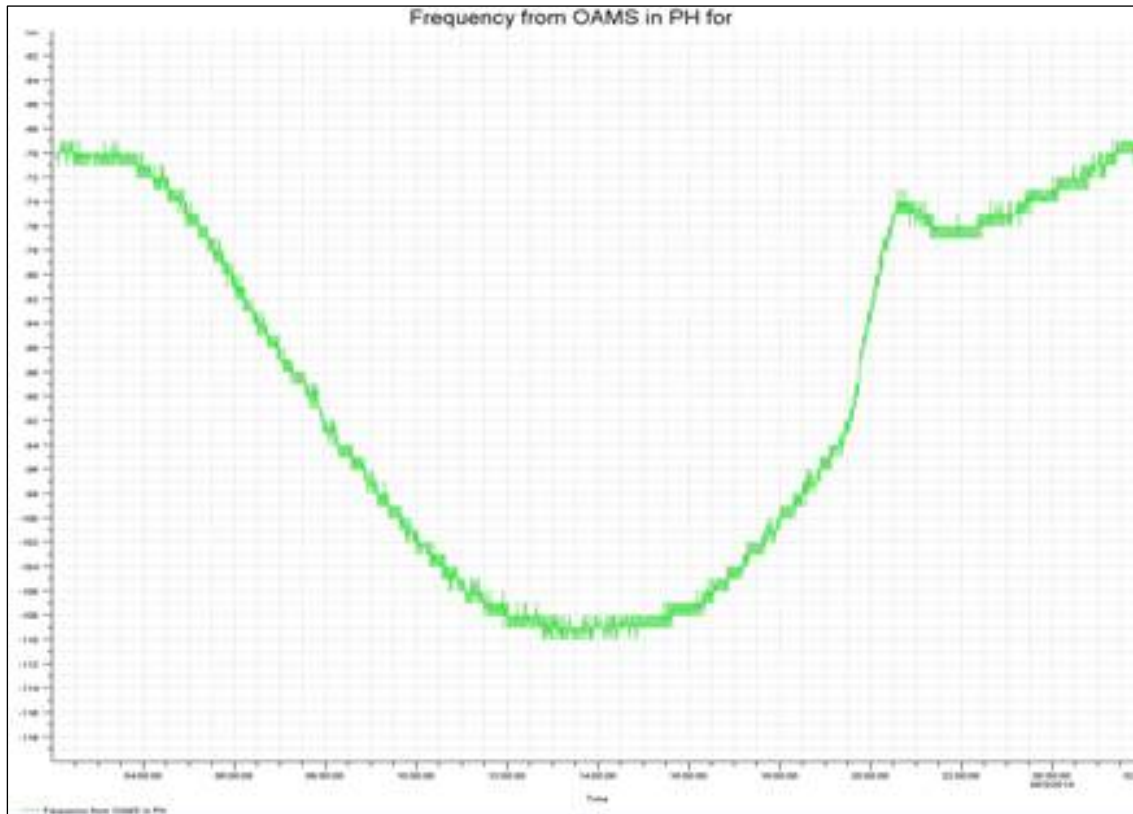


Source: Inmarsat

22 Mar 2014 *Differential Doppler Analysis Release 2 (OAMS)*

Updated analysis using measured data from Inmarsat's Off Air Monitoring System (OAMS) to improve the estimation of the Perth GES frequency correction. The OAMS measured data showed the receive frequency of a pilot signal after it had passed through the Perth receive system, and as well as showing the sinusoidal variation in frequency it showed the 'kink' caused by the satellite going through eclipse.

Figure 2: Measured pilot frequency error in Perth



Source: Inmarsat

The OAMS data was inverted and scaled to give a more representative indication of the overall frequency correction due to satellite eclipse (the kink in the curve) and the Perth GES correction (the 24 hour sinusoidal shape). The scaling/inversion mapped the 24 hour frequency variation to the 24 hour frequency variation measured/reported by the Perth staff in the previous model. The effect of eclipse on the satellite translation frequency was determined by the scaled version of the kink in the curve.

- Satellite translation frequency variation outside of the eclipse effects were not modelled by this approach, but were assumed to be small.

The model gave good results when applied to a number of 'calibration' flights and it formed the basis for the statement by the Prime Minister of Malaysia and the release of the BFO chart on 24 Mar 2014. Whilst satellite translation frequency uncertainty was known to be present, the difference between the North and South paths was significantly larger than these errors, as determined by the calibration flights.

25 Mar 2014 Differential Doppler Analysis EXT

A tidied up version of the previous analysis, which removed unnecessary and obsolete calculations. This was released to the wider Satcom Group for peer review and checking, and to form the basis for subsequent flight path reconstruction work.

3 Apr 2014 Differential Doppler Analysis ADJ_EXT

Internal Inmarsat model where Eclipse and diurnal (sinusoidal) contributions to frequency translation were separated.

8 Apr 2014 Differential Doppler Analysis ECLIPSE_1

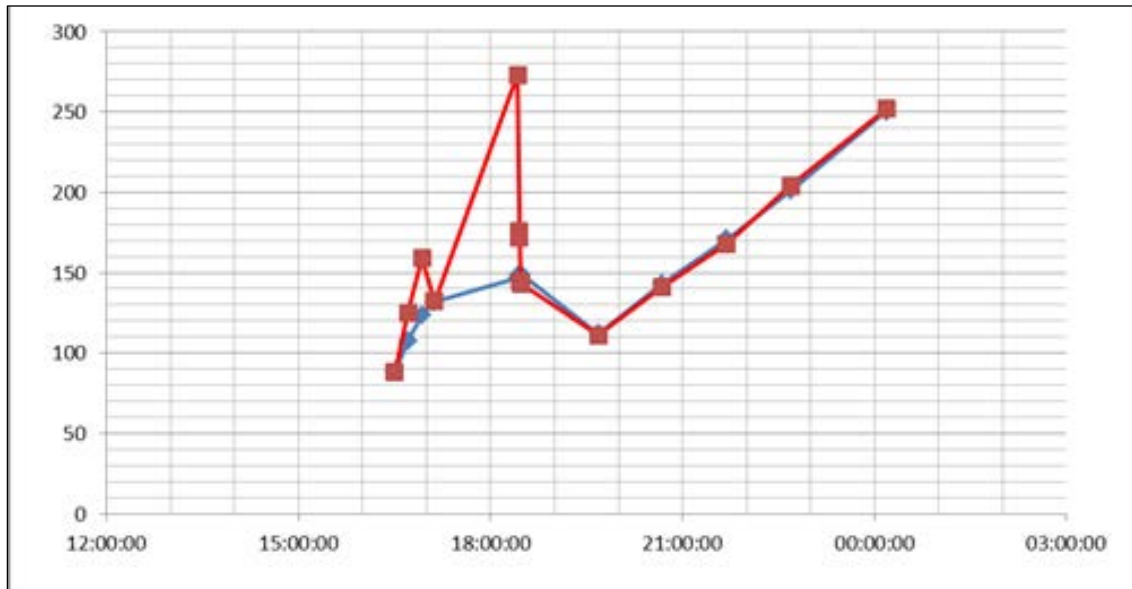
Formal release of previous model.

8 Apr 2014 Differential Doppler Analysis ECLIPSE_2

A tidied up version of the previous model distributed to the wider Satcom Group. The model incorporated all the frequency translations that Inmarsat were aware of, and they considered they had a good understanding and justification for all of them. The model indicated best fit agreement for a 400

kt ⁴ground speed flight which crossed the 19:41 arc at 2°N. This showed the predicted and measured frequencies agreeing to within an average of 2 Hz for all five measurement points between 20:41 and 00:11 UTC. The track was on a constant heading of 165.3°ETN for the first three hours, then swings slightly to the East, ending at 28.2°S, 99.6°E at 00:19 UTC. It should be noted that the model provided reasonably good matches for a range of ground speeds between 375 and 500 knots from this starting location.

Figure 3: BFO vs time. AFC/ Eclipse corrected best fit - 400 knots (ends 28.2°S, 99.6°E)



Source: Inmarsat

Eclipse 2 Sensitivity

The optimal fit was determined by starting from the 19:41 arc at different latitudes (in 1° steps from 4°S to 10°N). The best fit was clearly associated with the 2°N starting point. Ground speeds were varied in 25 knot steps from 350 knots to 500 knots, but were kept constant for each track analysed. Aircraft heading was kept constant between arc crossings, but was allowed to change as the ground track crossed each arc.

From the same starting point there were visible differences in quality of match for different ground speeds. For the (optimum) 2°N start point the match remained good across a range of ground speeds, but the gradient of the predicted (blue) and measured (red) lines diverge, indicating a 'sweet spot' in the range 375 to 500 knots, with end of flight between 25°S and 37°S:

Eclipse 2 Model Reference Data

The following reference data was used in the model:

- AES Frequency Compensation: used same algorithm as aircraft;
- AES induced Doppler: used location, ground speed & heading of AES and signal frequency and true satellite location;
- Satellite induced Doppler: used true satellite location/velocity and true AES and Perth GES location and frequency;
- Perth GES Frequency Compensation: calculated by comparing calculated pilot signal Doppler variation (known frequency, location and satellite velocity/location) with its variation after Perth GES frequency compensation applied;

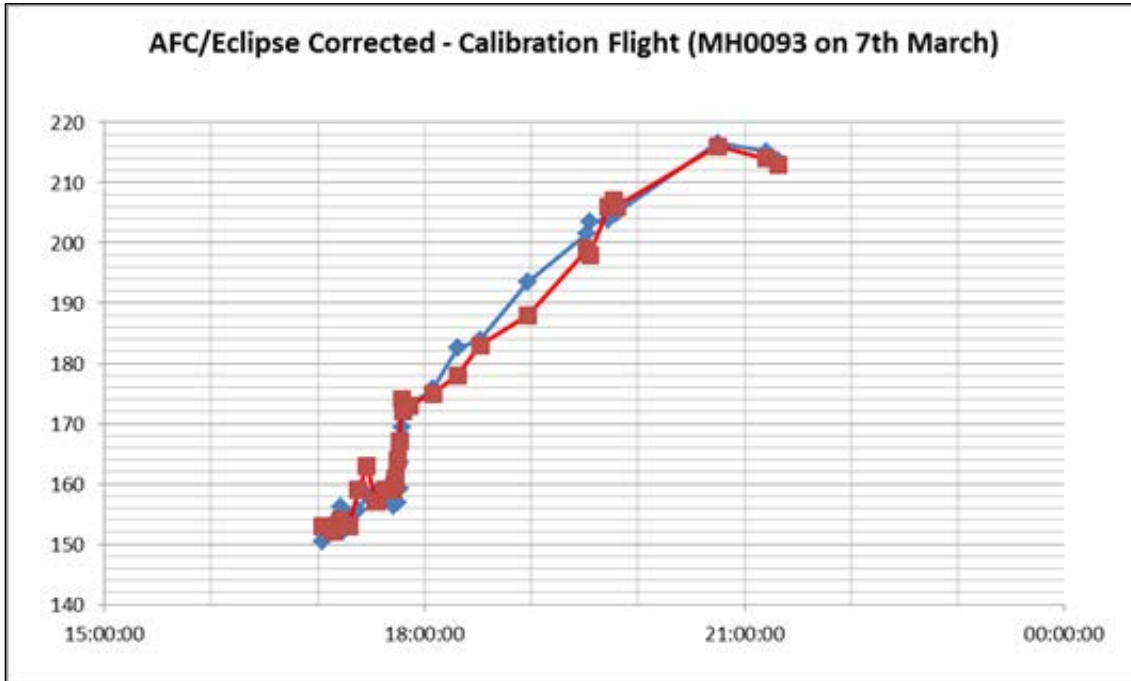
⁴ On 5 April 2014 the best fit speed was revised to 425 kts and the most probable path was adjusted

- Satellite eclipse frequency shift: measured from deviation of measured pilot frequency from residual Doppler related variations after GES frequency compensation applied (13 Hz variation measured, peaking around 19:40 UTC).

Verification

The model was verified using Malaysia Airlines Boeing 777 flight MH0093 from Narita to Kuala Lumpur on 7th March, which was in the air at the same time as MH370. It indicated a good match, but subject to errors of up to 3 Hz for individual measurement points.

Figure 4: BFO vs time. Eclipse 2 calibration



Source: Inmarsat

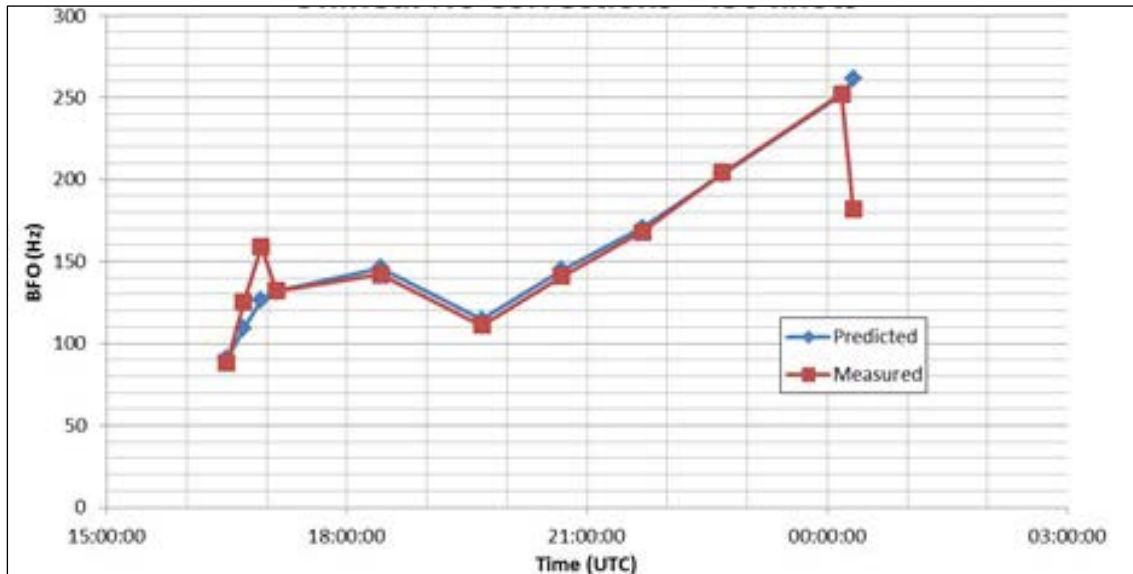
23 May 2014 *Differential Doppler Analysis ECLIPSE_3*

Internal Inmarsat model, refining curve fitting aspects of the ECLIPSE_2 model. Never released.

19 Jun 2014 *BFO Analysis UNIFIED*

The Unified model was developed when Inmarsat found out more about how the Miteq tracking receiver, used in the Perth GES, worked. The model avoided assumptions about the performance of the tracking receiver by processing the OAMS measured data in a different way to accurately measure the combined frequency shift of the Perth GES and the satellite, rather than trying to handle them separately. It fully modelled the pilot signal which forms the OAMS measured data to do this. The signal is transmitted at a constant frequency from the Burum GES (in the Netherlands) and is subject to Doppler shift due to satellite motion relative to both Burum (on the signal uplink) and Perth (on the signal downlink) which can be accurately predicted and removed from the OAMS measurement, leaving only the frequency variation related to the satellite frequency translation variation and the Perth GES translation frequency variation. This accurately calibrated out all frequency translations in the signal path and so was much more accurate than the previous ECLIPSE variants of analysis.

Figure 5: BFO vs time. Unified best fit 450 knots ends at 7th arc 32.7°S



Source: Inmarsat

The UNIFIED model was briefed to the Search Strategy WG on 19 June 2014, explaining why it was more accurate than the previous ECLIPSE variants, and the spreadsheet containing the model was distributed.

20 Jun 2014 BFO Analysis UNIFIED 2x

A timing error of 2 minutes 55 seconds associated with the labelling of OAMS data records was corrected in this model, which was otherwise identical to the original UNIFIED model. It was distributed to the Search Strategy WG later on the same day as the original model was sent out.

21 Jul 2014 BFO Analysis UNIFIED 3x

Internal Inmarsat minor refinement of UNIFIED 2x model. Not distributed.

30 Jul 2014 BFO Analysis UNIFIED 4x

Formal release version of UNIFIED 2x model but with more streamlined lookup tables.

Appendix D – Fugro Survey Pty Ltd Search for Malaysian Airlines Flight MH370 All Vessels Reconnaissance Bathymetric Survey, Deep Tow Wide Area Survey and AUV Wide Area Survey Volume 7 – Summary Report

FUGRO SURVEY PTY LTD

Search for Malaysian Airlines Flight MH370

All Vessels

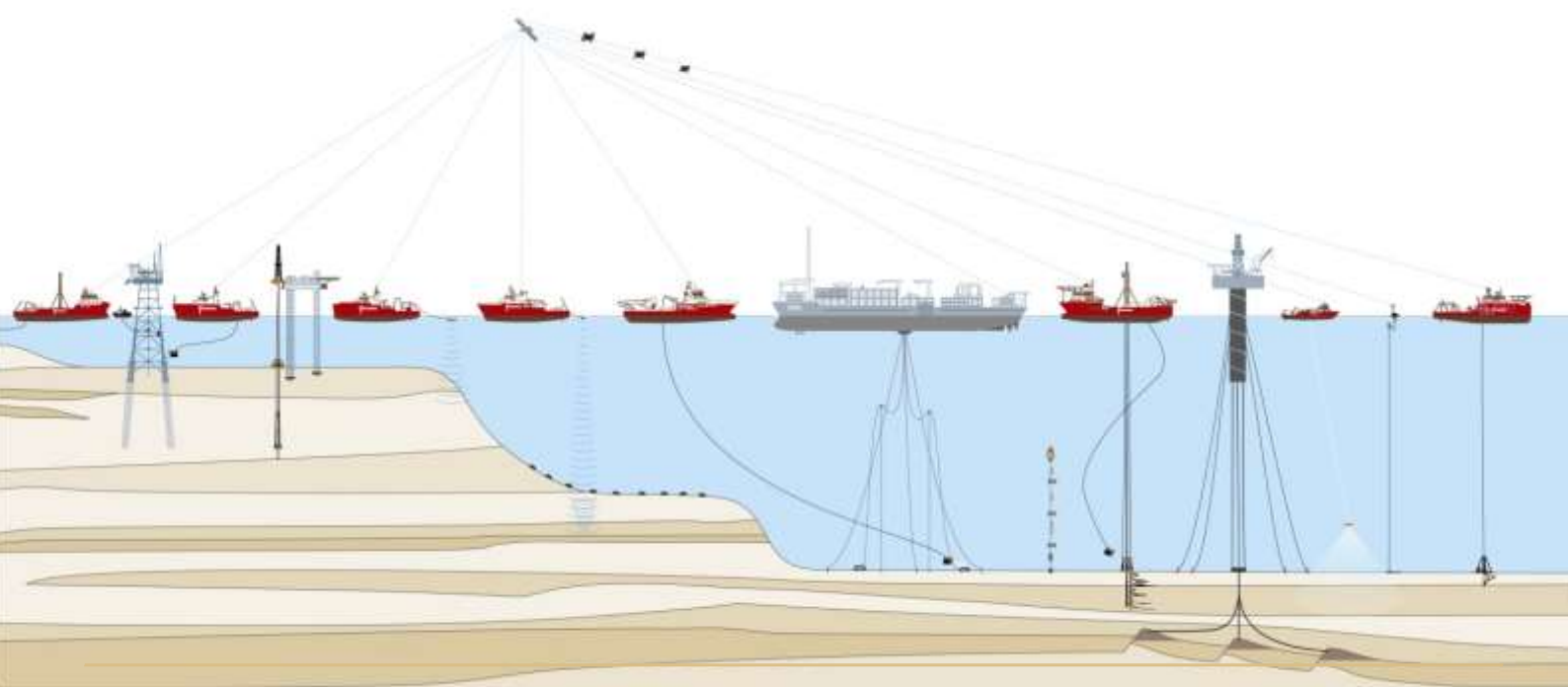
Reconnaissance Bathymetric Survey, Deep Tow Wide Area Survey and AUV Wide Area Survey

Volume 7 – Summary Report

Survey Period: 2 June 2014 – 24 January 2017

Fugro Document No: FRPT GP1500-SUM_Vol7_Summary Report

Australian Transport Safety Bureau



All Vessels

Reconnaissance Bathymetric Survey, Deep Tow Wide Area Survey and AUV Wide Area Survey

Volume 7 – Summary Report

Survey Period: 2 June 2014 – 24 January 2017

Fugro Document No: FRPT GP1500-SUM_Vol7_Summary Report

Prepared For: Australian Transport Safety Bureau
62 Northbourne Avenue
Canberra, 2601
ACT



0	Draft final with client's comments addressed	H. Ballantyne	M. Watson	M. Roberts	30 May 2017
A	Draft final for client's comments	H. Ballantyne	M. Watson	M. Roberts	18 April 2017
Rev	Description	Prepared	Checked	Approved	Date

CONTENTS

1.	INTRODUCTION	1
1.1	Project Description	1
1.2	Project Objectives	3
1.3	Scope of Work	3
1.4	Survey Operations	4
1.5	Report Structure	5
2.	HEALTH, SAFETY AND ENVIRONMENTAL MANAGEMENT	6
2.1	Health, Safety and Environmental Performance (HSE)	6
3.	SURVEY OPERATIONS	9
3.1	Sequence of Events	9
3.2	Vessel Swings	10
3.3	Mobilisations	11
3.4	Production Summary	12
3.5	Project Time Allocation	17
3.6	Survey Coverage	17
	3.6.1 Port Calls	19
3.7	Processing and Reporting	19
3.8	Data Transfer Ashore	20
3.9	Demobilisation	21
4.	STATISTICAL SUMMARIES	22
4.1	Data Holiday Types and Extents	22
	4.1.1 Remaining Holidays	22
4.2	Contact Summary	24
4.3	Findings	25
	4.3.1 Shipwreck #1	25
	4.3.2 Shipwreck #2	28
	4.3.3 Shipwreck #3	30
	4.3.4 Shipwreck #4	31
	4.3.5 Small Target Detection	32
4.4	Sound Velocity Profiles	33
4.5	Seabed Features	35
4.6	Transit Distance	36
4.7	Personnel Hours	36
4.8	Equipment – Deep Tow and AUV	37
4.9	MBES Coverage	39

4.10	Extreme Sea Condition	41
4.11	Time Spent On Line Turns	42
4.12	Fuel Consumption	43
5.	SURVEY PARAMETERS	44
5.1	Geodetic and Projection Parameters	44
5.2	Vertical Control	45
6.	SURVEY EQUIPMENT, VESSEL AND PERSONNEL	46
6.1	Vessels	46
6.1.1	Fugro Equator	46
6.1.2	Fugro Discovery	47
6.1.3	Fugro Supporter	48
6.1.4	Havila Harmony	48
6.2	Personnel	49
7.	DATA HANDLING	50
8.	DISTRIBUTION	52

APPENDIX

A. SOUND VELOCITY PROFILES

TABLES IN THE MAIN TEXT

Table 1.1: Report Structure	5
Table 2.1: Safety Performance Summary – Leading Indicators All Vessels	6
Table 2.2: Safety Performance Summary – Lagging Indicators All Vessels	8
Table 3.1: Dates of Vessels in Field	9
Table 3.2: Fugro Discovery – Dates of Individual Swings	10
Table 3.3: Fugro Supporter – Dates of Individual Swings	10
Table 3.4: Havila Harmony – Dates of Individual Swings	11
Table 3.5: Fugro Equator – Dates of Individual Swings	11
Table 3.6: Total Line km per Phase (DOR)	14
Table 3.7: Equator v Discovery km ²	16
Table 3.8: Number of Port Calls – All Phases	19
Table 4.1: Data Holiday and LPD Count	22
Table 4.2: Data Holiday and LPD Infill Statistics for the three AUV Campaigns	23
Table 4.3: Personal Hours All Vessels	36

Table 4.4: 'Spero' Deep Tow Sensors	37
Table 4.5: 'Dragon' DT-1 and 'Intrepid' DT-2 Sensors	38
Table 4.6: Hugin ES7 1000 AUV	38
Table 4.7: Total Bathymetric Coverage Compared to Countries and States	39
Table 4.8: Reconnaissance Bathymetric Coverage Compared to Countries and States	39
Table 4.9: Depth Range Histogram	40
Table 4.10: Fuel Used by Each Vessel During Each Phase	43
Table 5.1: Project Geodetic and Projection Parameters	44

FIGURES IN THE MAIN TEXT

Figure 1.1: General location diagram	2
Figure 2.1: Leading indicators (%) – all vessels	7
Figure 2.2: Lagging indicators (%) – all vessels	8
Figure 3.1: Dates and durations of vessels in field	9
Figure 3.2: Example line statistics showing Distance Cross Course (DCC) and Altitude at KP values	13
Figure 3.3: Total Line km (%) all phases (DOR)	15
Figure 3.4: Total line kms by all vessels by end of swing date	15
Figure 3.5: Equator v Discovery km ² (%)	16
Figure 3.6: Time allocations for the Fugro Equator Deep Tow	17
Figure 3.7: Combined Deep Tow and AUV coverage overlain over the Reconnaissance Bathymetric Survey	18
Figure 3.8: Deep Tow coverage overlain over the Reconnaissance Bathymetric Survey	18
Figure 3.9: AUV trackplots from data holiday infills overlain over the Reconnaissance Bathymetric Survey	19
Figure 3.10: Typical directory structure for data upload	20
Figure 4.1: Area of remaining Fugro data holidays	22
Figure 4.2: Data holiday and LPD infill statistics for AUV campaigns	23
Figure 4.3: Remaining data holidays for Fugro v non-Fugro vessels	24
Figure 4.4: Number of contacts per phase	24
Figure 4.5: Sidescan sonar over shipwreck #1	25
Figure 4.6: Shipwreck #1 – anchor	26
Figure 4.7: Shipwreck #1 – ship's capstan	26
Figure 4.8: Shipwreck #1 – possible water tank	27
Figure 4.9: Shipwreck #1 – chain	27
Figure 4.10: Shipwreck #1 – angular item	28
Figure 4.11: Shipwreck #2 – original Deep Tow image	28
Figure 4.12: Shipwreck #2 – bow on sidescan sonar image	29
Figure 4.13: Shipwreck #2 – side on image	29

Figure 4.14: Shipwreck #3 – sidescan sonar image	30
Figure 4.15: Shipwreck #3 – showing deck railing and nets	30
Figure 4.16: Shipwreck #4 – port bow	31
Figure 4.17: Shipwreck #4 – starboard bow damage	31
Figure 4.18: 200 litre drum – original Deep Tow sidescan sonar data, 690 m range	32
Figure 4.19: 200 litre drum – original Deep Tow sidescan sonar data, 1100 m range	32
Figure 4.20: 200 litre drum – ROV photo	33
Figure 4.21: Location of sound velocity profiles at the search area site	34
Figure 4.22: Location of sound velocity profiles at the trial site	34
Figure 4.23: The Geelvink fracture zone	35
Figure 4.24: Cross-section of Geelvink Fracture Zone (452 m Petronas Towers for scale)	35
Figure 4.25: 2500 km range ring from Fremantle	36
Figure 4.26: Personal hours all vessels	37
Figure 4.27: Cross-section through Diamantina Fracture Zone	40
Figure 4.28: Reconnaissance bathymetric survey by depths (%)	41
Figure 4.29: Maximum vessel heave recorded during the survey	42
Figure 4.30: Cumulative fuel consumption for each vessel for each swing	43
Figure 6.1: Fugro Equator	46
Figure 6.2: Fugro Discovery	47
Figure 6.3: Fugro Supporter	48
Figure 6.4: Havila Harmony	49
Figure 7.1: Vessel and Deep Tow raw and processed data formats	50

ABBREVIATIONS

AINS	Aided Inertial Navigation System
APOS	Acoustic Processor Operating Station
ATSB	Australian Transport Safety Bureau
AUSat	Australian Satellite
AUV	Autonomous Underwater Vehicle
CAT	Customer Acceptance Test
DGNSS	Differential Global Navigation Satellite System
DP	Dynamic Positioning
DVL	Doppler Velocity Log
Fugro	Fugro Survey Pty Ltd
GPS	Global Positioning System
GLONASS	Global Navigation Satellite System
HARS	HUGIN Alternative Recovery System
HDD	Hard Disc Drive
HiPAP	High Precision Acoustic Positioning System
HOC	Hazard Observation Card
HOS	Hugin Operating System
HSE	Health, Safety and Environment
IOR	Indian Ocean Region
JHA	Job Hazard Analysis
LARS	Launch and Recovery System
LPD	Low Probability Detection Zone
MBES	Multibeam Echo Sounder
NAS	Network Attached System
NCR	Non-Conformance Report
PP	Payload Processor
QC	Quality Control
SBP	Sub-Bottom Profiler
SSS	Sidescan Sonar
SVP	Sound Velocity Profile
TFI	Tile Fish Imagery
TRA	Task Risk Assessment
USBL	Ultra Short Baseline
UTC	Coordinated Universal Time
UTM	Universal Transverse Mercator
WGS84	World Geodetic System (1984)

1. INTRODUCTION

1.1 Project Description

Fugro Survey Pty Ltd (Fugro) has been contracted by the Australian Transport Safety Bureau (ATSB) on behalf of the Commonwealth of Australia to supply seafloor survey vessels, equipment and services to undertake a search for the wreckage of the Boeing 777 aircraft operated as Malaysia Airlines Flight 370 (MH370). The contract covers operations to locate, positively identify, map and obtain visual imagery of the wreckage.

Flight MH370 carrying a total of 239 persons onboard, disappeared on 8 March 2014, whilst en route from Kuala Lumpur, Malaysia to Beijing, China. Subsequent analysis of available satellite, radar and other data has determined that the aircraft most likely ended its flight in the southern Indian Ocean, on or adjacent to what is termed the “7th arc” within Australia’s search and rescue zone. The initial search area was an area of 30,000 km² on or adjacent to the 7th arc as advised by the ATSB.

The search area was extended several times including widening the search area adjacent to the 7th arc in the south, as well as the addition of blocks to the south of the search area. By the end of the search, in January 2017, the area covered was over 120,000 km².

A general location diagram highlighting the potential search areas is provided as Figure 1.1.

All survey services were conducted from the Fugro owned and operated vessels the Fugro Discovery and the Fugro Equator, both of which have been equipped and crewed as dedicated survey vessels. Each vessel was mobilised with an Edgetech DT-1 or DT-2 Deep Tow (DT) system comprising of a 6000 m rated Deep Tow, sidescan sonar (SSS), multibeam echo sounder (MBES), sub-bottom profiler (SBP), high definition camera and an aided inertial navigation system (AINS).

The Fugro Supporter equipped with a Hugin Echo Surveyor 7 autonomous underwater vehicle (AUV) joined the search in January 2015 and left the search in May 2015. The Havila Harmony replaced the Fugro Supporter until March 2016. Upon completion of Deep Tow operations the Fugro Equator was remobilised to operate the AUV. The AUV was rated to a depth of 4500 m and was equipped with full suite of survey sensors including sidescan sonar, multibeam echo sounder, sub-bottom profiler, high definition camera and an aided inertial navigation system (AINS). The AUV had a two-fold tasking; firstly, to search areas too difficult for the Deep Tow systems to safely or efficiently investigate, and secondly to carry out detailed investigations of sonar contacts that may represent debris from the lost aircraft.

This Summary Report summarises some of the significant statistical achievements from the search for MH370 in terms of the people and vessels involved and the data collected.

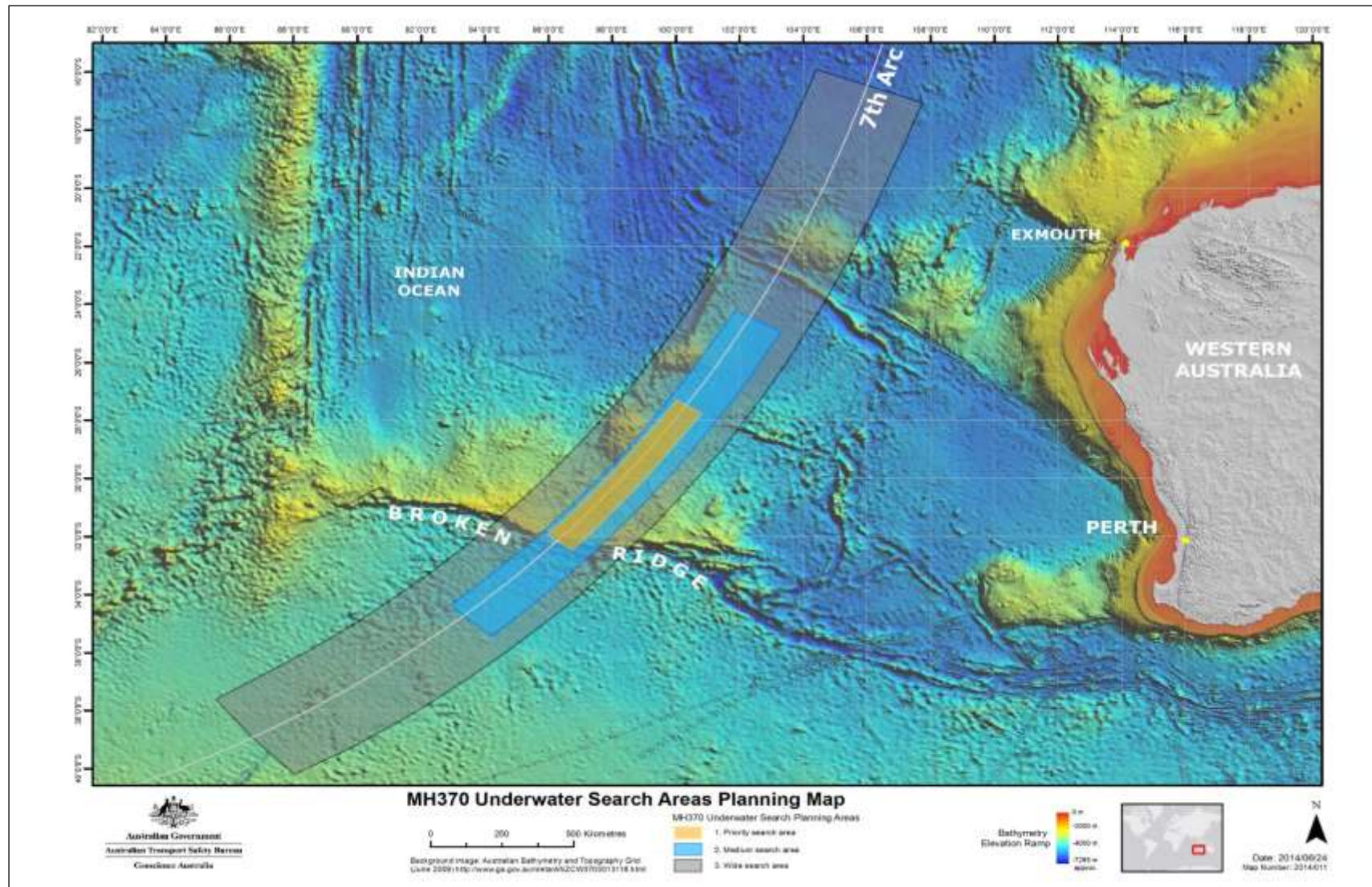


Figure 1.1: General location diagram

1.2 Project Objectives

The objective of the wide area search phase was to investigate the search area for all seafloor anomalies and discount natural geological or environmental features. In order to satisfy the ATSB requirements, Fugro was required, according to the Contract (570-04) to complete the following:

- i. Search for, locate and positively identify MH370 within the defined search area on the seafloor;
- ii. If MH370 is located, obtain optical imaging (photograph or video) of the aircraft debris field and, if possible, recover the flight data recorders; and,
- iii. Discount any area searched for the presence of MH370 with a high degree of confidence.

All search activities were conducted in an effective and cooperative manner which ensured the safety of the search vessels and the personnel onboard was paramount.

1.3 Scope of Work

For the Fugro Equator and the Fugro Discovery the wide area search for MH370 was carried out within the search areas defined by the ATSB around the 7th arc using a Deep Tow system.

The Deep Tow system was positioned using USBL aided INS and completed the seafloor investigation using the following main instrumentation:

- Edgetech 75 kHz and 410 kHz chirp sidescan sonar, to provide primary object detection over a large [2 km] swath;
- Kongsberg EM2040 multibeam, used to provide high resolution bathymetry and object detection coverage across the sidescan sonar nadir gap;
- HD camera system, to further confirm the object identification;
- Subsea fluorometer for polycyclic aromatic hydrocarbons sensing.

The primary purpose of the AUV survey onboard the Fugro Supporter, Havila Harmony and Fugro Equator was to carry out a wide area search using the low frequency sidescan sonar in areas where the Deep Tow systems had not been able to acquire data due to seabed terrain shadows and terrain avoidance. These areas where there was insufficient Deep Tow sonar coverage have been classed as "data holidays". The data holidays were collated and grouped together into polygons to provide defined areas for the AUV to acquire data.

Data holidays include the following:

- Shadow zones which were created by the topographical relief where the sidescan sonar signal could not reach the seafloor (acoustic shadow);
- Off-tracks, where the tow fish deviated from the line plan resulting in data gaps between adjacent lines;
- Equipment failure, where no data were recorded in certain areas;
- Terrain avoidance, where the Deep Tow sensor altitude was over 300 m, typically caused by large seafloor gradients.

In addition to these holidays another category was mapped, but not classified as data holidays:

- Lower probability detection zones (LPDs), which were generally areas of complex geology where the ability to detect plane debris was limited.

The second purpose of the AUV survey was to reinvestigate contacts using a high frequency sidescan sonar to provide a higher resolution image and where necessary, to then carry out an optical imaging mission in order to obtain photographs of the contacts in question.

1.4 Survey Operations

Prior to commencement of Deep Tow operations the Fugro Equator conducted five Swings of reconnaissance MBES. The existing bathymetry derived from scattered surveys and satellite bathymetry was not of a high enough resolution to allow for safe Deep Tow and AUV operation. Reconnaissance survey operations were conducted between 2 June and 22 December 2014, and also at periodic times up to demobilisation when weather did not permit Deep Tow or AUV operations or when tasked to do so by the ATSB. The data was initially processed using VBAProc onboard the Fugro Equator to ensure coverage and then sent to Geoscience Australia for final processing.

The Fugro Equator was then remobilised and then began Deep Tow operations from 5 January 2015, until 15 October 2016. After this the Equator was remobilised again to conduct AUV operations between 22 October 2016 and 23 January 2017 (arrival in Fremantle), before being fully demobilised upon return to Singapore on 7 February 2017.

The Fugro Discovery was mobilised on 5 October 2014, and after completing Deep Tow operations on 11 August 2015, was demobilised.

The Fugro Supporter was mobilised with the AUV in Bali, Indonesia on 4 January 2015, and conducted AUV operations until 17 May 2015.

The Havila Harmony replaced the Fugro Supporter conducting AUV operations from 23 November 2015, until 26 March 2016. The AUV was then taken ashore and mobilised on the Fugro Equator October 2016.

1.5 Report Structure

The report for the reconnaissance bathymetric survey and wide area search phase is presented in eight volumes outlined in Table 1.1.

Table 1.1: Report Structure

Fugro Report No.	Volume	Report Title
FRPT GP1500-1_FD_Vol1_ Operations Report	1	Fugro Discovery Deep Tow Wide Area Survey Survey Operations
FRPT GP1483_GP1500-2_FE_Vol2_ Operations Report	2	Fugro Equator Reconnaissance Bathymetric Survey and Deep Tow Wide Area Survey Survey Operations
FRPT GP1500-5_FS_Vol3_ Operations Report	3	Fugro Supporter AUV Wide Area Survey Survey Operations
FRPT GP1500-6_HH_Vol4_ Operations Report	4	Havila Harmony AUV Wide Area Survey Survey Operations
FRPT GP1500-6_FE_Vol5_ Operations Report	5	Fugro Equator AUV Wide Area Survey Survey Operations
FRPT GP1500-3_Vol6_ Processing, Interpretation and Results Report	6	Reconnaissance Bathymetric Survey, Deep Tow Wide Area Survey and AUV Wide Area Survey Processing, Interpretation and Results Report
FRPT GP1500_SUM_Vol7_ Summary Report	7	Summary Report (this report)
FRPT GP1483_GP1500_LL_Vol 8_ Lessons Learnt	8	Reconnaissance Bathymetric Survey, Deep Tow Wide Area Survey and AUV Wide Area Survey Lessons Learnt

2. HEALTH, SAFETY AND ENVIRONMENTAL MANAGEMENT

2.1 Health, Safety and Environmental Performance (HSE)

The total working personnel hours for all phases of this project, based on 24 man hours per day, was 625,488.

To better understand HSE during the course of the survey the events were split into two groups: Lagging Indicators and Leading Indicators. Lagging indicators are negative HSE events that occurred over the course of the project such as illness or first aid cases. Leading indicators are positive and proactive HSE events, such as Toolbox Talks and Marine Fauna Observations. Table 2.1 shows the leading indicators numbers from all vessels and Figure 2.1 shows the same data graphically as percentages.

Table 2.1: Safety Performance Summary – Leading Indicators All Vessels

Leading Indicator	Total
Toolbox Talks	4807
Permit to Work	852
HOC Unsafe Conditions	754
Vessel Inductions	433
Emergency Exercises/Drills	350
RA Reviewed	350
HOC Safe Act/Suggestions	343
Inspection/Reviews	342
Management Visits	326
HSE Meetings	154
HOC Unsafe Acts	118
Safety Training Conducted	75
Audits	41
RA Developed	36
Hazard Hunts	34
Marine Fauna Observations	29
GroSAFE Observations	14
Stop Work Exercised	13

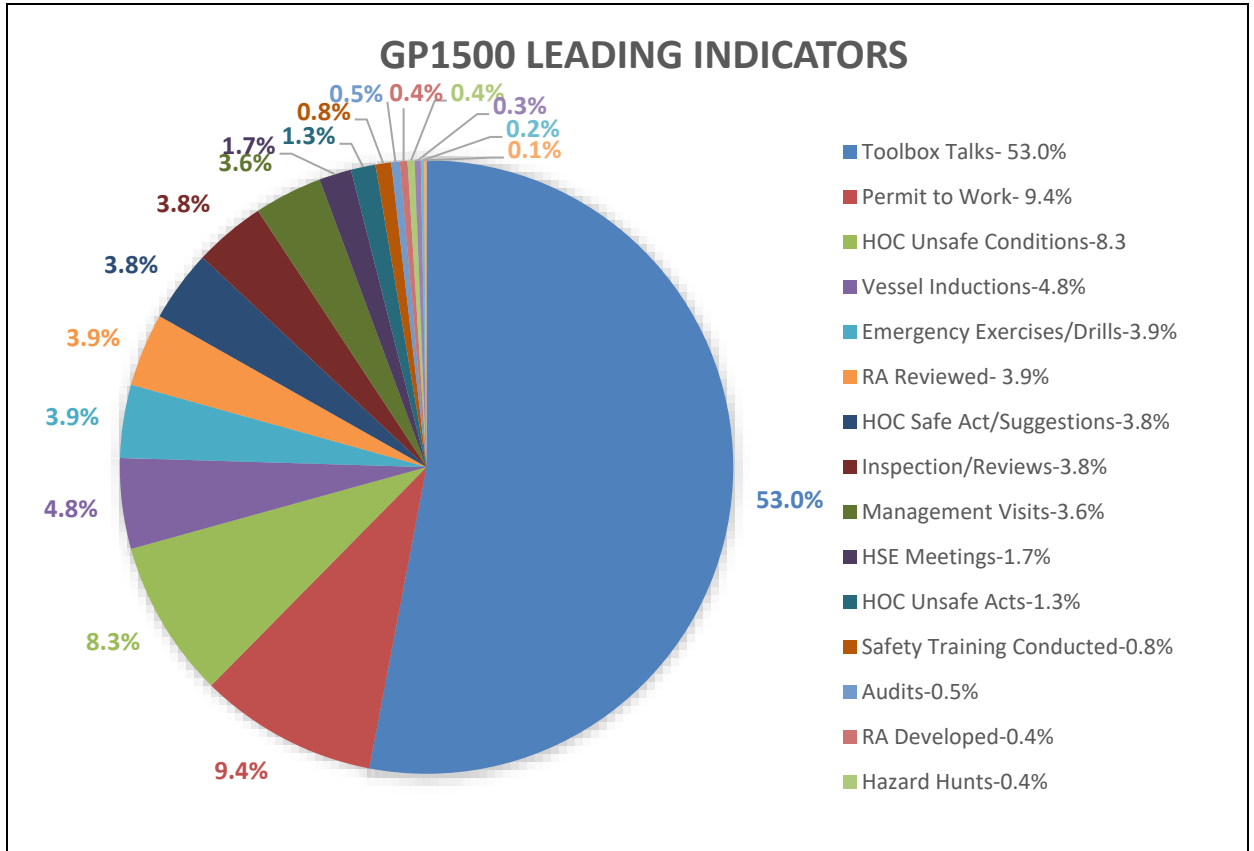


Figure 2.1: Leading indicators (%) – all vessels

Table 2.2 shows the lagging indicators numbers from all vessels and Figure 2.2 shows the same data graphically as percentages.

Table 2.2: Safety Performance Summary – Lagging Indicators All Vessels

Lagging Indicators	Total
Equipment Damage/Loss	46
Near Miss	35
Crew Boat Transfers	11
First Aid Case	6
Medical Treatment	6
Hi Potential Incident	3
NWR – Medical treatment	3
Environmental Incident	1
MOB Deployments	1
NWR – Injury/Illness	1
Occupational Illness	1
Restricted Work Case	1
EP Non-Compliance	0
Fatality	0
Lost Work Day Case	0
NWR – First Aid Case	0
Open Action Items	0
Overdue Action Items	0

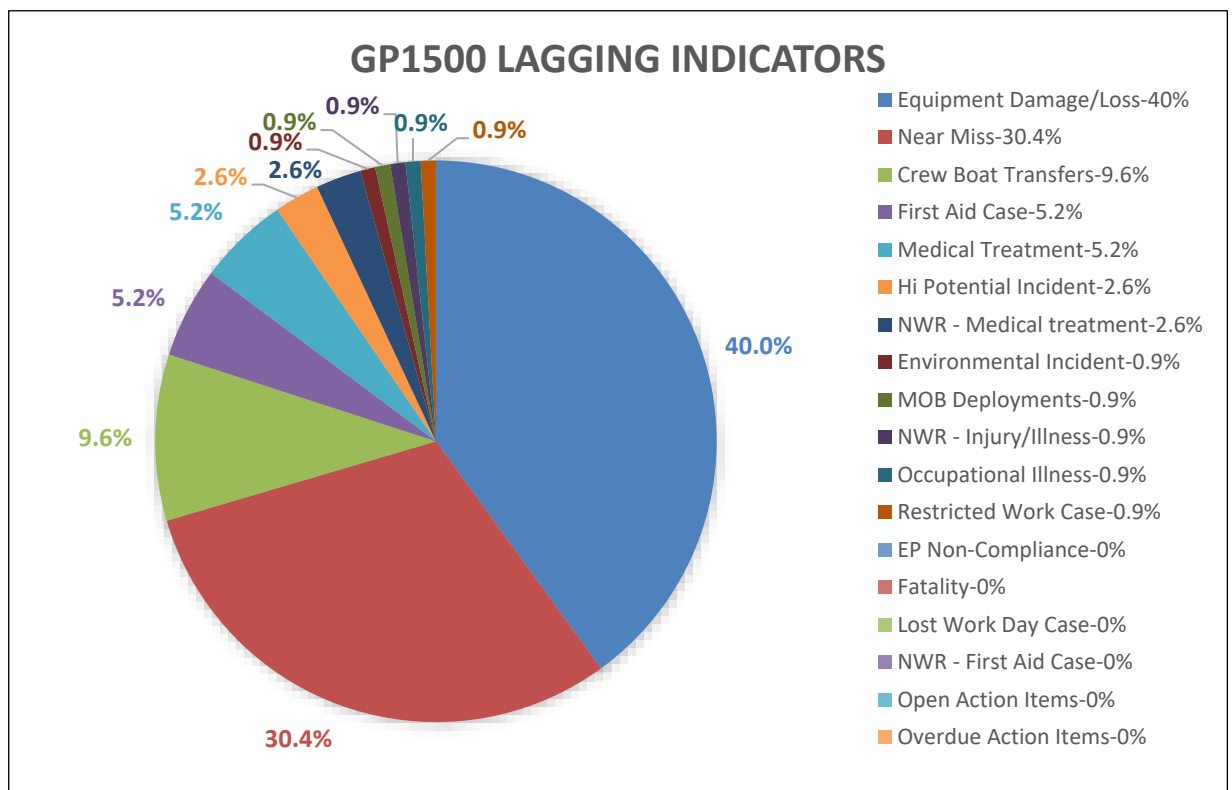


Figure 2.2: Lagging indicators (%) – all vessels



3. SURVEY OPERATIONS

Overall, survey operations were conducted successfully and the acquired data was of good quality.

3.1 Sequence of Events

The offshore phase of the Wide Area Search was undertaken between 2 June 2014, and 7 February 2017, when the vessel demobilised in Singapore.

A brief summary of significant survey events is presented in Table 3.1 and in Figure 3.1. The figures include time spent mobilising and in transit to and from the survey site. For more detail, refer the individual volumes for each vessel.

Table 3.1: Dates of Vessels in Field

Vessel	Dates in Field
Fugro Equator (Reconnaissance MBES)	2 June 2014 – 01 November 2014 and, 16 November 2014 – 22 December 2014
Fugro Discovery (Deep Tow)	05 October 2014 – 24 August 2016
Fugro Equator (Deep Tow)	01 November 2014 – 15 November 2014 and, 29 December 2014 – 21 October 2016
Fugro Supporter (AUV)	04 January 2015 – 17 May 2015
Havila Harmony (AUV)	23 November 2015 – 26 March 2016
Fugro Equator (AUV)	22 October 2016 – 23 January 2017
Fugro Equator (Final transit to Singapore)	24 January – 07 February 2017

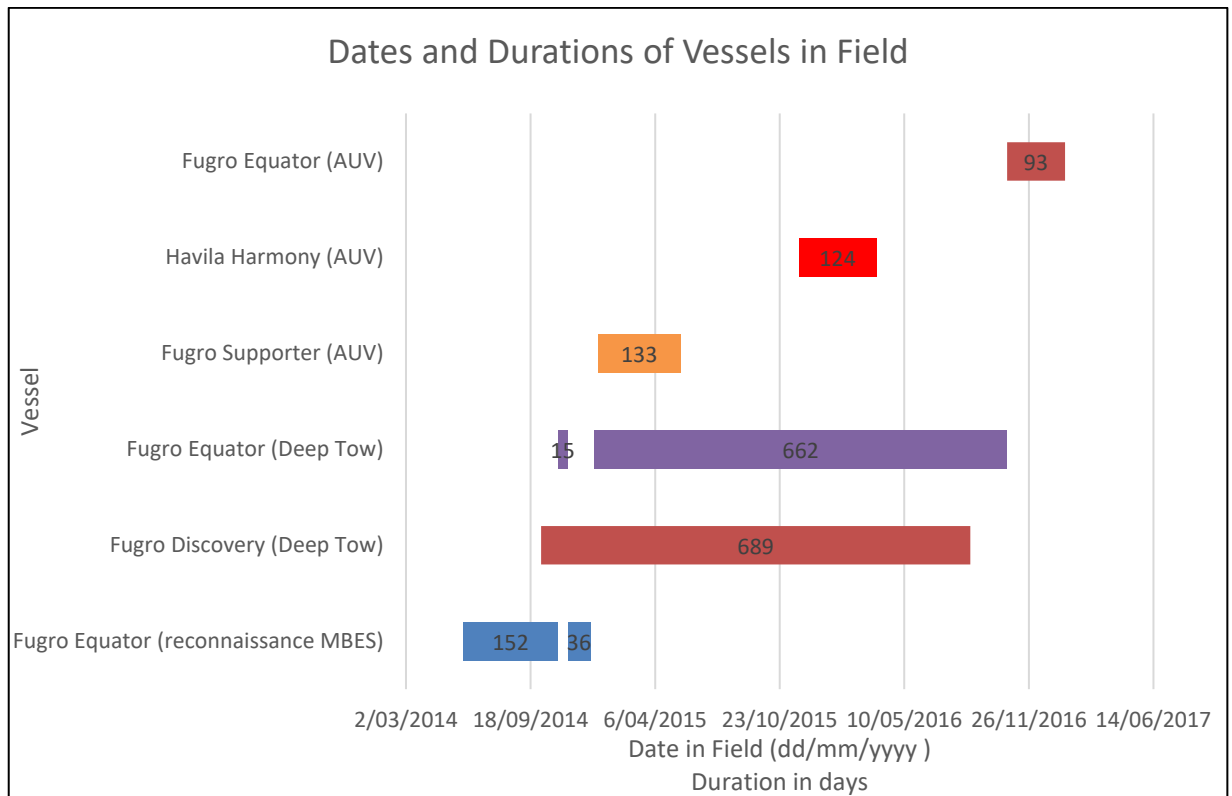


Figure 3.1: Dates and durations of vessels in field

3.2 Vessel Swings

Dates of the 16 swings carried out by the Fugro Discovery are shown in Table 3.2.

Table 3.2: Fugro Discovery – Dates of Individual Swings

Fugro Discovery Swing	Port to Port Dates	On Site
1	17 October 2014 – 24 November 2014	22 October 2014 – 17 November 2014
2	27 November 2014 – 06 January 2015	04 December 2014 – 30 December 2014
3	09 January 2015 – 18 February 2015	15 January 2015 – 11 February 2015
4	20 February 2015 – 30 March 2015	25 February 2015 – 24 March 2015
5	04 April 2015 – 13 May 2015	10 April 2015 – 08 May 2015
6	15 May 2015 – 23 June 2015	22 May 2015 – 18 June 2015
7	27 June 2015 – 01 August 2015	04 July 2015 – 24 July 2015
8	05 August 2015 – 16 September 2015	11 August 2015 – 15 September 2015
9	16 September 2015 – 27 October 2015	21 September 2015 – 22 October 2015
10	28 October 2015 – 28 November 2015	4 November 2015 and 14 – 22 November 2015 ¹
11	29 November 2015 – 11 January 2016	03 December 2015 – 06 January 2016
12	13 January 2016 – 15 February 2016	20 – 24 January 2016 and 06 – 10 February 2016 ²
13	18 February 2016 – 05 April 2016	25 February 2016 – 30 March 2016
14	07 April 2016 – 16 May 2016	12 April 2016 – 11 May 2016
15	17 May 2016 – 29 June 2016	24 May 2016 – 23 June 2016 ³
16	11 July 2016 – 22 August 2016	21 July 2016 – 11 August 2016

¹ On Swing 10 the Fugro Discovery had to return to port twice to relieve crew members for medical reasons
² On Swing 12 the Fugro Discovery had to return to port twice. Initially due to loss of towfish on 24 January 2016, then due to tow cable break on 9 February 2016
³ The port call between Swing 15 and Swing 16 was extended due to necessary maintenance

Dates of the three swings carried out by the Fugro Supporter are shown in Table 3.3.

Table 3.3: Fugro Supporter – Dates of Individual Swings

Fugro Supporter Swing	Port to Port Dates	On Site
1	18 January 2015 – 20 February 2015	29 January 2015 – 11 February 2015
2	23 February 2015 – 08 April 2015	28 February 2015 – 01 April 2015
3	10 April 2015 – 18 May 2015	18 April 2015 – 11 May 2015

Dates of the two swings carried out by the Havila Harmony are shown in Table 3.4.

Table 3.4: Havila Harmony – Dates of Individual Swings

Havila Harmony Swing	Port to Port Dates	On Site
1	30 November 2015 – 21 January 2016	05 December 2015 – 15 January 2016
2	25 January 2016 – 26 March 2016	03 February 2016 – 20 March 2016

Dates of the 20 swings carried out by the Fugro Equator are shown in Table 3.5.

Table 3.5: Fugro Equator – Dates of Individual Swings

Fugro Equator Swing	Port to Port Dates	On Site
1 GP1483	02 June 2014 – 08 July 2014	14 June 2014 – 03 July 2014
2 GP1483	09 July 2014 – 12 August 2014	13 July 2014 – 07 August 2014
3 GP1483	13 Aug 2014 – 18 September 2014	17 Aug 2014 – 13 September 2014
4 GP1483	19 Sept 2014- 31 October 2014	24 Sept 2014- 25 October 2014
5 GP1483*	16 Nov 2014 – 22 December 2014	21 Nov 2015 – 18 December 2014
1	05 January 2015 – 17 February 2015	15 January 2015 – 10 February 2015
2	20 February 2015 – 08 April 2015	27 February 2015 – 28 March 2015
3	09 April 2015 – 19 May 2015	16 April 2015 – 13 May 2015
4	23 May 2015 – 29 June 2015	28 May 2015 – 23 June 2015
5	30 June 2015 – 12 August 2015	06 July 2015 – 06 August 2015
6	12 August 2015 – 23 September 2015	19 August 2015 – 17 September 2015
7	25 September 2015 – 09 November 2015	05 October 2015 – 03 November 2015
8	10 November 2015 – 21 December 2015	15 November 2015 – 16 December 2015
9	28 December 2015 – 09 February 2016	03 January 2016 – 02 February 2016
10	10 February 2016 – 23 March 2016	16 February 2016 – 17 March 2016
11	24 March 2016 – 05 May 2016	30 March 2016 – 29 April 2016
12	06 May 2016 – 15 June 2016	14 May 2016 – 09 June 2016
13	15 June 2016 – 27 July 2016	21 June 2016 – 22 July 2016
14	28 July 2016 – 07 September 2016	04 August 2016 – 02 September 2016
15	08 September 2016 – 21 October 2016	15 September 2016 – 15 October 2016
16	28 October 2016 – 12 December 2016	02 November 2016 – 06 December 2016
17	12 December 2016 – 24 January 2017	19 December 2016 – 17 January 2017

* This swing was originally designated Fugro job number GP1500-4, and this appears in the DORs until 26 November 2014, but was retrospectively changed back to GP1483

3.3 Mobilisations

The Fugro Equator was initially mobilised in Benoa, Bali between 7 and 9 July 2014, where a patch test was undertaken before transit to the trial site for operations.

Mobilisation of the Fugro Discovery took place between 5 and 10 October 2014, whilst the vessel was alongside at Fremantle.



The original mobilisation of the Fugro Equator for Deep Tow operations took place alongside at the Port of Fremantle, Western Australia, between 1 and 8 November 2014. Problems were encountered with the installed winch which meant that a replacement had to be found. While the replacement winch was being sourced the Fugro Equator returned to site to conduct more reconnaissance MBES. On 28 December 2014, the Fugro Equator returned to Fremantle to complete Deep Tow mobilisation and commence Deep Tow operations.

The Fugro Supporter was mobilised with the Hugin 1000 AUV Echo Surveyor 7 in Benoa, Bali, Indonesia between 4 and 18 January 2015.

The Havila Harmony was mobilised between 23 and 26 November 2015, alongside the BAE Henderson, just south of Fremantle.

On 22 October 2016, the Equator was remobilised for ES7 AUV alongside the AMC4 Wharf, Henderson.

3.4 Production Summary

The survey work scope for each swing was defined by Tasking Requests issued by the ATSB which detailed the preferred order of survey lines to be run and whether Deep Tow or MBES reconnaissance operations were to be carried out. Similar Tasking Requests were issued to the AUV vessels for missions, although there was a great deal of input from the Mission Planners onboard each vessel as well.

The Deep Tow survey line spacing was initially set at 2000 m with a sidescan sonar range of 1250 m in order to acquire data efficiently. This was the case for lines 01-NW, 02-NW and 03-NW. Subsequently the line spacing was reduced to 1800 m with a sidescan sonar range of 1110 m in order to ensure data quality over the full scan range. This was the case up until completion of 05-SE. After this lines were acquired with 1700 m line spacing and sidescan sonar range 1110 m to reduce offtrack holidays (only the first 1000 m of the data was considered acceptable for object detection). This was the case for the remainder of the project, unless there were towfish positioning issues such as the USBL system dropping out. If this occurred the line spacing was reduced to 1600 m.

The survey required 100 % seafloor coverage by the sidescan sonar with the nadir gaps being filled by processed multibeam backscatter data. The online surveyor attempted to maintain the towfish within 100 m of the line being surveyed, with a maximum excursion of 150 m being acceptable to ensure data overlap and 100 % coverage of the seabed. On the completion of each line, statistics were produced to provide a summary of line keeping and towfish altitude for that line (see Figure 3.2).

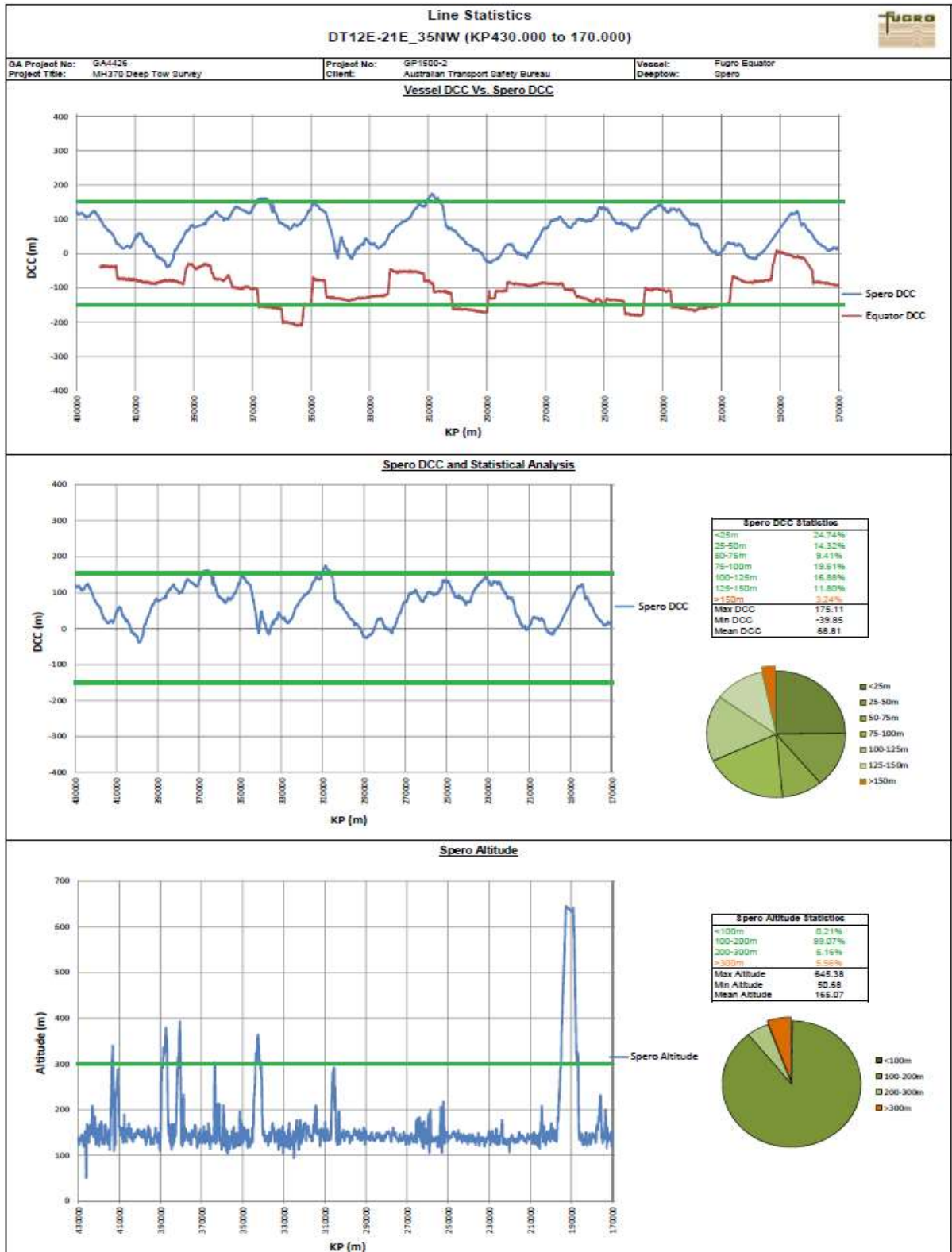


Figure 3.2: Example line statistics showing Distance Cross Course (DCC) and Altitude at KP values

Although each port to port swing was of six weeks duration for Deep Tow operations and eight weeks for swings onboard the Havila Harmony, the long transit of over 1000 Nm to and from the search area resulted in approximately 30 days on site each swing and 41 days for the Havila Harmony.

Operations to safely launch and recover the Deep Tow and AUV were restricted by the weather conditions, particularly during the winter months, and productivity was reduced as a result.

Daily weather forecasts were obtained from Fugro GEOS and from the Bureau of Meteorology (BOM) Defence Meteorological Support Unit (DMSU) and this allowed onsite planning of operations to maximise Deep Tow productivity. As the search area was in excess of 800 kms in length it was often possible to work in the north of the search area when weather conditions prevented safe operations in the south, and vice versa.

The Fugro Equator and Fugro Supporter also had the option to undertake reconnaissance MBES work when the weather was unsuitable for Deep Tow operations or it was tasked to do so by the ATSB. The vessels were able to continue acquisition of acceptable MBES data in often very poor weather conditions, although data quality was dictated by the relative direction of the surveyed line and prevailing weather conditions.

On completion of each swing a summary report was produced highlighting, amongst other things, the productivity achieved for that particular swing.

The combined Deep Tow sidescan sonar virgin territory coverage from both the Fugro Equator (Deep Tow and AUV) and, Fugro Discovery amounted to 104,033 km². The Fugro Supporter and Havila Harmony AUV covered 700 km². When combined with the data acquired by the DJ101 and the GO Phoenix, the total sidescan sonar coverage for the entire project amounted to 121,502 km².

Table 3.6 shows the total line kilometres for each phase with figures taken from the Daily Operation Reports submitted each day from each vessel.

Table 3.6: Total Line km per Phase (DOR)

Total Line km per Vessel (DOR)	
Vessel	[kms]
GP1483 – Equator Vessel MBES	33340
GP1500-2 – Equator Deep Tow	29635
GP1500-2 – Equator Vessel MBES	9488
GP1500-1 – Discovery Deep Tow	29884
GP1500-5 – Supporter AUV	5491
GP1500-5 – Supporter Vessel MBES	2733
GP1500-6 – Harmony AUV	7431
GP1500-6 – Equator AUV	5234
GP1500-6 – Equator Vessel MBES	2789
Total	126025

These kilometres are represented as pie chart percentages in Figure 3.3 and for all the Deep Tow and AUV swings as kilometres against dates in Figure 3.4.

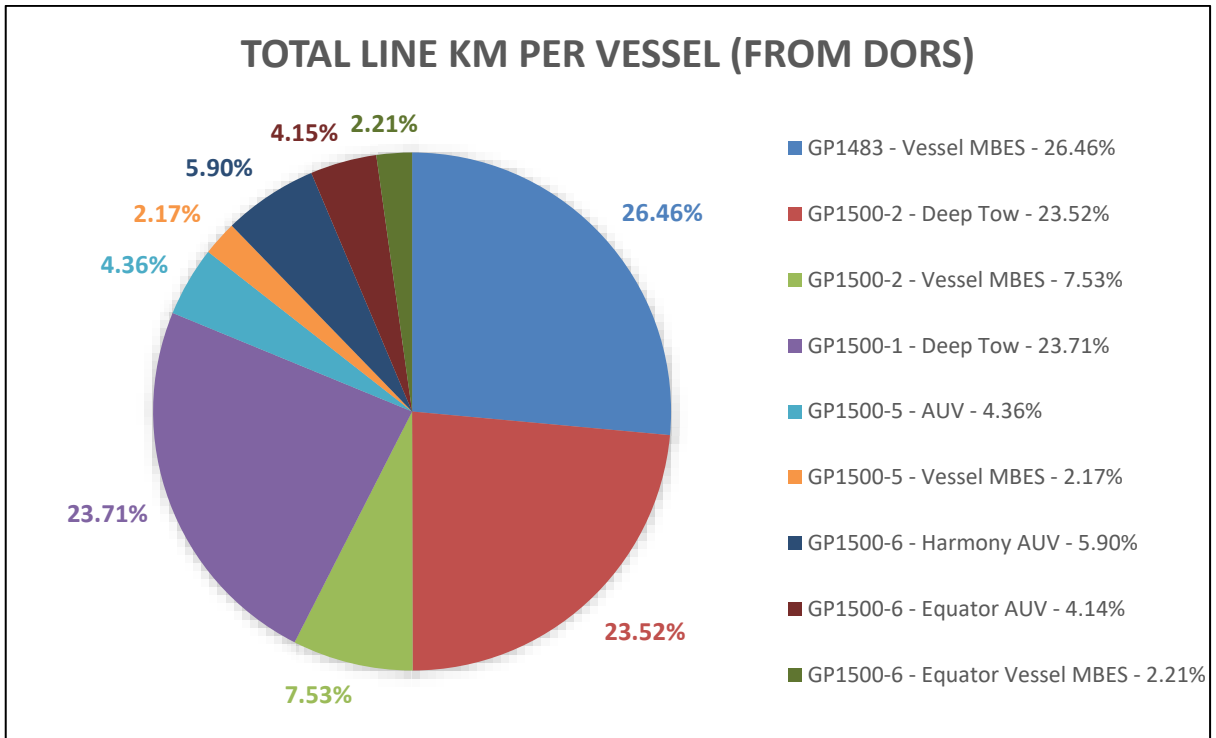


Figure 3.3: Total Line km (%) all phases (DOR)

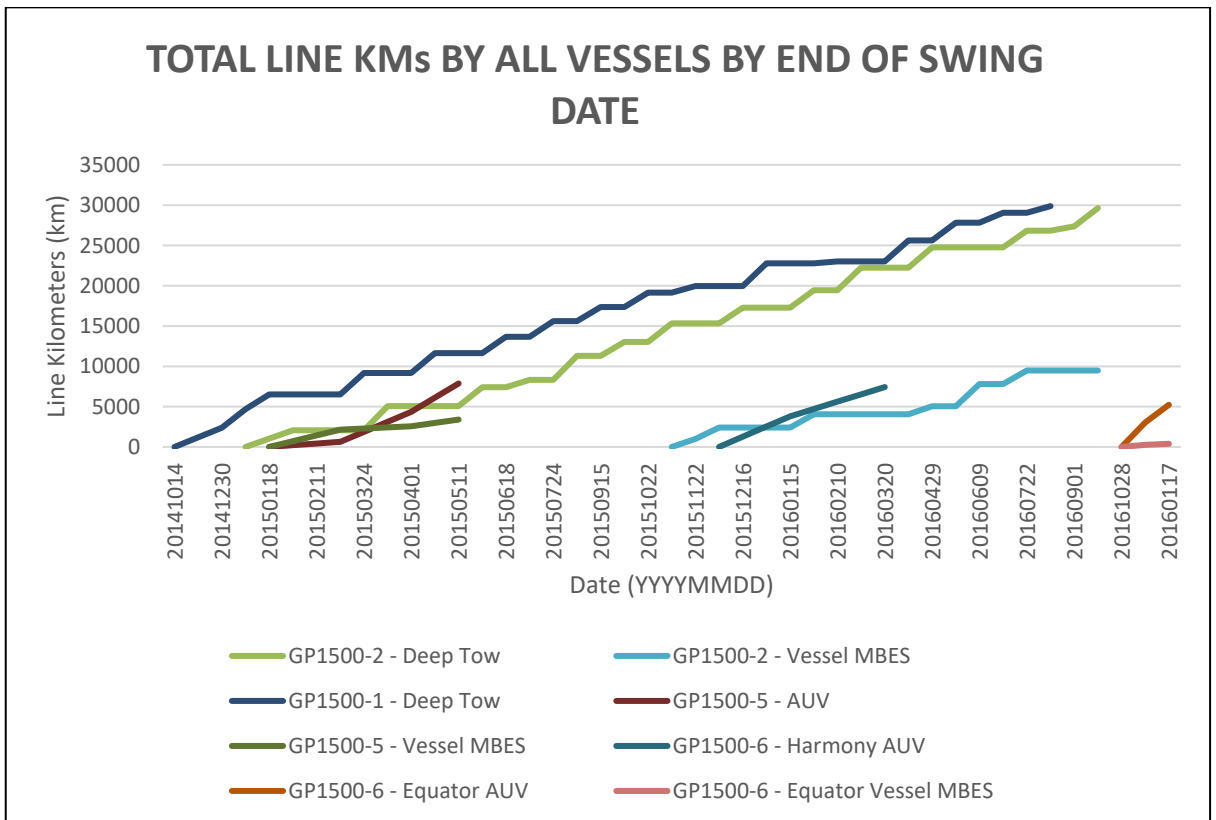


Figure 3.4: Total line kms by all vessels by end of swing date

After two years of Deep Tow acquisition between the Fugro Discovery and Fugro Equator the square kilometres survey by each were almost identical, the Fugro Discovery completing just 432 km (0.42 %) more than the Fugro Equator (see Table 3.7 and Figure 3.5).

Table 3.7: Equator v Discovery km²

Vessel	[km ²]	[%]
Equator DT	51389.6	49.79
Discovery DT	51821.9	50.21
Total DT km²	103211.5	

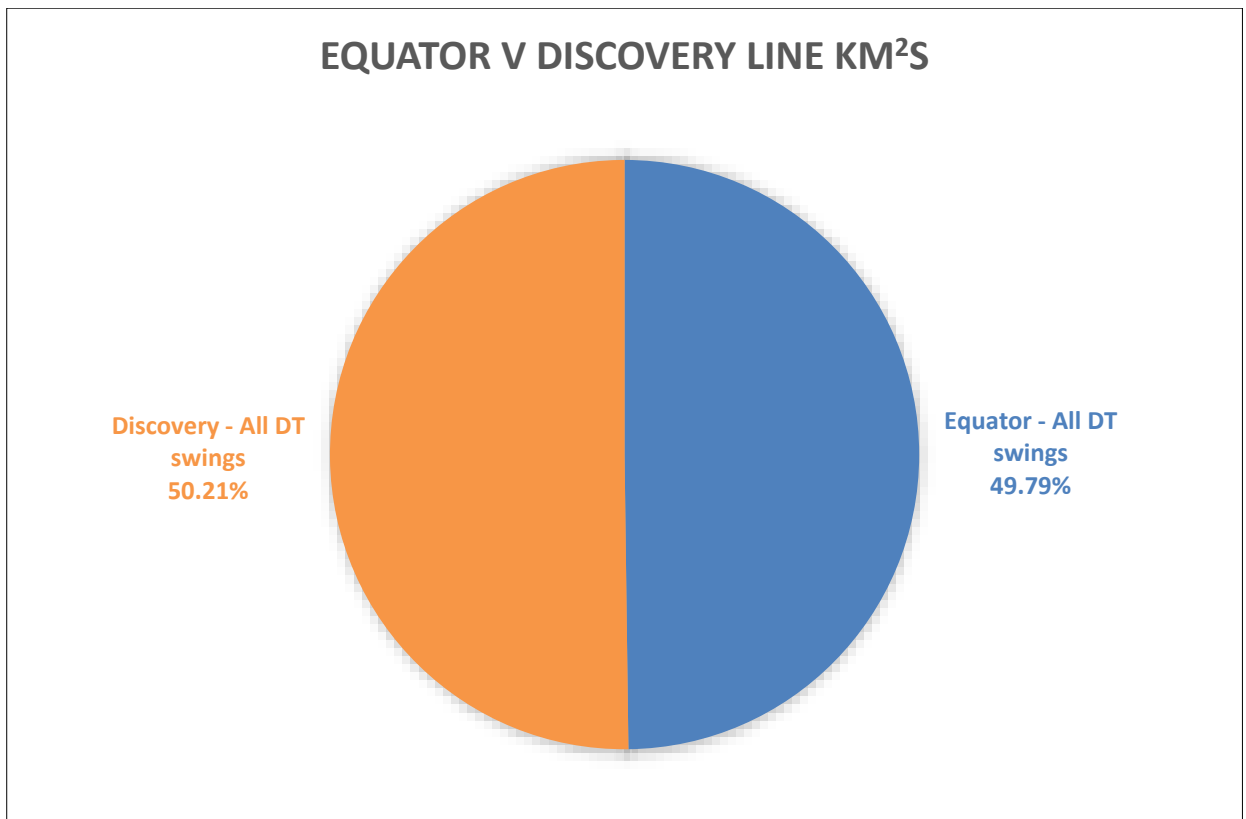


Figure 3.5: Equator v Discovery km² (%)

3.5 Project Time Allocation

Overall the project was conducted in an efficient manner with minimal amounts of down time attributable to equipment problems. A summary of the project time allocations, abstracted from the Daily Operations Report, is presented in Figure 3.6. In total there were 2099 Daily Operations Reports issued for all vessels involved in the search.

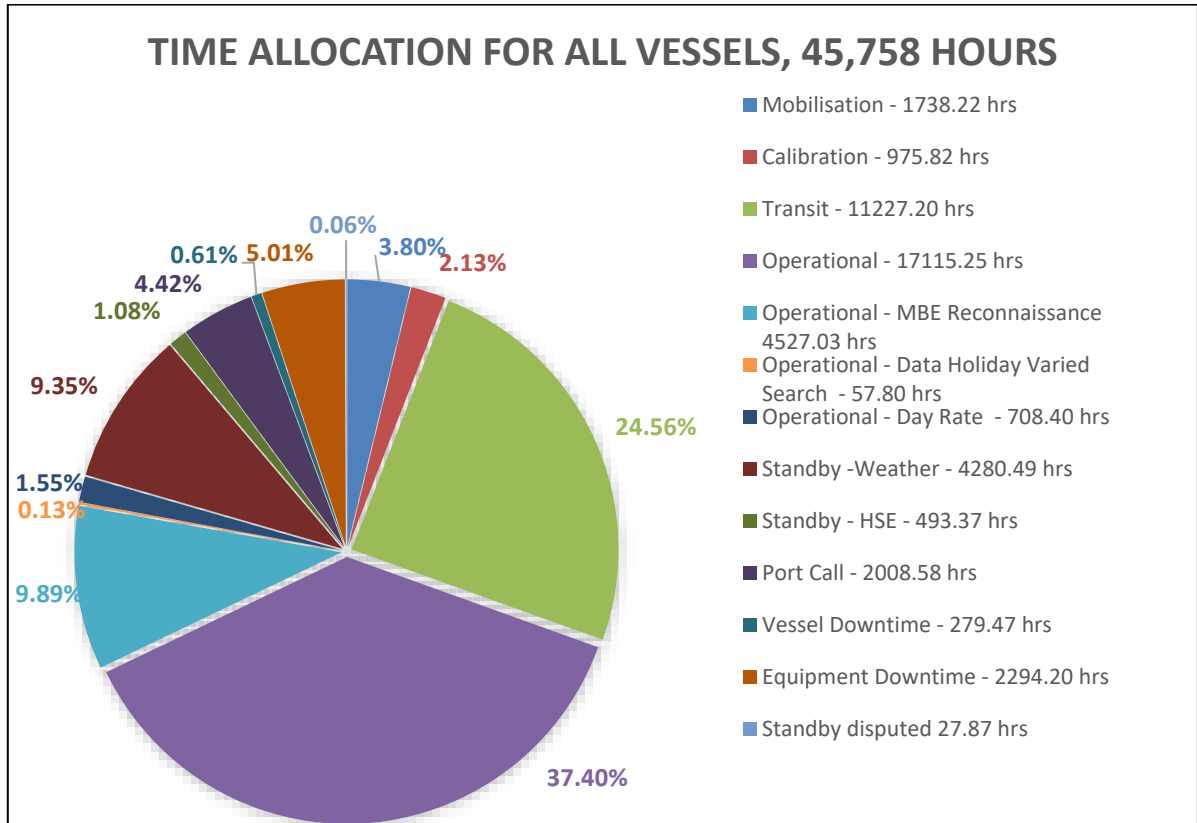


Figure 3.6: Time allocations for the Fugro Equator Deep Tow

The location of the MH370 search area, being more than 1000 Nm west of Fremantle, is reflected in the large percentage ≈25 % of project time devoted to vessel transit. Weather conditions on site varied throughout the year and a total of 10 % of time was lost to weather, particularly during the winter months. There was no production at all during Swing 12 of the Fugro Equator (May 2016 – June 2016) as the adverse weather prevented launch of the Deep Tow.

3.6 Survey Coverage

The Reconnaissance Bathymetric phase of the survey covered a much larger area than was achieved with all subsequent Deep Tow, AUV and ROV surveys combined. This is shown in Figure 3.7 which has the combined Deep Tow and AUV coverage, in purple, overlying the Reconnaissance Bathymetric area as a backdrop. The coverage achieved by just the Fugro Equator and Fugro Discovery Deep Tow operations is shown in Figure 3.8. The AUV tracks for the data holiday infill survey, the primary task during the three AUV phases, are shown in Figure 3.9.

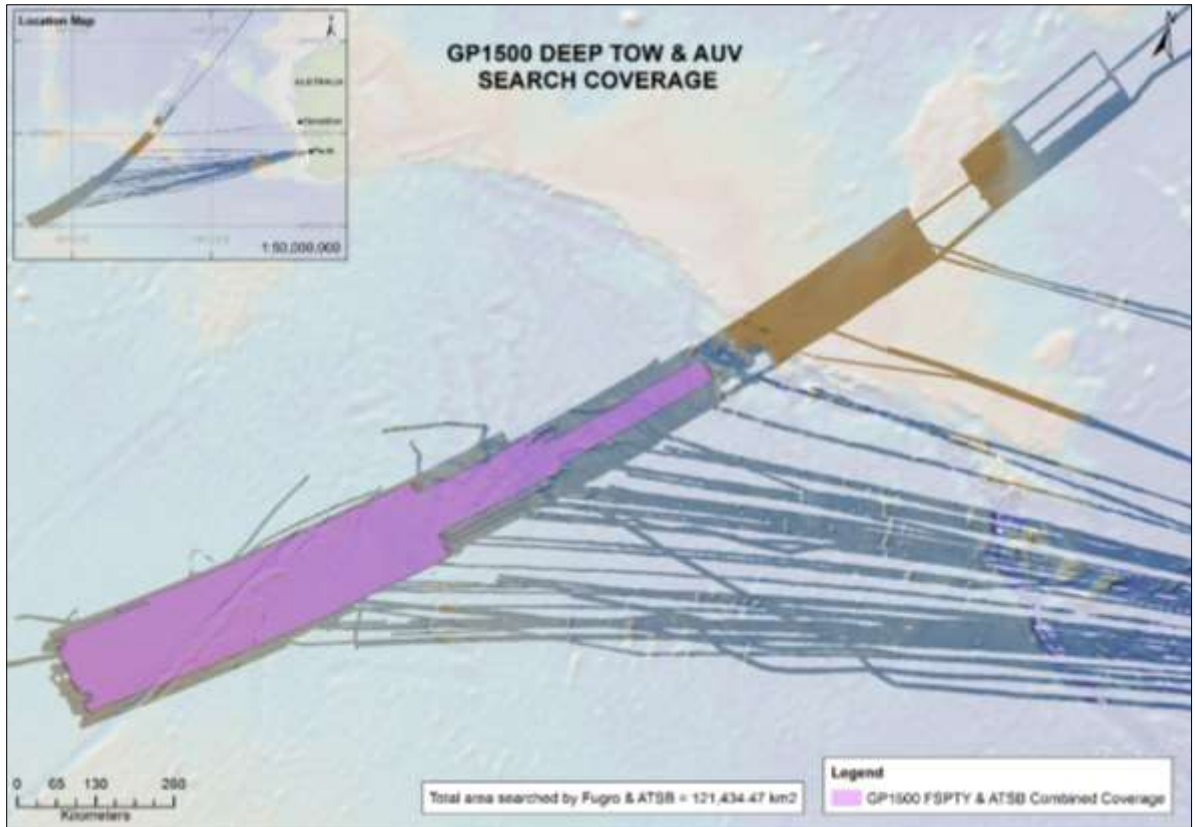


Figure 3.7: Combined Deep Tow and AUV coverage overlain over the Reconnaissance Bathymetric Survey

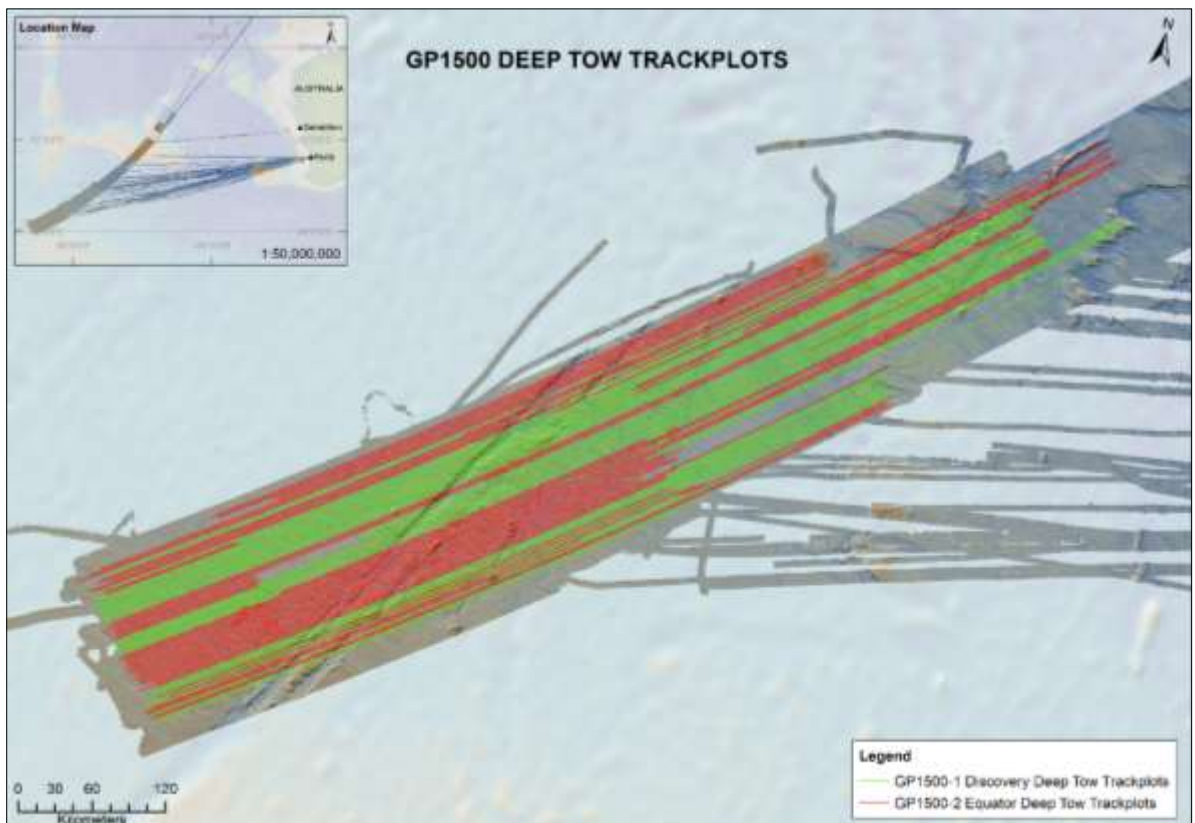


Figure 3.8: Deep Tow coverage overlain over the Reconnaissance Bathymetric Survey

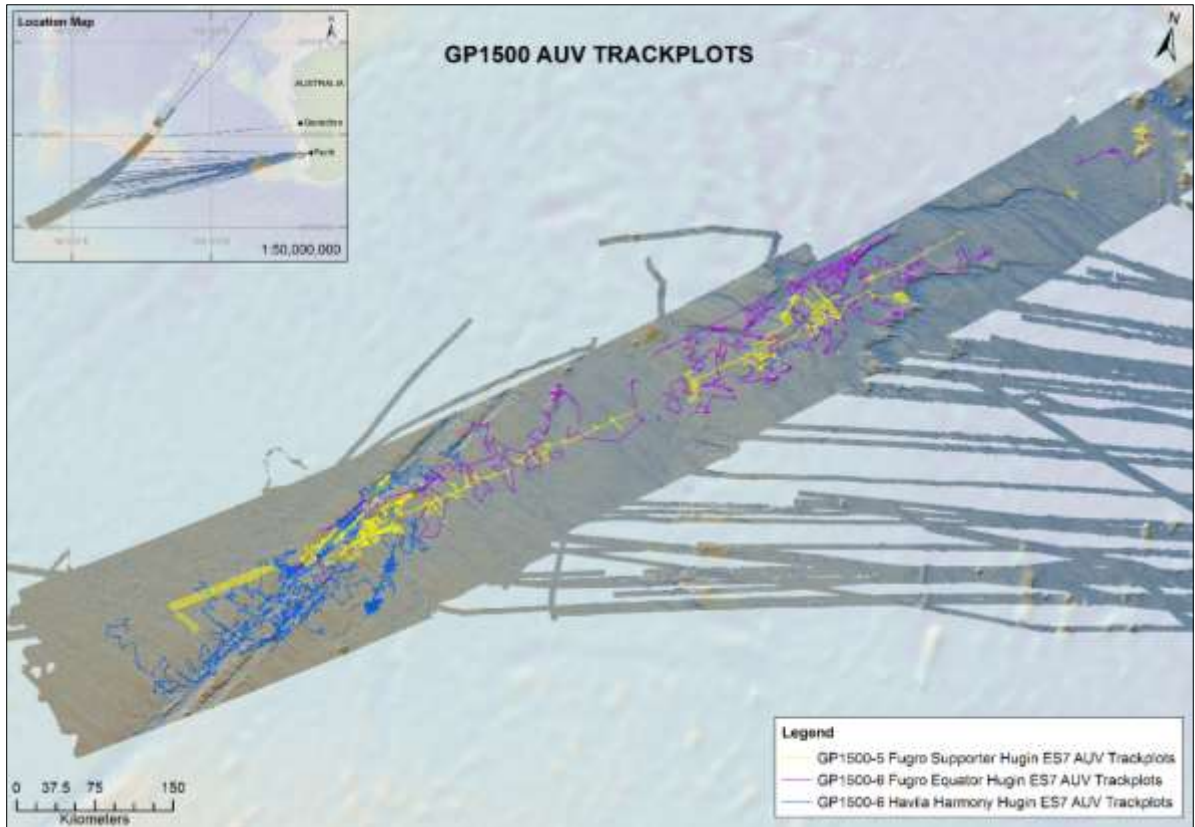


Figure 3.9: AUV trackplots from data holiday infills overlain over the Reconnaissance Bathymetric Survey

3.6.1 Port Calls

A total of 50 port calls were conducted over the course of the project at five different ports, as shown in Table 3.8.

Table 3.8: Number of Port Calls – All Phases

Port	Number of Port Calls
Bali – Indonesia	2
Geraldton – Australia	1
Fremantle – Australia	40
Henderson – Australia	5
Singapore	2
Total	50

3.7 Processing and Reporting

Multibeam data processing was undertaken onboard the vessels after each day of survey by the dedicated multibeam processor using CARIS processing software (see Section 7.2). A geophysical data processing work station was located in the geophysical laboratory to enable interactive data QC during the field work. The onboard geophysicist was able to complete QC of the sidescan sonar data whilst offshore. In addition the onboard geophysicist uploaded all processed geophysical data to Fugro’s server in Perth so that the data was available onshore for more thorough analysis. As the job progressed, the onboard geophysicist sent a brief Preliminary Contact Report ashore each day prior to analysis

onshore. A dedicated onshore team was then able to produce contact reports after reviews by three different people. Each contact report contained a picture of the data, where the contact was identified, and categorised the contact into one of three classifications:

- Classification 1: Marked with high interest and warrants further investigation;
- Classification 2: Marked with some interest but has low probability;
- Classification 3: Marked but not probable.

The onboard QC and onshore interpretation allowed the data quality to be confirmed and survey coverage to be monitored, thus ensuring that the survey objectives had been met prior to each port call and eventually demobilisation.

All onboard data (raw and processed) were regularly backed up to the vessel’s server and to removable storage media throughout the project. A copy of the agreed data deliverables was issued to the ATSB on an external hard drive after each swing. Data processed in the office and uploaded to the ATSB during each swing was also added to this hard drive.

Further details of the sequence of processing is contained in Volume 6 – Processing, Interpretation and Results Report.

3.8 Data Transfer Ashore

Survey data from the vessels was transmitted ashore using the vessel’s upgraded C-Band VSat system. Initial processing of the data was conducted onboard and a set of deliverables created for each 24 hour period. This data was uploaded to the Fugro Aspera Shares site in the Unites States on a daily basis.

The type of data uploaded depended on the operations being conducted on the vessel. Figure 3.10 illustrates the different directory structures for Deep Tow, Reconnaissance MBES and AUV operations. Only data directly relevant to the search and the identification of anomalies was transmitted ashore for final processing. All auxiliary data such as sub-bottom profile data and MBES water column data was retained onboard and copied to hard drive for delivery to the office at each port call.

<u>Deep Tow Data</u>	<u>MBES Data</u>	<u>AUV Data</u>
000_Navigation	001_MBES_ALL	000_Navigation
002_SSS_XTF	002_Logs	002_SSS_XTF
003_Logs	004_Delayed Heave	003_Logs
004_Track_Plot		004_Track_Plot
005_Weather		005_Weather
006_MBES_XYZ		006_MBES_XYZ
007_MBES_Backscatter		007_MBES_Backscatter
008_Sniffer		016_AUV_Mission_Settings_Plans

Figure 3.10: Typical directory structure for data upload

3.9 Demobilisation

The Fugro Supporter was demobilised in Fremantle on 17 May 2015, the AUV removed and then departed for Benoa, Bali.

The Havila Harmony was demobilised on 26 March 2016, in Fremantle.

The Fugro Discovery finished Deep Tow operations on 11 August 2016, and began transit to Singapore, arriving on 22 August 2016 for demobilising and preparation for dry docking.

On 16 October 2016, following completion of the Swing 15 Task Request, the Fugro Equator departed the search area and transited to Fremantle for demobilisation of the Deep Tow equipment, arriving alongside the Australian Maritime Complex in Henderson, Western Australia, on 21 October 2016. Preparation for the demobilisation was undertaken during transit to port and, on arrival, the Dynacon traction winch, HPU diesel generator and EdgeTech Deep Tow-2 towfish were quickly demobilised from the vessel.

The Fugro Equator was scheduled to continue working on the project, and mobilisation of Fugro EchoSurveyor VII Hugin 1000 AUV commenced immediately to make the vessel ready for AUV operations. After completion of its AUV campaign the Fugro Equator returned to Fremantle and was demobilised between 22 and 27 January 2017, before transiting to Singapore for dry docking.

4. STATISTICAL SUMMARIES

4.1 Data Holiday Types and Extents

4.1.1 Remaining Holidays

Table 4.1 shows the number and size of the remaining data holidays as well as the percentage of the total remaining holidays that resulted from the surveys carried out by Fugro. The table shows the effectiveness of survey operations conducted by Fugro. Equipment failure and offtracks are particularly low, especially considering the time spent surveying was over two years.

Table 4.1: Data Holiday and LPD Count

	Remaining Data Holidays and LPDs*		Remaining Fugro Data Holidays and LPDs		
	Polygon Count	Area [km ²]	Polygon Count	Area [km ²]	[%] of Total Remaining
Equipment Failure	88	17.1	40	3.49	20.41
Offtracks	8	19.2	2	0.07	0.36
Shadow Zones	5026	312.94	4521	264.09	84.39
Terrain Avoidance	146	218.79	120	116.34	53.17
Lower Probability of Detection	7440	2510.09	7285	2379.72	94.81

*Includes Go Phoenix and DJ101

Figure 4.1 shows the individual Fugro data holidays (not LPDs) in area (km²) as percentages of the total remaining data holidays.

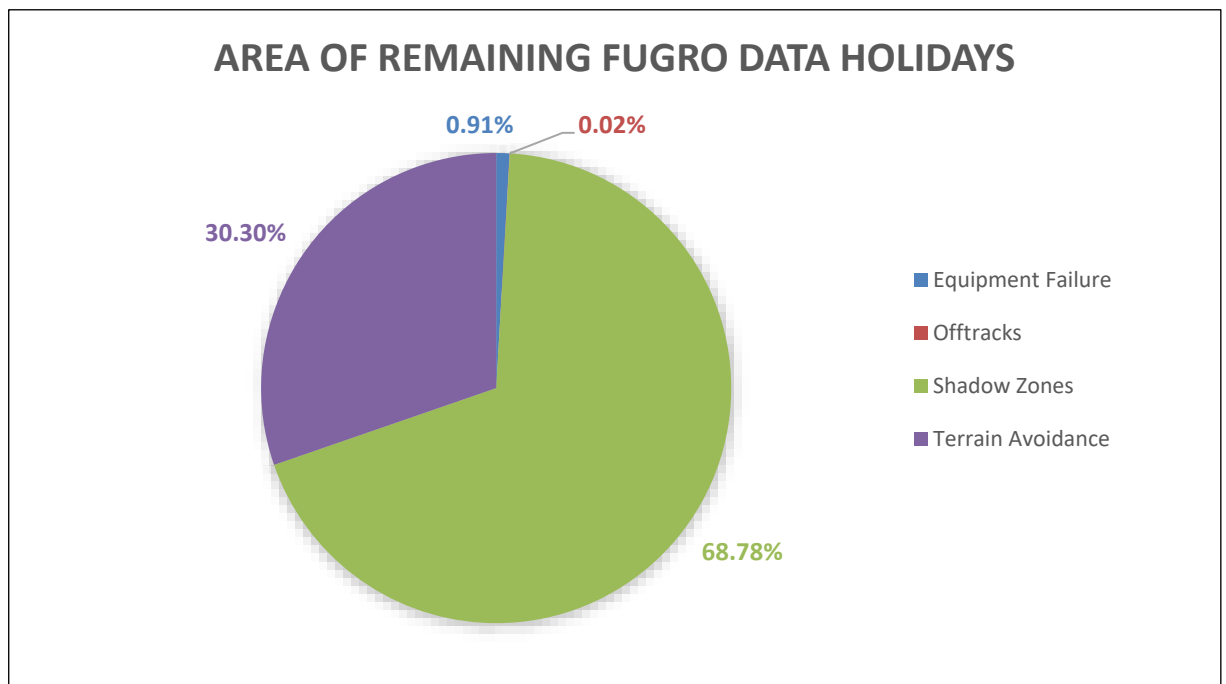


Figure 4.1: Area of remaining Fugro data holidays

The prime reason for the AUV phase of the survey was to fill in data holidays, though the AUV was used on a few occasions to cover virgin territory in the same manner as the Deep Tow was tasked.

Table 4.2 shows the infill statistics from the three AUV phases of the search. Between 73.5 % for the Havila Harmony and 85.4 % for the Fugro Supporter, of data holidays were successfully infilled by good AUV data. The next highest percentage is LPD, between 11.58 % for the Fugro Supporter and 24.05 % for the Havila Harmony. It should be noted LPDs, when resurveyed by the AUV, generally confirmed that the terrain consisted of complex geology and/or a dynamic sea floor environment which typically decreases the confidence of detection for delineating man made debris from geology.

Table 4.2: Data Holiday and LPD Infill Statistics for the three AUV Campaigns

	Fugro Supporter		Havila Harmony		Fugro Equator	
	Area [km ²]	[%]	Area [km ²]	[%]	Area [km ²]	[%]
No Change ¹	5.85	1.35	13.89	2.41	19.00	5.33
Filled ²	368.95	85.37	423.98	73.49	266.94	74.85
LPD ³	50.04	11.58	138.76	24.05	70.59	19.79
<100 m ⁴	7.35	1.70	0.29	0.05	0.10	0.03

¹Data holiday has not been filled in by good AUV data

²Data holiday has successfully been filled in by good AUV data

³Data holiday has turned into a LPD as a result of AUV data

⁴Data holiday has been cut down to a size which no longer classifies it as a holiday

Figure 4.2 shows the overall data holiday and LPD statistics for all three AUV campaigns in percentage terms.

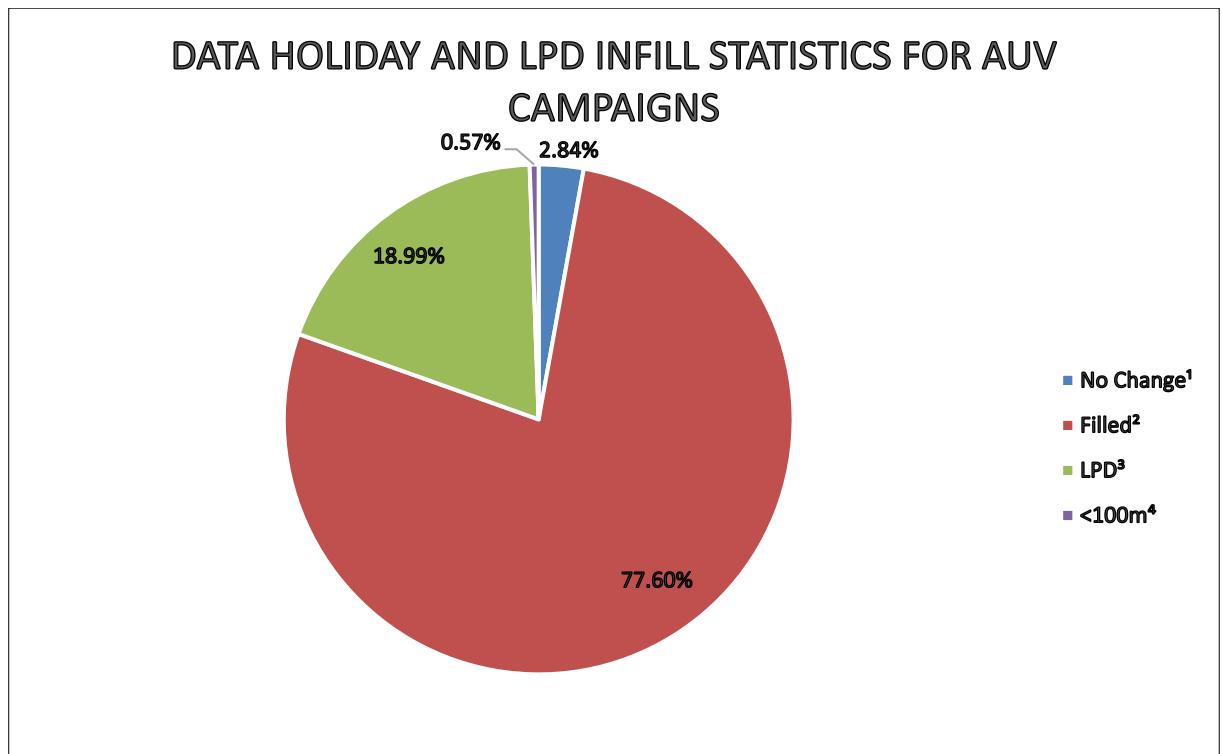


Figure 4.2: Data holiday and LPD infill statistics for AUV campaigns

Figure 4.3 shows the areas of all remaining data holidays for Fugro v non-Fugro vessels.

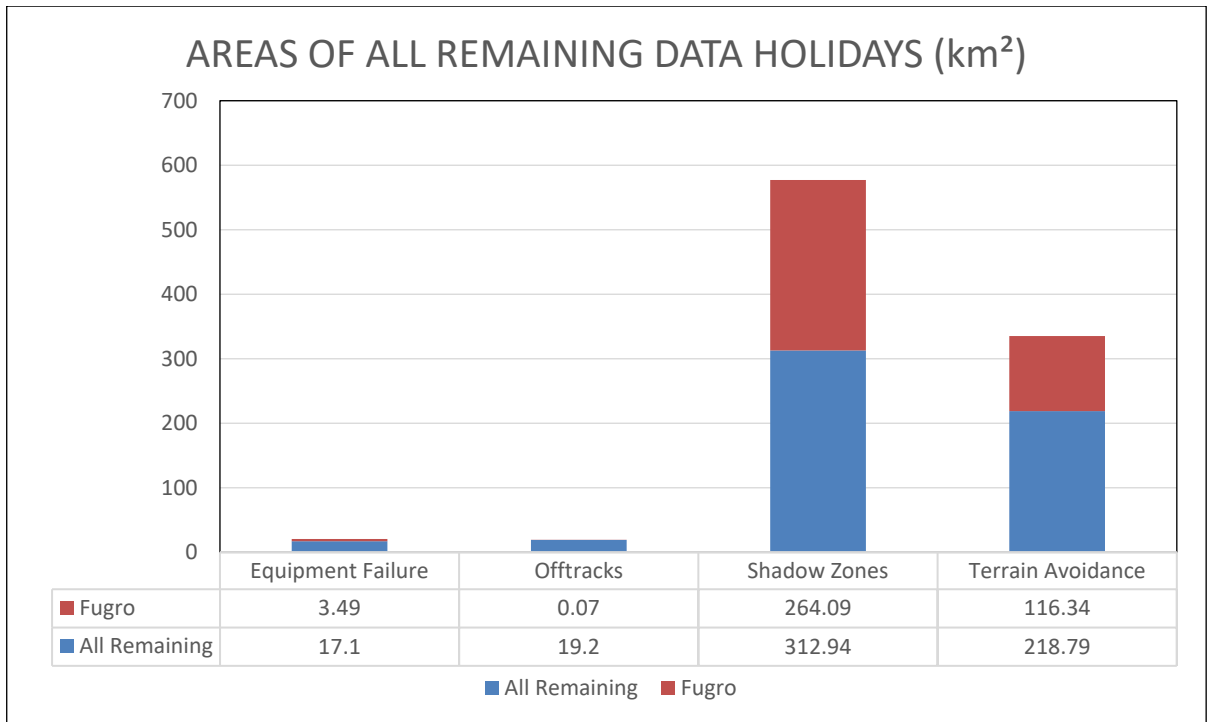


Figure 4.3: Remaining data holidays for Fugro v non-Fugro vessels

4.2 Contact Summary

A summary of the contacts for each phase of the survey picked by the two onshore based reviewers, those contacts that were subsequently forwarded to the ATSB and then the number of these contacts that were picked by both onshore reviewers is shown in Figure 4.4.

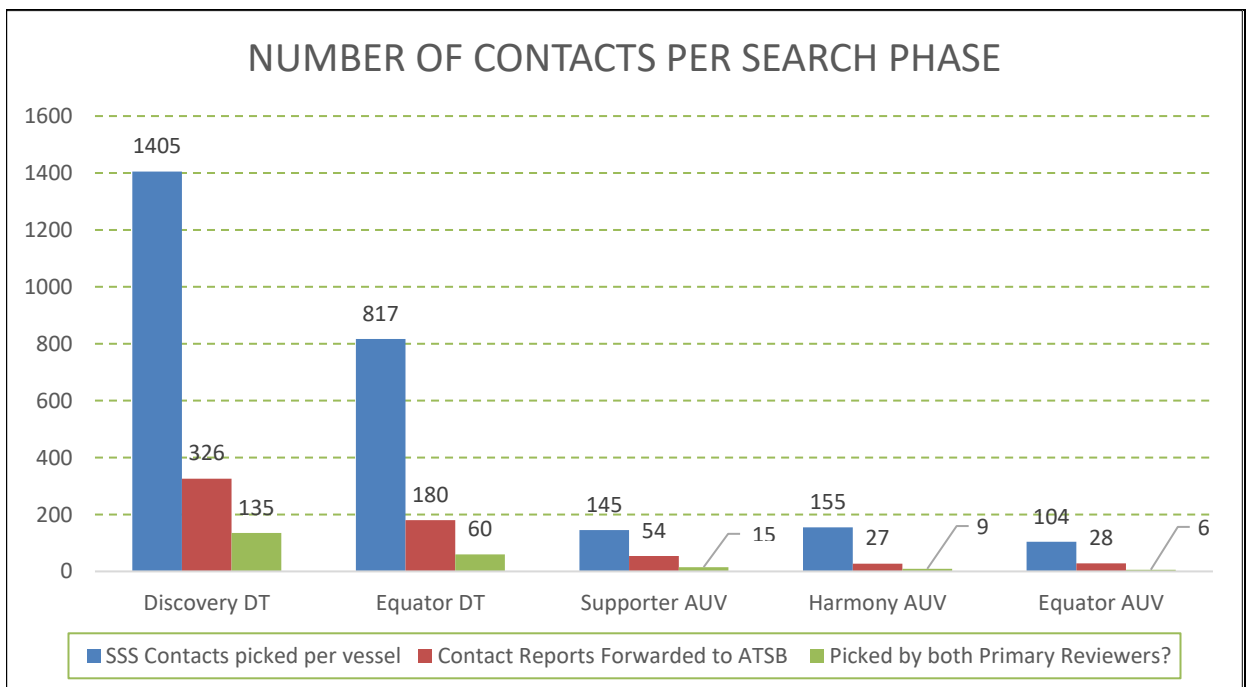


Figure 4.4: Number of contacts per phase

This graph demonstrates the process of narrowing down all possible contacts that were deemed interesting enough to warrant further investigation. All data were reviewed multiple times both offshore and onshore to identify all possible contacts and then reviewed again to ensure nothing of interest could be missed.

4.3 Findings

A number of contacts upon investigation by the AUV or ROV turned out to be shipwrecks.

4.3.1 Shipwreck #1

The sidescan sonar over the first shipwreck (designated Shipwreck #1) discovered on the search is shown in Figure 4.5. It shows the many bright and large returns that suggested that there might be something of interest to investigate.

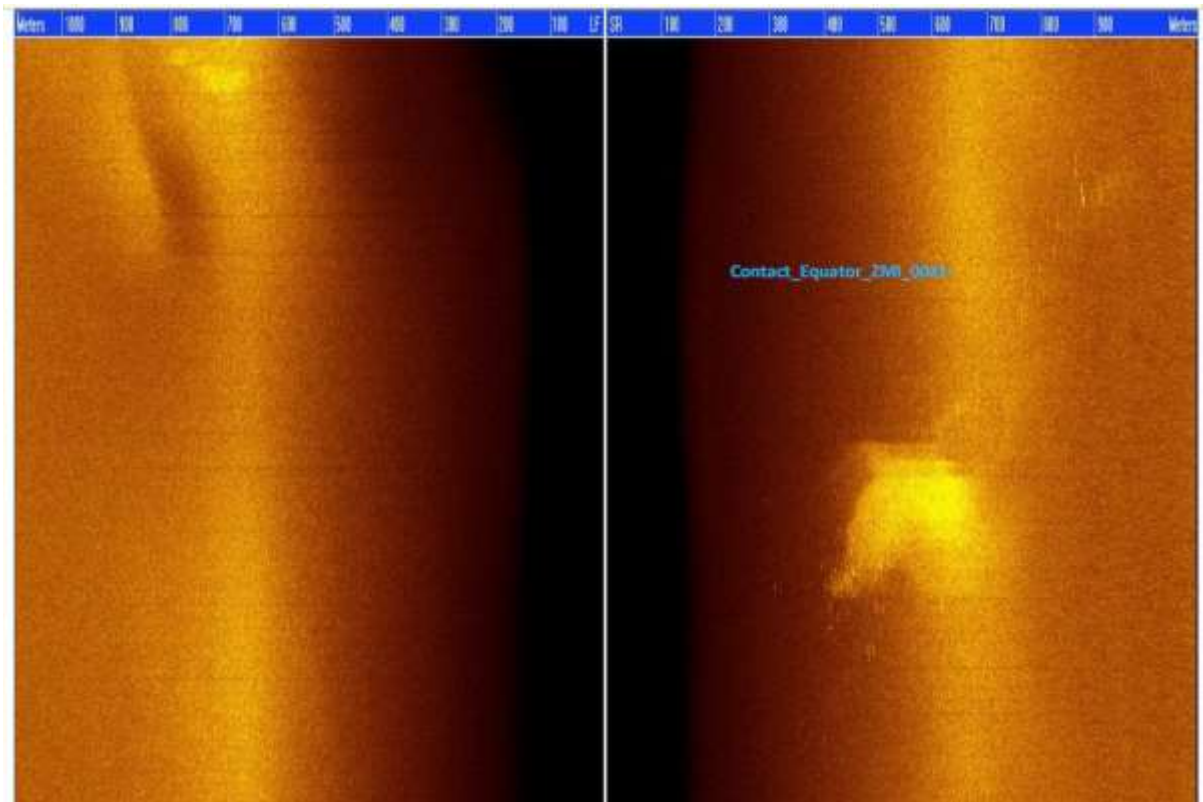


Figure 4.5: Sidescan sonar over shipwreck #1

Shipwreck #1 was in 3800 m of water and when investigated further by a camera survey from the AUV, very detailed images emerged of debris associated with the wreck.

Figure 4.6 to Figure 4.10 clearly shows identifiable images of an anchor, a capstan, a chest, a chain and many items of debris.



Figure 4.6: Shipwreck #1 – anchor

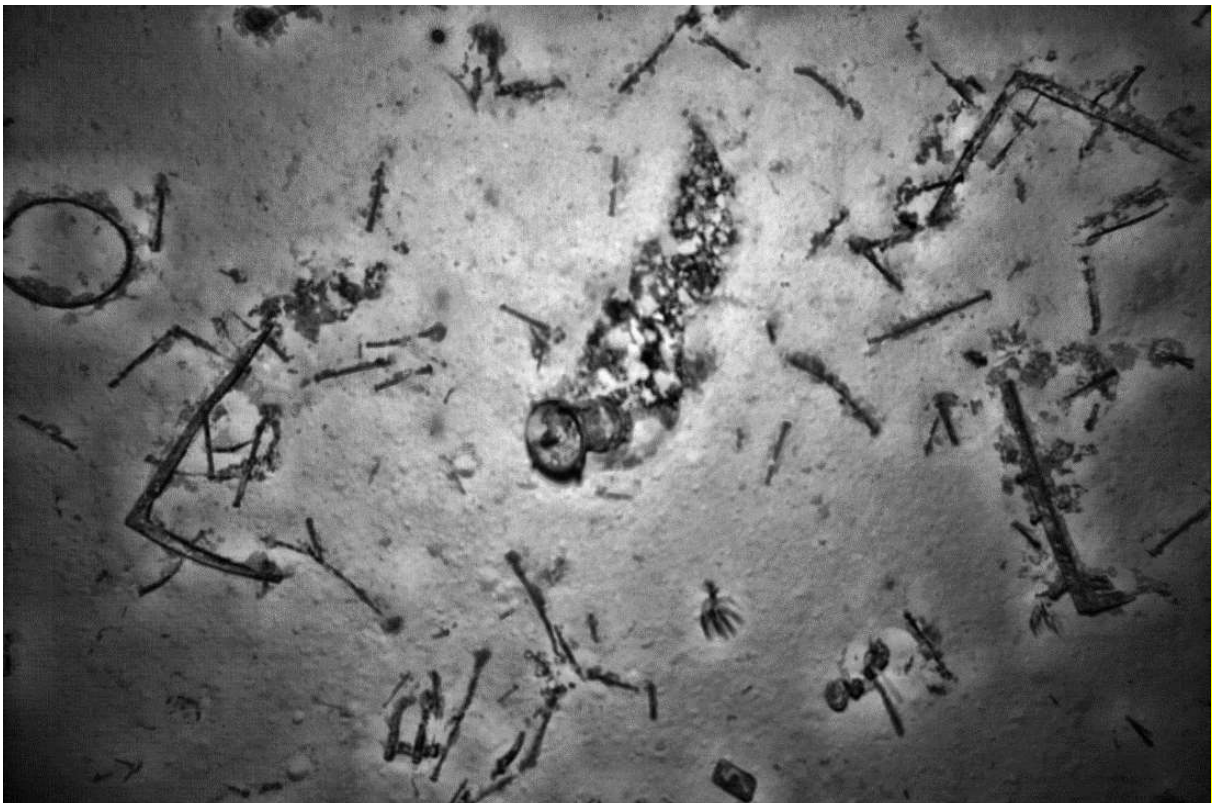


Figure 4.7: Shipwreck #1 – ship's capstan

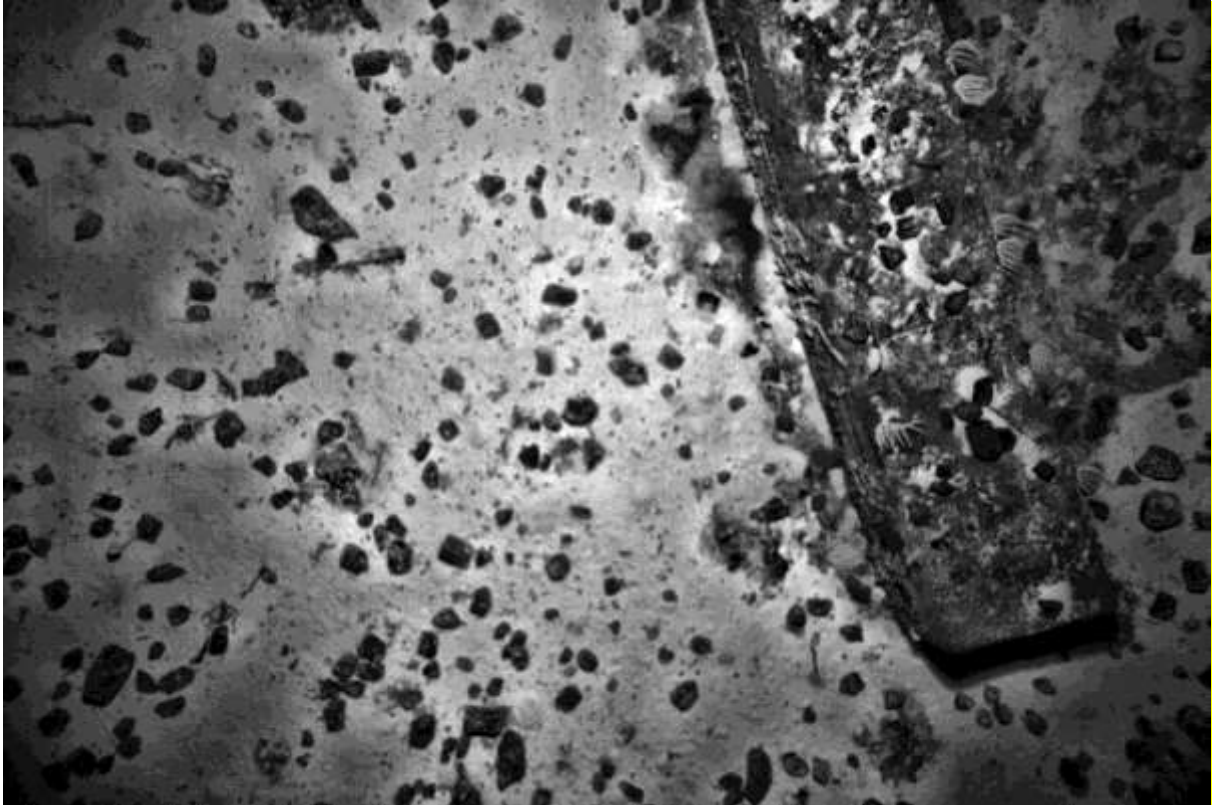


Figure 4.8: Shipwreck #1 – possible water tank

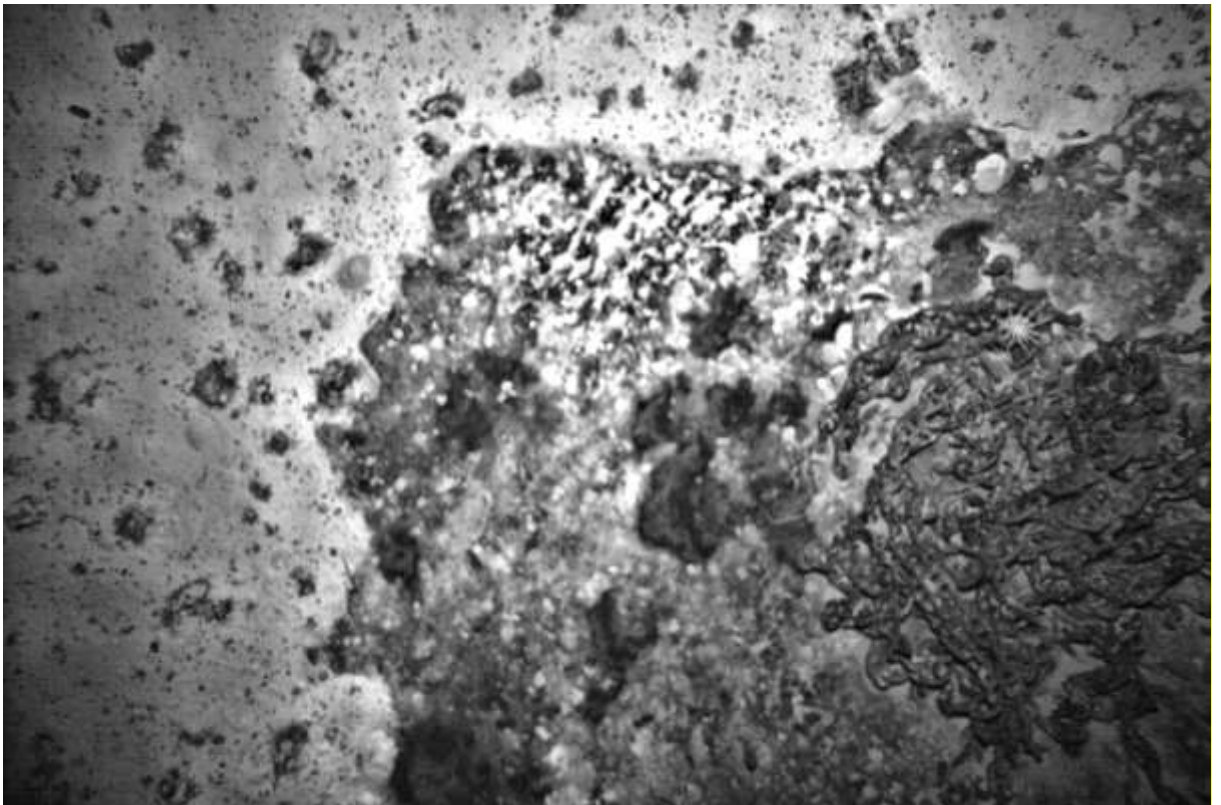


Figure 4.9: Shipwreck #1 – chain

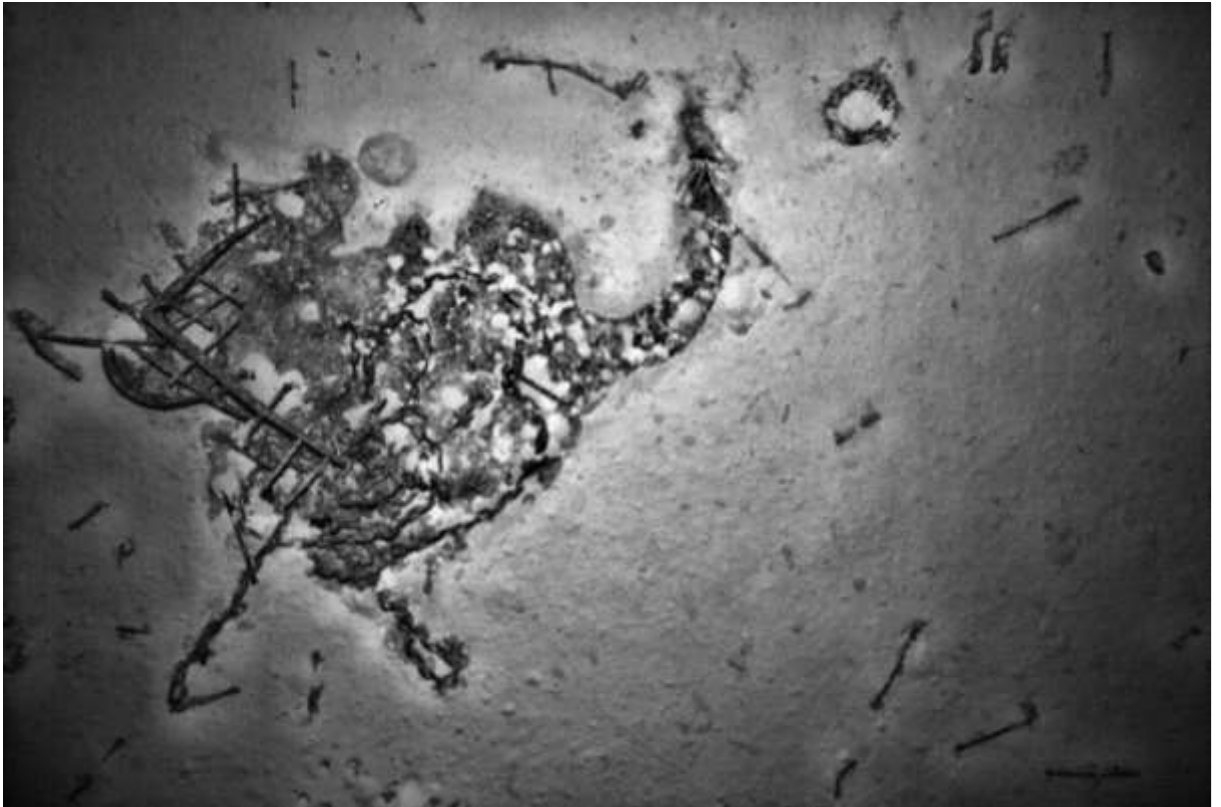


Figure 4.10: Shipwreck #1 – angular item

4.3.2 Shipwreck #2

The sidescan sonar from the Deep Tow over the second shipwreck (designated Shipwreck #2) is shown in Figure 4.11. It originally showed up as a bright patch centred on a brighter symmetrical body which had shadows, indicating it had a visible vertical dimension.

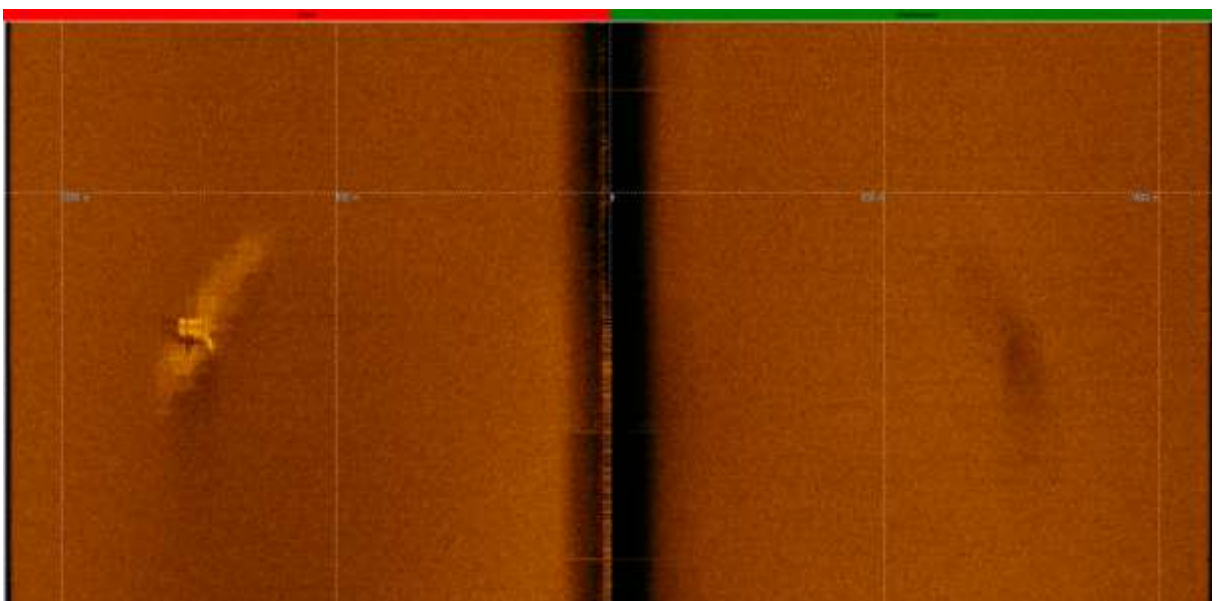


Figure 4.11: Shipwreck #2 – original Deep Tow image

Further investigation by the Deep Tow, flying at an altitude of approximately 35 m above the seabed revealed a complete steel hulled shipwreck sitting upright on the seabed (Figure 4.12 and Figure 4.13).

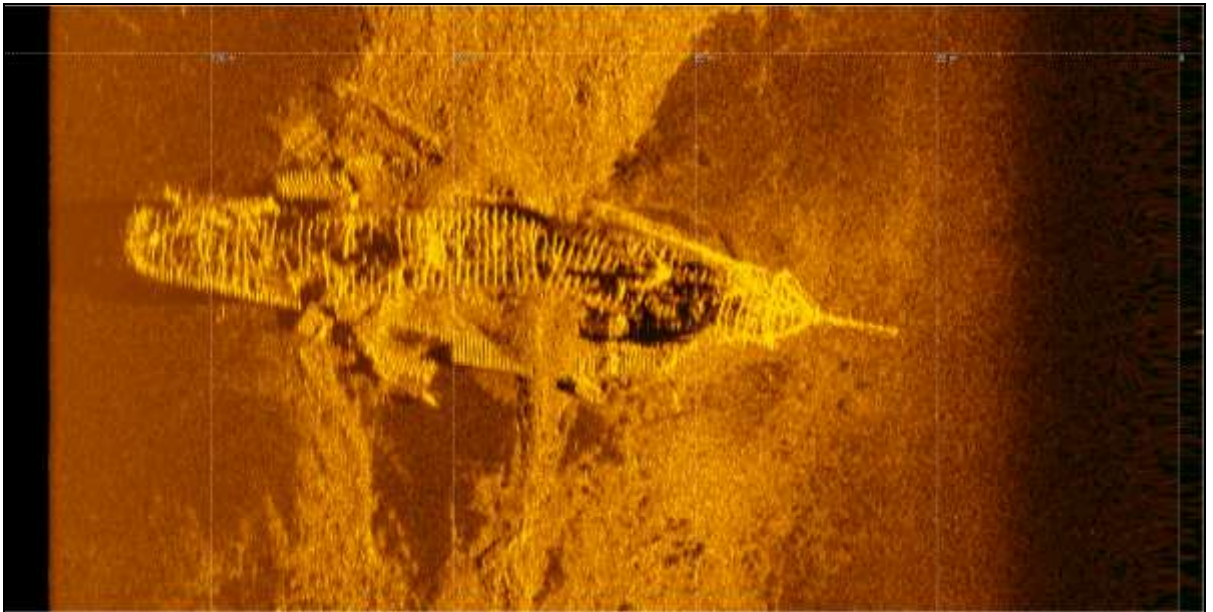


Figure 4.12: Shipwreck #2 – bow on sidescan sonar image

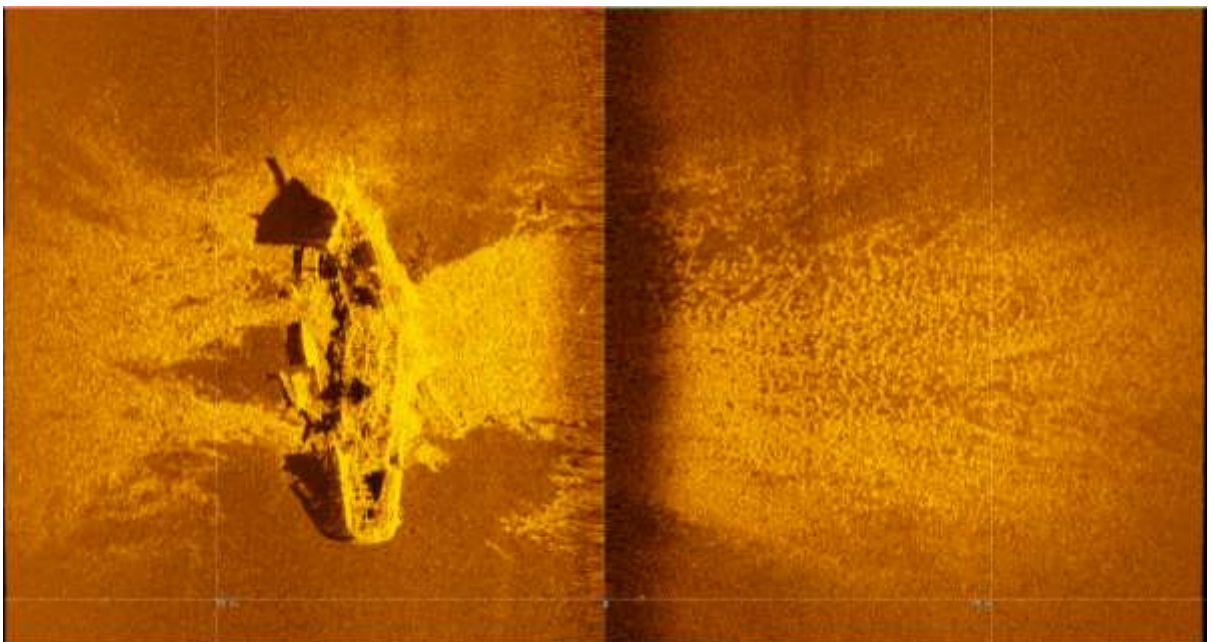


Figure 4.13: Shipwreck #2 – side on image

4.3.3 Shipwreck #3

Shipwreck #3 was a recent steel fishing vessel, found upright, intact and complete with nets, as shown in Figure 4.14 and Figure 4.15.

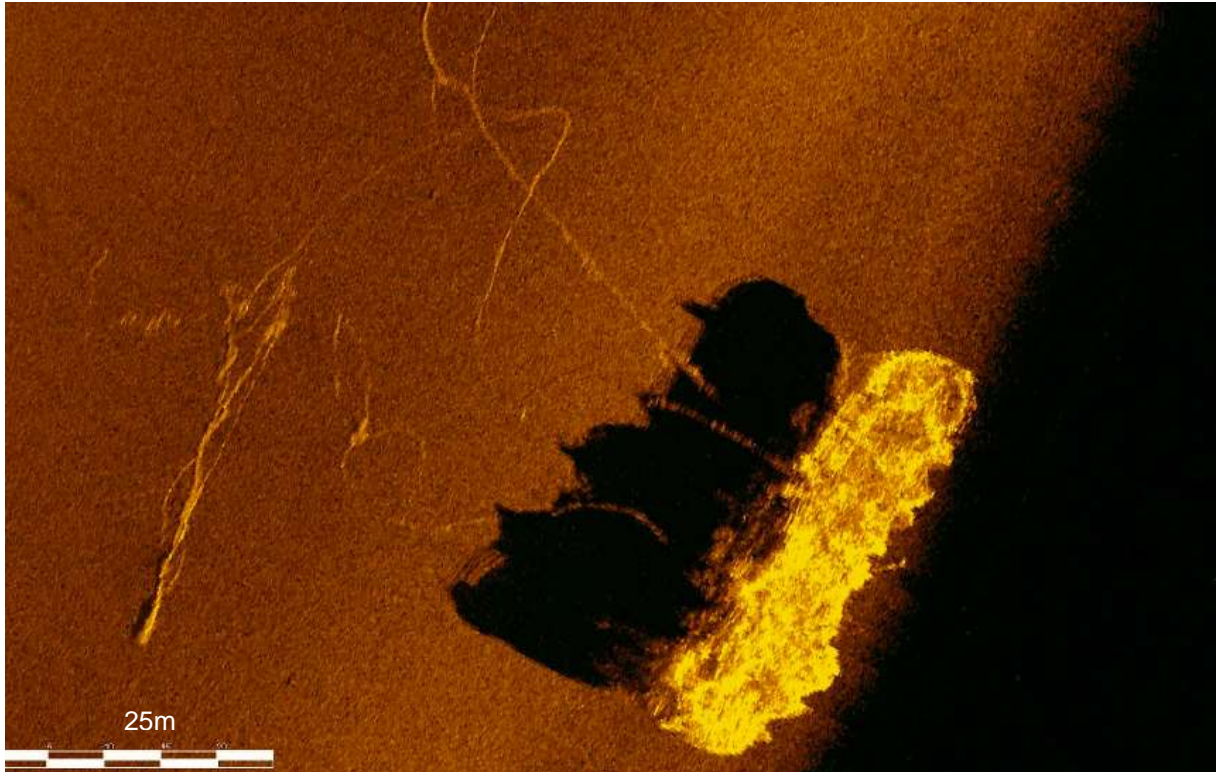


Figure 4.14: Shipwreck #3 – sidescan sonar image



Figure 4.15: Shipwreck #3 – showing deck railing and nets

4.3.4 Shipwreck #4

Shipwreck #4 was a small wooden fishing vessel with substantial damage to the bow as shown in Figure 4.16 and Figure 4.17.



Figure 4.16: Shipwreck #4 – port bow



Figure 4.17: Shipwreck #4 – starboard bow damage

4.3.5 Small Target Detection

Probably the clearest demonstration of the Deep Tow systems capability was the detection of a 44 gallon (200 litre) drum at a range of 690 m (see Figure 4.18). Clearly it helped that the seabed was smooth and free from outcrops. The drum was photographed during an ROV mission.

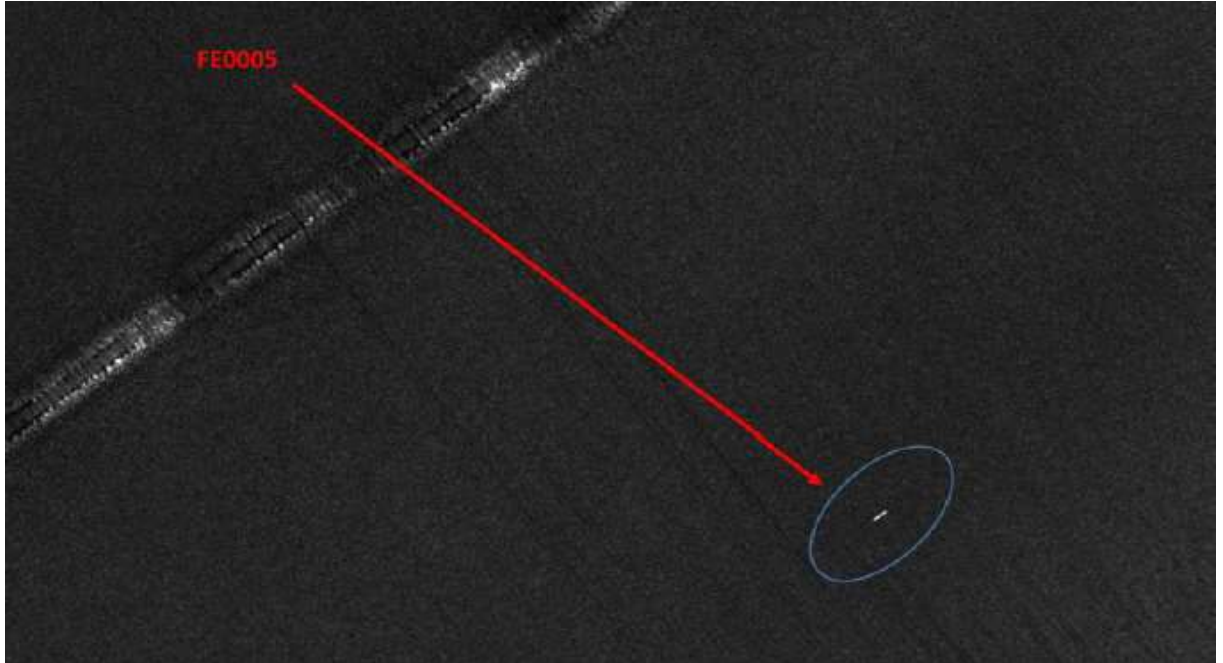


Figure 4.18: 200 litre drum – original Deep Tow sidescan sonar data, 690 m range

The drum was also observed on the adjacent line at 1100 m range as seen in Figure 4.19.

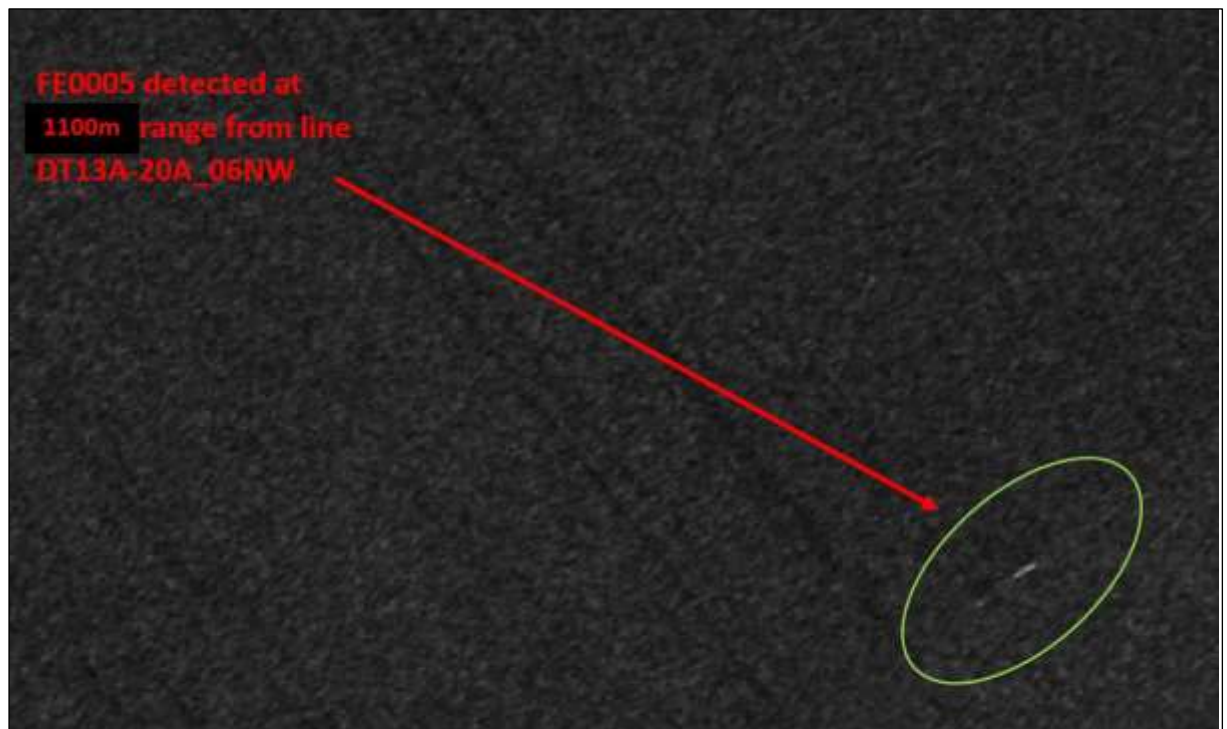


Figure 4.19: 200 litre drum – original Deep Tow sidescan sonar data, 1100 m range

The photograph of the drum taken from the ROV is shown in Figure 4.20.



Figure 4.20: 200 litre drum – ROV photo

4.4 Sound Velocity Profiles

Sound velocity profiles (SVPs) were required to accurately gather vessel based MBES data and to conduct USBL positioning of both the Deep Tow and AUV systems.

For the initial sound velocity profiles completed during the Reconnaissance phase a MIDAS SVX2 sound velocity sensor was lowered over the side of the Fugro Equator to near the sea floor. In total 29 SVPs were taken, all subsequent SVPs were taken from sensors mounted on the Deep Tow and AUV systems as they were raised and lowered.

It was important to conduct multiple sound velocity profiles as the speed of sound in water varied based on location and time of year and to this end results were shared between vessels so that all of the survey area was covered.

The tables provided in Appendix A, give a summary of the collected sound velocity profiles for each phase of the search.

In all, 195 SVPs were taken on the search area site, the spread of which is shown in Figure 4.21.

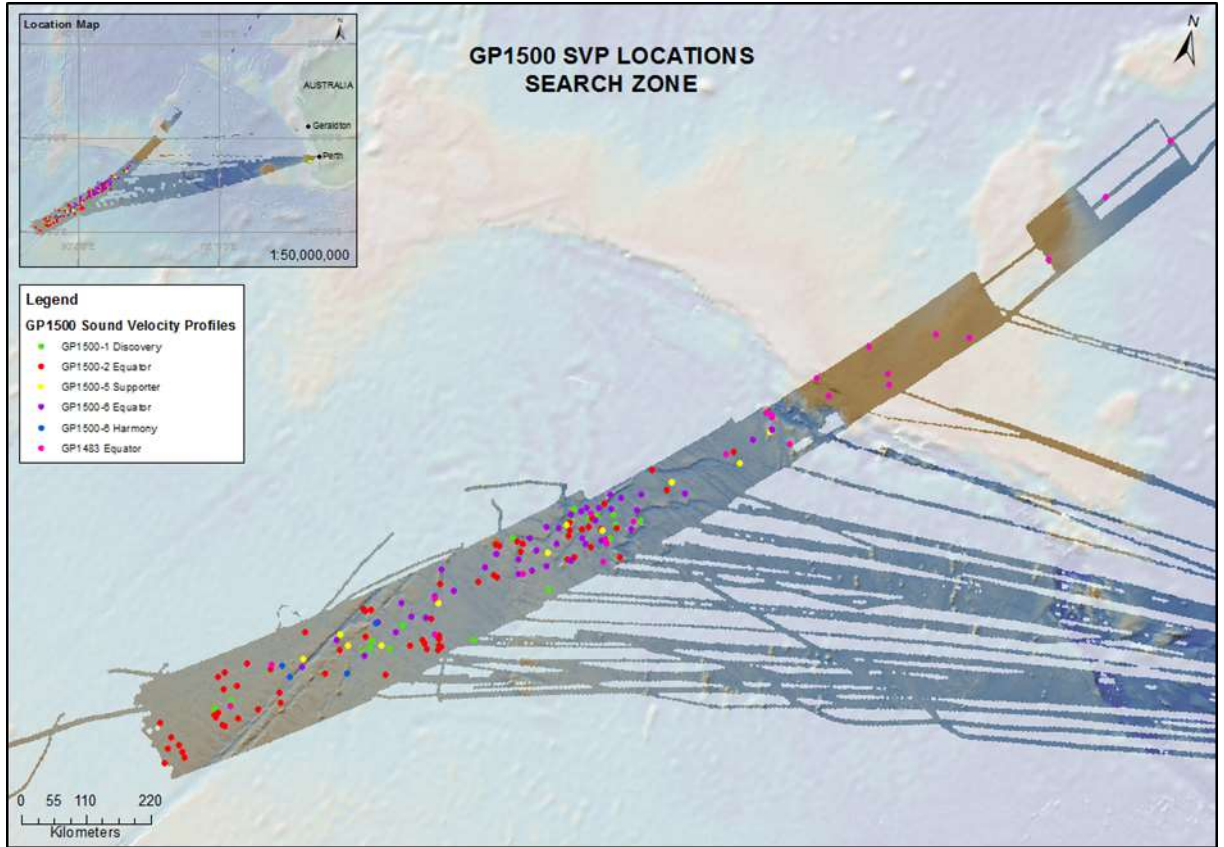


Figure 4.21: Location of sound velocity profiles at the search area site

There were also a number of sound velocity profiles carried out on the trials site off the coast of Fremantle, these are shown in Figure 4.22.

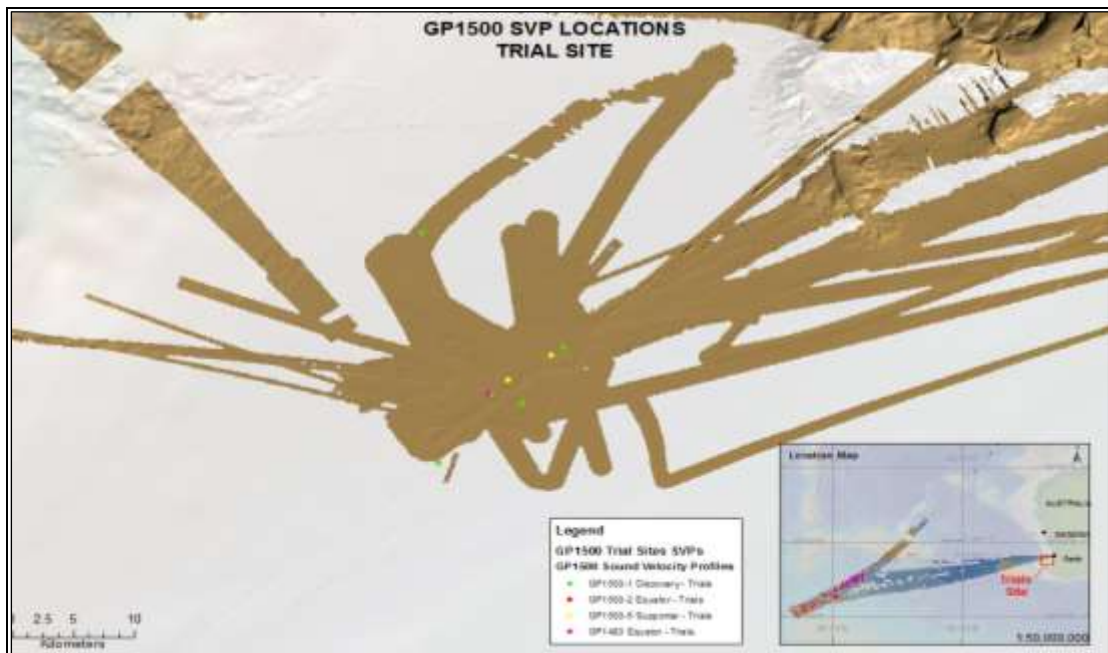


Figure 4.22: Location of sound velocity profiles at the trial site

4.5 Seabed Features

The reconnaissance bathymetric survey highlighted some significant seabed features the most significant being the Geelvink Fracture Zone, part of which is seen as a large canyon, shown in Figure 4.23.

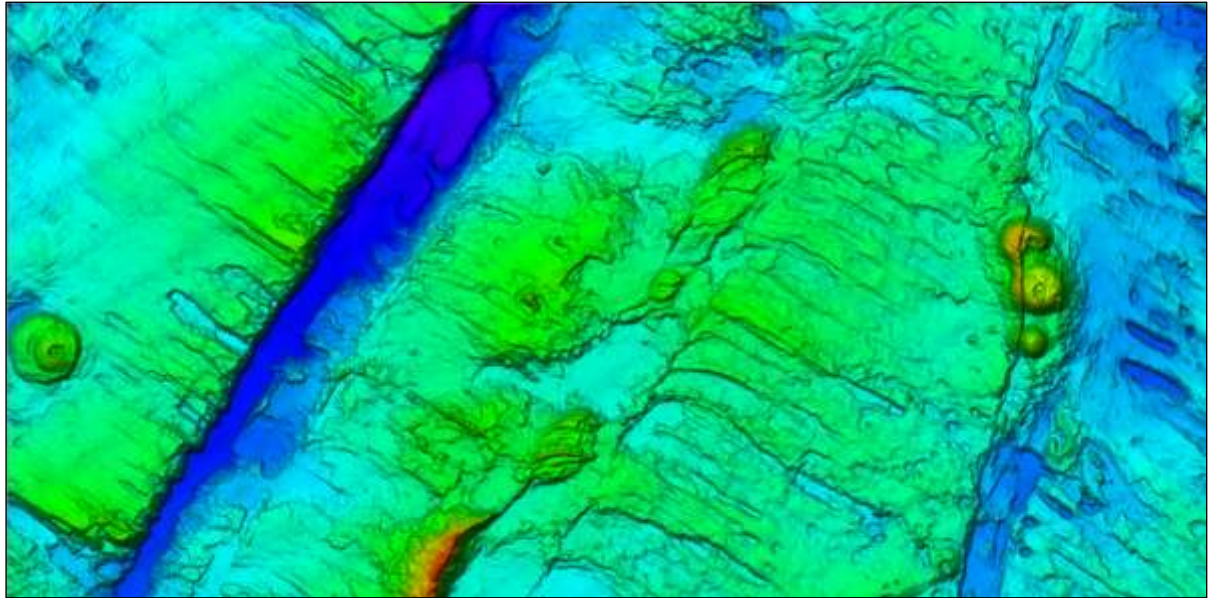


Figure 4.23: The Geelvink fracture zone

The Geelvink Fracture Zone could be a detachment fault associated with large scale extensional tectonic movement in the area. The presence of seamounts in the vicinity confirm volcanic activity which could be associated with very thin oceanic crust. On some of the sidescan files structures resembling pillow basalts can be seen. These clues hint at the possibility that the escarpment could represent an area of incipient oceanic crust. Close examination of the walls of the fault shows smaller faults which are shooting off perpendicular to the main fault strike. These are likely to be caused by brittle deformation whereby the crust is being stretched over the spherical surface of the earth and failing. There is some evidence for lateral displacement on the north-west/south-east striking faults suggesting a strike-slip component to the major fault movement.

The scale of the Geelvink Fracture Zone is shown in Figure 4.24, with the 452 Petronas Towers at 452 m for scale. In places it is up to 800 m deep.

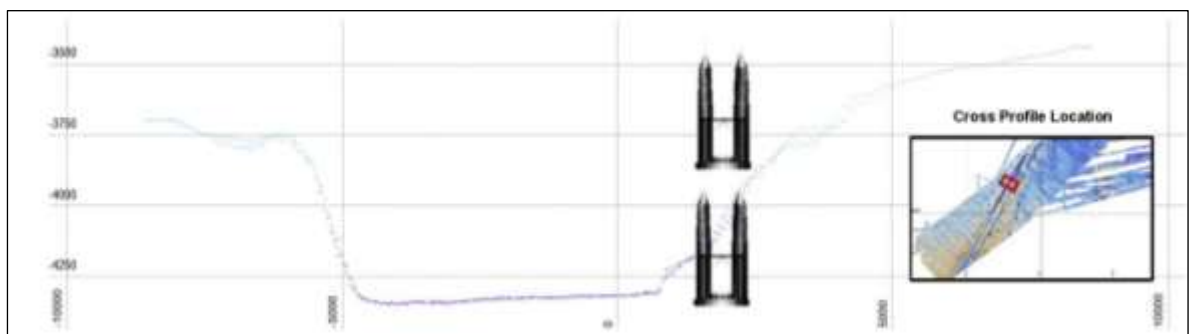


Figure 4.24: Cross-section of Geelvink Fracture Zone (452 m Petronas Towers for scale)

4.6 Transit Distance

The remoteness of the survey area from Australia is shown in Figure 4.25. The red ring is 2500 km radius centred on Fremantle. At approximately 9 knts it generally took the search vessels approximately six days to reach site, depending where on site search operations were to begin for each swing. Usually operations where practical started and ended with minimal transit (five days) to maximise operational time.



Figure 4.25: 2500 km range ring from Fremantle

Considering just the transit distance the search vessels combined completed 213,260 kms or 5.3 laps around the earth as measured at the equator (this distance was derived from transit multibeam data acquired. The Fugro Discovery and the Havila Harmony did not acquire data on their transits distances so their values were estimated). The distance covered by vessels on site was not factored into this equation as there was no detailed log for the vessels kilometres covered.

4.7 Personnel Hours

Table 4.3 and Figure 4.26 show how many billing hours each of the Fugro Operating Companies accrued during the entire duration of the search across all vessels.

Table 4.3: Personal Hours All Vessels

Personal Hours for all Vessels	
Operating Company	Hours
Fugro Survey Ltd	160860
Fugro Survey Pty Ltd	43392
Fugro Survey PTE Ltd	36648
ATSB	23712
Fugro Marine	326280
Contractors	23496
ISOS	11196

Personal Hours for all Vessels	
PT Fugro Indonesia	4692
Fugro GeoServices, Inc	17592
Fugro BTW Ltd	1596
Imtecc (Port Call only)	24
Fugro TSM	4320
Other (Harmony)	6912
Total	660720

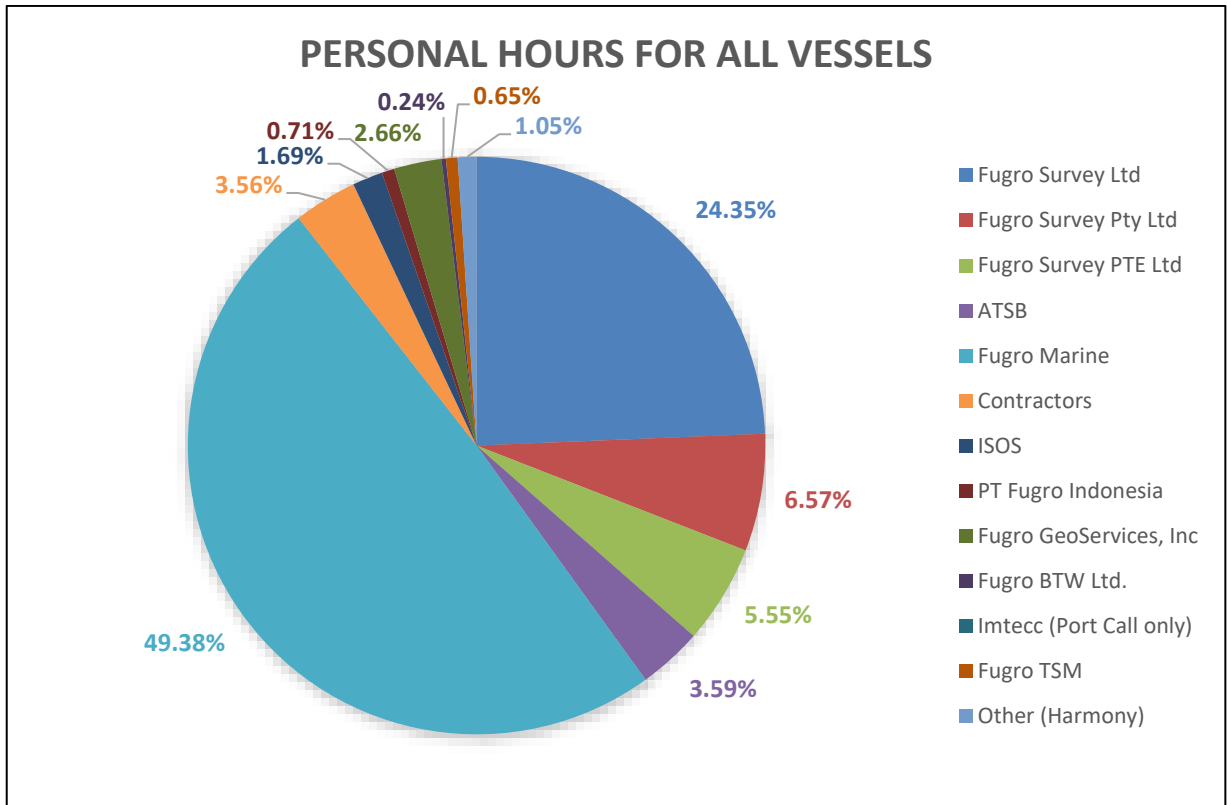


Figure 4.26: Personal hours all vessels

4.8 Equipment – Deep Tow and AUV

The Deep Tow system onboard the Fugro Equator is shown in Table 4.4.

Table 4.4: 'Spero' Deep Tow Sensors

Acoustic Navigation	
System	Hydroacoustic Aided Inertial Navigation (HAIN)
USBL	Kongsberg HiPAP 101, cNODE Maxi Transponder
Inertial measurement unit	Teledyne CDL MiniRLG
Doppler velocity log	RDI Teledyne Workhorse 300 kHz
Geophysical Sensors	
Multibeam	EM2040 200kHz
Sidescan sonar	EdgeTech Chirp FS 75 kHz and 410 kHz
Sub-bottom profiler	EdgeTech 2200-M, FS Chirp 1 kHz – 10 kHz
Communications	
Emergency communication system	Xeos Iridium Micro Beacon

Additional Sensors	
Speed of sound	Valeport Midas Bathypack
Altimeter	Valeport Midas Bathypack
HD camera	Kongsberg OE14-408-055 Camera
Hydrocarbon detection system	HydroC Subsea Fluorometer

The Deep Tow system onboard the Fugro Discovery is shown in Table 4.5.

Table 4.5: 'Dragon' DT-1 and 'Intrepid' DT-2 Sensors

Acoustic Navigation	Deep Tow-1	Deep Tow-2
System	Hydroacoustic Aided Inertial Navigation (HAIN)	
USBL	Kongsberg HiPAP 101, cNODE Maxi Transponder	
Inertial measurement unit	Teledyne CDL MiniRLG2	
Doppler velocity log	RDI Teledyne Workhorse	
Geophysical Sensors		
Multibeam	EM2040 200 kHz	
Sidescan sonar	Edgetech chirp FS 75 kHz and 410 kHz	
Sub-bottom profiler	Edgetech 2200-M, FS chirp 1 kHz to 10 kHz	
Communications		
Emergency communication system	Xeos Iridium Micro Beacon	Metocean AS-900A
Flashers	-	Metocean ST-400A
Additional Sensors		
Speed of sound	Valeport Midas Bathypack	
Altimeter	Valeport VA500 Altimeter	
HD camera	Kongsberg OE14-502-055 Camera	Kongsberg OE14-408-055 Camera
Hydrocarbon detection system	HydroC Subsea Fluorometer	

The systems onboard the Hugin Echo Surveyor 7 1000 AUV is shown in Table 4.6.

Table 4.6: Hugin ES7 1000 AUV

Acoustic Navigation	
System	Hydroacoustic Aided Inertial Navigation
USBL	Kongsberg HiPAP 501 system
Inertial measurement unit	Honeywell HG9900 inertial navigation system
Doppler velocity log	RDI Teledyne workhorse 300 kHz
Geophysical Sensors	
Multibeam	EM2040 200 kHz
Sidescan sonar	EdgeTech2400 75/410 kHz chirp
Sub-bottom profiler	EdgeTech 2200-DW 2 kHz – 16 kHz
Communications	
Emergency communication system	Xeos Iridium Micro Beacon
Additional Sensors	
Speed of sound	Valeport Midas Bathypack
Altimeter	Kongsberg Mesotech 1007 200 kHz Digital Altimeter
HD camera	Kongsberg NEO 11 megapixel 35 mm monochrome +
Hydrocarbon detection system	HydroC Subsea Fluorometer



4.9 MBES Coverage

The total area covered by search was 728,243 km². This figure is made up of Reconnaissance MBES data, while on weather standby, all transit data gathered while the vessels transited to and from the five ports of call, and while the Fugro Equator transited to and from Singapore when mobilising and demobilising for the search. To put this in perspective Table 4.7 gives comparable sizes of countries and states by area.

Table 4.7: Total Bathymetric Coverage Compared to Countries and States

MBES Coverage [728,243 km ²]		
Country/State ¹	Area [km ²]	Total Coverage Compared to Country/State
New Zealand	270,467	x 2.69
Australia	7,692,024	x 0.09
Malaysia – East and West	330,803	x 2.20
Chile	756,102	x 0.96
France	640,679	x 1.14
United Kingdom	242,495	x 3.00
Netherlands	41,850	x 17.40
Texas	695,662	x 1.05

¹ Figures derived from Wikipedia

For the Reconnaissance Bathymetric Survey a total of 277,082 km² was covered. To put this in perspective Table 4.8 gives comparable sizes of countries and States by area.

Table 4.8: Reconnaissance Bathymetric Coverage Compared to Countries and States

Reconnaissance MBES coverage [277,082 km ²]		
Country/State ¹	Area [km ²]	Total Coverage Compared to Country/State
New Zealand	270,467	x 1.02
Australia	7,692,024	x 0.04
Malaysia – East and West	330,803	x 0.84
Laos	236,800	x 1.17
United Kingdom	242,495	x 1.14
Netherlands	41,850	x 6.62
Minnesota	225,163	x 1.23

The maximum depth recorded was 6950 m during transit to site, over the Diamantina Fracture Zone. Figure 4.277 shows a cross-section through this deep transit data and a rapid 3165 m change in depth over 10 kms.

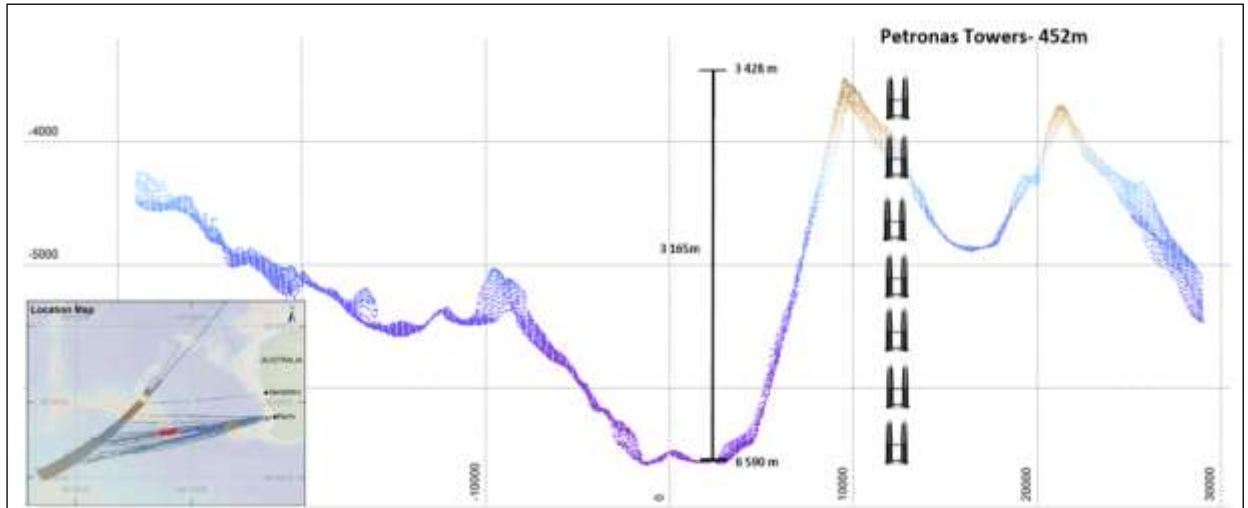


Figure 4.27: Cross-section through Diamantina Fracture Zone

The Reconnaissance Bathymetric Survey ranged in depths from 623 m to 5525 m.

Table 4.9 and Figure 4.28 show the variation in depths found within the search site. Both the table and the figure illustrate just how deep the majority of the search site was – 72 % of the area was deeper than 3500 m.

Table 4.9: Depth Range Histogram

Depth Range [m]	Depth Range [%]
500 – 1000	0.04
1000 – 1500	1.02
1500 – 2000	2.89
2000 – 2500	5.14
2500 – 3000	6.34
3000 – 3500	12.42
3500 – 4000	41.21
4000 – 4500	24.95
4500 – 5000	5.63
>5000	0.35

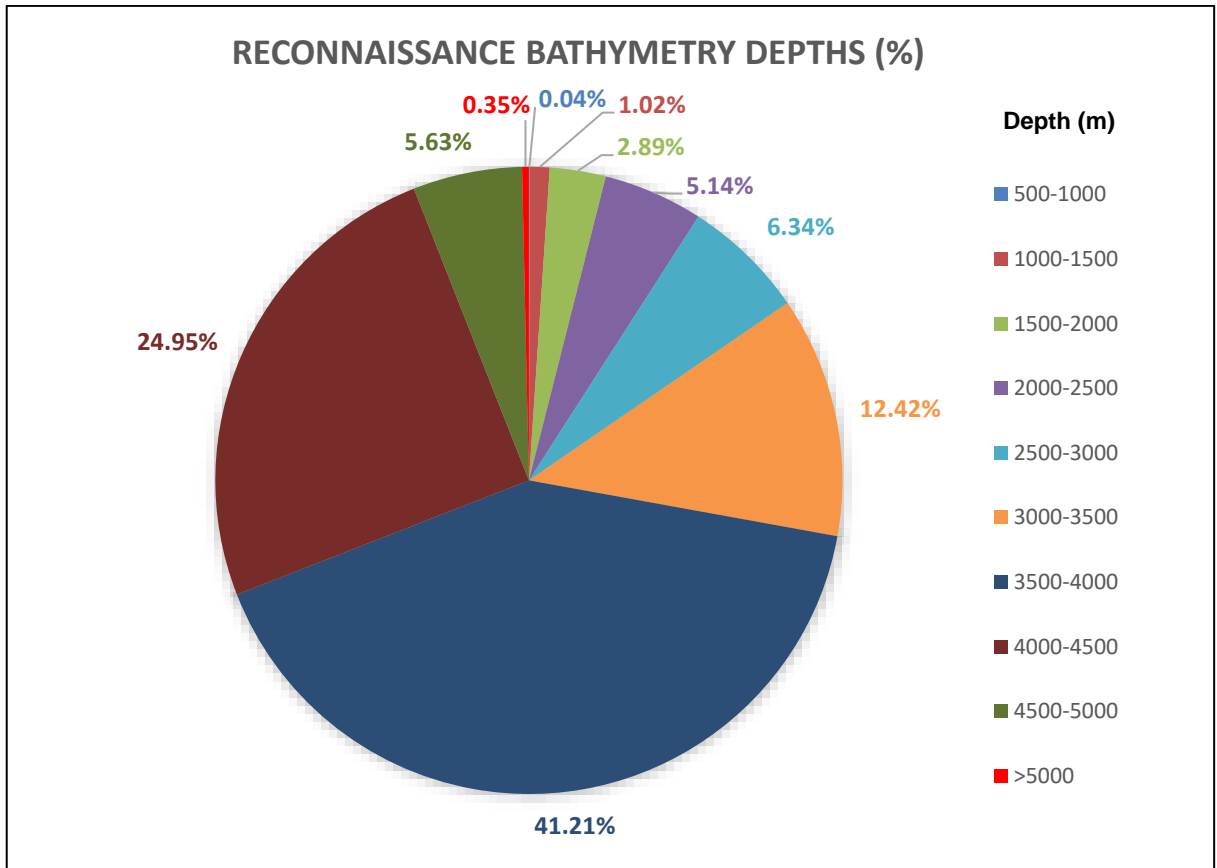


Figure 4.28: Reconnaissance bathymetric survey by depths (%)

4.10 Extreme Sea Condition

Sea state on site was the predominant factor in weather downtime during the survey. Launch or recovery of either the Deep Tow or AUV was determined by sea state, and planning for conditions when it was possible to recover and launch meant that weather forecasts were crucial.

During one whole swing of the Equator Deep Tow survey, Swing 12, between 6 May and 15 June 2015, the weather was so bad that the Deep Tow was unable to be launched at all.

The most extreme sea state measured by any of the vessels was recorded on the Fugro Equator on 13 July 2016, and measured at 23.99 m in height, from peak to trough over a period of 8 to 9 seconds. The heave was calculated from a motion sensor located above the MBES and tracked the actual movement of the boat from that position not the actual swell height, which could have been higher or lower than this. The graph of this particular heave is shown in Figure 4.29.

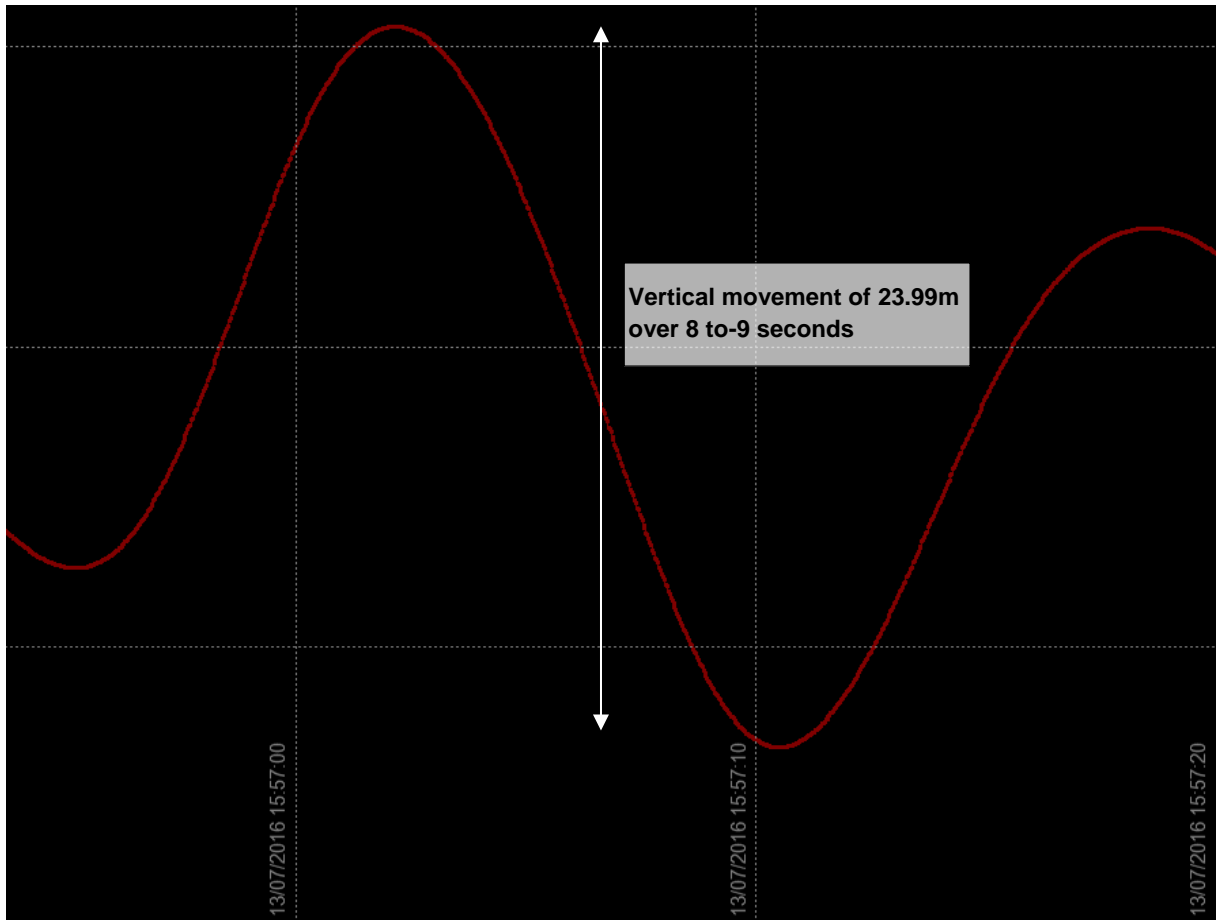


Figure 4.29: Maximum vessel heave recorded during the survey

4.11 Time Spent On Line Turns

Due to the extensive cable out for the Deep Tow survey, up to 9.5 km, depending on depth of the seabed, the vessel needed to go well beyond the end point of a survey line and ensure there was enough run in to the start of lines to enable the Deep Tow to get on line. This often meant elevating the Deep Tow to a safe height above the seafloor by pulling in cable in areas where there was no Reconnaissance Survey data. It also meant that there were more kilometres involved in line turns that there was cable out to the Deep Tow. Consequently line turns were very time consuming averaging, for instance, 10.2 hours over 60 Deep Tow line turns made by the Fugro Equator from Swing 1 through to Swing 15.

There are many factors that can determine the duration of a turn including; the difference between end KP and start KP between lines, the cross-track distance between lines, water depth, type of turn, equipment issues and weather.

4.12 Fuel Consumption

In total 9268 m³ was used by all five Fugro vessels during the survey, as set out in Table 4.10.

Table 4.10: Fuel Used by Each Vessel During Each Phase

Vessel	Phase (Fugro Job #)	Fuel [m ³]
Fugro Equator	Reconnaissance (GP1483)	988.6
Fugro Discovery	Deep Tow (GP1500-1)	2890.3
Fugro Equator	Deep Tow (GP1500-2)	3295.6
Southern Supporter	AUV (GP1500-5)	644.8
Havilla Harmony	AUV (GP1500-6)	1044.0
Fugro Equator	AUV (GP1500-6)	404.7
Total		9268.0

The cumulative breakdown of fuel consumption for each vessel for each swing is shown in Figure 4.30. (These figures do not include fuel figures to and from ports prior to mobilisation and after demobilisation).

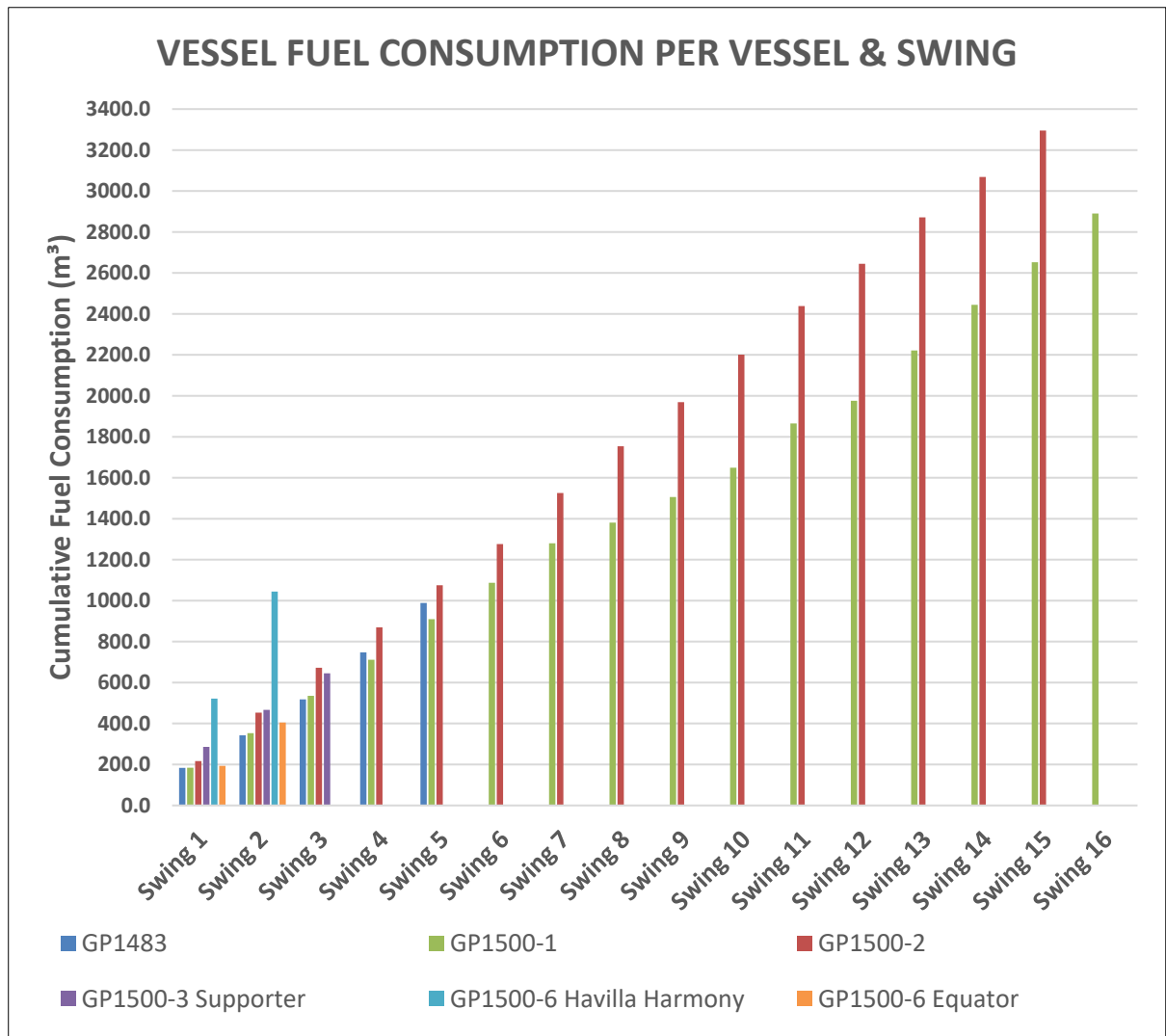


Figure 4.30: Cumulative fuel consumption for each vessel for each swing



5. SURVEY PARAMETERS

5.1 Geodetic and Projection Parameters

The search area covered Blocks 12 to 21 which traversed two projected Universal Transverse Mercator (UTM) Zones – 45 S (CM 87 °E) to 46 S (CM 93 °E). In addition the Fugro Equator was tasked to carry out Reconnaissance Surveys between Block 12 in the south to Block 7 in the north, adding another UTM Zones – 47 S (CM 99 °E). Having to log data over three projected coordinate zones was logistically untenable as it would have meant changing UTM zones at the UTM boundary whilst still surveying. As the projected coordinates were not a crucial issue in that real positions could be related to any coordinate system it was decided to adopt the westernmost Zone – 45 S – throughout. This had the advantage of never having negative eastings and the vessels would not have the problems associated with changing projections during a survey line.

The geodetic parameters used during this project are shown in Table 5.1.

Table 5.1: Project Geodetic and Projection Parameters

Global Navigation Satellite System (GNSS) Geodetic Parameters 1)		
Datum:	International Terrestrial Reference Frame 2008	
Ellipsoid:	Geodetic Reference System 1980 (GRS80)	
Semi-major Axis:	a = 6 378 137.000 m	
Inverse Flattening:	$1/f = 298.257\ 223\ 101$	
Local Datum Geodetic Parameters 2)		
Datum:	World Geodetic System 1984 (WGS84)	
Ellipsoid:	WGS84	
Semi-major Axis:	a = 6 378 137.000 m	
Inverse Flattening:	$1/f = 298.257\ 223\ 563$	
Datum Transformation Parameters 3) from ITRF2008 to GDA94		
Shift dX: 0.00000 m	Rotation rX: 0.00000arcsec	Scale Factor: 0.00000000 ppm
Shift dY: 0.00000 m	Rotation rY: 0.00000arcsec	
Shift dZ: 0.00000 m	Rotation rZ: 0.00000arcsec	
Project Projection Parameters		
Map Projection:	Transverse Mercator	
Grid System:	UTM Zone 45 South	
Central Meridian:	87° East	
Latitude of Origin:	0° (Equator)	
False Easting:	500 000 m	
False Northing:	10 000 000 m	
Scale Factor on Central Meridian:	0.9996	
Units:	Metres	
Notes:		
1. The geodetic datum of Fugro's global GNSS correction data is ITRF2008.		
2. Source: Client and Fugro.		
3. WGS84 has been refined on several occasions since its inception, the most recent update (G1762) aligns WGS84 with ITRF with an accuracy better than one cm-per-component, resulting in an overall difference of less than one cm.		

5.2 Vertical Control

Bathymetry data has not been tidally corrected since reducing water depths of between 2500 m and 4600 m to a particular datum was considered to be academic in terms of the purpose of this survey.

6. SURVEY EQUIPMENT, VESSEL AND PERSONNEL

6.1 Vessels

6.1.1 Fugro Equator

The survey vessel which was in the field longest was the Fugro Equator (Figure 6.1). The vessel is managed by Fugro Marine Services (FMS) and was built in 2012 specifically for survey operations. It is 65.7 m long, 14.0 m wide, with a draft of 4.2 m and can accommodate 42 people.

The vessel has a multi-role capability and can undertake pipeline and cable route surveys, high resolution seismic acquisition surveys, geotechnical surveys and environmental surveys. In addition, AUV and ROV systems can be mobilised to the vessel as required. The vessel is permanently fitted with a full suite of modern analogue and digital geophysical equipment, Fugro Starfix high precision DGNS positioning and through hull USBL for acoustic positioning. Deck equipment includes a variety of survey and oceanographic winches, port and starboard 2.5 T boom cranes and a 12.5 T hydraulic A-frame.



Figure 6.1: Fugro Equator

6.1.2 Fugro Discovery

The vessel which had the second longest duration was the Fugro Discovery (Figure 6.2). The vessel was originally built for the Norwegian Navy and is an Ice-Class vessel. It is 70 m long, 12.6 m wide, with a draft of 6.0 m and can accommodate 35 persons.



Figure 6.2: Fugro Discovery

The vessel is well appointed with a multi-role capability; ROV inspection, pipeline and cable route surveys, high resolution seismic acquisition surveys, geotechnical surveys and environmental surveys. The vessel is fitted with an auto positioning system, a full suite of modern analogue and digital geophysical equipment, and a comprehensive suite of deck equipment which includes a 16 tonne A-frame.

6.1.3 Fugro Supporter

The first Fugro vessel in the field with AUV capability was the Fugro Supporter (Figure 6.3) which carried the Echo Surveyor 7 AUV for three swings. The vessel is a 72 m multipurpose vessel owned and operated by Fugro Marine Services.



Figure 6.3: Fugro Supporter

The vessel is fitted with state-of-the-art geophysical and geotechnical equipment, this full-ocean depth vessel specialises in cable route surveys and is a versatile platform capable of deploying work class ROVs, AUVs, and both 2-D and 3-D High Resolution seismic spreads.

The vessel offers excellent deck handling facilities including a 15 tonne A-frame and 12 tonne deck crane. It has comfortable accommodations for 47 personnel with all cabins offering en-suite facilities, plus an extensive survey laboratory and client office space.

6.1.4 Havila Harmony

The second Fugro vessel in the field with AUV capability was the Havila Harmony (Figure 6.4) which carried the Echo Surveyor 7 AUV for two swings. The vessel is a 93 m multipurpose vessel owned and operated by Fugro-TSM. It can be used for construction support, ROV survey and inspection, geophysical surveys and AUV surveys.

It carries a 150 Te heave compensated crane, moonpool, helideck and extended accommodation for 86 people.



Figure 6.4: Havila Harmony

6.2 Personnel

The project extended from June 2014 to January 2017, with regular, six weekly, crew changes being conducted at the Port of Fremantle. The only exceptions were a crew change in Geraldton and two seven to eight week swings on the Havila Harmony.

The total number of Fugro personnel involved in the project was 390 from over 20 nationalities.

7. DATA HANDLING

From the beginning of the project it was identified that, due to the huge amount of data being logged each day, good data management was of paramount importance.

The Deep Tow system comprised a number of survey sensors and data is recorded in a variety of file formats. To help manage this aspect of the project a Data Management Plan was created (FDMP GP1500) as part of the project documentation.

In addition, a work instruction was developed offshore (GP1500_WI_000_General Project Data Management and Requirements) to provide a detailed description of the requirements for data logging and storage.

Figure 7.1 provides a summary of the directory structure used for data management and the raw and processed file types created from the Deep Tow vessels.

000_SPL_LOGGING	Fugro RAW logging formats
001_VESSEL_NAV	Vessel Navigation(GPS; Starpack)
002_VESSEL_USBL	Vessel Realtime USBL (Cartesian)
003_DEEPTOW_NAV_Raw	Deeptow Realtime Position
004_DEEPTOW_NAV_Processed	Deeptow Processed Position (from Navlab)
005_VESSEL_SBES_Raw	Vessel Single Beam Echo Sounder (Raw)
006_VESSEL_MBES_Raw	Vessel Multi Beam Echo Sounder (Raw- *.all files)
007_VESSEL_MBES_WaterColumn	Vessel Multi Beam Echo Sounder (WaterColumn- *.wcd files)
008_DEEPTOW_MBES_Raw	Deeptow Multi Beam Echo Sounder (Raw- *.all files)
009_DEEPTOW_MBES_RawPositioned	Deeptow MBES (Processed Position Applied *_P all files)
010_DEEPTOW_MBES_XYZ_Backscatter	Deeptow MBES (Processed XYZ and Backscatter files)
011_DEEPTOW_MBES_WaterColumn	Deeptow Multi Beam Echo Sounder Watercolumn (Raw- *.wcd files)
012_VESSEL_SBP_Raw	Vessel Sub-Bottom Profiler (Raw -*.segj)
013_DEEPTOW_SBP&SSS_Raw	Deeptow Sub-Bottom Profiler & Side Scan Sonar (Raw -*.jsf)
014_DEEPTOW_SBP&SSS_RawPositioned	Deeptow SBP & SSS (Processed Position Applied -*_P jsf)
015_DEEPTOW_SSS_Processed	Deeptow Side Scan Sonar (Processed Position Applied - *_P.tif)
016_DEEPTOW_SSS_ProcessedCompressed	Deeptow SSS (Processed Position Applied - *_P.compressed.tif) - compressed file
017_DEEPTOW_SBP_Processed	Deeptow Sub-Bottom Profiler (Processed Position Applied - *_P.segj)
018_VESSEL_Delayed_Heave	Vessel Delayed Heave or iHeave
019_DEEPTOW_SNIFFER	Deeptow HydroCarbon Detector
020_VESSEL_SVP	Vessel Sound Velocity Profiles
021_DEEPTOW_SVP	Deeptow Sound Velocity Profiles
022_TIDES_MSS	Tides (Raw SPM for Rinex from Starpacks)
023_TIDES_SPM_for_RINEX	Tides (Raw MSS from Fugro MSS Tides)
024_Weather	Weather (Realtime weather condition from vessel weather station)
025_DEEPTOW_Camera	DeepTow On Board Video camera

Figure 7.1: Vessel and Deep Tow raw and processed data formats

All raw data logged onboard the vessel was backed up to a central project directory located on one of the vessel’s three data servers. The project directory was also backed up to a second data server at least once every 24 hours. To provide multiple redundancy against any potential data loss the project data was also backed up to duplicate external hard drives, with progressive backups being completed on a daily basis.

At each port call two duplicate hard drives were removed from the vessel and transferred to Fugro's Perth office for data processing and archiving. An additional hard drive containing raw data and data uploaded from the Fugro office to the ATSB during the swing was supplied to the ATSB after each port call.

All survey data relevant to the seafloor search was initially processed offshore in order to assess data quality, coverage, and preliminary feature detection. Data directly relevant to the seabed search and identification of anomalies was transmitted to Fugro's Perth based processing centre using Aspera FTP software.

8. DISTRIBUTION

A copy of this report has been distributed as follows:

Australian Transport Safety Bureau

Attn: Mr Duncan Bosworth : 1 electronic copy



APPENDIX

A. SOUND VELOCITY PROFILES



A. SOUND VELOCITY PROFILES

FUGRO SURVEY PTY LTD
SUMMARY OF SOUND VELOCITY PROFILES



CLIENT: ATSB **LOCATION: Indian Ocean**

PROJECT: MH370 **Job No. GP1483/GP1500**

GP1483 Equator

SVP No.	Time Date	Latitude [S]	Longitude [E]	Sound Velocity [m/s]		
	[UTC +8]			Min	Max	Mean
1	17:24 on 07/06/2014	08° 59' 30"	115° 05' 01"	1485.41	1537.14	1494.28
2	16:04 on 08/06/2014	09° 30' 23"	115° 03' 59"	1485.55	1538.99	1495.53
3	10:00 on 16/06/2014	26° 55' 48"	100° 36' 27"	1484.4	1526.52	1501.88
4	15:02 on 18/06/2014	28° 02' 11"	99° 50' 40"	1484.23	1525.12	1496.4
5	15:52 on 25/06/2014	29° 11' 55"	99° 15' 27"	1483.99	1522.18	1495.36
6	01:35 on 14/07/2014	30° 41' 00"	098° 21' 24"	1484.95	1521.13	1496.21
7	10:44 on 18/07/2014	30° 47' 41"	97° 46' 46"	1484.45	1518.38	1494.35
8	10:44 on 23/07/2014	31° 16' 47"	96° 42' 32"	1484.31	1513.54	1493.46
9	19:07 on 27/07/2014	31° 35' 19"	97° 09' 41"	1484.56	1515.12	1494.4
10	19:07 on 01/08/2014	31° 57' 19"	95° 58' 21"	1484.12	1514.2	1492.58
11	12:58 on 17/08/2014	31° 43' 57"	97° 15' 16"	1485.54	1514.11	1491.48
12	15:36 on 23/08/2014	32° 09' 53"	96° 16' 13"	1484.76	1512.97	1492.59
13	20:47 on 26/08/2014	32° 41' 06"	95° 16' 57"	1484.17	1509.07	1494.65
14	16:16 on 01/09/2014	34° 50' 43"	93° 29' 07"	1484.59	1523.95	1500.72
15	11:46 on 09/09/2014	33° 27' 50"	94° 47' 27"	1485.71	1524.53	1501.21
16	08:29 on 23/09/2014	32° 41' 52"	95° 23' 38"	1484.84	1523.04	1500.31
17	04:36 on 29/09/2014	38° 18' 34"	87° 26' 59"	1486.16	1514.37	1497.98
18	16:28 on 01/10/2014	34° 54' 09"	92° 41' 05"	1484.5	1527.11	1501.35
19	18:45 on 08/10/2014	36° 45' 06"	90° 13' 47"	1485.27	1518.07	1498.63
21	15:52 on 19/10/2014	36° 03' 52"	91° 44' 06"	1485.57	1526.92	1501.55
22	17:39 on 23/10/2014	35° 13' 21"	93° 03' 56"	1484.63	1522.04	1499.79
Trial	0:54 on 06/11/2014	32° 31' 10"	114° 42' 25"	1484.28	1522.87	1501.23
24	04:42 on 21/11/2014	32° 44' 03"	95° 23' 54"	1484.31	1523.79	1501.38
25	13:56 on 24/11/2014	35° 16' 13"	93° 07' 13"	1485.15	1509.06	1493.02
26	14:00 on 27/11/2014	39° 03' 26"	86° 49' 26"	1484.39	1514.18	1496.65
27	10:05 on 04/12/2014	37° 17' 03"	90° 23' 12"	1484.59	1505.7	1492.44
28	04:00 on 09/12/2014	33° 02' 53"	95° 51' 20"	1485	1515.08	1494.04
29	16:00 on 16/12/2014	35° 33' 52"	93° 08' 19"	1485.4	1506.6	1493.45

GP1500-1 Discovery

SVP No.	Time Date	Latitude [S]	Longitude [E]	Sound Velocity [m/s]		
	[UTC +8]			Min	Max	Mean
1	07:25 on 13/10/2014	32° 35' 03"	114° 42' 04"	1495.41	1521.98	1508.93
2	09:16 on 22/10/2014	34° 49' 43"	93° 5' 25.4"	1484.26	1528.29	1512.82
3	00:00 on 17/12/2014	37° 16' 17"	89° 44' 32"	1484.4	1669	1495.84
4	17:30 on 15/01/2015	34° 57' 18"	93° 10' 44"	1484.74	1524.02	1499.95
5	17:30 on 31/01/2015	39° 08' 12"	86° 31' 33.3"	1484.94	1514.5	1497.33
6	00:00 on 25/02/2015	37° 37' 22"	89° 15' 32"	1485.93	1518.12	1500.7

FUGRO SURVEY PTY LTD
SUMMARY OF SOUND VELOCITY PROFILES



CLIENT: ATSB		LOCATION: Indian Ocean				
PROJECT: MH370				Job No.	GP1483/GP1500	
7	02:45 on 03/04/2015	32° 30' 55"	114° 44' 09"	1488.76	1530.25	1510.78
8	08:30 on 10/04/2015	37° 38' 13"	88° 37' 54"	1485.7	1517.77	1502.67
9	22:03 on 21/05/2015	35° 03' 29"	92° 20' 31"	1497.74	1519.53	1507.31
10	13:43 on 07/05/2015	34° 53' 51"	92° 21' 14"	1498.58	1507.15	1501.38
11	08:42 on 03/08/2015	32° 31' 07"	114° 42' 35"	1502.74	1524.85	1507.93
12	00:20 on 02/08/2015	34° 54' 38"	92° 48' 08"	1483.95	1528.56	1501.51
13	09:00 on 29/08/2015	34° 58' 51"	92° 39' 41"	1484.22	1529.43	1501.98
14	07:25 on 21/09/2015	35° 11' 07"	93° 08' 53"	1484.58	1526.92	1508.59
15	07:25 on 22/09/2015	35° 11' 07"	93° 08' 53"	1481.69	1523.33	1501.12
16	00:32 on 05/10/2015	34° 47' 38"	93° 36' 25"	1484.94	1533.03	1503.87
17	23:00 on 30/10/2015	32° 27' 46"	114° 44' 29"	1491.02	1521.01	1510.29
18	03:30 on 14/11/2015	36° 11' 02"	92° 17' 04"	1485.07	1558.2	1498.45
19	16:30 on 22/12/2015	38° 58' 00"	86° 48' 46"	1485.75	1537.71	1501.48
20	12:00 on 14/01/2016	32° 25' 39"	114° 35' 24"	1486.7	1528.08	1502.81
21	12:00 on 20/01/2016	37° 43' 25"	89° 14' 33"	1484.53	1519.3	1515.27
22	04:00 on 08/02/2016	37° 40' 15"	89° 37' 31"	1484.81	1522.1	1499.88
23	12:00 on 25/02/2016	37° 48' 36"	89° 07' 11"	1484.42	1517.99	1498.35
24	07:00 on 12/04/2016	37° 13' 54"	91° 08' 15"	1484.94	1533.03	1503.87
25	19:23 on 06/06/2016	35° 34' 03"	91° 23' 11"	1485.61	1517.32	1499.73

GP1500-2 Discovery

SVP No.	Time Date	Latitude [S]	Longitude [E]	Sound Velocity [m/s]		
	[UTC +8]			Min	Max	Mean
3	18:45 on 15/01/2015	35° 06' 39"	92° 42' 49"	1485.81	1519.99	1494.64
4	14:09 on 18/01/2015	36° 11' 27"	91° 13' 05"	1485.21	1519.02	1500.48
5	22:19 on 20/01/2015	36° 21' 17"	90° 57' 29"	1485.41	1517	1497.95
6	02:49 on 01/02/2015	35° 18' 34"	92° 23' 19"	1485.23	1519.77	1498.75
7	01:17 on 05/02/2015	35° 03' 29"	92° 20' 31"	1484.7	1518.29	1498.95
8	14:13 on 10/02/2015	38° 50' 03"	86° 37' 57"	1485.21	1514.96	1497.03
9	09:07 on 27/02/2015	37° 04' 46"	90° 15' 15"	1485.13	1514.93	1497.47
10	09:15 on 14/03/2015	39° 12' 00"	86° 36' 08"	1484.59	1512.56	1495.99
11	19:22 on 16/03/2015	39° 14' 49"	86° 33' 08"	1485.54	1511.39	1497.05
12	15:19 on 23/03/2015	39° 15' 54"	86° 35' 19"	1485.71	1511.64	1496.87
13	09:30 on 29/03/2015	38° 42' 16"	87° 42' 16"	1484.94	1520.18	1495.24
14	11:25 on 16/04/2015	38° 15' 48"	88° 29' 36"	1485.56	1509.97	1498.04
15	20:00 on 28/05/2015	39° 14' 36"	86° 32' 48"	1485.65	1509.97	1496.09
16	12:30 on 30/05/2015	39° 01' 05"	87° 21' 45"	1485.83	1512.82	1498.46
17	15:30 on 06/06/2015	38° 22' 21"	87° 26' 54"	1485.37	1512.08	1496.4
18	18:44 on 11/06/2015	39° 22' 30"	86° 44' 10"	1484.52	1510.62	1496.51
19	14:06 on 14/06/2015	37° 33' 12"	89° 59' 01"	1484.23	1515.63	1497.63
20	22:46 on 17/06/2015	37° 25' 13"	90° 11' 25"	1484.05	1514.35	1497.28

FUGRO SURVEY PTY LTD
SUMMARY OF SOUND VELOCITY PROFILES



CLIENT: ATSB		LOCATION: Indian Ocean				
PROJECT: MH370				Job No.	GP1483/GP1500	
21	22:19 on 19/06/2015	39° 13' 51"	87° 00' 57"	1484.93	1510	1496.5
22	07:13 on 20/06/2015	39° 23' 12"	86° 48' 01"	1484.98	1510.28	1496.6
23	03:10 on 21/06/2015	38° 51' 30"	87° 46' 13"	1485.17	1508.89	1495.91
24	08:10 on 07/07/2015	36° 30' 59"	90° 16' 06"	1484.47	1518.54	1499.74
25	12:03 on 09/07/2015	35° 36' 51"	91° 36' 23"	1485.12	1515.82	1498.52
26	02:12 on 11/07/2015	34° 41' 54"	92° 52' 19"	1483.43	1522.13	1501.11
27	02:52 on 14/07/2015	37° 18' 42"	90° 27' 46"	1483.92	1515.07	1496.8
28	04:21 on 18/07/2015	39° 53' 45"	85° 45' 50"	1487.12	1511.51	1506.01
29	00:29 on 22/07/2015	37° 28' 13"	90° 14' 33"	1484.17	1512.96	1496.97
30	08:57 on 22/07/2015	37° 20' 22"	90° 29' 02"	1483.84	1518.29	1498.25
31	02:45 on 26/07/2015	39° 48' 47"	85° 58' 29"	1484.61	1509.68	1496.31
32	02:29 on 30/07/2015	37° 32' 37"	90° 18' 43"	1484.18	1515.85	1498.16
33	11:27 on 30/07/2015	37° 18' 03"	90° 28' 38"	1484.06	1502.57	1492.94
34	16:53 on 31/07/2015	37° 09' 13"	88° 56' 37"	1484.13	1524.13	1500.98
35	09:14 on 19/08/2015	35° 00' 43"	93° 13' 34"	1480.97	1525.8	1498.74
36	23:32 on 04/09/2015	35° 24' 00"	92° 50' 50"	1480.43	1519.37	1497.66
38	08:12 on 12/09/2015	35° 39' 49"	92° 29' 32"	1481.7	1522.43	1499.11
39	11:53 on 17/09/2015	35° 36' 17"	92° 36' 05"	1480.53	1519.04	1497.25
40	12:03 on 05/10/2015	34° 21' 03"	93° 34' 12"	1485.12	1526.98	1501.48
41	12:34 on 06/10/2015	34° 58' 07"	92° 45' 29"	1490.33	1525.44	1506.53
42	14:13 on 07/10/2015	35° 13' 50"	92° 23' 03"	1481.37	1529.72	1500.25
43	19:41 on 08/10/2015	35° 25' 28"	93° 25' 52"	1485.06	1514.21	1496.91
44	23:07 on 09/10/2015	34° 56' 56"	92° 43' 50"	1481.93	1523.06	1498.13
45	19:46 on 12/10/2015	35° 07' 21"	92° 20' 27"	1482.35	1524.46	1500.7
46	19:06 on 26/10/2015	38° 34' 26"	86° 33' 56"	1485	1514.52	1498.24
47	07:37 on 17/11/2015	37° 26' 42"	90° 32' 10"	1484.58	1516.14	1498.05
48	02:04 on 21/11/2015	39° 53' 41"	86° 04' 06"	1483.06	1508.91	1494.57
49	22:05 on 26/11/2015	38° 43' 54"	86° 51' 35"	1485.03	1511.77	1497.1
50	04:21 on 09/12/2015	39° 31' 45"	85° 30' 33"	1482.91	1510.41	1495.17
51	08:37 on 10/12/2015	40° 06' 54"	85° 45' 16"	1483.07	1511.48	1497.31
52	08:16 on 13/12/2015	38° 04' 45"	89° 38' 41"	1486.19	1514.11	1499.04
53	18:27 on 06/01/2016	35° 44' 10"	91° 36' 01"	1484.38	1522.37	1498.11
54	19:00 on 16/01/2016	39° 42' 50"	85° 47' 40"	1483.11	1525.18	1499.37
55	06:26 on 27/01/2016	39° 58' 30"	86° 07' 20"	1482.95	1512.73	1494.19
56	08:59 on 16/02/2016	37° 27' 08"	90° 34' 52"	1484.21	1516.72	1497.85
57	16:11 on 17/03/2016	37° 30' 50"	90° 31' 01"	1485.92	1520.32	1499.86
58	01:19 on 04/04/2016	37° 11' 26"	88° 59' 27"	1484.54	1524.1	1499.81
59	08:51 on 19/04/2016	38° 39' 23"	86° 27' 29"	1483.51	1505.53	1492.43
60	01:59 on 22/04/2016	38° 21' 46"	86° 58' 06"	1480.64	1516.89	1496.39
61	21:52 on 28/04/2016	35° 43' 25"	91° 06' 16"	1485	1510.9	1496.52
62	20:55 on 21/06/2016	35° 43' 47"	91° 07' 30"	1487.67	1515.43	1501.2

FUGRO SURVEY PTY LTD
SUMMARY OF SOUND VELOCITY PROFILES



CLIENT: ATSB		LOCATION: Indian Ocean				
PROJECT: MH370				Job No.	GP1483/GP1500	
63	23:47 on 07/08/2016	35° 44' 07"	91° 10' 24"	1486.48	1517.42	1499.34
64	20:00 on 10/08/2016	37° 43' 06"	87° 57' 13"	1486.48	1515.19	1498.19
65	08:50 on 17/08/2016	37° 09' 15"	89° 05' 44"	1486.49	1517.01	1499.25
66	13:56 on 19/08/2016	35° 36' 05"	91° 28' 58"	1484.39	1515.29	1497.13
67	14:47 on 21/08/2016	35° 05' 38"	92° 56' 38"	1484.99	1518.62	1498.71
68	08:02 on 26/08/2016	37° 34' 45"	89° 06' 43"	1486.43	1513.21	1498.08
69	07:37 on 28/08/2016	36° 12' 39"	91° 17' 11"	1485.44	1519.02	1499.18
70	16:30 on 29/08/2016	34° 14' 23"	93° 55' 38"	1486.24	1526.83	1502.58
71	23:10 on 01/09/2016	33° 24' 08"	94° 55' 24"	1485.43	1524.06	1500.79
72	14:45 on 15/09/2016	37° 51' 48"	88° 40' 43"	1484.83	1513.64	1498.666

GP1500-5 Supporter

SVP No.	Time Date	Latitude [S]	Longitude [E]	Sound Velocity [m/s]		
	[UTC +8]			Min	Max	Mean
1	17:08 on 05/01/2015	08° 56' 59.6"	115° 10' 02.6"	1495.28	1543.68	1516.31
2	08:25 on 07/01/2015	08° 57' 26.58"	115° 11' 3.48"	1491.29	1543.5	1512.28
3	02:30 on 08/01/2015	08° 59' 12"	115° 08' 25"	1485.36	1543.27	1498.37
4	10:40 on 10/01/2015	08° 56' 38.21"	115° 10' 38.35"	1497.24	1543.69	1521.24
5	00:34 on 12/01/2015	08° 58' 57"	115° 08' 25"	1484.41	1543.45	1498.14
6	12:01 on 13/01/2015	09° 49' 09"	114° 48' 13"	1486.32	1543.75	1497
7	07:01 on 18/02/2015	36° 48' 33"	90° 18' 05"	1485.61	1514.13	1497.6
8	11:50 on 22/02/2015	32° 28' 22"	114° 44' 06"	1485.17	1515.54	1497.97
9	08:50 on 28/02/2015	35° 09' 29"	92° 17' 48"	1488.77	1529.62	1503.76
10	03:30 on 11/03/2015	35°38' 42"	92° 05' 00"	1485.72	1523.42	1499.24
11	16:25 on 18/03/2015	36°48' 33"	90°18'04"	1485.96	1523.44	1502.82
12	18:29 on 27/03/2015	37°46' 32"	88°48'56"	1486.34	1520.18	1507.64
13	16:25 on 01/04/2015	38°07' 02"	88°00'53"	1486.29	1526.94	1510.94
14	07:59 on 11/04/2015	32° 30' 12"	114° 42' 55"	1482.76	1530.85	1509.18
15	10:49 on 24/04/2015	37°37' 32"	88°36'51"	1486.85	1527.83	1510.01
16	16:15 on 30/04/2015	32° 56' 42"	95° 25' 30"	1483.57	1528.7	1502.3
17	12:53 on 02/05/2015	33° 32' 16"	95° 04' 26"	1481.02	1528.01	1502.22
18	01:59 on 04/04/2015	34° 06' 52"	93° 57' 54"	1481.02	1528.01	1502.22
19	14:08 on 05/04/2015	34° 06' 54"	93° 57' 53"	1485.56	1529.79	1509.69
20	01:56 on 06/05/2015	35° 05' 37"	92° 57' 51"	1486.25	1529.8	1508.75
21	16:12 on 08/05/2015	37° 38' 51"	89° 25' 44"	1487.09	1521.35	1501.62

GP1500-6 Havila Harmony

SVP No.	Time Date	Latitude [S]	Longitude [E]	Sound Velocity [m/s]		
	[UTC +8]			Min	Max	Mean
1	12:00 on 07/12/2015	37 20'34.595"	89 13'45.937"	1485.96	1514.28	1497.19
2	10:43 on 20/12/2015	38 11'16.789"	88 54'50.508"	1485.96	1514.28	1497.19

FUGRO SURVEY PTY LTD
SUMMARY OF SOUND VELOCITY PROFILES



CLIENT: ATSB		LOCATION: Indian Ocean				
PROJECT: MH370				Job No.	GP1483/GP1500	
3	11:00 on 27/12/2015	38 11'16.789"	88 54'50.508"	1486.16	1512.8	1495.9
4	02:40 on 02/01/2016	38 16'56.348"	87 38'49.186"	1486.52	1503.37	1496.71
GP1500-6 Equator						
SVP No.	Time Date	Latitude [S]	Longitude [E]	Sound Velocity [m/s]		
	[UTC +8]			Min	Max	Mean
1	04:47 on 02/11/2016	32° 53' 55"	95° 28' 02"	1476.63	1510.7	1495.71
2	23:40 on 02/11/2016	32° 53' 55"	95° 28' 02"	1476.31	1514.84	1498.15
3	19:17 on 04/11/2016	33° 07' 47"	95° 10' 45"	1477.07	1519.19	1495.68
4	19:09 on 05/11/2016	34° 12' 59"	94° 15' 27"	1483.4	1529.99	1506.08
5	04:01 on 07/11/2016	34° 24' 59"	93° 29' 04"	1485.04	529.89	504.28
6	10:41 on 08/11/2016	34° 40' 11"	93° 28' 54"	1484.82	1530.25	1505.97
7	11:03 on 09/11/2016	34° 32' 21"	93° 09' 18"	1485.42	1530.51	1504.86
8	04:12 on 10/11/2016	34° 44' 58"	93° 01' 51"	1505.57	1485.46	1530.61
9	06:25 on 11/11/2016	34° 58' 04"	93° 28' 27"	1485.44	1530.05	1504.99
10	08:36 on 12/11/2016	34° 59' 03"	92° 48' 26"	1486.19	1530.47	1504.85
11	16:38 on 15/11/2016	34° 47' 21"	92° 48' 05"	1485.9	1530.06	1505.95
12	06:01 on 19/11/2016	35° 17' 46"	92° 38' 53"	1486.42	1530.59	1508.96
13	11:14 on 20/11/2016	35° 14' 37"	93° 00' 11"	1486.05	1529.8	1506.28
14	17:39 on 21/11/2016	35° 21' 57"	92° 43' 56"	1486.19	1527.68	1507.28
15	22:18 on 22/11/2016	35° 40' 11"	92° 32' 40"	1486.52	1522.75	1503.16
16	11:26 on 23/11/2016	35° 40' 08"	92° 33' 01"	1486.52	1527	1505.67
17	16:14 on 24/11/2016	35° 50' 47"	92° 07' 34"	1486.14	1526.76	1505.2
18	05:23 on 26/11/2016	35° 28' 36"	92° 11' 36"	1485.86	1529.88	1507.27
19	10:23 on 27/11/2016	35° 14' 48"	92° 09' 57"	1486.02	1530.98	1506.97
20	15:24 on 28/11/2016	35° 30' 10"	91° 41' 31"	1485.54	1529.79	1504.85
21	01:27 on 30/11/2016	35° 51' 24"	91° 35' 18"	1485.58	1527.89	1507.49
22	12:32 on 01/12/2016	35° 39' 28"	91° 52' 21"	1485.32	1519.51	1500.29
23	16:34 on 02/12/2016	35° 57' 56"	91° 53' 33"	1486.1	1523.15	1503.51
24	20:51 on 03/12/2016	36° 04' 40"	91° 39' 16"	1486.6	1526.6	1503.94
25	23:23 on 04/12/2016	36° 05' 52"	91° 00' 37"	1486.24	1525.64	1504.47
26	14:10 on 19/12/2016	36° 34' 09"	90° 33' 11"	1486.24	1512.87	1497.13
27	07:29 on 24/12/2016	36° 18' 19"	90° 13' 36"	1486.38	1524.98	1504.89
28	15:23 on 25/12/2016	36° 43' 32"	90° 12' 36"	1486.05	1511.21	1497.45
29	16:49 on 26/12/2016	37° 04' 05"	90° 08' 35"	1485.79	1524.17	1505.49
30	19:27 on 27/12/2016	37° 06' 40"	89° 52' 27"	1477.38	1525.79	1504.38
31	22:10 on 28/12/2016	36° 56' 58"	89° 37' 58"	1485.84	1524.78	1506.2
32	00:04 on 30/12/2016	37° 23' 52"	89° 38' 56"	1485.74	1524.35	1504.33
33	01:44 on 31/12/2016	37° 19' 06"	89° 15' 39"	1485.85	1526.38	1505.54
34	08:19 on 01/01/2017	37° 52' 00"	89° 10' 17"	1485.8	1521.72	1502.35
35	09:47 on 02/01/2017	37° 43' 06"	88° 34' 34"	1485.45	1528.46	1510.22

FUGRO SURVEY PTY LTD
SUMMARY OF SOUND VELOCITY PROFILES



CLIENT: ATSB		LOCATION: Indian Ocean				
PROJECT: MH370				Job No.	GP1483/GP1500	
36	08:29 on 03/01/2017	38° 14' 32"	88° 01' 32"	1485.13	1524.21	1502.62
37	07:37 on 06/01/2017	35° 51' 55"	91° 09' 49"	1486.01	1516.57	1494.4
38	14:15 on 06/01/2017	35° 51' 55"	91° 09' 49"	1485.94	1529.99	1510.32
39	17:38 on 07/01/2017	34° 59' 08"	92° 19' 48"	1485.3	1530.47	1504.81
40	21:45 on 08/01/2017	35° 16' 09"	91° 56' 39"	1485.8	1529.71	1506.68
41	18:12 on 09/01/2017	34° 59' 08"	92° 19' 45"	1485.09	1530.57	1506.76
42	14:27 on 10/01/2017	34° 32' 28"	92° 56' 27"	1483.56	1530.69	1509.09
43	05:46 on 12/01/2017	34° 54' 02"	92° 29' 48"	1485.07	1530.21	1507.88
44	10:23 on 16/01/2017	34° 50' 05"	92° 35' 01"	1484.28	1530.21	1506.08

Appendix E – Phoenix International Holdings Inc. Malaysia Airlines Flight 370 (MH370) Search End of Contract Report



MALAYSIA AIRLINES FLIGHT 370 (MH370) SEARCH

END OF CONTRACT REPORT

10 May 2017

**Submitted to
AUSTRALIAN TRANSPORT SAFETY BUREAU**

**Attn: Mr. Duncan Bosworth
62 Northbourne Avenue
Canberra ACT 2601
Australia**

**By
PHOENIX INTERNATIONAL HOLDINGS, INC.**

**9301 Largo Drive
Largo, MD 20774
+1.301.341.7800
www.phnx-international.com**

TABLE OF CONTENTS

1.0	INTRODUCTION	1
2.0	BACKGROUND	1
3.0	MOBILIZATION AND ACCEPTANCE TRIALS.....	5
4.0	DEEP TOW SAS SEARCH ABOARD <i>DONG HAI JIU 101</i>	7
4.1	Swing 1.....	7
4.1.1	ProSAS Loss	8
4.1.2	ProSAS Recovery	9
4.1.3	ProSAS Repairs and Testing.....	10
4.2	Swing 2.....	10
4.3	Swing 3.....	11
4.4	Operational Stand Down	12
4.5	Swing 4.....	12
5.0	LESSONS LEARNED.....	14
5.1	Mobilization/Operation/Demobilization from a Vessel of Opportunity	14
5.1.1	Lesson Learned	14
5.2	Problem Encountered: ProSAS Umbilical Failure.....	14
5.2.1	Lesson Learned	14
5.3	Problem Encountered: ROV Load Release Shear Pin Failure	15
5.3.1	Lesson Learned	15
5.4	Problem Encountered: ProSAS-60 Cable Damage	15
5.4.1	Lesson Learned	15
5.5	Problem Encountered: Sonardyne iUSBL Failure	15
5.5.1	Lesson Learned	16
5.6	Problem Encountered: ROV Fiber Link Lost	16
5.6.1	Lesson Learned	16
6.0	CONCLUSION.....	17

1.0 INTRODUCTION

This End of Contract Report details Phoenix International Holdings, Inc. (Phoenix) operational search for Malaysia Airlines Flight 370 (MH 370) and Lessons Learned aboard the People's Republic of China (PRC) Rescue Salvage Bureau (RSB) vessel *Dong Hai Jiu 101*. Phoenix was contracted by the Commonwealth of Australia under the direction of Australian Transport Safety Bureau (ATSB) to provide deepwater towed side scan sonar and Remotely Operated Vehicle (ROV) services in support of continuing the underwater search for Malaysia Airlines Flight 370 (MH370).

The findings in this report are derived from Daily, Weekly, and Swing reports filed by the Project Manager deployed aboard *Dong Hai Jiu 101*. This End of Contract Report includes a summary of the key project events, i.e. engineering activities and vessel preparations in advance of project operations, mobilization/demobilization, operational swing reports, vessel, and lessons learned.

During the timeframe February – August 2016 Phoenix and teammate Hydrospheric Solutions, Inc. (HSI) conducted side scan sonar operations using the highly capable and technologically advanced SLH PS-60 (ProSAS-60), a 6,000 meter depth-rated synthetic aperture sonar (SAS) towed system onboard the Chinese Rescue Salvage Bureau (RSB) vessel *Dong Hai Jiu 101* (DJ101).

During the timeframe October – December 2016 Phoenix conducted Remotely Operated Vehicle (ROV) search operations using the Phoenix 6,000 meter depth-rated Remora III ROV onboard the *Dong Hai Jiu 101* (DJ101).

2.0 BACKGROUND

The Commonwealth of Australia (Commonwealth), as represented by the Australian Transport Safety Bureau (ATSB) and Phoenix International Holdings, Inc. (Phoenix) signed Contract 570-19 on 12 January 2016, for the provision of equipment and services for the search for Malaysia Airlines Flight 370 (MH370). Contract 570-19 supported the Commonwealth 's efforts to carry out seafloor search operations to localize, positively identify, map and obtain visual imaging of the wreckage of MH370 which is believed to have gone missing in the Indian Ocean on or around 08 March 2014. Objectives under the Contract were to search for, locate and identify MH370 within the defined Search Area on the sea floor.

The contract required Phoenix to provide the following key search equipment, with availability as noted in the table below:

SEARCH KEY EQUIPMENT		
Equipment	Description	Availability
ProSAS Deep Tow System	The deep tow systems comprise Key Equipment and Subsurface Equipment which includes; the towfish and its systems including SAS, MBES, the depressor, winch and wire and the towfish positioning equipment including	The ProSAS Deep Tow System will be mobilized and made available on board the Third Party Supplied Vessel in accordance with the directions of the Commonwealth Contract Authority.

	the USBL. Sonardyne positioning system.	
Remora 3 Remotely Operated Vehicle (ROV)	The ROV systems comprise Key Equipment and Subsurface Equipment which includes; the ROV and its launch and recovery system including colour video camera, winch and wire and the ROV positioning equipment including the USBL positioning system.	The Commonwealth Contract Authority may request in writing that the ROV and the Contractor will use its best endeavors to mobilize and make the ROV available on board the Third Party Supplied Vessel in accordance with the request.
Artemis Autonomous Underwater Vehicle (AUV)	The AUV systems comprise Key Equipment and Subsurface Equipment which includes; the AUV and its launch and recovery systems including SSS, MBES, black and white still photography camera, and the AUV positioning equipment.	The Commonwealth Contract Authority may request in writing that the AUV and the Contractor will use its best endeavors to mobilize and make the AUV available on board the Third Party Supplied Vessel in accordance with the request.

The People's Republic of China provided a crewed vessel *Dong Hai Jiu 101*, coordinated by the Commonwealth, as part of the search.

In advance of the contract signing, the ATSB and Phoenix participated in meetings with the Donghai Rescue Bureau/Ministry of Transport, and conducted a ship-check of the Chinese vessel *Dong Hai Jiu 101* during the period 19-20 November 2015 in Shanghai China. The ship-check was conducted on the 19th of November 2015, and follow-on meetings and briefings with the ATSB and senior level Chinese officials were conducted on the 20th of November 2015.

Meetings and discussions during this visit focused on three areas of interest, i.e. Vessel Ship-Check, Operational Considerations, and Mobilization Coordination issues/or concerns. Additional areas of interest included vessel GA drawing requirements, DP 24/7 operations and vessel ship handling, messing/berthing accommodation arrangement options, food requirements, non-smoking requirements, power supply/cable lengths and VFD location, ROV/AUV/ProSAS deck lay-out installation options, deck timber removal concerns/options, locator pole installation options, equipment stowage and data processing room options, vessel communications capabilities (512kb upload/1024Kb download), IMO/SILOS certifications, Communications (e.g. English-Chinese translation requirements), etc.

19-20 November 2015 Visit - Summary Findings

- *Dong Hai Jiu 101* was built in 2012, and was found to be very clean and well-maintained.
- The ship is a well-equipped, DP-2 towing/salvage vessel, with ~600m² total deck area (~328m² working deck area aft). Engine rooms were clean and well-lighted.
- Ship's power is adequate to support search equipment demands. China agreed to procure/install a Variable Frequency Drive (VFD) unit. Exact location of the VFD is TBD.
- Ship follows China Ship Class (CSC) rules.
- The ship does not have an A-frame, but agreed to fabricate an A-frame (20-ton capability) based on a Phoenix design and installation drawing.
- Deck area (aft deck and helicopter deck) is adequate to support installation of ProSAS, Remora III (optional), and Artemis (optional). Vessel deck area was adequate to support 10 tons/m² aft of frame 20, and approximately 6 tons/m² forward of frame 20.
- Phoenix tasking included the following:
 - A-Frame design/installation drawing (fabrication work in China).
 - Basic installation concept drawing(s).
 - Provide ATSB with ROM estimate on design/engineering services work to support mobilization effort.
 - Installation drawings/plan for CSC review and approval by surveyor. Separate installation drawings will be initiated for each system, i.e. ProSAS, Remora III, and Artemis.
 - List of computers and equipment (and power requirements) for data center room.
 - Mobilization and Demobilization cost estimate and timeline estimate to ATSB. Include engineering support (e.g. design effort, etc) in mobilization cost.
 - Stand-alone communications VSAT day-rate estimate to support corporate related message traffic.
 - Review/comment on indicative draft contract.

On 13 December 2015 Phoenix again met with the Chinese Rescue Salvage Bureau (RSB), Dong Hai Jiu 101 officers/crew, and the Shanghai Merchant Ship Design & Research Institute. Meeting participants (approximately 20-25 participants) included Mr. Wang (Deputy Director-General China Rescue Salvage/RSB), Mr. Guo (Deputy Director Rescue Bureau), Mr. Xu (Senior Engineer, RSB), Mr. Hueng (Deputy Director Rescue Bureau), Mr. Liu (Deputy Department Leader Rescue Bureau), Dong Hai Jiu 101 Captain/Chief Engineer/crew Han Qiang (Shanghai Merchant Ship Design & Research Institute), Shanghai Merchant Ship Design & Research Institute staff, and Robert Lohe and Jim Gibson (Phoenix).

13-15 December 2015 Visit - Summary Findings

- A-Frame. RSB provided a detailed engineering design status update. China purchased an existing (30 Ton) A-Frame from a commercial company. Engineering design drawing package was submitted to the CSC (vessel surveyor/classification society) for approval.
- Reviewed Power Supply System options for A-Frame and Winch
- Reviewed proposed Deck Lay-out (includes ProSAS plus Remora III ROV (option))
- Conducted Engineering Design Review, including A-Frame, locator pole, ROV platform drawing packages.
- Reviewed status of fabrication efforts, e.g. Locator Pole, ROV platform, deck risers, etc.
- A-Frame Padeyes. Phoenix provided lift padeye and towing padeye details.
- Storage Winch/Traction Winch. Phoenix provided additional details on traction winch and storage winch placement.
- Design Documentation. Phoenix provided additional engineering design documentation to include drawings and calculations.
- Locator Pole. Phoenix provided additional details on locator pole placement, fabrication, and installation.
- Van Placement. Phoenix – RSB conducted detailed discussion on placement of ProSAS/Remora III Ops and Maintenance Vans. Installation drawings will reflect the inclusion and placement of Remora III ROV Ops/Maintenance Vans.
- Equipment Foundation Elements. Phoenix – RSB reviewed details of equipment foundation elements, fabrication, and installation.
- Phoenix provided detailed presentation providing answers/or discussion points based on RSB list of clarification questions.
- RSB expressed interest in the mobilization schedule and delivery timeline for ProSAS. Phoenix took an action to provide a notional (~4 week) schedule for the delivery of ProSAS in Singapore.
- Reviewed 7 day installation/test schedule in Singapore.
- *Dong Hai Jiu 101* inspection/assessment. Conducted another detailed tour of fantail/deck areas affected by new installation plan.
- Discussed Singapore mobilization roles and responsibilities, to include work assignments and areas of responsibility, and logistics coordination, e.g. crane/welding services, etc.
- Discussed the timing on the arrival of ProSAS and arrival of *Dong Hai Jiu 101* in Singapore. Ship is reporting a projected SOA of ~17 kts during (6-day) transit to Singapore.
- Reviewed the timing on Remora III ROV platform fabrication/installation in Shanghai.
- Reviewed A-Frame static and dynamic load factors.

- Assigned Actions
 - **Rescue Salvage Bureau (RSB) Actions**
 - a. Engineering Design Drawings. The RSB was tasked to complete all engineering design fabrication and installation drawings. RSB assumed ownership and responsibility for all engineering drawing development and delivery of the final drawing package.
 - b. ROV Platform Fabrication and Installation. The RSB agreed to take an action to discuss further with Peter Foley (ATSB Program Director, Operational Search for MH370). Phoenix recommended completing the fabrication and installation of the ROV platform in Shanghai, even if the ROV was still being considered as an option. RSB completed the ROV platform fabrication design and installation drawings. Phoenix shared additional ROV platform drawings and calculations with the RSB.
 - c. The RSB was tasked to comment on Singapore Mobilization Roles/Responsibilities.
 - **Phoenix Actions**
 - a. Notional Mobilization Timeline. Phoenix was tasked to develop a notional timeline/schedule for the delivery of ProSAS to Singapore.
 - b. Engineering Design Support. Phoenix was requested to continue to provide engineering design support as required by the RSB.
 - c. Phoenix was asked to stop (as requested by Mr. Wang) all engineering design efforts and installation drawing work, to include modeling, load case studies, and fabrication and installation drawings, etc.

Phoenix met with the RSB and Shanghai Merchant Ship Design & Research Institute staff again on Tuesday, 15 December to continue the review and discussion on the drawing packages currently under development, and worked towards finalizing Singapore-based mobilization roles/responsibilities.

3.0 MOBILIZATION AND ACCEPTANCE TRIALS

Phoenix and HSI crew departed the United States on 21 January 2016 and arrived in Singapore on 23 January 2016 to begin mobilizing the *Dong Hai Jiu 101*. Mobilization of the equipment onto the vessel began on 25 January 2016 at Berth 12 in Singapore. During the mobilization period, HSI added a fourth array panel to the ProSAS system and updated the software on the system to allow operation with 4 panels per side vice the normal 3 panel configuration. The advantage of adding a fourth array panel enabled greater coverage (range scale) at the same tow speed (2 knots). The three panel array provided a 1000 meter range scale at 2 knots. The four panel array provided a 1300 meter range scale at 2 knots.

The vessel shifted to dry dock on 27 January 2016 and remained there until 29 January 2016 to have its hull cleaned, a shaft seal repaired and propeller work completed. Mobilization and equipment testing continued during this time.

Dong Hai Jiu 101 returned to Berth 12 on 29 January 2016 and completed mobilization and equipment testing on 31 January 2016 when the vessel departed for Fremantle Western Australia

During the transit to Fremantle Western Australia, the *Dong Hai Jiu 101* conducted launch and recovery practice, equipment testing, buoyancy and trim checks, INS alignment, data collection and Multibeam Echo Sounder calibration. *Dong Hai Jiu 101* arrived at Fremantle Western Australia's outer anchorage on 08 February, boarded the ATSB Data Quality Manager, and proceeded to the test range for acceptance trials.

The ProSAS-60 vehicle dove on the test range on 09 February 2016 and failed the acceptance test because of excessive noise in the data. The vessel returned to Fremantle Western Australia and moored at Berth E to take on fuel and troubleshoot the system.

Vehicle repairs and troubleshooting were completed and the *Dong Hai Jiu 101* departed for the test range on 15 February 2016. Acceptance trials were completed on 17 February 2016 and the vehicle data was accepted, however, the vehicle frame was damaged during the recovery and the vessel returned to Fremantle Western Australia, Berth E to conduct repairs on the vehicle frame.

Dong Hai Jiu 101 arrived Fremantle Western Australia on 18 February 2016 and the vehicle frame was transported to a local metal shop for repairs. The repairs were completed and the frame returned to the ship on 21 February 2016. The vessel got underway to return to the test range to insure the data was still acceptable. Trials were conducted on 21 February 2016 and the vehicle data was still of an acceptable quality.

The vessel proceeded to the Operations Area and arrived for dive operations on 25 February 2016 to begin Swing 1.

4.0 DEEP TOW SAS SEARCH ABOARD *DONG HAI JIU 101*

Phoenix International Holdings, Inc. (Phoenix) was contracted by the Commonwealth of Australia under the direction of Australian Transport Safety Bureau (ATSB) to provide deepwater towed side scan sonar services in support of continuing the underwater search for Malaysia Airlines Flight 370 (MH370). Phoenix and teammate Hydrospheric Solutions, Inc. (HSI) conducted side scan sonar operations using the highly capable and technologically advanced SLH PS-60 (ProSAS-60), a 6,000 meter depth-rated synthetic aperture sonar (SAS) towed system.

Team Phoenix mobilized aboard the Chinese Rescue Salvage Bureau (RSB) vessel *Dong Hai Jiu 101* in Singapore in late January 2016. Following a brief port call in Fremantle Western Australia, Phoenix commenced ProSAS-60 search operations in late February 2016.

Dong Hai Jiu 101 and the Phoenix/HSI crew were tasked by the ATSB to conduct a wide area search east of the 7th arc. Lines DT13A-21A_19SE thru DT13A-21A_25SE were assigned and bounded approximately between KP170 to KP355. ProSAS data was collected at the 1100m range scale to maintain at least a nominal 200m overlap, however overlap greater than 500m was consistently achieved throughout the operation.



Dong Hai Jiu 101

4.1 Swing 1

Swing 1 commenced 25 February 2016 with the first dive in the Operations Area and lasted until the *Dong Hai Jiu 101* returned to Fremantle Western Australia on 26 March 2016.

The towfish was first launched on 25 February 2016, but during descent the depth sensor failed and a recovery was conducted to change out the sensor. A second launch was conducted and the towfish began collecting data on line DT13A-21A_19SE on 26 February 2016, followed by line DT13A-21A_20SE a few days later.

During deep tow operation on line 13A-21A_21SE a fishing vessel was encountered. The vessel was on an intercept course based on the tow (search) direction. After repeated unacknowledged hails on the radio and flashing the vessel with the search light, the *Dong Hai Jiu 101* had to divert its heading slightly to avoid collision with the fishing vessel. Data collection during this encounter was not affected.

On 27 February 2016 the iUSBL transceiver experienced water intrusion and the connector pins were damaged beyond repair. The operators followed the recommendations of the manufacturer and did not use an O-ring in the connector which allowed water intrusion at depth. There were no spare connectors onboard and the operators used a layback calculation for positioning until a spare unit was received. The manufacturer later rescinded that recommendation and an O-ring was used on future operations.

On 07 March 2016 the vessel was unable to safely maintain speed and heading down line DT13A-21A_22SE due to high sea state and the ProSAS-60 was hauled back to 600 meters of cable out and laid to in the seas for a weather standby until 09 March 2016 when wide area search operations resumed on line DT13A-21A_22SE.

After completing line DT13A-21A_22SE, a decision was made to move onto line 13A-21A_24SE skipping over line DT13A-21A_23SE which would be completed after line DT13A-21A_25SE. This decision was made in an effort to maximize time on bottom collecting data and minimize time in turns and transit due to lines 24SE and 25SE being longer than line 23SE.

On 14 March 2016 the ProSAS-60 multibeam system experienced a synchronization failure which required a reboot of the system which took several minutes and caused a loss of data collection creating a 2km nadir gap. Due to this loss of data the towfish was hauled in to 300m of cable out and the vessel turned back to several kilometers before the data gap to acquire the missing data. After completing line DT13A-21A_25SE a turn was conducted onto the previously skipped line DT13A-21A_23SE to collect data along this line.

On 18 March 2016, during tow operations down line DT13A-21A_23SE, the ATSB sent an amended task request with instructions to conduct SAS imaging of shipwreck #1 at a 1300m range scale, followed by an LPD test line and concluding with infill lines. This amended task was to commence upon completion of Line 23SE. The shipwreck was imaged on 19 March 2016 followed by the LDP line SAS_DJ101_LPD_01 on 20 March 2016.

After completing data collection on the first infill line, DT13A-21A_02NW_125m_SE, on 21 March 2016, the towfish was being hauled in to approximately 300m cable out to conduct a turn onto the next assigned line. During the haul back, when the cable was at 608m of cable out and at a depth of 447m, the mechanical termination failed at 11:19 UTC. This failure caused the depressor to separate from the cable and descend uncontrolled to the bottom at a depth of water of approximately 3600m with the ProSAS in tow. The position was well logged and the decision was made to head to port to plan and refit for a recovery of the ProSAS-60. The vessel arrived in Fremantle Western Australia on 26 March 2016 ending Swing 1.

4.1.1 ProSAS Loss

At 1119 (UTC) on 21 March 2016, after completing line DT13A-21A_02NW_125m_SE, communication was lost to the ProSAS-60 vehicle and the vehicle tow cable tension went from over 2,000 lbs to approximately 700 lbs. The navigational position of this event was recorded immediately. The topside power reading was checked and found to be consistent with exposed power conductors on the tow cable, indicating a potential break or separation in the tow cable.

Phoenix recovered the tow cable to the surface and reported the ProSAS vehicle was disconnected and noted the exposed cable was pulled out of the depressor.

An accident/incident report was initiated and the accident reported to the ATSB. The following information was noted regarding the incident:

- Sea conditions at the time of loss recorded winds at 18-20 knots out of the SE and seas of approximately 3 meters.
- The winch speed at the time of the accident was approximately 30 m/s and the vessel speed was approximately 2.35 knots.
- The termination which failed was deployed for a total of 25 days, 2 hours, and 30 minutes. These values were determined from the daily search situational reports (SITREPS).
- The umbilical cable is a Tyco Electronics, Rochester Corporation electro-optical-mechanical steel armored cable. The umbilical is 0.681 inch nominal diameter cable.
- The weight of the depressor is between 1,800 and 2,000 pounds.
- The connection of the umbilical termination to the depressor is made with a shackle from the depressor padeye to a steel endless loop which is captured in the PMI EVERGRIP Termination by a pin.

The ProSAS had been in the water since 25 February 2016. The depressor had been recovered several times to inspect the cable and mechanical termination. Visual checks of the termination on ProSAS-60 were conducted on two previous occasions during the deployment prior to the loss. These previous observations occurred on 10 March 2016 at 0902 UTC (about 11 days prior) and on 14 March 2016 at 0926 UTC (about 7 days prior). No wear of the PMI EVERGRIP termination was observed during either of these inspections. There were no visible signs of damage or slippage of the termination noted.

4.1.1.1 Findings

The failure of the termination was the result of fatigue failures of all but two of the grip rods. The rod failure location corresponded approximately to the nose of the PMI EVERGRIP™ termination housing. The two intact rods had apparently pulled out of the housing after failure of the other rods.

The ends of the failed rods were examined under low power magnification. The broken rod ends exhibited classic fatigue failures, most likely caused by cable strumming also known as vortex-induced vibration.

The cable strength loss was likely due to the general corrosion observed on the outer armor wires, it was noted that the inner two armor layers had little to no corrosion present. This is consistent with vortex-induced vibration where the outer armor wires break and the adjacent inner wires will be called upon to carry more tension. During this process the cable will become less well torque balanced. Eventually, there could be a cascade effect that results in the failure of the outer wires.

4.1.2 ProSAS Recovery

In response to the loss of ProSAS, Phoenix began mobilizing the *Remora III* Remotely Operated Vehicle (ROV) aboard *Dong Hai Jiu 101* on 05 April 2016 for ProSAS recovery efforts. Mobilization was completed on 10 April 2016 and the vessel proceeded to the ProSAS-60 loss

location. *Dong Hai Jiu 101* arrived at the loss location on 14 April 2016 and conducted ROV test dives.

Between 15 April 2016 and 18 April 2016, the ProSAS-60 vehicle and depressor weight were located on the seafloor and after several attempts between weather fronts and rigging, both the vehicle and depressor weight were recovered to deck and secured for transit to Fremantle Western Australia.

Dong Hai Jiu 101 arrived in Fremantle Western Australia on 22 April 2016 and repairs to the vehicle began and the cable was re-terminated.

4.1.3 ProSAS Repairs and Testing

The ProSAS vehicle was disassembled and inspected for mechanical and electrical problems associated with the cable detachment and descent to the seafloor. This repair period took place in Fremantle Western Australia from 22 April 2016 until 05 May 2016. The primary corrective actions were focused on stabilizing the INS power supply and reducing the noise levels in the arrays. Vehicle repairs were completed by 05 May 2016 and the vessel departed for the test range to validate the data quality.

The vessel conducted multiple dives on the test range between 05 May 2016 and 08 May 2016. The data was accepted by the ATSB representative and the vessel returned to Fremantle Western Australia on 09 May 2016, disembarked the test crew and began transiting to the Operations Area.

4.2 Swing 2

Swing 2 commenced 09 May 2016 with the transit to the Operations Area and concluded on 21 June 2016 in Fremantle Western Australia. Swing 2 experienced very rough working conditions throughout. On 16 May 2016, the ProSAS-60 launch was aborted due to conditions above safe working limits.

After a prolonged weather standby period, Phoenix received an amended tasking from the ATSB on 19 May 2016 to identify contact FE0133 with REMORA III. Prior to arrival at FE0133, the vessel Master received a directive from RSB that no ROV operations are to be performed from the *Dong Hai Jiu 101* and the ROV dive was not conducted.

Attempts were made again to find an operable weather window for towed ProSAS operations by working in areas north or south of where the weather was the strongest. A negative ProSAS-60 launch assessment was made on 03 June 2016 and the weather standby continued. Finally the ProSAS-60 launched the morning of 12 June 2016 and during the early cable pay out the topside tow fish power tripped a breaker. The cause was found to be water intrusion into the rotating junction box and slip ring attributed to the heavy sea conditions. These components were cleaned and the unit resealed and operated nominally.

During the same descent, the cable pay out continued until 1950 m depth when the depth sensor failed and array P1 array began showing intermittent problems. The failed depth sensor was bypassed using depth from the iUSBL. The lead-in to line DT13A-20A_27SE was too short to continue cable payout so the cable was recovered to 1,000 meters for a racetrack turn to bring the vehicle onto the survey line to avoid a data gap.

During the transit to the final approach turn site, the tow fish was deployed to the seafloor for sample data collection and confirmed that only 7 of the 8 arrays were operable. The ATSB through their onboard Commonwealth Representative gave approval for operations with only 7 of 8 arrays functioning on line DT13A-20A_31SE. Towed ProSAS operations continued through 14 June 2016 when the failed slip-ring was replaced to insure continued operations which required a turn back up line to avoid any data gaps.

The search continued along line DT13A-20A_31SE until 15 June at KP 260 when the weather conditions quickly deteriorated. The ProSAS-60 was towed in the water with 2000 m cable out until 17 June when it was possible to recover to deck. After recovery the vessel began a transit to Fremantle Western Australia anchorage.

The vessel arrived at the Fremantle Western Australia anchorage on the morning of 21 June at 0220 UTC ending Swing 2.

4.3 Swing 3

Swing 3 commenced 26 June 2016 with the *Dong Hai Jiu 101* transit to the Operations Area and concluded on 07 August 2016 in Fremantle Western Australia. During the transit, launch and recovery training was conducted with the new crew, and the ProSAS-60 was also wet tested. After evolutions were completed, the vessel resumed transit to the search area.

On 27 June 2016, a crew member sleeping in an upper bunk fell from his bed and onto furniture below when the vessel rolled in heavy weather. The crew member received medical treatment from the ship's doctor for a laceration and bruised shoulder. A decision was made to return to Fremantle Western Australia and transfer the injured crew member to shore for further assessment and care.

Dong Hai Jiu 101 commenced the transit to Fremantle Western Australia on the morning of 28 June 2016. Arrangements were made to provide replacement crew member. *Dong Hai Jiu 101* departed Fremantle Western Australia on 01 July 2016 with the new crewmember onboard.

Upon arrival to search area on 06 July 2016, the vessel was met by adverse weather conditions. The weather continued deteriorating until the vessel departed search area to seek safer conditions. During the evening on 13 July 2016, severe weather caused water intrusion into the PDU supply for the deck equipment. Power was secured eliminating the internet connection and was not restored until 18 July 2016.

Once the weather subsided to safe working limits, the ProSAS-60 was launched on 22 July 2016. The tow cable was damaged during launch requiring recovery of the ProSAS-60. The cable was repaired and the vehicle was launched on 23 July 2016 then immediately recovered due to a problem with the projectors. Repairs were conducted and on 25 July 2016, the ProSAS-60 was launched for dive 14. The search survey continued until the vehicle was recovered on 25 July 2016.

Adverse weather returned and the *Dong Hai Jiu 101* began transit to an area with workable conditions (Block 10A) to conduct holiday infill. The ProSAS-60 was able to complete infill on the larger holiday areas before recovery in this region due to adverse weather. Weather standby conditions continued until ATSB direction was received to return to Fremantle Western Australia on 01 August 2016.

During the transit to Fremantle Western Australia, the depressor was launched to perform adjustments to the level wind system on the Dynacon winch. *Dong Hai Jiu 101* arrived in Fremantle Western Australia on 06 August 2016. On 08 August 2017, the ATSB directed Phoenix to demobilize the ProSAS-60 system, place the Remora III ROV system in storage, and stand down all operations until the weather improved.

4.4 Operational Stand Down

Equipment demobilization and storage preparations commenced on 09 August 2016 and continued until 13 August when the crew began their travel home. The operation stand down continued until 14 October 2016 when the crew began travel back to Fremantle Western Australia to begin the remobilization of equipment for Remora III ROV operations to investigate targets located during the sonar search.

4.5 Swing 4

The Remora III ROV equipment was mobilized onto the *Dong Hai Jiu 101*, and re-activated and tested between 17 October 2016 and 20 October 2016. *Dong Hai Jiu 101* was underway on 20 October 2016 and proceeded to a 1,000 meter water depth, where ROV test operations were successfully conducted.

The vessel arrived at the first target location on 24 October 2016 and conducted a dive on contact GP-001. Weather conditions remained an issue. *Dong Hai Jiu 101* continued to chart a course to investigate the list of targets, deploying the ROV on contacts GP-038, GP-042, FS0052A, FE0151, and FE0152. Occasionally weather conditions would increase delaying dives on average by 24 hours.

A problem was discovered during the first group of dives with the ROV umbilical. The cable was not conditioned to the current operating depth, which resulted in loss of two floats and re-terminations of the umbilical had to be performed.

On 30 October 2016 the vessel commenced a transit to a water of depth 4,900 meters to condition the ROV cable. The umbilical was paid out with a weight replacing the ROV to remove the turns in the cable which resolved the twist in the cable. The cable was recovered and the ROV re-terminated to the umbilical. *Dong Hai Jiu 101* then transited to the next target and successfully resumed ROV dive operations on 01 November 2016.

04 November 2016 weather conditions again deteriorated to the point of being not safe while diving on contact FD0268. The operation went into a standby weather condition until 06 November 2016 when ROV dive operations were resumed.

Operations continued on contacts FD0292 and FE0150 with no interruptions. Contacts FE0162, FE0164 and FD0319 were investigated with small weather delays. On 07 November 2016, after the investigation of contact FD0319 was completed, the weather conditions began deteriorating to an unsafe working condition and operations went to another weather standby condition. Once the weather improved, *Dong Hai Jiu 101* initiated a slow transit to contact RMSFD002 on 11 November 2016.

Poor weather conditions continued until 19 November 2016 when the ROV was finally deployed to investigate contacts RMSFD002 and HH0009A. Weather conditions deteriorated after recovery and operations were in a standby weather condition until 22 November 2016 while the ship held station at contact FE0154. The vehicle was deployed to investigate contacts FE0154A,

FE0154B, and HH0029 when the vehicle experienced water intrusion into the ROV motor causing a motor failure while simultaneously the light control board on the ROV failed and required replacement. The ROV was recovered, and the motor and light control board replaced with spares. Dive operations resumed on 23 November 2016.

During dive operations on 24 November 2016, the ROV camera began experiencing oil intrusion into the camera lens while working at depth. The camera was removed and drained during the transit between targets. Also on this day, the ROV transponder flooded and was not repairable. No further USBL tracking was available after this point. No spare was available. Weather conditions deteriorated and the operation went to a standby weather condition.

ROV dive operations resumed on 26 November 2016 when the weather subsided. During the dive operations the color camera connector failed and the camera had to be removed from service. The camera was replaced with a spare that did not have a zoom capability.

ROV operations concluded on 02 December 2016 and *Dong Hai Jiu 101* commenced the transit to Fremantle Western Australia for demobilization. *Dong Hai Jiu 101* arrived in Fremantle Western Australia on 07 December 2016 and system demobilization commenced immediately. Demobilization was completed on 10 December 2016 and the crew departed for home.

Overall, Remora III conducted a total of 33 dives to inspect targets of interest identified during previously completed side scan sonar search operations. The Remora III operated in depths down to 4,800 meters of seawater (msw) and provided investigators with clear imagery of the targets of interest, which were ultimately identified as a combination of seafloor geology and manmade objects, such as shipwrecks, a pile of wire rope, and a 55 gallon drum.

5.0 LESSONS LEARNED

This section discusses lessons learned while performing ProSAS-60 side scan sonar search operations and Remotely Operated Vehicle (ROV) operations onboard the Chinese Rescue Salvage Bureau (RSB) vessel *Dong Hai Jiu 101 (DJ101)*. The objective is to promote awareness and understanding and preclude the recurrence of any undesirable outcomes on future projects.

5.1 Mobilization/Operation/Demobilization from a Vessel of Opportunity

Phoenix operated from the vessel *Dong Hai Jiu 101 (DJ101)* from January 2016 until December 2016.

5.1.1 Lesson Learned

Well-coordinated and executed pre-planning activities well in advance of mobilization and operations onboard a Vessel of Opportunity is critical to the success of any at-sea operation. The ATSB/ Donghai Rescue Bureau/Ministry of Transport support and guidance in the conduct of the pre-mobilization ship-check of the Chinese vessel *Dong Hai Jiu 101*, and participation in the associated follow-on meetings and briefings was key to the transparency and efficiency, and safe execution of all key operational project events, to include vessel mobilization and at-sea operations.

Pre-planning activities provided a well-structured process for the review of several very important key project requirements, to include: vessel GA drawings, DP 24/7 operations and vessel ship handling, messing/berthing accommodation arrangement options, food requirements, non-smoking requirements, power supply/cable lengths and VFD location, ROV/AUV/ProSAS deck lay-out installation options, deck timber removal concerns/options, locator pole installation options, equipment stowage and data processing room options, vessel communications capabilities (512kb upload/1024Kb download), IMO/SILOS certifications, Communications (e.g. English-Chinese translation requirements), etc.

5.2 Problem Encountered: ProSAS Umbilical Failure

At 1119 (UTC) on 21 March 2016, after completing line DT13A-21A_02NW_125m_SE, communication was lost to the ProSAS-60 vehicle and the vehicle tow cable tension went from over 2,000 lbs to approximately 700 lbs. The navigational position of this event was recorded immediately. The topside power reading was checked and found to be consistent with exposed power conductors on the tow cable, indicating a potential break or separation in the tow cable.

5.2.1 Lesson Learned

1. Use of the PMI Everflex BSR (Bending Strain Relief) (<http://pmiind.com/rugged-cable-hardware/everflex-bsr-bending-strain-relief/>) will significantly deter the potential failure rate of the helical cable from 5,000 cycles to 5 million cycles.
2. PMI reports that high loads and large angles of deflection can induce strain near the rigid termination attachment point. During adverse weather conditions the ProSAS vehicle was put on a short tow and the vessel increased speed to maintain steerage way operating in a racetrack course to stay close to the last line surveyed. These actions induced higher loads and increased harmonic frequencies on the cable at the rigid termination point increasing the rate of cyclical fatigue. Phoenix made the following recommendations for operational changes during these conditions:

- a. During turns, only bring in enough cable to be above minimum water depth plus a safety margin to leave sufficient catenary in the wire to dampen any resultant forces.
 - b. During recovery, reduce speed to bare steerage way so that the vessel can maintain the proper sea/wind aspect and haul in the cable at a reduced speed to minimize the loading on the cable.
2. HSI reported that the ProSAS vehicle was 15 pounds buoyant, however, when the vehicle was recovered from the seafloor it took over 100 pounds of weight to sink the vehicle during the recovery. Phoenix recommended that the buoyancy be verified to more properly align with the ProSAS-60 designed flight profile.
3. As an added measure of safety, a keeper line was installed on the tow cable to avoid any potential future loss of the ProSAS and depressor weight as a result of the cable failure. Phoenix recommended the installation of a second torque grip up the tow cable with a safety wire going directly to the depressor weight. The safety cable was left slack and tie-wrapped to the tow cable to secure it so it fit through the sheave on a normal recovery.
4. Phoenix recommended the re-installation of a passive pinger on the ProSAS-60 vehicle to help locate the vehicle if it was lost again.
5. Phoenix recommended the installation of a remotely activated guillotine cutter on the ProSAS which when activated would allow the vehicle to float to the surface.

5.3 Problem Encountered: ROV Load Release Shear Pin Failure

The ROV load release shear pin is a fuse-able link that protects the umbilical from parting when load conditions exceed a limit.

5.3.1 Lesson Learned

The shear pin failed as designed when the dynamic loading conditions during the ROV recovery exceeded that limit. During the recovery in a moderate sea state, the swell action and ship motion created a dynamic load that momentarily exceeded the breaking strength of the shear pin and it released the load. The shear pin performed as designed and saved parting the cable or causing vehicle damage due to excessive load conditions. Recommend delaying heavy lift activities during excessive sea states to mitigate recurrence.

5.4 Problem Encountered: ProSAS-60 Cable Damage

While deploying the ProSAS-60, slack in the cable caused the cable in the traction sheaves to fall out of the grooves. When the winch operator started hauling in cable, the slack on the traction winch pulled tight onto the motor shafts for the sheaves causing damage to the cable outer armor.

5.4.1 Lesson Learned

The Project Team modified launch procedures by assigning a dedicated watch to the portions of the winch obscured to the winch operators line of sight to reduce risk of a recurrence.

5.5 Problem Encountered: Sonardyne iUSBL Failure

Sonardyne iUSBL failed due to a connector flooding and caused positioning loss for the ProSAS.

5.5.1 Lesson Learned

The Sonardyne iUSBL was rented from Seatronics. The unit was inspected upon receipt and found to not have an O-ring in the connector. Sonardyne (OEM) was contacted and queried about the need for an O-ring in this connector. Sonardyne stated that an O-ring was not needed for this type of connector. However, the Project Team discovered when the unit was submerged for an extended period of time water intruded this connection causing a ground fault and shorted out the iUSBL unit. Spares inventory should be confirmed to avoid single points of failure. System sparing and redundancy must be a top priority.

5.6 Problem Encountered: ROV Fiber Link Lost

During ROV dive #2 the fiber link to the ROV was lost at a depth of 3,300 msw requiring a dead vehicle recovery. The vehicle was kept outboard of the vessel and out of harm's way by correctly positioning the ship and adjusting the winch recovery rate. The fiber break was a result of the umbilical twisting and tangling the third and sixth floats together.

5.6.1 Lesson Learned

This was a new umbilical which was spooled onto the storage drum in Fremantle Western Australia by Green Monster according to manufacturer tensioning specifications. While all procedures were followed, experience has shown that new umbilical lines need to be conditioned using a swivel and weight in deep water at maximum depth to allow all the twists to come out of the cable. Operational schedules should be adjusted (if feasible) in coordination with the client to allow time for cable conditioning.

6.0 CONCLUSION

Phoenix's work aboard the *Dong Hai Jiu 101* was Phoenix's third effort to support the search for Malaysia Airlines Flight 370 (MH370). Phoenix was involved in the search for MH370 from March 2014 – December 2016. During this time Phoenix used a wide variety of underwater systems, including the U.S. Navy Towed Pinger Locator (TPL-25), the Phoenix 5,000 meter depth-rated AUV *Artemis*, Hydrospheric Solutions' 6,000 meter depth-rated ProSAS-60 towed synthetic aperture sonar system, and the Phoenix 6,000 meter depth-rated Remora III ROV.

During the course of this extensive search effort, Phoenix conducted operations on three different ships: the Australian Defence Vessel (ADV) *Ocean Shield*, the M/V *GO Phoenix*, and the Chinese Rescue Salvage Bureau (RSB) vessel *Dong Hai Jiu 101*.

In total, Phoenix completed 13 "swings" to the MH370 search area, which was approximately 1,500 nautical miles west of Fremantle Western Australia, Western Australia. Each swing consisted of a five-day transit to the search area, 30 days or more of search operations, and a five-day transit back to Fremantle Western Australia, Western Australia.

Phoenix proudly recognizes the dedication and professionalism of the many countries, Governmental Agencies, vessel crew, and private industry that have spent years in the search for MH370. Phoenix stands ready to assist and remains fully committed to supporting any future search effort to one day locate Malaysia Airlines Flight 370 (MH370).

Appendix F – Chemical investigations on barnacles found attached to debris from the MH370 aircraft found in the Indian Ocean

Chemical investigations on barnacles found attached to debris from the MH370 aircraft found in the Indian Ocean

Patrick De Deckker

Research School of Earth Sciences
The Australian National University
Canberra ACT 2601

Summary

Trace element analyses were conducted on calcified scuta plates of sessile pedunculate barnacles, belonging to the species *Lepas (Anatifera) anatifera striata*, found attached to debris of the MH370 aircraft. The Laser Ablation Inductively Coupled Plasma Spectrometer [LA-ICPMS] technique was used at the Australian National University to reconstruct the magnesium to calcium ratio [Mg/Ca] across the growth lines of several scutum plates in an attempt to reconstruct the water temperature [SST] at the sea-surface in which the barnacles grew during their drifting at sea while attached to the aircraft debris.

The reconstruction of the sea-surface temperature of the seawater in which the barnacles grew is hindered by a number of factors:

- (1) the correlation between SST and the Mg/Ca of the water in which barnacles grew is based on too few analyses carried out over sixty years ago by Chave (1954);
- (2) there is a large amount of organic matter in the scuta plates of the barnacles and it was found that this organic matter is rich in magnesium, thus preventing us from using the Mg/Ca in the calcite matrix of the scuta plates to reconstruct SST at the time of formation of the plates.

In addition, as so few observations have so far made on barnacles growth, we are unable to establish if rates of growth and calcification are controlled by temperature or food supply, or both. In addition, we are also unable to tell if the barnacles we examined grew continuously once attached to the aircraft debris or stopped growing at some stage for several possible reasons such as lack of food supply and/or temperatures unsuitable for growth, or exposure outside water.

We carried out chemical analyses on the same scuta specimens analysed by our French colleagues [see Blamart & Bassinot, 2016] following parallel lines to their sampling and our attempts at reconstructing past SST do not match the reconstructions based on oxygen isotope analyses, thus further suggesting the organic matter contamination in the scuta shells is hindering any possible reconstruction of water temperatures.

1. Introduction

Darwin (1851), in an extensive monograph, was first to establish the morphological nomenclature and systematics of barnacles which belong to the Crustacea in a very diverse class called Cirripedia. Crustaceans encompass prawns, shrimps and lobsters among others. The barnacle specimens found attached to the MH370 debris are sessile and use a peduncle to remain attached to material floating at sea such as wood and pumice, as well as other debris, such as those discussed here. During their life cycle, barnacles undergo metamorphosis, starting from an egg developing into a minuscule swimming larva, referred to as the cyprid larva, that eventually attaches itself to floating objects and, in the case of the specimens examined here, become securely attached with a fleshy peduncle. Pedunculate barnacles feed on the neuston, being floating particulate matter often found at the sea surface. Thus, the specimens examined here

are referred to as neustonic pedunculate barnacles or as epipelagic goose barnacles [*sensu* Schiffer & Herbig, 2016]. Several calcified plates made of calcite [= calcium carbonate: CaCO₃] progressively grow on the outside of the animals and thus cover and protect the soft appendages and organs. Rates of growth are thought to be dependant on water temperature, food supply and the conditions experienced while drifting with their 'substratum', but ecological observations on peduncular barnacles are unfortunately very few (de Graaf, 1952; Evans, 1958; Skerman, 1958; Patel, 1959; Thiel & Gutow, 2005; Inatsuchi et al., 2009).

2. The hard calcified plates of the barnacles

Pedunculate barnacles are commonly found on Australian beaches as they attach themselves to floating debris, such as wood, and also pumice. The fleshy peduncle is quite solid and even after death of the organisms - often as a result of 'beaching' – will permit the barnacle shell to remain attached for quite some time (see figure 1).

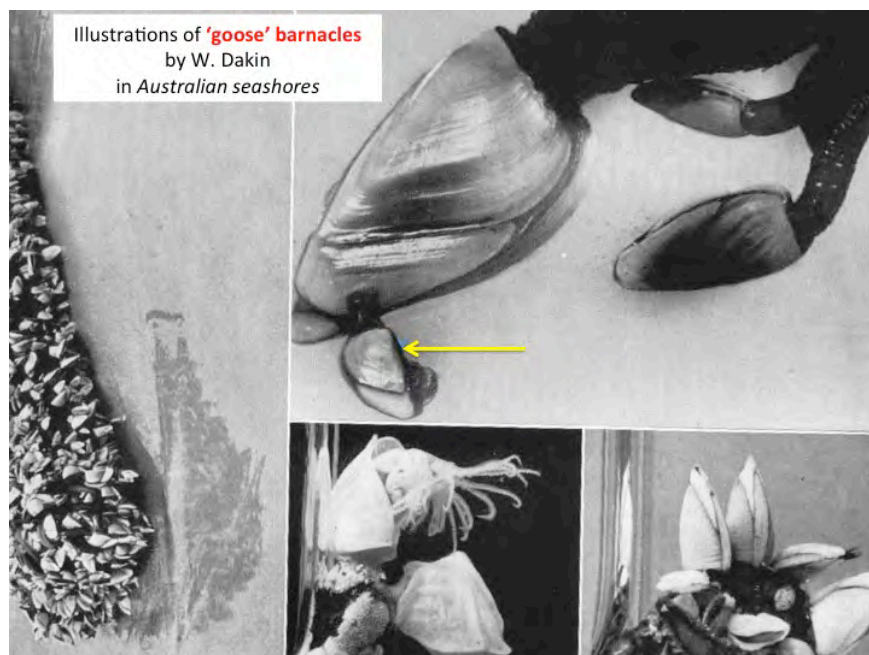


Figure 1. Photographs modified from the book “Australian Seashores” by Dakin (1973, plate 45) showing on left how barnacles accumulate on debris, in this case a drifting wooden log, on top right corner four generations of *Lepas anatifera* with their characteristic fleshy peduncle; [the arrow shows the youngest specimen], and on the bottom, in the middle image the appendages are clearly visible, and bottom right specimens of a different species of *Lepas* being the short – stalked *L. anserifera*.

We propose to use the terminology of the calcified plates first employed by Darwin (1851), an original sketch of which is presented in Figure 2.

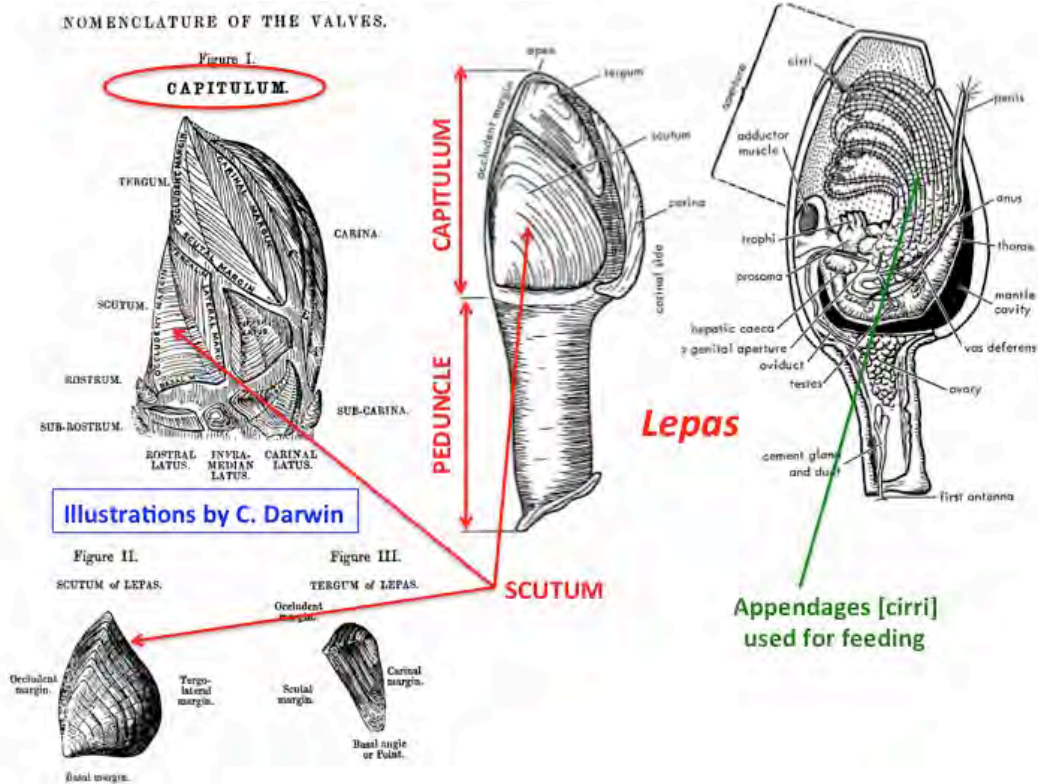


Figure 2. On left, copy of the original illustrations (1-3) of a pedunculate barnacle made by Darwin (1851) detailing the terminology used in this report. On the right are illustrations of the pedunculate barnacle *Lepas* showing the hard parts and peduncle, and next to it is a specimen showing the appendages which are used for feeding and aerating the inside of the shell. Illustrations modified from The Treatise of Invertebrate Paleontology Part R (1969).

The scutum plates which adorn the organism are the largest ones and therefore were used for chemical analyses. In fact, we received 3 scutum plates from Drs Dominique Blamart and Franck Bassinot from the Laboratoire des Sciences du Climat et de l'Environnement in Gif-sur-Yvette near Paris, one from La Réunion Island which had previously been “microdrilled” for stable isotope analyses. This specimen labelled A2 G1 is illustrated in Figure 3 and the location of the microdrilling is very obvious. Microdrilling involves extraction of the upper surface of the scutum plate and the resulting powder is then analysed for its isotopic composition [see report by Blamart & Bassinot, 2016]. The scutum plates of 2 barnacles recovered from Rodrigues Island [19° 44' 26.49”S] were also analysed, one being large and the other representing a much smaller specimen. Because these 2 specimens were not dissected - for fear of breaking them - we are unaware if they are juveniles or adults.

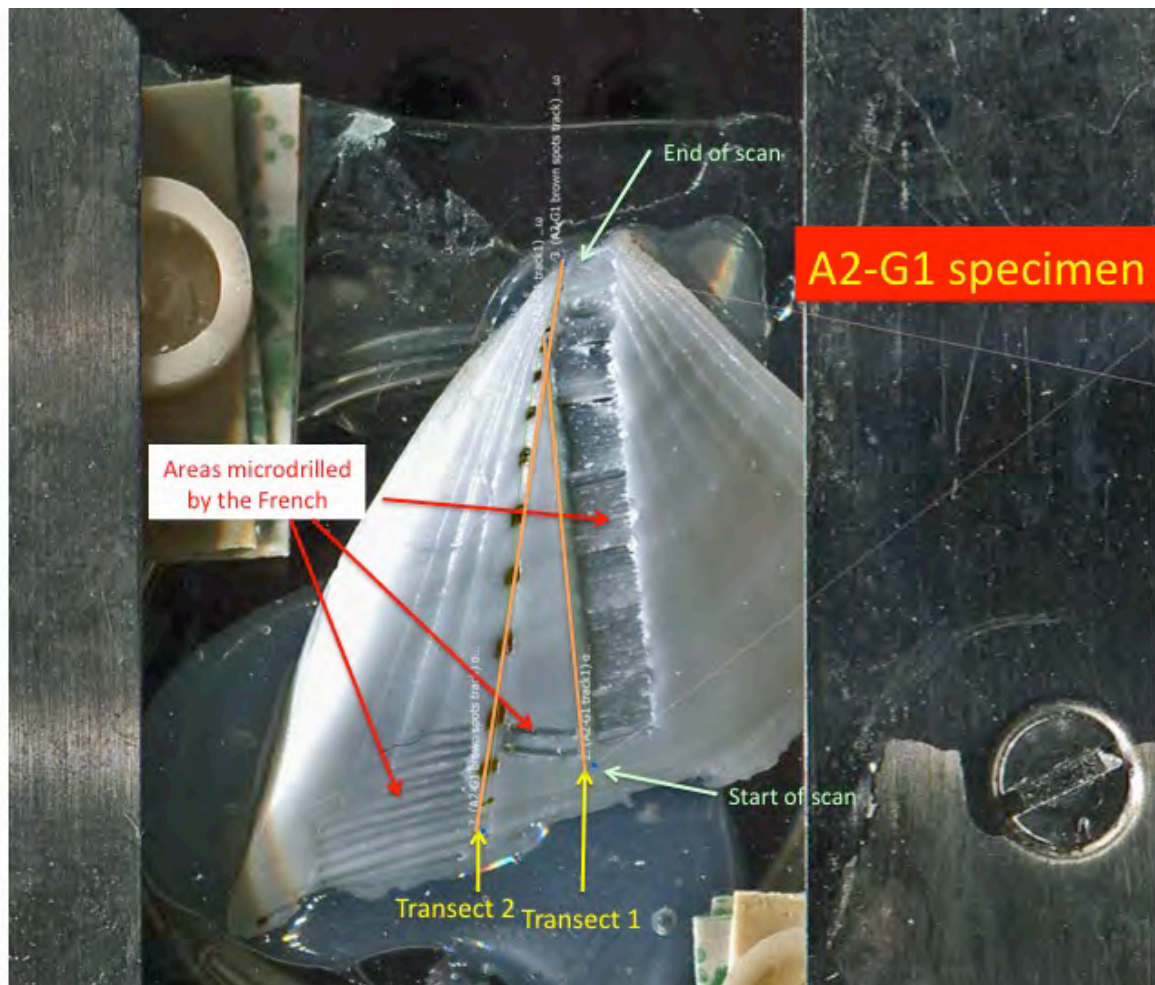


Figure 3. Photograph of the scutum plate of specimen A2-G1 collected at La Réunion and which was originally attached to the fragment of the aircraft. The red arrows indicate the parts which had been microdrilled by our French colleagues. The orange lines show the tracks followed by the laser ablation at the ANU. Transect 1 lies just outside the area microdrilled in France for oxygen isotope analyses. Transect 2 goes from the tip of the scutum at the top (which was formed in the early stage of growth) and ends near the last part of growth of the scutum. Note that transect 2 was arranged to pass over the brown spots that are almost equidistantly located. The dark part on either sides of the scutum plate belong to the metal holder in which the specimen was fixed.

The barnacle plates are made of low Mg calcite [viz. <5% Mg in CaCO₃] which allow them to remain intact in sea water. All the elements such as Ca and Mg are taken by the organism directly from seawater and possibly from the food it eats. As Ca is a bivalent cation, other bivalent cations (e.g. Mg²⁺, Sr²⁺, Ba²⁺ and Cd²⁺) can take its place and fit within the CaCO₃ lattice. Such elements can be It is now clear from observations made at the ANU that the calcite lattice contains numerous microlayers of organic matter that are visible under a powerful microscope. These layers are coloured pale brown and follow the obvious growth lines seen externally (See Figures 3-4).

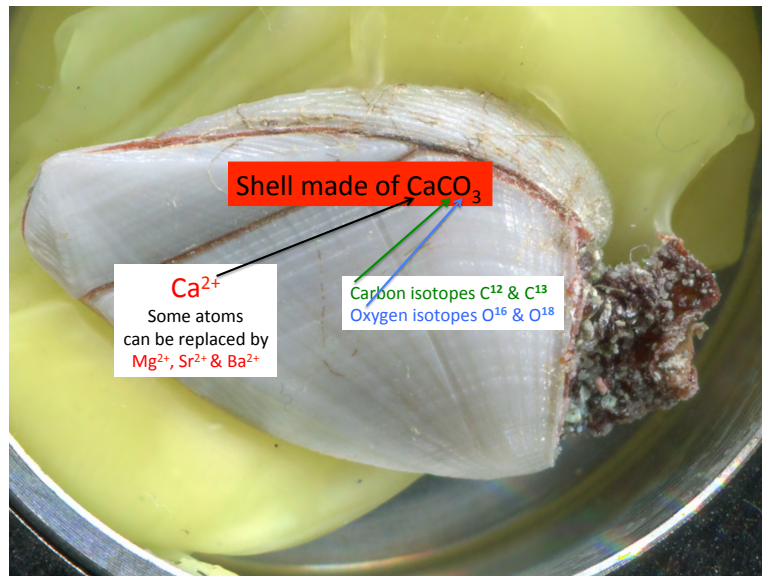


Figure 4. Photograph of an entire barnacle from Rodrigues Island showing the large scutum plate lying inside a metal holder and resting on (yellow) parafilm material for stable mounting of the sample while ablating the specimen. Note the broken piece of peduncle on the right hand side which is coloured brown and has shrunk substantially due to dehydration. Note the faintly visible microlayers that are almost parallel to the boundary between the scutum plate and the tergum (see Fig. 1) and which are representative of growth lines. Such lines are more obvious when the specimen is examined at high magnification.

3. Carbonate chemistry of barnacle plates

Chave (1954) was the first to systematically assess the Mg content in biogenic carbonates of many different phylogenies. His aim was to determine whether there is a link between ambient water temperature and the Mg composition of carbonates. Concerning barnacles, he used spectrography to determine the percentage of MgCO₃ in the calcite lattice and 2 of the data points he used came from Clarke and Wheeler (1917). All the samples had less than 5% magnesium carbonate, and Chave (1954) showed an obvious relationship between water temperature and the weight per cent MgCO₃ of barnacle valves (Chave, 1954). Note, however, that in his figure 12 Chave presented results for 6 samples of mixed barnacles. In our plot of Chave (1954)'s data (Figure 5-6), we eliminated 3 data points as they clearly represented outliers, especially since the fragments came from low temperatures; 2 samples were associated with 5.2°C from Adak Island in Alaska and the other from Mount Desert being a large island offshore Maine, USA. It also appears that there is a better relationship between water temperature and the Mg/Ca of barnacle shells by using a logarithmic correlation curve (red line in Fig. 6).

There is however an important observation to make as we do not know if the temperature values tabled by Chave (1954) represent an annual mean, or the temperature at the time of collection. Note also that 7 out of 9 specimens Chave (1954) listed were barnacle fragments.

4. Information on the growth of *Lepas anatifera*

Very little information is available in the scientific literature about the ecology of *Lepas anatifera*. Evans (1958) examined colonies of *Lepas hillii* and *L. anatifera* barnacles that had settled on the side of the yacht *Petula* between Dakar and Barbados during the winter season of 1953-54. It seems that none of the barnacles listed above had settled on the ship while in Dakar Harbour. On the way to Barbados, thirty days later, a sample of 20 of the largest *Lepas* barnacles growing on the topside of the yacht was collected

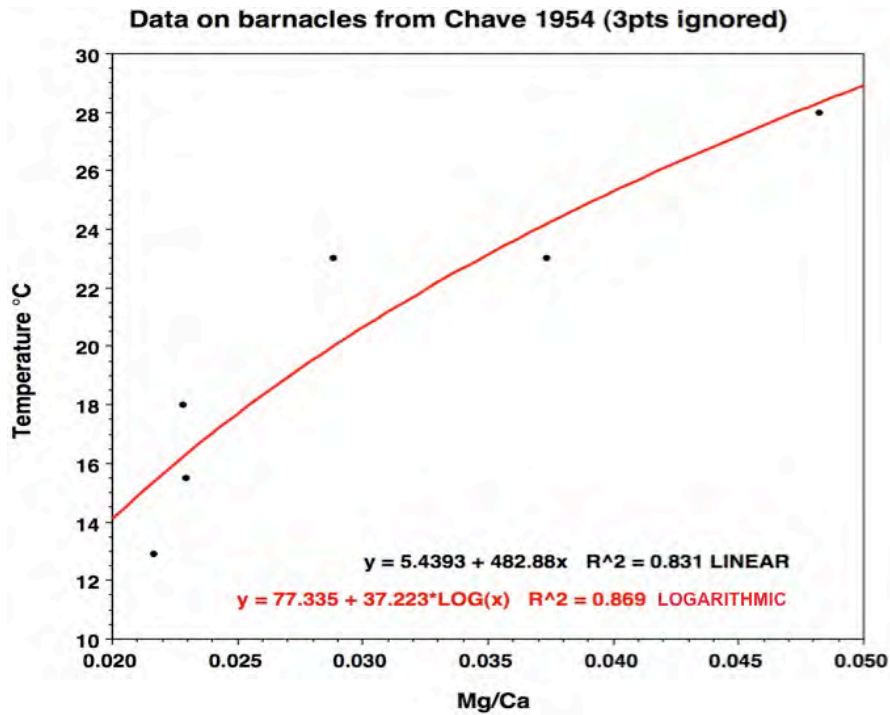


Figure 5. Plot of the Mg/Ca of complete barnacle shells against water temperature in which the barnacles grew. Data from Chave (1954) for which 3 outlier points were omitted [see text for explanation]. In red is the logarithmic correlation and the linear correlation value appears in black.

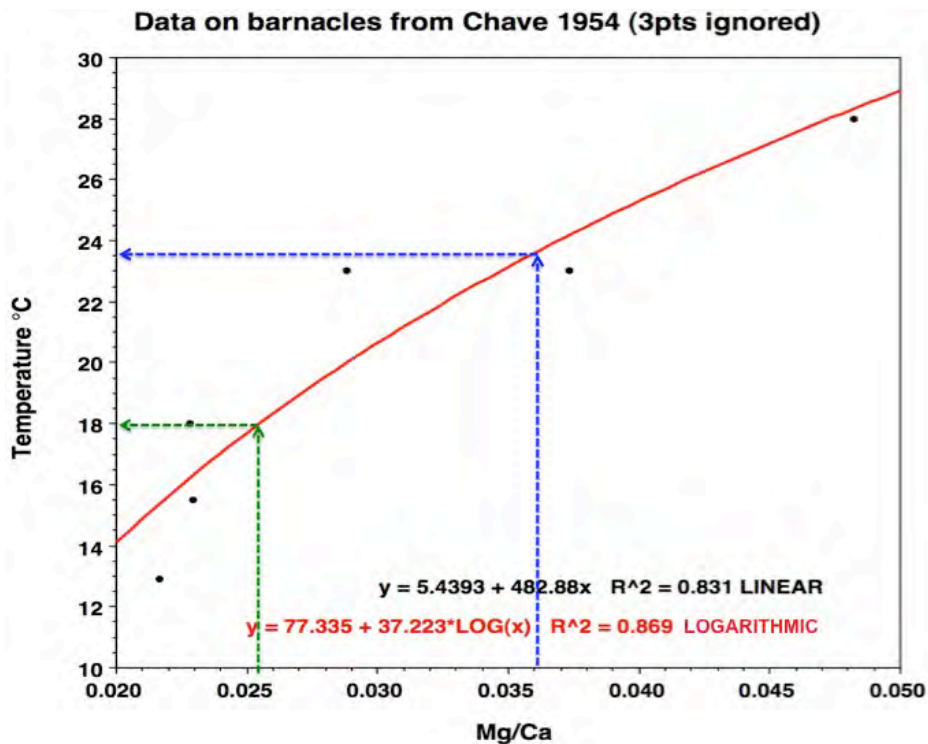


Figure 6. Copy of figure 4 showing how water temperature can be obtained from the Mg/Ca composition of the barnacle shell based on Chave (1954)'s data. Using the logarithmic correlation, a Mg/Ca ratio of 0.0361 would represent a temperature of 23.6°C [blue lines] whereas a Mg/Ca of 0.0254 would dictate a temperature of 18°C [green lines].

and preserved. A further collection of 60 of the largest specimens from an adjacent position on the ship was taken after 60 days. Evans (1958) estimated that average daily size increase was about 0.5mm in the first month and may have continued as such during ontogeny, generally on the 30th to 34th day. Afterwards, the growth rates near 0.3mm/day were interpolated. Apparently, the sea-surface temperature during the voyage ranged between 24.4° and 26.1°C. In addition, Evans (1958) cautioned about extrapolating growth rate and length of the barnacle juvenile phase in cooler waters. In a second study, MacIntyre (1966) collected *L. anatifera* barnacles after a [originally clean] buoy was recovered 17 days later in the Tasman Sea off the eastern coast of Australia in December 1960. Maximum lengths of the capitulum of the barnacles were recorded. Only 2 specimens had mature ovaries and these specimens were 23mm long (Figure 7) whereas a large range of sizes were recorded as shown in that figure. Hence, as indicated by MacIntyre (1966) 'it would be unwise to generalise about barnacle growth rates and their dependence on temperature'. Nevertheless, if we were to assume that the mature barnacles had grown over 17 days at the most, growth rate could be estimated to have been ~1.35 mm/day and the temperature range around the buoy was 25-28°C. Another study examining *L. anatifera* adhered to beacons in Hawke Bay on the east coast of the North Island of New Zealand looked at growth of the barnacles, this time at lower temperatures than for the Tasman Sea study (Figure 8 and comments). More recently, Magni et al. (2015) who attempted to evaluate the floating time of a corpse recovered in the Tyrrhenian Sea based on *L. anatifera* barnacles found attached to the body estimated a growth rate of 0.2mm/day, with temperatures having possibly ranged between 13° and 19°C, or less depending on when barnacles started growing on the body. Further, Magni et al (2015) estimated that within that temperature range, a capitulum may reach 12 mm after approximately 60 days. Hence, it seems likely that size is related to water temperature. However, once again, caution has to be exercised because other factors may contribute to growth, such as food availability. This issue was already partly addressed by Inatsuchi et al (2010) both in the ocean and in the laboratory, who concluded that both high temperature and high food availability contributed to greater growth.

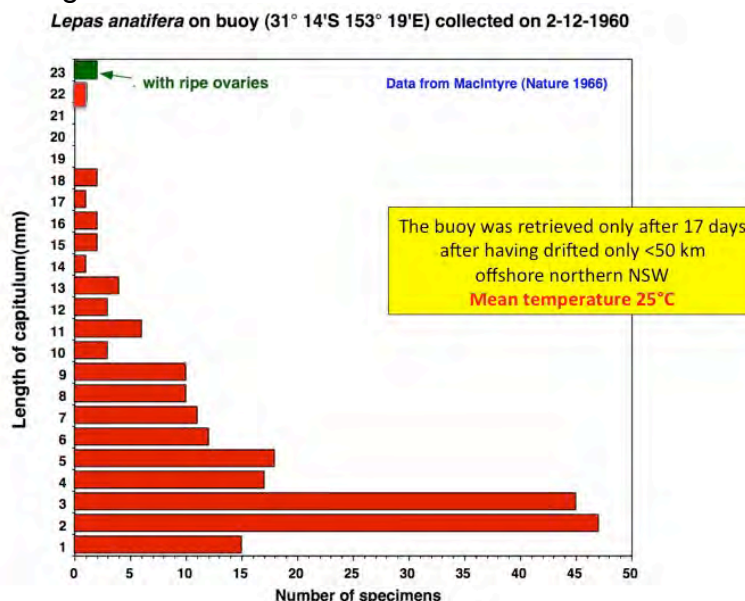


Figure 7. Histogram plot of the size of *L. anatifera* specimens found attached to a buoy offshore eastern Australia only after 17 days. Note that we do not know when the juvenile barnacles settled on the buoy within that 17 days period. Hence, growth rates may even be higher, but it is not possible to find out.

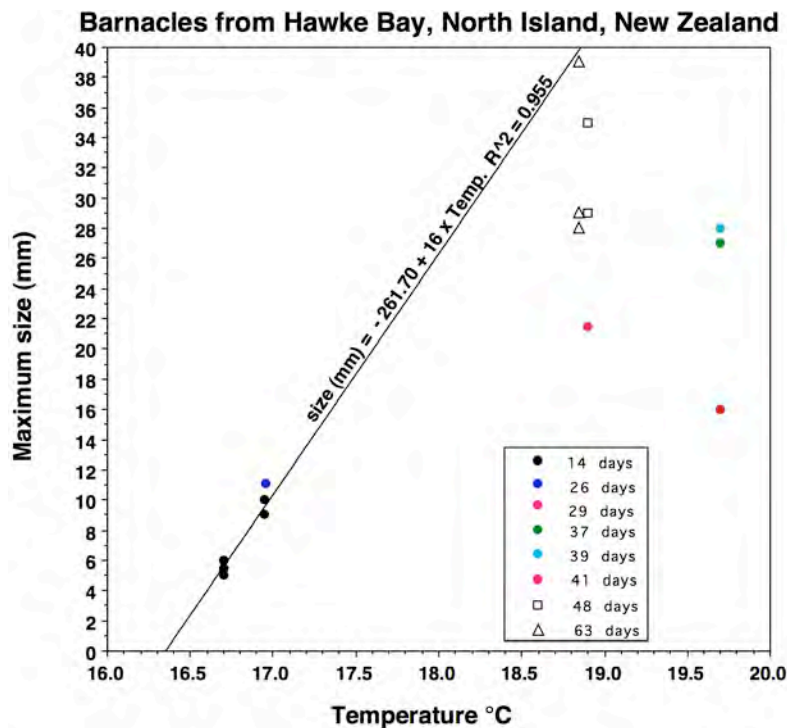


Figure 8. Plot of all maximum sizes of barnacles collected from beacons immersed in Hawke Bay along the North Island of New Zealand over the 1954-55 period (refer to Skerman, 1956 for more details). A regression line is provided here only for the barnacles that were collected from the beacons after 14 days. This indicates a substantial growth rate, viz ~1cm over 14 days at about 17°C. At slightly higher temperatures and over longer time periods, the growth rate appears to be slightly lower. Compare the data presented here with that of McIntyre in figure 7 which shows one barnacle having reached 22mm over 17 days when temperature was much higher, viz. 25°C.

5. Microanalytical techniques

We used a laser ablation inductively coupled mass spectrometer [LA-ICPMS] at the Research School of Earth Sciences at The Australian National University (Figure 9). We performed linear transects along the surface of the shells following the initially developed technique to analyse planktic foraminifera tests (Eggins et al., 2003), to investigate the nature and extent of the compositional variation along the growth lines of the barnacle scuta.

It proved unnecessary to clean the specimens and therefore, on each occasion and for every new profile, laser ablation was performed to clean the outer surface of the shells by “shaving off” the upper few microns of the outer surface.

More information on the technique is available in Eggins et al. (1998).

Nevertheless, below are some specifications of the technique we used. These were:

- Before proper analyses could be performed, a thorough cleaning of the outer surface of the shells had to be performed. As a result 50µm spots at 5 pulses per second were drilled, thus resulting in a 20-40µm deep groove. Following that procedure, analyses were performed in the groove.
- Continuous ablation at 20 microns per second, 10 Hertz at 20 kvolts;
- Elements and their respective isotopes being recorded: Be¹¹, Mg²⁴, Mg²⁵, Ca⁴³, Ca⁴⁴, Sr⁸⁶, Sr⁸⁸, Ba¹³⁸;
- Results were reported as ratios to calcium in the calcitic shells;
- Consequently, about 1400 continuous analyses covered approximately a 1.4 cm long transect.

- Hence, because so many analyses were performed for a single transect, there was a need to smooth the data at times due to 'analytical noise', we used 14 point smoothing.

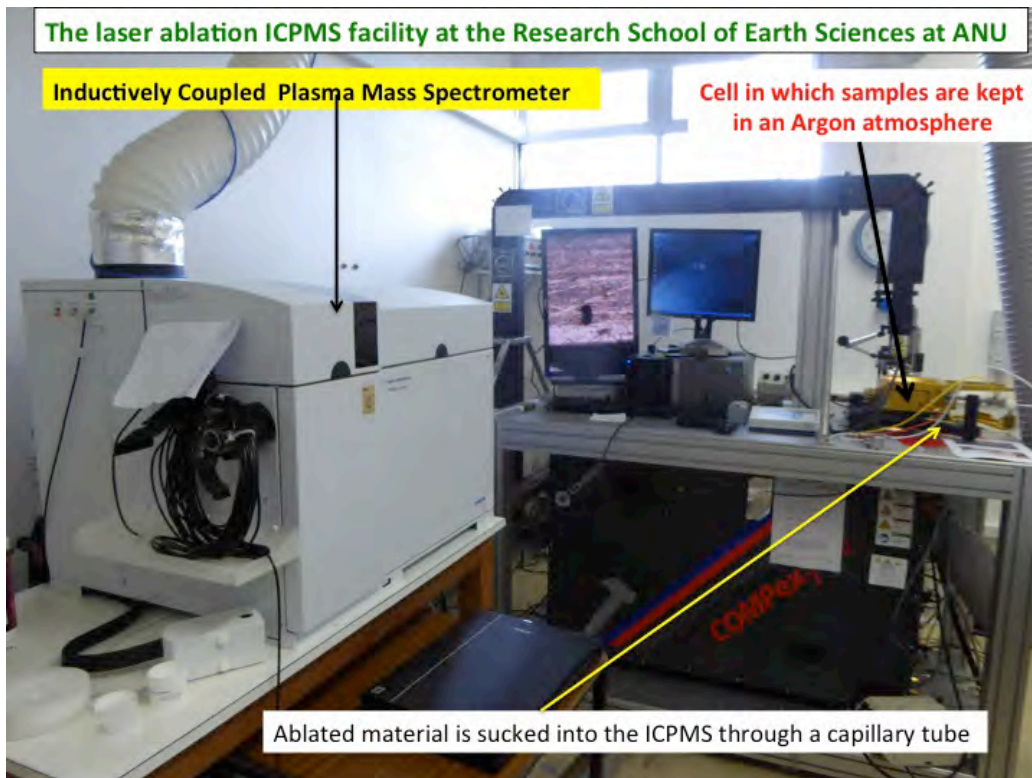


Figure 9. Photograph of the equipment used at the Research School of Earth Sciences.

6. LA-ICPMS results

It was decided to plot all the results in the figures presented below, having 'translated' the Mg/Ca into temperature values, using the correlation obtained from Chave (1954)'s data point shown in figures 5 and 6. This is to better visualise the results as sea-surface temperatures instead but, more importantly, for the reader to assess the veracity of the reconstructed temperatures.

Below is a presentation of the results from the laser ablation analyses, and their interpretation will be provided in section 7.

6.1 Specimens retrieved from La Réunion Island



Figure 10. Photograph of the metal holder showing cavities in which the barnacle specimens were placed prior to the laser ablations. The yellow material on which the barnacles rest is made of parafilm which was partly heated with a hair drier to soften it before allowing to cool so as to maintain the barnacles in a stable position. The yellow lines show the transect followed by the equipment before ablation could proceed. The surface of the coral standard displays numerous grooves related to previous ablations.

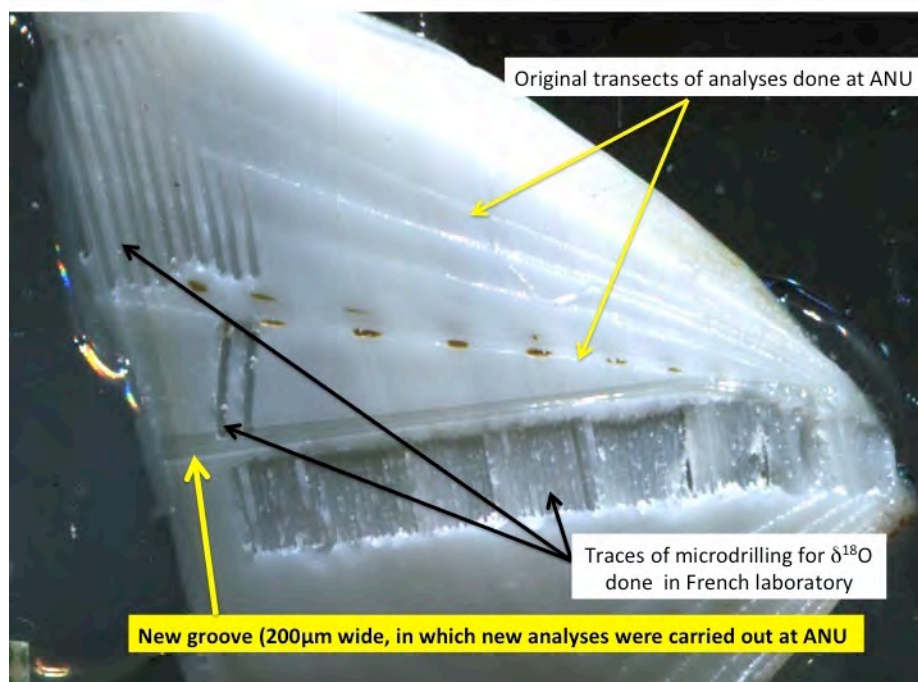


Figure 11. Photograph of the scutum of barnacle A2-G1 which shows the location of the microdrilling (indicated by black arrows) done in France (for oxygen isotope analysis) as well as the fine transects performed by the laser. Note that the middle transect passed over the brown 'spots' and consequently partly ablated them. These 'spots' coincide to sites of high Mg/Ca values (see Figure 12 and text for more explanation). The lowest and much wider 'groove', that partly ablated the brown spots, was performed before a new ablation of the calcite could be done. The results of the original ablation are presented in figure 12.

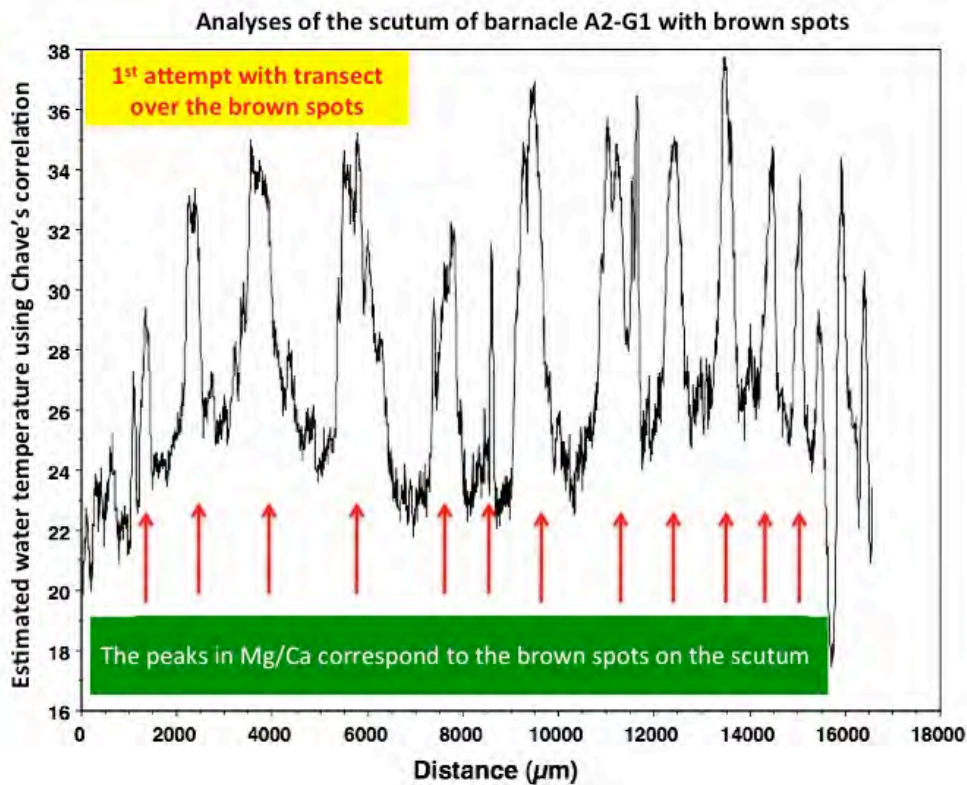


Figure 12. Plot of the analyses performed along the groove that passed over the brown spots on barnacle A2-G1 (shown in figure 11). The data was obtained as Mg/Ca ratios, but transformed into estimated temperatures based on the Chave (1954) correlation. This procedure is used to simply demonstrate the obviously implausible temperature reconstructions. The transect is almost 1.7cm in length.

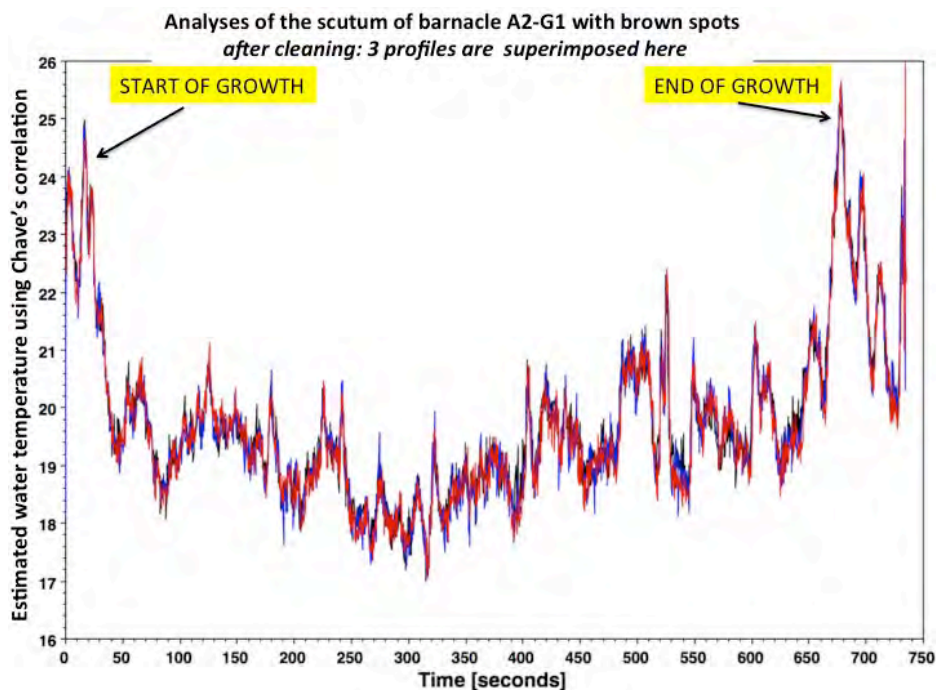


Figure 13. Plot of three sets of analyses performed along the groove that passed over the brown spots on barnacle A2-G1 after surface cleaning was performed by ablation. Once again the Mg/Ca data were translated into an estimates of water temperature based on the Chave (1954) correlation presented in figure 6. Note the horizontal axis gives the time used to obtain the profile.

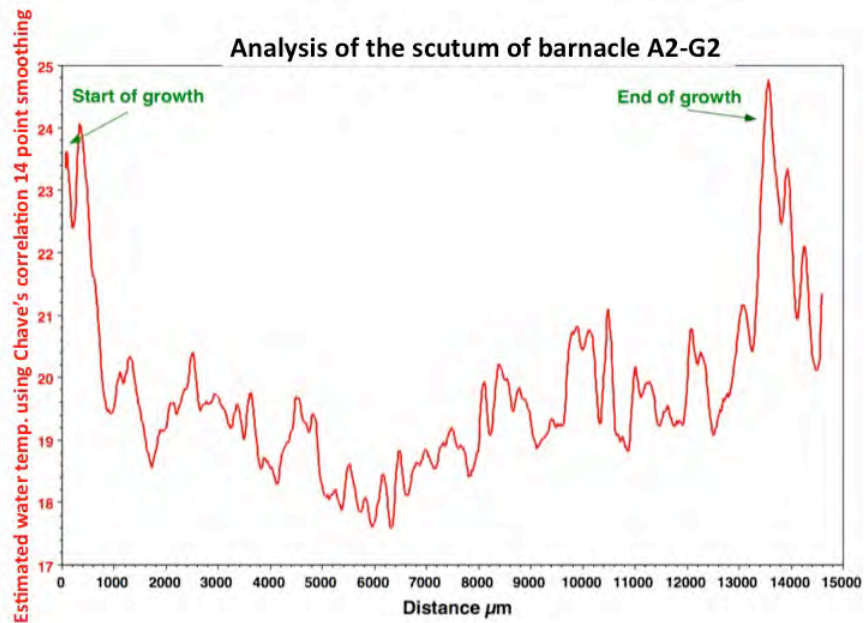


Figure 14. Plot of one set of analyses performed along the groove that passed over the brown spots on barnacle A2-G1 after cleaning was performed by a substantial amount of ablation was performed. Once again the Mg/Ca data were translated into an estimation of water temperature using Chave (1954)'s formula presented in figure 6. This time 14-point data smoothing was performed to clearly evaluate the temperature trends. Note that both the start and end of growth of the scutum 'report' higher temperature estimates.

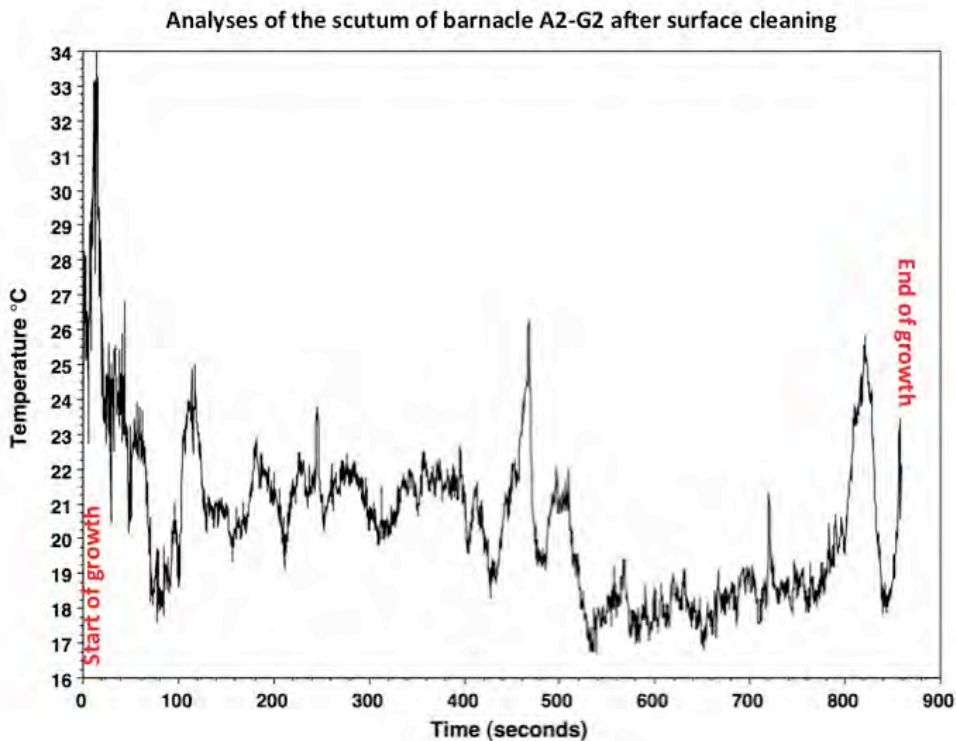


Figure 15. Plot of the analyses performed along the transect on barnacle A2-G2 after the strong cleaning procedure was performed with deep and wide ablation of the outer surface of the scutum shell. Once again the Mg/Ca values were translated into estimated water temperatures based on the Chave (1954) correlation shown in figure 6. Note the horizontal axis gives the time used to obtain the profile.

6.2 Specimens retrieved from Rodrigues Island

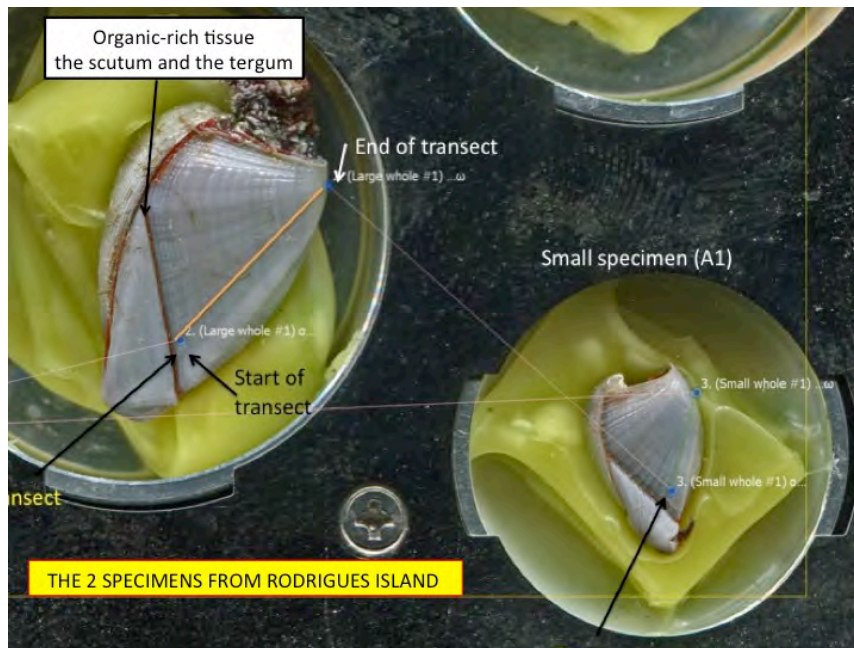


Figure 16. Photograph of the 2 entire barnacles collected on Rodrigues Island, mounted and kept inside the metal holder used of the LA-ICPMS analyses. The orange lines show the location of the transects performed on the scuta after strong ablation was performed before the analyses were performed. The results of the analyses are displayed in the following two figures.

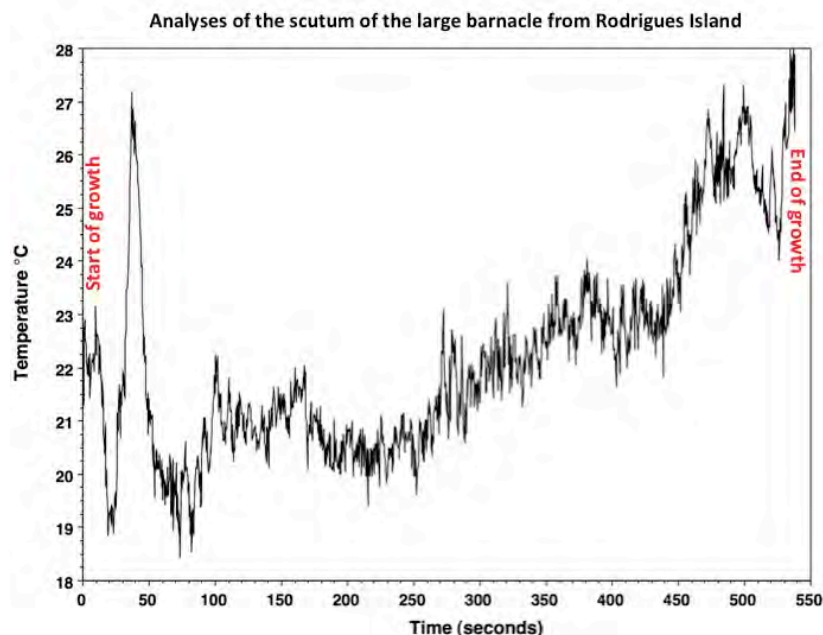


Figure 17. Plot of the analyses performed along the **large** barnacle collected on Rodrigues Island after the strong cleaning procedure was performed with deep and wide ablation of the outer surface of the scutum shell. Once again the Mg/Ca values were translated into estimated water temperatures based on Chave (1954)' correlation shown on figure 6. Note the horizontal axis gives the time used to obtain the profile.

7. Discussion and interpretation of the results

7.1 Growth rates of *Lepas anatifera*

Based on the limited data available in the scientific literature, it is very hard to come up with an age of the barnacles that were found attached to the aircraft debris from either islands. The prime factor that seems to determine rate of growth is temperature (as shown in figure 8). However, as mentioned in the study of Inatsuchi et al. (2010), nutrients can also intervene in growth rate. The study of MacIntyre (1965) demonstrates a very obvious point: barnacles may take time before settling on floating material, and therefore we are unable to tell when the barnacles that adhered to the aircraft debris 'anchored' themselves. It is unknown whether they grow continuously after settlement. If we follow the findings of Inatsuchi et al. (2010) barnacles that were living in the ocean within the range of 19 to 29°C reached a capitulum size of 12 mm within 15 days, ca. 0.7-1 mm/day. It could be assumed the specimens analysed here were quite young, perhaps less than one month, considering that some of the scuta we analysed would have been part of much larger capitula, but not more than ~ 20mm.

7.2 Reconstructed water temperatures based on barnacle shell chemistry

Significant difficulties were encountered in attempting to reconstruct the temperatures of the waters in which the barnacles grew for several reasons; including

1. The data on the Mg content of barnacles published by Chave in 1954 is limited to only 9 samples, of which and we decided to eliminate three were eliminated as outliers. Hence, with only too few samples analysed, we have to be cautious due to large uncertainties surrounding the formed uncertainty of the relationship between Mg/Ca and temperature.
2. Large amounts of organic matter/tissue occur in specific regions of scutum shells [i.e. the brown spots visible in figure 3] and throughout the shell. These regions associated with organic matter are enriched in magnesium.
3. After ablating the outer surface of scuta (see figures 11, 12), we are unsure if some organic layers remained in the calcite even after ablation to obtain Mg/Ca of the calcite.
4. It is also obvious that the extermities of the scuta are the sites of early growth and final growth, are characteristically coloured brown [figures 4, 10 and 16], indicating the presence of organic matter. These areas contain higher measured Mg/Ca and their higher estimated temperatures compared to the rest of the scuta [see figures 13-15, 16-17]. We do not know if these temperature values are accurate due to the presence of organic matter.
5. The observations made in several previous studies [Evans, 1958; Skerman, 1958; Patel et al., 1959; McIntyre, 1965; Inatsuchi et al., 2009; Magni et al., 2015] indicate that the rate of growth of *Lepas anatifera* barnacles is affected by temperature and other factors such as nutrient availability. The rate of growth may also determine incorporation of Mg into the CaCO₃ precipitated by the barnacle as in other crustaceans which also secrete low-magnesium calcite (e.g. ostracods). Chivas et al. (1983) who grew ostracods in the laboratory under controlled conditions [temperature and salinity] identified that the early stages of growth of the organisms [when shell growth is very rapid] yielded higher Mg concentration compared to when the shells reached a stable weight and size. Thus, in general, faster growth results in higher Mg/Ca. Consequently, if barnacle growth rate changed with life stage or with nutrient availability, the Mg/Ca of the barnacle shell may change accordingly. We were unable to assess the impact of growth rate on barnacle shell chemistry.
6. Further difficulty at assessing the results of the analyses on the shells is that we are unaware as to (1) when the barnacles first adhered to the aircraft debris, (2) if

they did possibly undergo a period of reduced or no growth during their life, and (3) if all the barnacles on a single debris grew synchronously. Comparison of the profiles for two barnacle scuta collected on the same aircraft debris provided different estimated temperature profiles, thus confusing our possible interpretation of the path in the Indian Ocean where the barnacles may have grown.

7. Reference to the distribution of the monthly average sea surface temperatures in the Indian Ocean obtained from the NOAA web site that span several years (see figure 19 below), indicates that if the aircraft had impacted the ocean at a high latitude in the lower half of the grey rectangle shown on the map, the estimated temperature should have been within the vicinity of 16 to 18°C in March. As circulation as the surface of the Indian Ocean follows an anticlockwise gyre on the eastern side of the Indian Ocean, temperatures at which the barnacle shells grew might be expected to increase (along the flow path) and eventually reach values of 24 to 27°C depending on the time when the debris reached the islands. If, on the other hand, the aircraft had impacted the ocean at a lower latitude, the profile of estimated temperature ought to have shown little variation.
8. Finally, we still do not know the timing of barnacle adherence to the debris, or the respective ages of the barnacle.

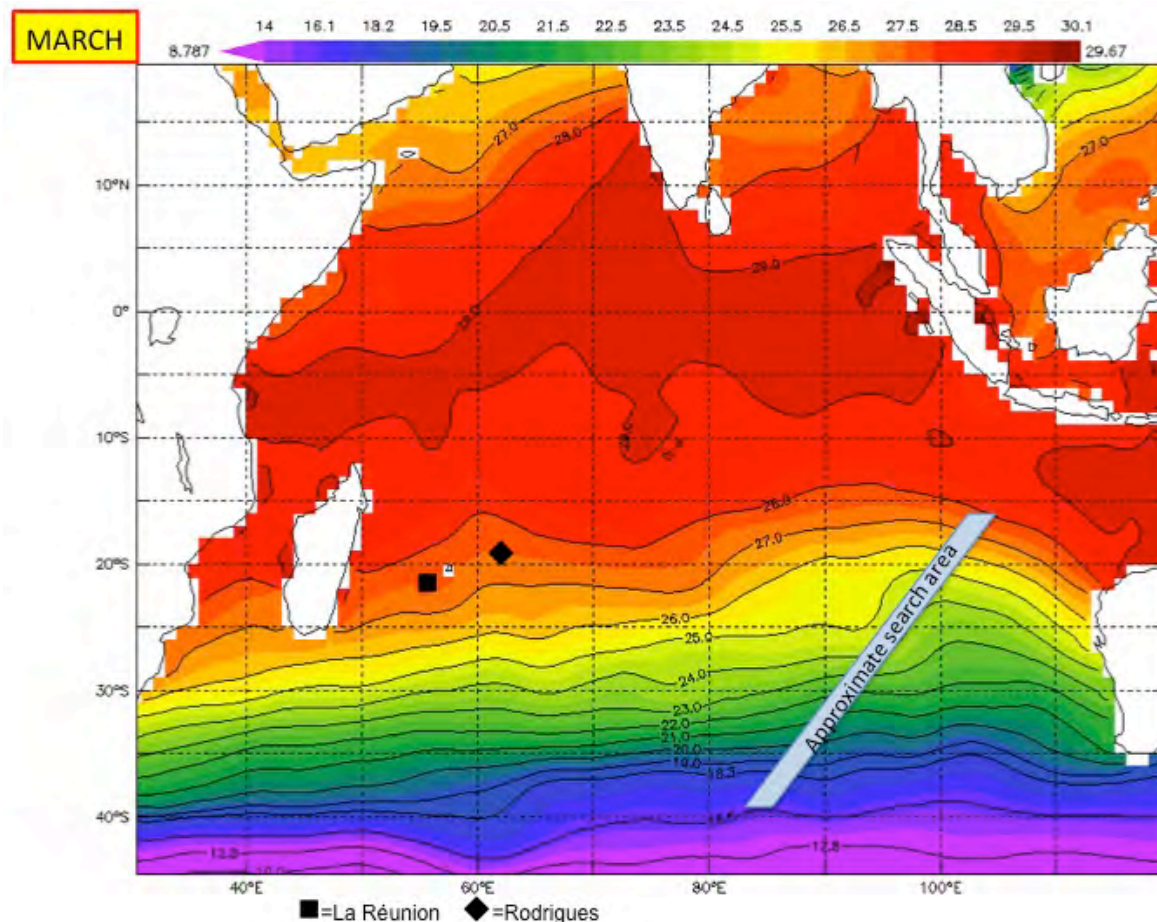


Figure 18. Average sea-surface temperature [SST] map for March for the Indian Ocean obtained from <http://ferret.pmel.noaa.gov>. The location of the 2 islands [La Réunion and Rodrigues] on which barnacles recovered from the aircraft debris were found. The approximate area of the search for the aircraft is shown in grey (although in reality it is arcuate in shape). Note also the colour schemes for the SSTs varies slightly between this figure and figure 19 below.

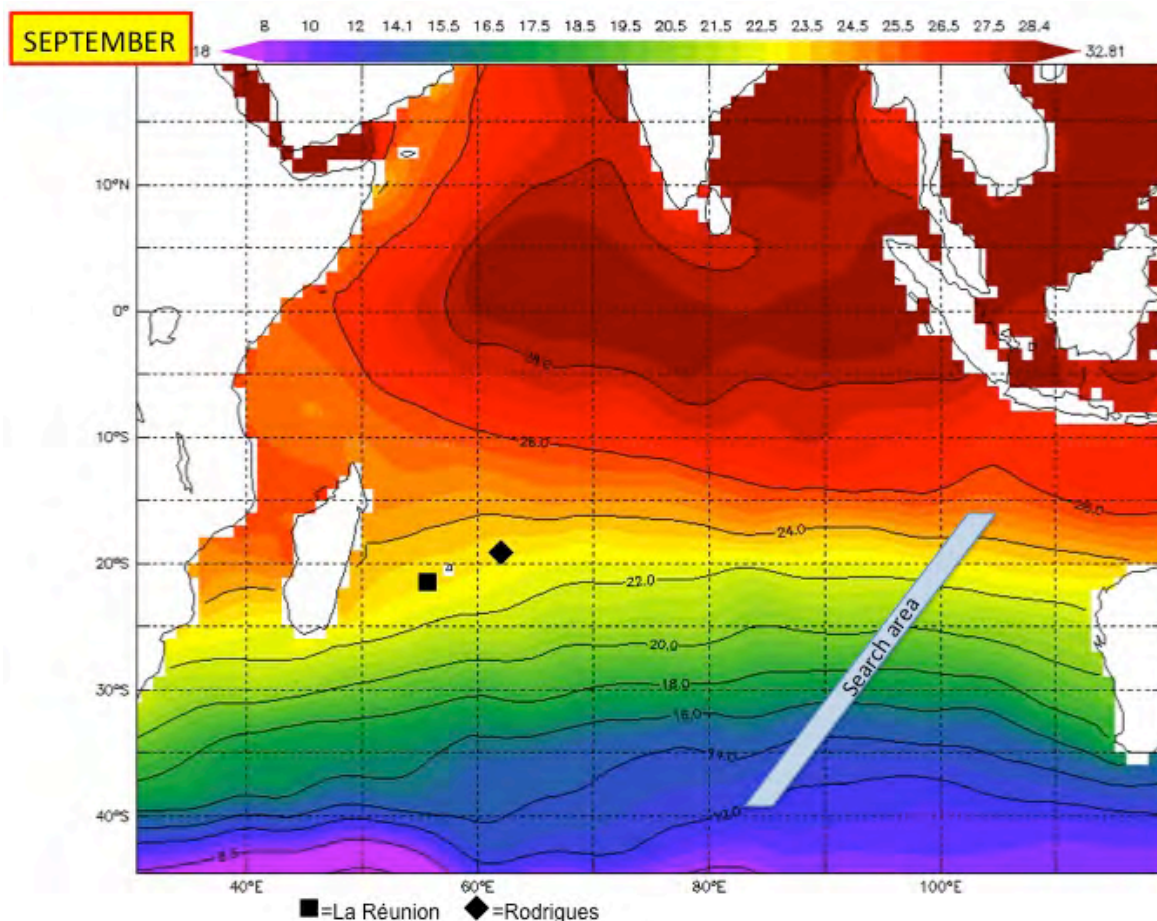


Figure 19. Average sea-surface temperature [SST] map for September for the Indian Ocean obtained from <http://ferret.pmel.noaa.gov>. This is displayed to identify the seasonality in SSTs between March and September. The location of the 2 islands [La Réunion and Rodrigues] on which barnacles recovered from the aircraft debris were found. The approximate area of the search for the aircraft is shown in grey (although in reality it is arcuate in shape). Note also the colour schemes for the SSTs varies slightly between this figure and figure 18 above.

8. Conclusions

If the aircraft had crashed at high latitude in the vicinity of the grey rectangle, and if the barnacle shells had commenced adhering to the plan debris soon after reaching the sea surface at that time, temperatures of the order of $\sim 18^{\circ}\text{C}$ should have been recorded by the shells. If on the other hand, the aircraft had impacted the ocean at a lower latitude in the rectangle, temperatures of $\sim 27\text{-}28^{\circ}\text{C}$ should have been recorded.

Note that seasonal changes of sea surface temperatures around La Réunion and Rodrigues Islands range between within a single year. So, if the barnacles had only started adhering to the aircraft debris in that region, the Mg/Ca of their shells ought to indicate values ranging between $\sim 23^{\circ}$ [for September; see figure 19] and $\sim 27.5^{\circ}\text{C}$ [for March; see figure 18].

Acknowledgements

I wish to thank Professor Stephen Eggins, Director of the Research School of Earth Sciences at the ANU for his permission to use ANU facilities. Mr Les Kinsley and Dr Pete Tollan also at ANU for expert help at using the Laser Ablation facility and processing the raw data.

Mr Joe Hattley from ATSB and Maggie Tran and John Pugh from Geoscience Australia, are all thanked for facilitating access to the barnacles and information on the missing

aircraft search. In addition, I wish to acknowledge the help of Professor Franck Bassinot and Dr Dominique Blamart of the Laboratoire des Sciences de l'Environnement et du Climat in Gif-sur-Yvette, France for providing barnacle specimens they also analysed and the many long phone conversations at night and on weekends concerning the interpretation of the results presented here.

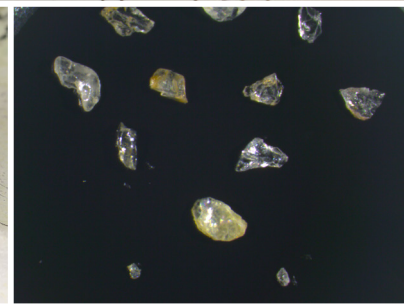
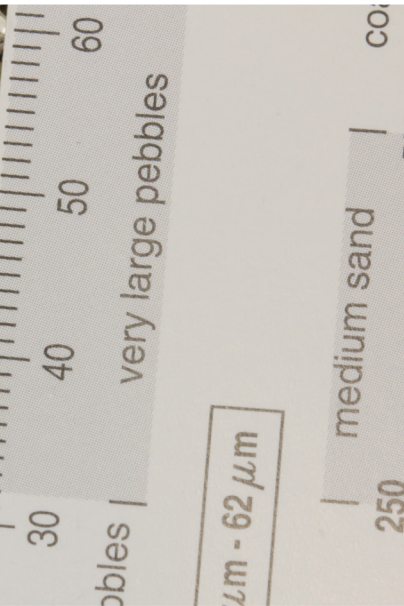
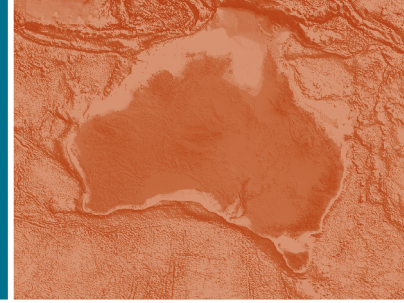
The interpretation of the results are my own responsibility.

References

- Blamart, D. Bassinot, F. 2016. Rapport d'expertise: Estimation des températures de croissance des valves de cirripèdes fixes sur le flaperon du vol MH370 à partir de l'analyse de leur composition isotopique $^{18}\text{O}/^{16}\text{O}$. Submitted to the 'Tribunal de Grande Instance de Paris' [unpublished].
- Chave, K.E. 1954. Aspects of the Biogeochemistry of Magnesium 1. Calcareous Organisms. *The Journal of Geology* 62, 266-283.
- Chivas, A.R., De Deckker, P., Shelley, J.M.G. 1983. Magnesium, strontium, and barium partitioning in nonmarine ostracode shells and their use in paleoenvironmental reconstructions – a preliminary study. In *Applications of Ostracoda* (R. F. Maddocks, ed.), University of Houston Geoscience, pp. 238-249.
- Clarke, F.W., Wheeler, W.C. 1917. The inorganic constituents of marine invertebrates. U.S. Geological Survey Professional Paper 124.
- Dakin, W.J. 1973. *Australian Seashores*. Revised edition, assisted by I. Bennett & E. Pope. Angus & Robertson Publishers, Sydney.
- Darwin, C. 1852. *A monograph of the subclass Cirripedia, with figures of all species. The Lepadidae, or pedunculated cirripedes*. Volume 1. The Ray Society, London, 400 pp.
- Eggs, S.M., De Deckker, P., Marshall, J. 2003. Mg/Ca variation in planktonic foraminifera tests: implications for reconstructing palaeo-seawater temperature and habitat migration. *Earth and Planetary Science Letters* 212, 291-306.
- Eggs, S.M., Kinsley, L.K., Shelley, J.M.G. 1998. Deposition and element fractionation processes occurring during atmospheric pressure laser sampling for analysis by ICPMS. *Applied Surface Science* 127-129 278-286.
- Evans, F. 1958. Growth and maturity of the barnacles *Lepas hillei* and *Lepas anatifera*. *Nature* 182, 1245-1246.
- Inatsuchi, A., Yamato, S., Yusa, Y. 2009. Effects of temperature and food availability on growth and reproduction in the neustonic pedunculate barnacle *Lepas anserifera*. *Marine Biology* 157, 899-905.
- Killingley, J. S. & Newman, W. A. 1982. O^{18} fractionation in barnacle calcite – a barnacle paleotemperature equation. *Journal of Marine Research* 40, 893-901.
- Magni, P.A., Venn, C., Aquila, I., Pepe, F., Ricci, P., Di Nunzio, C., Ausania, F., Dadour, I.R. 2015. Evaluation of the floating time of a corpse found in a marine environment using the barnacle *Lepas anatifera* L. (Crustacea: Cirripedia: Pedunculata). *Forensic Science International* 24 (doi.org/10.1016/j.forsciint.2014.11.016).
- McIntyre, R.J. 1966. Rapid growth in stalked barnacles. *Nature* 212, 637-638.
- Patel, B. 1959. The influence of temperature on the reproduction and moulting of *Lepas anatifera* L. under laboratory conditions. *Journal of the Marine Biological Association of the United Kingdom* 38, 589-597.
- Shiffer, P.H., Herbig, H-G. 2016. Endorsing Darwin: global biogeography of the epipelagic goose barnacle *Lepas* spp. (Cirripedia, Lepadomorpha) proves cryptic speciation. *Zoological Journal of the Linnean Society* doi: 10.1111/zoj.12373.
- Skerman, T.M. 1958. Rates of growth in two species of *Lepas* (Cirripedia). *New Zealand Journal of Science* 1, 402-411.
- Treatise of Invertebrate Paleontology (1969) Part R. Arthropoda 4, volume 1. The Geological Society of America Inc & The university of Texas.

Appendix G – Summary of Analyses Undertaken on Debris Recovered During the Search for Flight MH370

Note: When the samples were originally created for analysis, there was discussion about providing one of the samples to Boeing for analysis. However, the ATSB and Geoscience Australia later determined that no analysis by Boeing was necessary and retained the samples.
(Page 44)



Record 2017/11 | eCat 110564

Summary of Analyses Undertaken on Debris Recovered During the Search for Flight MH370

A collation of reports describing quarantine and parts analysis undertaken by Geoscience Australia

M. Tran, W.A. Nicholas, J. Chen, Z. Hong, J. Sohn, T. Whiteway, J. Pugh, and C. Thun

Summary of Analyses Undertaken on Debris Recovered During the Search for Flight MH370

A collation of reports describing quarantine and parts analysis undertaken by Geoscience Australia

GEOSCIENCE AUSTRALIA
RECORD 2017/11

M. Tran, W.A. Nicholas, J. Chen, Z. Hong, J. Sohn, T. Whiteway, J. Pugh, and C. Thun

Department of Industry, Innovation and Science

Minister for Resources and Northern Australia: Senator the Hon Matthew Canavan

Assistant Minister for Industry, Innovation and Science: The Hon Craig Laundy MP

Secretary: Ms Glenys Beauchamp PSM

Geoscience Australia

Chief Executive Officer: Dr James Johnson

This paper is published with the permission of the CEO, Geoscience Australia



© Commonwealth of Australia (Geoscience Australia) 2017

With the exception of the Commonwealth Coat of Arms and where otherwise noted, this product is provided under a Creative Commons Attribution 4.0 International Licence.

(<http://creativecommons.org/licenses/by/4.0/legalcode>)

Geoscience Australia has tried to make the information in this product as accurate as possible. However, it does not guarantee that the information is totally accurate or complete. Therefore, you should not solely rely on this information when making a commercial decision.

Geoscience Australia is committed to providing web accessible content wherever possible. If you are having difficulties with accessing this document please email clientservices@ga.gov.au.

ISSN 2201-702X (PDF) 110564

ISBN 978-1-925297-48-5 (PDF)

eCat 110564

Bibliographic reference: Tran, M., Nicholas, W.A., Chen, J., Hong, Z., Sohn, J., Whiteway, T., Pugh, J. & Thun, C. 2017. Summary of analyses undertaken on debris recovered during the search for flight MH370: a collation of reports describing quarantine and parts analysis undertaken by Geoscience Australia. Record 2017/11. Geoscience Australia, Canberra.
<http://dx.doi.org/10.11636/Record.2017.011>

Version: 1701

Abbreviations

AM	Australian Museum
ANU	Australian National University
ATSB	Australian Transport Safety Bureau
GA	Geoscience Australia
µm	micrometre
m	metres
MAGNT	Museum and Art Gallery of the Northern Territory
MTQ	Museum of Tropical Queensland
NIWA	National Institute of Water and Atmospheric Research (New Zealand)
SEM-EDS	Scanning Electron Microscope-Energy Dispersive Spectroscopy
WAM	Western Australian Museum

Acknowledgements

The authors thank the following people for their generous contributions to this report through advice, research, time and expertise. Peter Foley, Joe Hattley, Jason Mcguire, Rob Smith, Seb Davey (Australian Transport and Safety Bureau); Andy Sherrell (Sherrell Ocean Services); Diana Jones (Western Australian Museum); Richard Willan and Chris Glasby (MAGNT); Dennis Gordon (National Institute of Water and Atmospheric Research); Robyn Cumming (Museum of Tropical Queensland); Elena Kupriyanova (Australian Museum); Megan McCabe, Andrew Carroll, Rachel Przeslawski, Christian Thun, Abby Loiterton, Ian Long, Billie Poignand, Simon Webber, Keith Sircombe, Bruce Kilgour (Geoscience Australia); Patrick De Deckker (Australian National University); the crew from Fugro Equator, Fugro Supporter, Fugro Discovery, Go Phoenix, Havila Harmony, Dong Hai Jiu and onshore staff of Fugro; Aslam Basha Khan bin Zakaria Maricar, Mohan Sippiah, Dato Kok Soo Chon (Malaysian Ministry of Transport). We also thank Drs Stephanie McLennan and Scott Nichol for reviewing this report.

Contents

Abbreviations	iii
Acknowledgements	iv
Contents	v
1 Executive Summary.....	7
2 Review of Sediment on Aircraft Pieces from Mozambique, Mossel Bay and Mauritius (Items 2 to 5).....	9
2.1 Summary.....	9
2.2 Methods	9
2.2.1 Establishing Geological Context	9
2.2.2 Sediment Analysis.....	10
2.3 Results for Items 2 and 3.....	10
2.3.1 Geological Context: Mozambique	10
2.3.2 Sediment Analysis Results.....	12
2.3.3 Discussion	15
2.3.4 Conclusion.....	16
2.4 Item 4	17
2.4.1 Geological Context: Mossel Bay, South Africa.....	17
2.4.2 Sediment Analysis Results.....	17
2.4.3 Discussion	17
2.4.4 Conclusion.....	17
2.5 Item 5	18
2.5.1 Geological Context: Rodrigues Island.....	18
2.5.2 Sediment Analysis Results.....	19
2.5.3 Discussion	19
2.5.4 Conclusions	20
2.6 References.....	21
3 Review of Macrofauna on Pieces from Mozambique (Item 2 and 3)	24
3.1 Summary.....	24
3.2 Method	25
3.3 Results	25
3.3.1 Item 2: Recovered From Daghatane Beach, Mozambique.....	25
3.3.2 Item 3 (Right Horizontal Stabilizer Panel): Recovered From a Beach in the Mozambique Channel	28
3.4 References.....	39
4 Stable Isotope Analyses of Paints on Aircraft Pieces From Mozambique (Items 2 and 3) and Mauritius (Item 5).....	40
4.1 Summary.....	40
4.2 Method	40
4.2.1 Sub-Sampling Items 2 and 3.....	40
4.2.2 Sub-sampling Item 5 and Control Sample	41
4.2.3 Isotopic Analysis of Items 2, 3 and 5 and the Control Sample.....	41
4.3 Results	42

5 Analyses of Organic Compounds on Aircraft Pieces From Mozambique (Item 2).....	44
5.1 Summary.....	44
5.2 Methodology	44
5.3 Results	44
5.4 References:.....	48
6 Review of Macrofauna on Aircraft Pieces Found on Mauritius and South Africa (Item 5).....	49
6.1 Summary.....	49
6.2 Method	50
6.3 Results	54
6.3.1 Item 4 (External Engine Cowling).....	54
6.3.2 Item 5 (Door R1 Stowage Closet)	54
6.4 References.....	56

1 Executive Summary

On 8 March 2014, the Boeing 777-200ER aircraft registered as Malaysia Airlines 9M-MRO and operating as flight MH370 (MH370) disappeared from air traffic control radar after taking off from Kuala Lumpur, Malaysia on a scheduled passenger service to Beijing, China with 227 passengers and 12 crew on board.

After analysis of satellite data it was discovered that MH370 continued to fly for over six hours after contact was lost. All the available data indicates the aircraft entered the sea close to a long but narrow arc of the southern Indian Ocean.

On 31 March 2014, following an extensive sea and air search, the Malaysian Government accepted the Australian Government's offer to lead the search and recovery operation in the southern Indian Ocean in support of the Malaysian accident investigation.

On behalf of Australia, the Australian Transport Safety Bureau (ATSB) coordinated and lead the search operations for MH370 in the southern Indian Ocean. Geoscience Australia (GA) provided advice, expertise and support to the ATSB in sea floor mapping (bathymetric survey) and the underwater search. Geoscience Australia has also provided quarantine facilities for receipt of possible debris, and has undertaken laboratory analyses for a number of these pieces.

Over twenty debris items of interest to the ATSB investigation team have washed up on the east and south coast of Africa, the east coast of Madagascar and the Islands of Mauritius, Reunion and Rodrigues in the Indian Ocean. Of these, a number of items were sent to Australia for identification and examination. Items transported to Australia were received through Geoscience Australia's Quarantine Approved Premise prior to analysis and ATSB investigation (Table 1).

This record compiles reports produced during the course of the laboratory analyses and investigation. The record is divided into five sections (reports) and covers the results of each analytical technique that Geoscience Australia has applied to the debris items:

1. Analysis of sediment to identify if the items had beached at any other locations prior to their discovery, and
2. Analysis of marine fauna found on the items to assess:
 - a) the length of time the items were in the water (based on the age and growth rates of particular species present),
 - b) the possible location of the aircraft crash site (based on age and growth rates of marine fauna endemic to particular ocean areas),
3. Analysis of stable isotopes and organic compounds to identify if there were any unusual chemical signatures on the items.

Results from these analyses show that:

- The constituents of sediment found on Items 2 to 5 match the location at which the items were recovered and were comprised natural and loose aircraft material.
- Macrofaunal analyses of Items 2 and 3 showed that these aircraft pieces were colonized with opportunistic and cosmopolitan species originating from the tropical Indo-Pacific Ocean. No evidence of cool or cold-temperate molluscs or annelids was found.

- Stable isotope analysis of the paint on the aircraft items analyzed indicated that all samples tested might have come from the same source.
- Organic compound analyses on aircraft pieces indicated that results were consistent with organic compounds of grease, lubricants or lubricant additives and possibly derived from higher plant origin petroleum.

Table 1. Summary of analyses on pieces of debris undertaken by Geoscience Australia

Item Reference Number*	Date Received at GA	Analyses undertaken	Relevant Reports
2	21/03/2016	Sedimentology	Review of sediment on pieces from Mozambique, Mossel Bay and Mauritius (Items 2 to 5)
		Macroecology	Review of macrofauna on pieces from Mozambique (Items 2 & 3)
		Isotopes	Stable isotope analyses of paints on pieces from Mozambique (Items 2 & 3) and Mauritius (Item 5)
		Geochemistry	Analyses of organic compounds on the MH370 pieces from Mozambique (Item 2)
3	21/03/2016	Sedimentology	Review of sediment on pieces from Mozambique, Mossel Bay and Mauritius (Items 2 to 5)
		Macroecology	Review of macrofauna on pieces from Mozambique (Items 2 & 5)
4	14/04/2016	Sedimentology	Review of sediment on pieces from Mozambique, Mossel Bay and Mauritius (Item 2 to 5)
		Isotopes	Stable isotope analyses of paints on pieces from Mozambique (Items 2 & 5) and Mauritius (Part 5)
		Macroecology	Review of macrofauna on possible MH370 Aircraft pieces found on Mauritius and Mozambique (Items 4 to 5)
5	14/4/2016	Sedimentology	Review of sediment on pieces from Mozambique, Mossel Bay and Mauritius (Items 2 to 5)
		Macroecology	Review of macrofauna on possible MH370 Aircraft pieces found on Mauritius and Mozambique (Items 4 to 5)
		Isotopes	Stable isotope analyses of paints on pieces from Mozambique (Items 2 & 3) and Mauritius (Item 5)

* Item reference numbers are consistent with the Malaysian Ministry of Transport and further information on each of these items can be found at:

http://www.mh370.gov.my/phocadownload/3rd_IS/Summary%20of%20Debris%20Recovered%20-%2028022017.pdf

2 Review of Sediment on Aircraft Pieces from Mozambique, Mossel Bay and Mauritius (Items 2 to 5)

2.1 Summary

This report provides a review of the sediment found on aircraft pieces recovered from Daghatane Beach, Mozambique (Item 2), Mozambique Channel (Item 3), Mossel Bay (Item 4) and Rodrigues Island, Mauritius (Item 5). For consistency, the four pieces are labelled as Right wing No. 7 Flap Track Fairing (Item 2), Right Horizontal stabiliser panel piece (Item 3), Engine Nose Cowl (Item 4) and Door R1 Stowage Closet (Item 5). This report is structured into three sections to address the different locations of debris discovery. The key findings from the study are:

- Each of the sediment samples analysed was observed to have constituents that closely match either published evidence, or in the case of the sample from Rodrigues Island, to match what would broadly be expected at the location at which the piece was recovered.
- No material was observed that would indicate a source distal to the location from which the aircraft pieces were found.
- Each sediment sample examined had a minor component of honeycomb material from the aircraft. The presence of loose honeycomb material suggests that natural sediment and other material could have been transported within the aircraft pieces, but this was not able to be confirmed.
- Sediment grains from the Rodrigues sediment sample were examined by scanning electron microscope-energy dispersive spectroscopy (SEM-EDS) to determine if the grains were natural or man-made, with results confirming that only natural material was present in the sample.

Caveats: Some criteria were applied to the acceptance of samples analysed, these include:

- Any sediment within voids that could not be accessed without destructively breaking apart the pieces was not sampled, and
- Any sediment < 100 µm was not analysed.

2.2 Methods

The following procedures were followed for inspection of sediment samples from all aircraft items numbered 2 to 5 provided to Geoscience Australia.

2.2.1 Establishing Geological Context

The locations where the aircraft pieces were recovered are not locations normally studied at Geoscience Australia. Thus the first part of this investigation was to establish geological context for the material being studied. Once the geological background was broadly established, insight was gained by intensively analysing the first two samples. Once this baseline understanding of the sediment from the aircraft parts, and the sediment from locations where they were found was thoroughly understood, it was possible to more rapidly investigate the other samples.

2.2.2 Sediment Analysis

Two samples were sieved into three grain-size intervals (100-500 µm, 500-1000 µm and > 1000 µm) and inspected using a binocular microscope at Geoscience Australia. To compare the characteristics of the sediment with descriptions of the environment in which they were found a detailed assessment of the components of each sediment sample was made. Sand grains were identified and counted using standard point-counting techniques. A minimum of 300 grains were used to make inferences on sediment sample composition and history. The principal constituents of each sample were counted, both for the mineral grains, and for the total mineral and biogenic carbonate assemblage. Grain counts were limited to 10 identifiable components.

2.3 Results for Items 2 and 3

2.3.1 Geological Context: Mozambique

The coastal locations at which the pieces were found in Mozambique are situated within the adjacent Gaza and Inhambane provinces, set within an expansive coastal plain that stretches across south and central Mozambique. Two prominent rivers discharge on the Gaza-Inhambane coast. These are the Limpopo at Xai Xai, and the Save, which discharges at Nova Mambone (Figure 1). Additionally, 270 km north of the Save delta, the Zambesi river, the largest river in southeastern Africa, enters the Mozambique Channel south of Quelimane. Both the Zambesi and the Limpopo rivers incise Precambrian igneous, and to a lesser extent, metamorphic terranes and discharge large volumes of sediment to the continental shelf and Mozambique Channel. The Zambesi discharges northeast from its delta, away from the locations where aircraft pieces were found (Schultz et al., 2011). The precise route of sediment dispersal once it reaches the coast from the Limpopo River is uncertain. However, based on the evidence from sediment bedforms at Maputo, and the general form of the coastal geomorphology, it is likely the Limpopo discharges northwards, potentially in the same direction as the longshore drift. Thus, the locations of Items 2 to 3 lie along this northward route of Limpopo sediment transport (Figure 1).

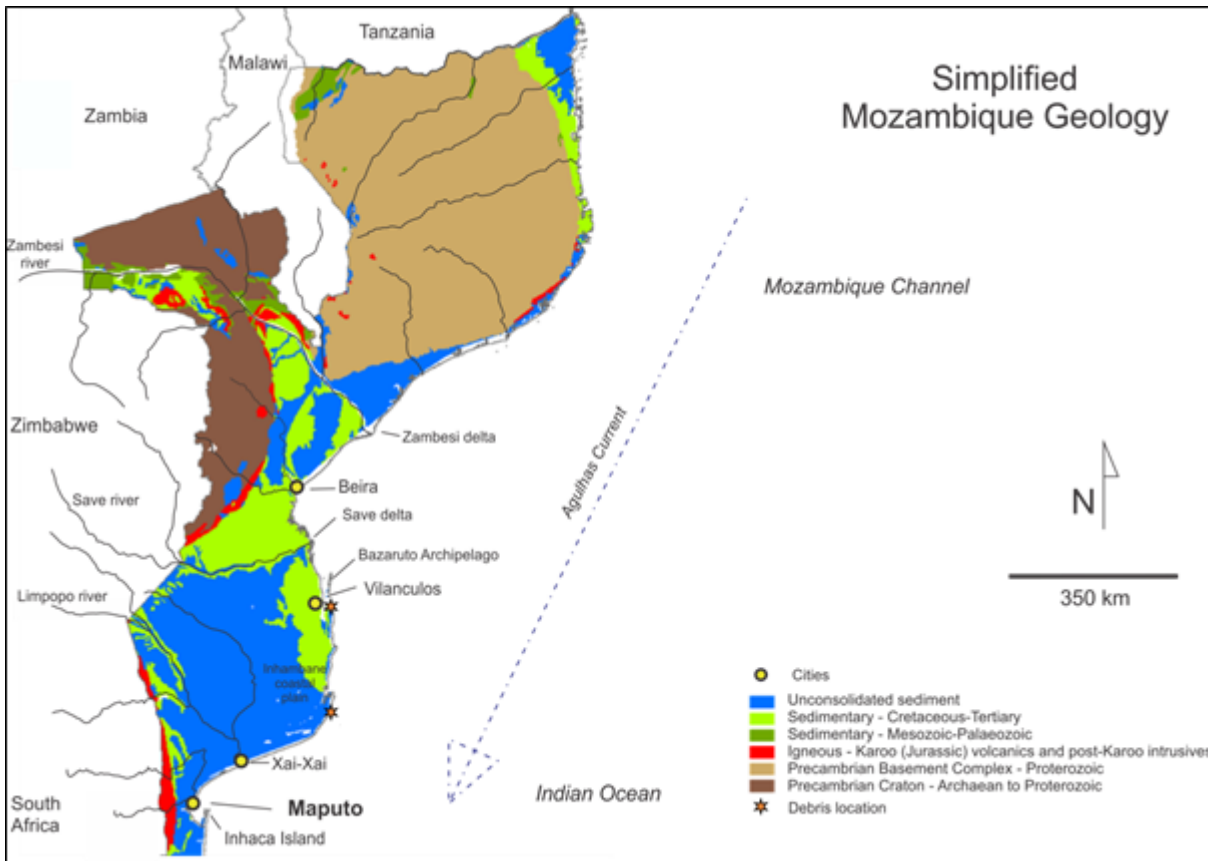


Figure 1. Geological context of the locations where aircraft pieces were found on the Mozambique coast. Map adapted from http://earthwise.bgs.ac.uk/index.php/Hydrogeology_of_Mozambique

Between the city of Maputo, southwest of the Limpopo estuary, and the Save delta, the coast is dominated by modern and Pleistocene age coastal dunes, underlain by Quaternary, Paleogene and Neogene sedimentary strata (Rutten et al., 2008). The principal landforms along this coast are parabolic dunes that in many instances are 1-2 km or more in length. These dunes also form the islands of the Bazaruto Archipelago, located approximately 12 km offshore from Vilanculos south of the Save delta, and where one aircraft piece was reported to be found at the southern end of the archipelago. The modern coastal parabolic dunes on Bazaruto Island are underlain by older unconsolidated reddish-yellow sands and aeolianite, suggesting long-term deposition, reworking and aeolian dune formation (Armitage et al., 2006). Bazaruto Island appears typical of the coastal sediments between Maputo and the Save river delta, and its geomorphology suggests considerable erosion of the coastal margin and redeposition of sediment inland has occurred in the past. Dune sands on the mainland coast opposite Bazaruto Archipelago are fine to medium grained (Avis et al., 2015). To the south, at the Mozambique-South Africa border, aeolian dunes rise up to 143 m above sea-level (Botha et al., 2003), and along the Inhambane coast active coastal dunes have been reported to be up to 191 m above sea-level (Tinley, 1985). Inland from the coast, between Maputo and the Save delta, calcrete is ubiquitous. In contrast, the coastal strata appear uncalcified, and the presence of several generations of dunes strongly suggests a long history of aeolian reworking of coastal sands. These reworked mineral grains tend to be fine to medium grained and rounded in shape.

At the location where Item 2 was found (Vilanculos), the Mozambique coast is characterised by dunes, mangrove swamps and shallow lakes, with seagrass meadows and coral reefs offshore. The Quaternary geology of the Bazaruto islands appears similar in composition and age to Inhaca Island, at Maputo (Armitage et al., 2006). Inhaca Island sedimentology, morphology, age and composition is well documented (Perry, 2005; Perry and Beavington-Penney, 2005; Peche, 2012).

Sediments comprise fine to medium quartz sand (monocrystalline) that is typically angular to rounded when observed in thin section (Peche, 2012). Accessory minerals include ilmenite and peridot (olivine). Similarly, tidal flats are characterised by sub-rounded to rounded quartz that comprises up to 90% of sediment.

On the inner to mid continental shelf, south of Maputo, seabed sediments comprise fine to medium-grained quartzose sand in the 20-50 m depth range (Green, 2009). Further south, surficial sands such as those to the south in Lake Sibaya, consist of well sorted, fine to medium grained quartz sand (Wright et al., 2000), that may be equivalent to those at Inhaca Island and Maputo. The key point here is that there appears to be a significant amount of terrestrial quartz within this part of the Mozambique coast and shelf, but detailed petrographic descriptions of these units are limited to those from Inhaca Island (Peche, 2012; Perry, 2005; Perry and Beavington-Penney, 2005). Maputo is ~ 50 km from the Limbombos Mountains to the west, where rhyolites and basalts are presently being eroded by numerous small creeks and streams that feed into the rivers discharging into Maputo Bay. It is highly likely that much of the quartz sediment present in Maputo Bay is sourced from the Limbombos mountains igneous units that are part of the regionally important Jurassic Karoo flood basalt province (Manninen et al., 2008). The Limpopo, Save and Zambezi rivers also incise the Karoo flood basalt province strata, and older igneous strata. Sediment chemistry indicate the Limpopo and its offshoot, the Olifants River, are both sourced from mafic (cf. basaltic) source rock while the Zambezi river to the north is largely sourced from felsic (cf. granitic) rock (Garzanti et al., 2014). Additionally, the Olifants River drains the huge Paleoproterozoic layered mafic intrusion of the Bushveld Complex and similarly incises through the Karoo Flood Basalts (Von Gruenewaldt et al., 1985; Garzanti et al., 2014).

2.3.2 Sediment Analysis Results

Both samples from Item 2 and Item 3 are dominated by low sphericity, angular to sub-rounded, clear, glassy, crystalline grains, most of which are quartz (Table 1). No clay or silt particles (silt + clay = mud) were observed in these samples, nor was mud observed on the aircraft pieces (from photographs). There are rare mineral grains that are clear, glassy, and crystalline and have one or two apparent cleavages. These are most likely zeolites (formed by chemical processes from original igneous minerals), but have been included in the quartz fraction for simplicity. In addition to these, a small proportion of rounded, anhedral yellow crystalline grains are present, many of which are likely reworked or secondary quartz. Also identified in the sample were rare grains of a pink crystalline mineral, a prismatic ilmenite, and olivine (anhedral), and an unidentified aquamarine coloured mineral (tentatively identified as the mineral aquamarine).

Table 1. Mineral grain counts from Items 2 & 3.

Sample and sieve size (µm)	Total count	Quartz clear, very angular to angular (%)	Quartz, clear, sub-angular to sub-rounded (%)	Quartz, clear, rounded to very rounded (%)	Yellow minerals Angular (%)	Yellow minerals rounded (%)	Green minerals angular (%)	Green minerals Rounded (%)	White Quartz (%)	Pink Minerals angular (%)	Pink minerals rounded (%)
1-1000	21	19.0	4.8	47.6	4.8	9.5	0.0	0.0	28.6	0.0	0.0
1-500	530	29.6	40.2	21.3	1.3	4.5	0.2	0.0	1.1	0.6	1.1
1-100	555	74.1	18.7	4.0	3.2	1.8	0.0	0.0	0.9	2.2	0.2
2-1000	13	7.7	30.8	38.5	7.7	15.4	0.0	0.0	0.0	0.0	0.0
2-500	315	36.5	47.0	15.9	0.6	1.3	0.0	0.0	0.6	0.0	0.0
2-100	516	59.9	27.9	7.0	0.4	0.6	1.0	0.6	0.6	2.7	0.4

Apart from minerals, the dominant constituent of the sediment samples, particularly from Item 3 (Table 2, Figure 2) is broken bryozoan pieces, which do not have any significant degradation. There are also trace amounts of benthic foraminifera and planktonic forams in both samples. In the fine-grained sediment of Item 3 (100 µm sieve) microscopic articulated bivalve molluscs were observed. A single juvenile (3 mm length) Goose Barnacle (*Lepas* sp) was present in the > 1000 µm sediment from Item 3. Broken specimens (n = 3) of the agglutinated foraminifera *Textularia hauerii* (Makled and Langer, 2010) are present in the 500-1000 µm subsample from both Item 2 and 3.

Table 2. Total assemblage counts for all pieces in representative sediment aliquots.

Sample and sieve size	Total # grains	Mineral grains (%)	Shells, unmodified, to sharp edges (%)	Shells, rounded, degraded (%)	Benthic Foraminifera (%)	Planktonic Foraminifera (%)	Ostracods, articulated (%)	Ostracods, disarticulated (%)	Bryozoan pieces (%)	Sponge spicules (%)	Echinoid spine pieces (%)
1-1000	24	16.7	4.2	41.7	4.2	8.3	0	0	25	0	0
1-500	542	90.2	0.7	8.7	0.2	0	0	0	0.4	0	0
1-100	413	98.8	0.2	1.0	0	0	0	0	0	0	0
2-1000	301	7.7	3.0	8.3	0.3	0	0	0	81	0	0
2-500	439	49.1	1.4	4.9	1.9	0.2	0	0	43.7	0.5	0.5
2-100	516	90.9	0.2	0	0.8	0	1.2	0.2	4.4	4.6	0

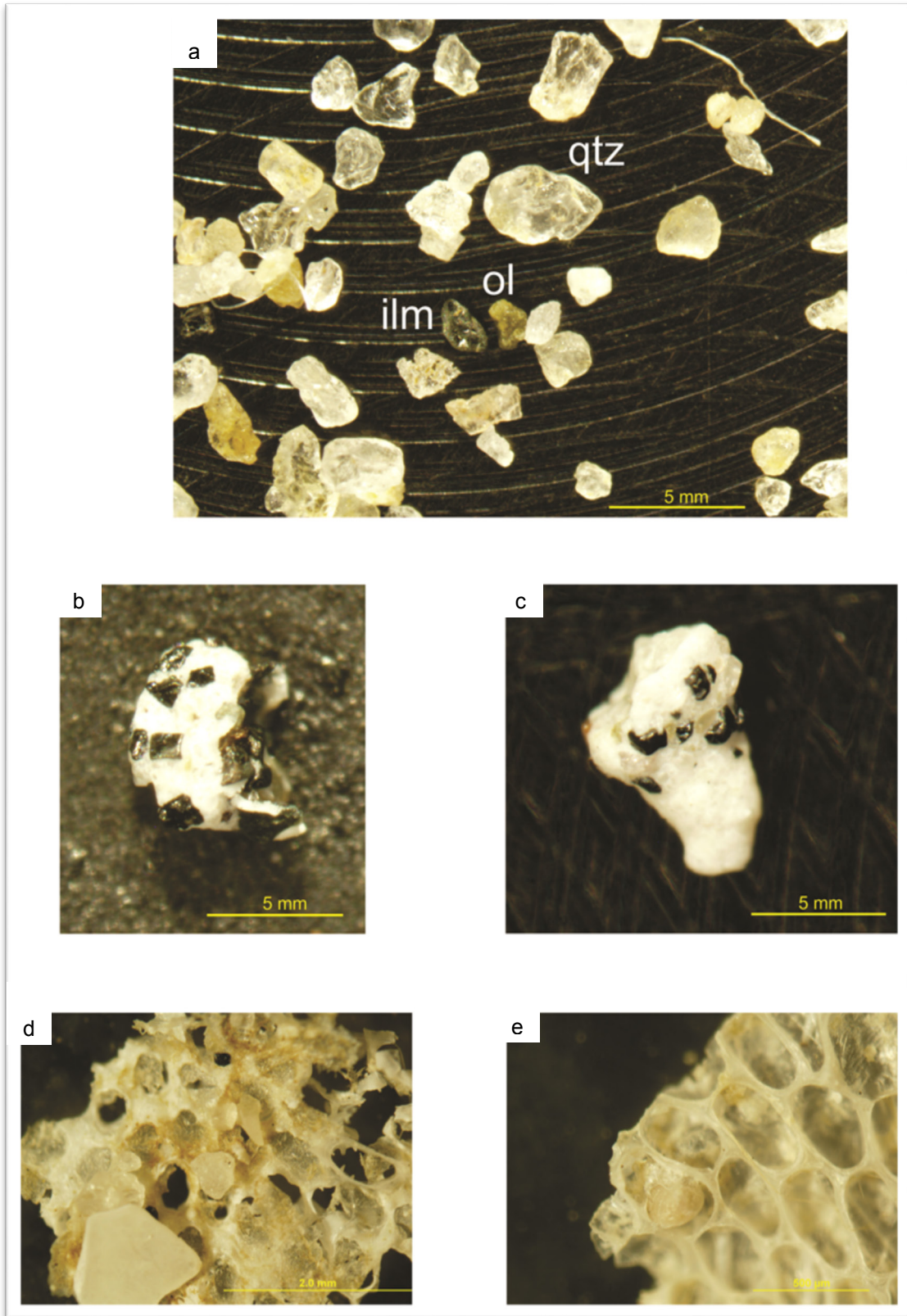


Figure 2. a) Example of clear crystalline grains of quartz (qtz), olivine (ol) and possible ilmenite (ilm); b) and c) examples of broken tests of agglutinated foraminifera that are possibly *Textularia hauerii* d'Orbigny with silt grains attached; d) and e) sediment grains attached underneath a bryozoan fragment and a benthic rotallid foraminifera overgrown by an enclosing bryozoan colony.

2.3.3 Discussion

The majority of quartz grains in samples from Item 2 and Item 3 appear young, unaltered, and angular to slightly rounded. The dominant proportion of minerals in the fine sediment fraction (100 µm sieve) are angular. The presence of minor amounts of ilmenite and olivine together with the juvenile nature of the quartz suggest the assemblage of minerals may potentially be from similar source material. The presence of pristine, angular mineral grains would require a crystalline, magmatic or high-grade metamorphic source rock, and either a proximal terrestrial source (e.g. volcanic rock or granites close to shore), or large rivers to deliver relatively unrounded sediment derived directly from the crystalline source rock, to the coast. All the rivers in the region where the debris pieces were recovered derive sediment from old igneous and metamorphic terrains, with the igneous Karoo Flood Basalt lavas and related igneous intrusive rocks west of Maputo for example, being closest to the coast.

The dominance of very angular to angular, juvenile quartz grains in fine sand-sized sediment is possible where the source rock is unaltered, where the transport distance is relatively short, and transport only occurs in water rather than in air. Ilmenite occurs in a wide variety of igneous and metamorphic rocks as a high-temperature accessory mineral (Wechsler and Prewitt, 1984) and is commonly found in placer deposits worldwide, because of its resistance to physical and chemical degradation (Riffel et al., 2016). In stark contrast, olivine is rapidly weathered to form clay minerals. Their presence together in the debris samples suggests they have either come from the same source via the same or similar pathways, or they are mixed from different sources. Both ilmenite and olivine are common to the basalt-rich igneous terrains of South Africa and Mozambique, but also to island basalt sources including Grand Comoros in the north of the Mozambique Channel, as well as La Reunion and Mauritius. Similar to the quartz sand at Maputo, igneous rock is the most likely source of any clear monocrystalline quartz along this coast, including any grains that remain angular. This is because comparatively little rounding and frosting of igneous silicic and lithic grains occurs while they are being transported in water (Haines and Mazzullo, 1988). In contrast, rounding, frosting and pitting and other degradation of quartz and similar minerals tends to be very rapid under aeolian conditions.

Skeletal carbonate in the samples from Items 2 and 3 is composed primarily of bryozoans and foraminifera. In the larger grained samples, quartz grains were trapped within some open bryozoan opercula, and underneath (on the base of) bryozoan pieces. One quartz grain was trapped by bryozoan mineralisation, indicating that the bryozoan had grown around the quartz grain. Some foraminifera are also encased by bryozoan mineralisation, indicating that the foraminifera were present before the mineralisation by bryozoans. The timing of bryozoan growth is not known, thus the foraminifera and quartz grains trapped may have been transported in a marine setting, or have been incorporated into the bryozoan structure within the aircraft piece at the shoreline where it was found. It is important to note however that the trapped foraminifera appear to be shallow-water benthic rotallids, with shallow water genera such as *Elphidium* present in the recovered sediment. Although occasional planktonic foraminifera are present, the trapped foraminifera are not planktonic. It would be possible for planktonic foraminifera to be trapped at any stage of the transport path of the aircraft pieces, but wherever the benthic foraminifera are sourced from must be shallow seabed. Thus at least some bryozoan growth occurred after the aircraft piece had passed through a shallow water setting.

The few foraminifera present are generally white in colour, commonly abraded, and are likely reworked benthic forms. These include genera such as *Elphidium* and *Amphistegina*. However, in these sediment samples foraminifera are few in number. Apart from one specific species, it is not possible to directly relate the examples found to a locality, as they are found globally. Additionally, it is commonly accepted that a relatively large number of microfossils are required to characterise an assemblage (≥300). As such it is not possible to infer whether one or more species are from locations distant to the locations at which the aircraft piece was recovered. However, foraminifera are marine organisms, and low numbers of foraminifera can be

present in areas of low salinity water, including estuaries and lagoons, either present as extant species or reworked from more marine settings.

In both samples (Item 2 and Item 3) fragments of an agglutinated foraminifera (*Textularia hauerii*; Makled and Langer, 2010) was observed, with ilmenite grains embedded within its test. This particular example of an agglutinated species with ilmenite grains attached has only been reported from the Bazaruto Archipelago, Mozambique (Makled and Langer, 2010). The presence of broken examples of *Textularia hauerii* may suggest transport from a zone where this species inhabits, either as part of the inspected sediment sample, or independent of it with post-transport incorporation into these samples. Onshore, to the south of Bazaruto Archipelago, a large ilmenite-rich placer deposit has recently been identified in surface (dredged) sediments at Mutamba (Riotinto.com) as well as extensive buried sands at Jangamo. This suggests that heavy minerals including ilmenite are readily available along the coast for agglutinated foraminifera to incorporate into their test structure because these dune sands are being eroded along the coast, and are incised into by local creeks and rivers.

The presence of rare planktonic foraminifera in these samples is of interest because benthic and planktonic foraminifera are not normally found together in shallow coastal sediments, unless the coasts are directly influenced by offshore water masses. Thus, their presence may indicate either that the coastal waters in which the aircraft pieces were recovered are influenced by offshore water masses and probably located close to open oceanic conditions, or that they are sourced and transported from a different area than where the debris was found.

The microscopic articulated bivalve molluscs in Item 3 are most likely derived from the coastal region of Mozambique because the post-mortem transport of these particularly fragile biogenic skeletal carbonate, very rapidly results in disarticulation and breakage. It may also be the case (although highly unlikely), that they have been transported to the Mozambique coast along with the aircraft pieces. If some of the biogenic carbonate material (foraminifera, ostracods, and bryozoans) represent material transported across an ocean, it indicates a transport pathway above the carbonate compensation depth (est -3000 m), below which CaCO_3 is dissolved. In the larger grain size samples, particularly Item 3 (1000 μm sub-sample), many mineral grains are attached, wrapped and partially encapsulated by a clear to translucent membrane. These agglomerated pieces are also attached to fibrous material that may be aircraft debris. The membrane in which the grains are fixed appears to be organic.

Fragments with metallic lustre and composed of plastic/polycarbonate of the same size as the mineral grains were also present. These had been variously torn, broken and twisted. The plastic/polycarbonate has low density (low specific gravity). These are believed to be pieces of aircraft, trapped within the large debris pieces. The colour and shape of these appear to be the same as the honeycomb structures that are present within the debris structure. The presence of these pieces, having been transported within the aircraft debris, suggests that sediment may also be transported from outside the locations at which the aircraft debris was found. Because of their similar geological composition, sediment from the Comoros Islands, Madagascar, and the Mascarene Islands could be present as part of the sediment recovered from the aircraft debris pieces. However, the weight of evidence suggests that the sediment recovered is derived from locations proximal to the recovery locations of the aircraft pieces.

2.3.4 Conclusion

There is insufficient evidence to identify a specific source for the sediment recovered from the two aircraft pieces. However, the Mozambique coast is logically the strongest candidate as the source of sediment in both cases. This is because the sediment petrology indicates a similarity between mineral grains in the recovered sediment, and the coastal sediment transported by large rivers from the Karoo Flood Basalts and

older igneous rock inland in Mozambique and South Africa. However, similar igneous rock is also present on La Reunion, the Comoros Islands, and Mauritius.

The evidence from biogenic carbonate is largely inconclusive, except that fragments of agglutinated benthic foraminifera (*Textularia hauerii*) were identified in the sediment from each piece of aircraft debris, with ilmenite grains embedded in the foram body wall. This association of ilmenite grains and agglutinated foraminifera is only known from one location, the Bazaruto Archipelago, on the southern Mozambique coast. Inland of Bazaruto Archipelago, an ilmenite placer deposit is present in surficial Cenozoic sediment, so it is likely these grains are locally derived at the site where the debris was recovered.

2.4 Item 4

2.4.1 Geological Context: Mossel Bay, South Africa

Mossel Bay is located near the eastern margin of the Southern Coastal Plain, South Africa (Cawthra, 2014; Cawthra et al., 2016). The coastal plain is relatively low-relief, bordered at its landward limit by the Cape Fold Belt (Locke, 1978), and at the seaward margin by the Indian Ocean. The coastal sediments along the Southern Coastal Plain are predominantly derived from the Cape Fold Belt mixed with marine carbonate and related cement formed at the coast during the Quaternary. Further landward of the Cape Fold Belt is the expansive Karoo Basin, where several of the large rivers that discharge to the Indian Ocean have their headwaters. Thus, the mineralogy of coastal sediments at Mossel Bay would potentially be similar to the coastal sediment of the southern Mozambique regions because they are ultimately sourced from very similar geology.

2.4.2 Sediment Analysis Results

The sediment in the sample from Item 4 is dominated by clear monocrystalline grains, most likely quartz, with some rounded yellowed grains, minor counts of foraminifera and a moderate proportion of multi-crystalline grains that are dominated by quartz. Shell and other bioclastic carbonate pieces were not common, except as broken, rounded grains that were commonly yellow (i.e. discoloured). In white light (i.e. normal daylight) the sample appears slightly yellow-brown. Under the microscope it is evident that because of the transparency of the clear grains the yellow colour of older and discoloured grains dominates the gross colour of the sample. This is similar to the samples from Mozambique.

2.4.3 Discussion

The angularity of sediment grains is very similar to those from the Mozambique coast, and the general composition (quartz rich with minor heavy minerals and low proportions of bioclastic carbonate) is also similar. The very low carbonate (i.e. lack of shelly sediment) is consistent with the general setting of Mossel Bay, and the position at which the aircraft piece was recovered (close to a river). Based on the composition and angularity of grains, this sediment sample resembles most closely the foreshore sample at the same location described by Cawthra (2014).

2.4.4 Conclusion

The sample of sediment from Mossel Bay is composed of very similar minerals and grains to that described in Cawthra (2014), a thesis describing the sediments, sedimentology and marine geology of Mossel Bay, South Africa. There is no evidence for any material from outside this location being present.

2.5 Item 5

2.5.1 Geological Context: Rodrigues Island

Rodrigues Island is the most isolated and easterly island of the Mascarene Island Group, which includes Mauritius and Reunion islands some 600 and 800 km to the east and southeast, respectively (Figure 3) (O'Leary and Perry, 2010). Rodrigues Island is a volcanic pedestal platform, with approximately 110 km² of land and a 240 km², 8 km wide lagoon. Lagoon water depths are typically less than 3 m and the lagoon is fringed by a near-continuous, 0.5-0.75 km wide, 90 km long barrier reef (O'Leary and Perry, 2010).

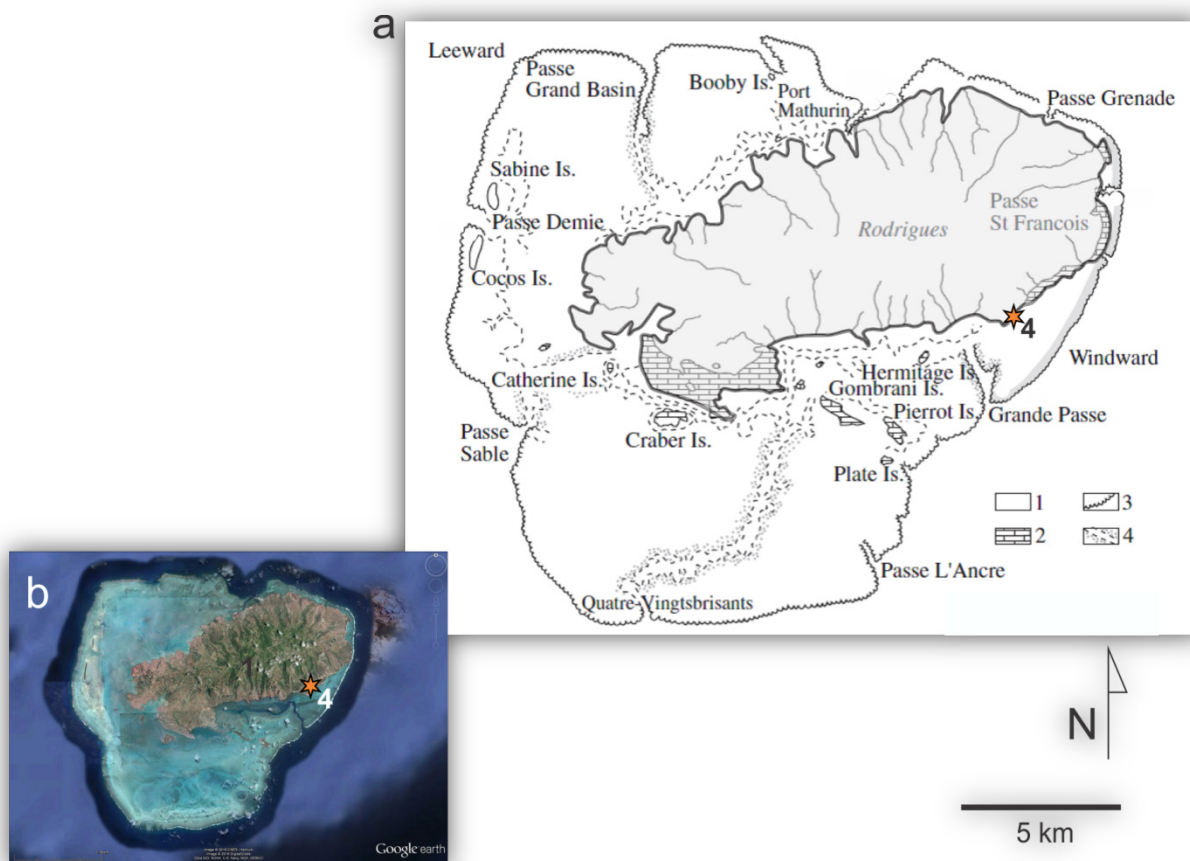


Figure 3. a) Map of Rodrigues Island, adapted from Rees et al., 2005, and b) Google Earth image of same. Location of debris (Item 5) is on the windward side of the island is shown.

Currents in the lagoon are wind-driven, flowing in a general clockwise direction (i.e. westerly to northwesterly) (O'Leary and Perry, 2010). At Port Mathurin, on the northern coast close to the reef margin, tidal amplitudes are up to 1.5 m, while at Mourouk, close to where the piece of debris was recovered, tidal amplitudes are broadly similar to Port Mathurin (Lowry, et al., 2008). Regionally, the South Equatorial Counter Current (SECC) flows east to west across the Mascarene plateau (Vianello, 2015; Badal et al., 2009; New et al., 2005). The southeast trade winds occur between June and October, and typically have accompanying swells of up to 2 m in amplitude (Naim et al., 2000, in Reese et al., 2004). For the rest of the year, winds are generally lighter, and produce swells less than 0.5 m amplitude. On nearby Mauritius, climate can be broadly divided into two seasons. These are the southeast lesser monsoon season, occurring between late June and late October, as on Rodrigues, and the northwest monsoon and cyclone season that extends from early December to May (Senapathi et al., 2010). Thus, because of their proximity, it would be

expected that Rodrigues Island also experiences a northwest monsoon and cyclone season during approximately the same season as Mauritius.

Large amplitude internal waves may be generated around the Mascarene Plateau (Lowry et al., 2008). Rodrigues Island is also affected by long wavelength swells from the southern ocean. Though the island is largely composed of basaltic rock, large areas of the southern and eastern coasts are covered with aeolian calcarenite, and these locations have many features typical of karst environments (Rees, et al., 2005; Burney et al., 2015).

2.5.2 Sediment Analysis Results

Approximately 60% of the sediment sample from Item 5 is composed of biogenic carbonate material, and most of this was broken and degraded. Most of the remainder consisted of sand-sized pieces of crystalline rock, commonly dark in colour and rounded, or sand-sized rock particles composed of a large proportion of variably rounded quartz-like minerals. This latter material is most likely to be aeolianite – a type of rock composed of carbonate cement and wind-blown sand grains. Of the biogenic components, only small barnacles were complete, unbroken, unaltered and intact.

Several grains were analysed to determine whether they are glass (i.e. man-made) or natural minerals. The results indicate all are natural, and all would potentially be associated with basalt or basalt-related igneous processes. In particular, the glass-like mineral grains were identified by the SEM-EDS analyser as zeolite – a chemical alteration mineral commonly formed by the interaction of basaltic minerals with seawater and/or groundwater (Figure 4).

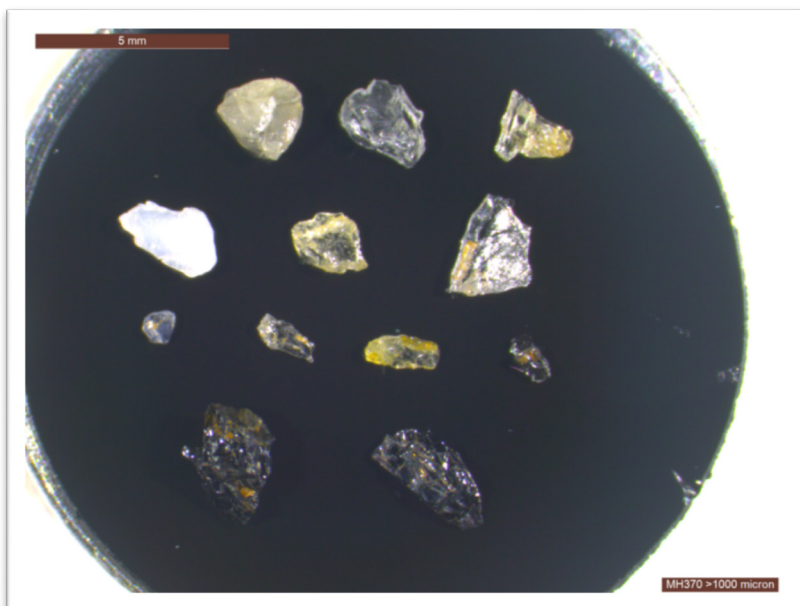


Figure 4. Photograph of mineral grains examined by SEM-EDS from the >1000 µm fraction from Item 5, Rodrigues Island.

2.5.3 Discussion

All the observed mineral grains and fine-grained pieces of rock (sand-sized sediment) are what would be expected at this location. No detailed sedimentological information was found in a literature search that would enable a direct comparison with the sediment sample examined.

2.5.4 Conclusions

The minerals and rock fragments in sediment from Item 5 are consistent with a source from Rodrigues Island. There are no minerals or biological material in the sample to indicate any other source of sediment.

2.6 References

- Armitage, S. J., Botha, G. A., Duller, G. A. T., Wintle, A. G., Rebêlo, L. P., Momade, F. J. 2006. The formation and evolution of the barrier islands of Inhaca and Bazaruto, Mozambique. *Geomorphology*, 82, 295-308.
- Armitage, S. J. 2003. Testing and application of luminescence techniques using sediment from the southeast African coast. PhD Thesis, University of Aberystwyth. 307 pp.
- Avis, T., Martin, T., Massingue, A. Buque, L. 2015. Nhangonzo coastal stream critical habitat biodiversity assessment: vegetation and floristic baseline survey. Sasol PSA development and LPG project, Inhambane province, Mozambique. Report No. 1521646-13550-24, EOH Coastal and Environmental Services. 57 pp.
- Badal, M. R., Rughooputh, S. D. D. V., Rydberg, L., Robinson, I. S., Patiaratchi, C. 2009. Eddy formation around south west Mascarene Plateau (Indian Ocean) as evidenced by satellite 'global ocean colour' data. *Western Indian Ocean Journal of Marine Science*, 8, 139-145.
- Botha, G. A., Bristow, C. S., Porat, N., Duller, G., Armitage, S. J., Roberts, H. M., Clarke, B. M., Kota, M. W., Schoeman, P. 2003. Evidence for dune reactivation from GPR profiles on the Maputaland coastal plain, South Africa. In: Bristow, C. S. and Jol, H. M. (eds): *Ground penetrating radar in sediments*. Geological Society, London, Special Publications, 211, 29-46.
- Burney, D. A., Hume, J. P., Middleton, G. J., Steel, L., Burney, L. P., Porch, N. 2015. Stratigraphy and chronology of karst features on Rodrigues Island, southwestern Indian Ocean. *Journal of Cave and Karst Studies*, 77, 37-51.
- Cawthra, H. C. 2014. The Marine Geology of Mossel Bay, South Africa. PhD Thesis, University of Cape Town. 256 pp.
- Cawthra, H. C., Compton, J. S., Fisher, E. C., MacHutchon, M. R., Marean, W. C. 2016. Submerged shorelines and landscape features offshore of Mossel Bay, South Africa. In: Harff, J., Bailey, G. & Luth, F. (eds.) *Geology and Archaeology: submerged landscapes of the continental shelf*. London: Geological Society.
- Garzanti, E., Padoan, M., Setti, M., Lopez-Galindo, A., Villa, I. M. 2014. Provenance versus weathering control on the composition of tropical river mud (southern Africa). *Chemical Geology*, 366, 61-74.
- Green, A. 2009. Sediment dynamics on the narrow, canyon-incised and current-swept shelf of the northern KwaZulu-Natal continental shelf, South Africa. *Geo-Marine Letters*, 29, 201-219.
- Haines, J. & Mazzullo, J. 1988. The original shapes of quartz silt grains: a test of the validity of the use of quartz grain shape analysis to determine the sources of terrigenous silt in marine sedimentary deposits. *Marine Geology*, 78, 227-240.
- Locke, B. E. 1978. The Cape Fold Belt of South Africa: tectonic control of sedimentation. *Proceedings of the Geological Association*, 89, 263-281.
- Lowry, R., Pugh, D. T. & Wijeratne, E. M. S. 2008. Observations of seiching and tides around the islands of Mauritius and Rodrigues. *Western Indian Ocean Journal of Marine Science*, 7, 15-28.
- Makled, W. A. & Langer, M. R. 2010. Preferential selection of titanium-bearing minerals in agglutinated Foraminifera: Ilmenite (FeTiO₃) in *Textularia hauerii* d'Orbigny from the Bazaruto Archipelago, Mozambique. *Revue de micropaleontologie*, 53, 163-173.

- Manninen, T., Eerola, T., Mäkitie, H., Vuori, S., Luttinen, A., Sévanno, A., Manhiça, V. 2008. The Karoo volcanic rocks and related intrusions in southern and central Mozambique. Geological Survey of Finland Special Paper 48, 211-250.
- New, A. L., Stansfield, K., Smythe-Wright, D., Smeed, D. A., Evans, A. J., Alderson, S. G. 2005. Physical and biochemical aspects of the flow across the Mascarene Plateau in the Indian Ocean. Philosophical Transactions of The Royal Society A: Mathematical, Physical & Engineering Sciences, 363, 151-168.
- O'Leary, M. J., Perry, C. T. 2010. Holocene reef accretion on the Rodrigues carbonate platform: an alternative to the classic "bucket-fill" model. *Geology*, 38, 855-858.
- Parker, J. H. & Gischler, E. 2011. Modern foraminiferal distribution and diversity in two atolls from the Maldives, Indian Ocean. *Marine Micropaleontology*, 78, 30-49.
- Peche, M. 2012. Geology of the KaNyaka barrier island system, Maputo Bay, Mozambique. MSc Thesis, University of Johannesburg. 247 pp.
- Perry, C. T. 2005. Structure and development of detrital reef deposits in turbid nearshore environments, Inhaca Island, Mozambique. *Marine Geology*, 214, 143-161.
- Perry, C. T., Beavington-Penney, S. J. 2005. Epiphytic calcium carbonate production and facies development within sub-tropical seagrass beds, Inhaca Island, Mozambique. *Sedimentary Geology*, 174, 161-176.
- Rees, S. A., Opdyke, B. N., Wilson, P. A., Fifield, L. K. 2005. Coral reef sedimentation on Rodrigues and the Western Indian Ocean and its impact on the carbon cycle. Philosophical Transactions of The Royal Society A: Mathematical, Physical & Engineering Sciences, 363, 101-120.
- Riffel, S. B., Vasconcelos, P. M., Carmo, I. O., Farley, K. A. 2016. Goethite (U-Th)/He geochronology and precipitation mechanisms during weathering of basalts. *Chemical Geology*, doi:10.1016/j.chemgeo.2016.03.033
- RioTinto.com
http://www.riotinto.com/documents/ReportsPublications/Titanium_mineral_sands_exploration_target_in_Mozambique.pdf (last accessed 14 April 2016)
- Rutten, R., Mäkitie, H., Vuori, S., Marques, J. M. 2008. Sedimentary rocks of the Mapai Formation in the Massingir-Mapai region, Gaza Province, Mozambique. Geological Survey of Finland Special Paper 48, 251-262.
- Schultz, H., Lückge, A., Emeis, K-C., Mackensen, A. 2011. Variability of Holocene to Late Pleistocene Zambezi riverine sedimentation at the upper continental slope off Mozambique, 15°-21° S. *Marine Geology*, 286, 21-34.
- Senapathi, D., Underwood, F., Black, E., Nicoll, M. A. C., Norris, K. 2010. Evidence for long-term regional changes in precipitation on the East Coast Mountains in Mauritius. *International Journal of Climatology*, 30, 1164-1177.
- Vianello, P. 2015. A Qualitative and physical analysis of processes around the Mascarene Plateau. Doctor of Philosophy, University of Cape Town, South Africa.
- Von Gruenewaldt, G., Sharpe, M. R., Hatton, C. J. 1985. The Bushveld Complex: introduction and review. *Economic Geology*, 80, 803-812.
- Wechsler, B. A., Prewitt, C. T. 1984. Crystal structure of ilmenite (FeTiO₃) at high temperature and high pressure. *American Mineralogist*, 69, 176-185.

Wright, C. I., Miller, W. R., Cooper, J. A. G. 2000. The late Cenozoic evolution of coastal water bodies in Northern Kwazulu-Natal, South Africa. *Marine Geology*, 167, 207-229.

3 Review of Macrofauna on Pieces from Mozambique (Item 2 and 3)

3.1 Summary

This report provides a brief review of the macrofauna found on the aircraft pieces from Mozambique, Daghatane Beach (Item 2) and Mozambique Channel (Item 3). For consistency, the two pieces are labelled Right wing No. 7 flap track fairing (Item 2) and Right horizontal stabilizer panel piece (Item 3). This report includes evaluation of external macrofauna collected off the pieces as well as the sieved fractions.

- Items 2 and 3 had evidence of barnacle peduncle attachment and other areas of sessile species attachment. Based on the visual similarities of the barnacle peduncle attachment, and from the samples from the peduncle attachment on the door R1 Stowage closet (Item 5), many samples that were collected from Items 2 and 3, could possibly be from barnacle pedunculated cement. The interior honeycomb of Item 2 was heavily colonised by encrusting bryozoans (*Jellyella tuberculata*).
- Identified mollusc species on Item 3 suggest that the item originated from, or picked up, macrofauna from the tropical Indo-Pacific Ocean. Most mollusc specimens found were recently dead or long-dead and possibly lodged into the item at the location where the item was found. Based on the species assemblage, the only taxon that could be significant in determining the oceanic waters that the aircraft piece had been in was *Petalconchus renisectus*. This specimen is estimated to be 8-12 months old and has a distribution that spans the tropical Indo-Pacific Ocean.
- From the species assemblage recovered and identified, there is no evidence of any cool- or cold-temperate mollusc or annelid in these samples that might suggest the aircraft pieces had been in the cold waters of the Southern Indian Ocean.
- One third of the identified molluscs on Item 3 are sufficiently opportunistic to grow on floating debris, and represent juveniles at approximately two months old.

Caveats: The aircraft pieces were retained over lengthy time frames (months), and under conditions that may not be conducive for faunal preservation. Therefore, some criteria were applied to the acceptance of samples analysed, these include:

- Any macrofauna within voids that could not be accessed without destructively breaking apart the pieces was not sampled
- Broken shells were not identified (only whole shells were identified)
- Any animals < 100 µm were not analysed
- Conclusions were based on the macrofauna found on the pieces

3.2 Method

1. The two pieces of aircraft were received on the 21st March 2016 and stored in Geoscience Australia Quarantine Approved Premises.
2. The pieces were visually examined for any obvious macrofauna then photographed with an SLR Canon 60D with a macrolens (EF 100mm).
3. Items were removed or scraped off and any biota collected was preserved in 75% ethanol.
4. The pieces were then washed and agitated in water to ensure any animals within cavities were flushed out. The resultant water was then passed through 3 sieves of sizes 100 µm, 500 µm and 1000 µm to ensure no spillage occurred in case of any obstruction. All material on each sieve was then carefully washed into a petri dish and then sorted under a microscope for any biological material. Any biota was then photographed with a Leica IC80 HD camera.
5. All waste material and liquids were disposed of via irradiation or a quarantine approved procedure.
6. Expert taxonomists from Australia were contacted via email and phone to ascertain species present in the images, including:
 - a. Dr Diana Jones for barnacles /other species (Western Australian Museum)
 - b. Dr Richard Willan for molluscs (Museum and Art Gallery of the Northern Territory; MAGNT)
 - c. Dr Chris Glasby for worms (MAGNT) and Dr Elena Kupriyanova (Australian Museum), Dr Katherine Yoo for photography of specimens (MAGNT), and Mr Neil Wright for assistance with post-production of images (MAGNT).
 - d. Dr Robyn Cumming and Dr Dennis Gordon for bryozoans (Museum of Tropical Queensland)

3.3 Results

3.3.1 Item 2: Recovered From Daghatane Beach, Mozambique

There was not a large amount of fauna found within the sieved fractions or attached to the surface of Item 2. However, evidence of barnacle peduncle and other sessile species attachment was clear on the bottom of the external rounded section (Figure 1). Based on the visual similarities of the barnacle peduncle attachment and physical evidence from the samples on the internal partition (Item 5) of the peduncle attachment, many samples collected on Item 2 and 3, are possibly barnacle pedunculated cement (Jones 2016; pers. obs; Table 1). At the time of writing this report, the species of barnacles could not be determined.

Crustacea:

One small juvenile barnacle (*Lepas anatifa anatifera*) was found within the sieved fractions attached to possible peduncle material (Table 1). *L. anatifera* is a species that commonly settles on floating animate or inanimate items in open water. It is a neustonic species (floating organism), which means

that only surface temperatures would need to be used to evaluate possible ages. *L. anatifera* has a cosmopolitan geographical range across the open water.

Mollusc:

One juvenile molluscan taxon was identified from Item 2; Mollusca: Bivalvia: Pteriidae: *Pinctada radiata* (Table 1 & 3). This mollusc is also known as the Atlantic pearl-oyster and is generally found throughout the Indo-Pacific at all depths but more commonly between 5-25 m. This species is also opportunistic and settles from plankton to grow on floating objects but detaches and falls off with age. This species is tolerant of a wide temperature range (13-30°C).

Bryozoa:

Bryozoa species found encrusting internal exposed honeycomb material are possibly colonies of *Jellyella tuberculata* (Table 1). This is a species that commonly settles on pumice, plastics and other floating substrata. It has been referred to as a 'pseudoplanktonic species'. These are small colonies that would achieve their size in a matter of weeks so it is difficult to ascertain how long the floating components were on the sea floor or at the sea surface based on bryozoan size alone (Gordon, 2016) (Table 1).

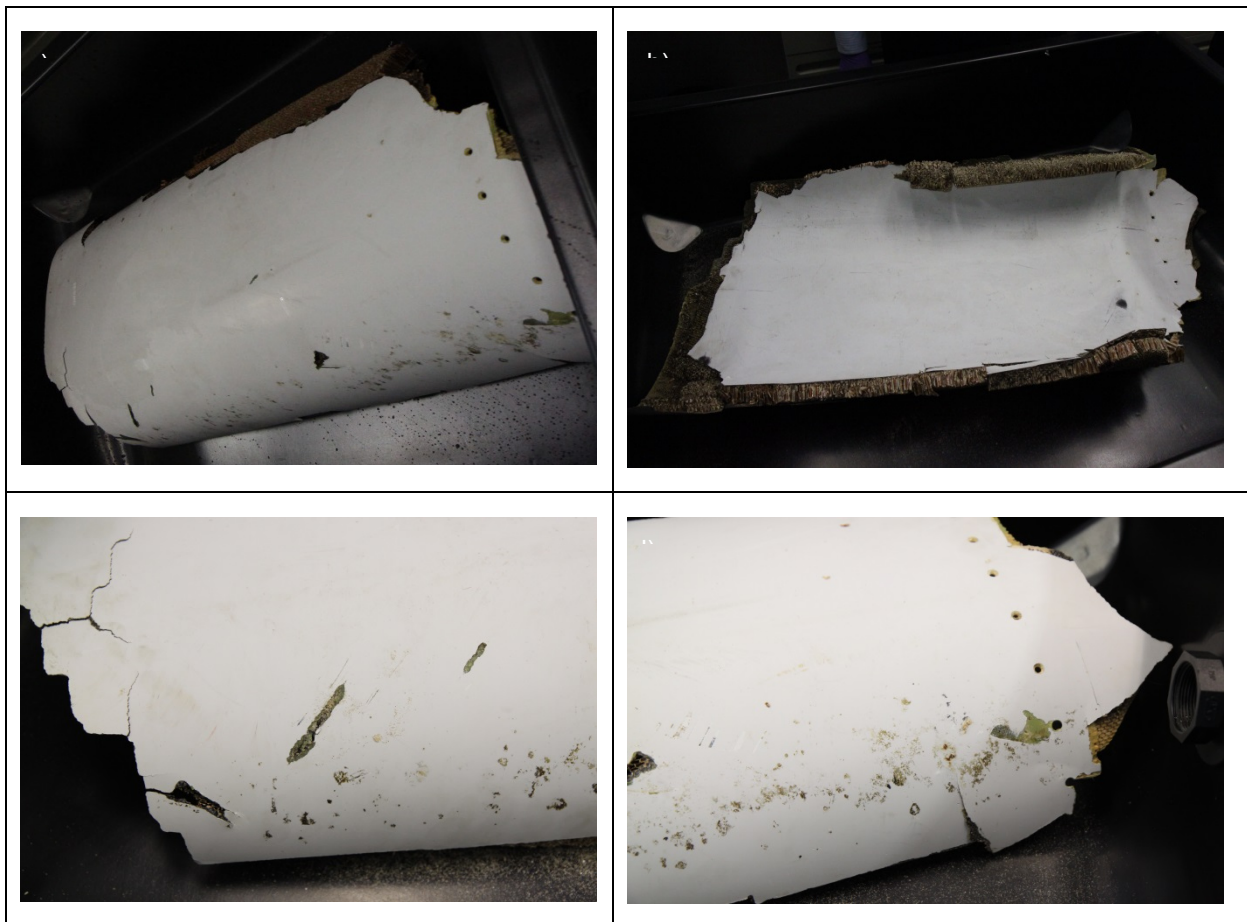
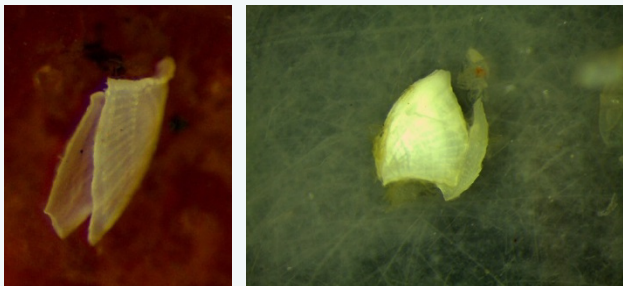
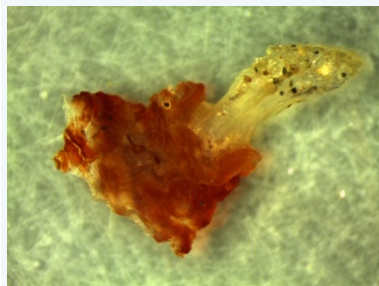
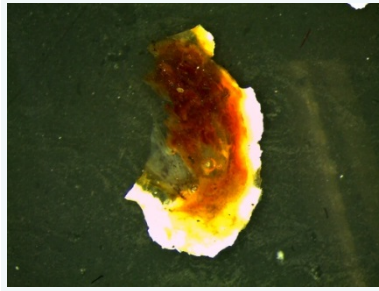


Figure 1 – Overview images of Item 2 (Right wing No. 7 flap track fairing); a) the external side of Item 2; b) internal side of Item 2; c) close up of bottom external side of Item 2; d) close up of possible remnants of barnacle cement.

Table 1: Images of species identified from Item 2 (Right Wing No. 7 Flap Track Fairing) originating from Mozambique.

Species	Image
Mollusca: Bivalvia: Pteriidae: <i>Pinctada radiata</i>	
Crustacea: Cirripedia: Lepadidae: <i>Lepas Anatifa anatifera</i>	
Bryozoa: Gymnolaemata: Cheilostomata: Membraniporidae: <i>Jellyella tuberculata</i> On Item 2 (left) and 3 (right) image	

Images of likely peduncle attachment images sent to Diana Jones (WA Museum) for analysis



3.3.2 Item 3 (Right Horizontal Stabilizer Panel): Recovered From a Beach in the Mozambique Channel

Item 3 had evidence of attached and unattached macrofauna within the sieved sections, and similar to Item 2, had evidence of barnacle peduncle and other sessile species attachment on the external facing section of the piece (Figure 2).

Molluscs and Annelids:

A total of 20 taxa (18 mollusc species and 2 annelid species) were identified from the sieved fractions, or attached on the surface of the aircraft piece. The majority of taxa (17 mollusc and 2 annelid species) were identified from Item 3.

Judging by its size and hence age, and by tendency to attach to floating objects, the only taxon that could be of possible significance in determining the oceanic waters that the aircraft piece had been in

is *Petaloconchus renisectus* (Table 2 & 3). This mollusc from the family Vermetidae is estimated to be 8–12 months old and is a species whose distribution encompasses the tropical Indo-Pacific Ocean. It is believed to have been living attached to the aircraft part prior to beaching at the discovery site because it has remnants of encrusting bryozoans on the under-surface consistent with those fouling the aircraft debris. Being a tropical species, it provides the only macrofaunal evidence that the debris had been in tropical waters at some early stage in its drift.

From the species identified on Item 3, there is no evidence of any cool- or cold-temperate mollusc or annelid that might suggest the aircraft debris had been in the cold waters of the Southern Indian Ocean. However, this does not rule out the possibility that the pieces did not travel through the Southern Indian Ocean, only that no species were retained on the piece after collection from Mozambique.

About two-thirds of the molluscs recovered from Items 2 and 3 must have been lodged onto the aircraft part(s) by waves when /they drifted ashore or were cast up on the beach(es) or by accidental human contamination [as in dragging the wreckage across the beach during its recovery]. Any handful of sediment, even a small one, from a tropical locality in the Indian Ocean would contain a very high diversity [hundreds] of dead shells of such species.. The natural habitat of the recovered molluscs is shallow water, on clean coral sand or in seagrass meadows. None of them could or would ever attach to drifting debris. These species are *Donax* cf. *nitidus*, *Ervilia* cf. *scaliola*, *Voorwindia* cf. *tiberiana*, *Nucinella* sp. 1, *Antosolarium* sp. 1, *Smaragdia souverbiana*, *Sigatica* sp. 1, *Hypermastus* sp. 1, *Pleuromeris* sp. 1 and *Spectamen* sp. 1 (Table 2 & 3) (Willan and Glasby, 2016).

About one-third of the molluscs and both the species of annelids in these samples are sufficiently opportunistic to settle out from the plankton and grow amongst fouling communities on floating objects. Some of them – the micromolluscs and *Neodexiospira* annelids – could grow to maturity (in six months or less) and reproduce on these floating objects. All of these species are only represented as juveniles in these samples, so they are assumed to be less than two months old. These species are *Cyclostrema* cf. *placens*, *Nozeba* sp. 1, *Iravadia* sp. 1, *Iravadia* sp. 2, *Diala semistriata*, “*Serpula* sp. 1” and *Neodexiospira* sp. 1. Again, partitioning these species into the opportunistic category does not negate their accidental lodgement onto the aircraft part(s) when it/they drifted ashore or were cast up on the beach(es) (Table 2 & 3) (Willan and Glasby, 2016).

One annelid tube from Item 3 belongs to a species of the genus *Vermiliopsis* (Saint-Joseph, 1894). The genus has a world-wide distribution and is found from subtidal to bathyal depths, mostly in tropical and subtropical areas, but this is typical for serpulid polychaetes in general. Species within the genus *Vermiliopsis* are morphologically recognised mainly based on the structure on the operculum (the specialised tube plugs). Thus, the animal, not just an empty tube is needed for positive identification. The tube, however, with its distinct longitudinal and transverse sculptural elements is quite typical for the genus. It resembles the tubes of species *Vermiliopsis monodiscus* Zibrowius, 1968 or rather *Vermiliopsis ex gr monodiscus* (one of the species from this group). *Vermiliopsis monodiscus* was described from the Mediterranean Sea, but then this identification seems unlikely given the region where the tube was found, so it might belong to one of the Indo-Pacific species.

Reproduction in this genus is also poorly known. Based on scarce egg size data, the larval development in *Vermiliopsis* appears to be lecithotrophic (= larvae rely on yolk provided in the egg at the time of spawning, do not feed independently on unicellular algae suspended in water column). Thus, larval growth is independent of food supply (algae), but the rate of larval growth and maturation mostly depends on water temperature. The sperm structure of *Vermiliopsis* suggests that fertilisation is external and larvae develop in the water column. Larvae have some limited swimming abilities, but mostly are distributed by water currents. Nothing is known about any substrate preferences by settling

larvae of *Vermiliopsis*. Most likely they are capable on settling on any available hard substrate, like many other serpulids. Life span (longevity) depends on body size: small serpulids have shorter life spans that large ones (the largest are estimated to live for 10-12 years). For a serpulid that inhabited the examined tube the life span is likely to be 2-3 years and the age of the animal is likely 6-8 months.

Crustacea:

One barnacle was found (*Lepas anatifera anatifera*) in the sieved sections. *L. anatifera* is a species that commonly settles on floating animate or inanimate items in open water. It is a neustonic species, which means that only surface temperatures would need to be used to evaluate possible ages. *L. anatifera* has a cosmopolitan geographical range across the open water (Table 2) (Jones, 2016).

Bryozoa:

Bryozoa species found encrusting on internal exposed honeycomb material are possibly colonies of *Jellyella tuberculata*. This is a species that commonly settles on pumice, plastics and other floating materials. It has even been dubbed a 'pseudoplanktonic species'. These are small colonies that would achieve their size in a matter of weeks so it is difficult to ascertain how long the floating components were on the sea floor or at the sea surface based on bryozoan size alone (Gordon, 2016) (Table 2).

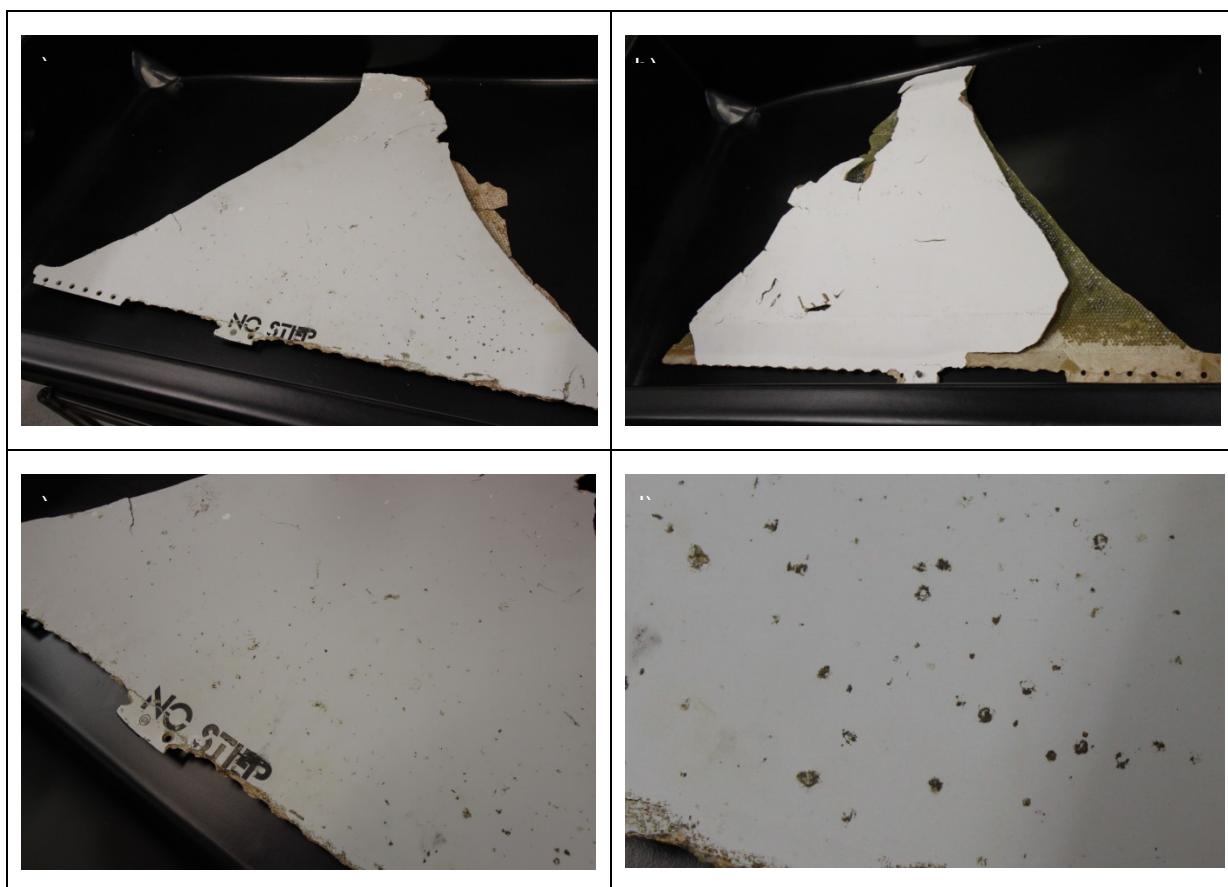


Figure 2 – Overview images of Item 3 (Right horizontal stabiliser panel piece); a) the external side of Item 3 indicating evidence of cementing structures; b) internal side of Item 3; c) close up of bottom external side of item 3; d) close up of possible remnants of barnacle cement.

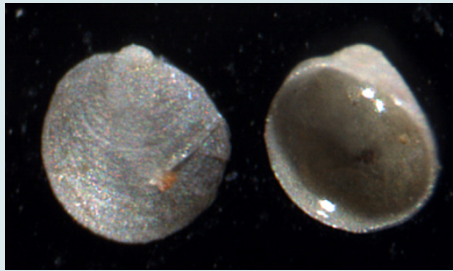
Table 2: Images of species identified from Item 2 and 3 originating from Mozambique. Images are sourced from Drs Richard Willan and Katherine Yoo, and Neil Wright from the Museum and Art Gallery of the Northern Territory.

Species	Image
Mollusca: Bivalvia: Donacidae: <i>Donax cf. nitidus</i>	
Mollusca: Gastropoda: Vermetidae: <i>Petalococonchus renisectus</i>	
Mollusca: Gastropoda: Liotiidae: <i>Cyclostrema cf. placens</i>	
Mollusca: Bivalvia: Semelidae: <i>Ervilia cf. scaliola</i> Found: HSP	
Mollusca: Gastropoda: Rissoiidae: <i>Voorwindia cf. tiberiana</i> Found: HSP	

Mollusca: Gastropoda:
Iravadiidae: *Nozeba* sp. 1



Mollusca: Bivalvia:
Nucinellidae: *Nucinella* sp. 1



Mollusca: Gastropoda:
Trochidae: *Antisolarium* sp. 1



Annelida: Polychaeta:
Serpulidae: *Neodexiospira* sp.
1



Mollusca: Gastropoda:
Iravadiidae: *Iravadia* sp. 2



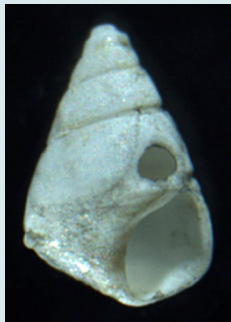
Mollusca: Bivalvia:
Semelidae: *Ervilia* cf. *scaliola*



Mollusca: Gastropoda:
Iravadiidae: *Iravadia* sp. 1



Mollusca: Gastropoda:
Dialidae: *Diala semistriata*



Mollusca: Gastropoda:
Liotiidae: *Cyclostrema* cf.
placens



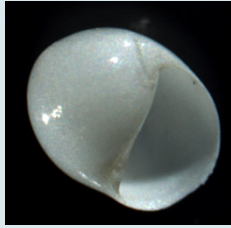
Mollusca: Bivalvia:
Donacidae: *Donax* cf. *nitidus*



Mollusca: Gastropoda:
Haminoeidae: *Haminoea* sp.
1



Mollusca: Gastropoda:
Neritidae: *Smaragdia
souverbiana*



Mollusca: Gastropoda:
Naticidae: *Sigatica* sp. 1



Mollusca: Gastropoda:
Eulimidae: *Hypermastus* sp. 1



Annelida: Polychaeta:
Serpulidae: *Neodexiospira* sp.
1



Mollusca: Bivalvia: Carditidae:
Pleuromeris sp. 1



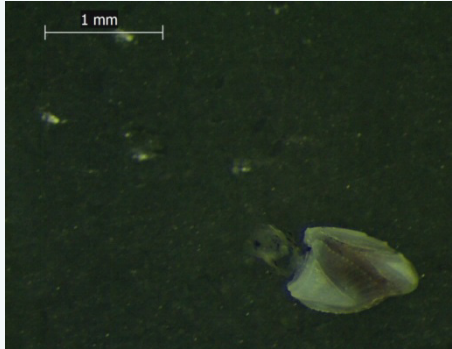
Mollusca: Gastropoda:
Solarieillidae: *Spectamen* sp.
1



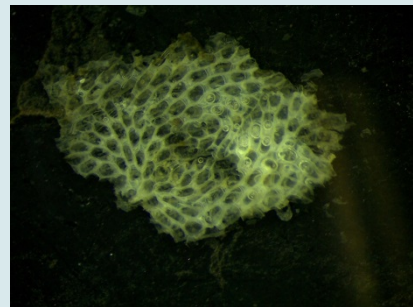
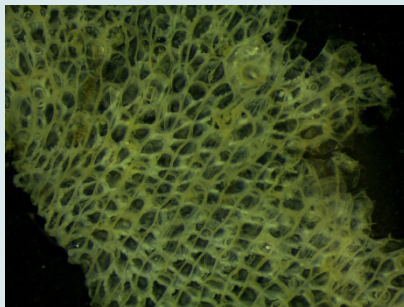
Mollusca: Gastropoda:
Dialidae: *Diala semistriata*



Crustacea: Cirripedia:
Lepadidae: *Lepas Anatifa anatifera*



Bryozoa: Gymnolaemata:
Cheilostomata:
Menbraniporidae: *Jellyella tuberculata*



Annelida: Polychaeta:
Sabellida:
Serpulidae: *Vermiliopsis* cf. *monodiscus*



Table 3 Identified mollusc and annelid species from Item 1 and Item 2.

Sample ID	Part	Identification	Comment	Significance for determining crash site	Habitat
HSP01	Horizontal Stabilizer Panel	Mollusca: Bivalvia: Donacidae: Donax cf. nitidus	One half valve from adult individual; long dead.	None	Tropical Indian Ocean. Shallow water, in clean coral sand or seagrass meadows
HSP02	Horizontal Stabilizer Panel	Mollusca: Gastropoda: Vermetidae: Petaloconchus renisectus	One adult or near-adult individual; freshly dead	Possible	Tropical Indo-Pacific Ocean. Shallow water, permanently attached to corals and rocks. Occasionally also grows on floating structures.
HSP03	Horizontal Stabilizer Panel	Annelida: Polychaeta: Serpulidae: "Vermiliopsis cf. monodiscus"	Specimen sent for precise determination and further comment to Elena Kupriyanova	Possible	Possible Indo-Pacific species, generally described from Mediterranean Sea. Generally found subtidal to bathyal depths, mostly in tropical and subtropical areas.
HSP100um 01	Horizontal Stabilizer Panel	Mollusca: Gastropoda: Liotiidae: Cyclostrema cf. placens	Three adult shells, all juveniles; freshly dead.	None	Tropical Indian Ocean. Shallow water, in clean coral sand or seagrass meadows.
HSP100um 02	Horizontal Stabilizer Panel	Mollusca: Bivalvia: Semelidae: Ervilia cf. scaliola	One half valve form adult individual; long dead.	None	Tropical Indian Ocean. Intertidal and shallow subtidal, on clean coral sand or seagrass meadows.
HSP100um 03	Horizontal Stabilizer Panel	Mollusca: Gastropoda: Liotiidae: Cyclostrema cf. placens	One subadult individual; long dead.	None	Tropical Indian Ocean. Intertidal and shallow subtidal, on clean coral sand or seagrass meadows.
HSP100um 04	Horizontal Stabilizer Panel	Mollusca: Gastropoda: Rissoiidae: Voorwindia cf. tiberiana	One juvenile individual; freshly dead.	None	Tropical Indian Ocean. Intertidal and shallow subtidal, on clean sand or seagrass meadows.
HSP100um 05	Horizontal Stabilizer Panel	Mollusca: Gastropoda: Irvadiidae: Nozeba sp. 1	One adult individual; freshly dead.	None	Tropical Indian Ocean. Intertidal and shallow subtidal, on clean coral sand or seagrass meadows.
HSP100um 06	Horizontal Stabilizer Panel	Mollusca: Bivalvia: Nucinellidae: Nucinella sp. 1	One juvenile individual; freshly dead.	None	Tropical Indian Ocean. Intertidal and shallow subtidal, on clean coral sand or seagrass meadows.
HSP500um 01	Horizontal Stabilizer Panel	Mollusca: Gastropoda: Trochidae: Antisolarium sp. 1	One juvenile individual; freshly dead.	None	Tropical Indian Ocean. Intertidal and shallow subtidal, on clean coral sand or seagrass meadows.

Sample ID	Part	Identification	Comment	Significance for determining crash site	Habitat
HSP500um 02	Horizontal Stabilizer Panel	Annelida: Polychaeta: Serpulidae: Neodexiospira sp. 1	One adult individual; freshly dead.	None	Cosmopolitan genus, well represented in tropical Indo-Pacific Ocean. Opportunistic, settling on a multitude of hard substrates.
HSP500um 03	Horizontal Stabilizer Panel	Mollusca: Gastropoda: Iravadiidae: Iravadia sp. 2	One adult individual; freshly dead.	None	Tropical Indian Ocean. Intertidal and shallow subtidal, on clean coral sand or seagrass meadows.
HSP500um 04	Horizontal Stabilizer Panel	Mollusca: Bivalvia: Semelidae: Ervilia cf. scaliola	One juvenile individual; freshly dead.	None	Tropical Indian Ocean. Intertidal and shallow subtidal, on clean coral sand or seagrass meadows.
HSP500um 05	Horizontal Stabilizer Panel	Mollusca: Gastropoda: Iravadiidae: Iravadia sp. 1	One adult individual; freshly dead.	None	Tropical Indian Ocean. Shallow water, in clean coral sand or seagrass meadows.
HSP500um 06	Horizontal Stabilizer Panel	Mollusca: Gastropoda: Dialidae: Diala semistriata	One subadult individual; long dead.	None	Tropical Indo-Pacific Ocean. Shallow water, in clean coral sand or seagrass meadows.
HSP500um_07	Horizontal Stabilizer Panel	Mollusca: Gastropoda: Liotiidae: Cyclostrema cf. placens	One adult individual; freshly dead.	None	Tropical Indian Ocean. Intertidal and shallow subtidal, on clean coral sand or seagrass meadows.
HSP500um_08	Horizontal Stabilizer Panel	Mollusca: Bivalvia: Semelidae: Ervilia cf. scaliola	One juvenile individual; freshly dead.	None	Tropical Indian Ocean. Intertidal and shallow subtidal, on clean coral sand or seagrass meadows.
HSP500um_09	Horizontal Stabilizer Panel	White inorganic particle - probable contaminant		None	Tropical Indian Ocean. Shallow water, in clean coral sand or seagrass meadows
HSP500um_10	Horizontal Stabilizer Panel	Mollusca: Bivalvia: Donacidae: Donax cf. nitidus	One juvenile individual; freshly dead.	None	Tropical Indian Ocean. Shallow water, in clean coral sand or seagrass meadows
HSP500um_11	Horizontal Stabilizer Panel	Mollusca: Gastropoda: Haminoeidae: Haminoea sp. 1	One juvenile individual; freshly dead.	None	Tropical Indian Ocean. Shallow water, amongst fine filamentous algae on clean coral sand or seagrass meadows
HSP500um_12	Horizontal Stabilizer Panel	Mollusca: Gastropoda: Neritidae: Smaragdia souverbiana	One juvenile individual; long dead.	None	Tropical Indian Ocean. Shallow water, in seagrass meadows

Sample ID	Part	Identification	Comment	Significance for determining crash site	Habitat
HSP500um_13	Horizontal Stabilizer Panel	Mollusca: Gastropoda: Naticidae: Sigatica sp. 1	One juvenile individual; live	None	Tropical Indo-Pacific Ocean. Shallow water, in clean coral sand or seagrass meadows
HSP500um_14	Horizontal Stabilizer Panel	Mollusca: Gastropoda: Eulimidae: Hypermastus sp. 1	One juvenile individual; freshly dead.	None	Tropical Indo-Pacific Ocean. Shallow water, in clean coral sand or seagrass meadows
HSP1000um 01	Horizontal Stabilizer Panel	Annelida: Polychaeta: Serpulidae: Neodexiospira sp. 1	One adult individual; freshly dead.	None	Cosmopolitan genus, well represented in tropical Indo-Pacific Ocean. Opportunistic, settling on a multitude of hard substrates.
HSP1000um 02	Horizontal Stabilizer Panel	Mollusca: Bivalvia: Carditidae: Pleuromeris sp. 1	One half valve from adult individual; freshly dead.	None	Tropical Indo-Pacific Ocean. Shallow water, in clean coral sand or seagrass meadows
HSP1000um 03	Horizontal Stabilizer Panel	Mollusca: Gastropoda: Solariellidae: Spectamen sp. 1	One adult individual; freshly dead.	None	Tropical Indian Ocean. Shallow water, in clean coral sand or seagrass meadows
HSP1000um 04	Horizontal Stabilizer Panel	Mollusca: Gastropoda: Dialidae: Diala semistriata	One adult individual; long dead.	None	Tropical Indo-Pacific Ocean. Shallow water, in clean coral sand or seagrass meadows.
CF01	Right Wing No. 7 Flap Track Fairing	Mollusca: Bivalvia: Pteriidae: Pinctada radiata	One juvenile individual; probably live when washed ashore	None	Tropical Indo-Pacific Ocean. Shallow water, permanently attached to corals and rocks. Juveniles occasionally grow on floating structures.

3.4 References

Gordon, D. 2016. Personal communication.

Hove, H.A. ten and Kupriyanova, E. K. 2009. Taxonomy of Serpulidae (Annelida, Polychaeta): the state of affairs. *Zootaxa* 2036: 1-126.

Jones, D.S. 2016. Personal communication.

Kupriyanova, E.K., E. Nishi, H.A. ten Hove, & A.V. Rzhavsky 2001. A review of life history in serpulimorph polychaetes: ecological and evolutionary perspectives. *Oceanography and Marine Biology: an Annual Review* 39:1-101.

Saint-Joseph, A. de 1894. Les annélides polychètes des côtes de Dinard, III. *Annales des Sciences naturelles*, Paris 17: 1-395.

Zibrowius, H., 1968b. Description de *Vermiliopsis monodiscus*. n.sp., espece Mediterranene nouvelle de Serpulidae (Polychaeta Sedentaria). *Bulletin du Muséum d'Histoire Naturelle, Marseille* 39: 1202–1210.

Willan, R. and Glasby, C. 2016. Personal communication.

4 Stable Isotope Analyses of Paints on Aircraft Pieces From Mozambique (Items 2 and 3) and Mauritius (Item 5)

4.1 Summary

This report provides the results of stable carbon isotope analysis for the paint samples collected from the three pieces from Mozambique, Daghatane Beach (Item 2), Mozambique Channel (Item 3) and Rodrigues Island, Mauritius (Item 5). This report also includes evaluation of control samples received from the Australian Transport Safety Bureau (ATSB).

- All the samples have similar $\delta^{13}\text{C}$ values, in the range of -29.5‰ to -30.6‰. The similar carbon isotopic compositions indicate that the paint samples may have come from the same source, and hence, Items 2 and 3 may also be from the same source.
- The decorative panel coating from Item 5 has a $\delta^{13}\text{C}$ value of -25.84‰, which is very close to the $\delta^{13}\text{C}$ value of the control sample, which is -25.151‰. The similar carbon isotope values indicate they may have come from the same source.

4.2 Method

Three pieces of debris Items 2 and 3 (from the Mozambique coastline) and Item 5 (from the Rodrigues Island, Mauritius) were supplied to Geoscience Australia Laboratory on the 21st March 2016 and the 14th of April 2016 (respectively) for geochemical analyses.

Stable isotopic analysis was undertaken on samples from all three items and on two 'control' samples which were supplied by the ATSB for analytical comparison. The control samples included painted plates and a sample of a new decorative panel.

4.2.1 Sub-Sampling Items 2 and 3

1. Paint samples from Items 2 and 3 were removed for analysis using an unused scalpel, and weighed into 8 capsules for analysis.
2. The prepared samples were loaded into 5 mm tin capsules on a Sartorius MC 5 micro balance using a thin metal spatula.
3. Weights of sample were recorded to $\pm 1\mu\text{g}$.
4. The paint samples were cleaned with mild detergent solution (HAEMO-SOL cleaner, Baltimore, USA) to remove obvious external dirt particles, potential grease and other contaminants, then rinsed well with deionised water and dried at room temperature.

4.2.2 Sub-sampling Item 5 and Control Sample

1. Scissors were used to prepare the following top coating layer samples:
 - a. One piece of top coating from the decorative panel of the inner cabin from Item 5.
 - b. One piece of Tedlar Polyvinyl fluoride (PVF) was collected from Item 5.
 - c. One piece of top coating from the decorative panel of the inner cabin from the control sample. The top coating was peeled off after immersing the part in dichloromethane (DCM).
2. The coating sample was rinsed with DCM before the analyses.

4.2.3 Isotopic Analysis of Items 2, 3 and 5 and the Control Sample

1. Bulk stable carbon isotopic analysis was performed using a Thermo Finnigan Elemental Analyser (Flash EA 1112) linked to Thermo Scientific MAT 253 Isotope-Ratio Mass Spectrometry (IRMS) with a Thermo Scientific ConFlo IV as an interface.
2. Approximately 0.3 mg of sample was weighed into tin capsules (SerCon) and introduced via an autosampler.
3. The Flash EA reactor tubes were comprised of two quartz glass tubes filled with chromium (III) oxide and copper oxide, held at 900 °C for combustion and a reduction reactor filled with reduced copper, held at 650 °C.
4. A post-reactor gas chromatography (GC) column was kept at 40°C. Measured $^{13}\text{C}/^{12}\text{C}$ isotope ratios are expressed in the δ notation [‰], relative to the international standard Vienna PeeDee Belemnite (VPDB).



Fig. 1: a. Item 2. Right wing No. 7 Flap Track and b. Item 3. Right Horizontal stabiliser panel, Outer Fairing, Outer Skin.

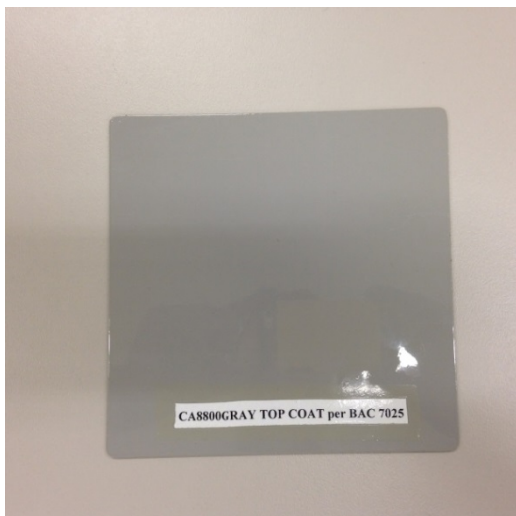


Fig. 2: Item 2. CA8800GRAY TOP COAT per BAC 7025 (from control sample)



Fig. 3: Item 3. CA8800GRAY TOP COAT per BAC 707 (from control sample)



Fig. 4: Sample of Tedlar and top coating from Item 5



Fig. 5: A roll of decorative panel used as a control

4.3 Results

- a. The stable carbon isotopic compositions of paint samples are listed in Table 1. All the samples have similar $\delta^{13}\text{C}$ values, in the range of -29.5% to -30.6% . The similar carbon isotopic compositions indicate that the paint samples may have come from the same source.
- b. The stable carbon isotopic results of decorative panel coating collected from Item 5, and from the control sample are displayed in Table 2. The sample from Item 5 has a $\delta^{13}\text{C}$ value of -

25.840‰, which is close to the $\delta^{13}\text{C}$ value of control sample, of -25.151‰. Similar carbon isotope values indicate they may have come from the same source.

- c. The sample of Tedlar from Item 5 has a $\delta^{13}\text{C}$ value of -24.778‰. The control sample for the Tedlar piece is unavailable for comparison.

Table 1. Stable carbon isotopic results of paint samples from two pieces of the Right Wing No. 7 Flap Track Fairing from Mozambique and control samples

Samples	$\delta^{13}\text{C}$ (‰)	Stdev (‰)	Comments
Item 2. CA8800GRAY TOP COAT per BAC 7025	-30.582	0.009	From control sample
Item 3. CA8800GRAY TOP COAT per BAC 707	-30.642	0.001	From control sample
Item 2. Flap Track Fairing, Outer Skin	-29.507	0.071	
Item 3. Stabiliser Stain Panel, Outer	-30.209	0.088	

Table 2. Stable carbon isotopic results of decorative panel coating for Item 5 and the control sample.

Samples	$\delta^{13}\text{C}$ (‰)	Stdev (‰)	Comments
Top Coating Outside	-25.840	0.092	
Top Coating Control	-25.151	0.118	
Tedlar (outside)	-24.778	0.199	No control supplied

5 Analyses of Organic Compounds on Aircraft Pieces From Mozambique (Item 2)

5.1 Summary

This report provides an analysis of the organic compounds detected on Item 2 (Right wing No. 7 Flap Track Fairing) of aircraft debris found in Mozambique.

- Higher n-alkanes (straight-chain alkanes; C21-C35) were detected in both debris samples (with and without solvent). These compounds are wax separated from petroleum and used as major constituents of grease and lubricants and indicate a possible source of higher plant origin petroleum.
- Four ester compounds were found with higher concentrations in the sample acquired with the application of organic solvent during sample collection (Table 1). These compounds contained grease, lubricants or lubricant additives.

5.2 Methodology

Cotton wool (pre-extracted with organic solvent to remove fat and grease and other organic materials) was used to collect the dust particles by wiping the surface of debris piece (Right Wing No. 7 Flap Track Fairing). Two samples were collected, the first (Sample #1) was the sample collected with dry cotton; the second (Sample #2) was collected with cotton soaked with organic solvent (mixture of dichloromethane and methanol 50:50). It was observed that more particles were collected with cotton soaked in solvent. The samples then were subsampled: one set was kept by Boeing for further analysis, and the other set was used for further analyses in the Geoscience Australia organic laboratory. Each sample was kept in individual 20 ml glass vials. The sample was covered with 10 ml hexane and extracted with sonication for 5 minutes. The hexane solution was transferred into a new 20 ml vial. The cotton was rinsed with 3 ml hexane and the solution was transferred into the same solution vial and performed 3 times. The total solution was concentrated to 4 ml with a nitrogen gas stream. A 2 mL aliquot was taken and concentrated further to approximately 100 µl which was then subjected to gas chromatography-mass spectrometry (GCMS) analyses with an injection volume of 0.5 µl. A full-scan was performed to measure the relative abundance and nature of detected compounds. Two blank samples (cotton wool with and without solvent) also underwent the same analytical procedures to trace any sources of contamination.

5.3 Results

Higher n-alkanes (straight-chain alkanes; C21-C35) were detected in both debris samples with much higher concentration (about 30 times) in Sample #2 (with solvent). The identifications are based on the comparison of GA's petroleum standard. These compounds are wax separated from petroleum and used as major constituents of grease and lubricants. The C27 is the most abundant compound among

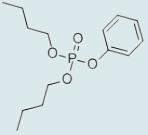
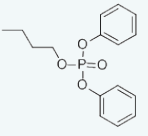
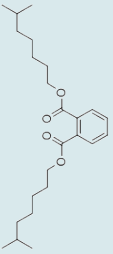
the n-alkanes. The n-alkanes demonstrate the pattern of 'odd-over-even' in the range of n-C27 to n-C35, indicating a possible source of higher plant origin petroleum.

Four ester compounds are detected in Sample #2 (with solvent) (Table 1). The identification of these ester compounds are based on the NIST mass spectrometry library search and comparison. These compounds have higher concentrations compared to n-alkanes. Some properties and usage of these esters are collected in Table 1 for reference. Please note that Compound 'D' (Nonanedioic acid, bis (2-ethylhexyl) ester) is used as grease and lubricant or as a lubricant additive. Other compounds, Phosphoric acid, dibutyl phenyl ester ('A') and 1,2-Benzenedicarboxylic acid, diisooctyl ester ('C') is toxic and can cause fire hazards.

These ester compounds are not detected in samples #1 (without solvent). This is possibly due to the use of organic solvents to sample the compounds from the surface of the debris, as physical sampling without solvent was not able to extract these compounds.

The results found on the aircraft items indicated that the higher n-alkanes indicate a possible source of higher plant origin petroleum and the ester results were consistent with organic compounds of grease, lubricants or lubricant additives.

Table 1. Some compounds detected in the sample #2.

Peak	Name	Structure	Chemical Formula	CAS Number	Synonyms	Molecular Weight	Properties and Usage (Refer to references)
A	Phosphoric acid, dibutyl phenyl ester		C ₁₄ H ₂₃ O ₄ P	2528-36-1	Dibutyl phenyl phosphate	286	Clear colourless liquid. Insoluble in water; Organophosphates, such as dibutyl phenyl phosphate, are susceptible to the formation of highly toxic and flammable phosphine gas in the presence of strong reducing agents such as hydrides. Partial oxidation by oxidizing agents may result in the release of toxic phosphorus oxides.
B	Phosphoric acid, dibutyl phenyl ester		C ₁₆ H ₁₉ O ₄ P	2752-95-6	butyl diphenyl phosphate; Phosphoric acid, butyl diphenyl ester; butyl diphenyl phosphate	306	Liquid; Industrial use: Flame retardants; Functional fluids
C	1,2-Benzenedicarboxylic acid, diisooctyl ester		C ₂₄ H ₃₈ O ₄	27554-26-3	1,2-Benzenedicarboxylic acid diisooctyl ester; DIISOCTYL PHTHALATE; alkylphthalates; Bis(6-methylheptyl) phthalate; Corflex 880; Flexol plasticizer diop; Hexaplas M/O; Isooctyl phthalate	390	Oily colourless liquid with a slight ester odour. Denser than water. Insoluble in water. Diisooctyl phthalate reacts exothermically with acids to generate isooctyl alcohol and phthalic acid. Strong oxidizing acids may cause a vigorous reaction that is sufficiently exothermic to ignite the reaction products. Heat is also generated by interaction with caustic solutions. Flammable hydrogen is generated by mixing with alkali metals and hydrides. Can generate electrostatic charges. [Handling Chemicals Safely, 1980. P. 250].

D	Nonanedioic acid, bis(2-ethylhexyl) ester		C25H48O4	103-24-2	BIS(2-ETHYLHEXYL) AZELATE; BIS(2-ETHYLHEXYL) NONANEDIOATE; AZELAIC ACID DIOCTYL ESTER; AZELAIC ACID BIS(2-ETHYLHEXYL) ESTER; AZELAIC ACID DI(2-ETHYLHEXYL) ESTER; DI(2-ETHYLHEXYL) AZELATE; DIOCTYL AZELATE; DIISOCTYL AZELATE	412	Industry use: Lubricants and lubricant additives; Consumer Use: Lubricants and Greases
---	---	---	----------	----------	--	-----	---

5.4 References:

Dibutyl Phenol Phosphate Chemical Description:

http://www.chemicalbook.com/ChemicalProductProperty_EN_CB9915709.htm

Butyl Diphenyl Phosphate Chemical Description:

https://pubchem.ncbi.nlm.nih.gov/compound/butyl_diphenyl_phosphate#section=Use-and-Manufacturing

Bis(2-Ethylhexyl Azelate Chemical Description:

https://pubchem.ncbi.nlm.nih.gov/compound/Bis_2-ethylhexyl__azelate#section=Use-and-Manufacturing

Dirthyl Phthalate Chemical Description:

<https://pubchem.ncbi.nlm.nih.gov/compound/6781#section=Wikipedia>

6 Review of Macrofauna on Aircraft Pieces Found on Mauritius and South Africa (Item 5)

6.1 Summary

This report provides a review of the macrofauna removed from aircraft pieces found on the coast of Mauritius and South Africa. For consistency, the two pieces are labelled as Engine Nose Cowling (Item 5) and Door R1 Stowage Closet (Item 5). This report only covers external macrofauna collected directly off the pieces, and not the sieved fractions.

The key points from investigations of Items 4 and 5 are:

- The smooth exterior engine cowling from Item 4 was not heavily colonised by macrofauna. Evidence of possible cementing structures was generally found on the external facing section of the piece. Macrofauna present suggest animals that are either cosmopolitan or resultant from terrestrial species from South Africa (grass stolons).
- Item 5 (Door R1 Stowage Closet) was heavily colonised by the *Lepas anatifera anatifera* barnacle, with evidence of cementing structures on the smoother sections of the part. Size plays an important role in age determination for *Lepas* sp.. The largest specimens were used to determine possible time periods, with evidence suggesting that Item 5 had active growth at a minimum of **45 to 105** days, but likely between **45 to 50** days due to surrounding sea surface temperature.
- The external facing section of Item 5 was colonised by more barnacles than the internal facing section.
- Based on the visual similarities of the peduncle (stalk-like) attachment and certainty from the samples on the Door R1 Stowage Closet from the peduncle attachment, many samples that were collected on Item 2 and 3 (Right wing No. 7 Flap Track Fairing and Right Horizontal stabiliser panel piece), could possibly be from barnacle pedunculated cement. Most of the barnacles were attached to exposed internal honeycomb, whereas only larger barnacles were found attached to smooth exposed materials.

Caveats: The sampling procedure to acquire macrofauna attached to the pieces highlights some possible deficiencies. The pieces were retained over different time frames, and under conditions that may not be conducive for faunal preservation, therefore, some criteria were applied to the acceptance of samples analysed, these include:

- Any macrofauna within voids that could not be accessed without destructively breaking apart the pieces was not sampled
- Broken shells were not identified
- Broken barnacle shells were not counted or measured
- Any animals < 100 µm were not analysed

6.2 Method

The two pieces (Items 4 and 5) were received on the 14th April 2016 and examined in Geoscience Australia's Quarantine Approved facilities.

The pieces were photographed with an SLR Canon 60D with a macrolens (EF 100mm) and visually examined for any obvious macrofauna.

The pieces were then washed and agitated in water to ensure any animals within cavities were flushed out. The resultant water was then passed through 3 sieves of sizes 100µm, 500µm and 1000µm to ensure no spillage occurred in case of any obstruction. All material on each sieve was then carefully washed into a petri dish and sorted under microscope for any biological material. The biota was photographed with a Leica IC80 HD camera.

For Item 5 (Door R1 Stowage Closet), due to the large number of barnacles present on internal and external parts, barnacle counts were separated into 6 grids. An examination of where the barnacles had colonised the item were recorded and the results separated into:

- Grids A1, A2, B1, B2, C1 and C2 (internal and external),
- Unattached barnacles (these had fallen off either through transit, transportation or physical movement), and
- Barnacles collected around the edges within honeycomb (Figure 3).

Barnacles were then measured with digital callipers and counted per grid.

Biological items were scraped off and any biota was preserved in 75% ethanol¹. Barnacles were stored in 100% ethanol for DNA preservation. Barnacles were removed manually and stored in allocated containers, however not all barnacles were stored in ethanol due to possible future analyses requiring different preservation techniques².

Sea surface temperature values around Mauritius were determined using monthly means available from the NASA MODIS ocean data website (NASA, 2016; Savtchenko et al., 2004).

¹ Expert taxonomists from Australia were contacted via email and phone to ascertain species present in the images. These specialists included: Dr Diana Jones for barnacles, barnacle cement remnants and other species (Western Australian Museum) Dr Robyn Cumming and Dr Dennis Gordon for bryozoans (Museum of Tropical Queensland)

² All waste material and liquids will be disposed of via irradiation or a quarantine approved procedure.



Figure 1 Overview images of Item 4 (Engine Nose Cowl); a) the external side of Item 4 indicating evidence of cementing structures; b) internal side of Item 4; c and d) close up of bottom external side of item 4





Figure 2 Examples of biota found on Item 4; a) unknown; b) possible remnant barnacle peduncle attached to the honeycomb from the exterior section; c) remnant barnacle scars on external facing section; d) possible *Jellyella tuberculata* colonies on internal facing section; e) stolon of terrestrial grass species; f) leaves of the terrestrial grass species.



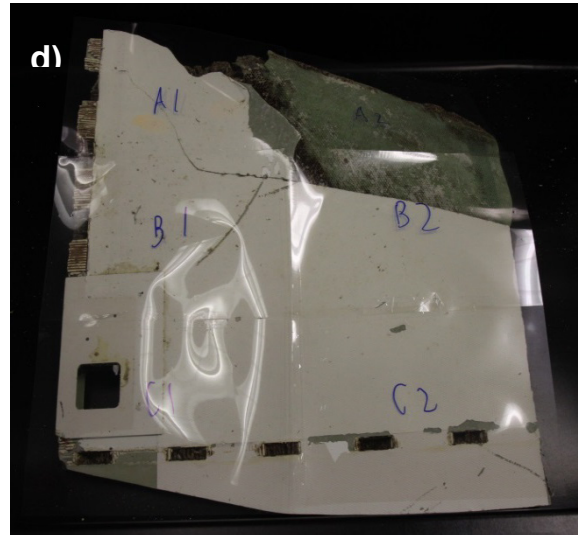
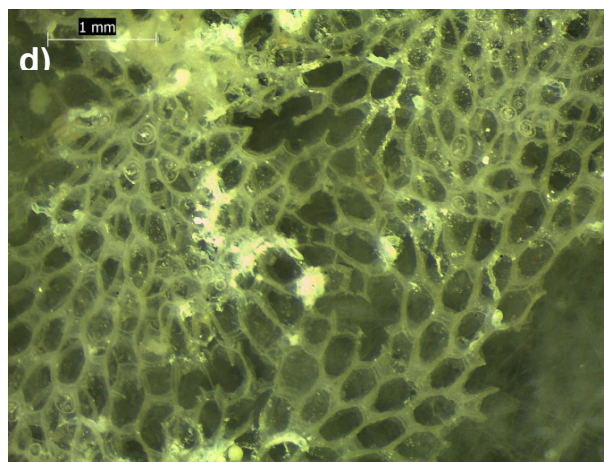
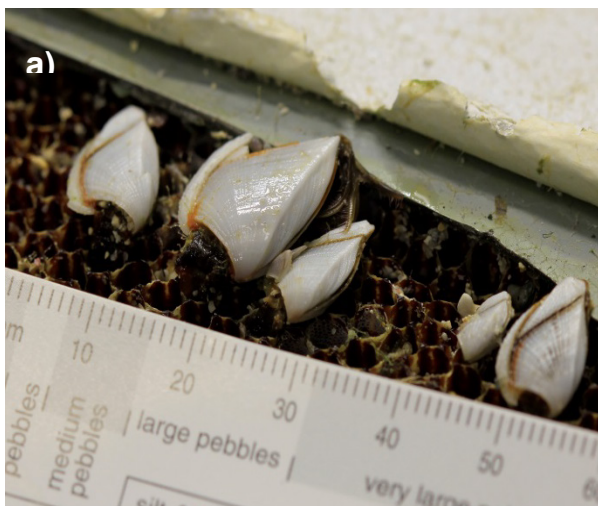


Figure 3 Images of Item 5; a) internal facing section of Item 5, b) external facing section of Item 5, c) grid of labels overlaid on the internal d) and external facing section of Item 5.



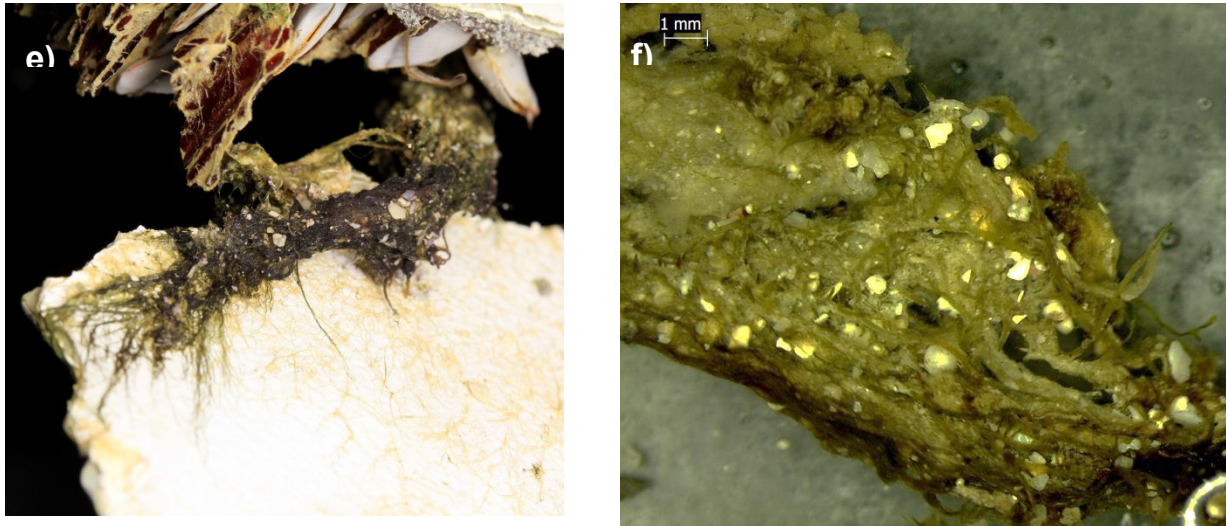


Figure 4 Examples of biota found on Item 5; a) colonies of barnacles attached to the more complex honeycomb of the Door R1 Stowage Closet); b) bryozoan colonies (possibly colonies of *Jellyella tuberculata*) on internal honeycomb structure; c) barnacle of *Lepas anatifa anatifera*; d) close up image of possible *Jellyella tuberculata* colonies; e) possible dried and matted filamentous green algae; f) close up image of dried and matted filamentous green algae entwined with *Caulerpa* sp.

6.3 Results

6.3.1 Item 4 (External Engine Cowling)

The Engine Nose Cowl (with the RR insignia) of Item 4 had evidence of many possible areas of attachment on the lower section. These include remnant scars with biological material (66) and remnant scars without any remnant material (15) (Figure 1). These areas are possibly related to peduncle attachment from barnacles. However, without any evidence of barnacle shells for size and identification, the species cannot be resolved.

In contrast, the internal facing section of Item 4 was relatively barren. Bryozoan colonies, possibly of species *Jellyella tuberculata* were found encrusted on the internal honeycomb and the black exterior of Item 4 (Figure 2).

6.3.2 Item 5 (Door R1 Stowage Closet)

A larger number of barnacles were found on the external section of the Door R1 Stowage Closet ranging between 1.39 mm to 20.05 mm in size (Figure 3; Table 1). Based on visual analysis:

- The barnacle species present on the Door R1 Stowage Closet is *Lepas anatifa anatifera* (Figure 4)
- Eleven 'adult' barnacles were found (between 13-23 mm capitulum length) (3% of collected barnacles)
- The size of the largest barnacle present corresponds to a growth period of approximately **45-50 days**, based on data by Evans (1958) for a growth rate of *Lepas* (*L. anatifera*), or **105 days** (based on the lower end 19 to 25°C sea surface temperature for optimum growth at 0.2 mm/day for the species) (Magni et al., 2015). However, it is likely that the higher growth rate of

age 45-50 days at approximately 0.44-0.55 mm/day can be assumed as sea surface temperatures surrounding Mauritius fluctuated between 26°C to 30°C during March 2016, 25°C to 30°C during February 2016 and 23°C to 29°C during January 2016 (NASA, 2016)

- Assumed minimum time for attachment of approximately 5 days for *Lepas* attachment to the debris (Magni et al., 2015)

Lepas anatifera anatifera is a species that commonly settles on floating animate or inanimate items in open water. It is a neustonic species (living on top of the water or right below the surface (Jones, 2016)), which means that only surface temperatures need to be used to evaluate possible ages. *L. anatifera* has a cosmopolitan geographical range across the open water. An understanding of growth rates of this species is summarised by Jones (2016), as follows:

“There are few studies on the growth rate of *Lepas anatifera* as the species lives in open marine environments and is difficult to culture under laboratory conditions. Whilst there are many qualitative observations that indicate fast growth in *Lepas* species, quantitative growth estimates are few or are based on laboratory experiments. In most *Lepas* species, growth is rapid and individuals achieve sexual maturity within a few weeks after settlement”

“The growth of barnacles varies with several factors, such as water temperature (mainly water surface), latitude, speed of movement of the item on which the barnacles are settling (Dalley & Crisp 1981) and the availability of food. In general, the growth rate of barnacles increases with increased temperature and current flow. However, this growth rate can be restricted with increased population density, competition from other species and adverse local environmental conditions (Bertness et al. 1991, Sorg et al. 1997).” (Jones, 2016)

Bryozoa species found encrusted on internal exposed honeycomb material are possibly colonies of *Jellyella tuberculata*. This is a species that commonly settles on pumice, plastics and other floating substrata. It has even been dubbed a ‘pseudoplanktonic species’. These are small colonies that would achieve their size in a matter of weeks, and as such it is difficult to ascertain how long the floating components were on the sea floor or at the sea surface based on bryozoan size alone (Gordon, 2016).

Algae species found on Item 5 are possibly from the genus *Caulerpa* sp., which is a common species found on Rodrigues Island (Coppejans et al., 2004), and filamentous green algae.

Table 1 Summary table highlighting statistics on macrofauna (barnacles) identified on Item 5 (Door R1 Stowage Closet). *I after the sample name indicates that the sample is from the internal facing components of the item (section with decorative decal), whereas E indicates external section of the item.

Sample location	Total Count	Minimum (mm)	Maximum (mm)	Median (mm)	Adult count
A1I*	1	11.53	11.53		0
A2I	6	2.41	9.03	3.655	0
B1I	0	N/A	N/A	N/A	0
B2I	17	1.95	15.84	4.27	2
C1I	26	1.39	15.95	5.7	3
C2I	13	1.91	4.63	2.62	0
Internal	63	1.39	15.95	4.27	5
A1E	117	2.27	20.05	5.23	3
A2E	48	1.88	7.76	3.56	0

Sample location	Total Count	Minimum (mm)	Maximum (mm)	Median (mm)	Adult count
B1E	33	1.82	10.67	3.56	0
B2E	NA	NA	NA	NA	0
C1E	4	3.88	11.26	4.71	0
C2E	NA	NA	NA	NA	0
External	202	1.82	20.05	4.135	3
Unattached	30	2.9	16.34	6.19	3
Exterior Honeycomb	91	2.06	11.72	3.6	0
Total	386	1.39	20.05	4.203	11

6.4 References

Bertness, M.D., Gaines, S.D., Bermudez, D. & Sanford, E. (1991). Extreme spatial variation in the growth and reproductive output of the acorn barnacle *Semibalanus balanoides*. *Marine Ecology Progress Series* **75**: 91-100.

Coppejans, E., Leilaert, F., Verbruggen, H., De Clerck, O., Schils, T., De vriese, T. and Marie, D. (2004). The marine green and brown algae of Rodrigues (Mauritius, Indian Ocean). *Journal of Natural History* **38**: 2959-3020.

Dalley, R. & Crisp, D.J. (1981). *Conchoderma*: a fouling hazard to ships underway. *Marine Biology Letters* **2**: 141-152.

Evans, F. (1958). Growth and maturity of the Barnacles *Lepas hillii* and *Lepas anatifera*. *Nature* **182**: 1245-1246

Gordon, D. 2016. Personal communication.

Jones, D.S. 2016. Personal communication.

Magni, P.A., Venn, C., Aquila, I., Pepe, F., Ricci, P., Di Nunzio, C. et al. (2015). Evaluation of the floating time of a corpse found in a marine environment using the barnacle *Lepas anatifera* L. (Crustacea: Cirripedia: Pedunculata). *Forensic Science International* **247**: e6-e10.

NASA Earth Observations. (2016). Sea surface temperature (1 month – AQUA/MODIS). Retrieved from <http://neo.sci.gsfc.nasa.gov/view.php?datasetId=MYD28M>

Savtchenko, A., Ouzounov, D., Ahmad, S., Acker, J., Leptoukh, G., Koziana, J., Nickless, D. 2004. Terra and Aqua MODIS products available from NASA GES DAAC. *Advances in Space Research*. **34**: 710-714

Sorg, M.H., Deaborn, J.H., Monahan, E.I., Ryan, H.F., Sweeney, K.G. & David, E. (1997). Forensic taphonomy in a marine context. In: Haglund, W.D. & Sorg, M.H. (eds), *Forensic taphonomy. The post mortem fate of human remains*. Pp 567-604. (CRC, Boca Ranton.)

Appendix H – Analysis of Low Frequency Underwater Acoustic Signals Possibly Related to the Loss of Malaysian Airlines Flight MH370



Curtin University

Centre for Marine Science and Technology

**Analysis of Low Frequency Underwater Acoustic Signals
Possibly Related to the Loss of Malaysian Airlines Flight
MH370**

Prepared for:
Australian Transport Safety Bureau

Prepared by:
Dr Alec J Duncan, Dr Alexander Gavrilov, Dr Rob McCauley

PROJECT CMST 1308
REPORT 2014-30

June 23rd 2014

Executive Summary

Malaysian Airlines flight MH370 disappeared in the early hours of 8th March 2014 and its whereabouts remain unknown. Current search efforts are based on position information derived from a satellite communication system and are focussed on the Indian Ocean, within Australia's search and rescue zone. The Australian Transport Safety Bureau (ATSB) has asked the Centre for Marine Science and Technology (CMST) to analyse signals received on underwater sound recorders operated by CMST that form part of the Australian Government funded Integrated Marine Observing System (IMOS), and on hydroacoustic stations operated by the Comprehensive Nuclear Test Ban Treaty Organisation (CTBTO) in an attempt to detect and localise underwater sounds that could be associated with the impact of the aircraft on the water or with the implosion of wreckage as the aircraft sank.

One acoustic event of particular interest has been identified that occurred at a time that could potentially link it to MH370 and appears to have been received on one of the IMOS recorders near the Perth Canyon (RCS) and at the CTBTO hydroacoustic station at Cape Leeuwin (HA01).

A detailed analysis of these signals has resulted in an approximate localisation for the source that is compatible with the time of the last satellite handshake with the aircraft, but incompatible with the satellite to aircraft range derived from this handshake. There appear to be three possible explanations for this discrepancy:

1. The signals received at HA01 and RCS are from the same acoustic event, but the source of the signals is unrelated to MH370.
2. The signals received at HA01 and RCS are from different acoustic events, which may or may not be related to MH370.
3. The signals received at HA01 and RCS are from the same acoustic event, and the source of the signals is related to MH370, but there is a problem with the position line determined from the satellite handshake data.

Of these, the first explanation seems the most likely as the characteristics of the signals are not unusual, it is only their arrival time and to some extent the direction from which they came that make them of interest.

If the second explanation was correct then there would still be some prospect that the signal received at HA01 could be related to the aircraft, in which case the combination of the HA01 bearing and the position arc derived from the satellite handshake data would provide an accurate location on which to base a search. However, the analysis carried out here indicates that, while not impossible, this explanation is unlikely.

The third explanation also seems unlikely because of the intense scrutiny the satellite handshake data has been subjected to. However, should the arc defined by the handshake data be called into question, the various timing and acoustic considerations discussed here would suggest that a reasonable place to look for the aircraft would be near where the position line defined by a bearing of 301.6° from HA01 crosses the Chagos-Laccadive Ridge, at approximately 2.3°S , 73.7°E . If the source of the detected signals was the aircraft impacting the sea surface then this would most likely have occurred in water depths less than 2000m and where the seabed slopes downwards towards the east or southeast. These considerations could be used to further refine the search area. If, instead, the received sounds were due to debris imploding at depth it is much less certain where along the position line from HA01 this would have occurred.

Contents

1	Introduction	5
2	Signal descriptions and analysis	6
3	Automated signal detection algorithm	11
3.1	General description	11
3.2	Mathematical derivation.....	12
3.3	Results.....	13
4	Independent time calibration check	14
5	Estimate of the probability that events at HA01 and RCS are from the same source.....	17
6	Analysis of data from HA08S	20
7	Discussion	25
8	Conclusions	31

1 Introduction

Malaysian Airlines flight MH370 disappeared in the early hours of 8th March 2014 and its whereabouts remain unknown. Current search efforts are based on position information derived from a satellite communication system and are focussed on the Indian Ocean, within Australia's search and rescue zone. The Australian Transport Safety Bureau (ATSB) has asked the Centre for Marine Science and Technology (CMST) to analyse signals received on underwater sound recorders operated by CMST as part of the Integrated Marine Observing System (IMOS) and on hydroacoustic stations operated by the Comprehensive Nuclear Test Ban Treaty Organisation (CTBTO) in an attempt to detect and localise underwater sounds that could be associated with the impact of the aircraft on the water or with the implosion of wreckage as the aircraft sank. This report collects together the results of various analyses that have been carried out by CMST, several of which have previously been reported to ATSB in summary reports.

One acoustic event of particular interest has been identified that occurred at a time that could potentially link it to MH370 and appears to have been received on CMST's acoustic recorders near the Perth Canyon (RCS), and at the CTBTO hydroacoustic station at Cape Leeuwin (HA01). Section 2 describes the signals associated with this event and the attempt made to localise it. Section 3 details an automatic detection algorithm that was developed to search for the same event in data from HA08S and was also used to characterise all events arriving at HA01 within an eight hour time period. HA08S and HA01 were the only operational CTBTO hydroacoustic stations in the Indian ocean at the time, The use of two of the separate events to check the calibration of the clock offset between RCS and HA01 is described in Section 4, while Section 5 details an initial attempt to estimate the probability that the signals at RCS and HA01 originated from the same source. Section 6 details the results of a search for the same event in data from HA08S, Section 7 provides a discussion that attempts to draw these various strands together, and the conclusions that can be drawn from this work are detailed in Section 8.

2 Signal descriptions and analysis

An underwater sound recorder operated by the Centre for Marine Science and Technology as part of IMOS and located at the seabed in 450 m water depth in the Perth Canyon (Rottnest Trench) received a transient signal at approximately 01:34:00 UTC on 8th March 2014. (This receiver is referred to as RCS in what follows.) After correction for clock drift the time of arrival of the peak energy in this signal has been calculated to be 01:33:44 UTC \pm 4 seconds. The signal and its spectrogram are shown in Figure 1.

A search of data from the Comprehensive Test ban Treaty Organisation's hydroacoustic station off Cape Leeuwin, Western Australia (HA01) carried out by the authors has revealed a signal believed to be from the same source, with a peak energy arrival time of 01:34:50 UTC \pm 3seconds. The signals and their spectrograms are shown in Figure 2.

Although the signal to noise ratio was poor on a single HA01 hydrophone, the signal at HA01 was strongly correlated between the station's three hydrophones which allowed the bearing of the source to be calculated with considerable accuracy. The result was a bearing of $301.6^\circ \pm 0.75^\circ$.

Projecting this bearing back from HA01 towards the source, computing the expected time difference between signals arriving at the two receiving stations as a function of distance along the track, and matching this to the measured time difference results in a most probable position for the sound source of 5.93°S , 77.22°E (see Figure 3). Calculations were carried out using Matlab's mapping toolbox and the WGS84 ellipsoid. Further details of this result are given in Table 1.

Uncertainties of $\pm 0.75^\circ$ in bearing from HA01 and ± 4 s in travel time difference result in the bounding box shown in Figure 3 and uncertainties of $\pm 1^\circ$ in bearing and ± 7 s in time difference result in the somewhat larger bounding box shown in Figure 4.

Calculated latitudes and longitudes of the vertices of the bounding box are given in Table 2. The bounding box is very elongated along the bearing from HA01 which is a result of the hyperbolic position line obtained from the arrival time difference being almost parallel to the bearing from HA01 at that range.

If the source was at the most probable position, then the signal would have been emitted at approximately 00:39:11 UTC.

The travel time differences have been calculated using acoustic group velocities estimated from numerical waveform modelling using an adiabatic normal mode model and climatological sound speed profiles for the appropriate time of year from the World Ocean Atlas 2005, (NOAA 2005). This gave a mean group velocity of 1486.20 m/s along the path from the most probable source location to HA01 and 1486.35 m/s along the path from the most probable source location to RCS.

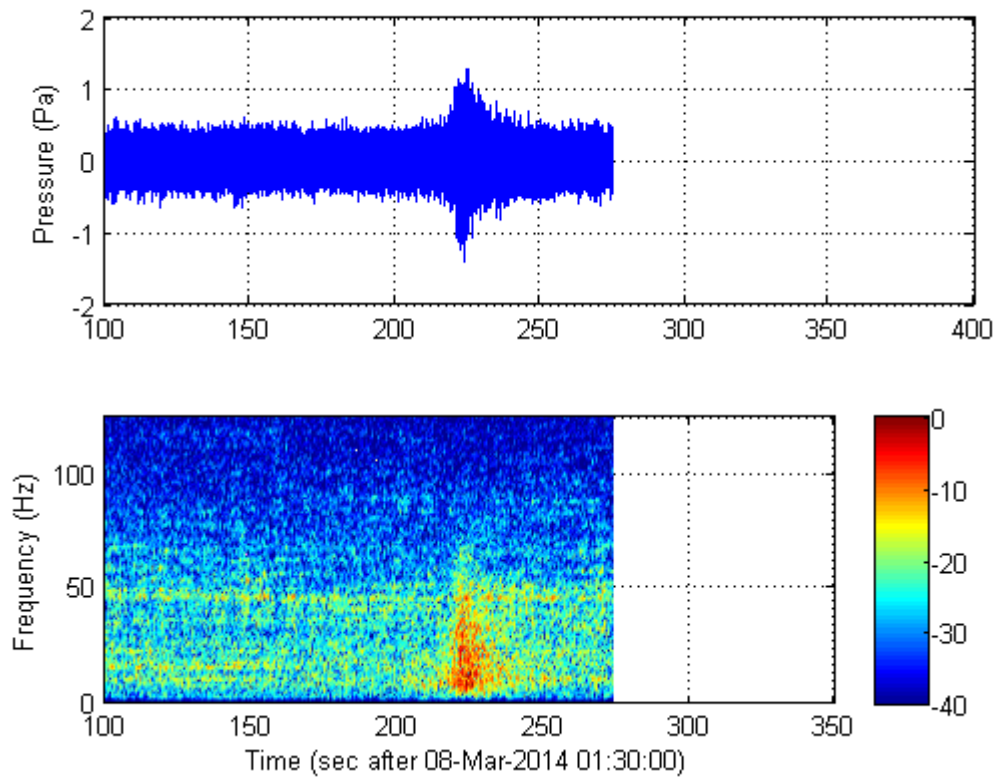


Figure 1. Time series (top) and spectrogram (bottom) showing the signal received at the Perth Canyon logger at 01:33:44 UTC on 8th March 2014. The spectrogram colour scale is in dB relative to the largest value in the spectrogram.

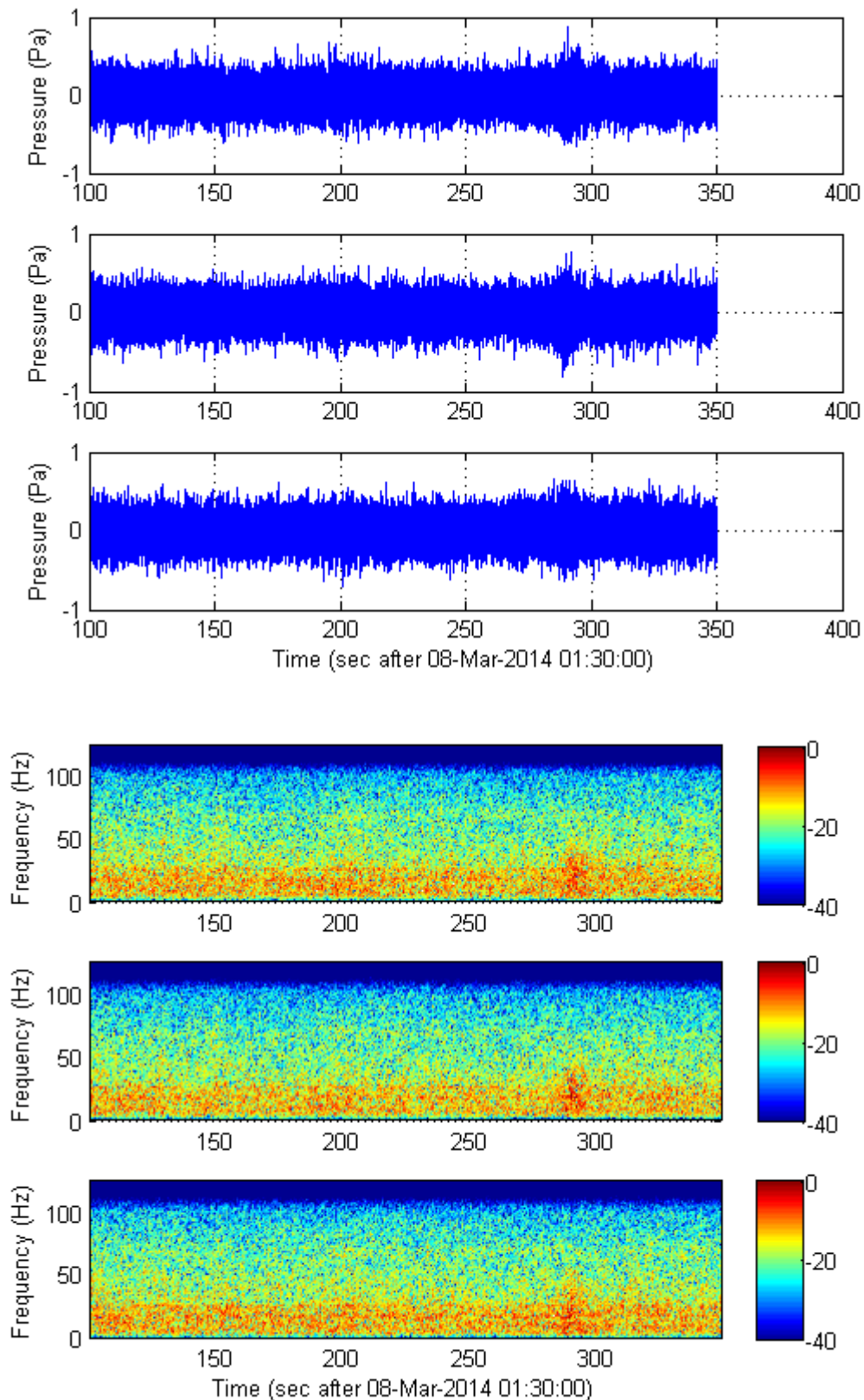


Figure 2. Time series (top) and spectrograms (bottom) showing the signals received at the three hydrophones of HA01 at 01:34:50 UTC on 8th March 2014. The spectrogram colour scales are in dB relative to the largest value in each spectrogram. Times scales are the same as for Figure 1.

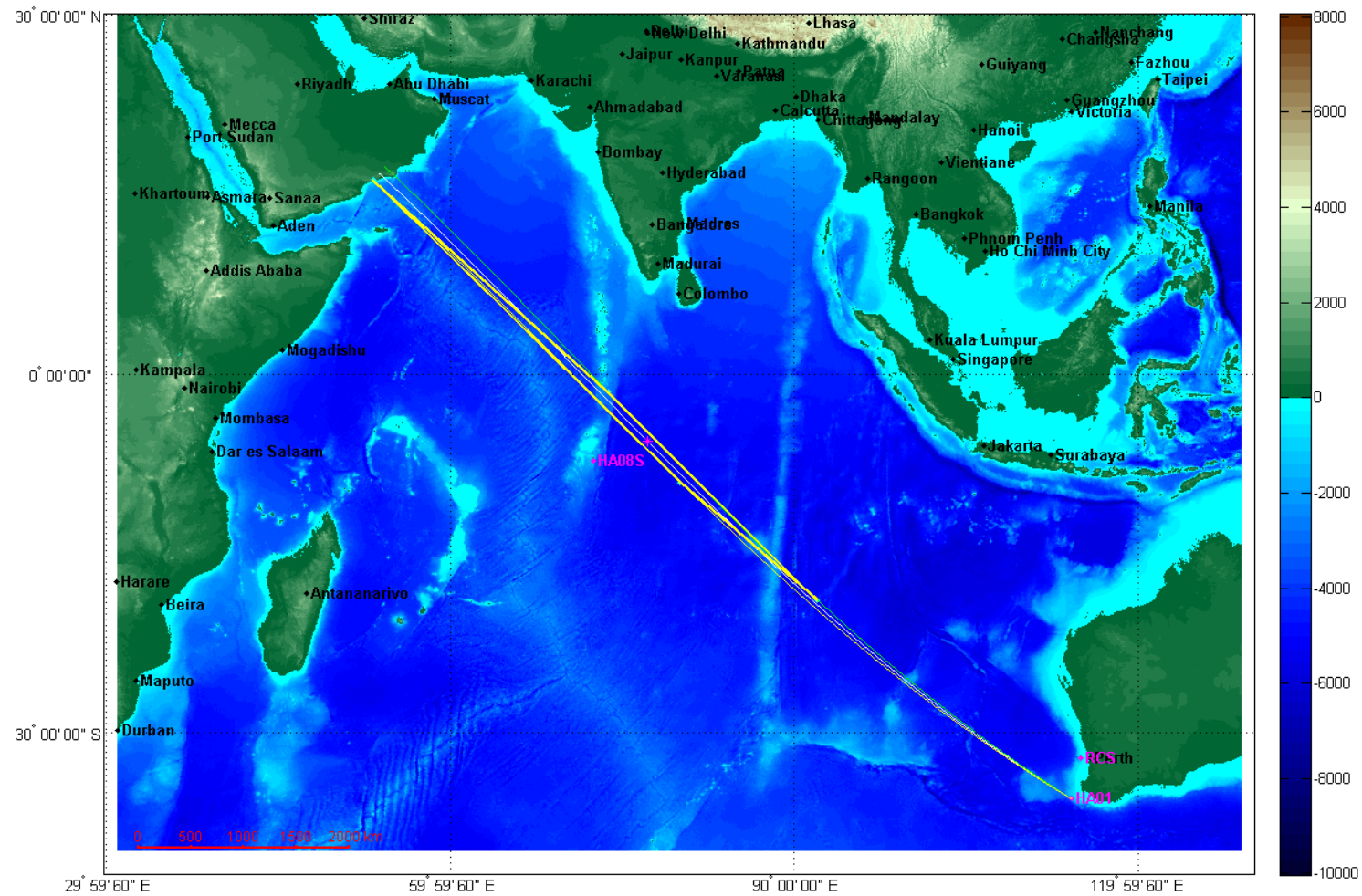


Figure 3. Map showing most probable location for the source of the received sound signals (magenta asterisk) and the uncertainty region (yellow polygon) based on an uncertainty of $\pm 0.75^\circ$ in the bearing from HA01 and a $\pm 4s$ uncertainty in the difference between signal arrival times at RCS and HA01.

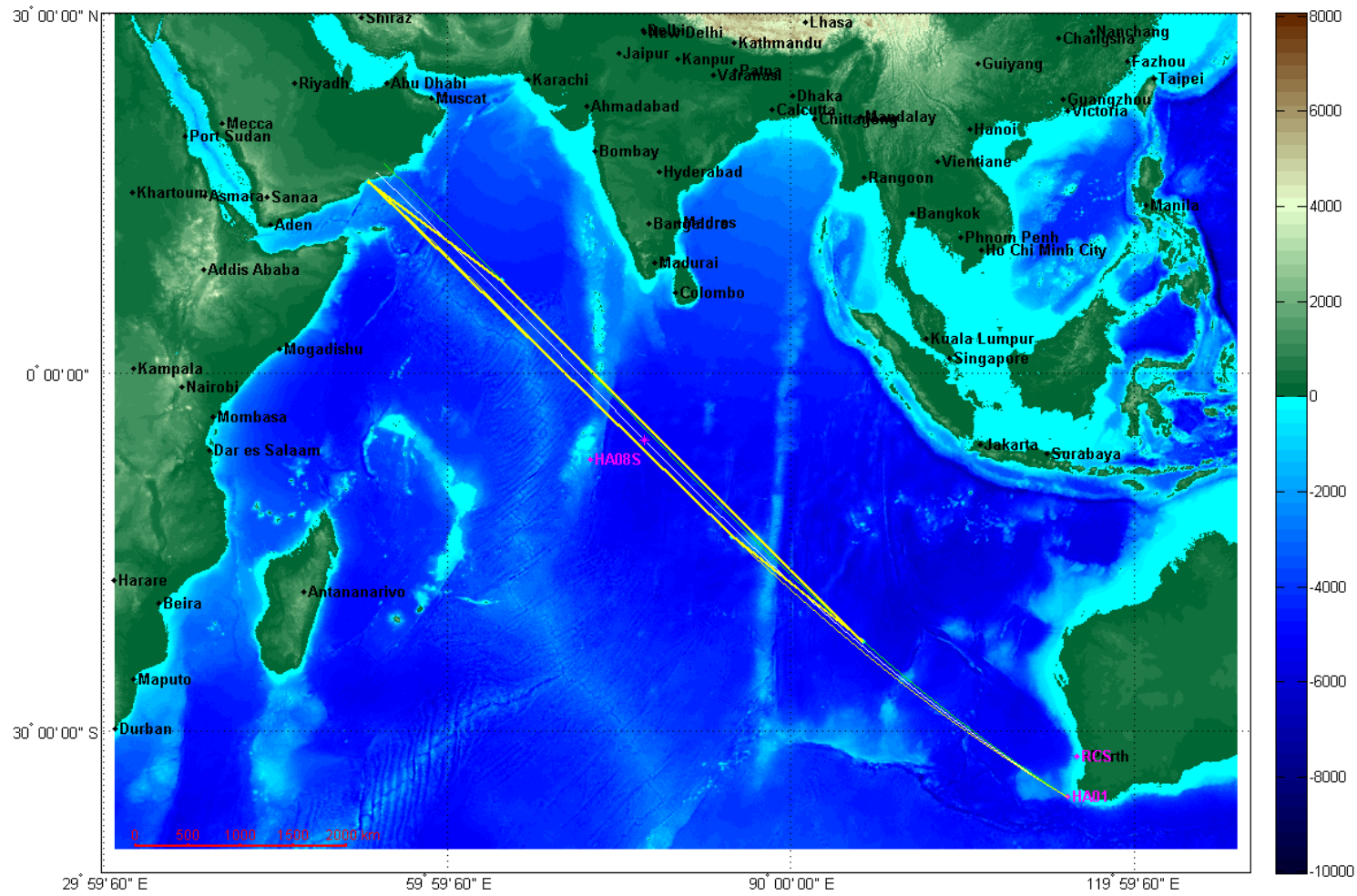


Figure 4. As for Figure 3 except the uncertainty region is based on $\pm 1^\circ$ in bearing and $\pm 7s$ in arrival time difference.

Table 1. Details of most probable position.

Position	5.93°S, 77.22°E
Distance to HA01 (km)	4961.6
Distance to RCS (km)	4864.0
Signal travel time to HA01 (s)	3338.4
Signal travel time to RCS (s)	3272.4
Calculated arrival time difference (s)	66.0
Measured arrival time difference (s)	66.0

Table 2. Uncertainty box bounds

Vertex	Position with +/-0.75° bearing error and +/-4 s timing error	Position with +/-1° bearing error and +/-7 s timing error
Northwest	16.8°N, 53.3°E	16.6°N, 53.1°E
Northeast	1.6°S, 73.8°E	8.1°N, 64.7°E
Southwest	9.5°S, 80.1°E	14.2°S, 84.9°E
Southeast	19.5°S, 92.0°E	23.0°S, 96.3°E

3 Automated signal detection algorithm

3.1 General description

To provide an efficient means of searching for other arrivals a Matlab program was written that breaks the signals received at a CTBTO hydroacoustic station into short blocks and then iteratively calculates the bearing to any sources. A 95% block overlap was used so that any genuine signal should appear as a detection in multiple blocks.

Each block was processed by computing the bearing to the strongest source using the conventional plane-wave fitting method (Menke, 1984, del Pezzo and Giudicepietro, 2002), estimating that signal using a least squares process, subtracting the estimated signal from the received signals (with appropriate time adjustments) to produce modified signals, and then applying the plane wave fitting method to the modified signals. This process can be repeated an arbitrary number of times, but it was found that there was little point in proceeding beyond three iterations.

At each stage the integrity of the fitted bearing was checked by requiring a discrepancy in the arrival time differences of no more than 10 ms, a fitted group velocity in the range 1420m/s to 1550m/s, and at least one neighbouring detection with a bearing within +/- 0.5°. The last criterion is based on the expectation that, because of the 95% block overlap, any genuine detection would occur in multiple adjacent blocks.

3.2 Mathematical derivation

Working in the horizontal (X, Y) plane, assume the incoming signal is made up of N plane waves coming from different directions. Then the received signal at time t at receiver $m \in \{1 \dots M\}$, located at x_m, y_m can be written:

$$p_1(x_m, y_m, t) = \sum_{n=1}^N s_n(t - v_{xn}x_m - v_{yn}y_m) + \varepsilon(x_m, y_m, t) \quad (1)$$

where

$v_{xn} = \frac{1}{c_{gn}} \cos \theta_n$ is the X-component of the slowness (inverse sound speed),

$v_{yn} = \frac{1}{c_{gn}} \sin \theta_n$ is the Y-component of the slowness,

c_{gn} is the plane wave group velocity,

θ_n is the direction in which the wave is travelling

$s_n(\cdot)$ is the waveform of signal n , and

$\varepsilon(x, y, t)$ is random noise that is assumed uncorrelated between receivers.

If the signals are ordered such that $|s_1| \gg |s_2| \gg |s_3|$ etc. then v_{x1} and v_{y1} can be estimated using the plane-wave fitting method (Menke, 1984, del Pezzo and Giudicepietro, 2002) and can therefore be considered known. We can write:

$$p_1(x_m, y_m, t) = s_1(t - v_{x1}x_m - v_{y1}y_m) + p_2(x_m, y_m, t) \quad (2)$$

where $p_k(x_m, y_m, t) = \sum_{n=k}^N s_n(t - v_{xn}x_m - v_{yn}y_m) + \varepsilon(x_m, y_m, t)$.

So:

$$p_1(x_m, y_m, t + v_{x1}x_m + v_{y1}y_m) = s_1(t) + p_2(x_m, y_m, t + v_{x1}x_m + v_{y1}y_m). \quad (3)$$

Defining $t'_{m1} = t + v_{x1}x_m + v_{y1}y_m$ we can rewrite (3) as:

$$p_1(x_m, y_m, t'_{m1}) = s_1(t) + p_2(x_m, y_m, t'_{m1}). \quad (4)$$

If the $p_2(x_m, y_m, t'_{m1})$ are treated as noise that is uncorrelated between sensors then equation (4) defines a set of three equations in terms of the unknown $s_1(t)$. The assumption that the $p_2(x_m, y_m, t'_{m1})$ are uncorrelated between sensors is justified because, by definition, all signal components that are correlated between sensors when the time delays associated with t'_{m1} are applied are included in $s_1(t)$. The least squares estimate of $s_1(t)$ is simply the average over the appropriately delayed sensor outputs:

$$\hat{s}_1(t) = \frac{1}{3} \sum_{m=1}^M p_1(x_m, y_m, t'_{m1}) \quad (5)$$

Once $\hat{s}_1(t)$ has been estimated, the residual signals can be calculated using a rearrangement of (2):

$$p_2(x_m, y_m, t) = p_1(x_m, y_m, t) - \hat{s}_1(t - v_{x1}x_m - v_{y1}y_m) \quad (6)$$

The plane-wave fitting algorithm can then be applied to $p_2(x_m, y_m, t)$ and the process repeated to estimate $\hat{s}_2(t)$, and so on.

3.3 Results

The results of applying two iterations of this algorithm to the HA01 data from 00:10:00 UTC on the 8th March to 08:00:00 UTC on the same day are shown in Figure 1. These

results were obtained a block duration of 20s and a block overlap of 19s. A zero-phase high pass filter with a cut-off frequency of 3 Hz was applied to the data prior to processing to remove very low frequency flow noise.

The vast majority of the detections originated from the Antarctic sector, which extends from 158° to 209° , or from just outside it. The majority of these are likely to be ice cracking events, although some may be some seismic events along a seafloor spreading ridge between Australia and Antarctica.

The 01:34:50 arrival (indicated by the orange arrow) stands out as being the only signal over this time period that originated from a northerly direction.

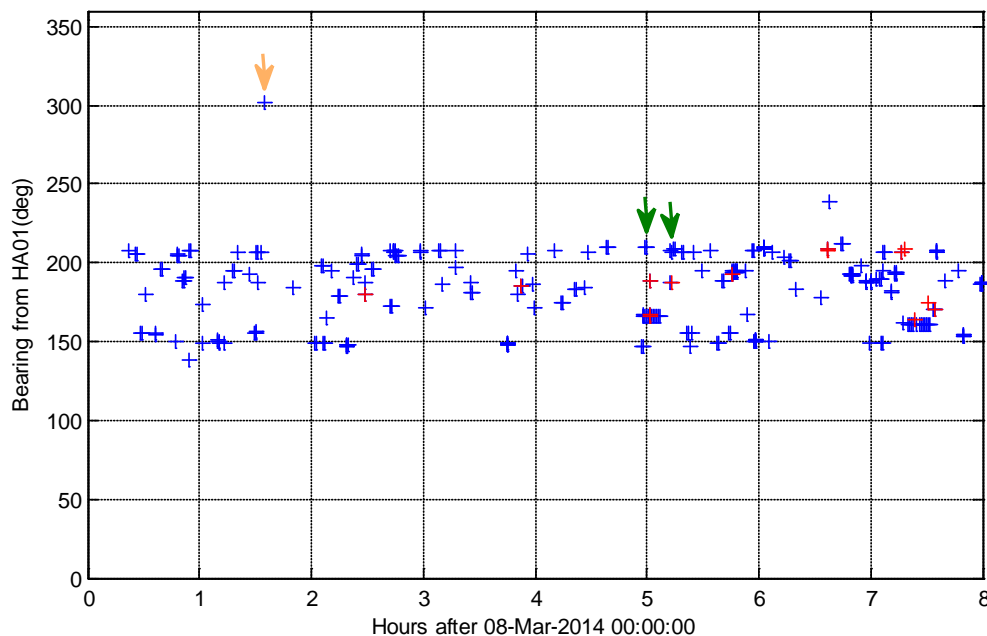


Figure 5. All automatic detections at HA01 between 00:00:10 and 08:00:00 UTC on 8th March 2014. The detection possibly associated with MH370 is indicated by the orange arrow. Blue crosses indicate detections made on the first iteration, red crosses are detections made on the second iteration. The dark green arrows indicate the two detections used for cross-checking the clock drift calibration.

4 Independent time calibration check

The estimate of the range of the source from HA01 is strongly dependent on the measured difference between the signal arrival times at RCS and HA01. The RCS recorder was deployed for a period of approximately three months during which its internal clock, which was set to UTC time prior to deployment and checked against UTC time after

deployment, gained 31.76 seconds (this is done in the noise logger hardware software using an external GPS and its UTC transmitted time). The time reference in both cases was the 1 pulse per second output from a GPS receiver. Assuming this drift rate was constant throughout the deployment, early on the 8th March 25.8 seconds must be subtracted from times according to the recorder clock in order to convert them to UTC.

An independent check of the accuracy of the drift correction of RCS compared with HA01 was carried out using two events other than the primary signal of interest, that resulted in signals that were received at both HA01 and RCS. The first of these resulted in a signal that was received at HA01 at 04:59:21 UTC on 8th March 2014 (17961 seconds after midnight) and came from a bearing of 210.2°. The corresponding signal arrived at RCS at 05:03:01 (18181 seconds after midnight). Both signals had high signal to noise ratio.

The second event was of much lower amplitude but came from a similar direction, and resulted in a signal that was received at HA01 at 05:14:28 UTC (18868 seconds after midnight) on the same day from a bearing of 208.5°. The corresponding signal was received at RCS at 05:18:13 (19093 seconds after midnight).

For each event, the arrival times and bearings at HA01 were used to compute a predicted arrival time at RCS, which was then compared to the measured arrival time. The results were computed using an assumed source range of 5000 km and an assumed group velocity of 1484 m/s and are given in Table 3.

Both arrivals came from a direction that is only about 15° from the direction of the line joining RCS and HA01, so the predicted arrival times at RCS depend only weakly on the source range assumption. A sensitivity study showed a 2 second increase in predicted arrival time if the assumed source range from HA01 was reduced to 1,000km, and a 0.2 second decrease if the source range was increased to 10,000km.

The assumed group velocity of 1484 m/s was obtained from numerical propagation modelling for a signal arriving from this direction and is considered accurate to within +/- 5 m/s. The effect of this uncertainty is considered along with other sources of error in the following analysis.

The uncertainties in the predicted arrival times at RCS were estimated based on a local plane geometry approximation to the ellipsoidal Earth in the vicinity of HA01 and RCS,

and the assumption that the source is an infinite distance away from the two stations. Note that this approximation has only been used to estimate the uncertainties. The actual arrival time calculations are based on ellipsoidal geometry and were carried out using Matlab's Mapping Toolbox.

With this approximation the arrival time at RCS is given by:

$$t_{RCS} = t_{HA01} + \frac{d \cos(\theta - \alpha)}{c_g}$$

where t_{HA01} is the arrival time at HA01 (seconds), d is the distance between HA01 and RCS (m), θ is the bearing of the source from HA01, α is the bearing of RCS from HA01 (13.65°), and c_g is the group velocity of the sound. The uncertainty in the predicted arrival time is given by:

$$\delta t_{RCS} = \left| \frac{\partial t_{RCS}}{\partial t_{HA01}} \right| \delta t_{HA01} + \left| \frac{\partial t_{RCS}}{\partial c_g} \right| \delta c_g + \left| \frac{\partial t_{RCS}}{\partial \theta} \right| \delta \theta$$

where $\delta \theta$ is the uncertainty in the bearing to the source (radians) etc. This leads to:

$$\delta t_{RCS} = \delta t_{HA01} + \Delta \frac{\delta c_g}{c_g} + \Delta \tan(\theta - \alpha) \delta \theta$$

where $\Delta = \left| \frac{d \cos(\theta - \alpha)}{c_g} \right|$ is the absolute value of the time delay between the signal

arriving at HA01 and at RCS in seconds.

In both cases the predicted and actual arrival times agree within uncertainties, with the maximum discrepancy being 3.2 seconds. This provides strong evidence that the clock synchronisation between HA01 and RCS is at least this accurate.

Table 3. Times are in seconds after 00:00:00 UTC on 8th March 2014.

Arrival time at HA01 (seconds)	Source bearing from HA01 (degrees)	Predicted arrival time difference (seconds)	Predicted arrival time at RCS (seconds)	Actual arrival time at RCS (seconds)	Predicted - actual (seconds)
17961 +/-2	210.2 +/-1	223.2 +/-2	18184.2 +/-4	18181 +/-2	3.2 +/-6
18868 +/-3	208.5 +/-1	225.0 +/-2	19093.0 +/-5	19093 +/-2	0 +/-7

5 Estimate of the probability that events at HA01 and RCS are from the same source

The estimate of the range of the source from HA01 depends on the assumption that the signals received at HA01 and RCS were generated by the same source and at the same time. An estimate has therefore been made of the probability that two signals arriving within a time window that would result in a valid fix, did so purely by chance. It should be noted that this estimate is based on very limited data and should therefore be treated as indicative only.

Let $P(A)$ be the *a-priori* probability that the HA01 and RCS arrivals are from the same source, and $P(B)$ be the *a-priori* probability that an arrival is observed at the RCS within a time interval of the arrival at HA01 that results in a valid fix.

Then $P(\bar{A}) = 1 - P(A)$ is the *a-priori* probability that the arrivals are from different sources and $P(\bar{B}) = 1 - P(B)$ is the *a-priori* probability that there was no arrival in the time interval required for a valid fix.

We want to calculate the *a-posteriori* probability that the arrivals are signals from the same source, given that the arrival at RCS occurred within the required time interval for a valid fix, i.e. $P(A | B)$, based on estimates of the probability of observing an arrival in the required time interval given that the signals are from the same source, i.e. $P(B | A)$, and

the probability of observing an arrival in the required time interval given that the signals are not from the same source, $P(B | \bar{A})$.

This can be done using Bayes Theorem (Walpole & Myers, 1985) :

$$P(A | B) = \frac{P(A)P(B | A)}{P(B)} \quad (7)$$

which can also be written:

$$P(A | B) = \frac{P(A)P(B | A)}{P(A)P(B | A) + P(\bar{A})P(B | \bar{A})} \quad (8)$$

So the problem reduces to estimating the various probabilities on the right hand side of Eq. (8).

If the signals are from the same source, then the RCS arrival must occur within the valid time interval, so $P(B | A) = 1$.

$P(B | \bar{A})$ can be estimated by looking at the statistics of similar arrivals at RCS over a long period of time. So far we have only looked at five hours of data, which is only enough for a very rough estimate, however even this is potentially useful as a starting point. There were two arrivals at RCS in that five hour period with broadly similar characteristics (duration and bandwidth) to the HA01 arrival – the one within the feasible time interval and another about 3 hours later. (The second arrival was actually a bit different in that it had a different pulse shape and a somewhat broader bandwidth, but for the purposes of this analysis we'll consider them as two events from the same process.) If we assume these pulses originate from a Poisson process, then an estimate of the process's rate parameter is $\lambda = 2/(5 \times 3600) = 1.11 \times 10^{-4}$ events per second. The probability of receiving k arrivals within a given time interval T is then given by the Poisson probability mass function:

$$P(X = k) = \frac{(\lambda T)^k}{k!} e^{-\lambda T} \quad (9)$$

The probability of receiving one arrival within the feasible time interval is then:

$$P(B | \bar{A}) = P(X = 1) = \lambda T e^{-\lambda T} \quad (10)$$

where T is the duration of the feasible time interval and can be determined from the geometry. Valid arrival time differences range from -200 s (for a source 40km from HA01, negative indicates the signal arrives at HA01 first) to +80 s for a source at 15,000km range, giving an interval duration of $T=280$ s. Substituting this into Eq. (10) with the previously calculated value of λ gives $P(B | \bar{A}) = 0.030$.

The other term required in order to evaluate Equation (8) is $P(A)$, the *a-priori* probability that the HA01 and RCS arrivals are from the same source. This can be interpreted to mean the probability that one would assign given only information about the characteristics of the two signals and without any knowledge of their relative arrival times. The arrivals at HA01 and RCS have very similar durations and spectra that are unlike the majority of other signals received at HA01, and the ratio of their amplitudes is consistent with model predictions. $P(A)$ should therefore be reasonably high, however as it is unclear (at least to the author) how this could be determined from the available data, results are plotted below in Figure 1 with $P(A)$ as a parameter.

It can be seen that providing $P(A)$ is greater than 0.03, $P(A | B)$ will be greater than 0.5. Furthermore, if $P(A) > 0.5$, then $P(A | B) > 0.97$.

Although the dependence of the final result on the difficult to determine *a-priori* probability, and the small amount of data used to estimate $P(B | \bar{A})$ make this analysis somewhat unsatisfactory, it does indicate that it is quite likely that the signals received at HA01 and RCS are from the same source. Analysis of considerably more data from both HA01 and RCS would provide a more robust result, but this has not been attempted.

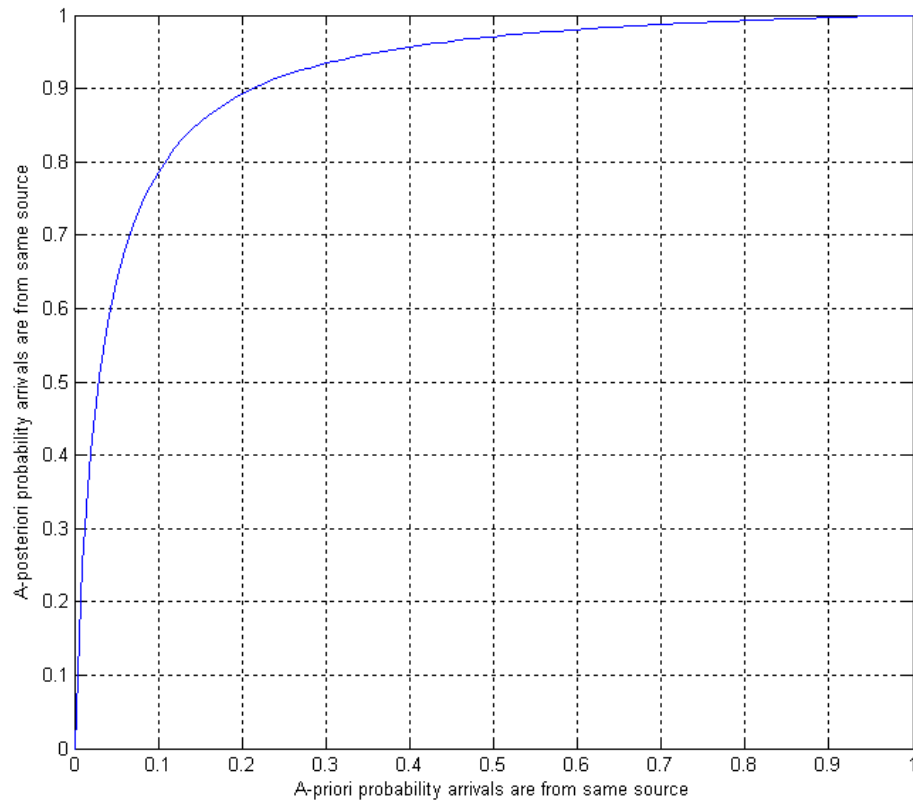


Figure 6. Plot of the a-posteriori probability against the a-priori probability that the arrivals at the two stations are from the same source.

6 Analysis of data from HA08S

Figure 6 shows the automatically calculated arrival bearings as a function of arrival time for all detections at HA08S. These results are summarised in Table 1. The two lines of detections that occur at almost constant bearings of 35° and 113° have characteristics consistent with offshore seismic surveys, which appear to have been taking place off Sri Lanka or in the Bay of Bengal, and off the northwest coast of Australia respectively. There were two other detections, one at about 700 seconds from a bearing of 168.1° and one at 7135 seconds from a bearing of 93° . Position lines corresponding to these various detections are shown in Figure 8.

A curve showing the expected arrival bearing at HA08S as a function of arrival time for the signal detected at HA01 at 01:34:50 on 8/3/2014 UTC is overlaid on Figure 6. It can be seen that neither of the discrete detections is consistent with the HA01 data.

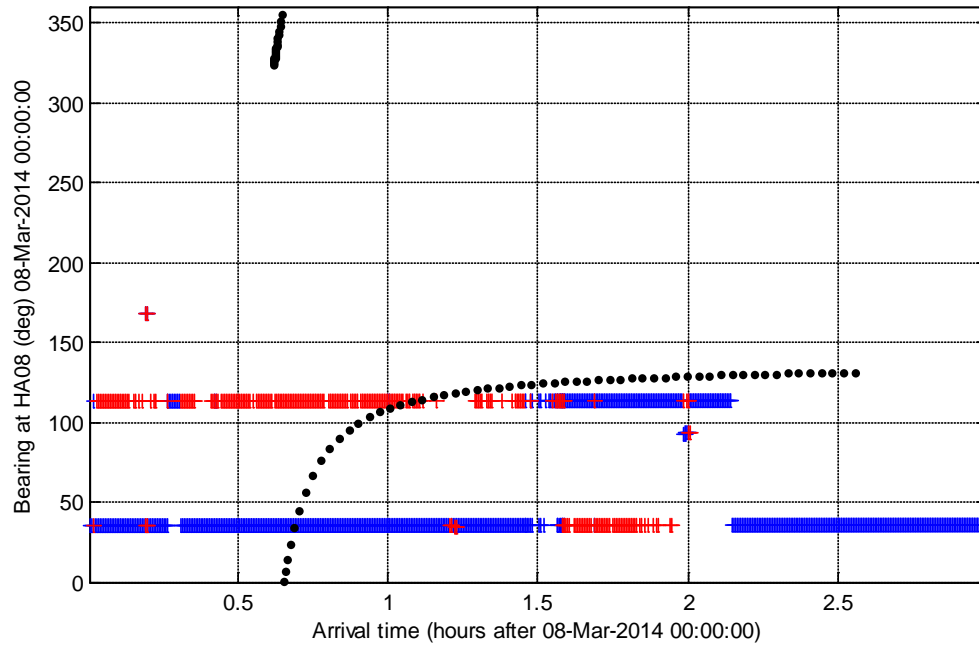


Figure 7. All automatic detections at HA08S between 00:00:00 and 03:00:00 UTC on 8th March 2014. The black dotted line shows the expected arrival bearing at HA08S as a function of arrival time for the signal detected at HA01 at 01:34:50 on 8/3/2014 UTC.

Table 4 Summary of HA08S detections

Time range (hours after 00:00:00 on 8/3/2014 UTC))	Bearing range (deg)	Figure 7 line colour	Likely source
0 to 3.00	34.9 - 35.4	Yellow	Seismic survey off Sri Lanka or in Bay of Bengal
0 to 2.14	113.0 - 113.6	Green	Seismic survey off NW Australia
0.19 to 0.20	168.05	White	Unknown. Possibly ice cracking noise or a small seismic event.
1.98 to 2.00	92.5 to 93.5	Red	Small earthquake in the Java Trench

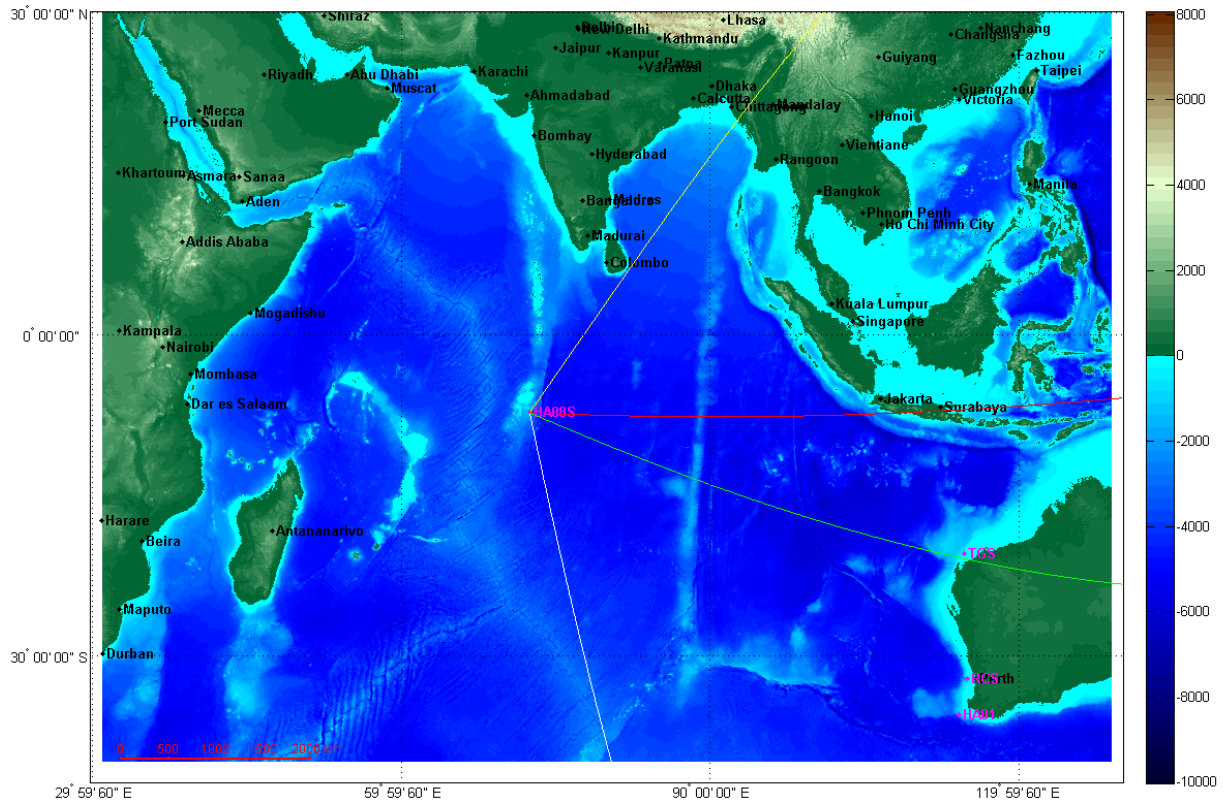


Figure 8. Map showing position lines for the HA08S detections listed in Figure 4. The location of the TGS seismic survey is shown by the magenta dot labelled "TGS".

Enquiries with industry contacts revealed that at the time MH370 is thought to have crashed, two seismic surveys were taking place off the northwest coast of Australia, close to the position line based on the 113° bearing from HA08S. These were the Woodside Centaurus 3D Survey and the TGS Huzzas 3D Survey. Both operators have provided the navigation data from the relevant survey lines, which are plotted in Figure 8.

The Woodside survey line was over a fairly flat seabed in just over 1000 m of water, whereas the TGS survey was over the continental slope in about 260 m of water. The time of reception of the last shot and the change in bearing with time both clearly indicate that the signals received at HA08S were from the TGS survey. The Woodside survey was not detected. This is consistent with the physics of acoustic propagation which requires a shallow sound source, such as a seismic survey airgun array, to be over a favourably sloping seabed in order to efficiently couple the sound into the Deep Sound Channel and achieve very long range propagation.

The navigation data provided by TGS allowed a check to be made of the bearing accuracy of HA08S. The results are plotted in Figure 9 and show a mean bearing offset of 0.6° . The resolution of the bearing measurement is sufficient to clearly track the northeast to southwest motion of the survey vessel.

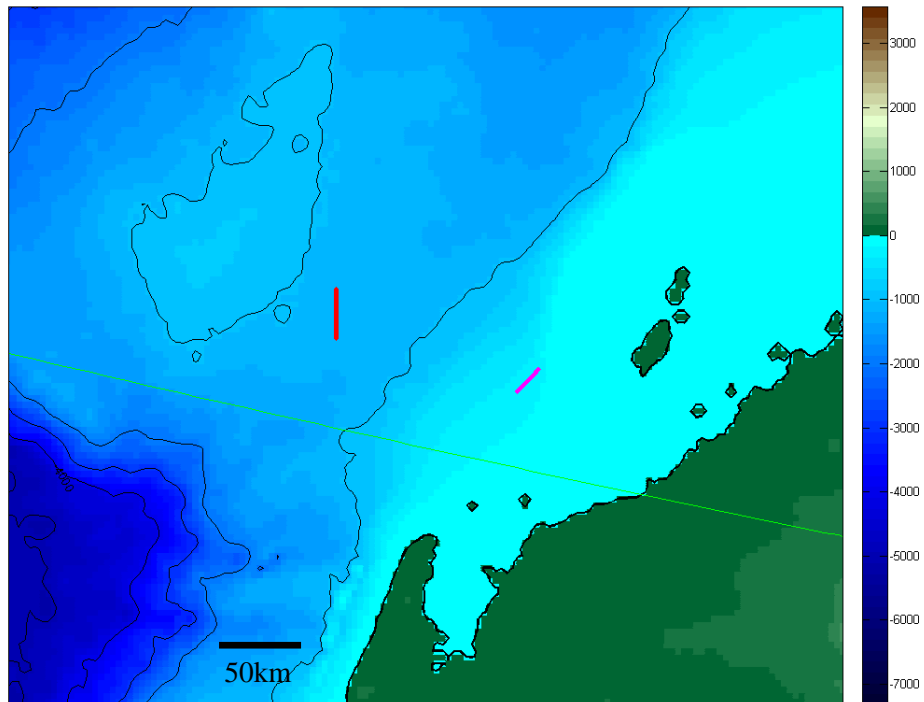


Figure 9. Map of Northwest Cape region, Australia, showing seismic survey lines being shot by Woodside (red) and TGS (magenta) around the time MH370 is thought to have crashed. The green line is the position line from HA08S

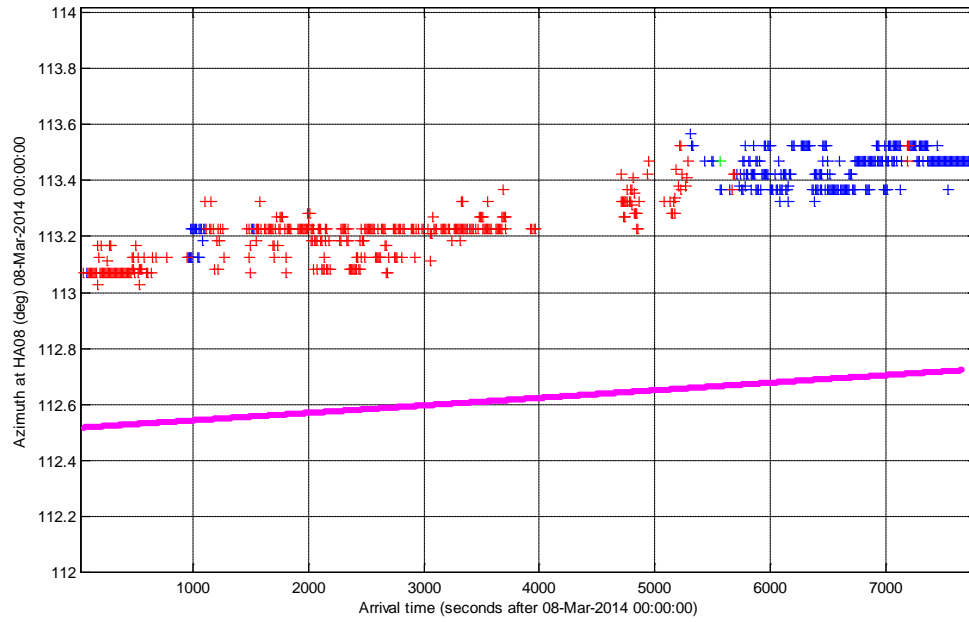


Figure 10. Plot of bearing vs. time for detections at HA08S that correspond to the TGS Huzzas 3D seismic survey (crosses). The magenta line is the calculated bearing based on the survey navigation data provided by TGS.

7 Discussion

Even with the largest likely uncertainties of $\pm 1^\circ$ in the bearing from HA01 and ± 7 s in the difference between the times of arrival of the signals at HA01 and RCS, the uncertainty region for the source location does not intersect the arc defined by the last satellite handshake (see Figure 11). An investigation of the timing error required to place the source location on the satellite handshake arc indicated that the arrival time difference would have to be 17 seconds less than measured, which is well outside uncertainties. Our estimate of the time of arrival of the signal at HA01 has been confirmed by Mark Prior from the CTBTO in Vienna, and the correction for clock drift in the RCS recorder has been checked and rechecked. Furthermore, the time calibration checks described in Section 4 provide independent confirmation that time of arrival measurements made at the two stations are consistent once the clock drift correction has been applied.

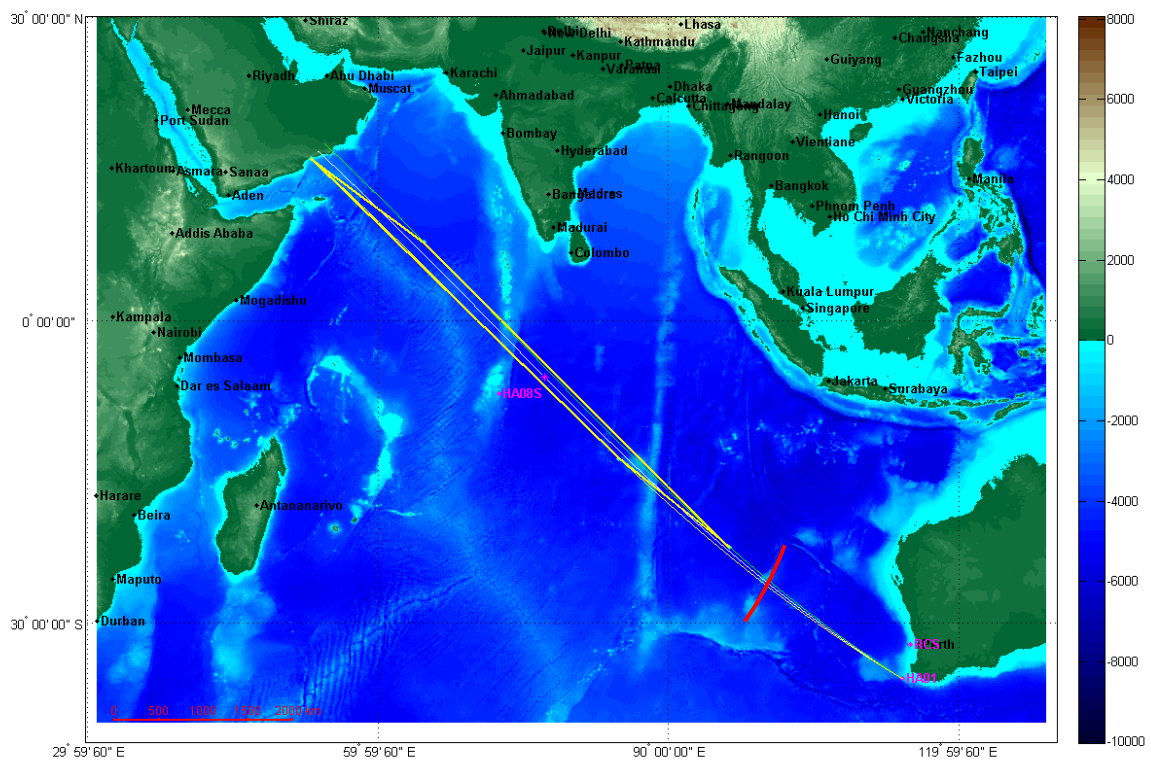


Figure 11. Map showing the uncertainty region (yellow polygon) based on an uncertainty of $\pm 1^\circ$ in the bearing from HA01 and ± 7 s in the arrival time difference, with the approximate location of the arc defined by the satellite handshake data superimposed (red line).

It is therefore apparent that the acoustic measurements are inconsistent with the satellite handshake data. We consider three possible explanations for this:

1. The signals received at HA01 and RCS are from the same acoustic event, but the source of the signals is unrelated to MH370.

This seems the most likely explanation as the characteristics of the received signals are similar to those of some natural events. The origin of these events is not certain, but they are thought to be of natural seismic origin. Events from this particular direction are not particularly common, but do occur. An analysis of five years of historical data from HA01 that was available to the authors indicated that over that period there was an average of about one event per day from this direction. However, on closer inspection it became apparent that most of these events occurred on one day, and then became progressively less frequent. (This is a common pattern with natural seismic events.) It would be useful to analyse data from the year or so leading up to 8th March 2014 in order to obtain a better estimate of the statistics relevant to that date, but this has not been done.

2. The signals received at HA01 and RCS are from different acoustic events, which may or may not be related to MH370.

If this were the case then the distance determination would be invalid and the source of the signal received at HA01 could be anywhere along the position line defined by the measured bearing from HA01, including on the satellite handshake arc. However, the analysis carried out in Section 5, while imperfect, indicates that it is more likely that the signals received at the two stations are from the same event. Also, if the sound source was on the satellite arc the signal would have been generated at 01:16:19 UTC on 8th March, some 25 minutes after the latest time it is thought that MH370 could have hit the water (00:51:00 UTC according to ATSB). The signal could, however, have been generated by the implosion of sinking debris if this occurred well after the initial impact, although this would be expected to be within a few km of the surface impact site.

3. The signals received at HA01 and RCS are from the same acoustic event, and the source of the signals is related to MH370, but there is a problem with the position line determined from the satellite handshake data.

If this were the case then the location of the aircraft would be much further from the Australian coast than the satellite handshake data would indicate. This explanation seems unlikely given the intense scrutiny that the satellite handshake data has been subjected to, however it is worth noting that the time at which the signal was received at HA01 is consistent with the time the aircraft is thought to have crashed if the impact occurred in the central portion of the uncertainty box plotted in Figure 3. To make this explicit, Figure 12 plots the source locations for a signal generated at the earliest possible impact time (00:19:49 UTC - north-western triangle), at the latest possible impact time (00:51:00 UTC - south-eastern triangle) and following the arc given by the signal received at HA01, based on the computed acoustic travel time to HA01 assuming a mean group velocity of 1486 m/s. These extreme locations can be seen to bracket the most probable position obtained solely from the acoustic data.

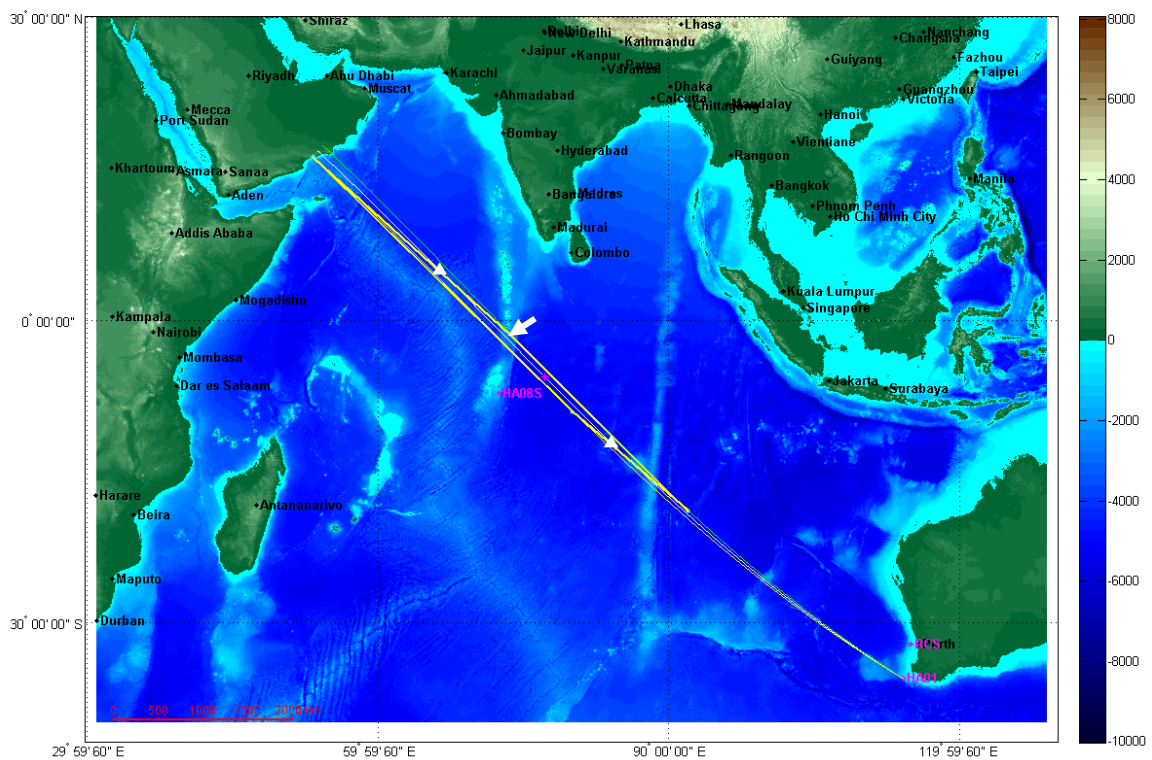


Figure 12. Map showing the smaller uncertainty box with range limits based on the earliest and latest times it is thought the aircraft could have hit the water superimposed (white triangles), assuming the aircraft crash was along the arc from HA01 given by the signal of interest. The arrow indicates the only area between these range limits that also satisfies the requirements for efficient coupling of sound from a near-surface source into the Deep Sound Channel.

Another consideration is that for sound from a near-surface sound source to be detectable at ranges of thousands of kilometres it must couple into the Deep Sound Channel well. A near surface source will generate sound in the water mostly at steep angles and will not efficiently couple into the Deep Sound Channel unless the seabed bathymetry is favourable. For the signal sound energy to couple into the Deep Sound Channel it is necessary for the seafloor at the source location to be sloping downwards towards the receiver. This allows sound reflected from the seabed to be directed into the Deep Sound Channel where it can propagate with very little attenuation. This process is most effective when the water depth is also shallow enough that the seabed intersects the Deep Sound Channel, the axis of which lies somewhere between 800-1200 m depth depending on latitude.

The only area between the locations defined by the earliest and latest impact times along the arc from HA01 given by the signal of interest that satisfies this criterion is on the Chagos-Laccadive Ridge, the submarine ridge that extends northwards from HA08S. The bearing from HA01 crosses this ridge at approximately 2.3°S, 73.7°E, just south of the Maldives, as indicated by the arrow in Figure 12.

The water depths along this bearing of 301.6°, and bearings 0.75° either side of it are plotted as a function of range from HA01 in Figure, along with plots of the computed acoustic transmission loss between a 20 Hz sound source, 30 m below the water surface, and HA01. Note that the way the transmission loss is plotted, an upward excursion corresponds to a reduction in transmission loss, which corresponds to an increase in the received signal. The transmission loss was computed using the Parabolic Equation acoustic propagation model RamGeo (Collins 1993), using range-dependent sound speed profiles from the World Ocean Atlas, 2005 (NOAA 2005), and assuming a low reflectivity, silt seabed with geoacoustic parameters from Jensen (2011). The effect would be enhanced if the seabed were harder and more reflective. Transmission loss calculations were also carried out for frequencies of 10 Hz and 40 Hz and produced similar results.

As expected, oceanographic features that result in sharp reductions in water depth give rise to corresponding reductions in transmission loss, which would correspond to an improved likelihood of detecting a signal for a source at that location. The effect does, however, depend critically on water depth. It can be seen that the Chagos-

Laccadive Ridge is too deep to have much effect along a bearing of 301.6° where it reaches a minimum depth of about 2200 m, but reduces the transmission loss by 20 dB along 302.36° where it rises to a minimum depth of just over 1000m.

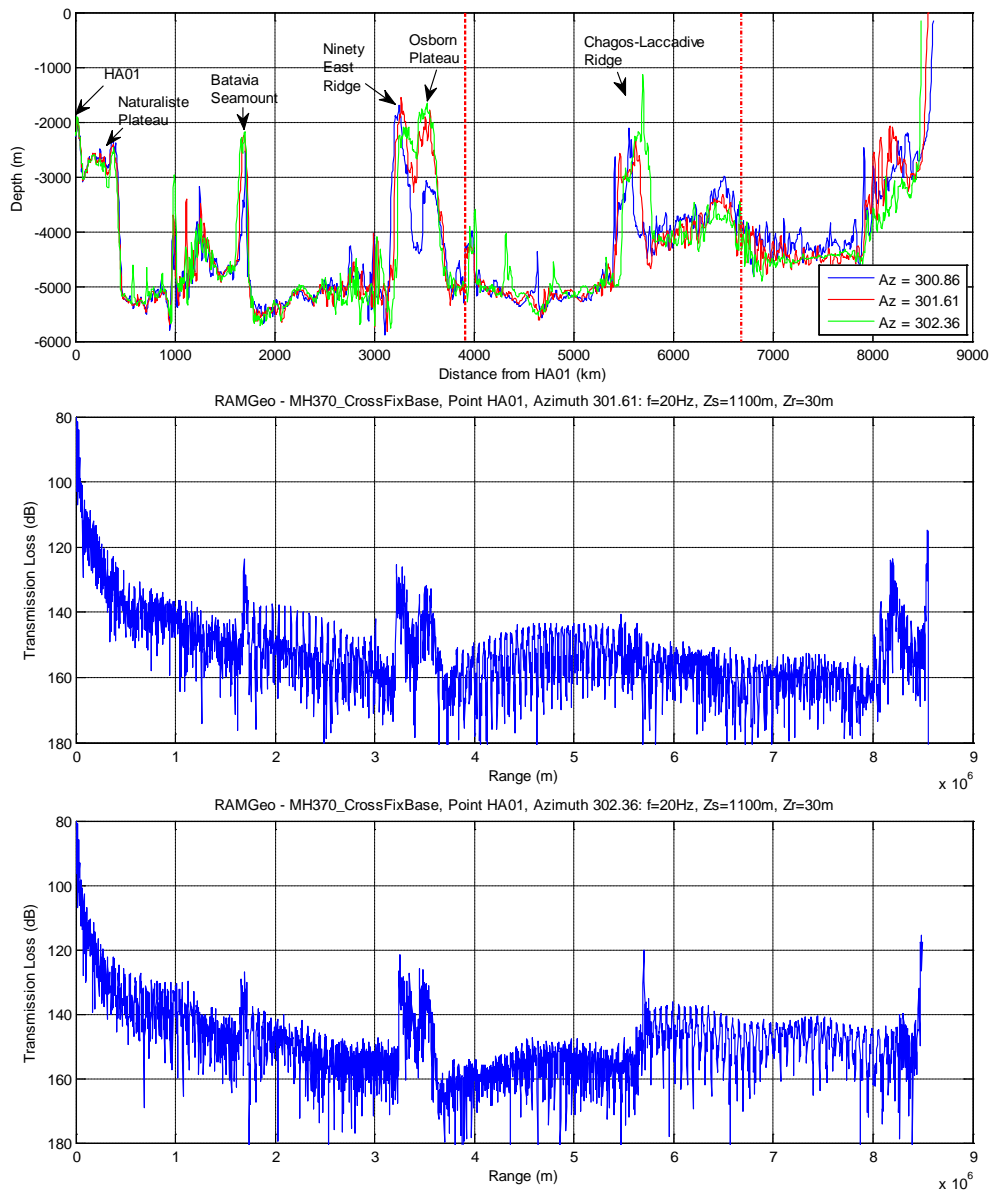


Figure 13. Top panel shows the bathymetry along the position line defined by a bearing of 301.61° from HA01, and bearings 0.75° either side of this as a function of distance from HA01. Red vertical lines indicate the range limits computed from the earliest and latest possible impact times. Various oceanographic features are indicated. The middle and lower panels show the computed transmission loss between a 20Hz acoustic source, 30m below the water surface, and HA01 as a function of range from HA01. Middle panel is for a bearing of 301.61° , lower panel is for 302.36° .

The above argument applies only if the source of the sound was the impact of the plane on the water surface. If it was the implosion of sinking debris, some time after

the impact, then the location could be closer to HA01 than the range limits based on the impact time would indicate. If the implosion occurred in the upper one hundred metres or so of the water column then the same considerations regarding bathymetry would apply, and other possible locations for the aircraft would include the Ninety East Ridge and the Osborn Plateau. However, if an implosion occurred deeper, then efficient deep sound channel propagation would be possible irrespective of the bathymetry. This effect is illustrated in Figure 14, which plots the transmission loss as a function of the distance of the source from HA01, and the source depth.

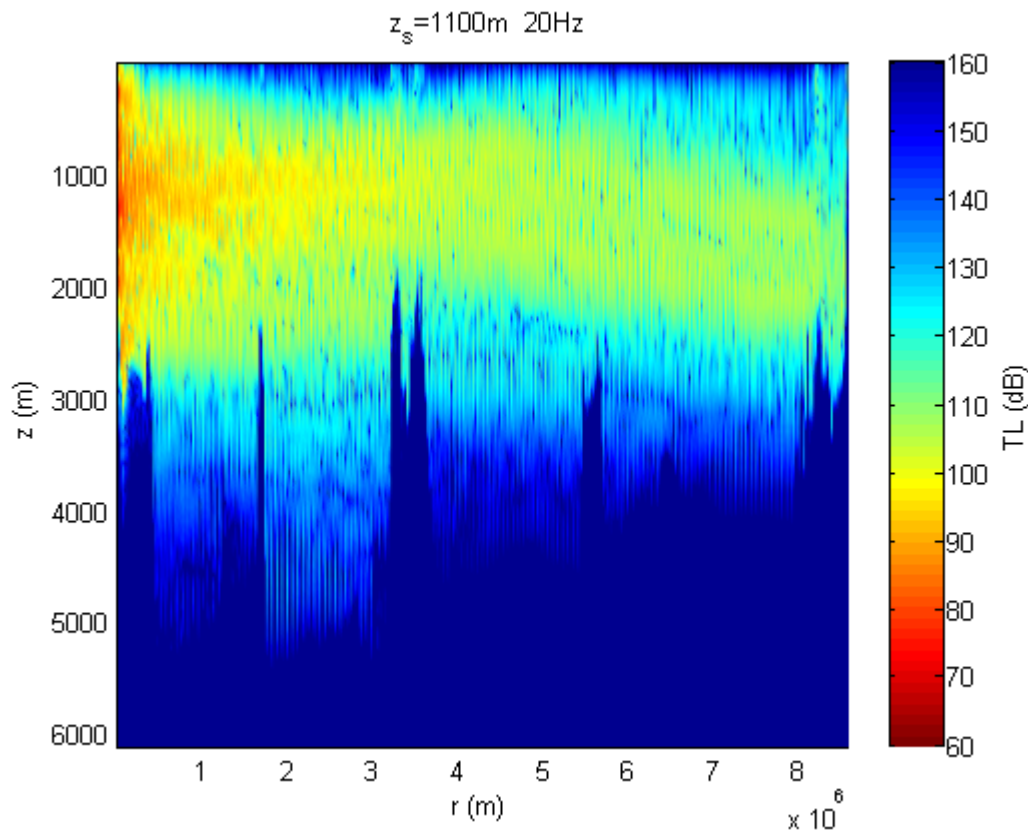


Figure 14. Transmission loss for 20 Hz acoustic signals arriving at HA01 at a bearing of 301.61° as a function of the distance of the source from HA01 and the depth of the source.

CMST are attempting to obtain other sources of acoustic data from the Indian Ocean which may contain the signals discussed here and may allow a better definition of the acoustic data discussed here. These sources are:

1. IMOS passive acoustic recorder located west of Dampier, North Western Australia (19° 23.06' S, 115° 54.92). This mooring is expected to be recovered in early August 2014. This receiver is on a 33% duty cycle.
2. IMOS passive acoustic recorder located north of Broome, North Western Australia (15° 29.002' S, 121° 15.06' E). This mooring is expected to be recovered in early August 2014. This receiver is on a 33% duty cycle.
3. Marine seismic survey recordings operating in the northern Indian Ocean over the time frame of aircraft impact. We have had an excellent response from the marine seismic community with regard to searching for seismic surveys operating in this area over the time frame of interest. If we can locate seismic surveys which were operating over the time frame of interest in areas where it is possible they may have received the signals discussed here we will request their streamer data to check for signals of interest. Marine seismic surveys typically collect data at a 60-80% duty cycle although analysis would be complicated by the presence of the intense marine seismic source signals.

8 Conclusions

Analysis of the low frequency acoustic signals that were received at RCS and HA01 around the time that MH370 disappeared has identified one acoustic event that could possibly be linked to the loss of the aircraft. It is also possible that this was a natural event and unrelated to the aircraft.

A detailed analysis of these signals has resulted in an approximate localisation for the source of the signals that is compatible with the time of the last satellite handshake with the aircraft, but not compatible with the satellite to aircraft range derived from this handshake which is being used to guide the search. There appear to be three possible explanations for this discrepancy:

1. The signals received at HA01 and RCS are from the same acoustic event, but the source of the signals is unrelated to MH370.
2. The signals received at HA01 and RCS are from different acoustic events, which may or may not be related to MH370.

3. The signals received at HA01 and RCS are from the same acoustic event, and the source of the signals is related to MH370, but there is a problem with the position line determined from the satellite handshake data.

Of these, the first explanation seems the most likely as the characteristics of the signals are not unusual, it is only their arrival time and to some extent the direction from which they came that make them of interest.

If the second explanation was correct then there would still be some prospect that the signal received at HA01 could be related to the aircraft, in which case the combination of the HA01 bearing and the position arc derived from the satellite handshake data would provide an accurate location on which to base a search. However, the analysis carried out here indicates that, while not impossible, this explanation is unlikely.

The third explanation also seems unlikely because of the intense scrutiny the satellite handshake data has been subjected to, however, should the arc defined by the handshake data be called into question, the various acoustic considerations discussed here would suggest that a reasonable place to look for the aircraft would be near where the position line defined by a bearing of 301.6° from HA01 crosses the Chagos-Laccadive Ridge, at approximately 2.3°S , 73.7°E . If the source of the detected signals was the aircraft impacting the sea surface then this would most likely have occurred in water depths less than 2000 m and where the seabed slopes downwards towards the east or southeast. This consideration could be used to further refine the search area. If, instead, the received sounds were due to debris imploding at depth it is much less certain where along the position line from HA01 this would have occurred.

The CMST are still to receive further passive acoustic data which may improve the location estimate provided here and allow a better definition of the signal source.

References

- Collins, M. D. (1993), A split-step Pade solution for the parabolic equation method. *The Journal of the Acoustical Society of America*, 93(4), 1736-1742.
- del Pezzo, E., and Giudicepietro, F. (2002), Plane wave fitting method for a plane, small aperture, short period seismic array: a MATHCAD program, *Computers & Geosciences*, Vol. 28, pp 59-64.
- Jensen, F. B., Kuperman, W. A., Porter, M. B., & Schmidt, H. (2011). *Computational Ocean Acoustics*, Springer, ISBN 978-1-4419-8677-1.
- Menke W., (1984), *Geophysical Data Analysis: Discrete Inverse Theory*, Academic Press, New York.
- Walpole, R. E., and Meyers, R. H. (1985), *Probability and Statistics for Engineers*, Macmillan, ISBN 0-02-946950-3.
- NOAA. (2005), *World Ocean Atlas*, National Oceanic and Atmospheric Administration, National Environmental Satellite, Data, and Information Service 61-62, U.S. Government Printing Office, Washington, D.C., 182 pp., CD-ROM

Appendix I – Results of analysis of Scott Reef IMOS underwater sound recorder data for the time of the disappearance of Malaysian Airlines Flight MH370 on 8th March 2014

Results of analysis of Scott Reef IMOS underwater sound recorder data for the time of the disappearance of Malaysian Airlines Flight MH370 on 8th March 2014.

Alec Duncan, Rob McCauley, Alexander Gavrilov
Centre for Marine Science and Technology, Curtin University
4th September 2014

Introduction

An underwater sound recorder that forms part of the Integrated Marine Observing System (IMOS) and was located off Scott Reef, Western Australia has recently been recovered. Data from the recorder was downloaded on 3rd September 2014. The recorder was located at 15° 29.002' S, 121° 15.060' E. This data set is of interest because the recorder was operational at the time that Malaysian Airlines Flight MH370 went missing on 8th March 2014.

Results

Signals and their spectrograms recorded between 01:00:00 UTC and 02:20:00 UTC on 8th March 2014 are plotted in the Appendix. Each recording is of five minutes duration and recordings started every 15 minutes, commencing approximately 15 seconds before the hour. The 15 second offset was due to drift of the noise recorder's internal clock relative to UTC. Drift was corrected by comparing the noise recorder's clock to UTC from a GPS receiver before deployment and after recovery, and assuming a constant drift rate during deployment.

The recordings are dominated by Bryde's whale calls in the 25Hz to 50 Hz frequency range, and also contain a number of short, impulsive signals of unknown but probably local origin. Of particular interest is a signal with considerable energy below 20 Hz commencing at 01:32:49 UTC. This signal and its spectrogram are shown in Fig. 1. The structure of the low frequency arrival is shown more clearly in Fig. 2, which is the same data after filtering with a 15 Hz, 4th order, low pass Butterworth filter to remove the whale calls and other higher frequency signals. It appears to consist of an initial high amplitude arrival of about ten seconds duration followed by a lower amplitude tail that lasts for at least another 100 seconds (the logger stopped recording before the end of the signal). The duration and frequency content of the initial high amplitude arrival are consistent with the signals received at the Comprehensive Nuclear Test-ban Treaty hydroacoustic station, HA01 at 01:34:50 UTC, and with the corresponding signal received at the IMOS underwater recorder off Rottneest Island (Duncan et. al. 2014).

The arrival time of this signal at the Scott Reef recorder is also within the range of possible times of arrival of signals from the event that generated the signal received at HA01, at 01:34:50 UTC.

A least squares fix was calculated based on the signal arrival time and arrival direction at HA01 and the arrival times at the Rottneest and Scott Reef IMOS recorders. The results are given in Table 1 and plotted in Fig. 3. The estimated position is close to the

Carlsberg Ridge, a geologically active mid-ocean spreading ridge, and is about 400km southeast of the position obtained by Dall'Osto and Dahl (2014) based on a low frequency arrival at HA08S, and the HA01 direction and arrival time data.

Conclusions

It is impossible to be certain that the Scott Reef IMOS recorder arrival at 01:32:49 UTC is from the same event as the arrivals at HA01 and the Rottneest IMOS recorder that have been analysed previously, however they share enough characteristics that it seems plausible that they are from the same event. Assuming this is the case results in an event location that is near the geologically active Carlsberg Ridge southwest of India. This location, together with the lower amplitude tail that appears to extend at least 100 seconds after the initial onset makes it likely that the event is of geological origin.

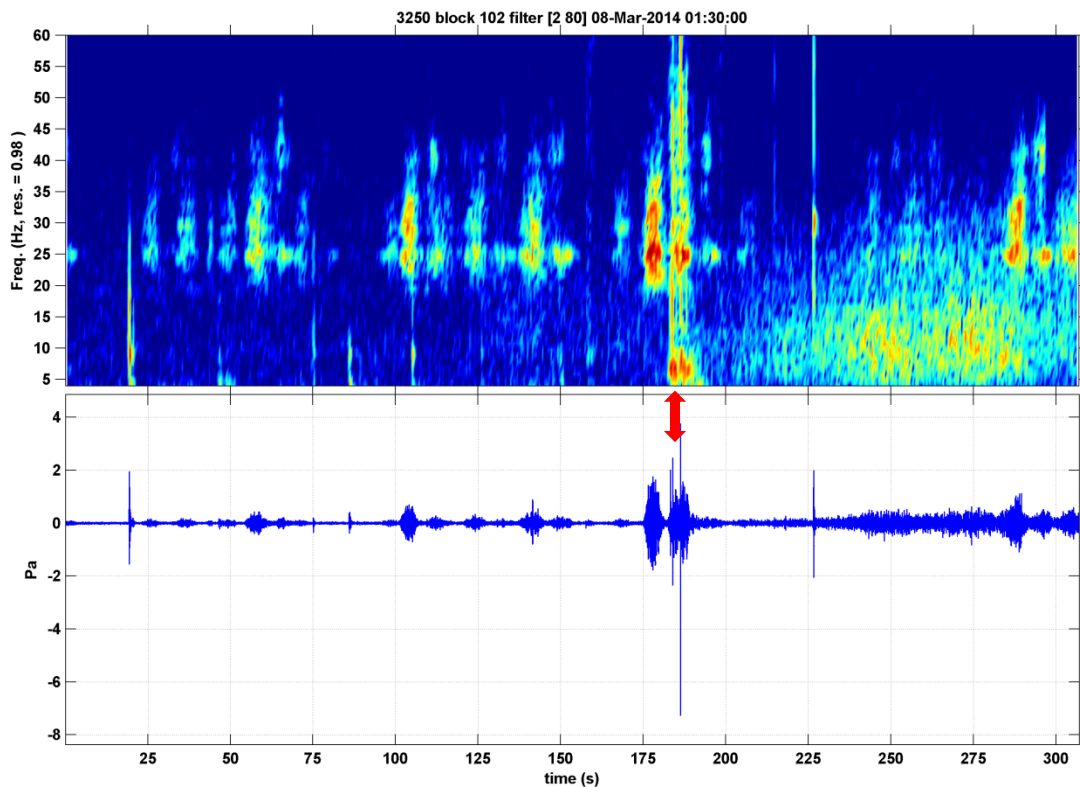


Fig. 1. Signal and spectrogram of the recording commencing at 01:29:45.9 UTC (drift corrected). The beginning of the 01:32:49 arrival is marked by the red arrow at about 180 seconds.

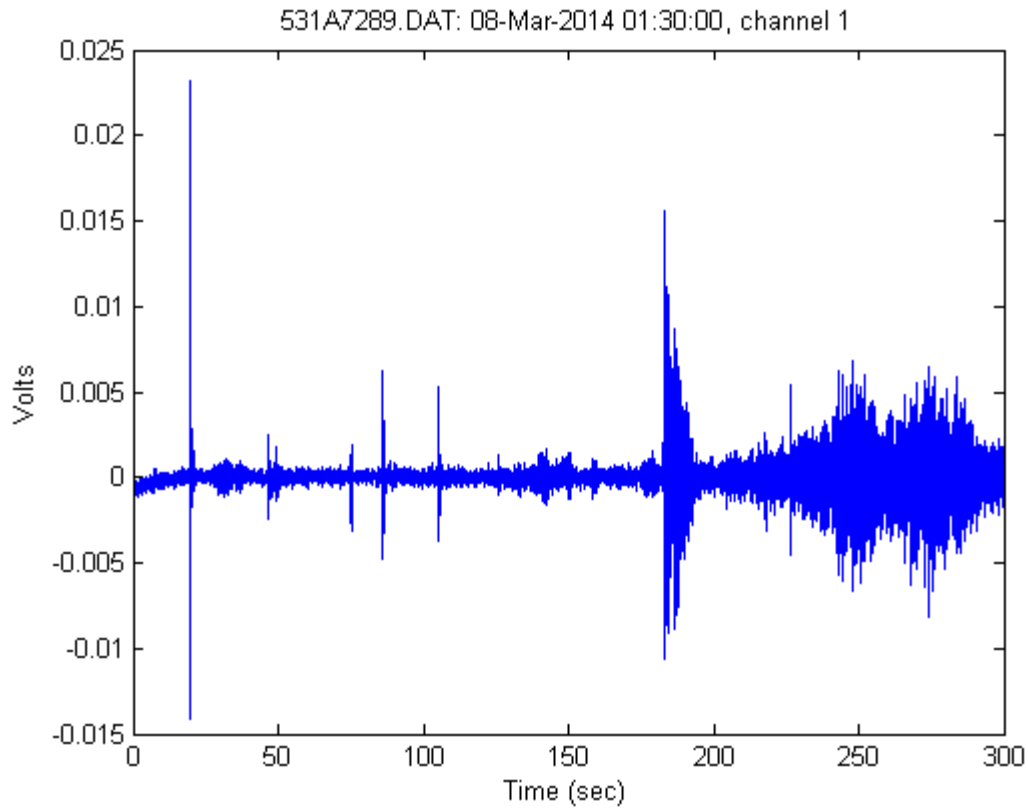
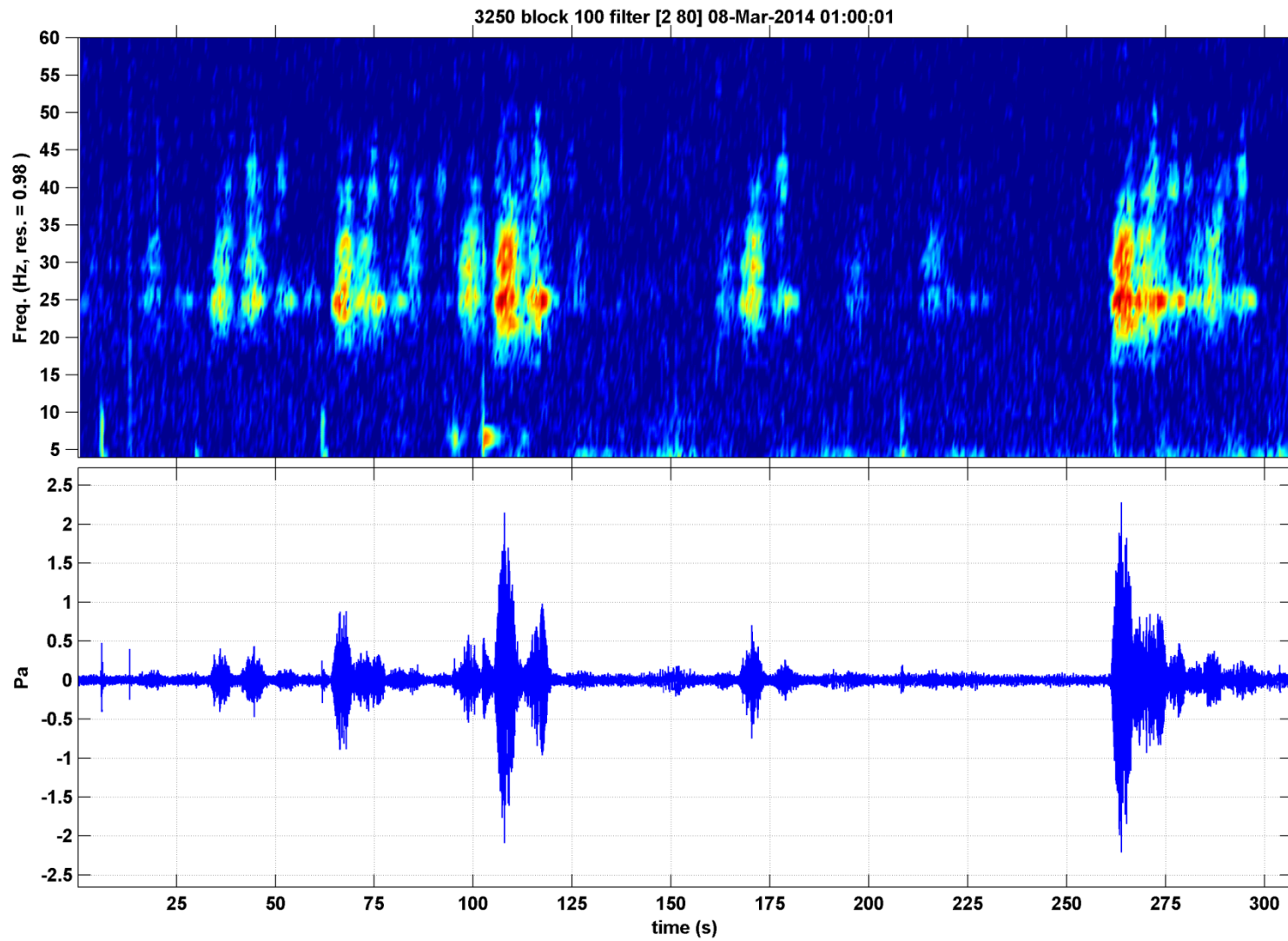


Fig. 2. The same signal after filtering with a 4th order low pass Butterworth filter with a 15Hz cutoff frequency. Times are relative to 01:29:45.9 UTC (drift corrected).

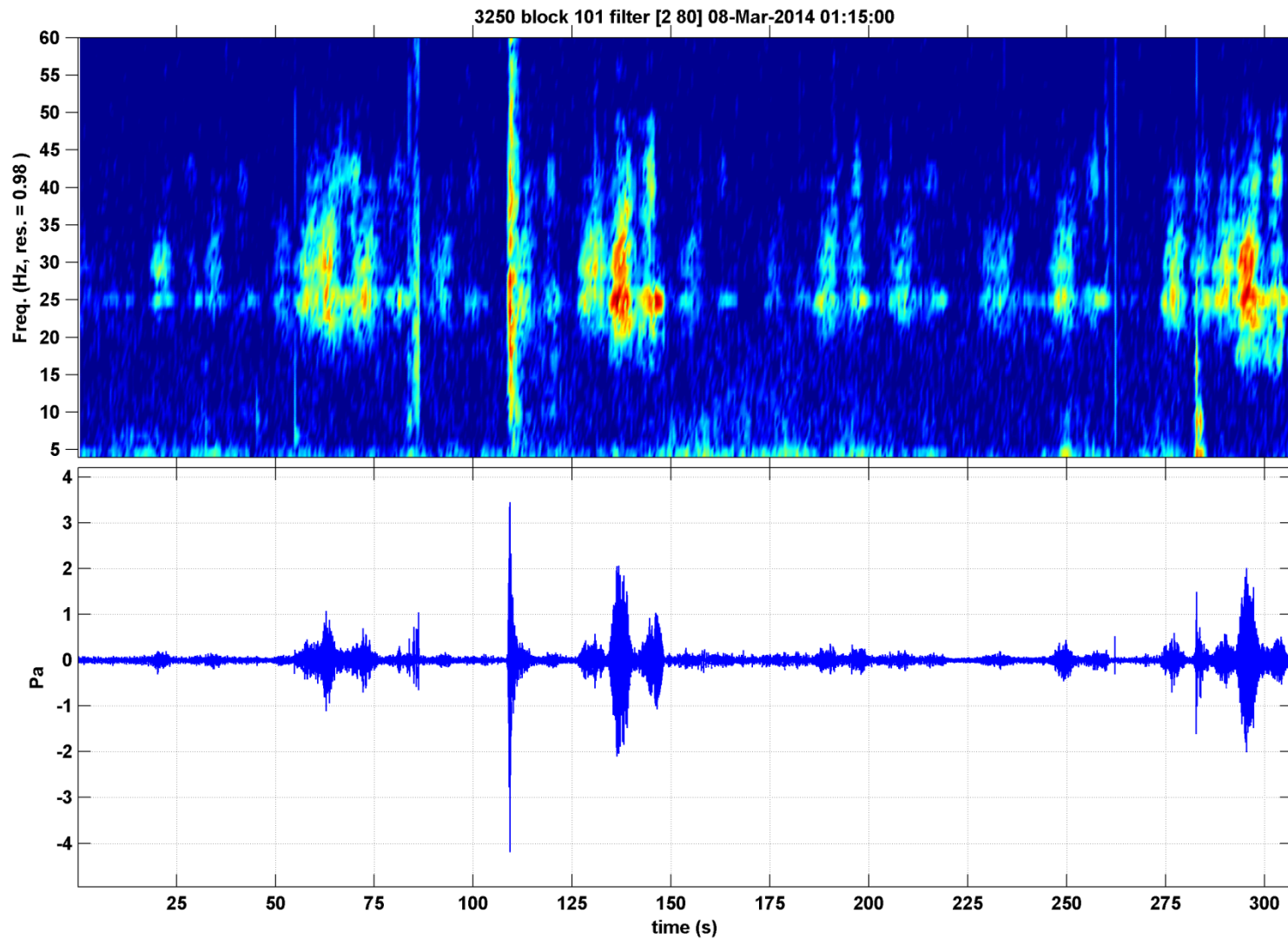
Table 1. Least squares fix results

Estimated event position (WGS84)	2.11°N, 69.31°E
Standard deviation in estimated latitude, longitude	0.67°, 0.96°
Covariance between latitude and longitude estimates	-0.63 (°) ²
Estimated event time	00:25:13.3 UTC on 8 th March 2014
Standard deviation in estimated event time	85 s
HA01 angle measurement residual	0.06°
HA01 time measurement residual	-0.2 s
Rottneest time measurement residual	1.7 s
Scott Reef time measurement residual	-0.04 s

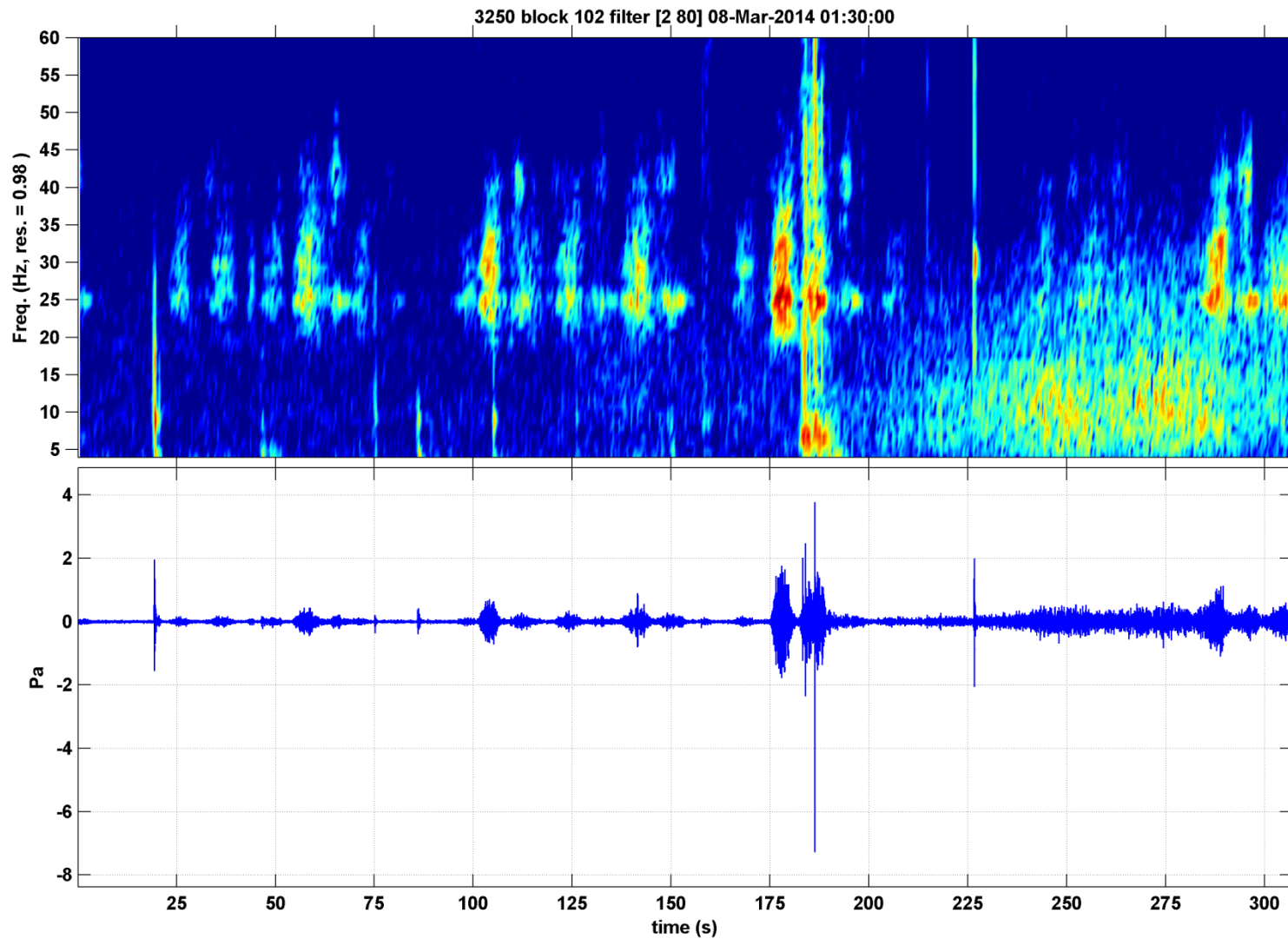
APPENDIX: All Scott Reef Logger Recordings from 01:00:00 UTC to 02:20:00 UTC on 8th March 2014



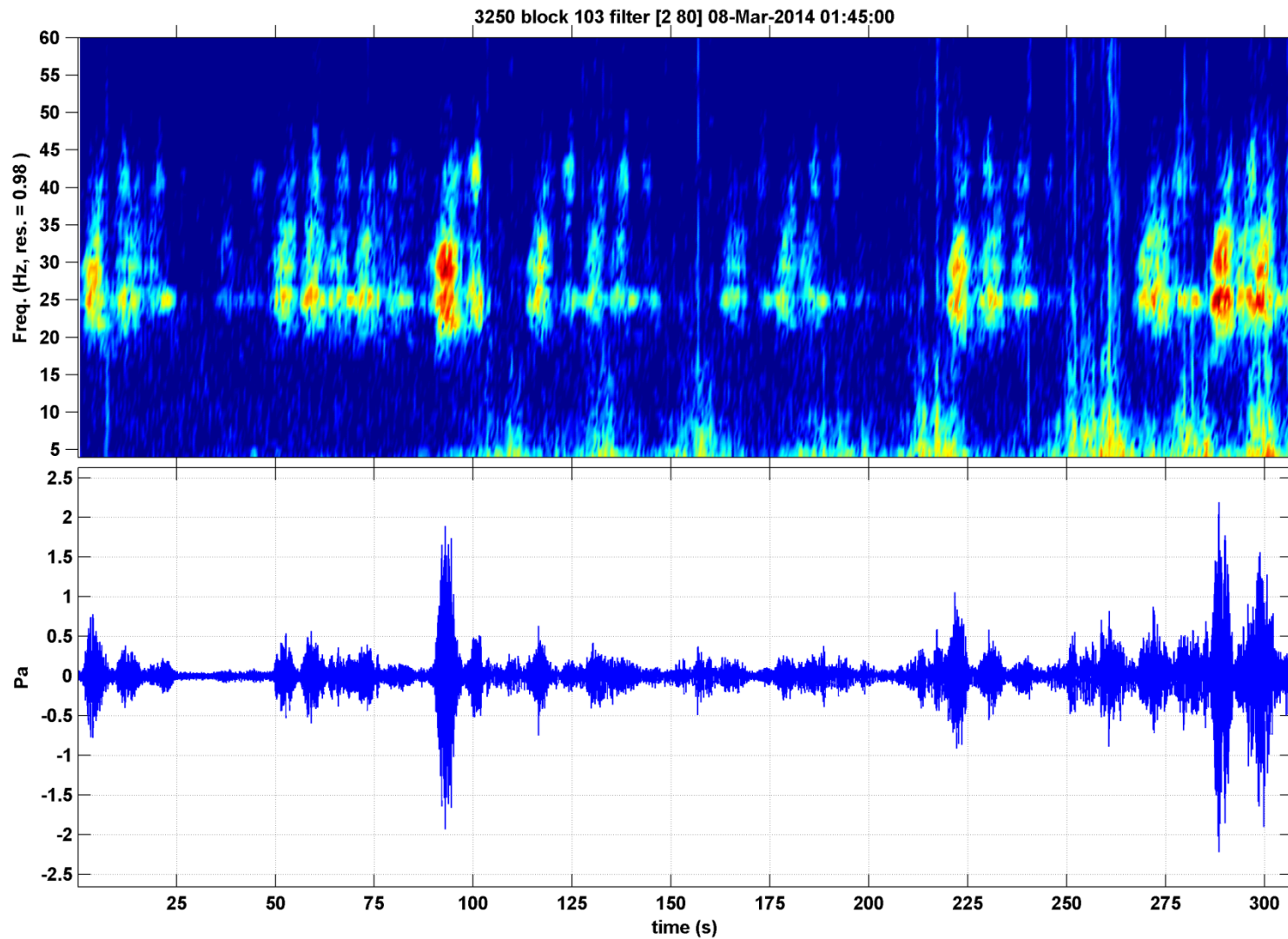
Block 100. Times are relative to 8-03-2014 0:59:46.3 UTC (drift corrected)



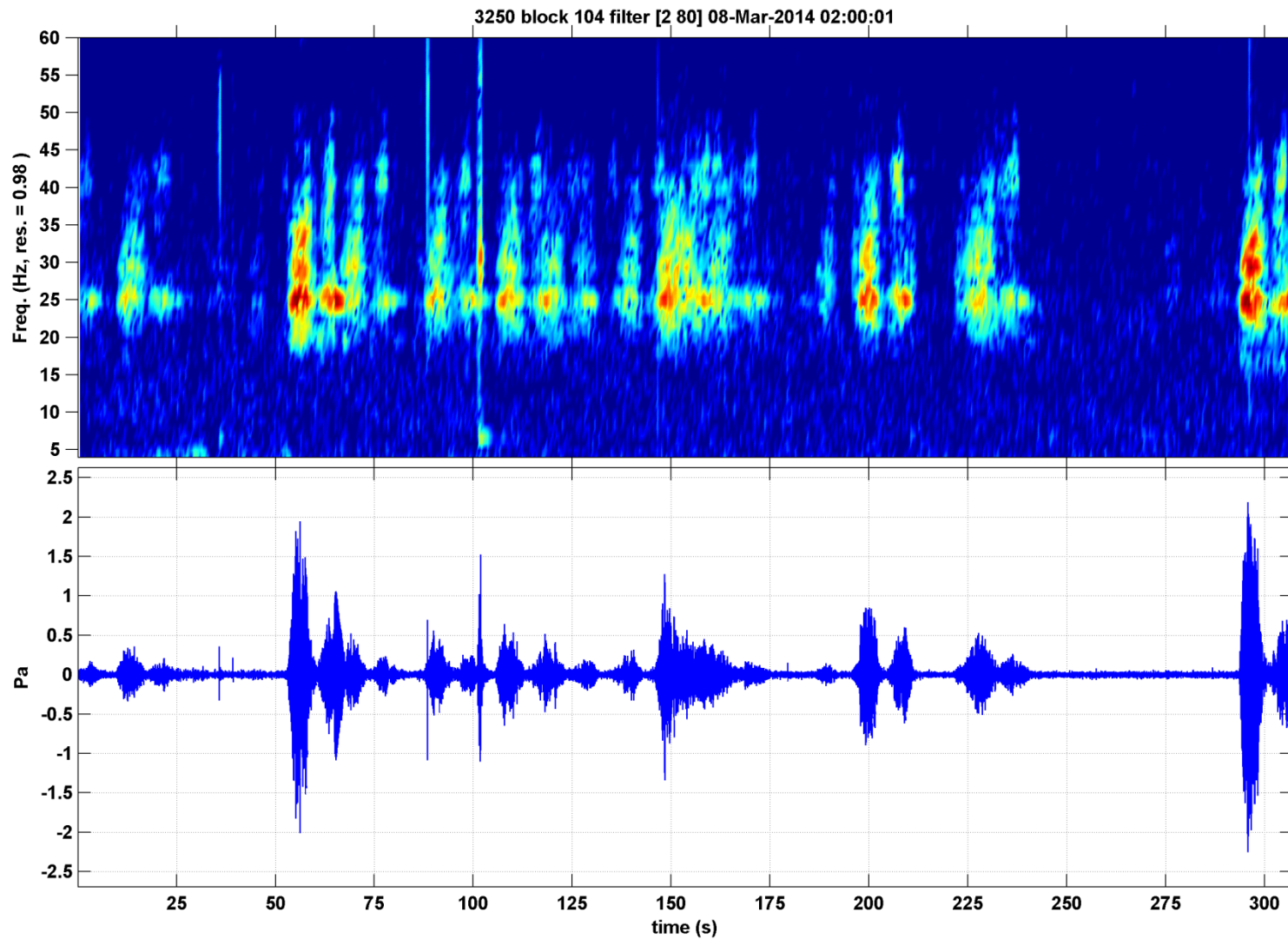
Block 101. Times are relative to 8-03-2014 1:14:45.8 UTC (drift corrected)



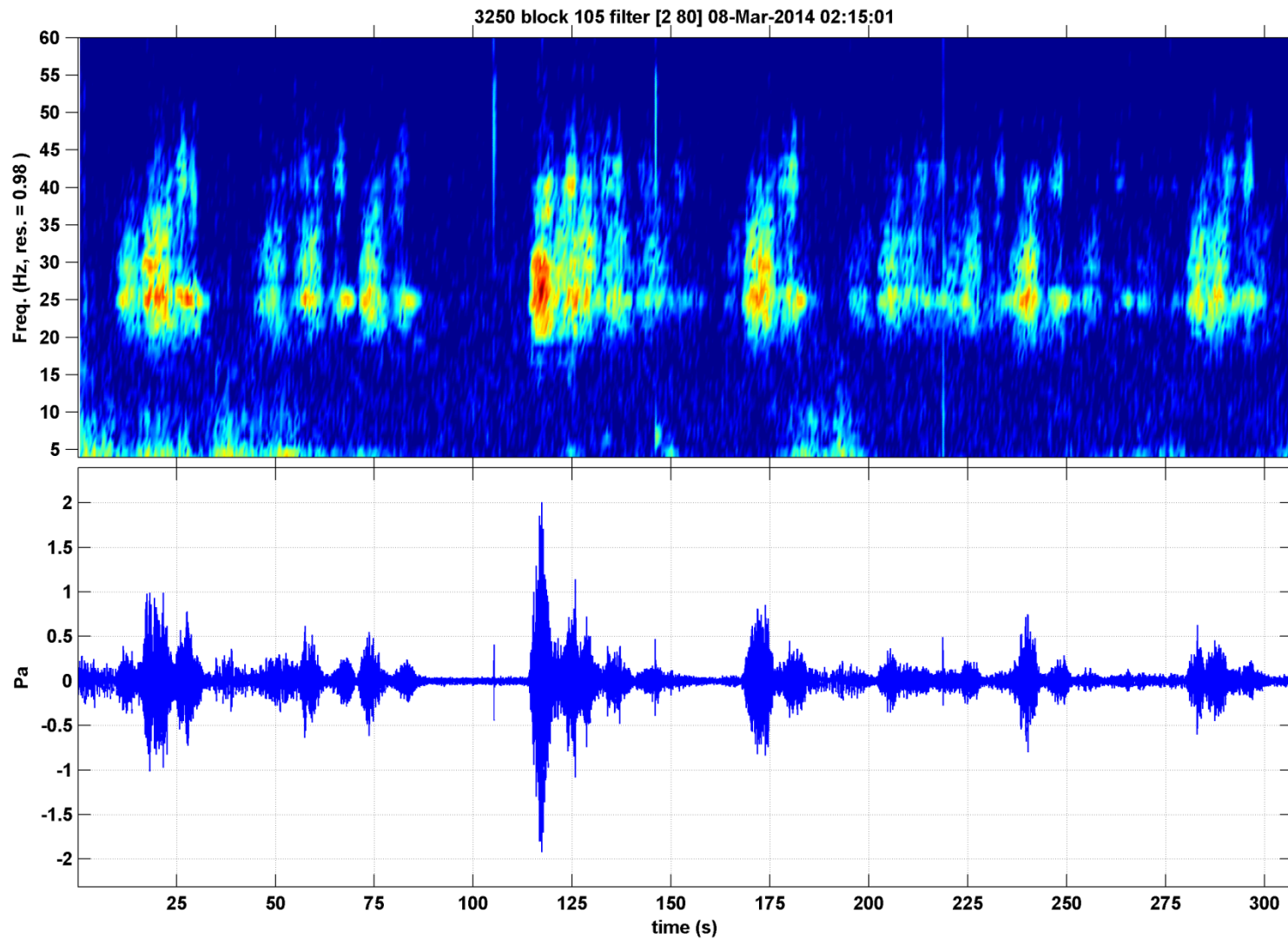
Block 102. Times are relative to 8-03-2014 1:29:45.9 UTC (drift corrected)



Block 103. Times are relative to 8-03-2014 1:44:45.7 UTC (drift corrected)



Block 104. Times are relative to 8-03-2014 1:59:46.1 UTC (drift corrected)



Block 105. Times are relative to 8-03-2014 2:14:46.4 UTC (drift corrected)

References

Dall'Osto, D. R., and Dahl, P. H. "Analysis of hydroacoustic signals from Diego Garcia South CTBTO station in support of Curtin University analysis of Cape Leeuwin CTBTO data regarding possible location of MH370 crash", Applied Physics Laboratory, University of Washington, Seattle, July 2014.

Duncan, A. J., Gavrilov, A. N., McCauley, R. D., "Analysis of Low Frequency Underwater Acoustic Signals Possibly Related to the Loss of Malaysian Airlines Flight MH370", Centre for Marine Science and Technology Report 2014-30, June 2014.

Appendix J – Seismic and hydroacoustic analysis relevant to MH370

LA-UR-14-24972

Approved for public release; distribution is unlimited.

Title: Seismic and hydroacoustic analysis relevant to MH370

Author(s): Stead, Richard J.

Intended for: Report

Issued: 2014-07-03

Disclaimer:

Los Alamos National Laboratory, an affirmative action/equal opportunity employer, is operated by the Los Alamos National Security, LLC for the National Nuclear Security Administration of the U.S. Department of Energy under contract DE-AC52-06NA25396. By approving this article, the publisher recognizes that the U.S. Government retains nonexclusive, royalty-free license to publish or reproduce the published form of this contribution, or to allow others to do so, for U.S. Government purposes. Los Alamos National Laboratory requests that the publisher identify this article as work performed under the auspices of the U.S. Department of Energy. Los Alamos National Laboratory strongly supports academic freedom and a researcher's right to publish; as an institution, however, the Laboratory does not endorse the viewpoint of a publication or guarantee its technical correctness.

Seismic and hydroacoustic analysis relevant to MH370

Abstract

The vicinity of the Indian Ocean is searched for open and readily available seismic and/or hydroacoustic stations that might have recorded a possible impact of MH370 with the ocean surface. Only three stations are identified: the IMS hydrophone arrays H01 and H08, and the Geoscope seismic station AIS. Analysis of the data from these stations shows an interesting arrival on H01 that has some interference from an Antarctic ice event, large amplitude repeating signals at H08 that obscure any possible arrivals, and large amplitude chaotic noise at AIS that obscures any arrivals at lower frequencies while the low sample rate at AIS precludes any analysis at higher frequencies of interest. The results are therefore rather inconclusive but may point to a more southerly impact location within the overall Indian Ocean search region. The results would be more useful if they can be combined with any other data that are not readily available.

Introduction

MH370 is a Malaysian Airlines flight that was lost over the Indian Ocean, and assumed to have crashed sometime shortly after 00:00 UTC on 2014/03/08. The impact of a large passenger jet with the ocean surface should create a signal that could be observed on hydrophones or nearby seismic stations. The study discussed here is an analysis of the hydroacoustic and seismic data readily available, in an effort to determine if such signals are present and if they can provide any information regarding the hypothesized impact event.

Data

The Indian Ocean is a relatively poorly monitored region of the globe. For sources near the ocean surface, the best records would be hydrophone stations, followed by near-shore seismic stations (to look for signals that result from the conversion of hydroacoustic energy to seismic energy, known collectively as T phases). In the southern Indian Ocean, there are only 2 hydrophone stations readily available, both from the CTBT IMS network: Cape Leeuwin, Australia, having the code H01, and Diego Garcia, an island in the British Indian Ocean Territory (BIOT), Chagos Archipelago, having the code H08. Both hydrophone stations have 3-element triangular arrays of hydrophones installed well offshore and positioned in the SOFAR channel. Other hydrophone stations in the Atlantic and Pacific are generally blocked from this source region. There is only one nearby seismic station for the expected region of impact, and that is Amsterdam Island, code AIS, a Geoscope station (Geoscope is a French international seismic network). This station has a

three-component broadband seismometer. The IMS data are available from the CTBTO located in Vienna, Austria. The data from AIS are available at the IRIS DMC located in Seattle, Washington, USA.

Analysis

H01

H01 is the closest hydrophone station, and as such has the highest likelihood of recording any signal that may have been generated by the expected impact event. H01 consists of a single 3-element array.

We started with a scan of the raw, broadband hydrophone data, for approximately 2 hours around the expected time of impact, adjusted for some travel time from the point of impact to the station. This scan revealed only one set of signals that was significantly above the background noise, including various small signals. These signals were observed at approximately 00:52 UTC, and shown in Figure 1. We focus all further analysis on these signals.

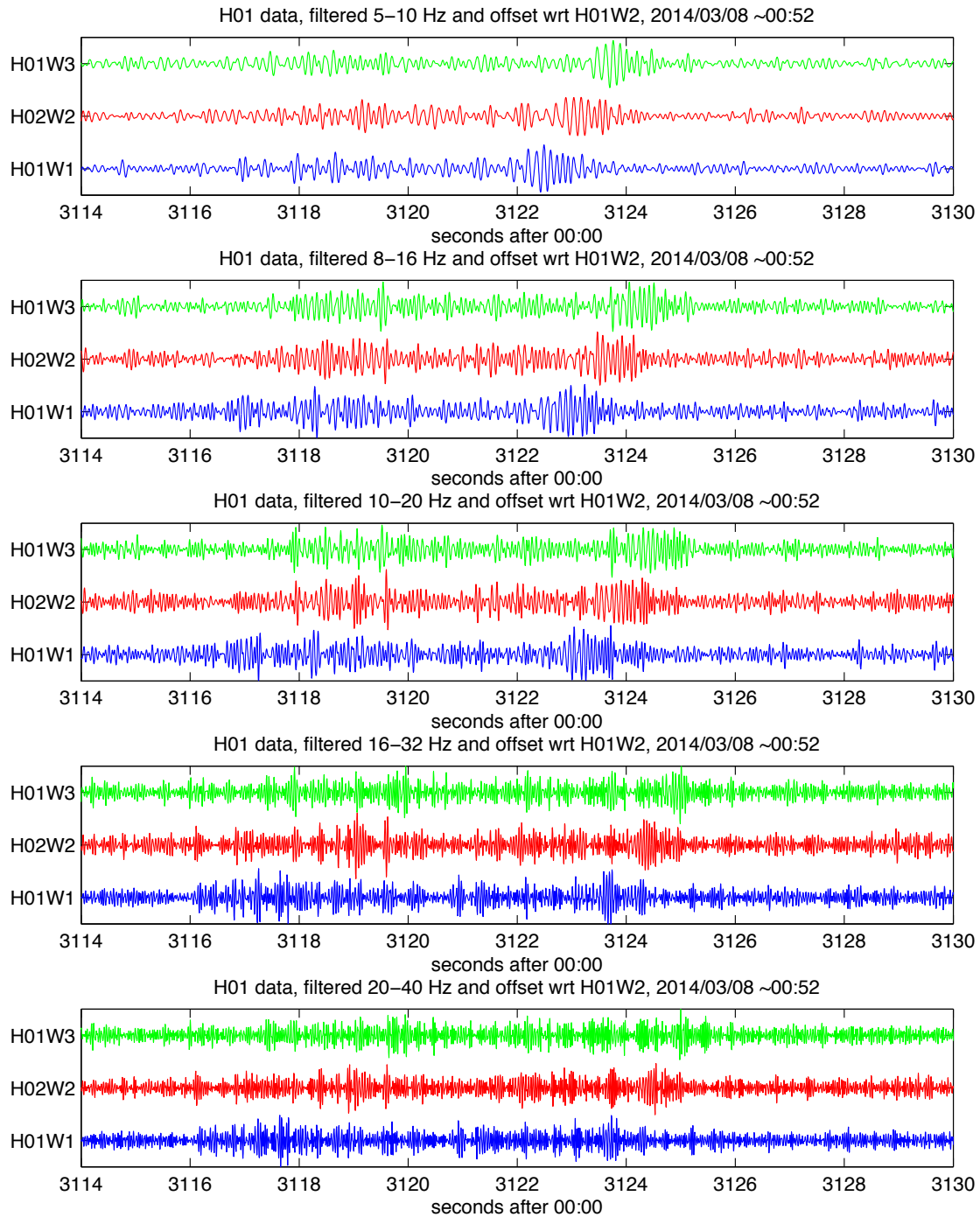


Figure 1: Filtered waveforms from all three elements of H01 around the time 00:52 UTC on 2014/03/08. The filters are 1-octave bands as indicated above each subimage. The features and alignment of the traces will be discussed later in the text.

The signals visible in figure 1 comprise two groups. The largest is the latter group showing large amplitudes and significant dispersion. We begin our analysis with that group. Using a time window relatively tight to just the late signals, we perform

a cross-correlation analysis to find the correct alignment of this group. The results are shown in figure 2. All further analysis of these signals is performed in the 10-20 Hz band. Figure 1 shows that the latter signal dominates the waveform at lower frequencies, and the signal-to-noise ratio is poor at higher frequencies. Thus 10-20 Hz is the best band in which to analyze all of the signals present.

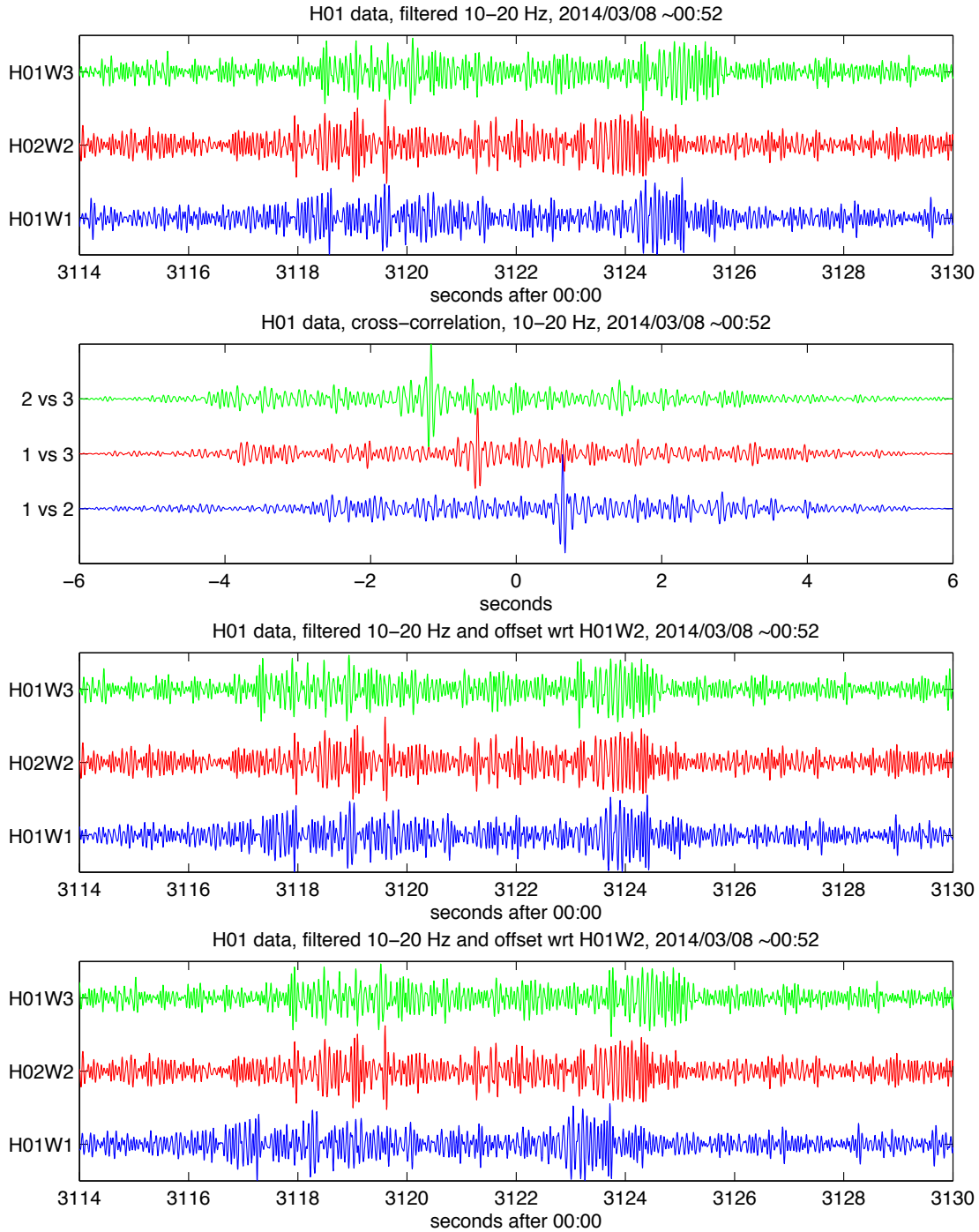


Figure 2: Cross-correlation analysis of the signals at H01. The first subimage shows all 3 elements, filtered 10-20 Hz and aligned on true time. The second shows the

cross-correlation analysis of just the 6 seconds surrounding the latter, large, dispersive signal, also performed in the 10-20 Hz band. The third subimage is aligned using the results of the cross-correlation analysis. Note the excellent alignment of the latter signal, particularly frequency dispersion, but the lack of alignment of earlier features. The alignment of the fourth subimage is discussed later in the text.

The cross-correlation analysis works very well on the latter, large-amplitude, dispersive signal. But it does not work well on the earlier signals. This leads us to conclude that the two sets of signals may originate from different sources. Other characteristics seem to support this conclusion, since the earlier signals seem to lack significant dispersion and also lack significant energy in the lower frequencies, such as 5-10 Hz, as can be seen in Figure 1. Using the offsets for the latter phase, we compute the direction of arrival (DOA, always given here as a 2D horizontal DOA measured in degrees clockwise from north) and observed phase velocity for that phase. DOA is 190.5° , and the phase velocity (inverse of apparent slowness) is 1.46 km/s, quite consistent with expected SOFAR channel phase velocities. For that direction, it is most likely that this signal originated in an ice-related event in the vicinity of Antarctica.

Cross-correlation was attempted on the earlier signals, without success – there were no significant peaks found, unlike the clear peaks shown in figure 2 for the latter signal. This is not surprising, since the separation of the array elements, which is on the order of 2 km, represents multiple wavelengths at this phase velocity and frequency. Most signals would not be expected to have strong coherence between the elements, especially those that are more impulsive and not dispersed. Instead of cross-correlation, we rely on a manual alignment of key features. Beginning with elements W2 and W3, which seem the most coherent for the earlier energy, we align 4 prominent peaks in the energy observed in the signals. This is shown in the lower part of figure 2. The third element of the array, W1, is then aligned by constraining the phase velocity to be that observed for the ice signal, 1.46 km/s. Geometrical constraints and the assumed phase velocity then determine uniquely the offset for W1. W1 is clearly not very coherent with either W2 or W3 for this signal, but in general, the bulk of the energy for this arrival appears in the same time window as it does on W2 and W3, with the exception of an early pulse of energy, which could be unrelated. Note that figure 1 is also created with this alignment, and the 8-16 Hz band shows good alignment for the timing of the bulk of the energy, again with the exception of spurious energy early on W1. Attempts to align the early energy on W1 result in unphysical phase velocities, which also leads us to conclude that this early energy on W1 is unrelated. The final alignment of the first arrivals produces a DOA of 246.9° (with the phase velocity fixed at 1.46 km/s). The source for this arrival would then be WSW of the array, in the general direction of the region in which MH370 may have impacted the ocean, and has an arrival time that could be consistent as well. Although the arrival is weak and is interfered by a strong ice source arrival, there is evidence that this could be an arrival from an impact of MH370 with the ocean surface. Figures 3 and 4 show spectrograms aligned with the

computed cross-correlation for the latter arrival and the manual alignment of the first arrival. The alignment of energy in these figures also supports the direction of arrival conclusions.

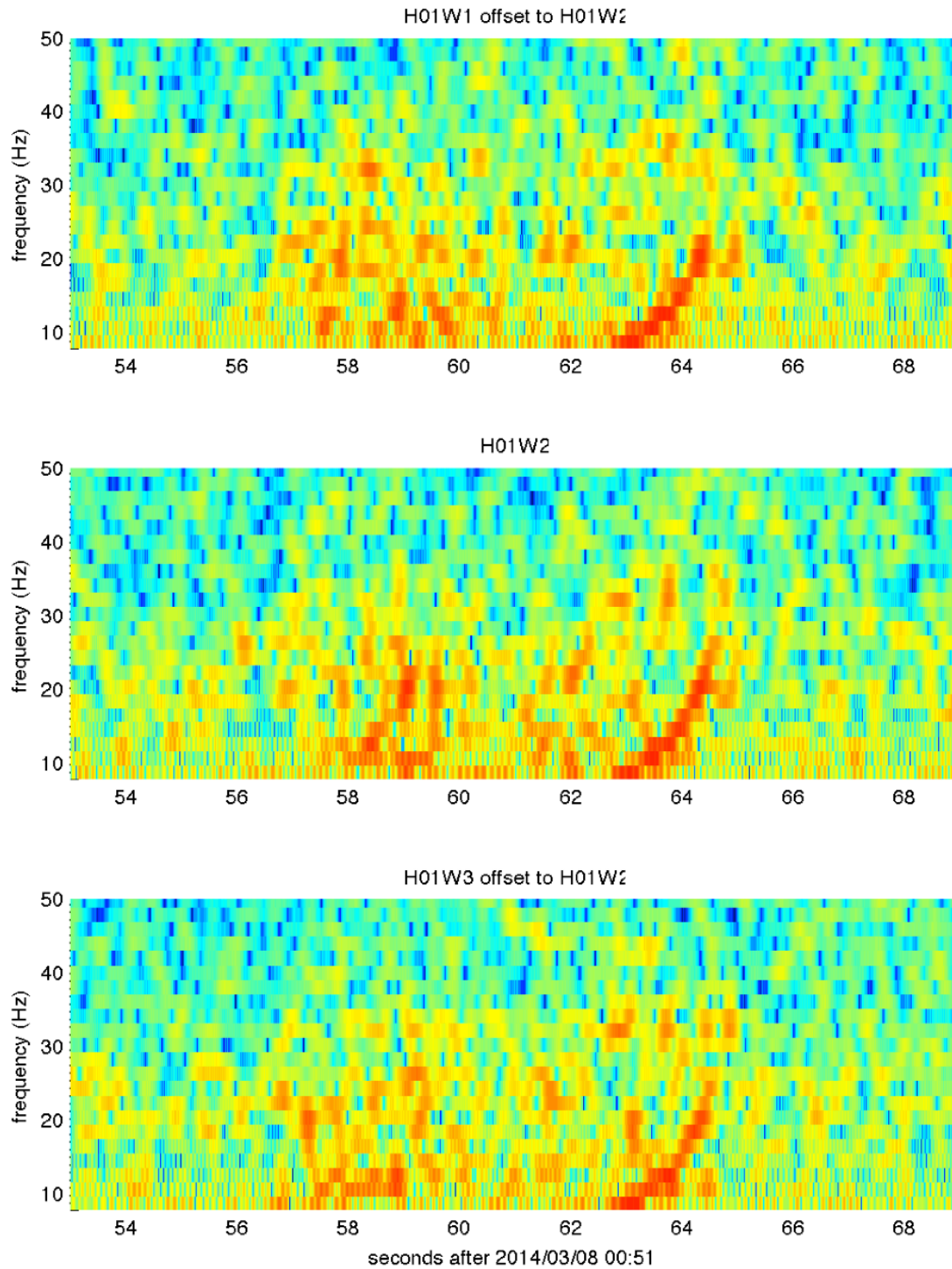


Figure 3. Spectrograms, 8-60 Hz, around 2014/03/08 00:52 UTC for hydroacoustic array H01. The spectrograms for the three elements of the array are aligned on the computed cross-correlation offsets for the latter arrival (the large-amplitude highly

dispersed arrival between about 63 and 65 seconds after 00:51). Note the apparent lack of alignment for the earlier energy.

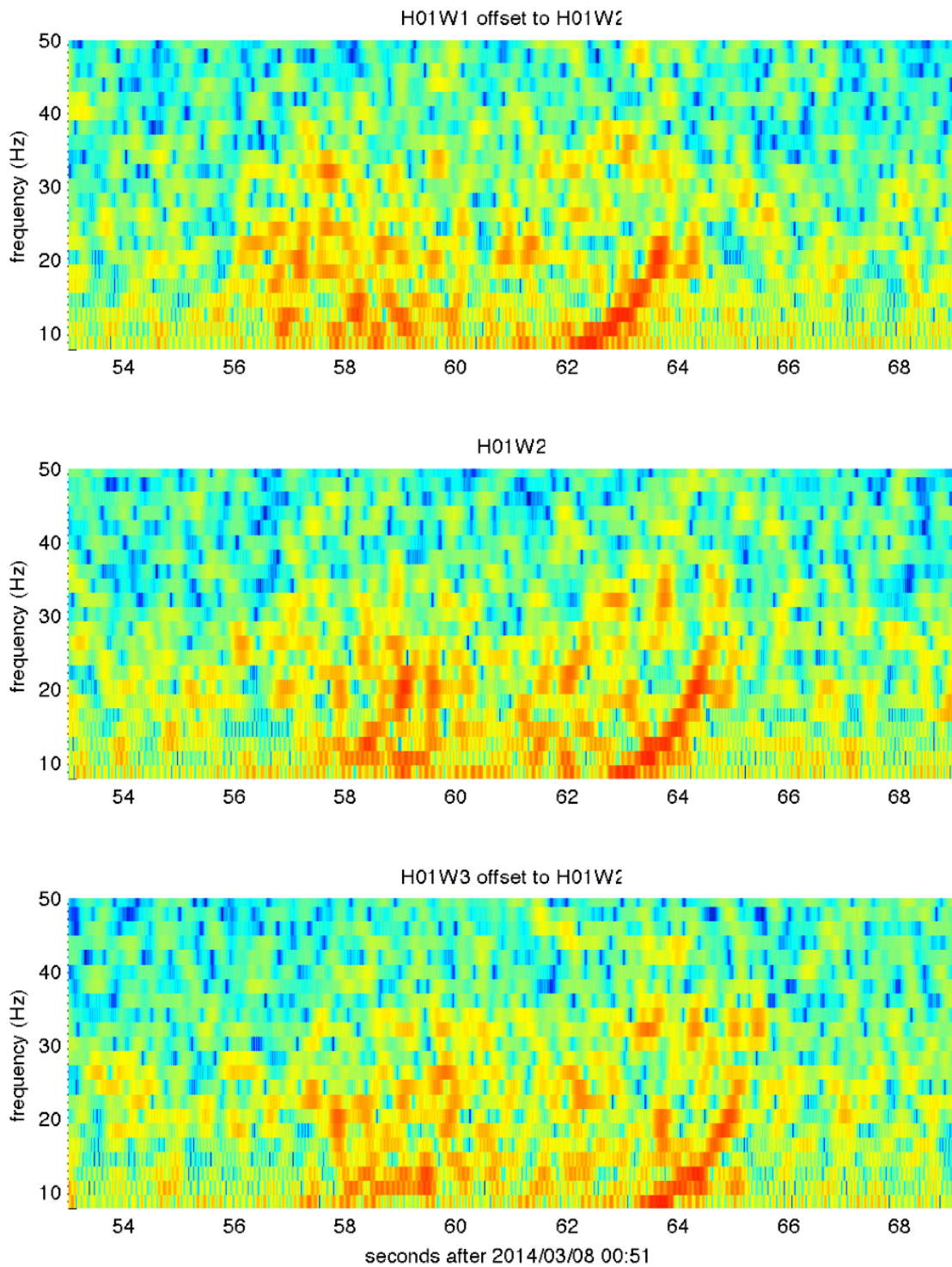


Figure 4: Spectrograms aligned according to manual alignment of early features. Apart from some early energy on H01, features of the earlier energy appear better aligned, particularly between W2 and W3 elements. All elements now show

features between 57.8 and 58.5 and again between 59 and 60 that appear to be well aligned. A feature between 58 and 58.5 may show some evidence of identical dispersion on elements W2 and W3.

H08

H08 is a hydrophone station that is quite a bit further from the potential impact region than H01. We started with the same type of time scan as we did on H01, applied to the southern 3-element array from H08. However, this analysis revealed a long set of two large-amplitude, broadband, repeating signals, one at approximately 10-second intervals and one at approximately 8-second intervals, that dominate the record throughout. These signals continue for hours both before and after the time of interest, and, as can be seen in the figure, are very broadband. In addition, they are larger in amplitude, relative to background, than the signals of interest observed on H01. These signals preclude any possibility of identifying any signal from the impact that might have arrived at H08. The signals arrive from two separate directions. They are both coming from the sea so they are either anthropogenic (airgun surveys or something similar) or biogenic (whales, for example).

A sample of H08 data is shown in figure 5. The same 5 filters are used as were used for H01 data in figure 1. The large amplitude signals appear at approximately 10-second intervals. The smaller amplitude signals are at about 8-second intervals and can be seen progressively interfering with the larger signals. To see this most clearly, look at element S2 at 10-20 Hz. The small signal clearly follows the large one at about 3707 (seconds after 2014/03/08 00:00), has about the same arrival time as the large one at 3715, arrives before the larger signal at 3723 and is almost completely before the larger signal at 3731, and these are 8-second intervals (the large arrivals are at 3704, 3714, 3724, 3734, which are 10-second intervals). The traces in figure 5 are aligned on the expected direction of arrival (and a fixed phase velocity of 1.46 km/s, as observed at H01) for a source in the vicinity of the MH370 expected impact. It is readily apparent that neither of the repeating signals arrivals are from that direction, and that they arrive from 2 different directions. The DOA for the larger 10-second signal is 29.8° , and the observed phase velocity is 1.485 km/s. For the smaller 8-second phase, the DOA is approximately 117° (determination is less reliable due to interference from larger signal). Therefore, H01 will not be useful for investigation of potential arrivals from an MH370 impact. H08 also has a northern array, but it would be blocked by Diego Garcia Island for any arrivals coming from the vicinity of the expected impact site.

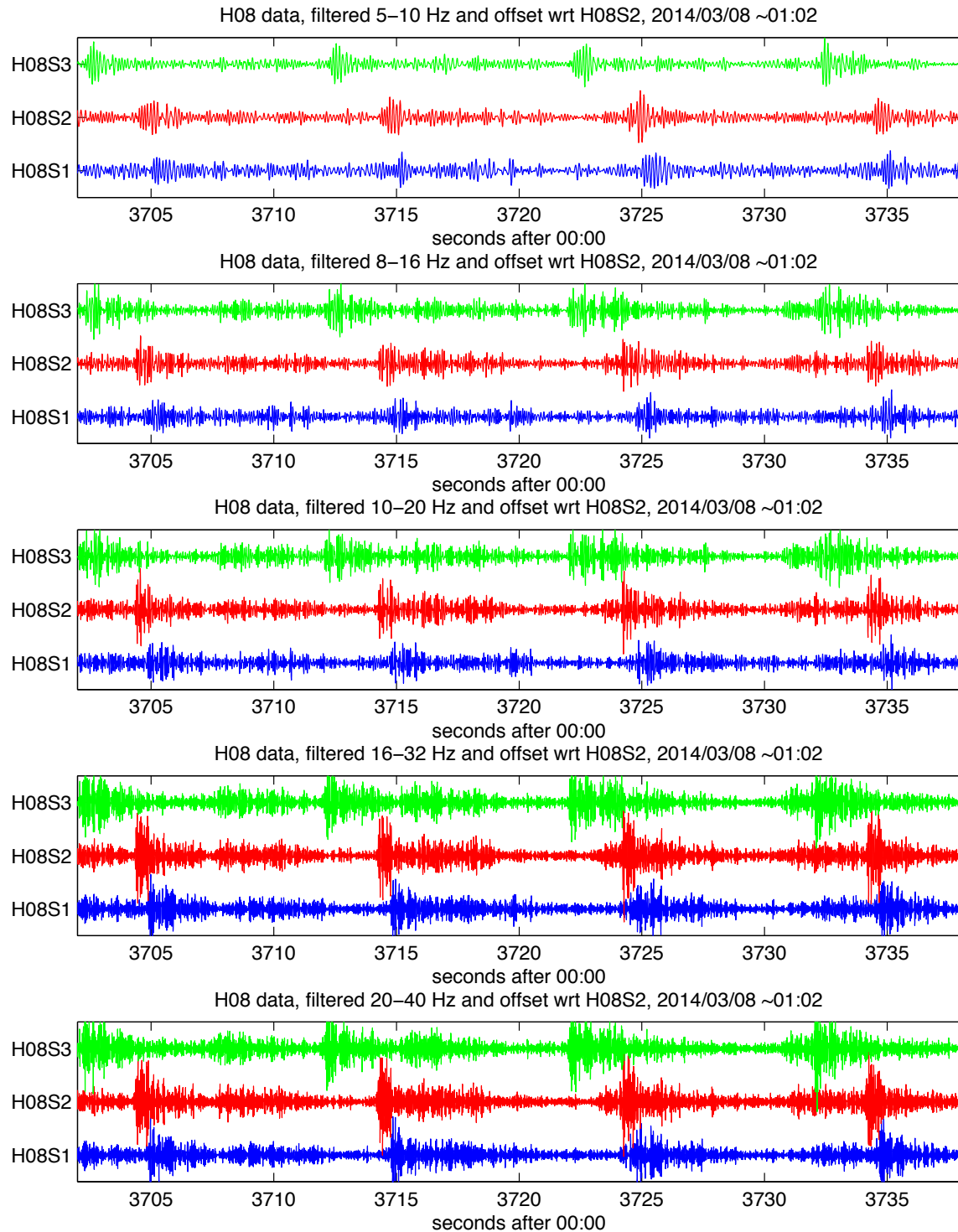


Figure 5: H08 data near expected arrival time. Data are shown filtered into 5 1-octave bands, same filters as figure 1. Note large amplitude signals repeating at 10-second intervals and smaller amplitude signals at 8-second intervals. Also note the broadband nature of the signals, having significant signal-to-noise ratio in all bands from 5 to 40 Hz here. These signals completely obscure any other signals that may be present.

AIS

As expected, AIS is a noisy site. It is close to shore on an island often buffeted by large breakers and exposed to strong winds. We again scanned the waveforms, looking for any signals that might stand out from the noise in any characteristic; however none could be found. Part of the problem is that the station has a low sample rate (20 samples per second) that precludes examining the waveforms in the band of interest, 10-20 Hz (as indicated by the signal of interest observed at H01), since the Nyquist is only at 10 Hz. One could well expect that if the suspected impact signal is not above the noise below 10 Hz at the hydrophones of H01, it then could not be above the noise when converted to a T phase, even without the excessive noise at these frequencies at AIS. As for higher frequencies, since AIS is likely closer to a potential impact site, then frequencies above 20 Hz may be above noise here that are not above noise at H01. But again, the low Nyquist frequency precludes any opportunity to investigate that possibility.

Figure 6 shows a sample of the waveforms around the time of the expected arrival. It was chosen to show one of the common noise bursts (at about 00:36) observed at this station. Several of these appear in the record every hour, so this is not unique and likely represents a local nature noise source, such as large waves crashing on a nearby shore or something similar. The waveforms were filtered at 2-9 Hz to eliminate most of the longer period ocean noise while retaining all available data above 2 Hz (and below the effects of the anti-aliasing filters at the station). We performed a polarization analysis on the data to look for any signals that might appear both above noise and with the correct DOA. The expected DOA here is approximately 137° . The polarization results for approximately the same time intervals as the waveforms in figure 6 are shown in figure 7. As can be seen, the large noise burst has a DOA (labeled 'az' on the figure) of approximately 40 degrees, which is about 100 degrees off from that expected. It is also similar to most of the background noise. Rectilinearity (labeled 'rect' on the figure, a measure of how closely the particle motion conforms to a plane wave, on a scale of 0-1, with 1 being a perfect plane wave) is slightly elevated for this phase, but not particularly distinct from the background noise. The incidence angle (labeled 'inc' on the figure, and is the angle the 3D DOA vector makes with respect to horizontal plane in a vertical plane that includes the vector) is also not distinct from the background noise. In all three measures, the polarization is not distinct from the background noise, indicating that this noise burst is merely a large-amplitude version of the background.

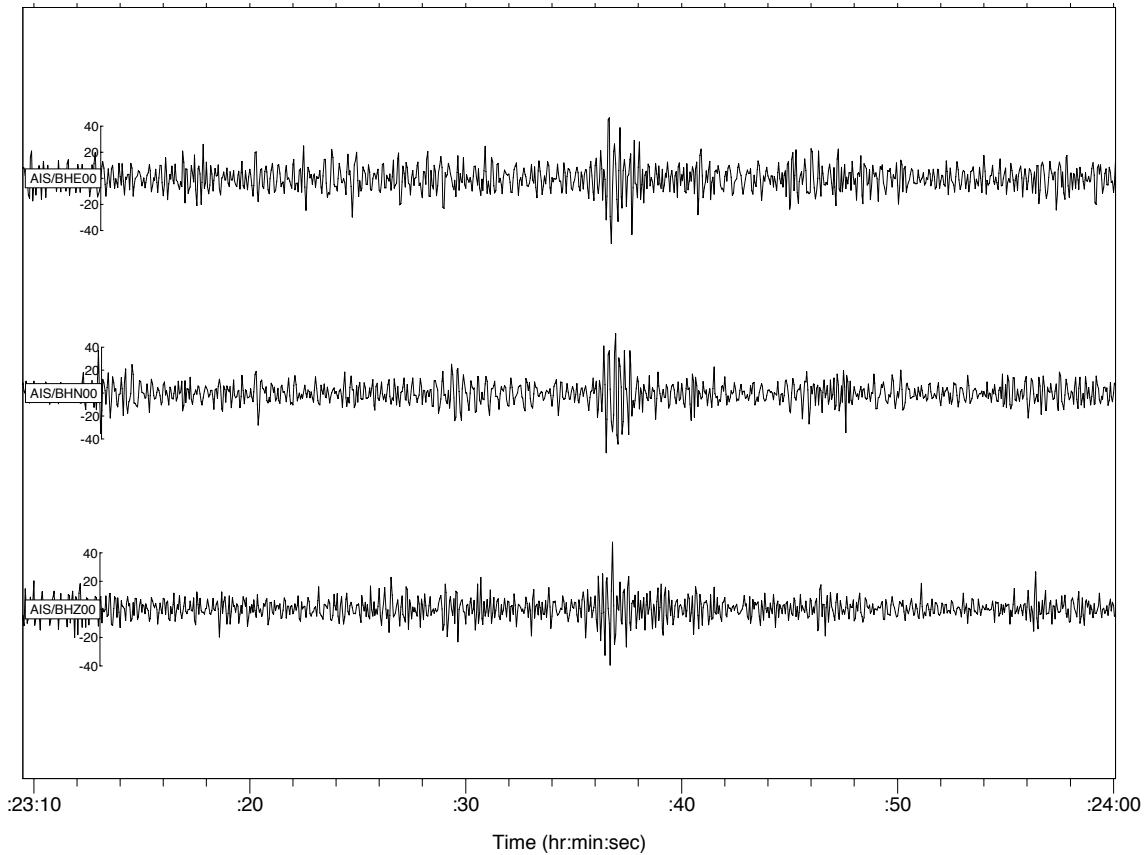


Figure 6: Waveforms from the seismic station at Amsterdam Island (AIS), filter at 2-9 Hz. For the channel names, “BH” indicates a broadband seismometer recorded at high gain, the “00” indicates that these are all components of a single instrument designated “00”, and the “E, N and Z” indicate the component of motion: E is positive east, N is positive north and Z is positive down. Time is given as hour:minute:second after 2014/03/08 00:00 UTC.

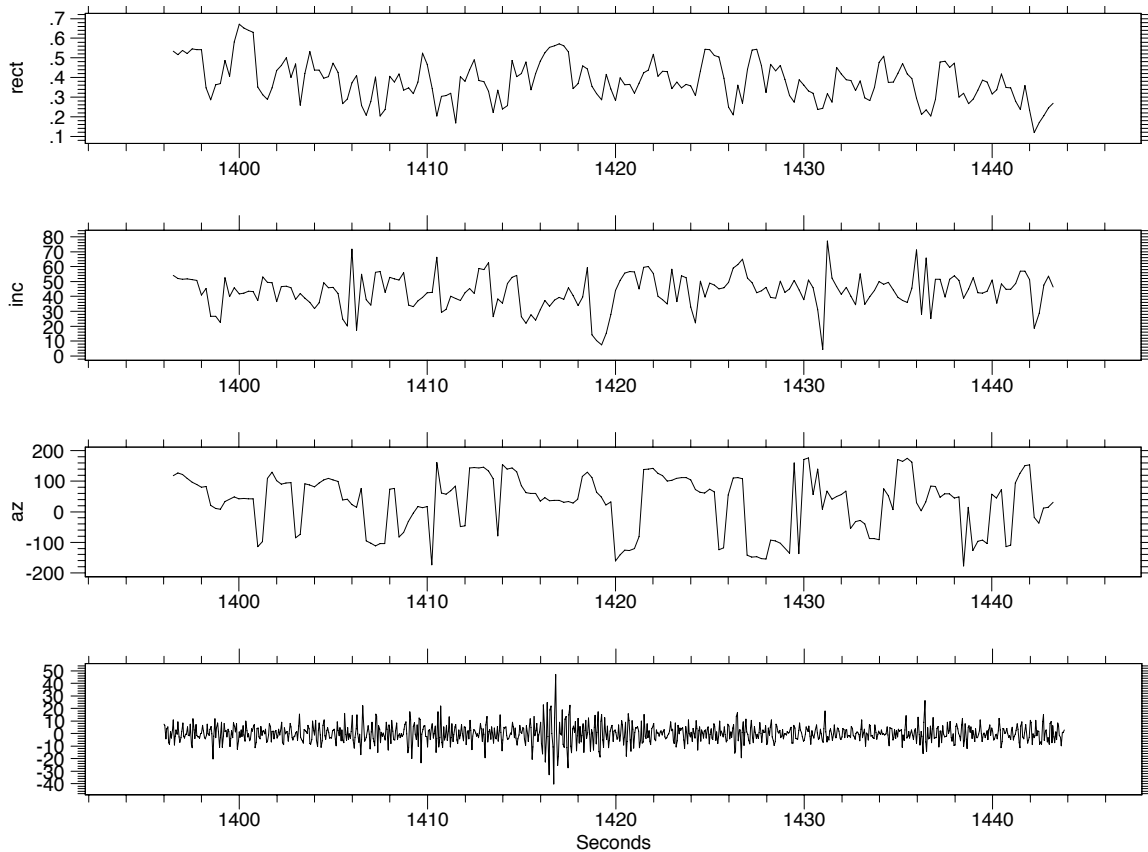


Figure 7: Polarization analysis of Amsterdam Island (AIS) seismic data. Data have been pre-filter to 2-9 Hz. The plots, in order from top to bottom, show rectilinearity, incidence angle, DOA and the seismogram from the vertical component. Time is given in seconds from 2014/03/08 00:00 UTC.

Given that no reasonable signals seem to be present above the noise and from the roughly expected azimuth, it is worth examining the orientation of the station to confirm that it is correctly oriented and would provide accurate azimuths. To do this we chose a large teleseism that is close to the day in question for an analysis to confirm the orientation of the instrument. We chose a M6.5 event near Japan, in the subducting slab of the Philippine Sea plate NW of Okinawa in the Ryukyu Islands. This event occurred on 2014/03/02 at 20:11:23 UTC at the geographic coordinates 27.431°N 127.367°E and a depth of 119.0km (magnitude, location and time from the USGS National Earthquake Information Center).

The P-wave from this quake would be expected to be strong in approximately 1-5 Hz at this range. We observed an arrival around 1-2 Hz at the expected P wave time of approximately 20:23:21, but signal-to-noise ratio was only about 2, which is insufficient to get a good horizontal polarization, especially for near-vertical incidence as this arrival would be. However, The dominant crustal surface waves near 20 seconds (0.05 Hz) would be well excited by this event and are also well below the microseism frequency band that creates so much noise at AIS. A plot of the waveforms with a 1-octave filter across 20 Hz is shown in figure 8. As can be

seen in the figure the north and east components show clear Love and Rayleigh waves well above the noise. The amplitudes on both horizontal components for both waves are roughly equivalent as would be expected for an approximately 45° DOA, clockwise from north. In addition, the motion of the Love wave is NW-SE as expected, and the horizontal motion of the Rayleigh wave is NE-SW, also as expected. This confirms the orientation of the station.

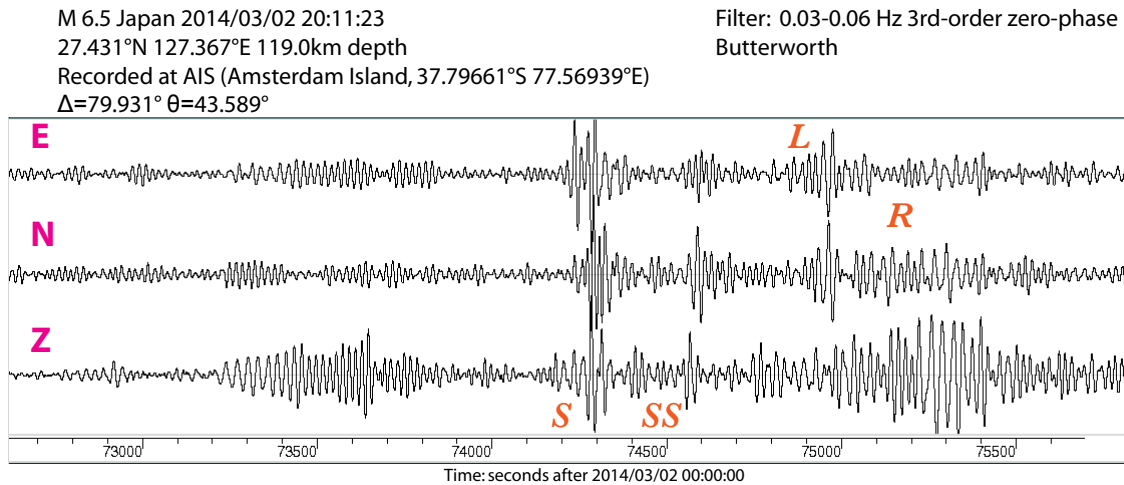


Figure 8. Orientation analysis of AIS using the M6.5 Japan quake from 2014/03/02. E, N, and Z label the 3 components of the instrument. S and SS are body-wave shear arrivals. L and R are the Love and Rayleigh surface waves, respectively. Waveforms have been filtered in a 1-octave band around 20 Hz.

Further information regarding possible flight paths indicated that a time of arrival at AIS of approximately 00:26:30 might be possible. For completeness, we looked at this time in more detail as well. We applied the same tools, including polarization, and careful review as we have done above. No useful signals were discovered; the time includes only the common noise found at this site. Figure 9 shows approximately 1 full minute of data around 00:26:30, filter in 4 bands. The 4 bands from top to bottom are octave bands 2-4, 3-6, 4-8 and 5-10 Hz. The Nyquist frequency is 10 Hz, so it is unnecessary to attempt any higher bands. The figure shows the relatively constant background at 2-4 Hz that is similar to what is seen at all lower frequencies as well. As the frequencies get higher, the more impulsive signals from wave strikes and similar weather-driven phenomena become more prominent. But none of this energy corresponds to seismic body waves that would be expected from the conversion of hydroacoustic energy in the SOFAR channel to seismic energy at the island's offshore slope. Very likely, small signals from converted hydroacoustic phases will be completely obscured in this much noise. The only signal that is not noise in the figure is a seismic surface wave, Rg, visible at about 00:26:25, identified as a surface wave from its dispersion. This would be from

some small seismic source on the island, and not from a more distant ocean surface impact.

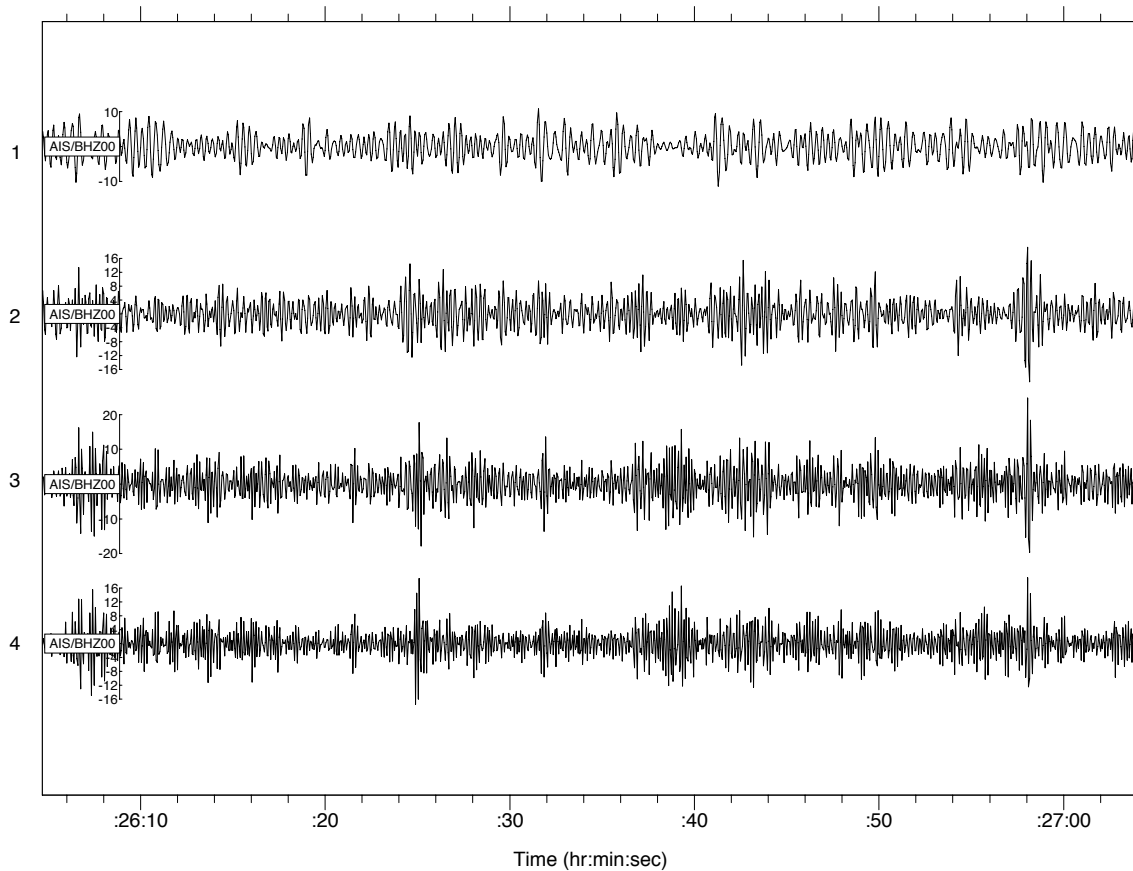


Figure 9. This figure shows a closer look as the seismic waveforms from around the time 00:26:30 at AIS. The vertical component is shown filtered to 4 1-octave overlapping bands. The time interval displays a variety of large-amplitude noise.

Conclusions

The seismic and hydroacoustic data readily and openly available for analysis are quite limited. Only Three potentially applicable station were identified: H01, H08 and AIS. Of these, H01 has a very interesting and potential applicable arrival. H08 is contaminated by a long series of large-amplitude repeating and interfering signals that completely obscure any possible applicable arrival. AIS is contaminated by natural noise sources and has a sample rate sufficiently low as to likely exclude any signals of interest. Thus, at most, we were able to identify a candidate arrival from only a single station. This arrival also has problems in analysis, since it is interfered with by a large-amplitude arrival that follows it with only a small delay. That arrival is clearly associated with some sort of ice event from Antarctica. Continued analysis and further confirmation of the arrival at H01 would only be possible if there are additional sources of data that are either not open or not readily available. The

arrival at H01, if it is indeed from the impact of MH370, would indicate that the impact is toward the southern portion of the broad search area previously declared and likely south of the area in which possible pings were briefly recorded.

In addition it is concluded that the southern Indian Ocean is insufficiently monitored for events of any type, including events of interest for the CTBT. Relatively small but significant explosions could prove to be difficult to detect, locate and identify in this region due to the shortage of useful stations and the likelihood that one or more stations could be rendered useless for monitoring purposes by various types of common noise sources in their vicinity.

Glossary

Accredited Representative

A person designated by a State, on the basis of his or her qualifications, for the purpose of participating in an investigation conducted by another State. Where the State has been established an accident investigation authority, the designated accredited representative would normally be from that authority.

Air-ground communication

Two-way communication between aircraft and stations or locations on the surface of the earth.

Airspace

Any part of the earth's atmosphere that can be used by an aircraft. It is a three-dimensional space where aircraft can operate.

Annex 13

Annex 13 of the Convention on International Civil Aviation (Chicago, 1944) provides the international Standards and Recommended Practices for Aircraft Accident Inquiries and was developed by ICAO. These practices are the basis for aviation accident, serious incident and incident investigations, accident prevention and accident and serious incident reporting.

Australian Search and Rescue Region

Australia, as signatory to the Convention on International Civil Aviation, 1944; the International Convention for the Safety of Life at Sea, 1974; and the International Convention on Maritime Search and Rescue, 1979, is responsible for search and rescue over a vast area (52.8 million square kilometres) made up of the East Indian, South-west Pacific and Southern oceans. Australia has the same boundaries for aviation and maritime search and rescue.

Autonomous Underwater Vehicle

An autonomous underwater vehicle (AUV) is a battery-powered self-propelled underwater vehicle that can be launched and retrieved from a search vessel and is pre-programmed with a search mission. The vehicle may be fitted with instruments including sonar and optical imaging systems.

Bathymetry

The study and mapping of seafloor topography. It involves obtaining measurements of the ocean depth and is equivalent to mapping topography on land.

Beaufort Scale

A scale of wind force, developed in 1805 by Admiral Sir Francis Beaufort, which uses observations of the effects of wind on the sea surface to estimate wind speed. Measurements range from 0 (calm) through to 12+ (hurricane).

Burst Frequency Offset

BFO is a measure of the difference between the expected frequency of a satellite transmission and the frequency received at the ground station.

Burst Timing Offset

BTO is a measure of the time taken for a satellite transmission round trip (ground station to satellite to aircraft and back) and allows a calculation of the distance between the satellite and the aircraft.

Controlled air space

Airspace that is actively monitored and managed by air traffic controllers. To enter controlled airspace, an aircraft must first gain a clearance from an air traffic controller.

Cockpit Voice Recorder

A CVR is a recorder placed in an aircraft for the purpose of facilitating the investigation of an aircraft accident or incident. It records the total audio environment of the cockpit area.

Coordinated Universal Time (UTC)

Coordinated Universal Time (UTC) or Universal Time Coordinated. UTC is the worldwide standard for time and date.

Depressor

A steel weight that is towed behind a search vessel on a long cable in front of the tow vehicle, to help stabilise it. This allows the tow vehicle to ‘fly’ with less motion above the seafloor, while gathering detailed imagery.

Flight Data Recorder

An FDR is a recorder placed in an aircraft for the purpose of facilitating the investigation of an aircraft accident or incident. It records flight parameters such as indicated airspeed.

Ground earth station

A satellite ground station sends or receives data from orbiting satellites.

Handshake

Satellite log-on interrogation messages that originate at the ground earth station and are transmitted through the satellite to the aircraft’s satellite communication system.

Hydrophone

A microphone designed to be used underwater for recording or listening to underwater sound.

Joint Investigation Team

Convened by the Government of Malaysia, the group of international academics and government officials worked towards defining the most probable position of MH370 from early in the surface search until 2 April 2014.

Knot

A unit of speed that is equal to one nautical mile (1.852km) per hour.

Nadir

In sonar systems, a nadir is the region directly below a deep tow vehicle or AUV which is not covered by side scan sonar.

National Collaboration Framework

The National Collaboration Framework was created to assist Commonwealth entities, State, Territory and local jurisdictions to work collaboratively to achieve government objectives.

Nautical mile

A unit of distance based on the circumference of the earth, used for marine charting and navigating. One nautical mile (NM) is equal to 1.852 km.

Pilot-in-Command

The pilot responsible for the operation and the safety of the aircraft during flight time.

Ping

A pulse of sonar sound.

Primary surveillance radar

Primary (or terminal area) radar relies on radio waves reflecting off metallic objects and is effective within a short range from the radar head, which is usually located at an airport.

Remotely Operated Vehicle

A remotely operated vehicle (ROV) is an underwater vehicle which is tethered to a search vessel by a cable and operated remotely by an operator on a search vessel. ROVs are equipped with a range of cameras, lights and manipulator arms to cut and lift objects on the seafloor.

Satellite Communications Working Group

Convened by the Government of Malaysia from early in the surface search, the group of international satellite communications specialists, including Inmarsat and Thales, worked towards defining the most probable position of MH370.

Sea state

A description of sea conditions, recorded using the World Meteorological Organization Sea State Codes. Measurements range from 0 (calm) through to 9 (phenomenal).

Search Strategy Working Group

Coordinated by the ATSB since the completion of the surface search, the group of international satellite and aircraft specialists worked towards defining the most probable position of MH370, at the time of the last satellite communications.

Secondary surveillance radar

Secondary (or en route) radar returns are dependent on a transponder in the aircraft to reply to an interrogation from a radar ground station.

Self-Locating Datum Marker Buoy

A floating buoy equipped with a global positioning system and satellite communication system to periodically transmit its location to primarily aid in search and rescue missions.

Seventh arc

Independent analysis of satellite communications and aircraft performance confirms MH370 will be found in close proximity to the arc labelled as the 7th arc. The arc extends from approximately latitude 20 degrees south to approximately latitude 44 degrees south. At the time MH370 reached this arc the aircraft is considered to have exhausted its fuel and to have been descending.

Side Scan Sonar

A sonar system which uses acoustic pings to form an image of the seafloor. Typically, a side scan sonar consists of two transducers, located in either side of a tow vehicle, AUV or ROV, each of which generates a fan-shaped sonar ping perpendicular to the vessel track.

A sonar system which uses sophisticated post-processing of sonar data to combine a number of sonar pings to form an image with higher resolution than conventional sonar.

Sonar contact

Any anomaly on the seafloor identified in sonar data that looks non-geologic in nature or unusual when compared to the surrounding seafloor.

Sonobuoy

A floating buoy equipped with a hydrophone and a radio transmitter to transmit the underwater sounds to overflying aircraft.

State of Registry

The State on whose register the aircraft is entered.

Note: In the case of the registration of aircraft of an international operating agency on other than a national basis, the States constituting the agency are jointly and severally bound to assume the obligations which, under the Chicago Convention, attach to a State of Registry. See, in this regard, the Council Resolution of 14 December 1967 on Nationality and Registration of Aircraft Operated by International Operating Agencies which can be found in Policy and Guidance Material on the Economic Regulation of International Air Transport (Doc 9587).

Surface search

A surface search for MH370 was conducted from 18 March to 28 April 2014. Coordinated by AMSA and the JACC, it was carried out by an international fleet of aircraft and ships along the seventh arc.

Swath

The effective range of a sonar system.

Swing

The amount of time it takes a vessel to go from its port of departure, out to sea and return to port.

Synthetic Aperture Sonar

A sonar system which uses sophisticated post-processing of sonar data to combine a number of sonar pings to form an image with higher resolution than conventional sonar.

Towed Pinger Locator

A TPL is a device that is towed behind a vessel for detecting the signals being emitted from an underwater locator beacon fitted to an aircraft’s Flight Data Recorder and Cockpit Voice Recorder.

Tow Vehicle

A vehicle which is towed behind a search vessel. The vehicle may be fitted with instruments including sonar and optical imaging systems.

Transponder

A device that emits an identifying signal in response to an interrogating received signal from a communications satellite or ground station.

Tripartite

Shared by or involving three parties. Tripartite meetings that make decisions with regard to MH370 involve the Governments of Australia, Malaysia and the People’s Republic of China.

Underwater Locator Beacon

A device attached to aviation flight recorders that when immersed in water emits an acoustic signal, to assist with locating an aircraft’s Flight Data Recorder and Cockpit Voice Recorder.

Uncontrolled air space

Airspace that has no supervision by air traffic control, so no clearance is required.

Waypoint

A predetermined geographical position that is defined in terms of latitude and longitude coordinates, used for navigation.

Abbreviations

3D	Three Dimensional
ACARS	Aircraft Communications Addressing and Reporting System
ADFR	Automatic Deployable Flight Recorder
ADS-B	Automatic Dependent Surveillance – Broadcast
AF447	Air France flight 447
AFP	Australian Federal Police
AMSA	Australian Maritime Safety Authority
Annex 13	Annex 13 of the Convention on International Civil Aviation (Chicago, 1944)
ATC	Air Traffic Control
ATSB	Australian Transport Safety Bureau
AUV	Autonomous Underwater Vehicle
BASARNAS	Badan SAR Nasional, National Search and Rescue Agency Republic of Indonesia
BEA	Bureau d'Enquêtes et d'Analyses pour la Sécurité de l'Aviation civile (France)
BFO	Burst Frequency Offset
BOM	Bureau of Meteorology
BTO	Burst Timing Offset
CMST	Centre for Marine Science and Technology at Curtin University
CSIRO	Commonwealth Scientific and Industrial Research Organisation
CVR	Cockpit Voice Recorder
DCA	Department of Civil Aviation (Malaysia)
DST Group	Defence Science and Technology Group
DVL	Doppler Velocity Log
EASA	European Aviation Safety Agency
ELT	Emergency Locator Transmitter
FDR	Flight Data Recorder
FL	Flight Level
ft	Feet (dimensional unit)
GIS	Geographic Information System
GPS	Global Positioning System
HSE	Health, Safety and Environment
ICAO	International Civil Aviation Organization
ICT	Information and Communications Technology
IFR	Instrument Flight Rules
JACC	Joint Agency Coordination Centre
JIT	Joint Investigation Team

kHz	Kilo Hertz
KL ARCC	Kuala Lumpur Aeronautical Rescue Coordination Centre
km	Kilometre
km ²	Square kilometre
LPD	Lower Probability of Detection
MBES	Multibeam Echo Sounder
MH370	Malaysia Airlines flight 370
MHz	Mega Hertz
MOU	Memorandum of Understanding
NASA	National Aeronautics and Space Administration
NM	Nautical Mile
NTSB	National Transportation Safety Board (United States)
PDF	Probability Density Function
PIC	Pilot-in-Command
PSR	Primary Surveillance Radar
RAN	Royal Australian Navy
RMP	Royal Malaysia Police
ROV	Remotely Operated Vehicle
SAR	Search and Rescue
SAS	Synthetic Aperture Sonar
SATCOM	Satellite Communications
SATCOM WG	Satellite Communications Working Group
SDU	Satellite Data Unit
SLDMB	Self-Locating Datum Marker Buoy
SSR	Secondary Surveillance Radar
SSS	Side Scan Sonar
SSWG	Search Strategy Working Group
t	Tonne
TPL	Towed Pinger Locator
ULB	Underwater Locator Beacon
USBL	Ultra-Short Base Line
UTC	Coordinated Universal Time
VHF	Very High Frequency

Australian Transport Safety Bureau

The Australian Transport Safety Bureau (ATSB) is an independent Commonwealth Government statutory agency. The ATSB is governed by a Commission and is entirely separate from transport regulators, policy makers and service providers. The ATSB's function is to improve safety and public confidence in the aviation, marine and rail modes of transport through excellence in: independent investigation of transport accidents and other safety occurrences; safety data recording, analysis and research; fostering safety awareness, knowledge and action.

The ATSB is responsible for investigating accidents and other transport safety matters involving civil aviation, marine and rail operations in Australia that fall within Commonwealth jurisdiction, as well as participating in overseas investigations involving Australian registered aircraft and ships. A primary concern is the safety of commercial transport, with particular regard to operations involving the travelling public.

The ATSB performs its functions in accordance with the provisions of the *Transport Safety Investigation Act 2003* and Regulations and, where applicable, relevant international agreements.

Purpose of safety investigations

The object of a safety investigation is to identify and reduce safety-related risk. ATSB investigations determine and communicate the factors related to the transport safety matter being investigated.

It is not a function of the ATSB to apportion blame or determine liability. At the same time, an investigation report must include factual material of sufficient weight to support the analysis and findings. At all times the ATSB endeavours to balance the use of material that could imply adverse comment with the need to properly explain what happened, and why, in a fair and unbiased manner.

Developing safety action

Central to the ATSB's investigation of transport safety matters is the early identification of safety issues in the transport environment. The ATSB prefers to encourage the relevant organisation(s) to initiate proactive safety action that addresses safety issues. Nevertheless, the ATSB may use its power to make a formal safety recommendation either during or at the end of an investigation, depending on the level of risk associated with a safety issue and the extent of corrective action undertaken by the relevant organisation.

When safety recommendations are issued, they focus on clearly describing the safety issue of concern, rather than providing instructions or opinions on a preferred method of corrective action. As with equivalent overseas organisations, the ATSB has no power to enforce the implementation of its recommendations. It is a matter for the body to which an ATSB recommendation is directed to assess the costs and benefits of any particular means of addressing a safety issue.

When the ATSB issues a safety recommendation to a person, organisation or agency, they must provide a written response within 90 days. That response must indicate whether they accept the recommendation, any reasons for not accepting part or all of the recommendation, and details of any proposed safety action to give effect to the recommendation.

The ATSB can also issue safety advisory notices suggesting that an organisation or an industry sector consider a safety issue and take action where it believes it appropriate. There is no requirement for a formal response to an advisory notice, although the ATSB will publish any response it receives.

Australian Transport Safety Bureau

Enquiries 1800 020 616

Notifications 1800 011 034

REPCON 1800 020 505

Web www.atsb.gov.au

Twitter @ATSBInfo

Email atsbinfo@atsb.gov.au

Facebook [atsbgovau](https://www.facebook.com/atsbgovau)

Investigation

ATSB Transport Safety Report
External Aviation Investigation

The Operational Search for MH370

AE-2014-054

Final – 3 October 2017